31 July 2009 | $10

Science

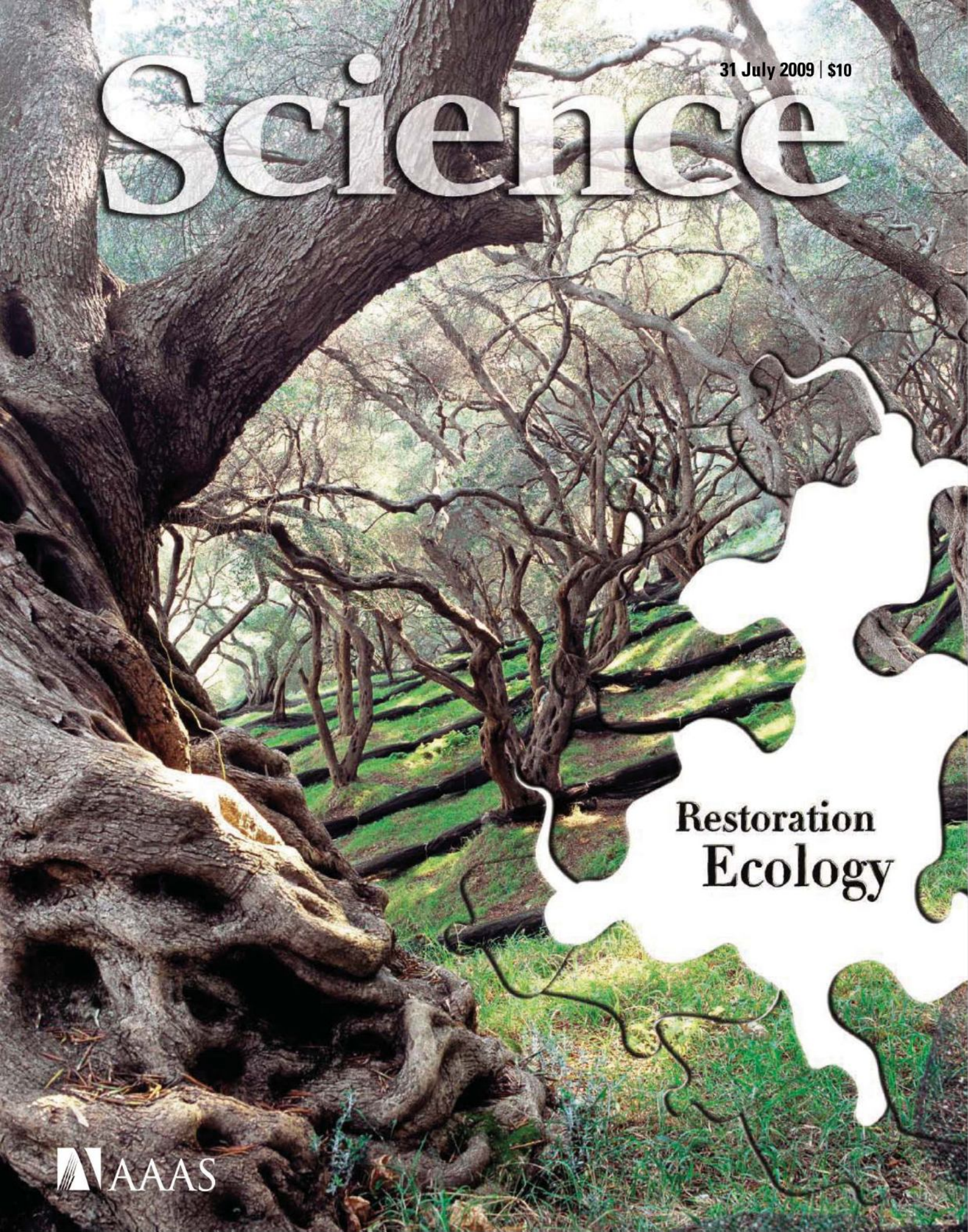

Restoration Ecology

AAAS

Coming Fourth Quarter 2009

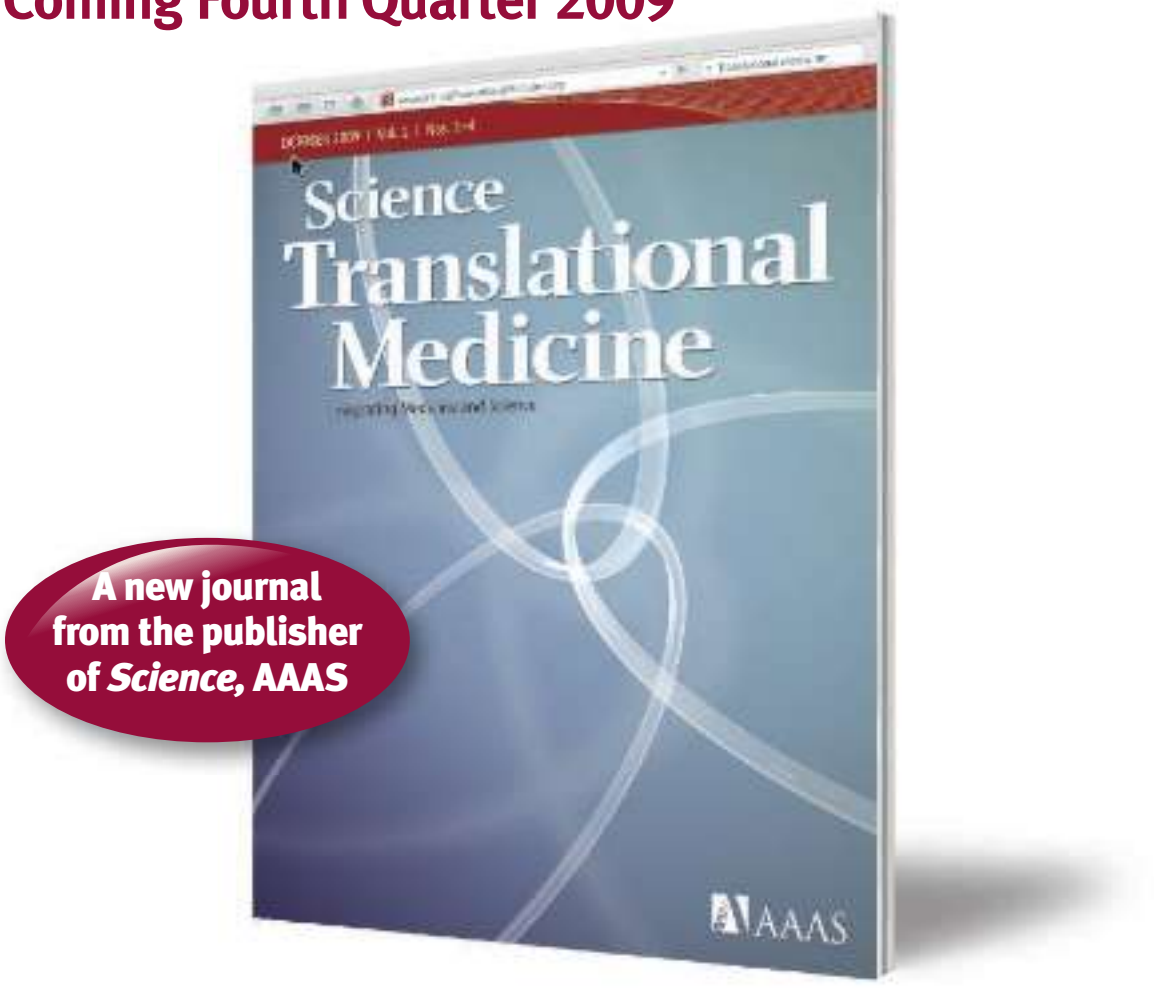

A new journal from the publisher of *Science*, AAAS

Introducing *Science Translational Medicine*, the new journal from AAAS and *Science*.

This fall, AAAS and *Science* will launch *Science Translational Medicine*, a new journal focused on how basic research knowledge can be applied to positively impact human health.

The goal of *Science Translational Medicine* is simple: to help the scientific community harness decades of progress in basic research and translate these complex biological discoveries into medical advances.

Headed by Editor Katrina Kelner, Ph.D., and Chief Scientific Adviser, Elias Zerhouni, M.D., former Director of the NIH, the journal will feature original research articles, in-depth reviews, and commentary. Both in print and online, *Science Translational Medicine* promises a unique forum where biologists, engineers, chemists, and physicians can come together to exchange ideas and information.

Science Translational Medicine is now accepting manuscripts. To submit your work for consideration please visit: **www.sciencemag.org/marketing/stm/papers.dtl.**

For information on institutional or individual subscriptions, please contact **sciencemedicine@aaas.org**.

Science Translational Medicine
AAAS

www.ScienceTranslationalMedicine.org

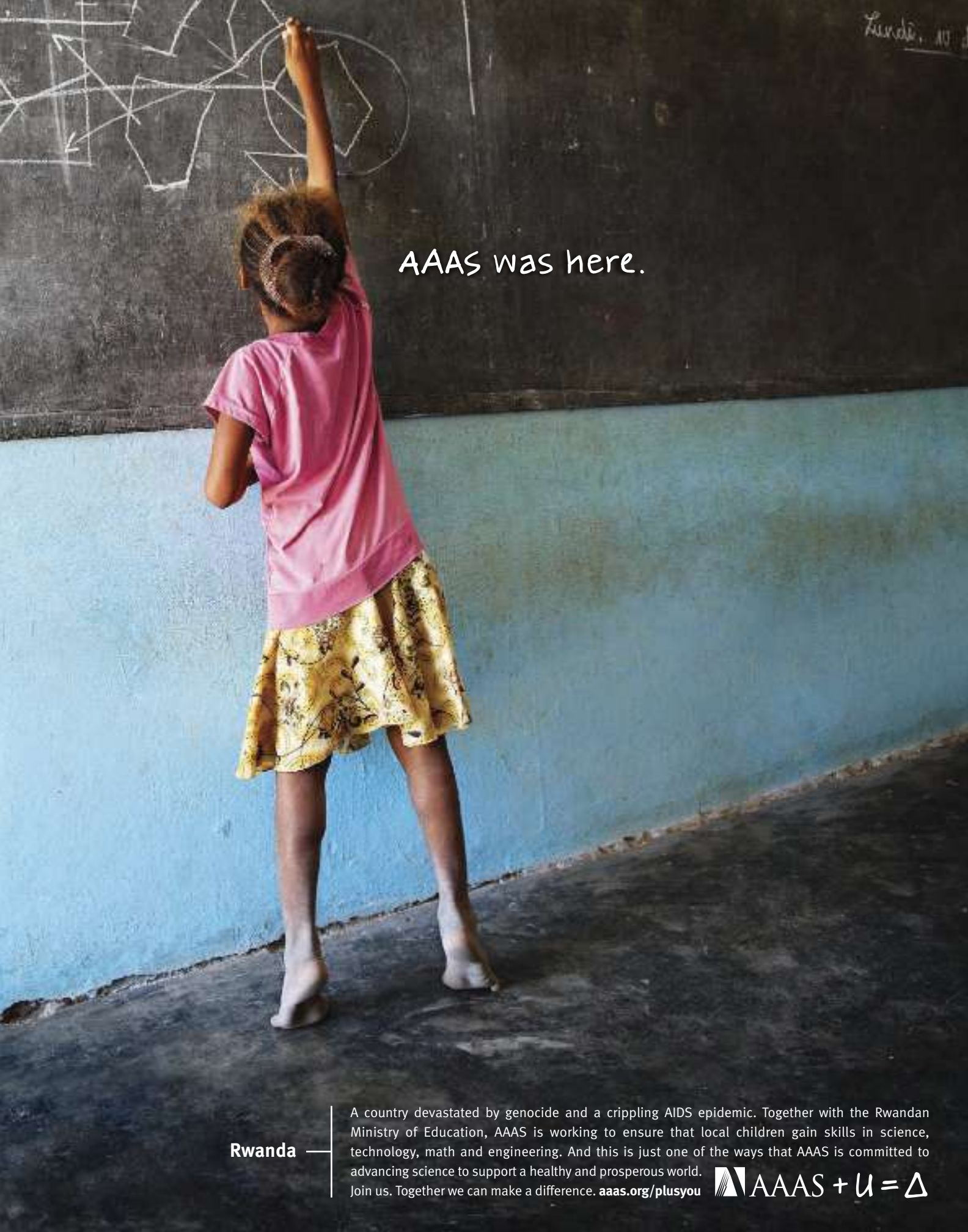

Rwanda

A country devastated by genocide and a crippling AIDS epidemic. Together with the Rwandan Ministry of Education, AAAS is working to ensure that local children gain skills in science, technology, math and engineering. And this is just one of the ways that AAAS is committed to advancing science to support a healthy and prosperous world.
Join us. Together we can make a difference. **aaas.org/plusyou**

AAAS + U = Δ

GE Healthcare

360° Service

"These days, productivity is everything in our business. Knowing that our scientists were losing valuable time due to service-related issues wasn't helping. To solve this problem and improve overall organizational efficiency, we looked at ways we could consolidate by purchasing from fewer suppliers. GE Healthcare was the only company that was happy to manage everything, regardless of the OEM; unbeatable flexibility that allows our teams to focus on what they are best at. Of course, GE Healthcare's track record in healthcare is world-class and it's a real benefit having a company that is happy to manage equipment of all types."

Richard Dickinson, Director of Operations, ERBI Ltd.

Pharmaceutical and biotech companies around the world rely on GE Service to deliver total coverage. From instrument service agreements — including systems from other manufacturers — to asset lifecycle management and facility validation. Now that's service in 360°. At GE Healthcare Life Sciences, our focus is on helping scientists achieve even more, faster. It's a commitment we have in our genes. And all this is backed by the service, support, and investment for the future that being part of GE can bring.

Find out more. Why not talk with us today.
Visit **www.gelifesciences.com/360service**

I ÄKTA I Amersham I Biacore I IN Cell I Whatman I **GE Service** I

imagination at work

First published June 2009
GE Healthcare Bio-Sciences AB, Björkgatan 30, 751 84 Uppsala, Sweden

GE07-09

SPECIAL SECTION

Restoration Ecology

INTRODUCTION

NEWS

PERSPECTIVES

>> See also Editorial p. 517; News stories pp. 525 and 526; Research Article p. 578; Science *Express Reports by J. M. Rey Benayas* et al. *and D. M. Schulte* et al.; Science *Express Perspective by M. W. Chase* et al.

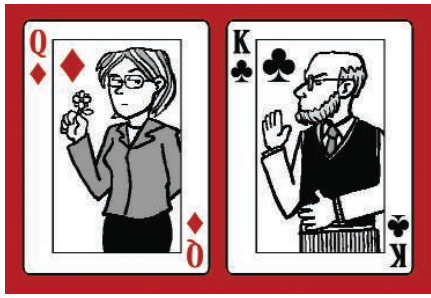

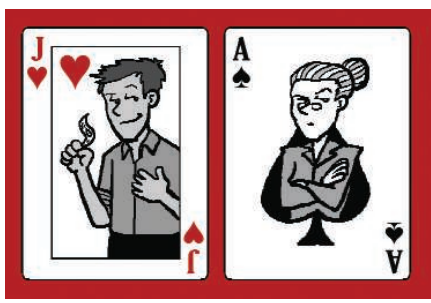

page 528

EDITORIAL

NEWS OF THE WEEK

NEWS FOCUS

LETTERS

BOOKS *ET AL.*

EDUCATION FORUM

CONTENTS continued >>

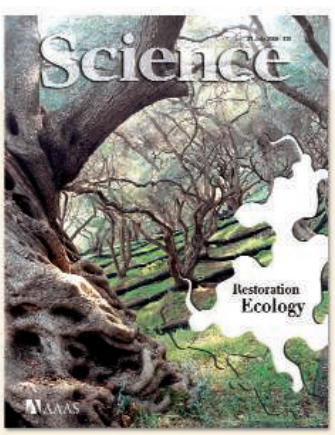

COVER

Like solving a puzzle whose pieces themselves change shape, ecologists around the world are developing techniques to restore degraded and exploited ecosystems. See the special section beginning on page 555.

Photo illustration: Nayomi Kevitiyagala (image: Grand Tour/Corbis)

DEPARTMENTS

Published by AAAS

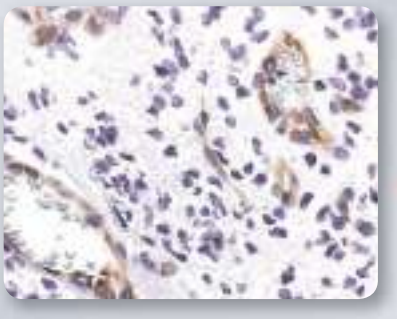

Immunohistochemical analysis of paraffin-embedded human astrocytoma using **VEGF Receptor 2 (55B11) Rabbit mAb #2479**.

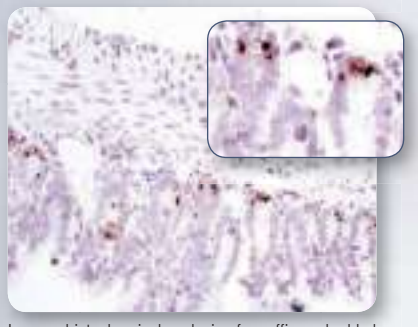

Immunohistochemical analysis of paraffin-embedded mouse small intestine using **MMP7 (D4H5) Rabbit mAb #3801**.

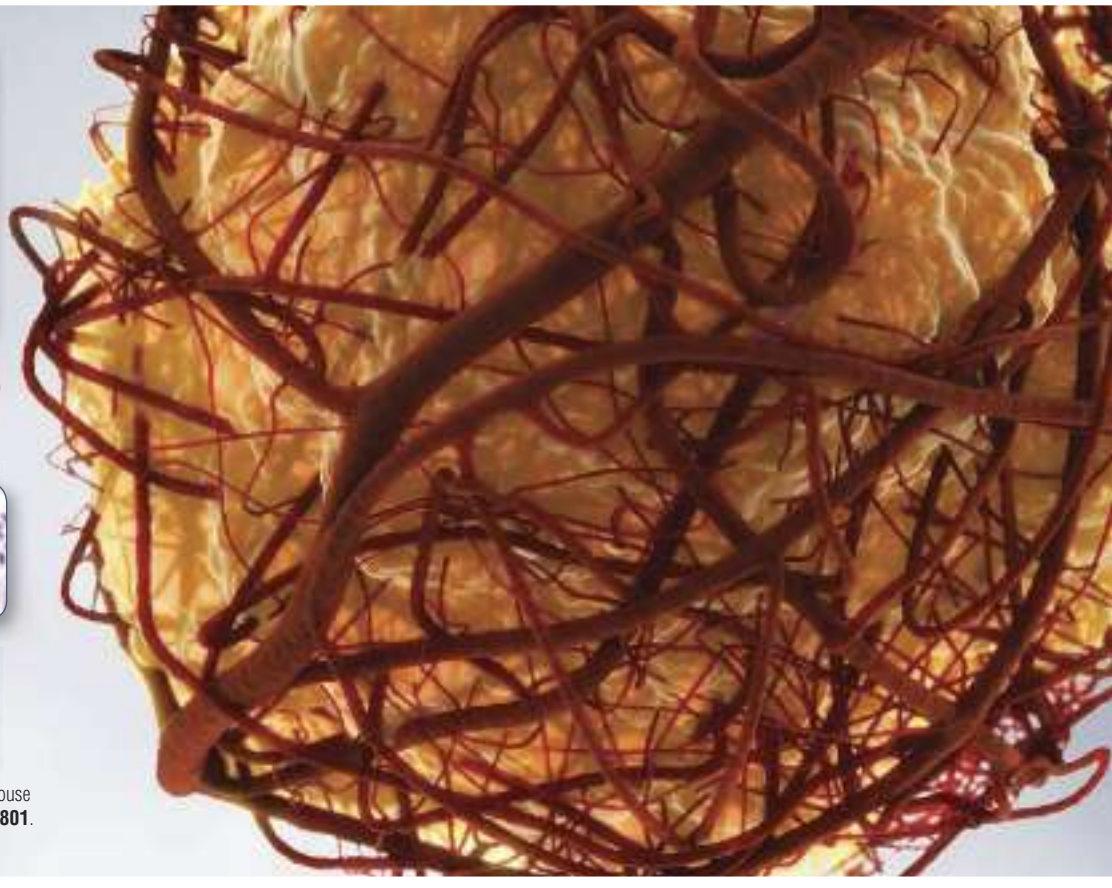

The Highest Quality Antibodies for the Study of

Angiogenesis

...from Cell Signaling Technology®

Unparalleled product quality, validation and technical support.

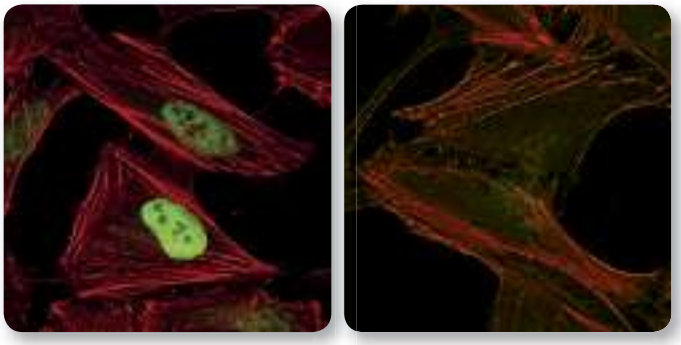

Confocal immunofluorescent analysis of HeLa cells, treated with either 10 µM MG132 (left) or 10 µM MG132 and 1 mM DMOG (right), using **Hydroxy-HIF-1α (Pro564) (D43B5) Rabbit mAb #3434** (green). Actin filaments have been labeled using DY-554 phalloidin (red).

- Cell Signaling Technology's innovative products offer unsurpassed sensitivity, specificity and performance.
- Extensive in-house validation means that optimization is not left up to you, the user.
- Technical support provided by the same scientists who produce and validate the products translates into a thorough, fast and accurate response.

for quality products you can trust...

www.cellsignal.com

Cell Signaling TECHNOLOGY®

PERSPECTIVES

BREVIA

RESEARCH ARTICLES

REPORTS

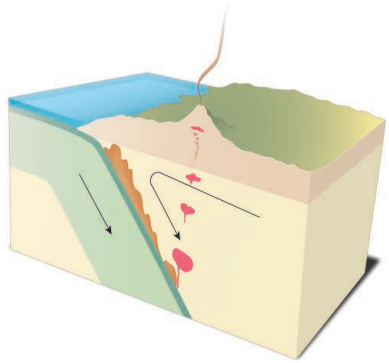

pages 545 & 605

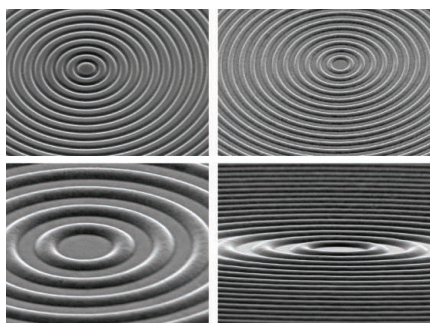

page 594

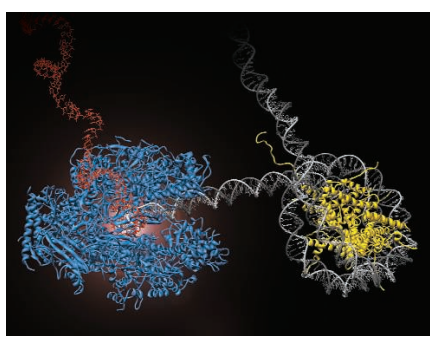

pages 547 & 626

CONTENTS continued >>

New Products, Services, and Solutions

SCIENCEONLINE

SCIENCEXPRESS

www.sciencexpress.org

Unprecedented Restoration of a Native Oyster Metapopulation

D. M. Schulte et al.

The height of oyster reefs above the river bed promotes their restoration in the Chesapeake Bay.

10.1126/science.1176516

>> *News story p. 525; Restoration Ecology section p. 555*

Enhancement of Biodiversity and Ecosystem Services by Ecological Restoration: a Meta-Analysis

J. M. Rey Benayas et al.

Restoration, biodiversity, and ecosystem services are positively linked in a wide range of ecosystem types across the globe.

10.1126/science.1172460

>> *Restoration Ecology section p. 555;* Science *Podcast*

Common Regulatory Variation Impacts Gene Expression in a Cell Type–Dependent Manner

A. S. Dimas et al.

Genetic variation in regulatory elements among humans affects gene expression in a tissue specific manner.

10.1126/science.1174148

Reassessing the Source of Long-Period Comets

N. A. Kaib and T. Quinn

Numerical simulations show that the inner Oort Cloud is a major source of long-period comets that cross Earth's orbit.

10.1126/science.1172676

Barcoding of Plants and Fungi

M. W. Chase and M. F. Fay

10.1126/science.1176906

>> *News story p. 526; Restoration Ecology section p. 555*

TECHNICALCOMMENTS

Comment on "Remeasuring the Double Helix"

N. B. Becker and R. Everaers

full text at www.sciencemag.org/cgi/content/full/325/5940/538-b

Response to Comment on "Remeasuring the Double Helix"

R. S. Mathew-Fenn et al.

full text at www.sciencemag.org/cgi/content/full/325/5940/538-c

SCIENCENOW

www.sciencenow.org

Highlights From Our Daily News Coverage

A 'Cloaking Device' for Earthquakes

Plastic rings could make buildings invisible to quake waves.

New Zealand Tree Stuck in a Time Warp

Plant still harbors adaptations that protected it from a long-dead foe.

Catching a Giant Wave

New insights into tsunami behavior may help researchers better track them with radar.

SCIENCESIGNALING

www.sciencesignaling.org

The Signal Transduction Knowledge Environment

EDITORIAL GUIDE: Unraveling Signaling Complexity

N. R. Gough and J. F. Foley

Dynamics adds to the complexity of signaling networks.

RESEARCH ARTICLE: Cell Type–Specific Importance of Ras–c-Raf Complex Association Rate Constants for MAPK Signaling

C. Kiel and L. Serrano

Ras–c-Raf association rates affect downstream signaling in the absence of negative feedback but not in its presence.

RESEARCH ARTICLE: Comparative Analysis Reveals Conserved Protein Phosphorylation Networks Implicated in Multiple Diseases

C. S. H. Tan et al.

Comparing the human phosphoproteome to that of flies, worms, and yeast reveals insights into evolution and disease.

RESEARCH ARTICLE: Integrating Proteomic, Transcriptional, and Interactome Data Reveals Hidden Components of Signaling and Regulatory Networks

S.-S. C. Huang and E. Fraenkel

Analysis of multiple "omic" data sets with a prize-collecting Steiner tree algorithm reveals components of signaling networks that are not obvious by analyzing the data individually.

PERSPECTIVE: Understanding Modularity in Molecular Networks Requires Dynamics

R. P. Alexander et al.

Relating structure and dynamics of molecular networks remains very challenging.

PERSPECTIVE: Proteomic Revelation—SUMO Changes Partners When the Heat Is On

K. Flick and P. Kaiser

A system-level view of SUMOylation dynamics shows the importance of SUMOylation to the heat shock response.

PERSPECTIVE: The Complexity of Cell Signaling and the Need for a New Mechanics

W. S. Hlavacek and J. R. Faeder

Studies that make sense of protein networks provide approaches to cope with complex signaling pathways.

PERSPECTIVE: Dynamic Advances in NF-κB Signaling Analysis

T. Kobayashi and R. Kageyama

Cytokine stimulation of cells at different time intervals produces distinct patterns of NF-κB–dependent gene transcription.

PODCAST

M. B. Yaffe and A. M. VanHook

Science Signaling's Chief Scientific Editor discusses complexity in signaling networks.

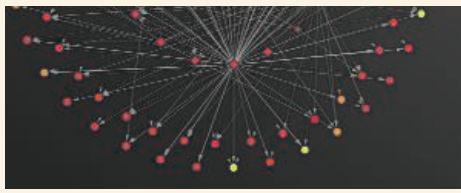

SCIENCESIGNALING
Kinase-substrate network.

CREDIT: (*SCIENCE SIGNALING*) CHRIS SOON HENG TAN/SAMUEL LUNENFELD RESEARCH INSTITUTE AND RUNE LINDING/THE INSTITUTE OF CANCER RESEARCH

SCIENCECAREERS

www.sciencecareers.org/career_magazine

Free Career Resources for Scientists

Perspective: How to Succeed in Big Science and Still Get Tenure

V. McGovern

You need to show that you are a serious scientist, separate from your work group.

Independent Postdocs: Early Autonomy

E. Pain

Demonstrate your independence by negotiating with advisers, seeking individual fellowships, or obtaining a junior-PI position.

Independent Postdocs: Resources

E. Pain

Here is a list of grants, fellowships, and junior-leader positions for postdocs in Europe and the United States.

SCIENCEPODCAST

www.sciencemag.org/multimedia/podcast

Free Weekly Show

Download the 31 July *Science* Podcast to hear about assessing ecological restoration, rethinking graduate student funding, science in Venezuela, and more.

ORIGINSBLOG

blogs.sciencemag.org/origins

A History of Beginnings

SCIENCEINSIDER

blogs.sciencemag.org/scienceinsider

Science Policy News and Analysis

SCIENCE (ISSN 0036-8075) is published weekly on Friday, except the last week in December, by the American Association for the Advancement of Science, 1200 New York Avenue, NW, Washington, DC 20005. Periodicals Mail postage (publication No. 484460) paid at Washington, DC, and additional mailing offices. Domestic individual membership and subscription (51 issues): $146 ($74 allocated to subscription). Domestic institutional subscription (51 issues): $835; Foreign postage extra: Mexico, Caribbean (surface mail) $55; other countries (air assist delivery) $85. First class, airmail, student, and emeritus rates on request. Canadian rates with GST available upon request, GST #1254 88122. Publications Mail Agreement Number 1069624. **Printed in the U.S.A.**

Change of address: Allow 4 weeks, giving old and new addresses and 8-digit account number. **Postmaster:** Send change of address to AAAS, P.O. Box 96178, Washington, DC 20090–6178. **Single-copy sales:** $10.00 current issue, $15.00 back issue prepaid includes surface postage; bulk rates on request. **Authorization to photocopy** material for internal or personal use under circumstances not falling within the fair use provisions of the Copyright Act is granted by AAAS to libraries and other users registered with the Copyright Clearance Center (CCC) Transactional Reporting Service, provided that $20.00 per article is paid directly to CCC, 222 Rosewood Drive, Danvers, MA 01923. The identification code for *Science* is 0036-8075. *Science* is indexed in the *Reader's Guide to Periodical Literature* and in several specialized indexes.

AAAS
ADVANCING SCIENCE, SERVING SOCIETY

EDITED BY STELLA HURTLEY

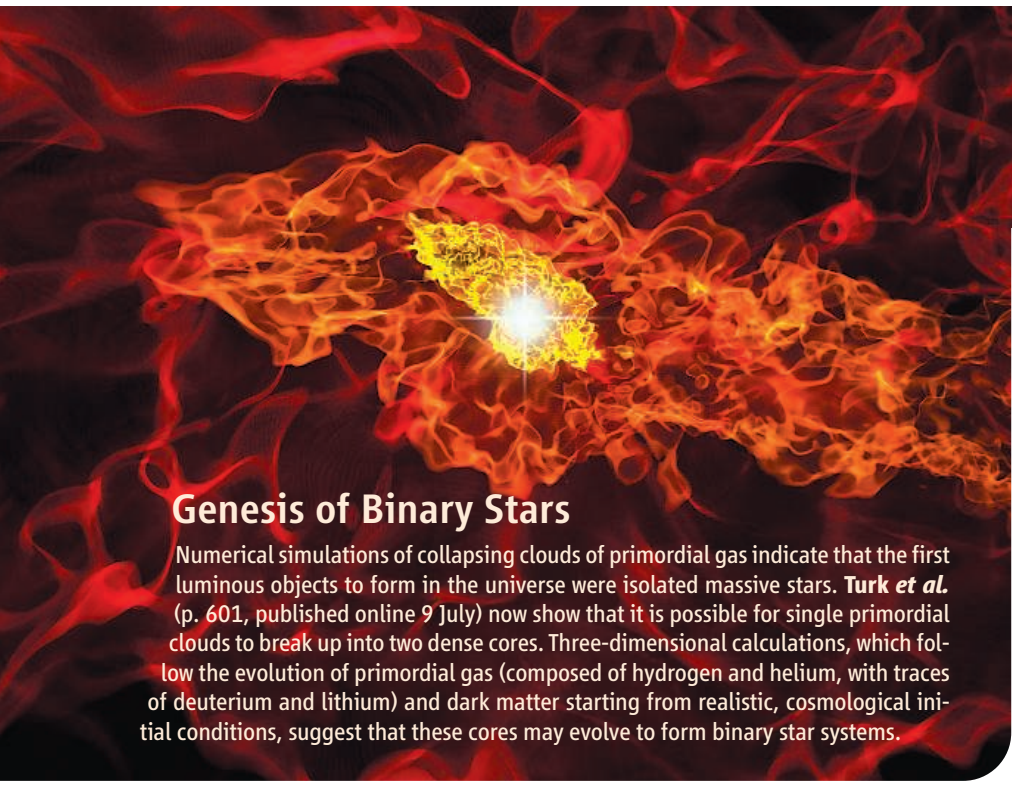

Genesis of Binary Stars

Numerical simulations of collapsing clouds of primordial gas indicate that the first luminous objects to form in the universe were isolated massive stars. **Turk *et al.*** (p. 601, published online 9 July) now show that it is possible for single primordial clouds to break up into two dense cores. Three-dimensional calculations, which follow the evolution of primordial gas (composed of hydrogen and helium, with traces of deuterium and lithium) and dark matter starting from realistic, cosmological initial conditions, suggest that these cores may evolve to form binary star systems.

Fighting for Fisheries

In the debate concerning the future of the world's fisheries, some have forecasted complete collapse but others have challenged this view. The protagonists in this debate have now joined forces to present a thorough quantitative review of current trends in world fisheries. **Worm *et al.*** (p. 578) evaluate the evidence for a global rebuilding of marine capture fisheries and their supporting ecosystems. Contrasting regions that have been managed for rebuilding with those that have not, reveals trajectories of decline and recovery from individual stocks to species, communities, and large marine ecosystems. The management solutions that have been most successful for rebuilding fisheries and ecosystems, include both large- and small-scale fisheries around the world.

Perfectly Flat?

Plasmonic devices, which exploit the interactions of light with surface electrons, show great promise for applications in sensing, communications, and energy conversion. A key hindrance is the deposition of patterned metals used for plasmonics, because, as deposited, the terminal surfaces are rough and not amenable to patterning by directional dry-etching techniques. **Nagpal *et al.*** (p. 594) use patterned silicon substrates on which they add gold, silver, or copper and then apply an epoxy layer to the deposited metal. When pulled apart, the metal separates from the silicon, where the adhesion is poorer, leaving an ultra-smooth surface. The resulting surface plasmon propagation lengths approach the theoretical values for perfectly flat films.

Optimizing Molecular Sieve Production

Microporous membranes composed of aluminosilicate minerals are known as zeolites and are often called molecular sieves because of their ability to filter or separate small molecules. The separation performance is partly governed by the selectivity for one species over another, and this can be compromised by defects, which allow for easy diffusion pathways. To create the porosity, structure-directing agents are used, which need to be removed during a long thermal treatment that can generate defects. **Choi *et al.*** (p. 590) show that for the silicalite-1 system, a rapid thermal treatment significantly reduces the defect density, with corresponding improvement in the filtration of very similar species, such as xylene isomers.

Tracing Mantle Oxidation

The chemical composition of the Earth's mantle varies with tectonic setting. For example, basaltic melts near subduction zones are more oxidized than magma near divergent plate boundaries. **Kelley and Cottrell** (p. 605; see the Perspective by **Hirschmann**) examined melts formed in different tectonic environments, using highly sensitive synchrotron-based analytical methods. The oxidation state of Fe increased with water content and mobile trace elements concentrations. Thus, fluids released from wet subducting plates drive mantle oxidation above subduction zones, which may help to explain the spatial differences in oxygen fugacity of the mantle.

Expanding Sulfonylurea Mechanisms

Sulfonylureas are important drugs used for treatment of diabetes that act through adenosine triphosphate–sensitive potassium channels to promote secretion of insulin from the pancreas. **Zhang *et al.*** (p. 607) present another mechanism by which the beneficial effects of sulfonylureas may also be obtained. Sulfonylureas were identified in a screen for substances that modify the activity of Epac2, a guanine nucleotide exchange factor for the small guanosine triphosphatase Rap1. Mice lacking Epac2 were less responsive to sulfonylureas, which may suggest that Epac2 would be a useful target for development of drugs for treatment of diabetes.

Young and Flexible

How an infant learns to understand and speak a language remains a deep scientific mystery even though millions of kids accomplish these feats each year. Furthermore, this learning capacity is apparently not even taxed to its utmost; children who grow up in bilingual families learn two languages just as rapidly as those who learn only one. **Kovács and Mehler** (p. 611, published online 9 July) have assessed the cognitive flexibility of preverbal 1-year-old children raised in monolingual versus bilingual households and find that the bilingual group displays an impressive facility in handling inconsistent, language-like, inputs. That is, the kids exposed to two distinct languages since birth were able to associate two distinct syllabic structures—AAB and ABA—

CREDITS (TOP TO BOTTOM): RALF KAEHLER, MATTHEW TURK, AND TOM ABEL (KIPAC/STANFORD); CHOI *ET AL.*

Published by AAAS

with looking leftward and rightward, whereas the monolinguals could only do so only with the simpler AAB structure.

Maintaining Mutual Ignorance

Our gut is colonized by trillions of bacteria that do not activate the immune system because of careful compartmentalization. Such compartmentalization means that our immune system is "ignorant" of these microbes and thus it has been proposed that loss of compartmentalization might result in an immune response to the colonizing bacteria. Microorganisms are sensed by cells that express pattern recognition receptors, such as Toll-like receptors, which recognize patterns specific to those microbes. **Slack *et al.*** (p. 617) show that Toll-like receptor–dependent signaling is required to maintain compartmentalization of bacteria to the gut of mice. In the absence of Toll-dependent signaling, intestinal bacteria disseminated throughout the body and the mice mounted a high-titer antibody response against them. This antibody response was of great functional importance because, despite the loss of systemic ignorance to intestinal microbes, the mice were tolerant of the bacteria. Thus, in the absence of innate immunity, the adaptive immune system can compensate so that host and bacterial mutualism can be maintained.

Mapping the Neuronal Map

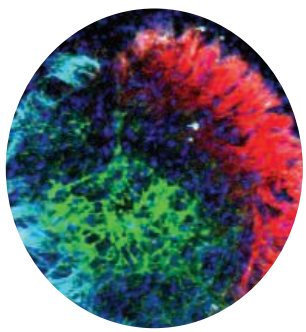

In vertebrates, sensory information is topographically represented as a neural map in the brain. How is the neural map formed in the brain? Nearly a half-century ago, Roger Sperry proposed the "chemoaffinity" model, in which the positional cues on the target determine the axonal projection site, thereby establishing the topographic neural map. However, molecular mechanisms of topographic map formation remain controversial. **Imai *et al.*** (p. 585, published online 9 July; see the Perspective by **Miyamichi and Luo**) now report that the topographic map is formed by axon-axon interactions before the axons reach the target. In the mouse olfactory system, the topography of the map is determined by the relative expression levels of a guidance receptor, Neuropilin-1, and its repulsive ligand, Semaphorin-3A, expressed in axons. Topographic organization occurs even in the absence of the target, the olfactory bulb. These findings require that Sperry's model, which suggests that only the targets determine the topography of neural maps, needs to be reconsidered.

Brain Rewiring After Stress

Chronic stress, mainly through the release of corticosteroids, affects executive behavior through sequential structural modulation of brain networks. Stress-induced deficits in spatial reference, working memory, and behavioral flexibility are associated with synaptic and dendritic reorganization in both the hippocampus and the medial prefrontal cortex. However, the effects of chronic stress on action selection strategies are unclear. **Dias-Ferreira *et al.*** (p. 621) examined whether chronic stress affects the ability of animals to select the appropriate actions based on the consequences of their choice, and found that rats exposed to chronic unpredictable stress rapidly shift toward using habitual strategies. The shift in behavioral strategies observed in chronically stressed animals corresponded to dramatic and divergent changes in connectivity in the associative and sensorimotor corticostriatal circuits underlying these behaviors.

Gradual Unpacking

Eukaryotic DNA is packaged onto nucleosomes, which form the main constituent of chromatin. This packaging material presents a barrier to accessing the genome by the various machineries that need to deal with the DNA: replication, recombination, repair, and transcription complexes, for example. **Hodges *et al.*** (p. 626; see the Perspective by **Otterstrom and van Oijen**) use single-molecule techniques to analyze how a yeast RNA polymerase II ternary elongation complex copes when it encounters a single nucleosome directly in its path. The polymerase does not actively peel the DNA from the nucleosome's surface but, instead, waits patiently until the DNA fluctuates off the nucleosome and then advances, increment by increment, until the nucleosome is destabilized. Under certain conditions the destabilized nucleosome, rather than being lost entirely from the DNA, can be passed back to the DNA behind the polymerase.

CREDIT: IMAI *ET AL.*

Eppendorf Consumables – it's your sample

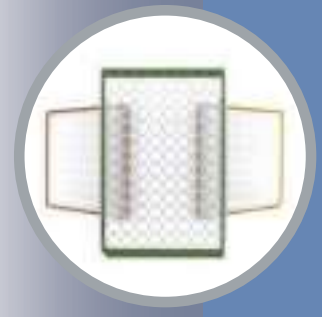

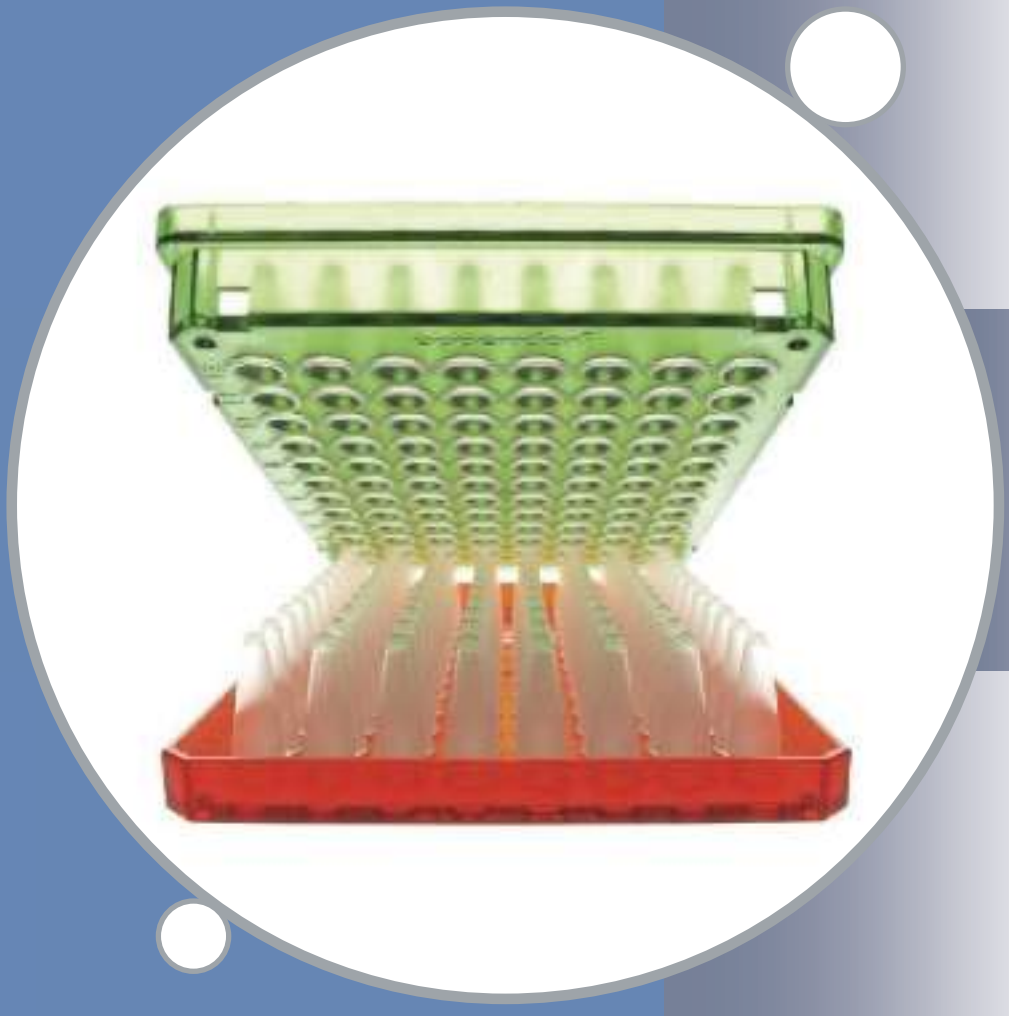

Make the best of it!

Top quality for your sample.

Each of your valuable samples deserves the best treatment. See for yourself how the eppendorf Plate® will save time and reduce costs.

Sample loss in plates can be time consuming and expensive. Therefore, the close environment of each sample should be adapted to its specific quality and purity needs. This can involve a specific purity level or the absence of certain substances, but also stability, reliability, or geometry. The eppendorf Plate® is designed to cover all of the specific needs of your samples!

Eppendorf twin.tec PCR plates*

- Rigid skirt for barcodes and automated handling
- Raised rims for effective sealing
- "skirted" (stackable) and "semi-skirted" plates
- Optimal heat transfer due to reduced wall thickness
- Autoclavable (121 °C, 20 min.)

* Eppendorf owns protective rights under European Patent EP 1 161 994 and US patents US 7,347,977 and US 6,340,589

Learn more about Eppendorf consumables:
www.eppendorf.com/consumables

eppendorf

In touch with life

Your local distributor www.eppendorf.com/worldwide · **Application Support** E-Mail: support@eppendorf.com
Eppendorf AG · Hamburg · Germany · Tel: +49 40 538 01-0 · Eppendorf North America, Inc. · USA · Tel.: +1 800 645 3050

M. S. Swaminathan is UNESCO Chair in Ecotechnology at the M. S. Swaminathan Research Foundation, Chennai, India.

Gene Banks for a Warming Planet

THE BICENTENARY OF CHARLES DARWIN'S LIFE AND WORK REMINDS US THAT THE GREAT biodiversity on Earth underlies natural selection, selective breeding, and the biotechnologies required to provide humanity with food, fiber, fodder, and fuels. In particular, biodiversity affords the development of plant varieties with novel genetic combinations, which will be required to meet the challenges arising from adverse alterations in temperature, precipitation, sea level, and the frequency of drought and floods—all of which are anticipated from human-induced climate change. The loss of each gene and species therefore limits our options for the future.

At the International Congress of Genetics in New Delhi in 1983, I stressed the need for a conservation continuum, beginning with revitalizing conservation of domesticated plants by farm families in all countries, and extending to the establishment of an international genetic resource repository maintained under permafrost conditions. Since then, thanks to the spread of participatory breeding and knowledge-management systems involving scientists and local communities, on-farm conservation and gene banks have become integral parts of national biodiversity conservation strategies. For example, there are now over 125,000 genetic strains of rice, of which over 100,000 are in a cryogenic gene bank maintained by the International Rice Research Institute (IRRI) in the Philippines. This gene pool is invaluable for adapting one of the world's most important cereal grains to the consequences of global climate change.

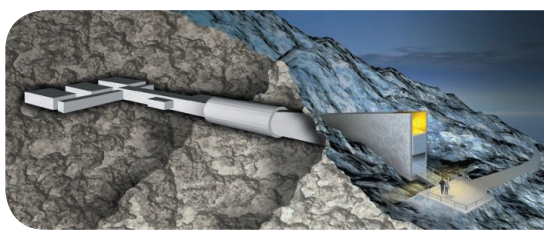

We now largely depend on a few crops such as rice, wheat, corn, soybeans, and potatoes for sustaining global food systems. However, their genetic homogeneity increases their vulnerability to abiotic and biotic stresses. If their production is affected by a natural calamity, their prices will increase and food-deficient countries are likely to face riots and worse. Important publications such as *Lost Crops of the Incas** and *Lost Crops of Africa*† document the historic role of agrobiodiversity in ensuring food and health security. Saving vanishing "orphan crops" has therefore become an urgent task. We also know that millets, tubers, and grain legumes are rich in micronutrients but require less irrigation than the major crops. These plants and others are also sources of genes that confer tolerance to drought, floods, and the increased salinity of soils.

Although plant conservation on farms and in the wild is the ideal approach to preserving genetic diversity in crop plants, these methods are constantly jeopardized by invasive species, human destruction of habitat, and market factors. Therefore, other preservation strategies become essential. There are many cryogenic gene banks around the world resembling that at IRRI, but each is very expensive to maintain. Now, thanks to an initiative of the government of Norway and the Global Biodiversity Trust that began in 2007, the Svalbard Gene Vault located near the North Pole will conserve over 4 million accessions without the need for expensive cryogenics. The remote isolation and capacity of this facility should be sufficient to preserve a sample of the existing genetic variability in all economically important plants, a vast resource generated over the past 10,000 years of agricultural evolution.

But what about species that lie outside the agrobiodiversity realm? We need specialized genetic resource centers to preserve them as well if science is to ameliorate the future consequences of a warming planet. For example, the M. S. Swaminathan Research Foundation in India is conserving genes from plants such as mangroves, which are unusually tolerant of saltwater, and from *Prosopis juliflora*, an excellent source of genes for drought tolerance.

The Global Biodiversity Convention (CBD) that was adopted at Rio de Janeiro in 1992 calls for the conservation and sustainable and equitable use of biodiversity. However, the extinction of species and erosion of genes continue to occur at an alarming rate. The agrobiodiversity conservation model of mobilizing the power of partnership may be useful for achieving the goals of the CBD, and initiating such international projects should be one of many important outcomes of the United Nations Climate Change Conference in Copenhagen this December.

– M. S. Swaminathan

10.1126/science.1177070

*http://books.nap.edu/openbook.php?isbn=030904264X. †www7.nationalacademies.org/dsc/Lost_Crops_of_Africa.html.

CREDITS: (TOP) M. S. SWAMINATHAN RESEARCH FOUNDATION; (RIGHT) GLOBAL CROP DIVERSITY TRUST

Published by AAAS

EDITED BY GILBERT CHIN AND JAKE YESTON

EDUCATION

From Journal to Classroom

Can cutting-edge science be taught in the classroom? Adapted primary literature (APL) retains the structure and results of original research papers while adjusting the content to fit high-school students. The use of APL in the classroom via conversation or group discussion introduces students to the idea that the written text serves both to construct arguments and to present them for evaluation by others.

In a case study at a girls-only religious high school, Falk and Yarden observed the coordination practices—which integrate elements from theory, methods, data, and applications—of eight 12th-grade biology students during an APL-based lesson. In text-oriented practices, the student connects different sections of the text, whereas in research-oriented practices, the student connects the scientific methods used to the data that were generated. The findings reveal not only that coordination practices enhanced APL-based learning but also that students are able to engage with this type of curriculum—learning science by inquiry and learning about science as a means of inquiry. Furthermore, developers of APL-based curricula need not avoid the complexity of the primary scientific literature because coping with ambiguous data through coordination practices expands the students' appreciation of scientific authenticity. — MM*

Res. Sci. Educ. **39**, 349 (2009).

PLANT SCIENCE

Making Salt-Tolerant Plants

Crops grown in salty soils yield less. Soils may be too salty naturally, as expanding land use presses hectares of marginal quality into agricultural service, and reasonable-quality lands can become too salty because of the effects of long-term irrigation. Plants respond to an excess salt in various ways: Some transport salt from the roots to the aboveground shoots; some sequester excess salt into vacuoles; and some are able to exclude excess Na^+ from the shoot tissues. As the first point of contact between the plant and salty soils, how the roots balance Na^+ influx and efflux determines how much Na^+ the plant has to deal with.

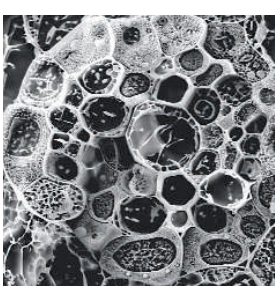

Møller *et al.* have manipulated Na^+ transport in the whole plant or only in the roots (cross section at left) and assessed the outcome in *Arabidopsis*. When the Na^+ transporter is overexpressed constitutively, the plants are, if anything, more sensitive to salt. In contrast, when the transporter is overexpressed specifically in the root stele tissue, which includes the vascular system that feeds the shoots, the plants become more salt-tolerant. In this case, less Na^+ is transported to the shoots, even though the amount of Na^+ taken up from soil into root remains unchanged. — PJH

Plant Cell **21**, 10.1105/tpc.108.064568 (2009).

APPLIED PHYSICS

Strained Graphene

When graphene (an extended two-dimensional layer of graphitic carbon) is adsorbed on substrates such as silicon dioxide (SiO_2), it can develop strong surface corrugations, and this buckling can create regions of high and low strain. Teague *et al*. examined the effect of this strain on the conductance properties of graphene adsorbed on SiO_2 by first making topographic measurements with a scanning tunneling microscope. A fast Fourier transform of these data produced a strain map of the surface. In unstrained regions, the conductance curves show a sharp inflection at the minimum conductivity and, as in suspended graphene samples, evidence Dirac-like behavior. In the strained regions, however, the effects of out-of-plane phonons mediate the inelastic electron tunneling and help create a broader "U-shaped" conductance curve. The authors note that the effects are relatively small and that strain effects should not prove a barrier to creating graphene devices. — PDS

Nano Lett. **9**, 2542 (2009).

*Melissa McCartney is an intern in *Science*'s editorial department.

CHEMISTRY

8 Legs or 8 Faces?

Octopi are so named because these intriguing sea creatures have eight legs. Lu *et al.* have prepared an "octapi" supramolecular complex, so named because it assembles through the stacking interactions of eight faces—more specifically, the faces of aromatic rings bearing delocalized pi-bonded electrons. The authors mixed palladium ions in solution with phenyl-substituted phosphine ligands and pyridine-substituted pyrazole ligands. When the latter ligands were properly sized (with a two-carbon bridge linking a pair of pyridylpyrazoles), crystals formed in which, at the molecular scale, two tightly interlocked macrocycles were held together by a 2.5-nm-long column of stacking interactions involving eight phenyl and pyridyl faces, supplementing phosphorus and pyridyl-nitrogen coordination to the metal centers. Extending the pyrazole bridge length by one carbon disrupted the geometric balance, leading to separated (rather than linked) macrocycles in the resultant crystal lattice. — JSY

J. Am. Chem. Soc. **131**, 10.1021/ja9041912 (2009).

CREDITS (TOP TO BOTTOM): ISTOCK PHOTO; MØLLER *ET AL.*, *PLANT CELL* **21**, 10.1105/TPC.108.064568 (2009)

BEHAVIOR

The Power of the Printed Word

A common belief in the United States is that the media exhibit a liberal bias, which generally aligns them with Democratic programs and politicians, in their reporting of the news and in their selection of what news to report on. In fact, one study estimates the effect of Fox News Channel, which was launched about a decade ago and is generally more conservative than other television outlets, as having increased the Republican share of the vote by half a percentage point.

One month before the November 2005 gubernatorial election in Virginia, Gerber *et al.* carried out a randomized field study in which several thousand households that did not already receive a daily newspaper were given trial subscriptions to either the *Washington Post* (liberal) or the *Washington Times* (conservative). Post-election telephone interviews established that receiving either newspaper had little impact on factual knowledge (such as Harriet Miers being a Supreme Court nominee) or political attitudes (such as President Bush's approval rating). What was affected was voter turnout (as measured by administrative records) and, surprisingly, actual voter choice, with both sets of newspaper-receiving households favoring the Democratic candidate by about seven percentage points. — GJC

The Washington Post

The Washington Times

Am. Econ. J. Appl. Econ. **1**, 35 (2009).

CELL BIOLOGY

Perfect Timing

For cell division to occur, DNA must be completely replicated during the S phase of the cell cycle. Replication is tightly controlled, and the timing of replication of different regions of the genome is linked to localization in the nucleus and gene expression; replication timing of some genetic loci changes during development.

Using a nuclear microinjection system, Lande-Diner *et al.* changed the timing and analyzed histone proteins, which package DNA into nucleosomes to form chromatin. Histones undergo extensive post-translational modifications, which correlate with gene activity. Chromatin replicating late in S phase is generally inactive and packaged with deacetylated histones. They found that when the replication timing of a reporter gene was switched from late to early during S phase, it was repackaged with acetylated histones, which are a marker of active chromatin, and that the opposite occurred when replication was switched from early to late. The switch is due to cell cycle regulation of the acetylation state of histones and indicates how alterations in replication timing, such as that occurring during development, affect chromatin organization and gene activity. — HP

Mol. Cell **34**, 767 (2009).

CHEMISTRY

The Breaking Point

A chemical reaction fundamentally involves the cleavage and formation of bonds between atoms. In general, the electrons and nuclei don't move at precisely the same time; more often than not, a rapid electronic rearrangement precedes a slower nuclear rearrangement, after which the electron distribution may adapt once again. In this context, the question arises of when exactly a bond can be considered broken. Should the criterion be electronic arrangement? Nuclear separation? Some combination of the two?

Wernet *et al.* explore this question in a study of the photoinduced dissociation of gaseous diatomic bromine. Specifically, they excite the molecule to a state that leads rapidly to dissociation and then use ultrafast laser pulses to track changes in the electronic distribution along the way. The probe pulses eject electrons from the valence shell of the dissociating molecule, and the measured kinetic energy variations of these photoelectrons reflect the evolving bonding framework. By shortening the probe pulses below their duration in prior studies of this system, the authors successfully map out the transition from a molecular (Br_2) electronic arrangement to an atomic (2 Br) arrangement, defining the bond-breaking point (~85 fs after excitation) based on the appearance of the atomic signature. — JSY

Phys. Rev. Lett. **103**, 13001 (2009).

CREDITS (TOP TO BOTTOM): THE WASHINGTON POST; THE WASHINGTON TIMES

www.sciencemag.org

Science

1200 New York Avenue, NW
Washington, DC 20005
Editorial: 202-326-6550, FAX 202-289-7562
News: 202-326-6581, FAX 202-371-9227
Bateman House, 82-88 Hills Road
Cambridge, UK CB2 1LQ
+44 (0) 1223 326500, FAX +44 (0) 1223 326501

Subscription Services For change of address, missing issues, new orders and renewals, and payment questions: 866-434-AAAS (2227) or 202-326-6417, FAX 202-842-1065. Mailing addresses: AAAS, P.O. Box 96178, Washington, DC 20090-6178 or AAAS Member Services, 1200 New York Avenue, NW, Washington, DC 20005

Institutional Site Licenses please call 202-326-6755 for any questions or information

Reprints: Author Inquiries 800-635-7181
Commercial Inquiries 803-359-4578

Permissions 202-326-7074, FAX 202-682-0816

Member Benefits AAAS/Barnes&Noble.com bookstore www.aaas.org/bn; AAAS Online Store www.apisource.com/aaas/ code MKB6; AAAS Travels: Betchart Expeditions 800-252-4910; Apple Store www.wapple/eppstore/aaas; Bank of America MasterCard 1-800-833-6262 priority code FAA3YU; Cold Spring Harbor Laboratory Press Publications www.cshlpress.com/affiliates/aaas.htm; GEICO Auto Insurance www.geico.com/landingpage/go51.htm?logo=17624; Hertz 800-654-2200 CDP#343457; Office Depot https://bsd.officedepot.com/portalLogin.do; Seabury & Smith Life Insurance 800-424-9883; Subaru VIP Program 202-326-6417; VIP Moving Services www.vipmayflower.com/domestic/index.html; Other Benefits: AAAS Member Services 202-326-6417 or www.aaasmember.org.

science_editors@aaas.org	(for general editorial queries)
science_letters@aaas.org	(for queries about letters)
science_reviews@aaas.org	(for returning manuscript reviews)
science_bookrevs@aaas.org	(for book review queries)

Published by the American Association for the Advancement of Science (AAAS), *Science* serves its readers as a forum for the presentation and discussion of important issues related to the advancement of science, including the presentation of minority or conflicting points of view, rather than by publishing only material on which a consensus has been reached. Accordingly, all articles published in *Science*—including editorials, news and comment, and book reviews—are signed and reflect the individual views of the authors and not official points of view adopted by AAAS or the institutions with which the authors are affiliated.

AAAS was founded in 1848 and incorporated in 1874. Its mission is to advance science, engineering, and innovation throughout the world for the benefit of all people. The goals of the association are to: enhance communication among scientists, engineers, and the public; promote and defend the integrity of science and its use; strengthen support for the science and technology enterprise; provide a voice for science on societal issues; promote the responsible use of science in public policy; strengthen and diversify the science and technology workforce; foster education in science and technology for everyone; increase public engagement with science and technology; and advance international cooperation in science.

Information for Authors
See pages 807 and 808 of the 6 February 2009 issue or access www.sciencemag.org/about/authors

EDITOR-IN-CHIEF **Bruce Alberts**
EXECUTIVE EDITOR **Monica M. Bradford**
NEWS EDITOR **Colin Norman**
MANAGING EDITOR, RESEARCH JOURNALS **Katrina L. Kelner**
DEPUTY EDITORS **R. Brooks Hanson, Barbara R. Jasny, Andrew M. Sugden**

Editorial senior editors/commentary Lisa D. Chong, Brad Wible; **senior editors** Gilbert J. Chin, Pamela J. Hines, Paula A. Kiberstis (Boston), Marc S. Lavine (Toronto), Beverly A. Purnell, L. Bryan Ray, Guy Riddihough, H. Jesse Smith, Phillip D. Szuromi (Tennessee), Valda Vinson, Jake S. Yeston; **associate editors** Kristen L. Mueller, Nicholas S. Wigginton, Laura M. Zahn; **online editor** Stewart Wills; **associate online editors** Robert Frederick, Tara S. Marathe; **web content developer** Martyn Green; **book review editor** Sherman J. Suter; **associate letters editor** Jennifer Sills; **editorial manager** Cara Tate; **senior copy editors** Jeffrey E. Cook, Cynthia Howe, Harry Jach, Barbara P. Ordway, Trista Wagoner; **copy editors** Chris Filiatreau, Lauren Kmec; **editorial coordinators** Carolyn Kyle, Beverly Shields; **publications assistants** Ramatoulaye Diop, Carlos L. Durham, Joi S. Granger, Jeffrey Hearn, Lisa Johnson, Scott Miller, Jerry Richardson, Jennifer A. Seibert, Brian White, Anita Wynn; **editorial assistants** Emily Guise, Michael Hicks, Patricia M. Moore; **executive assistant** Sylvia S. Kihara; **administrative support** Maryrose Madrid

News deputy news editors Robert Coontz, Eliot Marshall, Jeffrey Mervis, Leslie Roberts; Contributing Editors Elizabeth Culotta, Polly Shulman; **news writers** Yudhijit Bhattacharjee, Adrian Cho, Jennifer Couzin, David Grimm, Constance Holden, Jocelyn Kaiser, Richard A. Kerr, Eli Kintisch, Andrew Lawler (New England), Greg Miller, Elizabeth Pennisi, Robert F. Service (Pacific NW), Erik Stokstad; **interns** Michael Torrice, Brittany Johnson, Preyanka Makadia; **contributing correspondents** Dan Charles, Jon Cohen (San Diego, CA), Daniel Ferber, Ann Gibbons, Robert Koenig, Mitch Leslie, Charles C. Mann, Virginia Morell, Evelyn Strauss, Gary Taubes; **copy editors** Linda B. Felaco, Melvin Gatling, Melissa Raimondi; **administrative support** Scherraine Mack, Fannie Groom; **bureaus** New England: 207-549-7755; San Diego, CA: 760-942-3252, FAX 760-942-4979; Pacific Northwest: 503-963-1940

Production director James Landry; **senior manager** Wendy K. Shank; **assistant manager** Rebecca Doshi; **senior specialists** Steve Forrester, Chris Redwood; **specialist** Anthony Rosen; **Preflight director** David M. Tompkins; **manager** Marcus Spiegler; **specialist** Jason Hillman

Art director Yael Kats; **associate art director** Laura Creveling; **senior illustrators** Chris Bickel, Katharine Sutliff; **illustrator** Yana Greenman; **senior art associates** Holly Bishop, Preston Huey, Nayomi Kevitiyagala; **art associates** Jessica Newfield, Matthew Twombly; **photo editor** Leslie Blizard

***Science* International**

Europe (science@science-int.co.uk) **editorial: international managing editor** Andrew M. Sugden; **senior editor/commentary** Julia Fahrenkamp-Uppenbrink; **senior editors** Caroline Ash, Stella M. Hurtley, Ian S. Osborne, Peter Stern; **associate editor** Maria Cruz; **locum editor** Helen Pickersgill; **editorial support** Deborah Dennison, Rachel Roberts, Alice Whaley; **administrative support** John Cannell, Janet Clements, Louise Moore; **news: europe news editor** John Travis; **deputy news editor** Daniel Clery; **contributing correspondents** Michael Balter (Paris), John Bohannon (Vienna), Martin Enserink (Amsterdam and Paris), Gretchen Vogel (Berlin); **intern** Claire Thomas

Asia Japan Office: Asca Corporation, Eiko Ishioka, Fusako Tamura, 77 Tenjin-cho, Shinjuku, Tokyo 162-0808, Japan; +81 3 6802 4616, FAX +81 3 6802 4615, inquiry@sciencemag.jp; **asia news editor** Richard Stone (Beijing: rstone@aaas.org); **contributing correspondents** Dennis Normile [Japan: +81 (0) 3 3391 0630, FAX +81 (0) 3 5936 3531; dnormile@gol.com]; Hao Xin [China: +86 (0) 10 6307 4439 or 6307 3676, FAX +86 (0) 10 6307 4358; cindyhao@gmail.com]; Pallava Bagla [South Asia: +91 (0) 11 2271 2896; pbagla@vsnl.com]

EXECUTIVE PUBLISHER **Alan I. Leshner**
PUBLISHER **Beth Rosner**

Fulfillment Systems and Operations (membership@aaas.org); **director** Waylon Butler; **senior systems analyst** Nomuna Nyamaa; **customer service supervisor** Pat Butler; **specialists** Latoya Casteel, LaVonda Crawford, Vicki Linton, April Marshall; **data entry supervisor** Cynthia Johnson; **specialists** Shirlene Hall, Tarrika Hill, William Jones

Business Operations and Administration director Deborah Rivera-Wienhold; **assistant director, business operations** Randy Yi; **manager, business analysis** Michael LoBue; **manager, business operations** Jessica Tierney; **financial analysts** Priti Pamnani, Celeste Troxler; **rights and permissions: administrator** Emilie David; **associate** Elizabeth Sandler; **marketing director** Ian King; **marketing managers** Allison Pritchard, Alison Chandler, Julianne Wielga; **marketing associates** Aimee Aponte, Mary Ellen Crowley, Adrian Parham, Wendy Wise; **marketing executive** Jennifer Reeves; **director, site licensing** Tom Ryan; **director, corporate relations** Eileen Bernadette Moran; **publisher relations, eresources specialist** Kiki Forsythe; **senior publisher relations specialist** Catherine Holland; **publisher relations, east coast** Phillip Smith; **publisher relations, west coast** Philip Tsolakidis; **fulfillment supervisor** Iquo Edim; **fulfillment coordinator** Carrie MacDonald; **marketing associate** Mary Lagnaoui; **electronic media: manager** Lizabeth Harman; **project manager** Trista Snyder; **assistant manager** Lisa Stanford; **senior production specialists** Christopher Coleman, Walter Jones; **production specialists** Nichele Johnston, Kimberly Oster

Advertising director, worldwide ad sales Bill Moran

Product (science_advertising@aaas.org); **midwest/west coast/w. canada** Rick Bongiovanni: 330-405-7080, FAX 330-405-7081; **east coast/e. canada** Laurie Faraday: 508-747-9395, FAX 617-507-8189; **uk/europe/asia** Roger Goncalves: TEL/FAX +41 43 243 1358; **japan** Mashy Yoshikawa: +81 (0) 3 3235 5961, FAX +81 (0) 3 3235 5852; **senior traffic associate** Deiandra Simms

Commercial Editor Sean Sanders: 202-326-6430

Project Director, Outreach Brianna Blaser

Classified (advertise@sciencecareers.org); **u.s.: sales manager** Daryl Anderson: 202-326-6543; **midwest** Tina Burks: 202-326-6577; **east coast** Alexis Fleming: 202-326-6578; **west/south central** Nicholas Hintibidze: 202-326-6533; **sales coordinators** Rohan Edmonson, Shirley Young; **international: sales manager** Tracy Holmes: +44 (0) 1223 326525, FAX +44 (0) 1223 326532; **sales** Susanne Kharraz, Dan Pennington, Alex Palmer; **sales assistant** Lisa Patterson; **japan** Mashy Yoshikawa: +81 (0) 3 3235 5961, FAX +81 (0) 3 3235 5852; **advertising support manager** Karen Foote: 202-326-6740; **advertising production operations manager** Deborah Tompkins; **senior production specialist/graphic designer** Amy Hardcastle; **senior production specialist** Robert Buck; **senior traffic associate** Christine Hall

AAAS Board of Directors retiring president, chair James J. McCarthy; **president** Peter C. Agre; **president-elect** Alice Huang; **treasurer** David E. Shaw; **chief executive officer** Alan I. Leshner; **board** Alice Gast, Linda P. B. Katehi, Nancy Knowlton, Cherry A. Murray, Julia M. Phillips, Thomas D. Pollard, David S. Sabatini, Thomas A. Woolsey

AAAS
ADVANCING SCIENCE, SERVING SOCIETY

Graveyard Geology

The Geological Society of America (GSA) is pressing cemeteries into service as global climate monitors. This month, the society invited the public to measure gravestones to gain data on air pollution and climate change since the Industrial Revolution.

White marble gravestones are highly susceptible to erosion from acid rain. Because they bear dates, the stones can help scientists infer a region's climate and pollution history, says GSA's education director, Gary Lewis, in Boulder, Colorado. Marble headstones are mainly a Christian tradition, so Lewis expects the data to cluster in the Americas, Europe, and Oceania.

To participate, you'll need a GPS device to record a marker's coordinates and a micrometer to measure its weathering. That's easy in places such as the United Kingdom and Australia, where inscribed letters on headstones are often filled with lead that starts out flush with the stone and stays in place as the marble wears away. Lacking that clue, weathering can be measured by comparing the thickness at the stone's top and bottom.

Participants will log their data into the project's Web site (www.goearthtrek.org/Gravestones/Gravestones.html). Lewis says that after 2 years, GSA will create a global map to provide data for climatologists. Thomas Paradise, a geomorphologist at the University of Arkansas, Fayetteville, calls the project "a great idea, long overdue."

A FACE FOR PHINEAS GAGE

A 19th century photograph of a one-eyed man proudly holding an iron spike is causing a stir among neuroscientists. The unlabeled photo, held for decades in a private collection, turns out to be the only known image of Phineas Gage, the railroad worker who suffered one of the most famous brain injuries in medical history.

In September 1848, an explosion in Vermont drove a 100-centimeter tamping iron through Gage's skull (*Science*, 20 May 1994, p. 1102). A doctor saw "half a teacupful" of brain spill from the opening. Amazingly, Gage recovered, albeit with a radical change in personality, from personable and conscientious to irascible and rude.

Scientists have always wondered whether Gage's injury caused other mental problems. But this picture "confirms the popular accounts," says Johan Carlin, a neuroscience Ph.D. student at the University of Cambridge in the United Kingdom, and creator of The Phineas Gage Fan Club blog. "It is encouraging to see that he was indeed well enough to pose for a picture," Carlin says. "The pose with the iron rod is consistent with popular accounts that he toured as part of a freak show after his recovery." Carlin adds: "It's amazing to finally be able to put a face to the story."

Turning Rejection Into Success?

Are piles of unwanted lemmas and corollaries collecting dust in the depths of your office? Send them to *Rejecta Mathematica*, a new open-access online journal launched to publish mathematics papers that other journals won't. Mark Davenport, a Ph.D. student in electrical engineering at Rice University in Houston, Texas, says he and a colleague dreamed up the journal while discussing a rejected paper they had written about card counting in blackjack. "We realized this could be the sort of paper that people might find interesting and educational but also might have no natural home among existing journals," Davenport says.

"I think it's an entertaining way to publish some decent papers that haven't been published for whatever reason," says Richard Thomas, a geometer at Imperial College London, who sits on the editorial board of the peer-reviewed journal *Selecta Mathematica*. Rejected mathematical papers are already available on the Web, Thomas notes. But he says that if the new publication can encourage serious comments and "help the refereeing process while filtering the nutters, then this should be watched with interest." Davenport agrees that maintaining standards is key: "We do not intend to provide a home for the world's mathematical cranks."

Highland Wolves

No wolves have trod the Scottish Highlands for more than 250 years. Meanwhile, the local red deer, with no natural predators, have been grazing the hillsides bare. So the Scots have been talking about reintroducing the gray wolf. Now a U.S.–Australian research team says the experience of Yellowstone National Park in the United States shows that wolves might help restore Highland ecology—not just by eating deer but also by creating a "landscape of fear" that would alter deer behavior.

William Ripple, a professor of forest ecosystems and society at Oregon State University in Corvallis, says the return of wolves to Yellowstone in the 1990s after a 60-year absence brought an unforeseen bonus: Many plant and animal populations rebounded as elk—the same species as Highland deer—started avoiding areas where they might run into wolves (*Science*, 27 July 2007, p. 438). In a paper in press in *Biological Conservation*, Ripple and colleagues recommend a large-scale wolf-and-deer experiment, perhaps on an island.

Timothy Coulson, a population biologist at Imperial College London, thinks wolves in Scotland could exert the same ecological impact as wolves in Yellowstone did. But testing the idea would take a lot of land, he notes: The average wolf needs about 260 square kilometers of roaming room.

CREDITS (TOP TO BOTTOM): GARY LEWIS; JACK AND BEVERLY WILGUS; ALISON HESTER; (INSET) U.S. FISH AND WILDLIFE SERVICE

Agreement on a plant bar code
526

Rethinking graduate education
528

PARTICLE PHYSICS

More Bad Connections May Limit LHC Energy or Delay Restart

MEYRIN, SWITZERLAND—Last September, the world's highest-energy particle smasher—the Large Hadron Collider, or LHC—mangled itself when a splice in a superconducting electrical line melted and set off a chain reaction of mechanical failures (*Science*, 26 September 2008, p. 1753). Since then, physicists here at the European particle physics laboratory, CERN, have installed exquisitely sensitive warning systems to monitor the delicate splices and head off a similar catastrophe (*Science*, 12 December 2008, p. 1620). Now, however, researchers have found flaws in different electrical connections that will limit the LHC's energy.

The bad connections will restrict the current that can course safely through the 1232 superconducting magnets that guide protons around the 27-kilometer subterranean ring. That restriction will limit the energy that the countercirculating bunches of protons will reach before they smash together in the hearts of four enormous particle detectors spaced around the ring. As *Science* went to press, researchers were testing the last of the 10,000 connections and planned to evaluate the data within a week, says Stephen Myers, director of accelerators and technology at CERN. "We will know the safe current we can run at without fixing anything else," Myers says. "And that will tell us the maximum energy we can run at" for the first year.

If the problem is too bad, though, it could delay the restart of the gargantuan accelerator, which is now slated for November. Officials had hoped to power up in September, but that date has slid as workers patch a couple of leaks in the LHC's cryogenics system.

The faulty connections mark another bump in the road for the $5.5 billion collider, which was once supposed to turn on in 2005 but circulated its first particles only last year. The LHC aims to blast massive new particles into existence that could light the way to a deeper understanding of the universe. The current highest-energy collisions are produced by the Tevatron collider at the Fermi National Accelerator Laboratory in Batavia, Illinois, which fires protons into antiprotons at energies of 2 teraelectron-volts (TeV). The LHC is designed to reach 14 TeV, although CERN officials had already set 10 TeV as the maximum energy for this coming year. The new problems could limit the energy to 8 TeV or less.

The new problems lie literally right next to the old ones. In last year's mishap, a soldered splice between two ribbonlike superconductors melted. The rupture caused the 9000 amps of current flowing through the line to "arc" to other nearby metal parts within the machine. In an instant, that lightning strike burned through the surrounding tube that kept the superconducting line bathed in frigid liquid helium. Boiling liquid and gas flooded the magnets' sealed casings, whose emergency relief valves were not designed to cope with such a deluge. As a result, a pressure wave shot through the machine, damaging 53 magnets and tearing some of the devices, which weigh up to 35 metric tons, from their moorings.

The new worry involves not the superconducting splices but the ordinary copper that surrounds them. Within a magnet, the ribbonlike superconductor runs within a thick copper cladding. At the junction of two magnets, the ribbons lie exposed so that they can be soldered together, one on top of the other like the slices of bread in a grilled-cheese sandwich. The splice is then encased in a sleeve of "copper stabilizer," which must be soldered to the cladding at either end of the junction. Since May, researchers have found that some of these copper-to-copper connections are not up to standards.

The problem is not quite as serious as a flaw in the superconducting splices them-

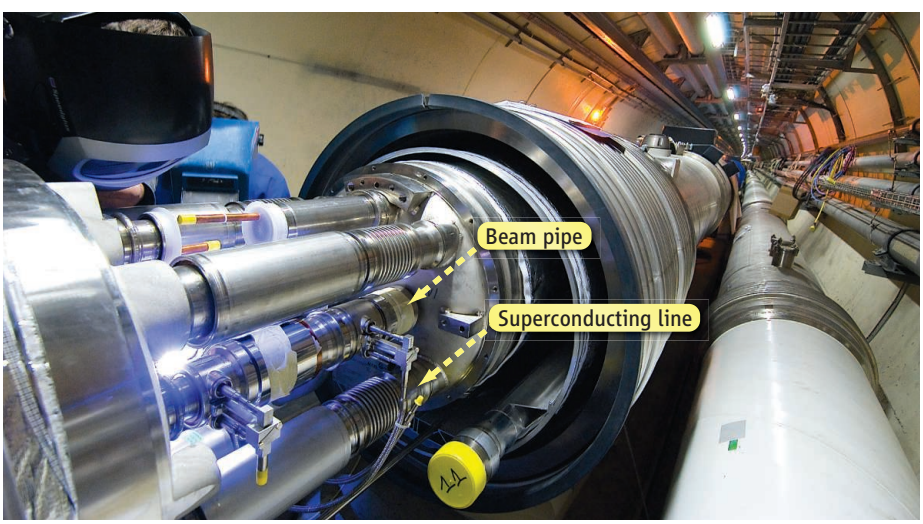

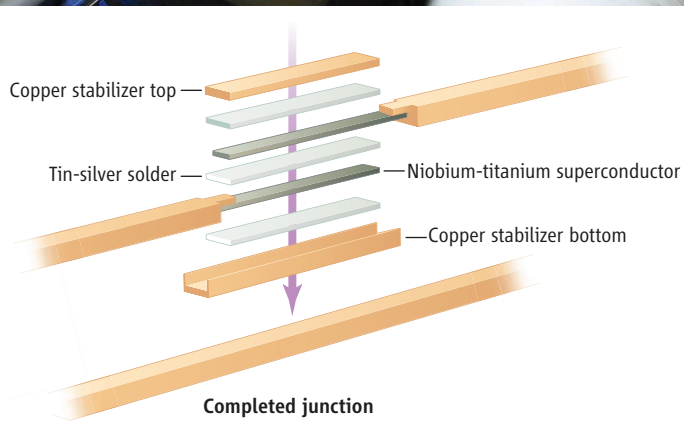

Weak link. The LHC has 10,000 connections between superconducting magnets. Faulty soldering between the nonsuperconducting copper parts of those junctions (bottom) will limit the accelerator's energy for the coming year.

CREDIT: CERN; (ILLUSTRATION) P. HUEY/*SCIENCE*

Published by AAAS

Saving the solenodon 531

Galactic limits to growth 532

selves. Ordinarily, all the current flows through the superconducting ribbon. It would flow through the copper stabilizer only if the superconducting wire got hot enough to "quench" and lose its ability to carry current without resistance. If a stabilizer were faulty, however, the current would continue to flow through the splice, which might melt like an overloaded fuse.

The iffy stabilizers are also far more numerous than the bad splices. After the 19 September accident, CERN researchers tested most of the splices and found only two more faulty ones. In contrast, they've found about 80 bad copper stabilizers, including 46 in one octant of the machine alone, Myers says.

Once accelerator physicists know how high in energy they can safely go, they will present that finding to the experimenters working with the particle detectors and ask them how to proceed, Myers says. If the energy is too low—significantly below 8 TeV—the experimenters may opt to delay the restart until the stabilizers can be fixed. But Myers says that between 8 and 10 TeV is likely and that experimenters probably will opt to run with that. "Both the machine people and the experimenters, we need to be running … to see what other problems might be out there waiting for us," he says.

That position resonates with experimenters working on the particle detectors. "It would still be very useful" to run at a lower energy, says Pauline Gagnon of Indiana University, Bloomington, who works on the ATLAS detector. "It will give us all the information that we need to calibrate our detector, and we will learn a lot about the LHC." Even so, she adds, "nobody wants to run at 4 TeV for a year."

Meanwhile, physicists at the lab are privately debating whether the problem constitutes a design error. Similar connections at other machines are secured with clamps, and in retrospect, the LHC probably should have employed a similar design, Myers says. But Lyndon Evans, the CERN engineer who oversaw the construction of the LHC, notes that in 1999 the current design passed an external review and that the use of clamps was discouraged as it would have impeded the flow of the surrounding liquid helium. Either way, some physicists grumble that the problem should have been caught earlier.

–ADRIAN CHO

Truth to power. European Commissioner Potočnik (*left*) calls the critical review by Vīķe-Freiberga (*right*) "good and honest".

EUROPE

Fix Funding Agency's 'Original Sin,' ERC Review Panel Demands

Timidity is not a trait that psychologist and former Latvian president Vaira Vīķe-Freiberga, nicknamed the Baltic Iron Lady, is known for. So when she was asked to chair a review of the European Research Council (ERC), the 2-year-old funding agency that many believe will be central to the competitive future of European science, no one expected her to come up with another serving of bland Brussels policy-speak. Her report,* presented on 23 July to Janez Potočnik, the European Commissioner for Research, didn't disappoint.

Despite a successful start—the ERC's grant calls have been flooded with applications, and scientists praise its focus on excellence as the sole criterion for picking proposals—the agency's structure is "a source of great frustration and ongoing low-level conflict" among its managers, opined Vīķe-Freiberga's panel. ERC's "over-regulation, over-control, and over-steering" of grantees has "tremendous detrimental effects." Scientists who have volunteered time to review grants are "surprised, not to say shocked," by ERC's procedures. "It's written in a rather unusual style, isn't it," says John Smith, deputy secretary general of the European University Association (EUA). "It's refreshing."

The review panel, which included former U.S. National Institutes of Health chief Elias Zerhouni, focused on the key question about ERC: Should scientists or bureaucrats run the show? With a €7.5 billion budget for the first 7 years, ERC funds frontier research irrespective of national boundaries, a rarity in the European Union, where funding is typically subject to political and economical considerations. To preserve that freedom, early advocates of such a U.S.-style grant agency argued that ERC needed to be independently run by scientists, with a minimum of bureaucracy and at a safe distance from the European Commission.

But when ERC got off the ground in early 2007, they got only half of what they wanted. ERC's scientific strategy is set by an independent Scientific Council, chaired by molecular biologist Fotis Kafatos of Imperial College London. Yet the management is in the hands of an Executive Agency, a body that ▶

* tinyurl.com/vaira

Published by AAAS

is formally autonomous but is, for all practical purposes, controlled by the commission. The Scientific Council has a permanent representative in the Executive Agency, called the secretary-general. But the position, which Spanish economist Andreu Mas-Colell took over on 1 July, comes with no formal power.

The review panel concludes that this "original sin" is at the source of many problems. The commission's recruiting system makes it hard to attract scientists to the agency, for instance, and E.U. rules designed to prevent fraud and waste clash with academic traditions. Grantees have to sign contracts that can keep them from switching research directions and force them to account for expenses or even keep time sheets; basic researchers need trust and flexibility, the panel says.

Strict rules are also threatening some scientists' willingness to review grant applications. They need to mail in a copy of their passport, which the panel calls "completely abusive"; travel expenses paid out of pocket can take a long time to be reimbursed. "I review for a large number of international funding bodies, and this was the worst experience I have had in 30 years," one scientist told the panel. "I would not agree to review again."

Unlike ERC's Scientific Council, which wants to wrestle control of the agency from the commission, Viķe-Freiberga's panel says that ERC should first try to fix its problems within the current structure. It recommends a range of measures, including merging the roles of secretary-general and director of the Executive Agency into a single post to be filled by a scientist. "It should not be acceptable today in Europe that non-scientists […] run major European research programmes!" the panel exclaims. (On occasion, it hits the Caps Lock button to hammer home the message, for instance when it demands "a true PROFESSIONALIZATION both at the scientific and managerial level.")

Going the independent route, which Article 171 of the European Community Treaty makes possible, should be done only if a new review in 2 years shows that the many "irritants" endure, the panel says. It's a recommendation that both sides can live with. "It's a very fair and balanced report, and the recommendations are wise," says Helga Nowotny, the Austrian vice-president of the Scientific Council. "It's a good, honest report that will help all of us a lot," says Potočnik.

Its strong language notwithstanding, the panel says ERC has done many things right. The agency was able to attract good reviewers—at least so far—and interest in its first grant calls was overwhelming. The panel's own survey also showed that most applicants and reviewers were happy, says Potočnik, who gets kudos himself for shielding ERC from political interference. An EUA consultation has shown that universities like the new agency, says Smith.

ERC has not done as well at attracting non-European research talents, who are eligible for the funds if they move to Europe, notes Wilhelm Krull, director of the Volkswagen Foundation, a German grantmaking agency, but that may improve as ERC becomes better known. Nor is it giving young researchers the best shot at getting grants, says Mas-Colell. ERC Starter Grants are available for researchers with less than 10 years of experience after their Ph.D., but most of them have gone to scientists at the upper end of that spectrum. In the future, the Scientific Council wants to reserve a portion of the grants for true starters with less than 5 or 6 years of experience, Mas-Colell says. As ERC now knows all too well, getting a good start in life can be difficult.

–MARTIN ENSERINK

ScienceNOW.org

From *Science*'s Online Daily News Site

Catching a Giant Wave
Like a shadow of death racing across the ocean surface, a tsunami churns the air and darkens the water along its path. Researchers now report that they can detect this activity with radar, improving the chances that coastal populations can escape these killer waves. http://bit.ly/oLcn5 ▼

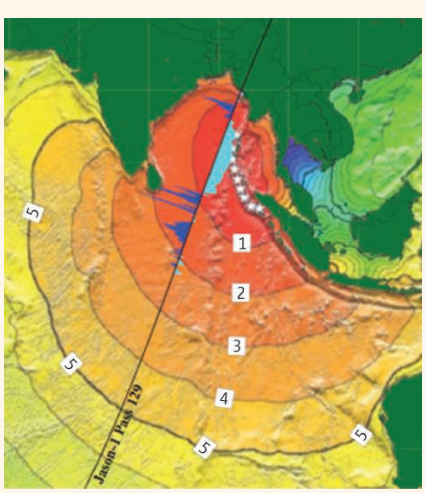

Can't Decide? Ask an Ant ▶
Classical philosophers called humans "the rational animal." Clearly, they never looked closely at ants. A new study suggests that ant colonies avoid irrational decisions that people and other animals often make. http://bit.ly/3O9D2C

Tree in a Time Warp
A eucalyptus-like tree that grows in New Zealand is still defending itself from a giant bird that died out about 500 years ago. The lancewood tree changes its appearance twice in its lifetime—an adaptation, a new study suggests, that prevented it from being eaten by flightless moas. http://bit.ly/LbXzu

A Cloaking Device for Earthquakes
Researchers say they have found a way to make buildings essentially invisible to earthquakes. If perfected, the technique could protect skyscrapers and homes alike from even the most devastating temblors. http://bit.ly/ek0B7

Microbe Evolution Gets a Push
Researchers report that they've come up with a new way to modify the genomes of billions of microbes simultaneously and then finger the ones with the most interesting changes. Because the technique will likely work with most types of genomes, it could turbocharge efforts to engineer microbes to produce everything from novel therapeutic drugs to vast quantities of biofuels. http://bit.ly/3oiVUb

Pump Up the Volume
Anyone who has woken to a cacophony of squawks and chirps knows that birdsong, no matter how melodious, isn't always a welcome sound. Past research suggests that birds aren't keen on human din either. But a new study finds that not all birds think alike: Some species actually appear to seek out noisy environments. http://bit.ly/U1LUH

Read the full postings, comments, and more on **sciencenow.sciencemag.org.**

CREDITS (TOP TO BOTTOM): STEPHEN PRATT/ARIZONA STATE UNIVERSITY; NOAA

Published by AAAS

Splashdown. Shells are sprayed into the Lynnhaven River in Virginia. Reefs now teem with oysters in the Wicomico River (*inset*).

CREDITS: PATRICK BLOODGOOD/U.S. ARMY CORPS OF ENGINEERS

RESTORATION ECOLOGY

Oysters Booming on New Reefs, But Can They Survive Disease?

Oysters were once so abundant in the Chesapeake Bay that they posed a navigation hazard. Perched on reefs made up of old shells, the filter-feeders had a sturdy spot to attach to and could avoid being covered by silt. But by the early 20th century, the reefs were nearly picked clean by humans, and the remaining oysters were ravaged by introduced diseases. Without a large population of oysters to keep them growing upward, the reefs sank and became topped with muck. Over the past 2 decades, restoration efforts to create new habitat have ramped up, but progress has been slow and patchy.

Now a group of researchers is claiming an "unprecedented restoration" in the Great Wicomico River, a small tributary. Thanks to a large network of reefs created in 2004, a booming population of native oysters has taken hold, the group reports in a paper published online by *Science* (www.sciencemag.org/cgi/content/abstract/1176516) this week. Some researchers herald the accomplishment as a model for restoration, but others say that the new populations have yet to prove they can survive now-endemic diseases. "It's very early in the game to call this a success," says Paula Jasinski of the National Oceanic and Atmospheric Administration's Chesapeake Bay Office.

Most efforts to restore native oysters (*Crassostrea virginica*) in the bay have been relatively small, 0.5 hectares or so, largely due to the expense of building reefs. To create new habitat, state natural resource agencies and other partners have dredged up old oyster shells and scattered them on river bottoms. These thin layers tend to sink and be covered with mud within 3 to 5 years, degrading the habitat.

David Schulte wanted to create something bigger and taller than the usual patches. A graduate student in marine biology at the Virginia Institute of Marine Science (VIMS) in Gloucester Point, Schulte also works for the U.S. Army Corps of Engineers. He helped designed the roughly $2 million project to build 35 hectares of subtidal reefs about 130 kilometers southeast of Washington, D.C. The Great Wicomico River is a good spot for restoration, in part because surviving oysters in it produce copious larvae.

In 2004, the corps created two kinds of reefs, one taller than the other. Researchers have built these so-called high-relief reefs elsewhere but not as expansively. Larvae from upstream settled on the new habitat, and within a year, young oysters were abundant. On average, they were five times more dense—up to 1000 oysters per square meter—on the taller reefs than on the shorter ones. The main reason, Schulte says: The extra height meant the reefs had less sediment and more exposed shell for larvae to settle on.

By March 2009, the estimated 185 million oysters constituted the largest known restored population of native oysters in the world, the authors say. And because there are already three generations of oysters present, the population is likely sustainable, says co-author Romuald Lipcius, an ecologist at VIMS.

With all the new oysters, the reefs themselves are accumulating shell debris, suggesting that they will grow in height on their own, as natural reefs used to. "It's very good news, especially for Chesapeake Bay," says Sean Powers, a fisheries scientist at the University of South Alabama in Dauphin Island who studies oyster restoration. "For marine ecology, restoration ecology, it really is an advance."

Most experts who work in the Chesapeake Bay are more cautious. They point out that the Great Wicomico River is a best-case scenario because of its plentiful larvae and its hydrology, which tends to prevent these larvae from drifting out to the bay. Jasinski says only a few other rivers would be as conducive to building up populations quickly. And so far, the new reefs don't have a large proportion of large oysters, longer than 75 millimeters, which are market-size and also the most fecund.

The biggest question is how well the new population will survive disease. Many oysters in the Chesapeake are afflicted with MSX, a condition caused by the protozoan *Haplosporidium nelsoni*, which was accidentally introduced in the bay in the 1960s. Young oysters catch the disease and are most likely to die after 3 to 4 years of infection, says James Wesson of the Virginia Marine Resources Commission in Newport News, who has been monitoring the population in the Great Wicomico River. There are already discouraging signs: Some adult oysters on the reefs, which now make up 80% of the new population, began to die last year. Based on past events, Wesson predicts 50% mortality among the adults by November.

Lipcius is more sanguine. "My firm belief is that the whole disease issue has been a red herring," he says. Although some deaths are to be expected, he thinks that overall, a population of healthy adults living in good habitat will resist disease better than other populations have.

The corps is also building high-relief reefs in the Lynnhaven River, farther south, and planning for a project in another small river, the Piankatank. But good habitat doesn't come cheap. Larger rivers—not to mention the bay proper—will require even bigger reefs stocked with billions of hatchery oysters. Everyone agrees that oysters have a long way to go. But steps like those in the Great Wicomico are promising, says Tommy Leggett of the Chesapeake Bay Foundation, a nonprofit based in Annapolis: "I think we're headed in the right direction."

–ERIK STOKSTAD

Published by AAAS

BOTANY

Plant Bar Code Soon to Become Reality

DNA bar-coding, the ambitious idea of using a short piece of DNA to tell every species in the world apart, is already a powerful tool for scientists studying animals. But for plant biologists, the idea has for the most part remained a pipe dream, stalling systematic studies of plants and efforts to conserve flora.

So far, every plant DNA sequence proposed as a marker has had problems, and the search for the "right" plant bar code has proven controversial (*Science*, 12 October 2007, p. 190). But at last, a solution appears within reach. A paper published this week in the *Proceedings of the National Academy of Sciences* (*PNAS*) proposes two genetic sequences, or loci, taken from chloroplast genes called *matK* and *rbcL*, as the official plant bar code. Although the new bar code works for some kinds of plants better than others, it identified 72% of all species on average and grouped 100% of plants into the correct genus.

The results comprise data from 25 major bar-coding labs, all part of the Plant Working Group (PWG), an organization set up in 2005 to help resolve the plant problem. It's now up to the Consortium for the Barcode of Life (CBOL) and a board of experts to endorse or reject the plant ID strategy within the next 2 months, says Peter Hollingsworth, chair of PWG. "I have a very strong hope that they will approve it, and we have worked very closely with CBOL throughout this process," says Hollingsworth, a conservation geneticist at the Royal Botanic Garden Edinburgh.

Plant bar-coding centers are eager for that approval. They could then finally "tag" wide varieties of plant species and share that information online through the Barcode of Life Data Systems Web site. In fact, many optimistic researchers have begun bar-coding using *matK* and *rbcL*, after the two loci were informally proposed at a PWG meeting in September 2008.

But PWG admits that the two-locus bar code is far from perfect, and a minority within the group believes the search is not over. W. John Kress, a co-author of the *PNAS* paper, endorses the proposed bar code, but he says his lab will continue to add another DNA sequence called *trnH-psbA* to *matK* and *rbcL*. From these three, the best two-locus bar code would then be selected at a later date. "We're finding that we still get some pretty good results with the three-locus bar code, and personally I'm not ready to give that up yet," says Kress, a botanist at the Smithsonian Institution in Washington, D.C.

The *PNAS* paper reports on seven candidate loci, including sections of genes and spacers (regions between genes), taken from work led by Kress; Ki-Joong Kim, a botanist at Korea University in Seoul; and Mark Chase at the Royal Botanic Gardens, Kew, in the United Kingdom. Each sequence was assessed on its ability to tell species apart and on factors such as its ability to be read rapidly by automated sequencers, says Robyn Cowan, a co-author and conservation geneticist at the Royal Botanic Gardens, Kew. Ultimately, four were ruled out, for reasons such as low discrimination rates or because the sequences were hard to read efficiently.

Of the remaining three, no individual sequence came up to scratch, so the loci were combined to bump up bar-code quality. The *rbcL* gene provides good-quality sequences and has effective primers (reagents used to "probe" or pick out the sequences) that work across a variety of plants, making it a good choice. Its ability to discriminate species hovers above the average at a rate of 61%. Both *matK* and *trnH-psbA* were better at telling species apart, with success rates of 66% and 69%, respectively. But *trnH-psbA* produced poorer quality sequences due to the presence of long mononucleotide repeats, in which one DNA base recurs excessively within the spacer. Such repeats can cause the sequence to be misread. On the other hand, *matK* doesn't have primers that allow it to be isolated in all plant groups. Although there is no immediate way to resolve the issues with *trnH-psbA*, the group expects the quality of *matk* primers to improve over time. Already, the current primers work well in angiosperms (flowering plants), being able to latch onto the loci in 90% of species, but are less successful with gymnosperms (cone-producing plants) at 83% and extremely poor with cryptogams (lower plants such as mosses and ferns) at 10%.

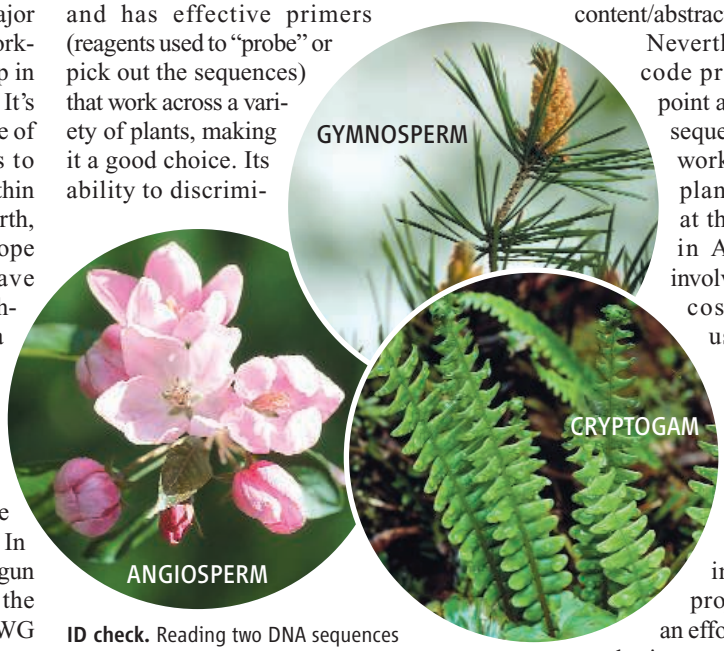

ID check. Reading two DNA sequences can tell most plants apart.

The proposed plant bar code remains less powerful than its animal counterparts, a gene called *CO1*, which averages upward of 95% discrimination. But PWG hopes to push up species discriminating power in the near future. One way of doing this is by using further supplementary bar codes in certain plant groups. For example, in protea, a group of flowering plants, botanists will use the ITS ribosomal spacer, says Chase. (For a Perspective on challenges in plant bar-coding by Chase and Fay, see www.sciencemag.org/cgi/content/abstract/1176906.)

Nevertheless, the proposed bar code provides a good "starting point and a reference for all subsequent plant DNA bar-coding work," says Andrew Lowe, a plant conservation biologist at the University of Adelaide in Australia who was not involved with the paper. As the cost of sequencing drops, using several genetic loci for bar-coding will become a more manageable exercise, he adds.

If the bar code is approved, it will open the way for a variety of plant tagging projects, including large-scale systematic projects such as Tree-BOL, an effort to bar code all trees, and the international grass bar-coding project. While Tree-BOL has been collecting *rbcL* and *matK* bar-code loci for some time, the formal approval of this bar code would make funding applications and publishing results easier, says Damon Little, chair of Tree-BOL and a plant biologist at the New York Botanical Garden in New York City.

For now, the plant community eagerly awaits CBOL's decision. "We [could] at long last move forward with sequencing" on a larger scale, says Little.

–CLAIRE THOMAS

CREDITS: JUPITERIMAGES

SCIENCE EDUCATION

Universities Begin to Rethink First-Year Biology Courses

Introductory biology courses are often the last academic exposure nonscience majors at U.S. colleges have to science. Unfortunately, say science educators, the courses too often leave a bad taste in the mouths of students who spend more time in lectures than on experiential learning and in regurgitating facts rather than understanding the concepts behind them. As voters, those graduates apply their misconceptions of science to shape national policies on everything from evolution to stem cell research. So improving introductory biology is seen as a critical step toward raising the nation's scientific literacy.

In 2006, the National Science Foundation (NSF) began an initiative to do just that. This month, 500 researchers, educators, and policymakers met in Washington, D.C., at a conference sponsored by NSF and AAAS (which publishes *Science*) to assess how far they have come. The consensus: There's still a long way to go.

Correcting the problem, speakers agreed, will require changing a deep-rooted academic culture that values research over teaching and makes little provision for doing a good job in the classroom. "We hire new faculty with big start-up packages and expect them to set up their labs and get going on their research," explained Joan Lorden, provost of the University of North Carolina, Charlotte. Then we say, 'Here's your course load. And by the way, we'd like you to be an innovative instructor.' But rarely do we give them the support they need to succeed."

NSF's education directorate funds a slew of programs aimed at improving undergraduate instruction across disciplines, and in recent years the agency's biology directorate has begun to tap into those efforts. At the conference, biology chief James Collins described his plans to ramp up support for improving undergraduate biology. Assuming congressional approval of NSF's 2010 budget, Collins hopes to spend an additional $10 million next year on a variety of activities, including mentoring, curriculum development, and research experiences for students as well as faculty development. This month, for example, NSF announced a new competition for $50,000 "incubator" grants that would allow researchers and educators to work up a full-fledged proposal to carry out such improvements. The biology directorate is also hoping to join the education directorate in funding a university-based center to improve undergraduate retention and graduation rates among science majors, with special attention to underrepresented minorities.

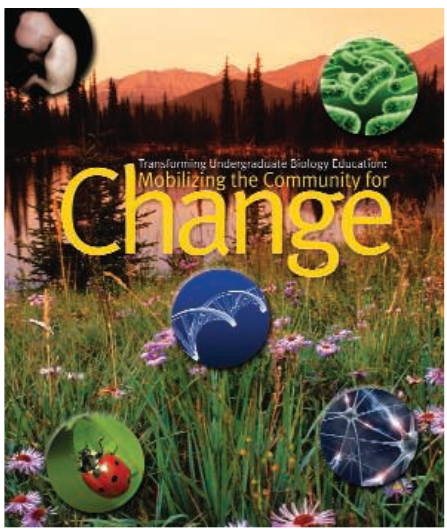

No small change. Conferees heard about many successful efforts already under way.

Online
sciencemag.org

To hear a discussion with conference leaders about transforming undergraduate biology, go to the online version of this article.

Participants said they hoped to use the conference to shore up support for reforms already under way on their campuses. But they were realistic about the availability of resources. "I heard about one terrific program that could be a model for us. But it costs $5 million over 5 years," notes Eric Stabb of the University of Georgia, Athens. "And I'm sure my dean doesn't have that kind of money lying around. But now we can use the conference to hammer the administration on the need to do more. And if we make a good case, maybe the state legislature can find the money."

Talk is cheap, agrees Collins, reminding participants that the burden is on them to sustain and scale up their reforms: "If anything is going to happen, it's because you will decide to do something."

–JEFFREY MERVIS

CREDIT: AAAS

ScienceInsider

From the *Science* Policy Blog

The U.S. House of Representatives dug into minutiae at the National Institutes of Health last week before passing a $31 billion NIH funding bill. At the behest of Darrell Issa (R–CA), members **okayed an amendment to kill three peer-reviewed grants** Issa doesn't like. They support efforts to understand the spread of HIV/AIDS by studying risky behavior among prostitutes in Thailand and China and alcoholics in Russia. Issa called them wasteful; biomedical groups protested. But rather than debate the issue, bill manager Representative David Obey (D–WI) accepted Issa's amendment. As with similar grant-killing measures a few years ago, many expect it to be stripped out in negotiations between the Senate and House on a final bill.

A stem cell paper that made international headlines earlier this month **has been retracted following charges of plagiarism**. The paper, which claimed to demonstrate how sperm could be made from human embryonic stem cells, was published online in *Stem Cells and Development* on 8 July with Karim Nayernia of Newcastle University in the U.K. as the corresponding author. Questions arose because of two paragraphs in the introduction that apparently were copied without attribution from a review article by another researcher. Graham Parker, editor-in-chief of *Stem Cells and Development*, told *Science*Insider that he decided to retract the paper on 21 July.

In other news, the U.S. Department of Homeland Security **used a scientifically flawed study** to justify its selection of Manhattan, Kansas, as the site for the proposed National Bio and Agro-Defense Facility, according to a draft federal report obtained by *The Washington Post*. And the Australian Stem Cell Centre hopes that **a new business plan that shifts the center's emphasis from commercialization to research** will help it regain momentum.

For more science policy news, go to **blogs.sciencemag.org/scienceinsider/.**

Published by AAAS

Reshuffling Graduate Training

Nobelist Roald Hoffmann believes that taking graduate students off grants and giving them fellowships would be good for U.S. science. But others say such a radical change isn't in the cards

DRESSED IN SATIN AND SEQUINS, ROALD Hoffman has ridden atop the first science-themed float in Rio's famed Carnival. Once a month, he appears on stage at a New York City café to host a revue of science and the arts. It's all part of what Hoffmann, a 1981 Nobelist for his work on the theory of chemical reactions, calls his "extreme outreach to the community."

"I think science should be fun," Hoffmann said in May to the National Science Board, the oversight body for the National Science Foundation (NSF), when it awarded him its prestigious Public Service Medal. But after flashing pictures of himself at Carnival and on stage at the Cornelia Street Café in Greenwich Village, Hoffmann got down to business: "Now I want to shift gears and talk about something serious."

Online
sciencemag.org
Podcast interview with author Jeffrey Mervis.

What Hoffmann wanted to discuss is a proposal for changing how the U.S. government supports the training of graduate students in the sciences. Federal research agencies now funnel most of their money for graduate students through grants to faculty members. That's the case for nearly 90% of the 39,000 graduate students whom NSF supports each year and for about two-thirds of those getting money from the National Institutes of Health (NIH). The remaining students are funded via fellowships, awarded directly to them, or through traineeships, in which universities compete for a grant to support a certain number of students in a particular area for a fixed period of time.

The commingling of education and research has created a system that is the envy of the world in terms of research productivity. It's also not a bad deal for the student, who typically doesn't pay a penny to earn her Ph.D. The university picks up the tuition for her required courses, and her research is funded through a federal grant awarded to her adviser, who then hires her to work in his lab. In return, she'll probably teach some undergraduate classes during her first few semesters, after which her adviser will receive several years of skilled labor at below-market rates.

But that wildly successful system comes at a high cost to both students and the profession, says Hoffmann, who also made his case in an 8 May editorial in *The Chronicle of Higher Education*. And it's not sustainable, he argues, especially during tough economic times like these. A better approach, says Hoffmann, would be for the government to stop supporting graduate students on research grants—roughly 30% of a typical NSF chemistry grant pays for graduate students, for example—and use the money for competitive fellowships that students could use at the university of their choice.

That seemingly minor shift could have huge consequences for universities and for the entire U.S. research enterprise. Although they admit Hoffmann's proposal faces long odds, some community leaders say that such a change is long overdue and that his suggestion offers a promising road map. "The real power of an individual fellowship is that it empowers a young scientist to act in a more independent manner, on something creative and for which they have a passion," says Thomas Cech, a Nobelist who recently returned to academia after a decade as head of the Howard Hughes Medical Institute (HHMI) in Chevy Chase, Maryland. "And that's what science is really about." Under the current system, he says, "a graduate student is told, 'Do experiment 2a because it's in our grant.' That turns the student into a pair of hands. So I think a shift to fellowships would be an excellent idea."

Shirley Tilghman, president of Princeton University and chair of a 1998 National Academies panel that offered advice on career paths in the life sciences, says a move away from supporting graduate students on research grants would also address two other major flaws. Although the current system has succeeded in maximizing the amount of research performed, she says, it

Published by AAAS

Bottom of the pile. Cartoonist Jorge Cham's view of lab hierarchy. (Twos are not wild.)

has also degraded the quality of graduate training and led to an overproduction of Ph.D.s in some areas. Unhitching training from research grants would be a much-needed form of professional "birth control," says Tilghman, who favors more federally funded traineeships. (Traineeships are grants awarded to institutions, which in turn promise to provide students with professional and career counseling as well as a chance to develop their scientific skills in specific areas.) Reducing the overall number of graduate students in the life sciences "is a price that I'd be willing to pay," she says, in return for a better training environment and improved job prospects.

Fellowships already have a strong following. Building on a 2007 proposal from economist Richard Freeman of Harvard University, President Barack Obama has promised to triple by 2013 the annual number of NSF's prestigious Graduate Research Fellowships, which run for 3 years and cover all fields that NSF funds. And another newcomer to Washington, HHMI President Robert Tjian, hopes to revive a graduate fellowship program that the institute terminated in 2003 when money became tight. Tjian sees the program, which would be open to the most talented students from around the world who are studying in the United States, as an important investment in the next generation of academic researchers.

However, other academic leaders worry that Hoffmann's proposal risks killing the goose that laid the golden egg. "Any radical shift away from what we do now is risky because it would jeopardize a strong innovation system," says Debra Stewart, president of the Council of Graduate Schools in Washington, D.C. Robert Berdahl, president of the Association of American Universities, also thinks that a wholesale shift to fellowships would be unwise because it would take the selection of graduate students out of the hands of investigators. "In effect, by making awards to individual researchers, we are asking faculty members to find the best students," says Berdahl, a former chancellor of the University of California, Berkeley. "Presumably, there is a correlation between the quality of an individual [scientist] and the quality of the students in his or her lab."

A system out of balance

Hoffmann, a professor at Cornell University, says he began to think about the need for changing the current system during a series of recent departmental meetings on coping with the economic downturn. Most of the suggestions from faculty members, he concluded, would erode undergraduate instruction, about which he is passionate. Although Cornell officials say they are still working on a long-term plan, Hoffmann fears that a one-time, 5% cut in the chemistry department's operating budget starting this fall will be extended for 3 years and that the result will be larger classes, fewer instructors, and limits on enrollment in some courses. "We're firing some of our best teachers," he says. In contrast, he adds, research programs are likely to be unaffected because they are funded by federal dollars that are beyond the university's control.

G. Peter Lepage, a physicist and dean of the College of Arts and Sciences at Cornell, says every university is struggling to educate undergraduates and maintain a strong research program in the face of shrinking endowments, reduced state subsidies, and pressure to hold down tuition increases. Lepage says he doesn't see how Hoffmann's suggestions would help undergraduates, and he worries that they could harm research. "I have to make sure I have enough money to cover our teaching responsibilities [to undergraduates]," he says. "And we'll figure out a way to do that. At the same time, our faculty need graduate students to do their research, and we need to admit enough of them to do the research as well as to teach the courses."

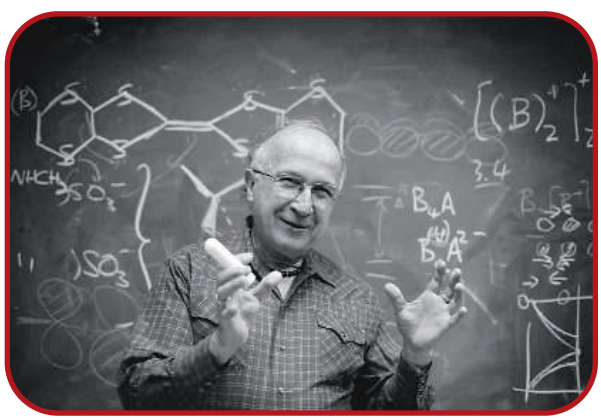

A radical redesign. Roald Hoffmann says supporting graduate students from grants benefits researchers and undermines instruction.

The current recession could have an impact on undergraduates, Lepage acknowledges. Graduate science students typically spend their first 2 years as teaching assistants while they take courses and explore research options, he says, whereas their final 3 years are devoted to research. "If you have more research money and less money for TAs, maybe we'll have to rejigger that balance and go from four to three semesters of teaching [per graduate student] and from six to seven semesters of research," he says. "But both missions will get done."

Hoffmann readily admits that a shift to fellowships, which are now limited to U.S. citizens, would have one major unfortunate consequence: It would drain the graduate pool of most students from China, India, and other nations. Foreign students fill a majority of the slots in many U.S. graduate programs in the natural sciences and engineering, but few could afford to come on their own dime. Hoffmann says he would regret losing those students but points to a silver lining. Having universities award fewer science Ph.D.s should force employers to pay higher salaries, he predicts, and attract more of the best U.S. students into science.

Tjian's plan would extend a helping hand to foreign students as well. (As a private philanthropy, Hughes doesn't have to answer to the political argument that U.S. tax dollars should be spent on Americans.) But the Hughes program will serve only a tiny fraction of the foreign graduate students now in the country.

Freeman, a labor economist who studies the dynamics of the scientific work force, sides with Cech and Hoffmann when it comes to the value of fellowships. However, Freeman thinks that Hoffmann's all-or-nothing plan ignores both economic and political realities. "We produce two things at our universities: education and science," says Freeman. "That's what society wants from us. And students will still want to work in a lab."

Freeman says Hoffmann's suggestions would result in "more expensive science, and that means fewer people doing it. That's not consistent with where most policymakers think we should be headed as a country. … I hate to reject something because it's radically different, but I think he needs to do a better job of modeling [the consequences]."

Getting the work done

What would fewer graduate students mean for research? Tilghman says that many scientists reacted in horror to the suggestion in her 1998 report that a typical 10-member lab might shed one graduate student as a way to reduce

CREDIT: COURTESY OF ROALD HOFFMANN

the overproduction of Ph.D.s and improve the quality of their training. "The PIs [principal investigators] told us that the lab's productivity would go way down if they left," she recalls.

Tilghman is dubious. "I think that's highly debatable, and in any case, it's never been rigorously tested," she says. "Every scientist knows that graduate students often go through long periods in which they are totally unproductive."

> "The real power of an individual fellowship is that it empowers a young scientist to act in a more independent manner."
>
> —THOMAS CECH, PRESIDENT EMERITUS, HHMI

Barbara Baird, the chair of Hoffmann's department of chemistry and biochemistry, thinks that her colleague is ignoring a fundamental rule of academic research. "Federal agencies hand out money based on what the PI says is needed to do a particular project," Baird explains. "If graduate students become a less dependable source of labor, then the tendency will be to simply hire postdocs. The work still needs to be done."

At NIH, the bulk of the training programs are run by the National Institute of General Medical Sciences. Its director, Jeremy Berg, says he shares Hoffmann's concern about maintaining high-quality undergraduate and graduate programs in the face of mounting pressure from faculty members to maintain their research programs. "The biggest driver for the production of Ph.D.s is not the perception that there is an undersupply but rather that there's work that needs to be done," says Berg. "However, even if they are cheap, I'd argue that students are also smart, committed, and hard-working labor."

Hoffmann says he assumes that a system of competitive fellowships would widen the already large gap between the elite universities and the rest of the nation's system of higher education, pointing to the fact that the top-20 research universities historically have attracted a disproportionate share of NSF's graduate research fellowships. Increasing that imbalance would bother him, he admits, but not enough to torpedo the idea.

For other scientists, however, that outcome would be a showstopper. "My fear is that you'd be creating a narrower base for the country's research enterprise and lose the geographic diversity of science that now exists," says Susan Gerbi, a biochemist at Brown University and an authority on training issues in the life sciences. "In addition, a school on the rise might not have access to the graduate students it needs."

A fellowships-only system, Gerbi says, would also lead to "wild swings in enrollment from one year to the next." On the other hand, say Gerbi and Tilghman, a shift to traineeships would reward universities that articulate a well-crafted approach to build up the talent pool in a particular area and also provide program stability.

> "I think he needs to do a better job of modeling [the consequences]."
>
> —RICHARD FREEMAN, HARVARD ECONOMIST

Berg says that striking the right balance between types of graduate support is a perennial issue for NIH and that Hoffmann's proposal is "a blunt instrument for a subtle problem." One complication, he says, is that federal research grants have become an increasingly important source of support for academic science "not just to support a research program but also to support institutional activities." That's code for the overhead charges—about 50% to 60%—that universities add to federal grants. In comparison, training grants and fellowships typically have overhead rates of 10% or less.

> "Any radical shift away from what we do now is risky because it would jeopardize a strong innovation system."
>
> —DEBRA STEWART, PRESIDENT, COUNCIL OF GRADUATE SCHOOLS

Is that difference large enough to make fellowships unattractive to most universities? "I'd like to know" what administrators think about that, says Berg.

Cech thinks the different overhead rates do influence how universities view support for graduate students. But he says those reimbursement rates aren't carved in stone. "There's no law that you can only give 10% in indirect costs for a fellowship," he argues. "You could make it 40%, on the grounds that they provide us with research results as well as training. Of course, that would cost more, so the money for training wouldn't go as far."

Senior NSF officials actually considered a variation of Hoffmann's proposal several years ago, notes Esin Gulari, dean of science and engineering at Clemson University in South Carolina and a former head of engineering at NSF. The plan would have allowed researchers to request money for a certain number of traineeships as part of their grant application; at the same time, support for graduate students would be excluded from their grant. "But it never went further than that," says Gulari, now a member of the science board and part of Hoffmann's target audience. "We were so focused on increasing the size of the stipends" for existing fellowships, she says, that the question of shifting the balance between various modes of support was never addressed.

Even those who agree with Hoffmann that changes are needed are not optimistic they will occur. Tilghman says the topic "is not high on the agenda" of most of her fellow university presidents. Instead, she's pinning her hopes on the heads of the various federal research agencies. But bringing about the changes Hoffmann has suggested, she adds, will require them to put the common good above the self-interest of their constituents, namely, individual scientists.

"We need to care most about the health of the overall scientific enterprise," she says. "If your only perspective is attracting the labor to run your lab, then the status quo works very well."

–JEFFREY MERVIS

Published by AAAS

Careful research. Kevlar gloves protect scientists working with the rare Hispaniolan solenodon.

ECOLOGY

Saving a Venomous Ghost

Despite periodic predictions that it will go extinct, the Hispaniolan solenodon endures, and scientists now want to ensure the rare mammal's survival

In 1907, explorer and naturalist Alpheus Hyatt Verrill went to the small island of Hispaniola in the West Indies to track down the elusive Hispaniolan solenodon (*Solenodon paradoxus*), one of the rare examples of a venomous mammal. Fellow scientists told Verrill the journey was "hopeless," saying he was "as likely to secure specimens of ghosts." However, the explorer managed to capture a pregnant female, which he sent back to the United States for examination by his father, zoologist Addison Emery Verrill. In a subsequent report, the father offered this pessimistic prediction: "Owing to the introduction of the mongoose and other causes this creature has become very rare and local. It is, without doubt, on the verge of extinction."

Back then, things didn't look good for *S. paradoxus*, and little has changed 100 years on for this shrewlike animal, as sightings remain rare. Still, the solenodon is a survivor; scientists have found fossils of it tracing back 76 million years.

Now, U.K. scientists are teaming up to help ensure this little-studied creature survives even longer. Starting in October, Richard Young of the Durrell Wildlife Conservation Trust (DWCT) in Bath, U.K., will lead the most extensive solenodon surveys so far in Hispaniola—an island shared by two countries: Haiti and the Dominican Republic—to find out more about these creatures with the hope of coming up with a conservation plan. Young and Samuel Turvey, a paleontologist and conservation biologist at the Zoological Society of London (ZSL), will also examine the animal's genetics and evolutionary history. "It represents an animal which has not changed much since the time of the dinosaurs," says Turvey.

In appearance, the Hispaniolan solenodon's tapered claws, stocky body, and long nose set it apart from most other modern mammals. It and the equally endangered Cuban solenodon—the landmasses of Cuba and Hispaniola were joined 25 million years ago—are also the only living mammals able to inject venom through grooved teeth, much the way a snake does, says Turvey.

In June and July of 2008, as part of a pilot study on Hispaniola to find out how best to catch or count the animals, Amy Hall, animal registrar of DWCT, set up movement-triggered cameras, looked for feces and hair, and deployed traps designed to ensnare live animals. Hall caught only one, protecting herself from the solenodon's poisonous bite with Kevlar gloves as she took pictures of its limbs and teeth and measured it. "It was fighting and letting out the most remarkable noise—a very loud, high-pitched cry—the loudest thing I've ever heard come out of an animal," she recalls.

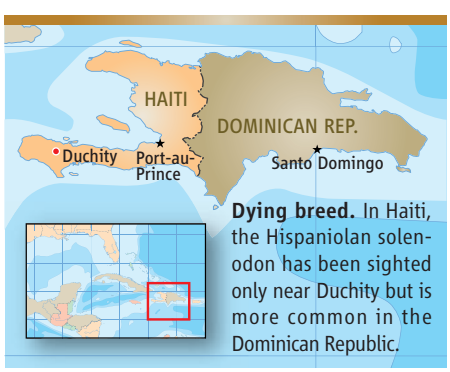

Dying breed. In Haiti, the Hispaniolan solenodon has been sighted only near Duchity but is more common in the Dominican Republic.

Before humans got to the island, Hispaniola was teeming with wildlife, with some 25 species of land mammals, including sloths and monkeys. But almost all of these have been driven to extinction, save the hardy solenodon and the hutia, a large-bodied rodent. "The region has experienced the world's highest level of mammal species extinctions, during both the historical era and the Holocene as a whole," says Turvey, who has been studying the island's fossil record. How the solenodon survived is unclear, he notes, but its varied diet and ability to cope in a range of habitats likely helped.

That flexibility may have been key, as once Amerindians arrived on Hispaniola about 6000 years ago, mammal habitats began to disappear, particularly as agriculture increased and human populations rose. The island's subsequent colonization by the Spanish in the late 1400s meant deforestation and the introduction of cats, dogs, and mongooses, all solenodon predators.

It wasn't until 1833 that the solenodon was first described in scientific literature, by German zoologist Johann Friedrich von Brandt. Even then, it was rare. Another specimen was not reported until Verrill captured his lone specimen more than 70 years later.

In an April 2007 survey in Haiti, Turvey led a team that spent 11 days looking for signs of the creatures and interviewing locals: The remains of three dead solenodons were brought to the team, one of which had been partly eaten by subsistence farmers. That evidence, plus Hall's catch of a live animal in 2008, was enough to persuade the U.K.'s Department for Environment, Food and Rural Affairs to allocate £223,341 (roughly $369,000) from its Darwin Initiative for a 3-year study of solenodons and hutias.

Starting this October, Young, Turvey, and others will investigate the abundance and distribution of solenodons across the island and evaluate what threatens the species. Local organizations, such as the Ornithological Society of Hispaniola, will help with fieldwork and raising public awareness. The ultimate goal is to develop a broad, long-term conservation plan for the solenodon.

Alongside this work, DWCT and ZSL teams are examining the DNA of 10 to 20 specimens, many provided by local partners, to figure out the genetic variation among various isolated solenodon populations across the island. Preliminary analyses suggest there may be up to three branches of solenodon species on Hispaniola, says Young. This would fit with earlier observations in 2001 by biologist Jose Ottenwalder, who described a distinct southern subspecies, *Solenodon paradoxus woodi*, which was markedly smaller than its northern counterparts.

Turvey hopes that in the end, studies of solenodons will provide insight into what primitive placental mammals were like. That's why he and other researchers believe saving the unusual species is so vital. "It's not really like anything else," says Turvey.

–CLAIRE THOMAS

Published by AAAS

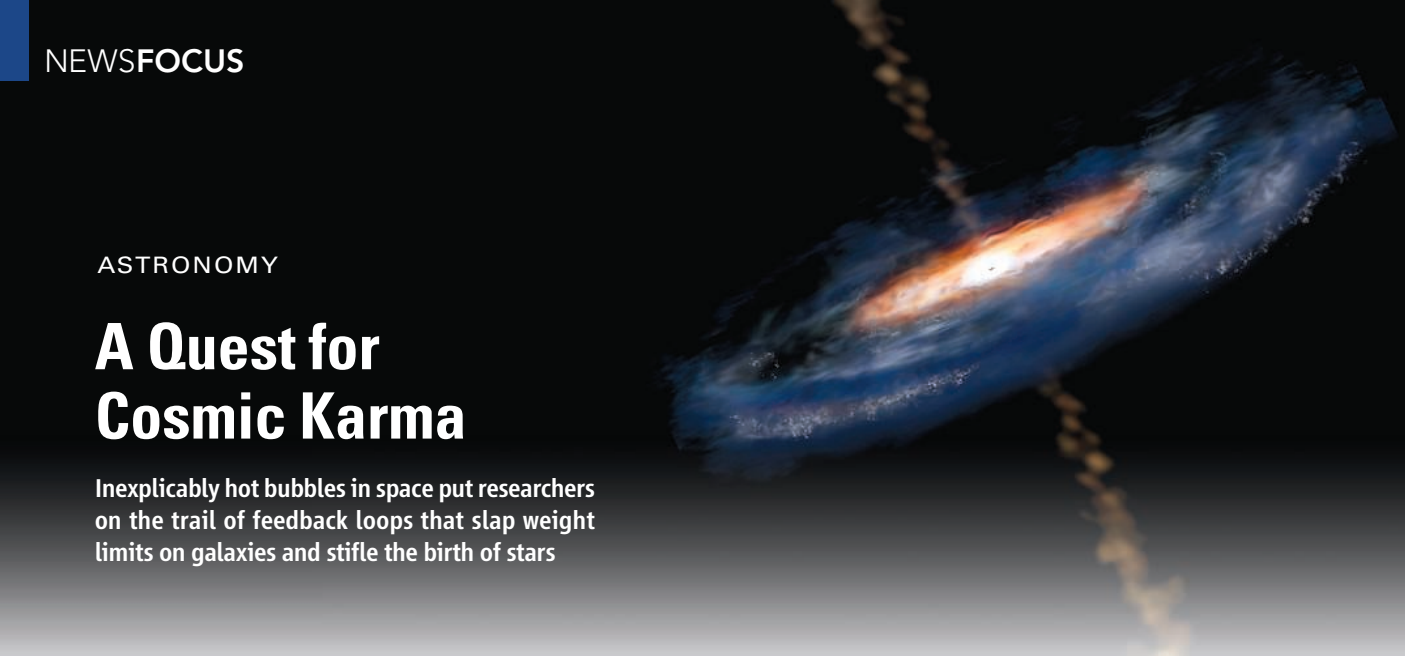

ASTRONOMY

A Quest for Cosmic Karma

Inexplicably hot bubbles in space put researchers on the trail of feedback loops that slap weight limits on galaxies and stifle the birth of stars

In the heart of a galaxy, a violent cosmic drama is unfolding. Streams of gas fall into a massive black hole at the galactic center like wisps of smoke being swallowed by a vent. As the black hole feeds, the core of the galaxy shines with the brilliance of many million suns—what astronomers call an active galactic nucleus (AGN). Then the black hole shoots out two opposing jets of particles at nearly the speed of light.

The shock from the jets drives gas away from the black hole, forming gigantic bubbles that send sound waves rippling through the galaxy's surroundings for millions of years. The process heats the gas farther out, preventing it from cooling and collapsing to form new stars. It also stops more gas from falling into the black hole, which, like a monster suffering from an extreme case of acid reflux, stops gaining mass and gravitational muscle. Both its growth and the growth of the galaxy come to a halt.

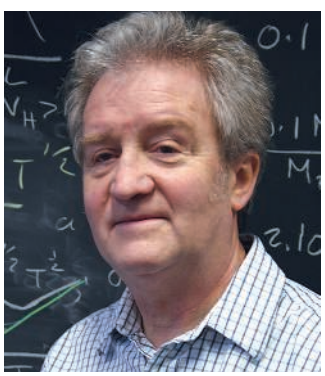

In the loop. Andrew Fabian saw feedback in the Perseus cluster.

Astronomers first glimpsed this cosmic shutoff valve in large galaxies in 2003 in high-resolution x-ray images of the Perseus cluster, a group of 500 galaxies about 250 million light-years from Earth. Since then, such "AGN feedback" has become one of the hottest topics in astrophysics. If it works the way some researchers think it does, AGN feedback is pivotal to understanding how galaxies evolve. It also appears to answer in one stroke two fundamental questions that have plagued researchers: Why are the masses of most galaxies so tightly connected to the masses of the enormous black holes at their centers? And why are very large and very small galaxies so much rarer than theory says they should be?

A plausible answer to the first question, at least in midsize-to-large galaxies, is that AGN feedback acts like "a thermostat, a regulator to keep things matched," says Meg Urry, an astronomer at Yale University. The mechanism also explains "why we don't see black holes bigger than 10 billion solar masses," says Avi Loeb, a theoretical astrophysicist at Harvard University. "As you go to high masses, AGN feedback shuts off galaxy growth; hence we see few massive galaxies."

In the past 5 years, new observational and modeling studies have convinced astronomers that AGN feedback is universe-wide and has influenced galaxy evolution through much of cosmic history. A conclusive, detailed picture of how it works, however, remains a long way off. Although many astronomers believe that the expansion and movement of bubbles inflated by jets is what transfers energy into the gas within and around the galaxy, some argue that the gas is heated mainly by radiation emitted by the AGN. "Although mechanical heating by jets is the popular view, we simply do not know yet which mechanism is dominant," says Loeb.

Too darned hot

When astronomer Andrew Fabian of the University of Cambridge in the United Kingdom took x-ray images of the Perseus cluster with the orbiting Chandra telescope, he expected to find its center awash in cold gas—a mere 10 million kelvin or below. The figure reflected how quickly the tenuous gas known as the intracluster medium was supposed to be cooling by emitting radiation. Fabian and his colleagues found that the gas in the core of the cluster, near the central galaxy, was tens of millions of degrees warmer than expected. Something must be heating it—but what?

The pictures themselves provided an answer. They showed large cavities in the gas extending out from the central galaxy, right along the path of jets previously observed in radio images. (The particles in the jets are so energetic that they can be detected only by their radio emission.) The x-ray photos also showed ripples around the cavities, which the researchers saw as the unmistakable signatures of mechanical energy in motion.

Other astronomers had suggested that jets shooting out from a galaxy might heat intracluster gas, but the idea had seemed as implausible as heating a house by shooting a laser up through the floorboards. The Perseus image, Fabian says, showed that "despite being radiatively inefficient, a jet could be extremely efficient in transferring kinetic energy." Connecting the jets, bubbles, and waves into one picture, "we could actually see a chain of cause and effect," he says. "If feedback didn't work, the central galaxy in Perseus would maybe have 10 times more stars than now observed." This picture of mechanical feedback is now called the "radio mode," because the jets emit strong radio waves.

Researchers glimpsed AGN feedback in higher definition 3 years later, when Harvard astronomers William Forman, his wife, Christine Jones, and others used the Chandra telescope to observe M87—a massive galaxy in the middle of the Virgo cluster, just ⅓ as distant as Perseus. M87 also revealed bubbles and waves, including a circular ring around a bubble floating several light-years from the galactic core. Forman and his colleagues were able to calculate the temperature and pressure change across the wave fronts, providing a ball-

Published by AAAS

Thermostat. Jets shooting from a galaxy's nucleus can limit its growth.

park estimate of how much energy the waves were pumping into the gas.

Using models developed with the help of Perseus and M87 observations, researchers have shown that the shock from the initial inflation by the jets, the propagation of waves, and the slow expansion of the bubbles into the intracluster medium can spread energy over vast distances to keep the gas from cooling. "The data imply that it's a relatively gentle process sustained over millions of years," Fabian says. In such a "steady boil" scenario, calculations show that even occasional jets can keep the gas warm over long periods.

Astronomers looking for more examples of feedback have seen several galaxies sporting ghost cavities or holes far from their centers. These bubbles probably formed when jets plowed through the intergalactic medium tens of millions of years ago and have since been slowly migrating through the gas. In a 2006 study, Fabian and colleagues spotted bubbles in 14 out of 20 galaxy clusters with unexpectedly warm gas at their centers.

Other astronomers have followed up with radio observations to confirm that these bubbles—many of which are tiny compared with those seen in M87—were in fact produced by jets. Somak Raychaudhury of the University of Birmingham, U.K., and his colleagues have detected the faint signature of ancient jets leading into these bubbles using observations made through the Giant Metrewave Radio Telescope in Pune, India, an instrument designed for low radio frequencies. "As particles travel along the jets, they radiate energy; as they age, they emit lower and lower frequencies," says Raychaudhury. "That allows us to reconstruct previous outbursts." Even if a galaxy lacks jets now, he says, those long-vanished energy sources could still be keeping nearby space bubbling away merrily.

On boil. Bubbles traveling outward from the core of galaxy M87.

CREDIT: NASA/CXC/CFA/W. FORMAN *ET AL.*

The quick and the dead

Although the broad outlines of the radio mode are not in dispute, the details are fuzzy and fraught with problems. One big stumbling block stems from geometry: The jets generally shoot out perpendicular to the galactic disk, sending the bubbles eddying away from that plane—not the most effective way to heat gas in and near the disk itself.

"The bubbles are not going to do much to the immediate galaxy," says Philip Hopkins, an astronomer at the University of California, Berkeley. Radio-mode effects might keep cluster gas from cooling and falling into the disk in the long run, Hopkins says. But to account for more-immediate processes—"things like shutting down the flow of material to the black hole or turning off the immediate star formation from gas that's already in the galaxy"—some other heating mechanism must be at work.

Researchers think the key is a different kind of feedback called the quasar mode. It involves direct heating by radiation from the AGN or by explosive winds from near the black hole that blow gas out of the galaxy. Hopkins and many other theorists think this kind of feedback may have been dominant in the early universe, "quenching" quasars (essentially highly luminous AGNs) and transforming them into what are now massive "red and dead" galaxies, with very low levels of new star formation. Applied to more-recent galaxies, the quasar mode can account for AGN feedback in galaxies without jets.

Some evidence for feedback on a large scale—possibly in the quasar mode—comes from a 2007 study by a group including Kevin Schawinski, now a postdoc at Yale, and Daniel Thomas of the University of Portsmouth in the U.K. By studying the spectra of some 16,000 galaxies with massive black holes at their centers, the researchers could infer which ones were still forming stars and which ones possessed the glowing core of an AGN. Most of the galaxies fell into one of two large bins: star-forming ones with no AGN activity and dead ones, also with no AGN activity. The remaining 10% of the galaxies bore the signatures of AGN activity and low levels of star formation.

Estimating the average age of the three kinds of galaxies, the researchers found they fell into evolutionary sequence that suggested AGN feedback in action over hundreds of millions of years. "When the black holes are dormant, the galaxies form stars," Thomas says. "Several hundred million years later, the black holes switch on AGN activity, suppressing star formation"—the 10% of galaxies in which the AGN had not yet completely stamped out the birth of new stars. The galaxies then move into the red-and-dead phase, the AGN eventually fizzling out.

In a follow-up study of 20 galaxies along this evolutionary sequence, published in the February issue of *The Astrophysical Journal*, Thomas, Schawinski, and others found a more direct link between AGN activity and the halt to star formation. In galaxies in which the AGN had switched on, the researchers found evidence of little molecular gas—the fuel needed to make stars. "The AGN is destroying the molecular gas," Thomas says: heating and blowing it out, as would be expected in the quasar mode.

If AGN feedback really is as large-scale and far-ranging as Fabian and others suspect, it could solve a couple of major problems in astrophysics. One is the discrepancy between models of the universe and astronomical observations. The models accurately predict the cosmic distribution of dark matter—the invisible stuff that makes up the bulk of the universe. But they also predict that the galaxies that sit inside the dark matter halos ought to range in size much more widely than astronomers observe.

The other problem is the surprising correlation between the mass of a galaxy and the mass of the black hole at its center. In the past decade, researchers have established that this ratio, known as the M-sigma relationship, is uniform for galaxies of different sizes throughout the universe. That regularity has led astronomers to wonder what physical process binds the destinies of the black hole and the galaxy. Cosmic limits to growth would explain those regularities of size and scale.

As promising as AGN feedback appears, however, many more studies are needed to pin down the mechanisms by which it works and the time scales on which it operates, says Jeremiah Ostriker, a theorist at Princeton University. Most current models of both the radio and the quasar modes of feedback are too simplistic, Ostriker says. For example, "the calculations of the mechanical and thermal components of feedback through bubbles are highly uncertain."

Fabian agrees that the list of unresolved questions is long and expects the quest for answers to simmer on for a while. "I don't think we can write QED at the bottom of this," he says.

–YUDHIJIT BHATTACHARJEE

Published by AAAS

CHINA

Help Wanted: 2000 Leading Lights To Inject a Spirit of Innovation

Reform-minded Chinese scientists hope a new program, *Qianren Jihua*, will reel in the sort of comrades who can help raise the nation's scientific game

Created just 5 years ago, the National Institute of Biological Sciences (NIBS) in Beijing is hailed—and envied—as a sanctuary where a select group of scientists is sheltered from China's patronage-driven funding system. So it was a major boost when officials announced earlier this month that biochemist Wang Xiaodong, a Howard Hughes Medical Institute investigator at the University of Texas Southwestern Medical Center at Dallas, not only would stay on for a second term at the helm of NIBS but also will close his lab in the United States and return to China for good. "There is no turning back," Wang says.

Wang is the biggest catch of a new program called *Qianren Jihua*, or Thousand-Person Plan, that aims to recruit up to 2000 top-notch scientists, entrepreneurs, and financial experts from abroad over the next 5 to 10 years. So far, *Qianren* status has been conferred on 96 "innovative talents," who will work at universities and institutes, and 26 "entrepreneurial talents," who will lead high-tech companies. The program was initiated by the Organization Department of the Central Committee of the Communist Party of China (*Zhongzubu*), which appoints and evaluates high-level cadres. *Zhongzubu*'s foray into headhunting underlines Beijing's belief that China must instill a more innovative spirit into its work force to sustain economic development.

Some scientists applaud *Qianren* as a timely effort to muster a critical mass of Western-trained researchers who, through strength in numbers, will gradually reform a scientific system rife with corruption, vested interests, and influence-peddling. "The plan aims to achieve two goals: to raise the level of research and to improve the academic environment," says *Qianren* recipient Shi Yigong, a structural biologist who left Princeton University last year to lead the schools of medicine and of life sciences at Tsinghua University in Beijing.

But the nascent program is under fire. Scientists who drafted and refined *Qianren Jihua* told *Science* the plan originally required recipients to work full-time in China; they were surprised, when the program rolled out last December, to see a minimum commitment set at 6 months a year for 3 years. Nor was the original plan limited to expats. "The idea was to establish government-endowed senior and junior faculty chair positions" to attract applications from qualified scholars from China or abroad, says Shi.

Another bone of contention is money. The original plan called for steady research support for successful candidates, but *Qianren* offers recipients only a one-time $146,000 relocation subsidy from *Zhongzubu*. The education and science ministries had been expected to foot salaries—suggested by the proposal to be about 60% of what expats receive overseas—and start-up funds of up to $1.2 million over 5 to 7 years, depending on the field. Instead, universities have had to pony up salaries and start-up packages, at least for the first batch of recipients.

Back for good. Wang Xiaodong is returning home to help put China on a solid research footing.

Not surprisingly, says *Qianren* awardee Xu Huaxi, Xiamen University, which nominated him, "has become less enthusiastic." Since 2003, Xu and fellow recipient Zhang Xiao-kun, both at the Burnham Institute for Medical Research in San Diego, California, have been volunteering to establish a biomedical research institute at the university along with three other overseas Xiamen alums. Xu says everything is still up in the air, from funding to how much time he will spend in Xiamen. Other *Qianren* recipients express similar uncertainty. "I am not sure how this will develop," says Shao Zhifeng, who returned from the University of Virginia in Charlottesville last year to Shanghai Jiao Tong University to head its Institute of Systems Biology.

Déjà vu

For more than a decade, China has made a concerted effort to woo talented expats to return home. In 1998, the education ministry launched the Changjiang Scholars Program, partly sponsored by Hong Kong real estate tycoon Li Ka-shing to provide incentives—$14,600 supplemental salaries, high by standards then—to lure talent under age 45 to teach and do research at Chinese universities. When officials realized that most overseas tenured professors did not want to return full-time, the program expanded to accommodate senior part-timers (*Science*, 22 September 2006, p. 1721). Since 2003, the science ministry has also provided Changjiang Scholars who commit to 9 months a year in China with start-up funding of $293,000 over 3 years. Also in 1998, the Chinese Academy of Sciences (CAS) shifted the focus of its *Bairen* (Hundred-Person) Plan—launched in 1994 to support young researchers trained locally or abroad—to attract expats. CAS requires institutes that recruit *Bairen* awardees to provide $100,000 in start-up funds. After 1 year of full-time work, awardees are evaluated for merit grants of $253,000 over 3 years and a $40,000 housing subsidy from CAS.

Together, the two ongoing programs have recruited some 2000 scientists to return full time, most of them newly minted Ph.D.s and postdocs (see graph, p. 535). The programs have also enticed several hundred associate or full professors with tenure overseas to spend up to 3 months a year in China.

Qianren Jihua is the first such program administered by the central government and the first to target entrepreneurs as well as academics. It is the brainchild of *Zhongzubu* chief Li Yuanchao, who has made recruiting talented people a priority. Li has been pushing leaders at universities, CAS, and industry—almost all of whom are Party cadres—to be more daring and reel in talent faster.

After notice went out last December, organizations scrambled to find *Qianren* candidates, mostly by going after colleagues already moonlighting in China. Tsinghua signed up four part-timers as candidates, including Hu

TALENT SEARCH

Program	MINISTRY OF EDUCATION (MOE)		CHINESE ACADEMY OF SCIENCES (CAS)		CPC ORGANIZATION DEPARTMENT
	Chanjiang Scholars Program		Outstanding Overseas Talent	Famous Overseas Scholars	Thousand-Person Plan (*Qianren*)
	Special Appoin't	Lecture Chair			
Year Began	1998	1999	1998	2001	2008
Target Audience	Domestic or returned scholars under 45	Overseas scholars with rank of associate professor or higher	Returned young researchers under age 45	Overseas scholars with rank of associate professor or higher	Overseas tenured full professors or equivalent under age 55
Commitment	Full-time	2–3 months per year	Full-time	2–3 months per year	Minimum 6 months per year
Outcome	1045 recipients as of 2008; 90% have overseas experience	511 recipients as of 2008	1122 recipients as of 2008	283 recipients as of 2008	96 academics and 26 entrepreneurs recruited in 2008

RACKING UP RECRUITS

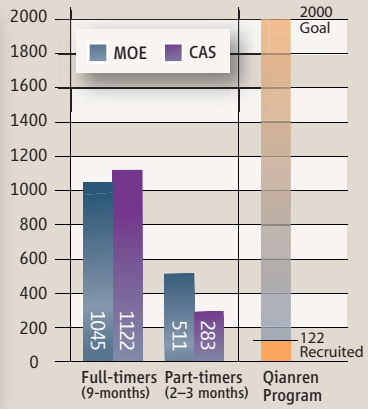

Xiaoping, a biomedical imaging expert at Emory University in Atlanta who has been helping Tsinghua establish a neuroscience imaging center. Hu is weighing his options: "The government wants us to decide quickly, but many policies are not clear," he says. Universities, CAS institutes, and national labs nominated candidates to either the education or science ministries. Both ministries appointed review panels, composed of academicians and science mandarins, which invited candidates to Beijing to give 20-minute presentations.

Although *Zhongzubu* has not released recipients' names, a dozen or so universities have publicized their *Qianren* awardees. The majority of them had been recruited by previous incentive programs. Two of Beijing University's (Beida's) three recipients have been recruited home before this. She Zhensu, an applied mathematician at the University of California, Los Angeles (UCLA), was one of the first Changjiang scholars in 1999 (*Science*, 21 January 2000, p. 417). Last year, he finally gave up his tenured appointment at UCLA to work full-time at Beida. Another recipient and former Changjiang scholar is She's boss, Chen Shiyi, Beida's engineering dean. Chen continues to keep one foot in the United States—at Johns Hopkins University's engineering school—after nearly a decade of shuttling across the Pacific Ocean. According to Andrew Douglas, associate dean of academic affairs at the engineering school, Chen is on "partial leave, [which] would allow him to work 6 months of the year in China." Chen declined and She did not respond to interview requests.

Overcommitted

Holding down simultaneous appointments in China and overseas might be manageable for theoreticians such as Chen, but it is hard for experimentalists to run labs on two continents. Those who try may discover that "it will be very tiring, and in the end both labs will suffer," says Hu. Wang Xiaodong thinks most U.S. universities would not allow tenured principal investigators in experimental sciences to work part-time for extended periods. "*Qianren Jihua*'s 6-month requirement is not workable; it will create conflicts of commitment," he says.

One *Qianren* awardee, Wang Peng, a carbohydrate researcher, is facing a review over his relationships with Chinese universities, according to documents obtained by *Science*. Wang has been an Ohio Eminent Scholar at the Ohio State University (OSU) in Columbus since 2003. Earlier that year, Shandong University in Jinan recruited Wang as a Changjiang-Scholar professor with a 9-month-per-year contract. Wang told *Science* that he "did not know what he was getting into" by accepting the Changjiang award; during his 5-year appointment, he says, he only spent short periods in Shandong. After the scholarship ended, Wang's name remained on the Shandong faculty roster as a Ph.D adviser. Wang says he resigned earlier this week from the Shandong position.

In 2007, Wang accepted an offer from Nankai University in Tianjin to set up a new school of pharmacy there and be its first dean. Nankai later nominated Wang for a *Qianren* award. Last March, Ohio State received a complaint about Wang's relationships with Chinese universities. Matthew Platz, interim dean of the colleges of biological sciences and of physical and mathematical sciences, says the matter is under review. In an April 2008 letter to OSU's biochemistry department chair, Wang explained that his activities at Nankai "are in the scope of consulting," the title of dean is "symbolic," and he would spend no more than 20% of the 9 months he is paid by OSU and 2 or 3 months in the summer when he is not paid by OSU or federal grants to consult at Nankai. As for his *Qianren* award, Wang says he has not decided what to do as Nankai has not made him an offer.

Unlike universities, CAS requires its *Qianren* recruits to work full-time in China, says Li Hefeng, director of CAS's Bureau for Human Resources and Education. Of the first batch of 122 *Qianren* recipients, 19 are affiliated with CAS, including five at the academy's University of Science and Technology of China in Hefei. CAS is providing $293,000 to each "innovative talent" and asks the recruiting institute to match the amount. No more than half of that sum may be used for salaries and fringe benefits for the recipient and lab members; the rest is for research overhead costs. A CAS *Qianren* recipient who previously received *Bairen* support will not get the $293,000, Li says.

A half-dozen university recruits told *Science* they will work full-time in China. Among them is mechanical engineer Robert Parker, who last September became associate dean for academic affairs at the University of Michigan–Shanghai Jiao Tong University Joint Institute in Shanghai. Parker says it wasn't the *Qianren* award that brought him to China but the challenge of building an institute from the ground up. "The goal," he says, "is to create a school of engineering which in quality and scope reaches the level of a major engineering school in the United States."

Other scientists who committed to working full-time in China—and who subsequently were given *Qianren* awards—echo that sentiment. Wang Xiaodong says he is returning to help like-minded colleagues steer Chinese academia toward a merit-based system. Wang, who was elected to the U.S. National Academy of Sciences in 2004 at age 41 for his research on mechanisms of cell death, says he is coming home to give it his all: "I do not want to leave any regrets." China's push to recruit good scientists, it seems, is already paying off.

–HAO XIN

With reporting by Li Jiao, a writer in Beijing.

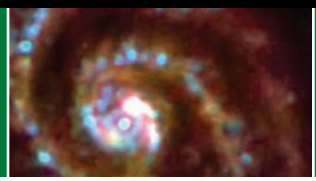

LETTERS

edited by Jennifer Sills

Mayas Live On

THE TITLE OF THE NEWS FOCUS STORY "A NEW LOOK AT THE MAYAS' END" (H. PRINGLE, 24 APRIL, P. 454) incorrectly characterizes the state of this American indigenous group. Maya people continued to exist after the decline of Tikal and other cities. They developed new civic centers, such as Mayapán in the north and Utatlán in the south. Kiché Mayas live in what is today Guatemala; Popol Vuh, a book that describes Maya cosmovision and history, serves as an example of their cultural strength in the late postclassical period. Today, seven million Maya-speaking people continue to live in Mexico, Guatemala, and Belize. Their vibrant culture has been noted by Noam Chomsky (*1*), Carlos Montemayor (*2*), and, of course, the Maya Nobel Prize winner Rigoberta Menchú (*3*).

JULIÁN M. PEÑA-CASTRO

Department of Botany and Plant Sciences, University of California, Riverside, CA 92521, USA. E-mail: julian.pena-castro@ucr.edu

References

1. Z. Vodovnik, Ed., *¡Ya Basta! Ten Years of the Zapatista Uprising* (AK Press, Oakland, CA, 2004).
2. C. Montemayor, D. Frischmann, Eds., *Words of the True Peoples: Anthology of Contemporary Mexican Indigenous-Language Writers* (Univ. of Texas Press, Austin, TX, 2004).
3. R. Menchú, Nobel Lecture (http://nobelprize.org/nobel_prizes/peace/laureates/1992/tum-lecture.html).

Mayas today. A Maya woman weaves traditional Maya fabric.

Venezuelan Science: A Professor's Defense

IN THE NEWS OF THE WEEK STORY "AS RESEARCH funding declines, Chávez, scientists trade charges" (B. Casassus, 29 May, p. 1126), the President of the Institute for Advanced Studies (IDEA) explains the reasons for my dismissal from the institution, after 27 years as an employee and a total of 41 years serving Venezuelan science. As the most senior professor at IDEA until my dismissal, I would like to defend myself, a right that has been denied to me in my country.

The accusation that while at IDEA from 2007 to 2009 I worked as an employee of another academic institution is false, as stated in my letter of resignation to that institution, dated 3 January 2007, the day I rejoined IDEA (*1*). The other accusation concerned the purchase of a piece of software in which, supposedly, I had a vested economic interest, before rejoining IDEA. Indeed, I was part of a team that was contracted to develop software for academic and bibliometric use. These programs are not my property, and I have never been entitled to receive any money for their commercialization (*2*). Nevertheless, because I was researching bibliometric output at IDEA, it seemed reasonable to request the purchase of the BIBLIOS software for use by the staff and students of my research unit in order to avoid software piracy. The software was never acquired.

JAIME REQUENA

Academia de Ciencias Físicas, Matemáticas y Naturales, Caracas, Venezuela. E-mail: requena.j@gmail.com

References

1. Letter of resignation, 3 January 2007 (www.hotlinkfiles.com/files/2564123_vtm2g/RenunciaFundamet2007enero.pdf).
2. Affidavit of the owner of BIBLIOS software regarding its commercialization (www.hotlinkfiles.com/files/2567098_p40tx/ConstanciaBiblios.doc).

Venezuelan Science: Government on Course

IN HIS LETTER ("VENEZUELAN SCIENCE AT RISK," 19 June, p. 1514), C. Bifano, speaking on behalf of the Venezuelan Academy of Physical, Mathematical, and Natural Sciences, enumerates their "fears for the present and future fate of science and higher education" in Venezuela. I believe that his concerns are unfounded.

Bifano worries about the fact that the government is establishing national research priorities, but it is the government's duty to make such decisions and to promote scientific research that addresses the country's problems. Bifano is concerned about the creation of new universities, but many young scientists, who would otherwise be excluded from the already crowded traditional universities, are now pursuing their careers through attending these new institutions. He speaks about budget cuts, but overall spending on science has quadrupled, reaching 2.1% of the gross domestic product in 2007 (*1*), in part due to private funds being allocated to science in response to the recently passed Organic Law on Science, Technology and Innovation. The government decided after wide consultations to centralize those funds and allocate them on a competitive basis, similar to the way in which the U.S. National Science Foundation allots funds.

GUILLERMO R. BARRETO

Biologia de Organismos, Universidad Simón Bolívar, Caracas, Venezuela. E-mail: guibarre@usb.ve

Reference

1. Editorial, *Nature* **450**, 922 (2007).

Published by AAAS

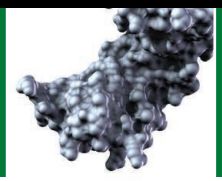

Splenic reservoir

549

Improving computer security

550

Venezuelan Science: Making Great Strides

WE WOULD LIKE TO REPLY TO THE NEWS OF the Week story by B. Casassus ("As research funding declines, Chávez, scientists trade charges," 29 May, p. 1126). The Bolivarian Republic of Venezuela is currently in the 10th year of a revolution aimed at improving the health, welfare, education, and culture of all Venezuelans. President Chávez has particularly emphasized the poorest sectors, who before 1999 had little access to the benefits from Venezuela's considerable oil production. Consequently, much larger fractions of our gross domestic product are now dedicated to health, education, and science and technology.

Because the world financial crisis has affected our country through the sharp decrease in oil prices, the government implemented a national budget reduction of 6.7% that includes all public institutions. This is substantially less than the budget cuts implemented in many other nations and is certainly not a measure directed against universities and research centers. In fact, the Bolivarian government has improved Venezuelan science in a number of ways:

(i) The number of researchers in the country has increased from 3597 in 1998 to 10,187 in 2008 (*1*).

(ii) The government passed the 2005 Organic Law on Science, Technology and Innovation, which stipulates that companies must devote a percentage of their income to Research and Development. This law increased the share of R&D from 0.39% of gross domestic product in 1999 to 2.69% in 2007 (*2*). The latter is probably the highest share in Latin America, and according to the Organisation for Economic Co-operation and Development (OECD), it is even higher than those of several developed countries in 2005, including Canada and Belgium (1.9%) and Australia and the United Kingdom (1.8%) (*3*).

(iii) The number of students in the country has increased from 6,233,127 in 1999 to 7,598,487 in 2008 (*4*). A massive effort has diminished illiteracy from 7% in 1999 (*5*) to 0.4% in 2008 (*6*). Similar enterprises have brought primary school, high school, and university education to many people who could not even dream of these educational opportunities before 1999.

(iv) Popular access to the Internet has increased from 5.43% in 2003 (*7*) to 27.04% in 2009 (*8*), through the installation of 3187 fully equipped "info-centers" throughout the country. Many are in remote areas thanks to the connectivity of our first satellite, "VENSAT-1, Simón Bolívar," launched last year by the Bolivarian Agency for Space Activities. The Ministry of the Popular Power for Science, Technology, and Intermediate Industries (MPPCTII) now incorporates the largest Venezuelan telecommunication companies, as well as a cell phone factory, which will enable most Venezuelans to own a cell phone for only US$13.95.

(v) A national computer factory, Venezolana de Industria Tecnológica, an Academy of Free Software, and the National Plan for Technological Literacy to reduce computer illiteracy have been established. These are initiatives by our government to guarantee free electronic access to information for all citizens.

Our ministry also funds the "Marcel Roche" Library at the Venezuelan Institute for Scientific Research (IVIC), allowing users to access more than 11,300 scientific journals (printed and electronic). To address the critical shortage of slots for higher education, this government created 40 new universities. It is astonishing that the president of the Academia de Ciencias Físicas, Matemáticas, y Naturales (ACFIMAN; Academy of Physical, Mathematical, and Natural Sciences) believes this to be a worrisome development or a national threat ("Venezuelan science at risk," C. Bifano, Letters, 19 June, p. 1514).

It is not true that there is a "loss of intellectual capital" in Venezuela. Despite the fact that good scientists have always been attracted to and recruited by academic institutions in the developed world, our largest research institute, IVIC, has increased its academic staff (including students) from 655 in 1998 to 1107 in 2008. It is also false that the government fired, demoted, or blacklisted dissident scientists. Since 1999, any scientist has been able to freely talk, write, demonstrate on the streets, vote, and work, as all Venezuelan citizens do in this evolving country. The short-term study (*9*) in the News Focus story was sponsored and published by a private foundation belonging to a consortium that participated in the economic sabotage orchestrated by the opposition before and during the April 2002 coup d'etat against President Chávez, and the subsequent commercial lockout in December of that year. For these reasons, the Bolivarian government considers this work biased and unreliable.

Finally, let us clarify that Venezuelan law stipulates that, as in most other countries, the appointment of presidents and directors of government research institutions is the responsibility and a prerogative of the MPPCTII, but requires the approval of the president.

JESSE CHACÓN-ESCAMILLO

Minister of the Popular Power for Science, Technology, and Intermediate Industries, Bolivarian Republic of Venezuela. E-mail: jchacon@mcti.gob.ve

References

1. Observatorio Nacional de Ciencia, Tecnología, e Innovación, "Indicadores–Venezuela, 2008" (www.oncti.gob.ve/pdf/PPI_SERIE_2008.pdf, p. 4).
2. Observatorio Nacional de Ciencia, Tecnología, e Innovación, "Boletin 2007" (www.oncti.gob.ve/pdf/SIDCAI_2007.pdf, p. 42).
3. OECD, "Stat Extracts, Gross domestic product" (http://stats.oecd.org/Index.aspx?DatasetCode=SNA_TABLE1).
4. Ministerio del Poder Popular para la Educación, *Memoria y cuenta 2008* (MPPE, Caracas, 2009).
5. J. B. Huerta, "El analfabetismo en Venezuela" (www.josebhuerta.com/analfabetismo.htm).
6. H. Chavez, Speech before the National Assembly, 13 January 2009 (www.parlatino.org.ve/paginas/sala_situacional/cuenta_2008.htm).
7. Tendecias Digitales, "Indicadores de penetración y uso de Internet en Venezuela" (www.cenit.gob.ve/cenitcms/servlet/com.mvdcomm.cms.andocasociado?58,72).
8. E. Táchira, Comisión Nacional de Telecomunicaciones, "Resultados del sector telecomunicaciones, I trimestre 2009" (www.conatel.gob.ve/Indicadores/indicadores2009/Presentaci%F3n_publica_Itrim_2009.pdf).
9. I. de la Vega, *Mundos en Movimiento: El Caso de la Movilidad y Migración de los Científicos y Tecnólogos Venezolanos* (Ediciones Fundación Polar, Caracas, 2005).

Letters to the Editor

Letters (~300 words) discuss material published in *Science* in the previous 3 months or issues of general interest. They can be submitted through the Web (www.submit2science.org) or by regular mail (1200 New York Ave., NW, Washington, DC 20005, USA). Letters are not acknowledged upon receipt, nor are authors generally consulted before publication. Whether published in full or in part, letters are subject to editing for clarity and space.

Published by AAAS

CORRECTIONS AND CLARIFICATIONS

News of the Week: "Appearances can deceive, even with standard reagents" by H. Xin (22 May, p. 997). The reference to a survey conducted with the biweekly magazine *Science News* should have made clear that the magazine is a Chinese publication unrelated to the U.S. magazine of the same name.

Reports: "Remeasuring the double helix" by R. S. Mathew-Fenn *et al*. (17 October 2008, p. 446). In Fig. 3B and fig. S4, a bending-derived variance estimate was added to the observed variances; it should have been subtracted from the observed variances. The corrected figures show the raw, experimentally observed variances. A corrected version of Fig. 3B and one sentence in the text are provided here. In the supporting online material, similar corrections have been made to fig. S4 and its caption. We thank N. Becker for pointing out these mistakes.

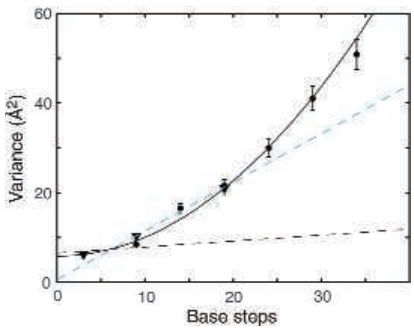

(**B**) Observed variance in nanocrystal-nanocrystal separation distance of end-labeled duplexes (circles) and internally labeled duplexes (triangles), plotted with respect to the number of intervening DNA base-pair steps. The variance predictions for an ideal elastic rod with a stretching modulus of 1000 pN (the value measured in single-molecule stretching experiments) are shown (dashed black line) and deviate grossly from the data. A linear relationship between variance and base-pair steps (dashed cyan line, two variables, $R^2 = 0.868$) is expected if the stretching of base-pair steps is uncorrelated along the DNA duplex (*24*). Alternatively, a quadratic relationship (solid black line, two variables, $R^2 = 0.989$) should hold if the DNA stretches cooperatively. The quadratic fit indicates that each base-pair step contributes 0.21 Å of standard deviation to the end-to-end length of a duplex. The y intercept of 5.8 Å^2 corresponds to variance arising from experimental factors. The variance data points derive from the Gaussian curves in Fig. 2B. The uncertainties in the variance values are estimated to be ±6.6%, based on the standard deviation of repeated measurements for the 25-bp duplex at independent beamlines and with independently prepared samples (fig. S3).

The fifth sentence of the third paragraph on page 448 should read, "The data fit a quadratic dependence to within this measurement error (black line; $\chi^2 = 9.95$ with 7 degrees of freedom; $P = 0.19$), but not to a linear dependence (cyan dashed line; $\chi^2 = 62.5$ with 7 degrees of freedom; $P = 4.8 \times 10^{-11}$)."

TECHNICAL COMMENT ABSTRACTS

COMMENT ON "Remeasuring the Double Helix"

Nils B. Becker and Ralf Everaers

Mathew-Fenn *et al*. (Reports, 17 October 2008, p. 446) reported unexpected distance fluctuations in short end-labeled DNA constructs and interpreted them as evidence for cooperative DNA stretching modes. We show that when accounting for a subtle linker leverage effect, their data can be understood within standard noncooperative DNA elasticity.

Full text at www.sciencemag.org/cgi/content/full/325/5940/538-b

RESPONSE TO COMMENT ON "Remeasuring the Double Helix"

Rebecca S. Mathew-Fenn, Rhiju Das, Timothy D. Fenn, Michael Schneiders, Pehr A. B. Harbury

We measured the mean and variance of end-to-end length in short DNA fragments in solution and reported evidence of DNA stretching that is cooperative over more than two turns of the double helix. Becker and Everaers suggest that the structural fluctuations we observed arise from bending motions of the DNA, rather than stretching. We present three experimental tests of this bending-based explanation.

Full text at www.sciencemag.org/cgi/content/full/325/5940/538-c

Published by AAAS

EARTH SYSTEMS

A Second Opinion for Our Planet

Lee R. Kump

He Knew He Was Right
The Irrepressible Life of James Lovelock and Gaia /
James Lovelock
In Search of Gaia
by John Gribbin and Mary Gribbin
Allen Lane, London, 2009. 262 pp. £20, C$42. ISBN 9781846140167. Princeton University Press, Princeton, NJ, 2009. 286 pp. $24.95, £16.95. ISBN 9780691137506.

The Vanishing Face of Gaia
A Final Warning
by James Lovelock
Allen Lane, London, 2009. 199 pp. £20, C$34. ISBN 9781846141850. Basic Books, New York, 2009. 288 pp. $25. ISBN 9780465015498.

Those rare Earth scientists with training in medicine have a more holistic view of the planet than their peers. James Hutton, the "father of geology," saw Earth as a superorganism and its proper study as physiology (*1*). His descendants, the geologists of the 19th and 20th centuries with little exposure to the life sciences, largely forgot or ignored this view. Then came James Lovelock, a Ph.D. in medicine with an eclectic career in research and innovation. Lovelock independently arrived at the view of Earth as a living organism, which he named Gaia, the Greek goddess of Earth. Importantly, Lovelock expanded Hutton's notion of a superorganism to include homeostasis, the self-regulation of critical components of the living Earth system. In their biography *He Knew He Was Right* (published in the United States as *James Lovelock: In Search of Gaia*), John and Mary Gribbin lead us on an exploration of how Lovelock came to his perspective of Earth. Their account prepares us for Lovelock's latest diagnosis of the planet's ills and dire prognosis for its future in *The Vanishing Face of Gaia: A Final Warning*.

This is not the first time that Lovelock's life history has been presented. Indeed, Lovelock himself has published an autobiography (*2*), a longer and more detailed exposition of him. Although the Gribbins rely heavily on Lovelock for much of their information, they provide an arm's-length perspective and a lucid style that repackages this material in an understandable and interpretive form. They offer valuable insights not only into how Lovelock came up with the idea for Gaia but more generally how his mind works and where the ideas for his scores of inventions come from. They describe how he begins with empathy for the subject, in one case imagining what it would be like to be a cell suspended in a liquid medium beginning to freeze. Those thoughts led to his revelation that freezing and desiccation are similar cellular experiences.

Nor is this the first time that Dr. Lovelock has called with the bad news: It was a focus of his 2006 book *Revenge of Gaia* (*3*). *Final Warning* seems to arise from frustration that society hasn't been roused by the wake-up call of *Revenge*. While revisiting many topics Lovelock discussed in the earlier book (including the history of Gaia theory and his views on global warming and alternative energy solutions), *Final Warning* has an elevated sense of urgency—stimulated in part by observations that anthropogenic influence and Earth's response are accelerating at a pace that exceeds the projections of the latest Intergovernmental Panel on Climate Change report.

Throughout his book, Lovelock decries American science. He refers to the "disastrous mistake" of assuming "that all we need to know about the climate can come from modeling the physics and chemistry of the air in ever more powerful computers." The geochemists' box models of global biogeochemical cycles and the atmosphere and ocean scientists' general circulation models ignore the physiology of a living planet. They assume linear parameterizations where life instills parabolas, with multiple equilibria and sharp transitions from homeostasis to positive feedback and system failure when pressed beyond optima. In Lovelock's view, American science is too compartmentalized into narrow disciplines, too reductionist in approach, so well funded as to stifle creativity, and too reliant on computer models. Lovelock places higher value on observation and experimentation than on modeling. To understand his perspective, imagine Marcus Welby, M.D., using computer models to generate a prognosis for progression of a serious disease.

According to Lovelock, America has largely ignored or rejected Gaia theory, a claim that is somewhat difficult to rectify with the Gribbins' conclusion that it has become increasingly respectable. In Lovelock's view, Gaia puts American scientists at professional risk. [Indeed, a reviewer of the manuscript of a 1994 paper I coauthored with Lovelock (*4*) claimed that its publication would likely ruin my career.] He believes that the concept casts doubt on the way science is divided into disciplines, presumably challenging the value of their associated administrative and educational bureaucracies. "Gaia is a holistic concept and therefore unpalatable to rational Earth and life scientists." As counterpoint, the Gribbins proffer the two American Geophysical Union Chapman Conferences on the topic and the elevated role that Earth system science has played in the scientific assessment of global warming. Yet we American scientists rarely utter the word Gaia except in critique of, or commentary on, these meetings or the writings of Lovelock, Lynn Margulis, and precious few others; *Science*'s internal search engine reveals no papers where Gaia was used except in this fashion.

Early in *Final Warning*, Lovelock rejects CO_2 and climate stabilization schemes, referring to them as "no better than planetary alternative medicine." Here he sees little prospect in alternative and renewable energy or in most

Gaia and her advocate.

CREDIT: BRUNO COMBY/ENVIRONMENTALISTS FOR NUCLEAR ENERGY

The reviewer is at the Department of Geosciences and Earth System Science Center, Pennsylvania State University, University Park, PA 16802, USA. E-mail: lkump@psu.edu

Published by AAAS

geoengineering schemes, with the exception of the burial of intentionally charred biomass (*5*). Later—perhaps reflecting an evolution of thought during the writing of the book and an expression of the inventor in him—he argues that we now have little option but to try various geoengineering schemes to moderate what he feels are the inevitable dire consequences of "global heating."

Do we do ourselves and society a disservice by ignoring Gaia? Are the intuitions of a planetary physician a more accurate prognosis for the future than those produced by supercomputers created by multidisciplinary teams of scientists? Climate scientists acknowledge the uncertainties of their projections and are working diligently to reduce them. But are we properly incorporating the feedbacks between climate and a globally potent biota? And do we even have time to refine these models? Lovelock thinks not. He calls for an immediate shift of focus to adaptation to a hothouse world, expecting that in the coming decades humanity will be forced to migrate to the few habitable refugia that remain (including the British Isles). The world population will be reduced from billions to millions, Gaia selecting those humans with the traits to live sustainably (her revenge). Models might come to serve an important alternative role even in this crisis phase, if and when it comes. Shifting from long-term projections to medium-term forecasting, future models with proper planetary physiology might identify the harbingers of the approach of a climate threshold, and if coupled to an expanded network of Earth observations, do so before it is too late.

In the end, Lovelock doesn't want to be viewed as a fearmonger and pessimist: "I am not a willing Cassandra and in the past have been publicly skeptical about doom stories, but this time we do have to take seriously the possibility that global heating may all but eliminate people from the Earth." This is a planetary physician's intuition rather than a projection from an integrated assessment model. Do we ignore it, or fill his prescription and call him in the morning?

References

1. D. B. McIntyre, in *The Fabric of Geology*, C. C. Albritton Jr., Ed. (Freeman, Cooper, Stanford, CA, 1963), pp. 1–12.
2. J. Lovelock, *Homage to Gaia: The Life of an Independent Scientist* (Oxford Univ. Press, Oxford, 2001).
3. J. Lovelock, *The Revenge of Gaia: Why the Earth Is Fighting Back—and How We Can Still Save Humanity* (Allen Lane, London, 2006).
4. J. E. Lovelock, L. R. Kump, *Nature* **369**, 732 (1994).
5. J. Lehmann, *Nature* **447**, 143 (2007).

10.1126/science.1175952

COMPUTERS

Civic Collaboration

Ben Shneiderman

Wiki Government
How Technology Can Make Government Better, Democracy Stronger, and Citizens More Powerful
by Beth Simone Noveck
Brookings Institution Press, Washington, DC, 2009. 246 pp. $28.95, £20.99. ISBN 9780815702757.

Conservatives and liberals alike will find things to cheer and things to fear in the upcoming changes to American political processes. Technology-mediated civic participation, electronically enhanced collaboration, and download-verifiable open government are rebalancing the power structure in federal, state, and local governments. At the same time, open journalism is empowering the universal investigative reporter while undermining the traditional news media.

Just as first movers have advantages that are respected by venture capitalists, first developers in political innovations deserve attention because they are ahead of the crowd. Beth Noveck went from law professor to user-interface designer for the Peer-to-Patent system, which allows public volunteers to provide guidance to the U.S. Patent Office. Getting the usability and the sociability right, she created a Web-based environment for experts in arcane patent issues to speed the work of patent examiners by discussing and selecting the ten most important examples of prior art. You might think that patent applicants, especially major companies, would fear having their patents turned down, but weeding out bad applications early and strengthening good patents benefits everyone. Noveck's emphases on interface design to promote participation and visualizations to provide feedback are increasingly recognized as the foundations for successful engagement of diverse users.

The author's good judgment and deserved success inspired many Peer-to-Patent imitations around the world. Now, she looks to bring similar benefits to other government processes, which she gets to do in her role in President Obama's Office of Science and Technology Policy. *Wiki Government* describes in detail how Noveck made Peer-to-Patent work and offers lessons for other federal agencies. Her tight, lawyerly writing provides a well-argued and fact-filled promotion of "expertocracy," the ways in which experts can contribute their narrow skills to specific problems.

All this makes for good reading and inspiration, but her case could be broadened by showing how these ideas work at more local levels, down to home owner associations. And although Noveck focuses on ways of engaging experts to provide their knowledge, there are additional means through which technology-mediated social participation can be put to work:

Citizen reporting of problems—through such systems as AMBER Alert, storm trackers, earthquake damage reports, forest fire alarms, and electronic suggestion boxes at government Web sites—has already demonstrated its value. More effective reward structures and increased social recognition could substantially expand the use of these avenues.

Volunteer service contributions have traditionally taken the form of material donations after disasters or participation in projects at museums, hospitals, schools, parks, and the like. Web sites such as http://serve.gov and http://nationalservice.gov now facilitate these service efforts. The Web can also be used to distribute tasks among volunteers, as in NASA's clickworkers site for image analysis of martian craters.

Public education (e.g., on personal health, flu pandemics, energy conservation, or environmental protection) can be promoted through well-designed user experiences and effective social norms.

Community building, at every level, is fostered by the rapidly growing social media and ubiquitous cell phones with their increasingly rich services. Communities can become energized by modern electronic versions of parent-teacher associations, neighborhood watches, and disaster planning teams.

Noveck summarizes her case in her closing paragraph: "Ordinary citizens have more to offer than voting or talking. They can contribute their expertise and, in so doing, realize the opportunity now to be powerful.… Collaborative governance is an idea whose time has come." Let's make it happen soon.

10.1126/science.1178326

The reviewer is at the Department of Computer Science, University of Maryland, College Park, MD 20742, USA. E-mail: ben@cs.umd.edu

EDUCATION

Computing Has Changed Biology—Biology Education Must Catch Up

Biologists need better computational education so that researchers can benefit from the bioinformatics revolution.

Pavel Pevzner[1]* and Ron Shamir[2]

Advances in computing have forever changed the practice of biological research. Computational biology, or bioinformatics, is as essential for biology in this century as molecular biology was in the last. In fact, it is difficult to imagine modern molecular biology without computational biology. For example, a difficult algorithmic puzzle had to be solved in order to successfully assemble the human genome sequence from millions of short pieces.

However, the computational components of undergraduate biology education have hardly changed in the past 50 years. New courses for biologists should be more relevant to their discipline, complementing the standard mathematical courses that were originally designed for physicists and engineers. Bioinformatics and biology communities should work together so that education of biologists in the 21st century may become as sophisticated as the computational education of physicists or economists.

For example, today's typical undergraduate economics curriculum may cover linear and integer programming, combinatorial algorithms, dynamic programming, game theory, and other computational concepts. These disciplines were in their infancy 40 years ago when the computational revolution started in economics. Because most biologists today (as most economists 40 years ago) do not know dynamic programming, for example, the idea of introducing such concepts into the biology curriculum may appear foreign and impractical. But the paradoxical result is that economics undergraduates may now be better prepared than biology graduate students to understand how DNA sequence alignment or gene prediction algorithms work (based on dynamic programming).

The RECOMB Bioinformatics Education Conference (http://casb.ucsd.edu/bioed/) explored ways to teach bioinformatics to undergraduate biology students. Attending biologists, computer scientists, and mathematicians from various branches of bioinformatics agreed that the time has come to shift the paradigm in biology education by adding new computational courses to standard curricula. This realization is not new: *BIO2010*, a National Research Council report (*1*), recommended substantial changes in the mathematics curricula for research-oriented biology undergraduates. Bialek and Botstein (*2*) and Pevzner (*3*) acknowledged the problem and outlined some creative approaches to its solution. However, the question of how best to deliver computational ideas to biologists remains.

Because bioinformatics is a computational science, courses should strive to present the ideas that drive an algorithm's design and to explain the crux of a statistical approach, rather than merely to recount the algorithms and statistical techniques. It is critical that bioinformatics is taught as a science that explains computational ideas and shows how they pertain to biological problems, rather than as a collection of cookbook-style recipes. A course must not be reduced simply to "Using Bioinformatics Tools," because a protocol-centric, how-to approach to teaching bioinformatics (without explaining computational ideas) is not unlike teaching how to take integrals in a calculus course without explaining what an integral is. For example, biologists sometimes use bioinformatics tools in the same way that an uninformed mathematician might use a polymerase chain reaction (PCR) kit, without knowing how PCR works and without any background in biology.

Many undergraduate bioinformatics programs at leading universities involve a grueling mixture of biological and computational courses that prepare students for follow-up bioinformatics courses and research. But many such courses aimed at bioinformatics undergraduates tend not to be ideally suited for biology students (undergraduate or graduate). This leads to a pedagogical challenge that, to the best of our knowledge, has not been resolved. How should the research and education community design a bioinformatics course that (i) assumes few computational prerequisites, (ii) assumes no knowledge of programming, and (iii) instills in students a meaningful understanding of computational ideas and ensures that they are able to apply them?

Consider the problem of analyzing gene expression data by principal component analysis (PCA), a powerful computational technique used by thousands of biologists. PCA is not typically covered in mathematics courses taken by biologists, so many may use PCA without understanding how it works or even what it does. A biologist who "blindly" uses PCA or other bioinformatics tools may misapply the method, miss important observations, misinterpret the results, and derive erroneous biological conclusions [see (*4*) for examples of misinterpretations of BLAST results].

Thus, we believe that undergraduate curricula should contain an additional course, "Algorithmic, Mathematical, and Statistical Concepts in Biology" to present the underlying ideas that drive computations in the field. This would not necessarily mean, for example, that biologists need an entire course in linear algebra to introduce eigenvalues, a fundamental aspect of PCA. At the RECOMB conference, Martin Vingron proposed ideas that can allow a simpler, elegant, and intuitive geometric interpretation of eigenvalues to address the problem of sorting a matrix so that similar rows are adjacent, a key problem in gene expression analysis [see (*5*)].

Some Biology departments have made progress toward introducing such courses. They focus on biological questions (e.g., "Did our ancestors interbreed with Neanderthals?" or "How do we distinguish between different forms of breast cancer and choose the appropriate chemotherapy?"), then follow with the computational ideas used to answer them. The best such courses are often designed by a team of faculty from different departments (e.g., Biology, Computer Science, and Mathematics). For example, Wingreen and Botstein (*6*) describe a course at Princeton that covers dynamic programming, clustering algorithms, Bayesian analysis, and other computational ideas relevant to original path-breaking papers in diverse areas of biology.

Or take, for example, the problem of selecting expression biomarkers that can be used to predict clinical outcomes of young breast cancer patients (*7*). The computa-

[1]Department of Computer Science, University of California, San Diego, 9500 Gilman Drive, La Jolla, CA 92093, USA. [2]The Blavatnik School of Computer Science, Tel Aviv University, Tel Aviv, 69978, Israel.

*Author for correspondence. E-mail: ppevzner@cs.ucsd.edu

Published by AAAS

tional ideas (hierarchical clustering, pattern classification, and feature selection) are introduced as part of the "story" to promote ease of understanding by students. Such examples may also instill in students the real-life impact of computational methods. This research, for example, led to the first cancer diagnostic chip to be approved by the U.S. Food and Drug Administration; it is currently used to determine which patients may benefit from additional chemotherapy.

The question of whether similar innovative courses can be implemented at the undergraduate level at many universities remains subject to debate (*8*, *9*). Nevertheless, such courses are pioneering steps toward developing a new computational biology curriculum.

We do not argue against the mathematical courses included in current undergraduate biology curricula. But we believe that these courses should be revised and extended. Many key computational ideas can be better communicated and absorbed by biology undergraduates with few prerequisites, in a way that will make the students excited about bioinformatics as a scientific discipline and more creative when they employ bioinformatics methods and ideas in the future. We feel that the best way to engage biology undergraduates in bioinformatics is to appeal to their innate intuition and common sense and to avoid mathematical formalism as much as possible. The proposed course may become a first step toward building the new computational curriculum for biologists.

References and Notes

1. National Research Council, *BIO2010, Transforming Undergraduate Education of Future Research Biologists* (National Academies Press, Washington, DC, 2003).
2. W. Bialek, D. Botstein, *Science* **303**, 788 (2004).
3. P. A. Pevzner, *Bioinformatics* **20**, 2159 (2004).
4. L. M. Iyer *et al.*, *Genome Biol.* 2(12), RESEARCH0051.1 (2001).
5. P. Grindrod *et al.*, *Math. Today* **44**, 80 (2008).
6. N. Wingreen, D. Botstein, *Nat. Rev. Mol. Cell Biol.* **7**, 829 (2006).
7. L. J. van 't Veer *et al.*, *Nature* **415**, 530 (2002).
8. L. J. Gross, *Cell Biol. Educ.* **3**, 85 (summer 2004).
9. R. Brent, *Cell Biol. Educ.* **3**, 88 (summer 2004).
10. We are grateful to all participants of RECOMB Bioinformatics Education conference (La Jolla, 14 and 15 March 2009) for many comments on various aspects of bioinformatics education. We are also grateful to V. Bafna, N. Bandeira, A. Tanay, and G. Tesler for many interesting discussions and suggestions. The conference was supported by the Howard Hughes Medical Institute Professors Program.

10.1126/science.1173876

EDUCATION

Mathematical Biology Education: Beyond Calculus

Training in developing algebraic models is often overlooked but can be valuable to biologists and mathematicians.

Raina Robeva[1]* and Reinhard Laubenbacher[2]

In 2003, the National Research Council's *BIO2010* report recommended aggressive curriculum restructuring to educate the "quantitative biologists" of the future (*1*). The number of undergraduate and graduate programs in mathematical and computational biology has since increased, and some institutions have added courses in mathematical biology related to biomedical research (*2*, *3*). The National Science Foundation (NSF) and the National Institutes of Health are funding development workshops and discussion forums for faculty (*4*, *5*), research-related experiences (*6*, *7*), and specialized research conferences in mathematical biology for students (*8*, *9*).

This new generation of biologists will routinely use mathematical models and computational approaches to frame hypotheses, design experiments, and analyze results. To accomplish this, a toolbox of diverse mathematical approaches will be needed.

Nowhere is this trend more evident than in systems biology. At the molecular level, this involves understanding a complex network of interacting molecular species that incorporates gene regulation, protein-protein interactions, and metabolism. Two types of models have been used successfully to organize insights of molecular biology and to capture network structure and dynamics: (i) discrete- and continuous-time models built from difference equations or differential equations (DE) models, which focus on the kinetics of biochemical reactions; and (ii) discrete-time algebraic models built from functions of finite-state variables (in particular Boolean networks), which focus on the logic of the network variables' interconnections.

Algebraic models were introduced in 1969 to study dynamic properties of gene regulatory networks (*10*). They have proven useful in cases where network dynamics are determined by the logic of interactions rather than finely tuned kinetics, which often are not known. Published algebraic models include the metabolic network in *Escherichia coli* (*11*) and the abscisic acid signaling pathway (*12*).

The use of algebraic methods is extending beyond systems biology. Methods from algebraic geometry have been used in evolutionary biology to develop new approaches to sequence alignment (*13*), and new modeling of viral capsid assembly has been developed using geometric constraint theory (*14*). Algorithms based on algebraic combinatorics have been used to study RNA secondary structures (*15*).

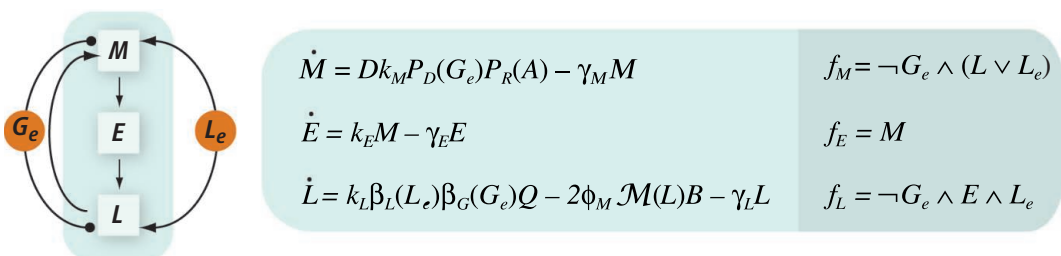

DE and Boolean models of the *lac operon* mechanism. Each component of the shaded part of the wiring diagram is a variable in the model, and the compartments outside of the shaded region are parameters. Directed links represent influences between the variables: A positive influence is indicated by an arrow; a negative influence is depicted by a circle.

[1]Department of Mathematical Sciences, Sweet Briar College, Sweet Briar, VA 24595, USA. [2]Virginia Bioinformatics Institute, Virginia Tech, Blacksburg, VA 24061, USA.

*To whom correspondence should be addressed. E-mail: Robeva@sbc.edu.

Because of the success of DE methods for modeling biochemical networks, they have been the primary focus of curriculum reform efforts, whereas algebraic models have received less attention. But algebraic models have many features needed to integrate mathematics and biology into the training of students at all levels; thus, their inclusion in curricula is necessary and timely.

DE Versus Algebraic Models

Many institutions now offer DE-focused courses that include problems from the life sciences, rather than just the traditional linkages with physics and engineering. For example, in bio-calculus and precalculus-level courses, differential and difference equations are used to model system dynamics. Textbooks emphasize development of DE models for various biological systems related to, e.g., population dynamics and the spread of an epidemic (*16*, *17*). In contrast, few curricular materials linking biology with modern algebra have been created. The courses "Mathematics for Computational Biology" (*18*) and "Algebraic Statistics for Computational Biology" (*19*) are two such examples targeting advanced undergraduate mathematics and biology students. A NSF curriculum development pilot project to produce algebraic educational modules is under way (*20*), as is a project to create an integrated biology curriculum, incorporating mathematics, statistics, and computational methods beyond calculus (*21*).

This relative lack of interest and investment in algebraic approaches compared with DE is due primarily to a lack of awareness of the importance of algebraic models in modern biology and mathematics research, as well as to a lack of appropriate educational materials on algebraic models, rather than to inaccessibility of the essential underlying mathematics.

Variables in a DE model can span a continuous range of biologically feasible values. Modelers need detailed knowledge of interactions between variables, for example, specifics of control mechanisms, rates of production and degradation, or highest and lowest biologically relevant concentrations. But in an algebraic model, only values from a finite set are allowed. The special case of a Boolean network allows only two states, for example, 0 and 1, representing the absence or presence of gene products in a model of gene regulation. In contrast to DE, the information necessary to construct a Boolean model requires only conceptual understanding of the causal links of dependency. Thus, continuous models are quantitative while Boolean models are qualitative in nature.

To illustrate, we use one of the simplest and best-understood mechanisms of gene regulation: the *lactose* (*lac*) *operon* that controls the transport and metabolism of lactose in *E. coli* (fig. S1). A wiring diagram is constructed to represent major components and causal interactions of the system (see figure, page 542).

The wiring diagram on the left of the figure depicts both DE and Boolean models of the *lac operon*. Although it involves only three variables, the DE model is complex, involving additional parameters reflecting the reaction kinetics. The Boolean model is simpler, reflecting only basic interactions depicted in the wiring diagram. Despite its simplicity, the Boolean model exhibits the same qualitative behavior as the DE model. Both are capable of reflecting the key feature of bistability of the operon (*22*).

In contrast with the high level of detail needed for the construction of the DE model, the Boolean model is relatively intuitive and was essentially obtained by translating a prose description of the molecular pathways depicted in fig. S1 and formalized by the wiring diagram into logical statements. This feature of algebraic models makes them particularly appealing as an entry into mathematical modeling.

Constructing algebraic models of biological networks requires only a modest amount of mathematical background, some of which is typically included in a college algebra course. This provides a quick path to mathematical modeling for students (and researchers, for that matter) in the life sciences. For mathematics students, algebraic models of biological networks provide a meaningful way to introduce many of the concepts in the discrete mathematics curriculum. And they are easily connected to more advanced topics in abstract algebra (*23*).

A Call for Change

Algebraic models should be considered critical for the professional development of biologists. Mathematics and biology educators must work to determine the best way of including these in undergraduate curricula. Because the mathematics involved is more easily accessible to faculty in the life sciences, relative to DE, this could lead to increased engagement on their part. Algebraic models will introduce problems from modern biology into the traditional mathematics courses, bringing life to the primarily theoretical abstract algebra curricula. Concurrent or subsequent introduction to DE models in the courses already in place will only reinforce the conceptual framework and further elevate students' mathematical sophistication.

References and Notes

1. National Research Council, *BIO2010: Transforming Undergraduate Education for Future Research Biologists* (National Academies Press, Washington, DC, 2003).
2. N. Wingreen, D. Botstein, *Nat. Rev. Mol. Cell Biol.* **7**, 829 (2006).
3. R. Robeva, *Methods Enzymol.* **454**, 305 (2009).
4. Over the Fence: Mathematicians and Biologists Talk About Bridging the Curricular Divide, Mathematical Biosciences Institute workshop, Columbus, OH, 1 and 2 June 2007.
5. Computational and Mathematical Biology, Mathematical Association of America, Professional Enhancement Programs, 2003, 2004, 2005, 2006, and 2007.
6. Expanding Biomedical Research Opportunities at the Undergraduate Level, in *Recovery Act Limited Competition: NIH Challenge Grants in Health and Science Research (RC1)* (National Institutes of Health Program Solicitation 12-DK-102, Challenge Grant Applications, 2009); http://grants.nih.gov/grants/funding/challenge_award/Omnibus.pdf.
7. Interdisciplinary Training for Undergraduates in Biological and Mathematical Sciences, (National Science Foundation Program Solicitation, NSF 08-510, 2008); www.nsf.gov/pubs/2008/nsf08510/nsf08510.htm.
8. Undergraduate Conference at the Interface between Mathematics and Biology, National Institute for Mathematical and Biological Synthesis (NimBioS), Knoxville, TN, 23 and 24 October 2009.
9. Undergraduate Research Conference in Quantitative Biology, Appalachian State University, Boone, NC, 2 and 3 November 2007 and 14 and 15 November 2008.
10. S. A. Kauffman, *J. Theor. Biol.* **22**, 437 (1969).
11. A. Samal, S. Jain, *BMC Syst. Biol.* **2**, 21 (2008).
12. R. Zhang *et al.*, *Proc. Natl. Acad. Sci. U.S.A.* **105**, 16308 (2008).
13. L. Pachter, B. Sturmfels, *Proc. Natl. Acad. Sci. U.S.A.* **101**, 16132 (2004).
14. M. Sitharam, M. Agbandje-Mckenna, *J. Comput. Biol.* **13**, 1232 (2006).
15. A. Apostolico *et al.*, *Nucleic Acids Res.* **37**, e29 (2009).
16. C. Neuhauser, *Calculus for Biology and Medicine* (Prentice-Hall, Upper Saddle River, NJ, ed. 2, 2003).
17. F. Adler, *Modeling the Dynamics of Life: Calculus and Probability for Life Scientists* (Thompson, Belmont, CA, ed. 2, 2005).
18. "MATH 127—Mathematics for Computational Biology" (University of California, Berkeley, CA, 2007); http://math.berkeley.edu/~bernd/math127.html.
19. "MATH, 295—Algebraic Statistics for Computational Biology" (Duke University, Durham, NC, 2005); www.math.duke.edu/graduate/courses/fall05/math295.html.
20. R. Robeva *et al.*, National Science Foundation DUE award 0737467, 2008; www.nsf.gov:80/awardsearch/showAward.do?AwardNumber=0737467.
21. Biology Through Numbers Howard Hughes Medical Institute Award, 2006; www.hhmi.org/research/professors/neuhauser.html.
22. E. M. Ozbudak, M. Thattai, H. N. Lim, B. I. Shraiman, A. van Oudenaarden, *Nature* **427**, 737 (2004).
23. R. Laubenbacher, B. Sturmfels, *Am. Math. Month.* arXiv:0712.4248v2, in press.

24. The authors thank R. Davies from Sweet Briar College for her review of the biological content. Support by the NSF under the Division of Undergraduate Education; NSF Course, Curriculum, and Laboratory Improvement (CCLI) award 0737467 is also gratefully acknowledged.

Supporting Online Material

www.sciencemag.org/cgi/content/full/325/5940/542/DC1

10.1126/science.1176016

NEUROSCIENCE

Brain Wiring by Presorting Axons

Specific molecular interactions among axons of mammalian olfactory neurons ensure their orderly arrival along the path from the nose to the brain.

Kazunari Miyamichi and Liqun Luo

Neurobiologist and Nobel Laureate R. W. Sperry proposed an influential chemoaffinity theory half a century ago (*1*) to explain the precision of neuronal wiring in the brain: "The cells and fibers of the brain must carry some kind of individual identification tags, presumably cytochemical in nature, by which they are distinguished one from another almost, in many regions, to the level of the single neurons" (*1*). He suggested that gradients of such identification tags on retinal neurons and on the target cells in the brain coordinately guide the orderly projection of millions of developing retinal axons. This idea was supported by the identification and genetic analysis of axon guidance molecules, including those that direct development of the vertebrate visual system (*2*). But axons not only perceive molecular cues on their targets; they also recognize those on fellow axons. On page 585 of this issue, Imai *et al*. provide a striking example of how axon-axon interactions organize olfactory axons before they reach their target in the brain (*3*).

In the mammalian olfactory system, each olfactory sensory neuron expresses a single type of odorant receptor. Those expressing the same odorant receptor are distributed widely in the nose but converge their axons onto a stereotypical location called the glomerulus in the olfactory bulb of the brain. This wiring results in a discrete map for odor processing (*4*), but how do 1000 different classes of olfactory sensory neurons converge their axons so precisely in the brain? Although odorant receptors may act as "identification tags" during axon targeting (*5*), many classic axon guidance molecules are involved in this process.

Olfactory sensory neurons are distributed in a convoluted two-dimensional nasal epithelium that can be viewed along two axes, anterior-posterior and dorsomedial-ventrolateral. Mapping along the dorsomedial-ventrolateral axis appears similar to that in the visual system (*2*): Odorant receptors are expressed in overlapping bands along this axis that correlate with the positions of target glomeruli along the dorsal-ventral axis of the olfactory bulb (*6*). Classical axon guidance molecules, such as Neuropilin-2, Slit-1, and Robo-2, have been implicated in establishing the coarse topography along this axis (*7*, *8*). By contrast, neurons expressing the same odorant receptor distribute randomly across the entire anterior-posterior axis. An important advance was made a few years ago (*9*). It was shown that odorant receptors define differential levels of cyclic adenosine monophosphate (cAMP) signaling, which results in differential gene expression. One such target is the gene encoding Neuropilin-1 (Nrp1), a receptor for the axon guidance molecule Semaphorin-3A (Sema3A) (*10*). Imai *et al*. reinforce this model by showing that genetic alteration of *Nrp1* expression in mouse olfactory sensory neurons indeed causes a corresponding shift of target sites along the anterior-posterior axis of the olfactory bulb.

Strikingly, Imai *et al*. found that axons that project to different regions of the olfactory bulb segregate before reaching their final target. Genetic experiments revealed that this pre-target sorting is mediated by Nrp1 and Sema3A. Interestingly, cAMP signaling regulates *Nrp1* and *Sema3A* expression in opposite directions: Higher cAMP signaling up-regulates *Nrp1* and down-regulates *Sema3A*. Thus, each olfactory sensory neuron class expresses complementary amounts of Nrp1 and Sema3A according to the level of cAMP signaling. This reflects the odorant receptor it expresses, regardless of the neuron's cell body position along the anterior-posterior axis of the nasal epithelium. As axons travel toward the olfactory bulb, repulsive interactions between Sema3A and Nrp1 gradually sort them according to the amounts of this ligand-receptor pair, and hence according to the odorant receptors they express (see the figure). Indeed, the absence of Sema3A from only olfactory sensory neurons affected not only pre-target axon sorting but also the final projection sites in the olfactory bulb.

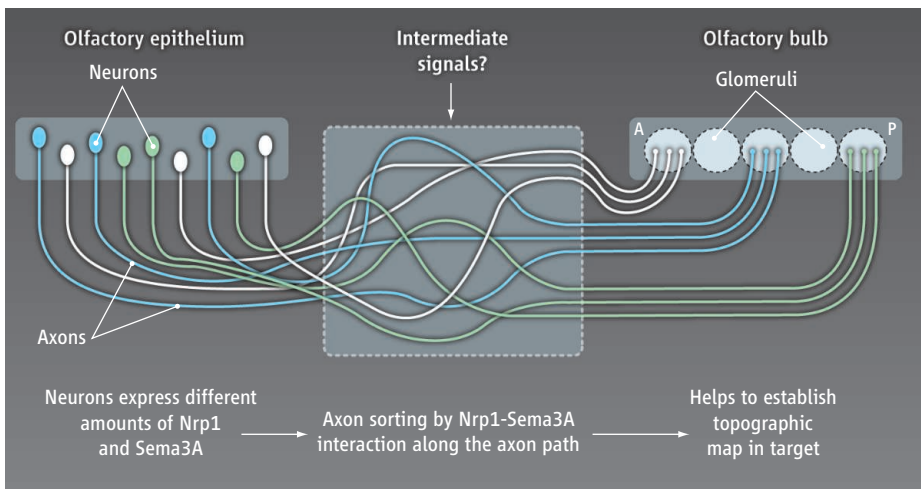

Wiring through sorting. Olfactory sensory neurons with different expression levels of Nrp1 and Sema3A are intermingled in the olfactory epithelium of the mouse nose. Repulsive axon-axon interaction by this ligand-receptor pair gradually sorts axons within the bundle before they reach their olfactory bulb target in the brain. Intermediate cues may orient the order of axons within the bundle. A, anterior; P, posterior.

Axon-axon interactions alone cannot provide the stereotyped polarity of axon order within the bundle projecting to the olfactory bulb. Imai *et al*. suggest that *Sema3A* expression in glia cells that surround the axon bundle is biased, which could orient the order of axons within the bundle to their environment. This hypothesis will be validated if the absence of *Sema3A* in these intermediate regions randomizes the polarity of axon order within the bundle.

The contribution of semaphorins to axon-axon interactions was first described in the fly olfactory system (*11*, *12*). In that model organism, pre-target axon sorting was not examined, but axon-axon interactions were shown to occur at the target (*11*). Two different olfactory sensory neuron populations project their axons with a temporal difference to the fly antennal lobe (corresponding to the mouse olfactory bulb). Sema1A that is expressed by early-arriving axons to the antenna constrains the target choice of late-arriving axons

Howard Hughes Medical Institute, Department of Biology, Stanford University, Stanford, CA 94305, USA. E-mail: lluo@stanford.edu

Published by AAAS

from the maxillary palp, likely through repulsive interaction with Plexin-A, a receptor for Sema1A (*11*). Thus, the same family of axon guidance molecules plays a role in axon-axon interactions in the fly and mouse olfactory systems, implying an evolutionally convergent strategy for olfactory circuit formation.

After the coarse olfactory map in the mouse is established by the processes described above, axon-axon interactions among those that target neighboring glomeruli further refine the map through attractive and repulsive interactions (*13*, *14*). Thus, wiring specificity of complex neural circuits is achieved through stepwise mechanisms, involving axon sorting along the path (*3*, *15*), at the targets (*11*, *13*), and pre- and postsynaptic recognitions. As well, the individual identification tags originally proposed by Sperry for pre- and postsynaptic matching can serve at multiple steps to ensure the precise wiring of the brain.

References and Notes

1. R. W. Sperry, *Proc. Natl. Acad. Sci. U.S.A.* **50**, 703 (1963).
2. L. Luo, J. G. Flanagan, *Neuron* **56**, 284 (2007).
3. T. Imai *et al.*, *Science* **325**, 585 (2009); published online 9 July 2009 (10.1126/science.1173596).
4. R. Axel, *Sci. Am.* **273**, 154 (October 1995).
5. G. Barnea *et al.*, *Science* **304**, 1468 (2004).
6. K. Miyamichi, S. Serizawa, H. M. Kimura, H. Sakano, *J. Neurosci.* **25**, 3586 (2005).
7. E. M. Norlin *et al.*, *Mol. Cell. Neurosci.* **18**, 283 (2001).
8. J. H. Cho, M. Lepine, W. Andrews, J. Parnavelas, J. F. Cloutier, *J. Neurosci.* **27**, 9094 (2007).
9. T. Imai, M. Suzuki, H. Sakano, *Science* **314**, 657 (2006); published online 21 September 2006 (10.1126/science.1131794).
10. T. S. Tran, A. L. Kolodkin, R. Bharadwaj, *Annu. Rev. Cell Dev. Biol.* **23**, 263 (2007).
11. L. B. Sweeney *et al.*, *Neuron* **53**, 185 (2007).
12. M. Lattemann *et al.*, *Neuron* **53**, 169 (2007).
13. S. Serizawa *et al.*, *Cell* **127**, 1057 (2006).
14. T. Kaneko-Goto, S. Yoshihara, H. Miyazaki, Y. Yoshihara, *Neuron* **57**, 834 (2008).
15. T. Bozza *et al.*, *Neuron* **61**, 220 (2009).

16. We thank L. Sweeney for helpful comments.

10.1126/science.1178117

GEOCHEMISTRY

Ironing Out the Oxidation of Earth's Mantle

Marc M. Hirschmann

Subduction processes cause magmas from volcanoes in island arcs to become more oxidized and may influence the oxidation state of the entire mantle.

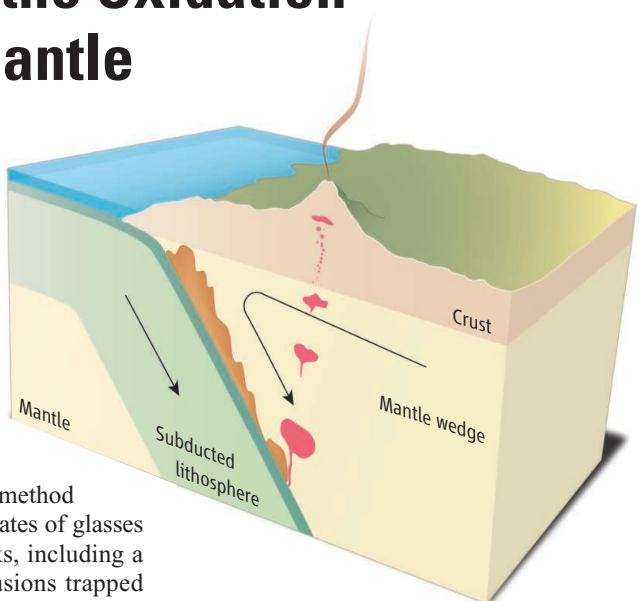

Oxidizing mantle rocks and magmas. Subduction of oceanic lithosphere carries oxidized surface rocks into Earth's interior. These rocks, including sediments and hydrothermally altered basalts, are rich in water, which is released into the overlying mantle wedge, as indicated by the region in brown. This process initiates melting in the mantle wedge, which in turn leads to formation of volcanoes in island arcs such as Japan and Indonesia. Regions where silicate melt is present are shown schematically in red. Kelley and Cottrell show that the subducted, volatile-rich geochemical component found in island arc volcanoes is also associated with oxidation, strongly suggesting that the fluids added from the subducted lithosphere to the mantle wedge are rich in an oxidizing agent such as ferric or sulfate ions. The mantle wedge is dragged into the deeper mantle by viscous coupling to the subducted lithosphere (curved arrow).

CREDIT: P. HUEY/*SCIENCE*

Lavas from island arc volcanoes form when the crust is recycled into the mantle at subduction zones (see the figure). These lavas are more oxidized than those produced at mid-ocean ridge volcanoes. On page 605 of this issue, Kelley and Cottrell (*1*) use a high–spatial resolution method to determine iron oxidation states of glasses from a suite of volcanic rocks, including a broad sampling of tiny inclusions trapped in minerals from arc volcanoes that have not undergone degassing. They correlate these measurements with dissolved water and trace element concentrations determined by other microanalytical techniques, and link the oxidation of arc volcano magmas with oxidants in the fluids that infiltrate the mantle wedge above subduction zones, as opposed to other processes, such as volcanic degassing in surface regions.

The lavas produced at arc volcanoes—adjacent to oceanic trenches in Japan, Chile, Indonesia, and other places around the Pacific "ring of fire"—are created when cold rocks from near Earth's surface are returned to the mantle at a subduction zone (see the figure). It may seem paradoxical that cold materials lead to volcanism, but the subducted rocks release fluids that rise and induce partial melting in the overlying mantle wedge. The partial melts are buoyant, and once they segregate from the mantle, they create arc volcanoes.

The fact that arc magmas are more oxidized than mid-ocean ridge magma has been attributed to subduction processes, but recently, new methods analyzing vanadium in arc lavas have challenged this supposition (*2*). Because vanadium takes on different oxidation states depending on its environment, its geochemical behavior can be used to infer the oxidation state during partial melting. Studies based on this method suggested that the mantle wedge beneath island arcs (see the figure) is no more oxidized than is the mantle in other regions (*2*). This could indicate that the oxidized character of arc volcanic rocks derives from near-surface processes, such as fractional crystallization or volcanic degassing.

However, the results of Kelley and Cottrell suggest a different explanation. Using microscale x-ray absorption near-edge spectroscopy, they determined the iron oxidation state of the lavas and found that it correlates with water content. They argue that the oxidation state of arc magmas is affected mainly by the proportion of subduction fluid added to the source. Thus, the oxidation process must occur near where the subducted rock meets the mantle wedge. The oxidation state is also proportional to trace element indicators of subduction influence, although more data will be required before a strong correlation can be established.

The study by Kelley and Cottrell shows that the increase in oxidation state is not an arti-

Department of Geology and Geophysics, University of Minnesota, Minneapolis, MN 55455, USA. E-mail: marc.m.hirschmann-1@umn.edu

fact of unrelated processes, such as fractionation, interaction with shallow rocks below the volcano, or volcanic degassing. However, their results do not fully resolve how subduction fluids oxidize the mantle wedge. In the mantle, water itself is a poor oxidant, and so the oxidation must be effected by chemical components associated with the water-rich fluid. Kelley and Cottrell explore several possibilities, including iron-containing brines, subducted sulfates, or hydrous silicate fluids or melts. However, it is unclear whether sufficient brine or sulfate is subducted in most places, and so the most likely candidate is ferric ion (Fe^{3+}) carried as a dissolved component in a silicate melt or silicate-rich fluid. The results of Kelley and Cottrell thus lend support to the hypothesis that the fluid leaving the slab is silicate-rich.

These studies of mantle oxidation raise another unresolved question. Subduction has been occurring on Earth for much of its history, and surface rocks have been oxidized at least since the rise of an oxygenated atmosphere ~2.5 billion years ago. Shouldn't billions of years of subduction have partly oxidized the mantle? At current subduction rates, deep recycling of a mantle wedge section, with an average thickness of 70 km (see the figure), would mean that 40% of the mantle has been flushed with comparatively oxidizing melts or fluids in the past 2.5 billion years. Yet investigations to date have not found evidence for an increase over time in the oxidation state of the mantle (*3*).

Why, then, is the mantle not more oxidized? Perhaps most of the oxidant released from the slab is extracted at arcs, leaving the mantle wedges relatively unaffected, or possibly oxidation has been offset by subduction of reduced surface materials, such as organic carbon. Indeed, the rise of oxidized surface conditions has been linked to sequestration of reduced carbon in the mantle (*4*). The work of Kelley and Cottrell firmly establishes that subduction oxidizes the source regions of arc magmas, but the long-term consequences for the evolution of Earth remain poorly understood.

References and Notes

1. K. A. Kelley, E. Cottrell, *Science* **325**, 605 (2009).
2. C.-T. Aeolus Lee, W. P. Leeman, D. Canil, Z.-X. A. Li, *J. Petrol.* **46**, 2313 (2005).
3. J. W. Delano, *Orig. Life Evol. Biosph.* **31**, 311 (2001).
4. J. M. Hayes, J. R. Waldbauer, *Philos. Trans. R. Soc. London Ser. B* **361**, 931 (2006).

10.1126/science.1176882

ASTRONOMY

Probing the Cold Universe

The launch of the Herschel infrared space telescope is expected to provide new vistas on the cold and dusty universe.

Michael Rowan-Robinson

The successful launch of the Herschel and Planck satellites on 14 April 2009 was a great achievement of the European Space Agency. With a mirror diameter of 3.5 m, the Herschel Space Observatory is the largest space telescope ever launched. The complex dual launch went perfectly, and both missions are performing well. After removing the cover of the cryostat housing the instruments on 14 June, Herschel was pointed to the famous M51 "whirlpool" galaxy and produced an impressive first image (see the figure), with an immediate resolution improvement over previous far-infrared missions.

From its final destination at the Lagrangian point between Earth and the Sun, Herschel will view the universe in the last unobserved wavelength band; the far infrared and sub-mm range from 60 to 600 μm. These wavelengths are inaccessible from the ground except for narrow windows at 350 and 450 μm. Herschel, named after the German musician turned British astronomer, William Herschel, who discovered infrared radiation in 1800, will penetrate the clouds of dust that shroud newly forming stars and galaxies. The stars and planets that form in these dense clouds do not emit visible light. It is only at infrared wavelengths that these processes can be observed. The molecules present in the clouds act as "probes" of the physical conditions, allowing Herschel to determine the physical and chemical details of these previously mysterious places.

Infrared space astronomy began in 1983 with the Infrared Astronomical Satellite (IRAS), a 60-cm telescope. Over 10 months of operation, it produced the first map of the entire sky at far infrared wavelengths. Following up on IRAS came the Infrared Space Observatory (ISO), launched in 1995, and then the Spitzer Space Telescope, launched in 2003, both general-purpose infrared observatories. Spitzer, with its 0.85-m diameter mirror, is still in orbit, but its coolant exhausted on 15 May this year, so it now continues operations as a survey instrument at 3.6 and 4.5 μm only. With its much larger size, Herschel presents a giant leap forward in infrared technology.

Herschel carries three scientific instruments. The Heterodyne Instrument for the Far Infrared (HIFI) (*1*) takes very high-resolution spectra in thousands of wavelengths simultaneously. It covers the bands 160 to 200 and 240 to 600 μm, using superconducting mixers as detectors. The Photoconductor Array Camera and Spectrometer (PACS) (*2*) is an infrared camera and a spectrometer operating at 60 to 210 μm, with bolometer and photoconductor array detectors. The Spectral and Photometric Imaging REceiver (SPIRE) (*3*) is a camera and spectrometer, providing broadband photometry simultaneously in bands centered on 250, 350, and 500 μm.

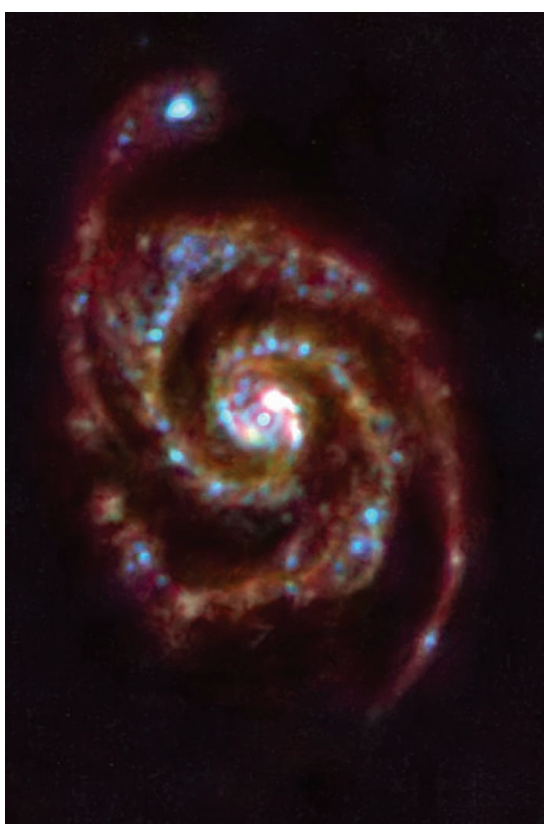

CREDIT: EUROPEAN SPACE AGENCY

First light. The Herschel-PACS instrument images the Messier 51 whirlpool galaxy, coded with blue for 70 μm, green for 100 μm, and red for 160 μm. The image was taken as soon as the cryostat cover was removed, while Herschel was still in transit to its final orbit at the Sun-Earth L2 Lagrangian point.

Astrophysics Group, Imperial College London, Prince Consort Road, London, SW7 2BZ, UK. E-mail: mrr@imperial.ac.uk

Herschel is an enormously versatile space telescope. It will study the physics and molecular chemistry of almost all types of cool celestial objects, from our own neighborhood to the edge of the Universe. The nearest objects it will study are within our own solar system, such as comets. These mountain-sized chunks of ice and rock are the leftovers from the formation of the planets, more than 4 billion years ago. They are the best fossils from the early solar system and can tell us what raw ingredients became the planets, including Earth.

It will also look into the dense clouds of matter that enclose stars in the process of formation. The ISO mission unveiled more than a dozen of these regions, but Herschel will find many more and will be able to look inside them to see the star-forming process happening. It will also look at the rings of debris that accumulate around forming stars, where it is believed that planets are completing the process of formation.

In addition, the telescope will look at young galaxies in the distant universe. Today, galaxies are giant collections of hundreds of billions of stars. The first objects that formed in the early universe were much smaller and then grew by merging together in dramatic collisions. These collisions triggered enormous bouts of star formation. The first census of star-forming galaxies will be made throughout the universe at the epoch of peak star formation, allowing the star-formation history and evolution of galaxies in the universe to be charted. The youngest stars in our Galaxy will be revealed, as will the vast reservoirs of gas and dust that constitute half the normal matter.

When the Hubble Space Telescope took its historic images of the distant universe in the 1990s, it saw a new population of distant, irregularly shaped galaxies. The James Clerk Maxwell Telescope on Hawaii also looked at these regions at a wavelength of 850 μm. It too saw distant galaxies, but different ones from Hubble. Herschel operates at wavelengths that bridge the gap between these two instruments and will show us the relationship between these apparently different young galaxy populations.

If Herschel were placed in orbit around Earth, heat from our planet would interfere with its instruments, reducing their sensitivity. Instead, Herschel will orbit a point in space about 1.5 million kilometers from Earth. Called the second Lagrangian point (L2) of the Sun-Earth system, it is a local gravitationally stable point providing an excellent place for Herschel to shelter from the heat being emitted by Earth, with a good view of the sky. A sun shield will protect the telescope from the Sun's radiation, which Herschel needs to be bathed in to power its solar arrays. Three years of routine science operations are planned, at the end of which there will be the option to extend the mission if the spacecraft is in good health and still has some of its 2400 liters of helium coolant left.

So far, about 60% of the observing time on Herschel has been allocated to 42 large Key Programs (*4*–*6*). Half are Guaranteed Time programs led by the instrument teams and half are Open Time programs competed for by the astronomical community. The remaining 40% of the observing time will be allocated by competition about a year into the mission. The 42 programs allocated so far cover an exciting range of science. In the solar system, the chemistry of water and trans-Neptunic objects will be studied. There will be studies of debris disks around stars, protoplanetary systems, and analogies of the solar system's distant Kuiper belt. Programs will study interstellar dust and molecules as well as star-forming regions in our Galaxy, and there will be a survey of the whole Galactic plane. There will be detailed studies of nearby galaxies, including the Magellanic Clouds, the Virgo cluster, and gravitational lens systems. There will be several large-scale cosmological surveys, of which the largest is the Hermes multilayered survey.

These two great missions, Herschel and Planck, were first proposed 13 years ago, in 1996, and had been studied for several years before that. Although their technical complexity has meant that the launch was later than originally planned, the expected insight they will provide into the cold and dusty regions from which planets, stars, and galaxies form, and into the early universe, means it has been well worth waiting for.

References

1. T. De Graauw *et al.*, *EAS Publ. Ser.* **34**, 3 (2009).
2. A. Poglitsch *et al.*, *EAS Publ. Ser.* **34**, 43 (2009).
3. M. Griffin *et al.*, *EAS Publ. Ser.* **34**, 33 (2009).
4. G. L. Pilbratt, *EAS Publ. Ser.* **35**, 15 (2009).
5. A. Pilbratt, *Proc. SPIE* **7010**, 1 (2008).
6. M. J. Griffin *et al.*, http://arxiv.org/abs/astro-ph/0609830v1 (2009).

10.1126/science.1177305

BIOCHEMISTRY

Nudging Through a Nucleosome

Jason J. Otterstrom and Antoine M. van Oijen

Single-molecule data suggest that RNA polymerase II moves a small step forward only when its DNA template briefly unwraps from the histone core.

Medieval monks feverishly transcribing Latin into Olde English would identify with the struggles that the eukaryotic RNA polymerase II complex must overcome in order to write DNA in the language of RNA. While theirs was a conceptual barrier, that of RNA polymerase II is quite physical and embodied by nucleosomes. Much like string wrapped around a spool, nucleosomes consist of a cylindrical protein core and DNA wrapped tightly around it. On page 626 of this issue, Hodges *et al.* (*1*) report single-molecule measurements that help to elucidate how the nucleosomal DNA is transcribed.

One of the nucleosome's functions is to compact genomes in eukaryotic nuclei. This compaction acts as a barrier to transcription (the process by which an RNA polymerase II enzyme converts a DNA sequence into mRNA). During transcription, RNA polymerase moves along double-stranded DNA, locally separating it into two single strands. One DNA strand is passed through the enzyme's active site, where its base sequence is read and the appropriate ribonucleotides are added to the end of a growing RNA strand. To transcribe nucleosomal DNA, the interactions between the nucleosomal core and the DNA backbone must be disrupted, because these interactions would otherwise cause the polymerase to slow down or stop transcribing.

To probe the dynamics of a single polymerase II molecule while it transcribes nucleosome-bound DNA, Hodges *et al.* used optical tweezers. In an optical tweezing experiment, a laser beam is tightly focused on a particle, typically a transparent polystyrene bead, suspended in solution. The change in the momentum of the photons refracted by the bead-solution interface pushes the bead to the center of the focused beam and traps it there. Movement of the bead away from the beam center by any external force is measured by monitoring the position of the bead. If a pair of laser beams holds two beads con-

Department of Biological Chemistry and Molecular Pharmacology, Harvard Medical School, Boston, MA 02115, USA. E-mail: antoine_van_oijen@hms.harvard.edu

nected to one another through a single DNA-protein tether, the entire system can be suspended in solution and separated from laboratory noise and drift, improving the resolution of force and distance measurements.

This type of setup has been used to show that the step size of a transcribing polymerase equals the separation between DNA base pairs and that during transcription, the polymerase moves forward via a Brownian ratchet mechanism: The molecule diffuses along the DNA template until it is rectified through binding of the next nucleotide called for by the DNA sequence (*2*). However, this mechanism is frequently interrupted by pauses that depend on the DNA sequence (*2*, *3*). These pauses have been attributed to a diffusive backtracking mechanism (*4*).

Backtracking of a polymerase occurs when the nascent RNA transcript becomes fed backward through the polymerase molecule, thereby occluding the enzyme's active site and prohibiting further nucleotide addition; with its active site blocked, the polymerase diffuses back-and-forth in one dimension along the DNA-RNA hybrid until the Brownian movement realigns the RNA 3′-end with the active site, allowing ribonucleotide addition and transcription to continue. Previous bulk biochemical work has shown that both sequence-dependent pausing and backtracking are exacerbated in the presence of a nucleosome (*3*, *5*), but the ensemble averaging in these studies occluded many of the mechanistic and kinetic details.

In their dual-trap assay, Hodges *et al*. first loaded a polymerase II molecule onto a DNA sequence that contained both intrinsic pause sites and a nucleosome-positioning sequence (either with or without a downstream nucleosome). At this point, the enzyme is stalled but poised to transcribe. They attached this stalled enzyme to one polystyrene bead and the DNA upstream of the enzyme to a second bead, thereby creating a DNA-based tether that was pulled taut by tuning the distance between the two beads (see the figure). Finally, they added a ribonucleotide-containing solution, thereby triggering polymerase transcription. The resulting lengthening of the upstream DNA could be measured by an increase of the distance between the two beads.

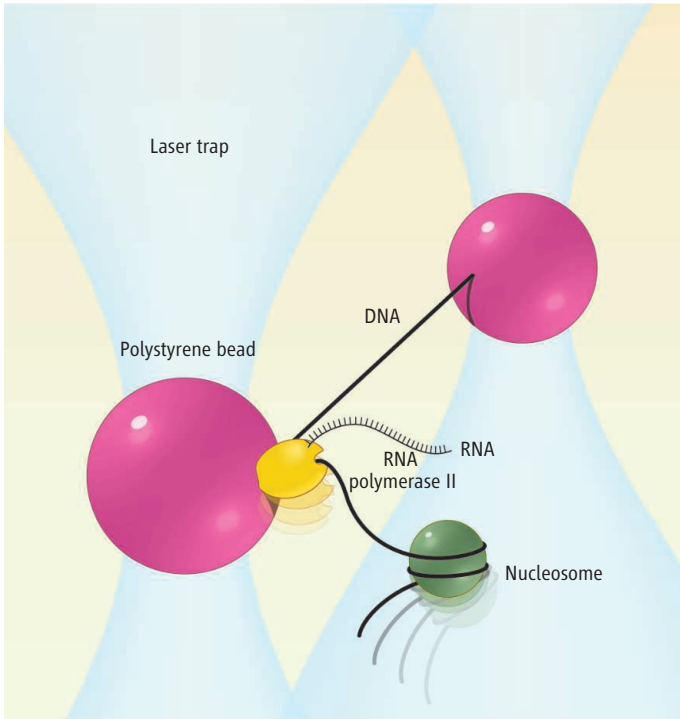

Dual trap. Hodges *et al*. attached a single RNA polymerase II molecule (preloaded onto 3 kb of double-stranded DNA) to an optically trapped bead (front). They affixed the upstream end of the DNA to another bead in a second optical trap (back). The movement of the polymerase II on the DNA can be measured by a lengthening of the tether length between the beads, allowing the interaction between the polymerase II and a downstream nucleosome to be studied.

This setup enabled Hodges *et al*. to quantify the effects of a nucleosome that lies in the path of a polymerase. They found that when transcribing through a nucleosome, the local probability for polymerase II to pause along the template tripled and that the region of highest pause density lies in the first half of the nucleosome-bound DNA. Further, the median pause duration doubled and the transcriptional velocity fell by 40%.

By comparing pause-duration distributions from many repeats of the experiment to a mathematical model describing the RNA polymerase II as a one-dimensional random stepper in the absence of any barriers (*6*), Hodges *et al*. were able to understand the role of polymerase II diffusion in bypassing a nucleosome. The authors incorporated the nucleosome barrier into the stepper model by assuming that the nucleosome fluctuates rapidly between two states: one in which the DNA is partially unwrapped in front of the polymerase, and another in which it is completely wrapped around the nucleosome core. Because the stepper (polymerase II) can move forward only when the nucleosome is partially unwrapped, the authors scaled the probability of moving forward by the fraction of time the nucleosome is in the partially unwrapped state. This assumption successfully predicts transcriptional and pausing kinetics in very good agreement with those measured experimentally. They conclude that during both backtracking and forward transcription through a nucleosome, the polymerase advances by taking advantage of fluctuations that partially unwrap nucleosomal DNA. In this manner, polymerase II acts to rectify brief nucleosomal openings as it ratchets through nucleosomal DNA.

The observation that polymerase II behaves as a diffusion-based Brownian ratchet when it pauses and backtracks is in agreement with previous single-molecule studies demonstrating this ratchet mechanism during normal transcription (*2*). It is also consistent with previous work suggesting that as the nucleosome rewraps, it can induce backtracking and push the polymerase backward through the reformation of contacts between DNA and the nucleosomal core (*3*).

These observations could have an impact on the field of transcriptional regulation and epigenetics. When nucleosomes in human embryonic stem cells and in *Drosophila melanogaster* are posttranslationally modified in a certain pattern, polymerase II will begin to transcribe a gene but soon becomes arrested. With the addition of a single nucleosomal modification, the gene is quickly transcribed in its entirety (*7*–*9*). Such nucleosomal modifications, or factors recognizing them, could affect polymerase II's nucleosome passage simply by altering the fraction of time a nucleosome fluctuates into an unwrapped state. It remains to be seen whether nucleosome modifications play such a mechanistic role, but Hodges *et al*. show that whether transcribing words or DNA, you've just got to ratchet through one bit at a time.

References

1. C. Hodges, L. Bintu, L. Lubkowska, M. Kashlev, C. Bustamante, *Science* **325**, 626 (2009).
2. E. A. Abbondanzieri, W. J. Greenleaf, J. W. Shaevitz, R. Landick, S. M. Block, *Nature* **438**, 460 (2005).
3. M. L. Kireeva *et al*., *Mol. Cell* **18**, 97 (2005).
4. E. A. Galburt *et al*., *Nature* **446**, 820 (2007).
5. M. L. Kireeva *et al*., *Mol. Cell* **9**, 541 (2002).
6. M. Depken, E. A. Galburt, S. W. Grill, *Biophys. J.* **96**, 2189 (2009).
7. M. G. Guenther, S. S. Levine, L. A. Boyer, R. Jaenisch, R. A. Young, *Cell* **130**, 77 (2007).
8. G. W. Muse *et al*., *Nat. Genet.* **39**, 1507 (2007).
9. J. Zeitlinger *et al*., *Nat. Genet.* **39**, 1512 (2007).

10.1126/science.1177311

IMMUNOLOGY

Dispensable But Not Irrelevant

Heart injury triggers the release of monocytes from an unexpected reservoir, the spleen.

Ting Jia[1] and Eric G. Pamer[1,2]

In the left upper quadrant of the abdomen lies the spleen, functioning in two major capacities—filtering and storing blood cells, and acting as an immune tissue, where antibody synthesis occurs and certain pathogens are eliminated. Yet the spleen lacks the gravitas of neighboring organs because we can survive without it, albeit with some inconveniences. Its surgical removal causes modest increases in circulating white blood cells and platelets, diminished responsiveness to certain vaccines, and increased susceptibility to infection with certain bacteria and protozoa. But on page 612 in this issue, the organ gains some new respect, as Swirski *et al*. (*1*) show that in the mouse, the spleen serves as a reservoir for immune cells (monocytes) that function in repairing the heart after myocardial infarction.

Circulating monocytes were postulated by Florence Sabin and Charles Doan, over 80 years ago, to play an important role in defense against infection (*2*), and recent work has confirmed this (*3*). Indeed, monocytes are essential for immune defense against potentially lethal microbial pathogens (*4*). Clearance of microbial infection requires dispatching monocytes from their reservoir, thought to be the bone marrow, in adequate numbers toward the site of infection. Monocytes are guided to their proper destination by chemokines, inflammatory cytokines, and adhesion molecules (*3*). But how adequate numbers of monocytes are mustered for their mission is less well understood. Swirski *et al*. demonstrate that after induction of inflammation—in their case, by myocardial infarction in mouse—monocytes rapidly exit the spleen, enter the bloodstream, and infiltrate the inflamed myocardium to remodel damaged tissue.

Circulating monocytes are a heterogeneous population (*5*), and in humans, can be divided into at least two subsets: one that expresses a high amount of the surface protein CD14 and no CD16, and a more mature subset that expresses a lower amount of CD14 and higher amount of CD16. The latter subset shares similarities with tissue macrophages, which are derived from monocytes. In mice, circulating monocytes also can be divided into subsets on the basis of chemokine receptor expression and the presence of the Ly-6C surface protein (*3*). One subset of murine monocytes (Ly-6C^{high}) expresses high amounts of the CCR2 chemokine receptor and the surface protein Ly-6C, and has been implicated in inflammatory responses. The second murine monocyte subset expresses a high amount of the chemokine receptor CX3CR1 and a low amount of Ly-6C (Ly-6C^{low}) and is similar to macrophages.

Although Ly-6C^{high} monocytes contribute to antimicrobial defense, they have also been implicated in the pathogenesis of atherosclerosis (hardening of the arteries). High blood cholesterol increases the frequency both of circulating monocytes and those that infiltrate lesions (plaques) in arterial walls (*6*). Furthermore, mice in which the CCR2 chemokine receptor or its major ligand, monocyte chemotactic protein-1 [(MCP-1); also called CCL2] are genetically deleted have markedly reduced atherosclerosis (*7*, *8*). Recruitment of monocytes to plaques depends on CCR2-mediated signaling, perhaps in response to MCP-1 produced by cells within the arterial wall. Ly-6C^{high} monocytes lacking CCR2 that are "adoptively transferred" into recipient mice do not traffic as efficiently into plaques of hypercholesterolemic mice as do CCR2-expressing Ly-6C^{high} monocytes (*6*, *9*). Although the most obvious explanation for this is that monocytes use CCR2-mediated signals to enter the arterial wall, it is also possible that CCR2-deficient monocytes return to the bone marrow and become trapped there, because CCR2 is required for monocytes to emigrate from the bone marrow (*10*, *11*). Adoptive transfer studies with Ly-6C^{high} monocytes have shown that they rapidly return to bone marrow in the absence of active recruitment to sites of inflammation (*12*).

Monocytes have also been implicated in the repair of damaged myocardium after myocardial infarction (*13*). In this scenario, Ly-6C^{high} monocytes are first to infiltrate damaged heart tissue and contribute to the

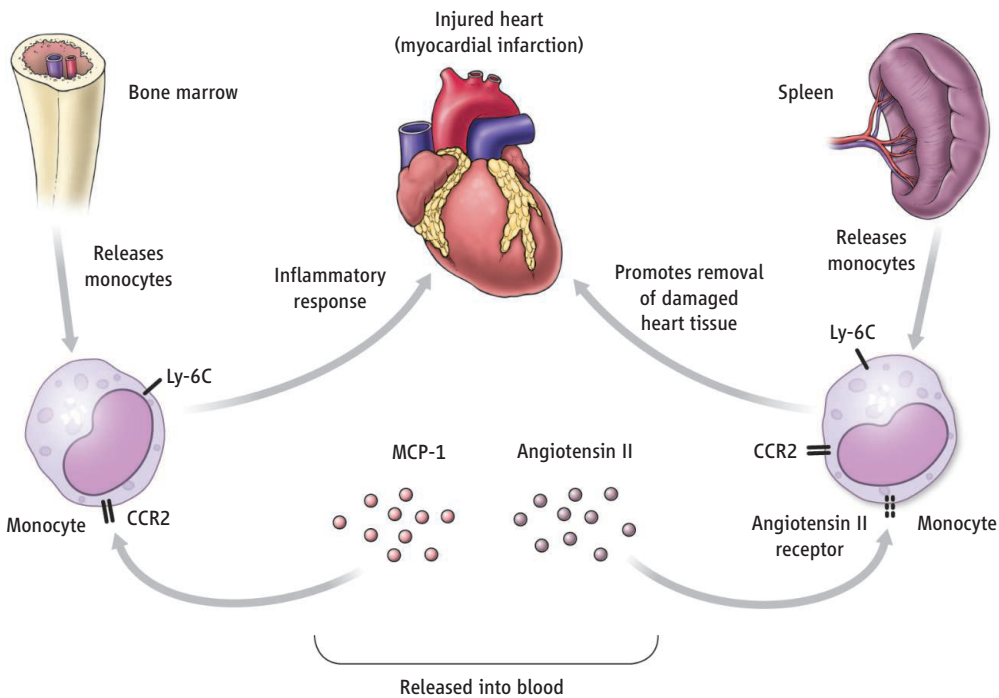

Calling up the reserves. In response to heart injury (myocardial infarction), specific subsets of monocytes are recruited from the bone marrow and spleen to remove and repair damaged tissue.

CREDIT: C. BICKEL/*SCIENCE*

[1]Immunology Program, Sloan-Kettering Institute, New York, NY 10065, USA. [2]Infectious Diseases Service, Memorial Hospital, Memorial Sloan-Kettering Cancer Center, 1275 York Avenue, New York, NY 10065, USA. E-mail: pamere@mskcc.org

Published by AAAS

fragmentation and recycling of necrotic and apoptotic tissues, whereas Ly-6C^{low} monocytes arrive at the scene later to promote revascularization and collagen deposition. Recruitment of Ly-6C^{high} monocytes to damaged myocardium is dramatically diminished in CCR2-deficient mice. Swirski *et al*. used the mouse myocardial infarction model to further characterize Ly-6C^{high} monocyte recruitment and identified the subcapsular red pulp of the spleen as a major source of recruited monocytes. Interestingly, angiotensin II, a circulating peptide that regulates vascular tone and blood pressure, promotes CCR2-independent emigration of splenic Ly-6C^{high} monocytes into the circulation.

Corticosteroid administration and vigorous physical exertion both result in abrupt increases in the number of circulating white blood cells, including monocytes. It has been assumed in these circumstances that white blood cells are released from endothelial surfaces. The finding by Swirski *et al*. that an increase in the circulating concentration of angiotensin II after myocardial infarction induces the dimerization of the angiotensin receptor on Ly-6C^{high} monocytes reveals a novel mechanism to boost circulating white blood cells in times of stress.

The findings by Swirski *et al*. raise questions about whether other types of stress or injury draw upon the spleen's reserve of monocytes as well. In the meantime, although the study does not make the spleen any less dispensable for mammalian survival, it does make this easily dismissed immune system organ seem a bit more purposeful and deserving of recognition.

References

1. F. K. Swirski *et al*., *Science* **325**, 612 (2009).
2. F. R. Sabin, C. A. Doan, *J. Exp. Med.* **46**, 627 (1927).
3. C. Auffray, M. H. Sieweke, F. Geissmann, *Annu. Rev. Immunol.* **27**, 669 (2009).
4. N. V. Serbina, T. Jia, T. M. Hohl, E. G. Pamer, *Annu. Rev. Immunol.* **26**, 421 (2008).
5. H. W. Ziegler-Heitbrock, B. Passlick, D. Flieger, *Hybridoma* **7**, 521 (1988).
6. F. K. Swirski *et al*., *J. Clin. Invest.* **117**, 195 (2007).
7. L. Boring, J. Gosling, M. Cleary, I. F. Charo, *Nature* **394**, 894 (1998).
8. L. Gu *et al*., *Mol. Cell* **2**, 275 (1998).
9. F. Tacke *et al*., *J. Clin. Invest.* **117**, 185 (2007).
10. N. V. Serbina, E. G. Pamer, *Nat. Immunol.* **7**, 311 (2006).
11. C. L. Tsou *et al*., *J. Clin. Invest.* **117**, 902 (2007).
12. C. Varol *et al*., *J. Exp. Med.* **204**, 171 (2007).
13. M. Nahrendorf *et al*., *J. Exp. Med.* **204**, 3037 (2007).

10.1126/science.1178329

COMPUTER SCIENCE

Is Your Computer Secure?

Security must be built in to software from the outset rather than added on later.

Frederick R. Chang

Cybersecurity is a pressing global issue today and increasingly affects all of us. According to a recent estimate, each U.S. adult had a 66% chance of experiencing at least one data exposure in 2008 and a 30% chance of experiencing multiple such exposures (*1*). A key motivator for cyber attackers is financial gain; a study of the underground economy observed advertisements for over $276 million in total "goods" (such as stolen credit card information) during a recent 1-year period (*2*). The annual cost to companies due to intellectual property theft and repair after data breaches has been estimated at over $1 trillion globally (*3*). Yet, in a study of consumer's personal computers, only 37% had up-to-date anti-malicious software (malware) protection; of those, 23% had active malware infections (*4*). What are the key cybersecurity dangers today, and how can they be addressed?

Computers can be infected merely by surfing the Web. By attacking a single Web site, attackers can potentially infect the computers of all visitors to that site. Using a technique known as SQL (Structured Query Language) injection, an attacker can insert malicious code into the database associated with the Web site. If the victim's browser is vulnerable, that malicious content is transmitted to the victim's computer. Using another technique, cross-site scripting, the software toolkit known as "Mpack" recently caused considerable damage (*5*). Users visiting legitimate Web sites were invisibly redirected to a server that downloaded malicious software onto the user's machine. Various types of malware can be downloaded to the victim's machine in this way, including keyloggers (which steal account and password information), rootkits (which hide the presence and activity of malicious software), and software enlisting the computer in a botnet.

Botnets are responsible for attacks including spam, phishing, distributed denial of service, data harvesting, click fraud, and password cracking. A bot is a computer that has been infected such that it can be remotely controlled; a botnet is a large network of bots. Up to 25% of the world's network-connected computers may be part of a botnet (*6*). In 2008, the botnet Srizbi sent out an estimated 60 billion spam messages per day—about 50% of the world's total (*7*). At the end of 2008, Srizbi's impact was much reduced when a suspect Web hosting company was cut off from the Internet. The botnet made a comeback, but in early 2009 a software patch was released that could remove the Srizbi software from client computers.

Another recent botnet, Storm, was estimated to have infected 1 million to 5 million computers; each infected computer sent out an average of 1200 spam messages an hour (*8*), generating healthy revenue for the botnet owners (*9*). Storm successfully evaded antivirus protection, had a decentralized control structure that made it difficult to shut down, and had a built-in self-defense mechanism (it launched denial of service attacks against researchers trying to access and study it). Storm also made sophisticated use of social engineering techniques: It was highly effective at inducing people to take action (such as to download and execute files), thereby infecting their computers with malware.

Social engineering here refers to manipulating a computer user to take an action with undesired consequences, such as downloading a file containing malware, clicking on a link that takes them to a fraudulent Web site, or divulging confidential information. Many users are easily manipulated in this way. In a study (*10*), university computer science students were sent an e-mail explaining that the system password database had been compromised and that they should reply with their password so that they could be validated in the database. No such database compromise had in fact occurred. The students were advised that they should never reveal their passwords to anybody, yet 41% of the students sent their passwords. Most were suspicious, changing their passwords in the 2 weeks after the study, but very few reported the incident (*10*).

In another study, a credit union hired a security firm to perform a social engineering "penetration test" on itself. When

Department of Computer Sciences, The University of Texas at Austin, Austin, TX 78712, USA. E-mail: chang@cs.utexas.edu

a group of the credit union's employees found "free" USB drives near their place of work, they brought them into the workplace and plugged them into their computers. The drives contained malicious software and infected the users' computers (*11*). Malware authors have also used phony security software or fraudulent electronic greeting cards. As attackers target the "human layer" with social engineering, it will be increasingly important to ensure that users are educated as to current cybersecurity risks and dangers.

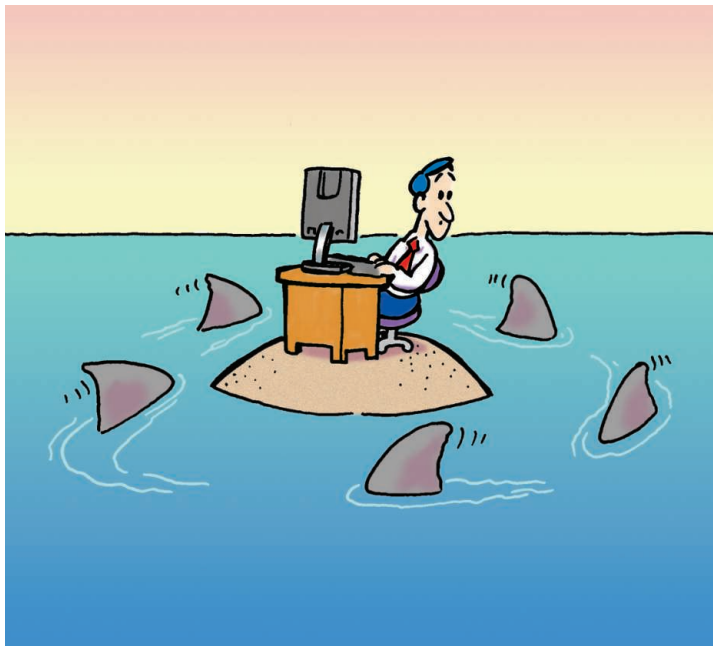

A key problem is that too much software today is insecure. Reports of software vulnerabilities are increasing rapidly (*12*), and attackers can easily exploit these vulnerabilities to cause harm. Even when a specific software vulnerability is reported, it can take months for an appropriate patch to be released and even longer for that patch to be installed to repair the vulnerable system. Antivirus software, firewalls, and intrusion detection systems are important and useful technologies, but they are symptomatic of the fact that security is often an afterthought.

The traditional goals of software quality and reliability must be expanded to include the fact that software must operate dependably in the face of malicious attack. As a result, increasingly, security must be built in to software from the very beginning (*13*). This is not to say that all software needs to be made nearly "hacker proof," but rather that much more software needs to be made more "hacker resistant." It is critical to know how secure the system needs to be.

If security is to be built into the software, then the software must be free of known bugs that can be exploited to compromise security. There are lists of common programming errors that can help the programmer, as well as powerful "bug finding" tools that can automate the identification of serious bugs (*14*). Security must be a part of the design of the software, and rigorous mathematical analysis techniques should be used whenever possible to ensure that the designs are adequate. The goal of security leads to different questions for the software designers. Can the software withstand a malicious attack? Are there multiple layers of defense to make it more difficult for attackers to succeed? For example, access to a sensitive file might require proper permissions, a strong password and a decryption key. What happens if the software is compromised? Does the system degrade gracefully— that is, does it continue to operate, albeit at a possibly reduced level? Finally, security should be integrated into the entire software development life cycle (requirements, design, coding, testing, deployment and operations) (*13*).

Building security in is not a new problem. Fortunately, important technical advances (*15*) over the past 25 years have improved the ability of developers to build more fundamentally secure systems. Better decision methods such as BDDs (binary decision diagrams) and SAT (propositional satisfiability) along with advances in model checking and theorem proving have greatly improved the ability to reason about complex system abstractions. Combined with greater computational power, these sorts of advances, among others, have led to tangible improvements in the ability to produce more fundamentally sound hardware and software systems. Numerous modern tools have been developed based on these advances and are increasingly being implemented, with positive results. Indeed, the UK-based software company Praxis High Integrity Systems uses rigorous mathematical methods to reduce software defects and improve the quality of their software. This company offers a software warranty to their customers—a rather rare occurrence in the software industry (*16*).

Technology advances alone will not solve all the problems. Indeed, critical insights into the limitations of technical solutions are being gained at the intersection of information security and the social sciences. In economics (*17*), a key issue relates to incentives: How people are motivated to behave regarding system security may be more important than how the system itself behaves. In psychology (*18*), a key question is why social engineering techniques continue to be so successful. As technical measures improve the security of systems, the end-user will increasingly become the weakest link.

As the attractive economics of cloud computing trigger yet another wave of valuable services over the Web, software security will become even more urgent. Perfectly secure software is impossible, but that does not mean that we should not try.

CREDIT: JOE SUTLIFF/WWW.CDAD.COM/JOE

References and Notes

1. D. E. Geer, D. G. Conway, *IEEE Secur. Privacy* **6**, 87 (2008).
2. *Symantec Report on the Underground Economy* (Symantec Corporation, Cupertino, CA, November 2008).
3. www.mcafee.com/us/about/press/corporate/2009/20090129_063500_j.html
4. *Malware Infections in Protected Systems* (Panda Security, Glendale, CA, 2007).
5. BBC News, "Hackers target 'legitimate' sites," 20 June 2007; news.bbc.co.uk/2/hi/technology/6221306.stm
6. T. Weber, "Criminals 'may overwhelm the web,' " BBC News, 25 January 2007, news.bbc.co.uk/2/hi/business/6298641.stm.
7. J. Stewart, *Top Spam Botnets Exposed* (SecureWorks, April 2008); www.secureworks.com/research/threats/topbotnets
8. P. Porras *et al.*, *A Multi-Perspective Analysis of the Storm (Peacomm) Worm, CSL Technical Note* (SRI International, Menlo Park, CA, October 2007).
9. C. Kanich *et al.*, *Spamalytics: An Empirical Analysis of Spam Marketing Conversion* (CCS'08, 27 to 31 October 2008, Alexandria, VA), see www.sigsac.org/ccs/CCS2008/program.html.
10. T. Greening, *SIGSAC Review* **14**, 9 (1996).
11. DarkReading, "Social engineering, the USB way," 7 June 2006; www.darkreading.com/security/perimeter/showArticle.jhtml?articleID=208803634.
12. *IBM Internet Security Systems X-Force 2008 Trend & Risk Report* (IBM Global Technology Services, Somers, NY, January 2009).
13. G. McGraw, *IEEE Secur.w Privacy* **2**, 80 (2004).
14. B. Chess, J. West, *Secure Programming with Static Analysis* (Addison-Wesley, Boston, MA, 2007).
15. R. E. Bryant, *IEEE Trans. Comput.* **c-35**, 677 (1986).
16. C. Jones, P. O'Hearn, J. Woodcock, *IEEE Compu.* **39**, 93 (2006).
17. R. Anderson, T. Moore, *Science* **314**, 610 (2006).
18. B. Schneier, *The Psychology of Security*, January 2008; www.schneier.com/essay-155.html.

19. I thank J Moore, M. Dahlin, W. Hunt, P. Acosta, and two anonymous reviewers for comments.

10.1126/science.1168661

EDUCATION

National Science Ed Standards—The Key to Improved Learning?

With concern about U.S. science education extending from corporate boardrooms and top research centers to local school districts, a bipartisan coalition of political leaders has moved in recent months to provide new school funding and support for teachers. Now momentum is building behind a proposal that many advocates see as a natural next step: voluntary national science education standards for students in elementary and high schools.

Long a pioneer in innovative science education, AAAS has taken a high-profile role in devising and assessing standards—and, most recently, in supporting voluntary national standards. Top AAAS officials have advanced the argument in scholarly journals and newspaper commentaries and have urged President Barack Obama to embrace standards that define a baseline of science knowledge expected of students.

Shirley Malcom

"The base of those who believe that we have to move to national science education standards definitely has grown broader," said Shirley Malcom, head of Education and Human Resources at AAAS. "There's a recognition that for life and work in the 21st century, students have to have a higher level of science knowledge and understanding."

The quality of U.S. science education has been a persistent concern over the past half-century. In 1983, the seminal study "A Nation at Risk" warned of shortcomings in science and math education. A major 2007 report, *Rising Above the Gathering Storm*, described improvements in science and math education as critical to economic strength and national security.

AAAS's Project 2061 science literacy initiative laid the groundwork for the science standards movement with its landmark 1989 report *Science for All Americans,* which described a coherent set of ideas in science, mathematics, and technology that all high school graduates should know, and its 1993 *Benchmarks for Science Literacy,* which set out detailed K–12 learning goals that could be used by educators to develop a core curriculum. In 1996, the U.S. National Research Council published the *National Science Education Standards,* the result of 4 years of work by 22 science and science education groups, including AAAS, and over 18,000 contributors.

Are you ready for today? SUNNY, HIGH 68, LOW 51 / PAGE B8 ROCKETS LOOK TO REGAIN SWAGGER / PAGE C1

HOUSTON CHRONICLE

Adopt national standards to help children compete

U.S. needs uniform goals to prepare lagging students

By ALAN I. LESHNER and JO ELLEN ROSEMAN

OFFICIALS in 46 states and the District of Columbia agreed June 1 to move toward uniform learning goals in reading and mathematics for children nationwide. The effort, led by the National Governors Association and the Council of Chief State School Officers, was applauded by U.S. Secretary of Education Arne Duncan.

Sadly, science was left out, and education leaders in Texas — along with Alaska, Missouri and South Carolina — have so far de- ...the plan.

for International Student Assessment. Even among college freshmen, nearly 30 percent need remedial science and math classes.

Our top-performing science students are still among the world's elite. But other young people are lagging. That's bad for the U.S. economy: McKinsey & Co. consultants say that closing the science gap between U.S. and international students could have increased America's gross domestic product by $1.3 trillion to $2.3 trillion in 2008. Closing the racial gap in science scores among U.S. students might have added another half-trillion dollars, the firm reported.

One promising strategy for improving science-learning standards will soon be reintroduced by Sen. Chris Dodd, D–Conn., and Rep. Vernon Ehlers, R-Mich. Their SPEAK Act ("Standards to Provide Educational Achieve- ...All Kids

The importance of standards. In the *Houston Chronicle,* AAAS CEO Alan I. Leshner and Project 2061 Director Jo Ellen Roseman wrote that voluntary national science standards promise economic dividends.

State educators drew heavily from those guides as they developed their own standards, but the results have been mixed, at best.

The most recent national scorecard on science performance found that 34% of American 4th graders and 43% of 8th graders scored below basic achievement levels. On the 2007 Programme for International Student Assessment, U.S. 15-year-olds ranked 21st among students in 30 developed nations, just behind Iceland and just ahead of the Slovak Republic.

Jo Ellen Roseman

Such scores suggest that "the majority of U.S. students are destined to graduate from high school without even a basic understanding of core concepts and skills in science," Project 2061 Director Jo Ellen Roseman and Communications Director Mary Koppal wrote in an analysis last November in *The Elementary School Journal.*

While inconsistent state standards have "resulted in curriculum frameworks and textbooks that are unfocused and ineffective," they said, national standards could focus and strengthen those materials—and help improve student learning.

The National Science Board (NSB), which oversees the U.S. National Science Foundation, came to a similar conclusion. The NSB drafted a broad framework for improving science education that was sent to Obama's transition team in January.

The new administration, it said, "should lead the process of articulating the core concepts and skills that all students should master." State and local educators could then adapt curricula to local needs, while the federal government helps develop assessments to measure students' progress.

Obama has been a strong proponent of improved science education, but the effort also has attracted bipartisan support in Congress and beyond.

The National Governors Association and the Council of Chief State School Officers last month announced an effort—involving 49 U.S. states and territories—to create common K–12 standards in English and mathematics. U.S. Secretary of Education Arne Duncan pledged $350 million "to support states in the creation of rigorous assessments linked to the internationally benchmarked common standards." Some see another opportunity to advance national standards in the No Child Left Behind Act, which is due for reauthorization later this year.

Meanwhile, U.S. Senator Chris Dodd (D–CT) and U.S. Representative Vernon Ehlers (R–MI) reintroduced their Standards to Provide Educational Achievement for All Kids (SPEAK) Act to encourage states to adopt national science standards.

The plan offered by the governors and state school officers did not include science, but in a commentary first published in the *Houston Chronicle,* Roseman and AAAS CEO Alan I. Leshner cited it as a signal of hope for addressing the general confusion among state standards. And the SPEAK Act, they said, "suggests an effective template for establishing science-education guidelines."

Their conclusion: "Voluntary, nationwide education standards in science, along with reading and math, are the next logical step [in education reform], promising dividends for tomorrow's workforce and for our economy."

Versions of the op-ed were subsequently published in the *St. Louis Post-Dispatch,* the *Greenville News* in South Carolina, and the *Fairbanks Daily News-Miner* in Alaska. Each of those states, like Texas, declined to sign on to the common standards effort developed by the governors and school officers.

Published by AAAS

ENVIRONMENT

AAAS HQ Goes Green, Earns Gold Award

An intensive, multiyear effort to make AAAS headquarters more energy efficient and environmentally friendly has earned the building honors from the U.S. Green Building Council.

The headquarters is the first building in Washington, D.C. to earn gold-level certification in the existing building category through the Council's Leadership in Energy and Environmental (LEED®) program. AAAS has also received the Council's Award of Excellence for Operations & Management for an existing building.

The award reflects the association's response to some of "the most important challenges of our time, including global climate change and dependence on nonsustainable and expensive sources of energy," said Rick Fedrizzi, the Council's president, CEO and founding chair. "The importance of retrofitting existing buildings, and the work of innovative projects such as the AAAS headquarters facility, is a fundamental driving force in the green building movement."

In pursuit of an environmentally sensitive workplace, the headquarters has reduced daily water consumption by 39% since 2007, recycled nearly half of all its solid waste in 2008, and now meets 50% of its energy needs using renewable sources such as wind power, according to Robert Zayas, the AAAS building manager.

"The AAAS mission is to advance science, engineering, and innovation throughout the world for the benefit of all people," said AAAS CEO Alan I. Leshner, who also serves as executive publisher of *Science*. "We are therefore extremely proud and honored to be able to demonstrate environmental leadership within our headquarters' facility."

The LEED program provides an internationally recognized, independent verification of a building's performance with regard to energy savings, water efficiency, carbon emission reduction, and other measures of environmental impact. Buildings can score up to 110 LEED points in these categories; buildings that score 60 or more points receive gold-level certification.

Along with improvements in recycling and water usage, AAAS has significantly decreased its carbon footprint and energy use. Operations at AAAS now release much less carbon dioxide into the atmosphere—1518 fewer tons of atmospheric carbon dioxide per year as of 2008—compared with the industry standard for a similar building, according to data available through the U.S. Environmental Protection Agency's Energy Star program.

As of 2008, the headquarters was using about 96,000 British Thermal Units of energy per square foot (BTU/SF) per year, said Zayas, compared to the industry standard of 162,000 BTU/SF for similar buildings.

Going green. Innovative projects in energy efficiency and recycling have made the AAAS headquarters a model for the green building movement.

Unique architectural features such as ribbons of extra windows, a pair of 10-story notches that cut vertically into the building, and an extensive system of sensors all help to reduce artificial lighting requirements in the AAAS facility.

"AAAS management believes that when occupants and tenants have access to natural daylight and views to the exterior, they may be able to work more comfortably and efficiently," Zayas noted. "We estimate that 90% of all regularly occupied spaces in the building have a direct line-of-sight to the outdoors."

Built in 1996 from a design by noted architect Henry N. Cobb of Pei Cobb Freed & Partners, the headquarters building has received several awards for its design and management. In 2007, AAAS became an Energy Star recipient, an honor recognizing outstanding contributions in energy efficiency from the U.S. Environmental Protection Agency. In addition, the headquarters facility was named "Building of the Year" in 1998 and "Corporate Building of the Year" in 1999 by the Apartment and Office Buildings Association.

The new honors reflect an "ongoing commitment" to environmental stewardship at AAAS, said Phillip Blair, the association's chief financial officer. He called the LEED gold certification "a great tribute to our Board and to staff members who have worked so hard to maintain an environmentally responsible facility."

—Ginger Pinholster and Becky Ham

REGIONAL DIVISIONS

Environment, Evolution Featured at Meetings

The effects of rapid climate change on human health in the Arctic, the decline of amphibians across the globe, and the emergence of life on Earth are some of the topics to be explored at upcoming annual meetings for three of the AAAS Regional Divisions. For more information on the conferences, visit www.aaas.org/go/divisions/.

Pacific Division Annual Meeting
"Sustainability in an Evolving World"
14 to 19 August 2009
San Francisco State University and the California Academy of Sciences
San Francisco, CA

Arctic Division Annual Meeting
"Impact of Environment on Human Health: Interdisciplinary Science and Education"
14 to 16 September 2009
Westmark Baranof Juneau Hotel
Juneau, AK

Caribbean Division Annual Meeting
"Astronomy and the Origin of Life"
24 October 2009
Puerto Rico Convention Center
San Juan, PR

2008 ANNUAL REPORT

The AAAS 2008 Annual Report has been published and can be downloaded at www.aaas.org/publications/annual_report/.

Published by AAAS

WHERE THE BASIC SCIENCE

WORLD MEETS THE WORLD

OF MEDICINE

Submit your work to *Science Translational Medicine* today!

This fall, AAAS and *Science* will launch *Science Translational Medicine*, a new journal focused on applications of basic research knowledge that will improve human health.

The goal of *Science Translational Medicine* is simple: to help the scientific community harness decades of progress in research at the basic level and translate these biological discoveries into medical advances. Take this opportunity to have your work recognized in this groundbreaking new journal.

Papers in the following areas will be reviewed and considered for publication:

- Animal & Human Studies
- Applied Physical Sciences
- Behavior
- Bioengineering
- Biomarkers
- Cancer
- Cardiovascular Disease
- Cell Culture
- Chemical Genomics/Drug Discovery
- Data Mining
- Drug Delivery
- Gene Therapy/Regenerative Medicine
- Imaging
- Immunology/Vaccines
- Infectious Diseases
- Medical Informatics
- Medical Nanotechnology
- Metabolism/Diabetes/Obesity
- Neuroscience/Neurology/Psychiatry
- Pharmacogenetics
- Policy
- Toxicology & Pharmacokinetics
- And other interdisciplinary approaches to medicine

To submit your work for consideration, please visit: **www.submit2scitranslmed.org**

Science Translational Medicine AAAS

www.ScienceTranslationalMedicine.org

INTEGRATING MEDICINE AND SCIENCE

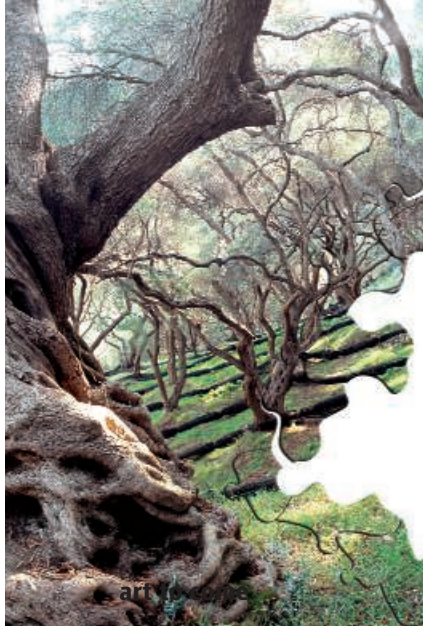

CREDIT: GRAND TOUR/CORBIS

INTRODUCTION

The Rise of Restoration Ecology

IN ART, RESTORATION INVOLVES RECAPTURING AN OBJECT'S AESTHETIC VALUE. In ecology, the stakes are arguably much higher: Our planet's future may depend on the maturation of the young discipline of ecological restoration. In this issue, we sample restoration projects around the world and consider the state of the science of this emerging field.

The goal of restoration ecology is not necessarily to restore an ecosystem to a pristine, prehuman ideal, but a long-term view is still important. In the opening Perspective, Jackson and Hobbs (p. 567) highlight paleoecology as a component of restoration science. Two more Perspectives focus on aspects of terrestrial ecosystems that are vital to the success of restoration. Harris (p. 573) considers the role of the soil microbial community: the bacteria and fungi that degrade organic matter and provide nutrients to the system. Dixon (p. 571) highlights the role of pollinators, whose activities are essential to natural and restored plant communities. The struggle to balance ecosystem complexity and economic reality is the theme of three News features: two that examine efforts to restore functional forest ecosystems in southern China (p. 556) and Borneo (p. 557) and a third that probes the ecological consequences of burgeoning rubber plantations in Southeast Asia (p. 564).

How successful is restoration? In a Perspective, Palmer and Filoso (p. 575) caution that it is unlikely to lead to the full recovery of the biodiversity and ecosystem services of undisturbed systems. A meta-analysis by Rey Benayas *et al.*, published on *Science* Express this week, confirms this view but shows that well-done restoration consistently enhances biodiversity and ecosystem services. In another Perspective, Norton (p. 569) considers the limits to restoration posed by invasive species, and a News story examines the success of a national program targeting invasives in South Africa (p. 562). Also on *Science* Express this week, Schulte *et al.* report an unprecedented restoration of oysters in the Chesapeake Bay in the eastern United States, which bodes well for the health of the entire estuarine ecosystem. Coral reefs, meanwhile, are under attack from human insults and climate change; a News feature (p. 559) gives an overview of important efforts to restore damaged reefs. Finally, in a Research Article, Worm *et al.* (p. 578) review current efforts to restore marine ecosystems and fisheries, concluding that making fisheries sustainable is an achievable goal.

Restoration ecology is a relatively new science—the Society for Ecological Restoration International (www.ser.org/default.asp) celebrates its 21st birthday this year—but in its short life it has assumed a major role in sustainable development efforts across the globe.

– LESLIE ROBERTS, RICHARD STONE, AND ANDREW SUGDEN

Restoration Ecology

CONTENTS

News

Perspectives

See also Science *Express Reports by J. M. Rey Benayas* et al. *and D. M. Schulte* et al. *on p. 513, and Research Article on p. 578.*

Science

Published by AAAS

Brave new forest. An experimental stand in Guangxi.

Nursing China's Ailing Forests Back to Health

A lauded effort to create mixed forest stands is giving villagers and loggers a chance to make a living while restoring ecosystem vitality

PINGXIANG, CHINA—The swath of hilly terrain looked like a man's face after a poor shave. A few days earlier, villagers had clear-cut a fir forest and burned the stumps. Soon they will uproot the charred stubble and repopulate the barren land with eucalyptus, a fast-growing Australian import. "The timber is low quality," says Lu Yuanchang, a forester at the Research Institute of Forest Resource Information Techniques of the Chinese Academy of Forestry (CAF) in Beijing. But after 5 years or so, the villagers who manage this community forest in southern China's Guangxi Zhuang Autonomous Region, near the border with Vietnam, will hack down the eucalyptus and pulp it for paper. "They should turn a quick profit," Lu says.

Ecological expediency of this sort has been rampant in sections of southern China, as villagers and local governments conspire to transform vibrant forests into plantations for money-spinners such as eucalyptus, rubber, and oil palm. "In recent decades, no other country in the world has established more forest plantations than China," says Heinrich Spiecker, director of the Institute for Forest Growth in Freiburg, Germany. Yet forests cover only about 18% of China's landmass, and timber yield and quality are lower than in many other places.

China's enthusiasm for monocultures has taken a heavy toll. "Converting large areas into single-species plantations is destroying the environment," Lu says. "There has been large-scale degradation of China's forests." Monocultures are often susceptible to pests and diseases, Spiecker notes. According to Lu, the most insidious effects stem from soil degradation, which destabilizes ecosystems. Monocultures, he says, were largely to blame for widespread forest losses inflicted by last year's ice storms (*Science*, 7 March 2008, p. 1318).

The problem is likely to get worse before it gets better. In 2003, the central government approved a regulation that grants Chinese citizens an extension of how long they can farm or manage a community forest—from 30 to 70 years. That enormous policy change effectively grants people land ownership for their lifetimes. "The policy is meant to stimulate families to take care of the land," says Cai Daoxiong, director of CAF's Experimental Center of Tropical Forestry in Pingxiang. However, notes Bernhard von der Heyde, director of the sustainable forest management project of the German nonprofit development group GTZ in Beijing, "there is a big rift between national will and local implemen-

CREDITS (TOP): R. STONE/*SCIENCE*

Published by AAAS

tation." Seduced by easy money, many individuals do as they please with forest patches under their control. "Many people just concentrate on short-term economic benefits," Cai says.

Lu hopes to restore China's forests before it's too late. Less than a kilometer from the budding eucalyptus plantation in Pingxiang is a CAF effort to engineer a "multipurpose" forest. In 2005, instead of clear-cutting, the Pingxiang center selectively harvested stands of Chinese fir (*Cunninghamia lanceolata*) and brought in seedlings of more than 20 hardwoods prized for their timber, including species of *Castanopsis*, a genus in the beech family, Ceylon ironwood (*Mesua ferrea*), and *Michelia hedyosperma*, a kind of magnolia. "It's really a simple concept," Lu says. "We are transforming single-species stands into mixed stands for economic and ecological benefit."

Near a *Castanopsis* sapling, Lu brushes away leaf litter and runs his fingers through rich humus. "In a good forest, you should not see the soil. You should only see humus," he says. For this particular forest revival, Lu selected a complementary mix of pioneer and mid- to terminal-succession tree species that play different ecosystem roles, from enriching the soil to forming the kind of canopy and fruits that attract birds and other wildlife. In several years, CAF can harvest fir trees that reach a target girth and in a few decades start logging valuable hardwoods tree by tree. Selective logging, Lu says, is slightly more expensive in China than clear-cutting, but in time the greater profit from the hardwood timber will more than compensate for the higher costs. "And we save the ecosystem," Lu says.

The science behind Lu's approach is not novel, but its impact on the restoration of China's forests could be revolutionary. And it's getting rave reviews. "Pingxiang is the best research model in China," says Li Nu Yun, deputy director general of the afforestation department of China's State Forestry Administration in Beijing. Multipurpose forestry, Von der Heyde says, "will increase carbon stocks in the ground tremendously." Lu and colleagues have launched multipurpose forest experiments in Guangxi, on the tropical island-province of Hainan, in the arid plains of Shanxi Province, and near Beijing. Experts say it should be possible to persuade government entities that oversee logging in state forests—more than 40% of China's forest cover—to set aside more and more land for multipurpose forestry. But persuading villagers to buy into the concept—and forgo quick profits—is more daunting. "It will take tremendous will and patience to implement this program," says Von der Heyde.

Nature's way

In the early 1980s, soon after China's devastating Cultural Revolution, researchers cast around for a more scientific approach to forest management. "We planted some high-value trees, and that was it,"

CREDIT: W. SMITS

RESTORING A 'BIOLOGICAL DESERT' ON BORNEO

FOR 30 YEARS IN INDONESIA, WILLIE SMITS OBSERVED HOW ONE CONSERvation project after another would fail without local community support. Finally, Smits hit upon a solution: An economic incentive for area residents became a cornerstone of his Samboja Lestari project, an ambitious effort to transform a clear-cut site in Borneo into a mix of agroforestry plots and orangutan habitat.

"The extent and depth of his integration of ecological [restoration] with economic restoration is unique in my experience," says Amory Lovins, an expert on sustainability at Rocky Mountain Institute, a think tank in Snowmass, Colorado. "It's the most important such project I know of in the tropics, if not in the world."

Born in the Netherlands and now a citizen of Indonesia, Smits founded the Borneo Orangutan Survival Foundation in 1991 to rescue orphans. He says he realized that the underlying problem affecting orangutans and other wildlife is habitat loss. So in 2002, Smits purchased 2000 hectares of deforested land in eastern Borneo, near Balikpapan. The site was "a biological desert," he says, and the district, with a 50% unemployment rate, was the province's poorest. Villagers who sold land to the project received a plot in a zone ringing the site where they planted acacia trees, which will provide timber, and sugar palms for sap to be processed into ethanol. Cash crops grown among the trees include ginger, papayas, cocoa, and chilies.

In the inner zone, teams of villagers were paid to plant fast-growing tree species to kick-start reforestation as well as slower-growing rainforest species. Enormous diversity—some 1600 tree species in all—has created a multilayered canopy that makes the most of sunlight and maximizes biomass. Smits has sunk about $4.5 million, raised from a foundation he directs and from small contributions, into the project. So far, the reforested habitat has attracted 137 bird species and is now home to orangutans and sun bears, a species found in Southeast Asian rainforests. The greenery has lowered air temperatures by 3° to 5°C in the immediate vicinity and increased rainfall by 25%.

Samboja Lestari's legal status as a nongovernmental project means it can avoid Indonesia's slow-moving bureaucracy and avoid compromises with commercial concerns eager to tap the region's coal deposits, Smits says. Community members know they, not the government, own the land, and the construction, replanting, and the Borneo Orangutan Survival Foundation's rescue and rehabilitation operations have generated 3000 jobs. Governance based on local traditions (Smits's wife is a tribal leader in North Sulawesi) means that the community, primarily through peer pressure, ensures that its own members do not fell trees and that they cooperate with project officials to keep poachers and loggers at bay.

Although Smits hopes Samboja Lestari will set an example, he warns that there is no single recipe for forest restoration. "You have to do detailed design for each location," he says. The key, he adds, is striking the right balance between suitable ecological methods and local needs. **–DENNIS NORMILE**

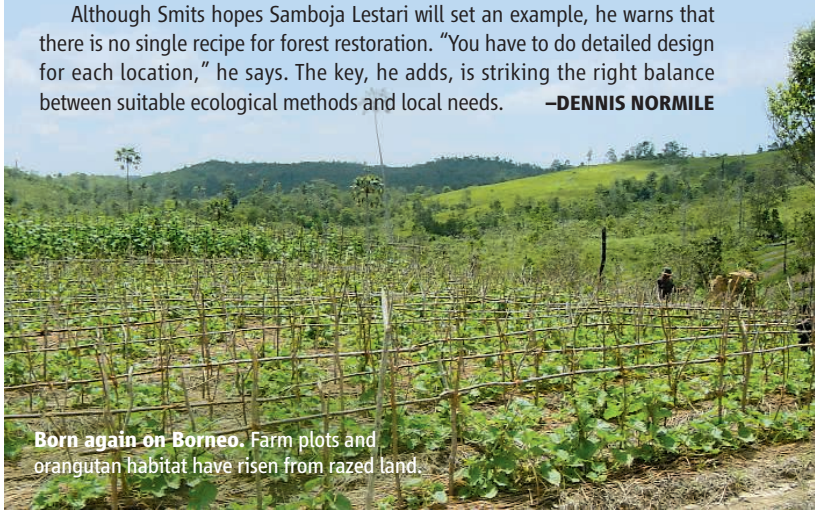

Born again on Borneo. Farm plots and orangutan habitat have risen from razed land.

Published by AAAS

Cai says. "But we really did not know how to practice sustainable forestry. Then Professor Lu came along."

Lu had trained in Germany in the 1990s, where he had become steeped in the country's "close to nature" approach to forestry. Like other central European nations, Germany lost its old-growth forests to centuries of agriculture and industrial development. During his stint in Germany, Lu gained an appreciation for the country's methodical approach to managing secondary stands: selecting complementary tree species and minimizing the impact of timber harvests on ecosystem health.

The benefits of this approach are many and varied, Lu says. The better the mix of trees, the richer the humus and the greater the soil's capacity to retain water. Reducing runoff stabilizes not only the hydrology of the watershed but also the local climate, he says. And the ecosystems are more resistant to pests and disease.

When Lu returned to Beijing in 2000, he proposed that China adopt the close-to-nature approach. He encountered plenty of resistance: "People thought that 'close to nature' is only a luxury. It was the hardest thing in the world to change people's minds." While a few centers like Pingxiang were tinkering with multifunctional forestry, the vast majority of state forests were managed according to the rotation system, in which stands are clear-cut and replanted, for example, with *Pinus radiata* pines, firs, or other fast-growing species. "That is the way it has been done for years," Lu says. "China has had a very hard time coming around to the idea of multipurpose forestry."

The Teutonic way. Forester Lu Yuanchang cut his multifunctional teeth in Germany.

For 3 years after Lu's return to China, one grant proposal after another that he wrote was rejected. But his superiors tolerated his close-to-nature proselytizing, and in 2003 Lu finally won funding for a multipurpose forestry experiment near CAF's headquarters in Beijing's northwestern suburbs. The small plots are meant to be pleasant arboreal getaways for smog-choked Beijingers rather than a proof of principle that multipurpose forests make economic sense. To make that case, Lu needed to find colleagues who managed larger acreages and who could demonstrate that multipurpose forests, after a few decades, would pad the bottom line of timber concerns. When Lu paid a visit to Pingxiang in 2005, he realized that he and Cai "were of one mind."

The duo immediately launched some multipurpose plots. "Lu introduced to us a scientific idea of forestry," says Cai. "We now believe this management system is better than a rotation system." Although the stands cover only about 100 hectares—a tiny fraction of the Pingxiang center's 20,000 hectares of land—"I am now convinced that all of our forest should be managed in a sustainable way. Gradually, we'll reduce the clear-cut area," Cai says. "We want to make this forest center a model for all of China."

Reasonable facsimiles

Gently stirred by a light breeze, the canopy casts an ever-changing mottled pattern on a *Castanopsis* trunk in one Pingxiang stand. In 20 years or so this tree, like others of its kind here, will be ready for harvest. Like an adoring father, Lu gives it a pat. "We'll come back in a few years and check on it, see how it's doing," he says.

Multipurpose forests in Guangxi and other regions will resemble, rather than imitate, original primary forests. It's hard to pin down what a forest in any given locale should look like: Its "potential natural vegetation" depends on local climate and therefore changes as the climate shifts. "Trying to determine past, present, and future potential natural vegetation is like a detective story," says Lu. In Guangxi, he says, there may be no forests left with species assemblages that existed here 1000 years ago. Logging is not permitted near the Vietnam border, he says, but even those forests are at most a century old. "The fact is, forests are dynamic," Lu says.

Rather than strive for an ideal that does not exist and may never have existed, Lu favors a more practical restoration target of achieving a healthy forest ecosystem that's a reasonable facsimile of potential natural vegetation. That doesn't require the wholesale abolition of plantations. Rather, it means convincing forest managers—and villagers—that multipurpose forests, by improving overall ecosystem health, will make many existing plantations viable. "A well-arranged mixture of forest types adapted to site conditions and local needs may best serve society," says Spiecker. Li of the State Forestry Administration agrees. "Now local people can decide themselves what kind of species to plant over their lifetime," she says. "They can think about what will be best for the next generation."

–RICHARD STONE

Close shave. This clear-cut ridge in Pingxiang was to be replanted with eucalyptus.

CREDITS (TOP AND BOTTOM): R. STONE/*SCIENCE*

Bringing Coral Reefs Back From the Living Dead

A smattering of efforts are aiming to prove that degraded coral reefs can be restored to functionality, if not pristine beauty

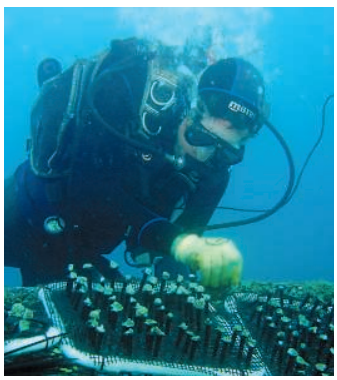

Wet nurse. A diver adjusts a nursery net studded with coral nubbins.

ISHIGAKI, JAPAN—Last April on the northern edge of Sekisei Lagoon, Japan's largest coral reef, five divers placed dozens of stainless steel cages packed with custom-made ceramic disks on the sea floor near a patch of healthy coral in the ailing reef. All had to be ready before a mass spawning event expected during the new moon in May, in hopes that millions of coral larvae would settle on the disks. The high-tech operation went according to plan, and earlier this month the divers moved the cages to sheltered lagoon waters to enable the larvae to mature and form colonies. In another 18 months or so, the disks will be cemented into parts of the reef where a process known as bleaching, triggered by unusually warm waters, had killed the coral. In 30 years or so, researchers hope, the 27,000-hectare reef will be fully restored.

One year earlier and 1000 kilometers to the southwest, the Philippine coastal community of Bolinao set out to restore its bleached and overfished reef. Residents decked out in homemade plywood flippers dove without air tanks from outrigger canoes. They broke off fragments of a robust coral from one part of the reef and wedged pieces into cracks in bleached sections. Six months later they returned, snapped off bits of the healthy transplanted coral, and repeated the process.

The Bolinao reef restoration may be the most inexpensive in the world, whereas that in Sekisei Lagoon is probably the costliest. But both projects are important experiments in an urgent effort to stabilize the world's embattled coral reefs, which provide habitat for some 9 million species, including 4000 kinds of fish. Roughly 100 million people in developing countries depend on reefs for subsistence fishing and tourism, estimates the Global Environmental Facility (GEF). The "rainforests of the sea," however, are threatened by human activity and natural disasters. About 19% of our planet's original global coral reef area has been destroyed; another 15% could be lost in the next 2 decades, according to the Global Coral Reef Monitoring Network's *Status of Coral Reefs of the World: 2008*.

As losses mount, restoration projects are only just getting off the ground. "The science of reef restoration is in its infancy," says Alasdair Edwards, a reef scientist at Newcastle University in Newcastle upon Tyne, U.K. "There are tens of thousands of square kilometers of degraded reefs apparently out there, and almost all restoration trials are working at subhectare scales." The immediate challenge, he and others say, is to show that promising techniques can be scaled up.

Underwater silviculture. A coral nursery suspended above the sea floor.

CREDITS (LEFT TO RIGHT): S. SHAFIR; J. B. RINKEVICH

Published by AAAS

That will require resources that are by no means guaranteed: A good share of recent restoration projects has been funded by GEF's Coral Reef Targeted Research program, which ends this year.

Some experts are skeptical that restoration can make much of a difference. Healthy reefs lightly disturbed by humans typically recover from bleaching and natural disasters on their own, Edwards notes. But reefs pummeled by pollution, destructive fishing practices, or land reclamation are often pushed beyond recovery by bleaching or storms. "The only way to help is to reduce stresses that made [such reefs] degrade in the first place," says David Fisk, a coral reef scientist and consultant in Geneva.

Saving Sekisei

The daunting challenges facing restoration scientists are evident at Sekisei Lagoon, cradled by Ishigaki and Iriomote, the two southernmost large islands of Okinawa prefecture. Sekisei's predicament has been documented by Mineo Okamoto, a specialist in marine assessment techniques at Tokyo University of Marine Science and Technology, who in 1993 started mapping coral in the lagoon using echo sounders and cameras to add detail to satellite images. Back then, Sekisei was in pristine condition, thanks to its remote location and status as a national park. But Okamoto sensed that change was coming from global warming, with its threat of more-frequent bleaching events, and rising ocean acidification, which is caused by the uptake of carbon dioxide from the atmosphere and weakens corals (*Science*, 4 May 2007, p. 678). Okamoto set out to document how such climate changes affect a coral reef.

Okamoto completed his first coral map in 1998. That year an El Niño followed by a La Niña warmed the eastern Pacific to the point that zooxanthellae—algae that live symbiotically with coral and provide nutrients—deserted their hosts. Without zooxanthellae, corals blanch and unless the algae return within a few weeks, the colony starves and perishes. The 1998 bleaching event killed 16% of corals worldwide (*Science*, 27 October 2000, p. 682).

Sekisei Lagoon's northern edge was hit hard. But the interior and southern rim were spared, which enabled coral to recolonize bleached sections without human intervention. Three bleaching events since 2001 devastated the interior and southern sections even as the northern rim recovered. But prevailing currents tend to sweep larvae produced on the northern edge away from the lagoon, impeding recolonization of recently damaged areas.

To speed the reef's recovery, Okamoto custom-made ceramic disks with grooves on the undersides that coral larvae can nestle in while avoiding algae that foul the disks' tops. Okamoto placed limited numbers of disks—which are small enough to fit in the palm of a hand—in the lagoon in 2002. Two years later, Japan's environment ministry made Sekisei Lagoon's restoration "a big public works project" and bestowed a budget of about $430,000 a year, says Okamoto, who now serves as a consultant. Teams have been placing cages filled with disks along the ocean side of the reef's 10-kilometer-long northern rim before the annual mass coral spawning. Months later, they move disks hosting juveniles to the lagoon's interior, where the corals mature. Okamoto estimates that the May 2008 spawning yielded about 10,000 colonies that will be placed on the lagoon's southern edge in December.

Coral babe magnet. Mineo Okamoto's ceramic disks offer a haven for Sekisei larvae to form colonies.

"We have set a long-term period of 30 years for this restoration project," says Takanori Satoh, a ranger for the ministry's Coral Reef Research and Monitoring Center in Ishigaki. In 7 or 8 years, he says, researchers will be able to ascertain whether larvae from the transplanted corals have begun to recolonize the lagoon's interior.

Economizing

Few projects can expect such unstinting support as Sekisei. "At the end of the day, [reef restoration] has got to be something low-cost and low-tech that involves the local communities," says Edgardo Gomez, a marine biologist at the University of the Philippines in Diliman, who has worked with fishers in Bolinao, where the university has a marine lab, to restore reefs. Degraded by decades of blast fishing, Bolinao's reefs were devastated by the 1998 bleaching and have recovered only spottily. "The fish catch greatly diminished, and people had to resort to other ways of making a living," Gomez says.

To restore the reef, Gomez needed to find a coral species that thrives even when handled roughly. "The villagers can't afford adhesives, and nobody in the town of Bolinao, save for the dive shop, has scuba equipment," Gomez says. He settled on *Porites cylindrica*, a fast-growing branching coral. During their first training workshop in April 2008, Bolinao spear fishers planted about 400 square meters of reef. Six months later, 80% of transplanted coral was growing nicely and was big enough for bits to be broken off to replant another 400 square meters. The process was repeated in spring 2009. "If we keep doubling the areas we are restoring, in time it will become significant," Gomez says.

Gomez is planning to introduce these methods elsewhere in the Philippines and in other countries. He admits that the patched-up reefs will lack the diversity of natural reefs. "What is most important is that you build back the [roughness] of the reef so fish and invertebrates have refuges," he says. The promise of a healthy fishery gives locals an incentive to stick with an effort that may take years before they see a payoff.

Another approach to restoration on the cheap is what Baruch Rinkevich, a marine biologist at the National Institute of Oceanography in Haifa, Israel, calls "underwater silviculture." Just as foresters rear trees in nurseries for transplantation, Rinkevich and colleagues have pioneered coral nurseries: mesh nets or even lengths of rope raised off the sea floor to avoid predators and sedimentation. Students, technicians, or local fishers collect donor corals, chop them into nubbins as small

CREDIT: D. NORMILE/*SCIENCE*

as 0.5 centimeters across, and glue these onto a substrate—anything from seashells to bits of plastic piping—that is then attached to the nursery nets. Rinkevich says up to 99% of nubbins survive, depending on the species, and 12 to 18 months later they are big enough to transplant onto a reef.

Rinkevich worked out the kinks of the technique in Eilat, on the Red Sea, starting in the mid-1990s. More recently, he has experimented in Jamaica, the Philippines, Singapore, Thailand, and Zanzibar. "The results are more than just promising; they are beautiful," he says. Rinkevich claims that under optimal conditions in countries with cheap labor, he can produce a colony ready for transplantation for as little as 18 cents. So far, Rinkevich has built nurseries with 10,000 corals and transplanted up to 3000 colonies. He envisions nurseries with up to 200,000 corals and similarly supersized transplantations. "By doing that, I'm pretty sure we can change completely denuded reefs," he says. Newcastle's Edwards agrees that nurseries are one of the most promising approaches. "You're minimizing the collateral damage [by cutting donor material into small pieces], getting transplants, and maximizing the effect you can have," he says.

One drawback is that a reliance on nubbins from a single donor coral results in limited genetic diversity. To address that, Rinkevich and others are investigating a variation on the theme in which they capture eggs and sperm from the ocean during mass spawning events or from colonies taken into the lab just before spawning (*Science*, 14 December 2007, p. 1715). The gametes are mixed, and the resulting larvae settle onto substrates in tanks. The juvenile corals are moved into the nursery and transplanted to a reef a year or so later. Although this procedure boosts genetic diversity, it is more costly than nubbins and requires more expertise.

One recent trial in the Philippines led by James Guest, a marine biologist at the National University of Singapore, yielded about 1.6 million larvae from 19 colonies in tanks with 2000 concrete pins as substrates. Based on work in 2008, they expect about 1000 colonies to survive the first year. "We still have lots of work to do to improve these survival levels," Guest says.

Another approach is more like animal husbandry than silviculture. Researchers have "got a bit of a handle on the process of sexual reproduction in corals," which opens up the possibility of manipulating larvae, says Andrew Heyward, a coral reproductive specialist at the Australian Institute of Marine Science in Perth.

In a 2008 experiment in Palau, Heyward's team collected gametes from lab colonies and cultured larvae in improvised tanks: aboveground swimming pools. Each day they tested a few larvae to see if these were ready to settle and form a colony by exposing them to a reef chemical that triggers settlement in "competent" larvae. When half the batch was primed to settle, the researchers funneled larvae into an enclosure over an artificial reef. Six months later, they found five times as many juvenile corals on the treated rock as on nearby rocks that relied on natural recruitment. The equation is simple, says Heyward: More larvae in a given area mean better recruitment. "It takes almost no technology," he says.

With the future of reefs hanging in the balance, coral scientists are eagerly following the nascent restoration efforts. The various techniques being deployed "are still basically unproven in the long term," Edwards cautions. Fisk in Geneva is pessimistic about any restoration effort reaching a critical scale that would make a reef resilient. "You can't build big enough to withstand natural and manmade disturbances," he says.

Others insist that reef restoration will ultimately prevail. Rinkevich compares reef rehab to terrestrial reforestation. Although most present-day forests in North America and Europe are human cultivated, they nonetheless provide habitat for wildlife and prevent soil erosion. "In similar ways, transplanted corals change the environment in an area around a reef: Fish arrive, and invertebrates arrive," Rinkevich says. The detrimental impact of global warming and rising ocean acidification is "going to get worse before it gets better," adds Gomez. But "waging a rear-guard action" through restoration should lessen the harm inflicted on reefs and on livelihoods.

Such debates might be settled "as soon as someone can come up with a large-scale restoration that has worked," says Edwards. It may be up to Sekisei Lagoon and bootstrapping community efforts to prove that the world's battered coral reefs can be saved.

–DENNIS NORMILE

Vital signs. Coral fragments wedged into cracks in a reef in Bolinao thrived (*bottom*), as did larvae cultured in swimming pools in Palau (*top*).

CREDITS (TOP TO BOTTOM): A. HEYWARD; E. GOMEZ

Unleashing an Army to Repair Alien-Ravaged Ecosystems

South Africa has scored decisive victories in its grassroots assault on invasive species. But will the war ever end?

When fires devastated 10,000 hectares of the Cape Peninsula's Table Mountain range in 2000, South Africa faced a race against time to prevent fast-growing invasive plants from overwhelming native flora. Its solution: Ukuvuka, a campaign that deployed hundreds of workers to uproot aliens and rehabilitate and reseed sensitive tracts of the rugged terrain. Nine years later, native vegetation is flourishing.

Ukuvuka, from a Xhosa word meaning "to rise up," is one of more than 300 projects initiated by a pioneering program called Working for Water (WfW). Since 1995, WfW has restored ecosystems by taking aim at some 200 alien plant species that clog waterways, degrade farmland, and heighten wildfire threat. Major efforts have included campaigns to control South American pompom weed, a meter-high plant that threatened to run rampant in KwaZulu-Natal province; clear invasive plants for ecosystem restoration along Kruger National Park's major rivers; and facilitate production of "eco-coffins" and school desks made from cleared invasives. At the same time, WfW has created tens of thousands of jobs in a country where one out of every four adults is unemployed.

After centuries of colonization and trade, South Africa is now home to "a witches' brew of alien species" from Australia, Europe, Asia, and the Americas, says ecologist Richard N. Mack of Washington State University, Pullman. As an antidote, WfW has cleared about 1 million hectares of invasive species in 15 years. "In terms of its reach, its intensity, longevity, and the number of invasive species it targets," Mack says, "I can't think of another ongoing project quite as ambitious."

Shock troops

Alien species got a toehold in South Africa in the 1800s, when European settlers established sprawling plantations of Australian eucalyptus and European pine. Those species are thirstier than native trees and placed a heavier demand on the watershed, a problem compounded by the expanding agricultural sector. Many rivers and streams shriveled as banks became overgrown with invasive trees and weeds that arrived as imported seeds.

In 1994, the year that apartheid ended and Nelson Mandela became president, a panel of South African scientists and resource managers predicted a water crisis unless aggressive steps were taken to manage catchments and control invasive vegetation. Mandela's first minister for water affairs, human rights activist Kadar Asmal, hired ecologist Guy Preston, research chief at the University of Cape Town's Environmental Evaluation Unit, as an adviser. Together they launched WfW, which combined a public works campaign with water preservation and the fight against invasives. They initially focused on riverbank foliage, but the program soon expanded to a $100-million-per-year effort that tackles "the whole spectrum of alien plant invasions," Preston says.

To mount their campaign, Asmal and Preston enlisted an army: in the beginning, about 7500 part-timers whose ranks have since swelled to 29,000 per year. At a starting wage of $6 a day, the workers donned yellow WfW T-shirts and fanned out across the country, wielding chain saws, slash hooks, and herbicides against invasive plants. WfW scientists have also deployed more than 75 imported insects to eat their way through 45 invasive plant species, with generally good results so far. Harold Mooney, an ecologist at Stanford University in Palo Alto, California, who helped establish the Kenya-based Global Invasive Species Programme, calls WfW "an innovative program that addresses invasive species, water, and job creation in an integrated way."

Basket-weaving aliens. Villagers earn income from cleared invasives, such as using the bark of *Acacia* for baskets.

Preston says WfW has "made science relevant to poor people," but that was only possible by making the program relevant to the new government. WfW has managed to win steady funding on the argument that ripping out water-slurping invasive plants costs less than building reservoirs to augment water supplies. "Invasive plants have a massive impact" on water levels, soaking up 7% of mean annual runoff water, Preston says. If left uncontrolled, research indicates, invasives could soak up 20%.

CREDITS (TOP TO BOTTOM): WORKING FOR WATER

Published by AAAS

Long, hard slog. WfW workers clear invasive hyacinths from the Queen's River in eastern South Africa.

Buttressing that argument, scientists at South Africa's Council for Scientific and Industrial Research used field-mapping, biomass, and catchment studies to estimate that alien plants had invaded about 10 million hectares and consumed 3.3 billion cubic meters of water per year—about 75% of the volume of one of South Africa's largest river systems. "Alien plant control is expensive," the council concluded in its 2000 report, but "control programs are cost-effective compared with alternative water-supply schemes."

Weed-whacking writ large was only part of the solution. WfW also had to face down tree plantation companies. With prodding from WfW, the government, and the Forestry Stewardship Council, plantations were persuaded to remove some trees in riparian, wetland, and upper catchment areas and pay fees to offset the value of water their trees absorb.

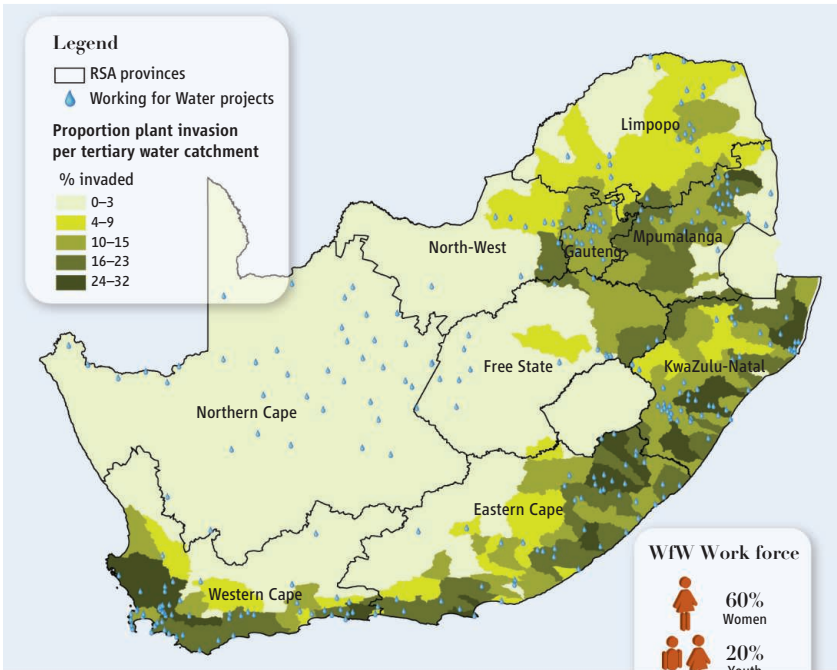

Battle lines drawn. Invasive species have dug in along South Africa's coast and in its northeastern interior; WfW has enlisted a diverse demographic profile to fight the scourge (*inset*).

Invasive marathon

Restoring natural ecosystems after an alien invasion is "an ultralong-distance race," Preston says. How that race is run depends on landscape, climate, the alien species, and the available native seed bank.

One common approach called "fell and remove" involves cutting down, weeding out, or burning alien species. Restorers assume that the indigenous seed bank will survive and the native plants will regrow. "In most cases, there are enough seeds of native species in the area to replace invasive plants that were removed," Preston says. Sometimes, however, reseeding of native species is necessary. That was the case in restoring the native fynbos ecosystem, a highly diverse mix of heath and shrubland plants in the Table Mountain range where intense fires roasted indigenous seeds.

Even areas cleared of invasives tend to revert. Invasive alien plant surveys by the Agricultural Research Council's Institute for Soil, Climate and Water in Stellenbosch have noted progress in some regions but accelerating invasions in others, primarily where clearing has not taken place (see map). "The fact that 9 million to 10 million hectares are currently invaded and under 1 million has been cleared means that more resources need to be allocated," says entomologist Dennis Rangi of the Commonwealth Agricultural Bureau International in Nairobi.

One challenge is that most invasive plant seed banks are healthy, allowing the aliens to grow back year after year. WfW sends out regular patrols to areas previously cleared by its shock troops to rip out return visitors. Another problem is that ridding an area of one invasive species can pave the way for another. After workers in 2004 cut down *Eucalyptus grandis* trees along the Sabie River, bugweed and a whole suite of other stubbier trees and shrubs sprouted in their place.

"Many invasives will quickly return unless the eradication effort is continued on a regular, or at least periodic, basis," says Jeffrey McNeely, chief scientist at the International Union for Conservation of Nature in Gland, Switzerland. Adds plant ecologist Mark Lonsdale of Australia's Commonwealth Scientific and Industrial Research Organisation: "You have to be strategic because of long-lived seed banks, regrowth, and re-encroachment."

That means WfW must grind on indefinitely to remain effective. "To the extent you can compel landowners to participate and shoulder the cost and generate revenue and indirect benefits from the project [as WfW has], you have something more sustainable," says Jeffrey Waage, an invasive-plant expert who directs the London International Development Center.

Water savings is not the only benefit from WfW: Clearing invasive plants from threatened habitats has also helped save some native insect species. Dense canopies of woody invasive plants provide more shade than dragonflies and damselflies are accustomed to, says entomologist Michael Samways of the University of Stellenbosch. As a result, Preston says, "over half of our endemic species of dragonflies and damsel flies were facing extinction" before WfW began. Recently, two species written off as extinct—the Ceres Stream damselfly and the Cape Bluet dragonfly—have been spotted near ponds purged of invasive trees. Getting rid of alien flora has "absolutely" benefited these insects, Samways says.

WfW has expanded its resources by partnering with provincial and local governments: Cape Town's municipal authority has taken over the Ukuvuka fire-restoration campaign in the Table Mountains, and KwaZulu-Natal province's Invasive Alien Species Programme is running the campaigns against pompom and other invasives.

Trying to extend its success to related areas of ecological restoration, WfW has spawned a trio of programs in South Africa with a narrower focus: Working on Fire, Working for Wetlands, and Working for Energy (using biomass to produce energy). A key link between the Water and Fire initiatives is that "some invasives burn at an intensity of 10 times or more the indigenous vegetation they displace," says Preston. He concedes that alien plants "are spreading and growing" in many regions where WfW has not had the resources to reach. Still, he says, "it's important to take action. It's like a cancer: What would happen if you do nothing?" **–ROBERT KOENIG**

SOURCE CREDIT: IAN KOTZE *ET AL.*

Published by AAAS

Addicted to Rubber

A rising tide of rubber plantations is eating away at Southeast Asian ecosystems. Can an ancient forest crop help wean the region off its monoculture habit?

Milking the cash crop. Rubbermakers tap latex in Xishuangbanna, China.

PHOTO CREDIT: CHARLES C. MANN

BAN NAMMA, LAOS—When the man from Huipeng Rubber visited, most of the village's men came to meet him. They hunkered down in sandals and worn T-shirts on the bare ground in front of the village headquarters, as the company agent, dressed in a sports coat, distributed cigarettes. Then the rep used a stick to sketch in the dirt the next step in the company's plan to remove 540 hectares (ha) of village forest and fields and replace them with rubber trees.

Ban Namma is at the edge of the Golden Triangle, the mountainous, thickly forested intersection of Laos, Myanmar (formerly Burma), and China. Long infamous for heroin, opium, and other poppy products, the region is now becoming known for another plant: *Hevea brasiliensis*, the Pará rubber tree. China has spread rubber across as much as 300,000 ha of Yunnan, replacing most of the southern province's lowland tropical forest. But now the nation is running out of land warm and wet enough for *H. brasiliensis*. In response, according to a 2008 report by economist Weiyi Shi for the German nonprofit development group GTZ, smallholders with Chinese connections and, more recently, Chinese companies have begun to clear large swaths of Laos for rubber. A single holding company, China-Lao Ruifeng Rubber, plans to cut and plant 300,000 ha; a second company, Yunnan Rubber, plans to convert 167,000 ha. As the tide of rubber sweeps from China into Laos, says Tang Jianwei, an ecologist at Yunnan's Xishuangbanna Tropical Botanical Garden (XTBG), the entire region is being transformed into an "organic factory"—with alarming environmental consequences.

Natural rubber is found suspended as minute particles in latex, a saplike substance made in hundreds of plants. Only a few, though, produce rubber suitable for human use, and the most important by far is the Amazonian tree *H. brasiliensis*. Rubbermakers tap the trees and—in a process reminiscent of making maple syrup—boil down the latex to draw out rubber. A problem, say ecologists, is that large-scale latex extraction is draining the water table in Yunnan's southern foothills. "Already, streams are running dry," Tang says. "Villages are being forced to move because they've lost their water supply."

Also alarming, rubber trees in China and Laos are mainly drawn from a small pool of parent stock, which means that their genetic diversity is low. In the 1930s, Henry Ford created huge rubber plantations in the lower Amazon, part of *H. brasiliensis*'s home range, only to have them wiped out by a fungal disease, South American leaf blight (*Microcyclus ulei*). Studies have indicated that Asian rubber plantations, including those in China and Laos, are vulnerable to leaf blight. In the age of jet travel, the fungus should eventually find its way to Asia. "An outbreak could effectively strip the forest bare," says Horst Weyerhaeuser of the National Agriculture and Forestry Research Institute in Vientiane, Laos. "It would take years—maybe decades—to recover."

Putting the brakes on *H. brasiliensis* will not be easy. Southern Yunnan has vastly profited from its production; in a 2006 XTBG study,

rubber sales increased one typical township's income almost 10-fold between 1988 and 2003. The region will continue to benefit; some forecasters believe that by 2020, global demand for natural rubber will outpace supply by as much 1.4 million metric tons (MT). (Total 2008 consumption was 9.9 million MT, according to the International Rubber Study Group.)

Rubber in the Golden Triangle has been a classic standoff between economics and ecology: Monocultural plantations are so much more profitable than any other lawful agricultural system in these hills that they have inevitably prevailed, no matter the environmental cost. But in a forthcoming article, Nicholas Menzies of the Asia Institute at the University of California, Los Angeles, argues that at least some smallholders have found out how to both make a living and restore forests to a healthier state. Surprisingly, their way forward is a return to one of the region's most ancient products: tea. Not only that, they are growing tea in a way that until recently was derided as backward and inefficient—in the forest, under the canopy of larger trees.

"Tea forests aren't pristine tropical ecosystems," Menzies says. "But they are far more diverse—and probably far more stable—than gigantic monocultures of rubber."

Rubber bandwagon

Although synthetic rubber has existed since World War I, natural rubber is superior—and much cheaper—for high-stress purposes. Only natural rubber can be steam-cleaned in a medical sterilizer, then thrust into a freezer—and still adhere flexibly to glass and steel. Jet and truck tires are almost entirely natural rubber. Militaries are major rubber consumers—which is why the United States imposed a rubber blockade on China during the Korean War. The blockade helped persuade the Chinese to prioritize growing rubber in 1951. Among the few areas in the nation warm enough for this tropical species is Xishuangbanna prefecture, at the southern tip of Yunnan.

Xishuangbanna prefecture has long been China's most biologically diverse area. Although it comprises just 0.2% of the nation's landmass, it contains 25% of its higher plant species, 36% of its birds, and 22% of its mammals, report biologists at Yunnan's Kunming Institute of Ecology. In the 1950s and 1960s, the People's Liberation Army turned this richly forested area into a rubber haven. The plantations became, in effect, army bases; labor was provided by more than 100,000 workers, many of them urban students. As the Cultural Revolution ground on, student workers were awakened every day at 3:00 a.m. and sent to clear the forest, one recalled to anthropologist Judith Shapiro, author of *Mao's War Against Nature*: "Every day, we cut until 7:00 or 8:00 a.m., then ate a breakfast of rice gruel sent by the [Yunnan Army] Corps kitchen. We recited and studied Chairman Mao's 'Three Articles' and struggled against capitalism and revisionism. Then it was back to work until lunch break, then more work until 6:00. After we washed and ate, there were more hours of study and criticism meetings."

Scoffing at botanists' admonitions as counterrevolutionary, the youths repeatedly planted rubber trees at altitudes where the trees were killed by storms and frost. Then they planted them again in the same locations—socialism would master nature, they insisted. The frenzy laid waste to parks, exacerbated erosion, and destroyed streams. But it didn't yield much rubber.

When China began its economic reforms in the late 1970s, the educated young people fled back to their home cities, precipitating a severe rural labor shortage. Yunnanese villagers were finally permitted to establish rubber farms. Between 1976 and 2003, the area devoted to rubber expanded 10-fold, shrinking tropical montane forest in that time from 50.8% of the prefecture to 10.3% as Xishuangbanna planters learned how to adapt to hostile conditions at the edge of rubber's geographic range. According to Hu Zhouyong of the Tropical Crops Research Institute in Jinghong, the prefecture capital, the relatively cold climate forces them to select for exceptionally robust trees. "Xishuangbanna is ahead of everywhere else in the world in terms of productivity," Hu says.

Even as China became the world's biggest rubber consumer, its rubber producers were running out of space. They began to eye Laos, which has about 6 million people in an area the size of the United Kingdom. A few villages in northern Laos had begun planting on their own as early as 1994. But the real push didn't begin until the end of the decade, when China announced its "Go Out" (*zou chu qu*) strategy, which pushed Chinese companies to invest abroad. Beijing had already changed the old military farms into private enterprises—corporations with abundant clout. As part of Go Out, the central government announced that it would treat rubber-growing in Laos and Myanmar as an opium-replacement program, making the former Yunnan military farms eligible for subsidies: up to 80% of initial costs for companies to grow rubber across the border, as well as the interest on loans and exemption from most tariffs for imported rubber.

Companies and smallholders flooded across the border. Most northern Laotian villagers live in hamlets without electricity or running water; schools and hospitals are a distant dream. Seeing a chance to improve their material conditions, villagers jumped on the rubber bandwagon, cutting deals with Chinese companies and farms. "In China, they were as

Where the rubber meets the land. Morning fog hangs over a hillside cleared for rubber in Laos's Luang Namtha Province (*right*). Fog dissipates earlier in the day than in the past in the Golden Triangle, altering the area's hydrology. Young rubber trees in Xishuangbanna (*left*).

CREDITS (LEFT AND RIGHT): CHARLES C. MANN

Published by AAAS

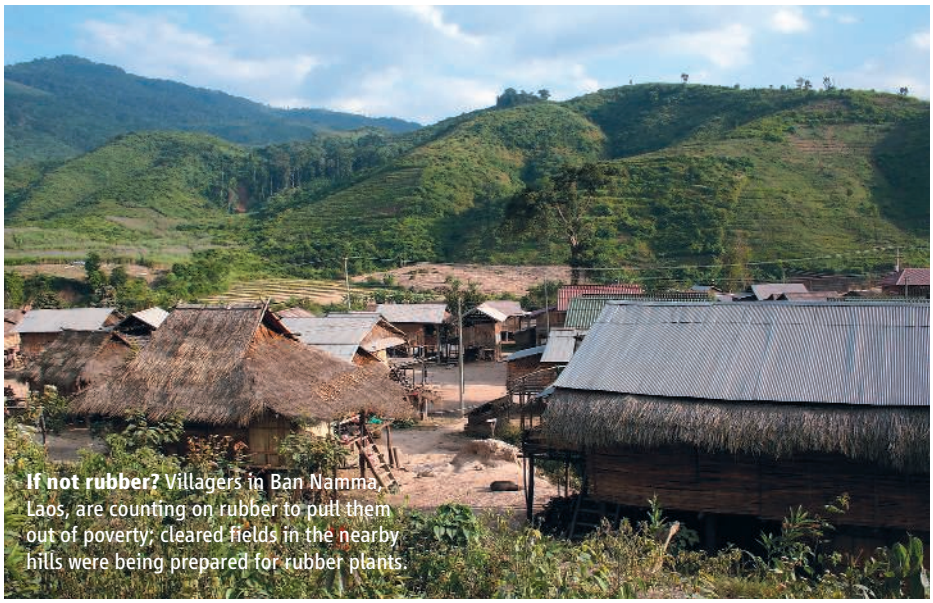

If not rubber? Villagers in Ban Namma, Laos, are counting on rubber to pull them out of poverty; cleared fields in the nearby hills were being prepared for rubber plants.

poor as us," the village head of Ban Namma told *Science*. "Now they are rich—they have motorcycles and cars—because they planted rubber. We want to have the same."

Partly backed by funds for opium eradication, Chinese investors provided Lao farmers with seeds, fertilizer, and training for growing cash crops. "The most important by far was rubber," says Jefferson Fox of the East-West Center in Honolulu, who is working with colleagues to evaluate rubber's impact in Southeast Asia. "It just exploded."

According to anthropologist Yayoi Fujita of the University of Chicago in Illinois, in 2003 rubber covered about 1 square kilometer in Laos, all near the border. It covered 45 km^2 in 2006. The Laotian government has estimated that by 2010, rubber will cover 1800 km^2 of the nation. Although the global economic crisis has slowed the pace of clearing, most researchers believe it will accelerate in the long run—along with the ill effects of that clearing.

Rubber, hit the road?

Although the Golden Triangle receives as much as 254 cm of rain a year, three-quarters of it falls between May and October. The rest of the year the forest survives largely on dew from morning fog. "Back in the 1980s and 1990s, there was still fog at lunchtime," says XTBG ecologist Tang. "Now it's gone by 11:00"—a symptom, he says, of a profoundly altered hydrological regime.

Tang and others blame rubber. In 2006, XTBG ecologist Wu Zhaolu and colleagues from Yunnan University and Xishuangbanna National Nature Reserve showed that converting tropical forest to rubber plantations increased surface water runoff by a factor of 3—which in turn jacked up soil erosion by a remarkable factor of 45.

The greatest effect may be underground. *H. brasiliensis* usually sheds its leaves in February, and new leaves begin budding in late March, at the peak of the dry season. The leaf loss means that the forest has lower albedo and fewer surfaces to retain dew. To propel growth, according to a 2007 study, the roots suck water from 1 to 2 meters below the surface. Tapping begins as new leaves appear and continues until they fall. To replace lost latex, the roots suck up still more water—annually, roughly 5000 kilograms per hectare, according to XTBG estimates. The result is to lower the region's water table. Rubber, Wu and colleagues argue, is making the forest both gather less moisture from the air and lose it—and soil nutrients—more quickly.

Beginning to heed ecologists' worries, Xishuangbanna effectively banned new rubber planting in 2006 by freezing all land rotation. The scheme is unlikely to have much effect, Shi notes, as it seems to violate China's newly reformed land laws. But even if Xishuangbanna farmers were to stop planting *H. brasiliensis* tomorrow, its area would keep rising as rubber trees invade remaining forest (*Science*, 21 March 2008, p. 1604).

Rubber's economic benefits may offset the ecological risks—but not if leaf blight arrives. Because rubber trees are grafted from high-yielding specimens, the great majority of plantation trees are clones. But as the area of rubber increases, it becomes an increasingly inviting target for *M. ulei*. For a century, isolation has spared rubber plantations, but a recently opened highway now links Singapore and Kunming, Yunnan's capital. If and when *M. ulei* appears, this corridor will provide transportation.

In the rubber tree's native Brazil, diversity protects the species from leaf blight; *H. brasiliensis* is usually widely dispersed throughout the forest, surrounded by other tree species. Ecologists have long argued that the best way to protect rubber plantations is to situate them in a larger, more diverse forest. That would require persuading some rubber planters to turn to something else.

Menzies argues for an alternative to monoculture plantations as a cash crop in these areas. In a forthcoming article in *The Social Life of Forests*, the proceedings of a May 2008 restoration conference, Menzies notes that Xishuangbanna was until recently best known for "big-leaf" tea (*Camellia sinensis var. assamica*), of which the most famous variety is pu-er. When the Communist era began, farmers were pushed into "people's communes" and instructed to create massive monocultures of short, clipped bushlike tea plants on terraces. Traditional methods were dismissed as primitive and backward.

Beginning in the 1990s, Menzies says, upscale tea fanciers, lured by tales of old-style pu-er tea, have sought out the remnants of ancient plantations of tea trees. Farmers have rebuilt them, creating a new market for what high-end merchant Peet's sells as "ancient trees organic pu-erh." The price of shade-grown tea rose from about 20 yuan per kg in the early 1990s to 1200 yuan (about $175) per kg in 2007, Menzies says.

Because forest tea is grown beneath a variety of other trees, it promotes more tree diversity than a typical tea or rubber plantation. And because it grows relatively tall, it can tolerate more understory plants than a monoculture, which is generally kept as free as possible of other plants.

Neither the central government nor Yunnan authorities have endorsed shade-grown tea as an alternative to monoculture plantations. Moreover, Menzies cautions, *C. assamica* cannot grow at very low altitudes, which means that tea could not be readily substituted for rubber across the lowlands. But in his view, "the rise of green markets and niche markets shows that traditional methods can economically compete with intensive, high-volume production." Tea is not a perfect replacement for rubber, Tang agrees. Still, he says, "every tea plant in the forest is one less rubber tree." **–CHARLES C. MANN**

With reporting by Josh D'Aluisio-Guerrieri.

CREDIT: CHARLES C. MANN

PERSPECTIVE

Ecological Restoration in the Light of Ecological History

Stephen T. Jackson[1]* and Richard J. Hobbs[2]*

Ecological history plays many roles in ecological restoration, most notably as a tool to identify and characterize appropriate targets for restoration efforts. However, ecological history also reveals deep human imprints on many ecological systems and indicates that secular climate change has kept many targets moving at centennial to millennial time scales. Past and ongoing environmental changes ensure that many historical restoration targets will be unsustainable in the coming decades. Ecological restoration efforts should aim to conserve and restore historical ecosystems where viable, while simultaneously preparing to design or steer emerging novel ecosystems to ensure maintenance of ecological goods and services.

> "[Nature] is ever shaping new forms: what is, has never yet been; what has been, comes not again." –Johann Wolfgang von Goethe, 1783, *On Nature* (*1*)

Ecological restoration is rooted in ecological history. To facilitate the recovery of degraded or damaged ecosystems, knowledge of the state of the original ecosystem and what happened to it is invaluable. However, systematic monitoring of ecosystems, whether deeply degraded or nearly pristine, rarely spans more than the past few decades. Restoration ecologists are forced to assess ecological history by indirect means, ranging from documentary sources (e.g., written descriptions, historical photographs, maps, and paintings) to paleoecological records from natural archives (e.g., tree-rings, rodent middens, and sediments of lakes, peatlands, oceans, and estuaries). Fortunately, both documentary and natural archives can provide records of environmental variables and ecosystem properties in many parts of the world.

Restoration ecology looks to ecological history as a means of identifying appropriate restoration targets—the state of the ecosystem before disruption—and assessing sources of damage (e.g., fire suppression, acid rain, and cultural eutrophication). Restoration targets in the "New Worlds" of the Americas, Australia, and Oceania are identified as the "natural" states existing at the time of European discovery and conquest, that is, just before disruptions associated with land clearance, agriculture, grazing, and wildfire control. Ecological history plays a straightforward role in these applications in identifying the natural state of the landscape and constituent ecosystems (*2*–*4*), including the range of variability in disturbance and other properties (*5*–*7*).

Deeper consideration of ecological history is leading to revision of this approach. First, the notion of "natural" is being redefined based on increasing awareness that pre-European native cultures often exerted substantial influence on ecosystems, from simple hunting/harvesting to fire management and direct vegetation alteration (*8*–*11*). The nature, duration, and intensity of these impacts varied widely in space and time (*10*, *12*), but few terrestrial or estuarine ecosystems escaped some effects of human activity. Second, climate has changed in the past 500 years, owing to natural causes and more recently to human activities (*13*). For many ecosystems, restoration to a historic standard is anachronistic. The environment has drifted, and so too have the targets. Ecosystems of even the recent past may be unsustainable under an early 21st-century climate. Finally, human activities leave ecological legacies that may be difficult or impossible to override in restoration. These legacies include extinctions (moas, mastodons) and industrial activities (brownfields, minelands). Moreover, more subtle human imprints are being revealed, including the *terra preta* soils of the pre-Columbian Amazon (*12*) and soil-nutrient mosaics dating to 17th- to 19th-century English settlers in Massachusetts and 2nd- to 3rd-century Roman settlers in France (*14*, *15*). For many parts of Europe, Asia, and Africa, undisturbed landscapes are too remote in time to provide restoration targets, which may instead comprise cultural landscapes (*16*, *17*).

Despite these complications, predisturbance restoration targets remain worthy goals in many contexts. A key task for the future will be to determine where this remains viable and, conversely, where alternative targets must be considered. Historical studies will remain valuable in determining ecosystem structure and function before disruption (*2*–*5*) and in assessing the nature and timing of ecosystem responses to disruptions (*4*–*9*, *18*–*20*). Paleoecology, together with observational, experimental, and modeling studies, can identify factors that prevent spontaneous or assisted ecosystem recovery once the obvious factors have been eliminated or mitigated.

Paleoecological and paleoenvironmental records spanning the last 10,000 to 20,000 years are now available for much of the globe, most densely in glaciated terrain but also in many other regions (*21*, *22*). These records provide important perspectives for restoration, not all of them comforting. First, environmental and ecological changes are normal; perhaps the most natural feature of the world in which we find ourselves is its continual flux. The past 20,000 years witnessed a transition from a glacial to an interglacial world, with numerous climatic excursions throughout. Few major terrestrial ecosystems have existed in situ for more than the past 12,000 years (*23*, *24*), and most are considerably younger, some arising only within the past few centuries (*24*). Every terrestrial locale has been occupied by a series of ecosystems—often contrasting in structure and function—since the

Fig. 1. The Big Woods (Minnesota) landscape, dominated by mesic forest, was savanna and prairie until about 1300 C.E., when droughts and consequent fine-fuel reduction led to reduction of surface fires, allowing tree invasion and expansion (*27*). [Photo: S. T. Jackson]

[1]Department of Botany and Program in Ecology, University of Wyoming, Laramie, WY 82071, USA. [2]School of Plant Biology, University of Western Australia, Crawley, WA 6009, Australia.

*To whom correspondence should be addressed. E-mail: Jackson@uwyo.edu (S.T.J.); rhobbs@cyllene.uwa.edu.au (R.J.H.)

last glacial period. In the long run, no inherent natural ecosystem or landscape configuration exists for any region. Second, a multitude of ecological realizations arise and dissolve as the environment changes. Different species assemblages develop, leading to ecosystems with differing structure and function. The late-glacial "no-analog" communities—assemblages of plants, vertebrates, and insects with no modern counterpart—are the most dramatic example, but community assembly and disassembly are characteristic of the entire Quaternary (*25*). Third, the paleoecological record provides numerous case studies of multiple, alternative "natural" states, owing to historical contingencies affecting species migration, site colonization, and extirpation (*26*). These cases are not always subtle, involving contrasting ecosystems (forests, grasslands, woodlands, and steppe) (Fig. 1) (*26*, *27*).

These observations have the potential for setting restoration ecology adrift from its moorings in notions of objectively identifiable natural states of ecosystems. If natural states are elusive, if the environment is always changing and ecosystems are always coming and going, and if multiple realizations are normal, then the premises underlying ecological restoration to a historic standard come under question. Does ecological history render ecological restoration "quaint"?

Ecological restoration finds new moorings in emphasizing restoration of ecosystem function, goods, and services. Restoration ecologists increasingly recognize the ongoing and often inevitable development of novel ecosystems, resulting from species invasions, climate change, land-use legacies, and altered biogeochemical cycles (*28*, *29*). Restoration efforts emphasize managing for change, which is accepted as inevitable, and interventions are directed toward ensuring that desirable ecological goods and services, including aesthetic values, are maintained (*7*, *30*).

The paleoecological record gives restoration ecologists permission to accept environmental and ecological change and to intervene in ways that will foster biodiversity and vital ecosystem functions. In many cases, this will lead to ecosystems unlike those of the past (*7*, *25*, *28*). Restored ecosystems may have combinations of species that have never cooccurred. Many such ecosystems will be contingent not only on scientific and societal judgments but also on particular combinations of climate events, disturbances, extinctions, and immigrations (*26*). As artificial or capricious as these ecosystems may seem, they must be embraced insofar as environmental change is inevitable, multiple ecological realizations are natural, and contingencies and legacies are embedded in virtually all natural ecosystems.

Even in the face of inevitable environmental change and ecological novelty, efforts to conserve and restore historical ecosystems should be continued and even accelerated in the immediate future. This presents a seeming paradox, given the increasingly anachronistic nature of historical targets. However, preventing damage is more cost effective than trying to repair damage. Furthermore, our understanding of historic ecosystems is typically far greater than for most novel or engineered systems. An unstated aim in restoration is to avoid creating bigger problems than those we seek to solve. Short-term targets of known, historic ecosystems may minimize the risk of making things worse. Restoration efforts might aim for mosaics of historic and engineered ecosystems, ensuring that if some ecosystems collapse, other functioning ecosystems will remain to build on. In the meantime, we can continue to develop an understanding of how novel and engineered ecosystems function, what goods and services they provide, how they respond to various perturbations, and the range of environmental circumstances in which they are sustainable (*28*, *29*).

Clearly, rapid environmental change renders these tasks daunting, and a major challenge for ecologists is to develop effective means of assessing the status of, and prognosis for, ecosystems in varying states of alteration (Fig. 2). Which historic ecosystems provide viable targets? Under what circumstances will combined forces of climate change, invasive species, and other global-change elements require that alternative ecosystems be considered? Can we develop the tools and wisdom to support these decisions?

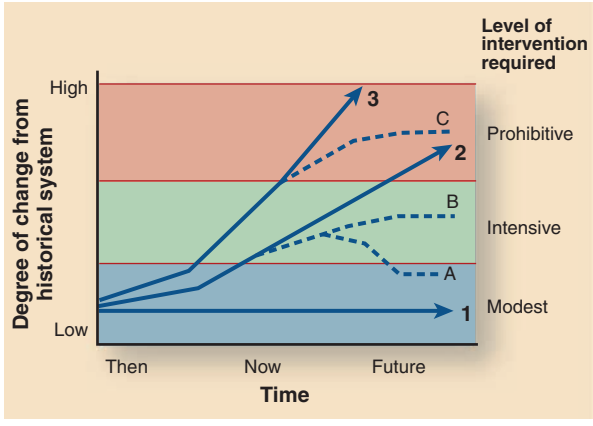

Fig. 2. Contrasting ecosystem trajectories from historic through present to future configurations, indicating degree of change from the historic ecosystem (e.g., physical environment and species pool). Trajectories 1 to 3 indicate systems in three different states today: relatively unchanged (1), moderately altered (2), and severely altered (3). Colored bands indicate costs of restoration to the approximate historic state. Dotted lines represent realistic interventions for each trajectory; pursuit of A is more difficult and expensive than B. For trajectory 3, the only viable option is to slow the rate of change and direct the system to maintain or improve its value in terms of ecosystem services (C). Paleoecology can help assess viability of different levels of intervention by identifying historical states and their range of variability, determining how far existing systems have drifted from these historic states, assessing the thresholds between required levels of intervention, and guiding design of novel and sustainable ecosystems capable of providing ecological goods and services.

Paleoecology will play important roles in all of these efforts. Paleoecological and paleoenvironmental studies inform our understanding of existing and historical ecosystems, determining the circumstances under which they arose, gauging the range of environmental variability they have experienced, and identifying environmental thresholds at which they will require different levels of intervention. By integrating the "reverse monitoring" of paleoecology with conventional "forward monitoring" and targeted experiments, we can diagnose the point(s) at which existing ecosystems will be unsustainable. At the same time, paleoecological studies will continue to reveal past ecosystem realizations and their properties at local, regional, and global scales. Paleoecological insights, together with modeling, experimentation, and observation, will advance our capacity to engineer ecosystems successfully. Obviously, the more time we purchase by slowing the rates of global change in all its dimensions, the more we increase our capacity for successful adaptation. We face serious risk that global change will outpace our scientific capacity to prescribe adaptive strategies, let alone implement them.

References and Notes

1. Translation by T. H. Huxley, *Nature* **1**, 9 (1869).
2. E. Gorham, L. Rochefort, *Wetlands Ecol. Manage.* **11**, 109 (2003).
3. D. A. Burney, L. P. Burney, *Front. Ecol. Environ* **5**, 483 (2007).
4. D. A. Willard, T. M. Cronin, *Front. Ecol. Environ* **5**, 491 (2007).
5. T. W. Swetnam, C. D. Allen, J. L. Betancourt, *Ecol. Appl.* **9**, 1189 (1999).
6. G. Motzkin, D. Foster, in *Forests in Time*, D. R. Foster, J. D. Aber, Eds. (Yale Univ. Press, New Haven, CT, 2004).
7. C. I. Millar, N. L. Stephenson, S. L. Stephens, *Ecol. Appl.* **17**, 2145 (2007).
8. D. M. J. S. Bowman, *New Phytol.* **140**, 385 (1998).
9. J. B. C. Jackson *et al.*, *Science* **293**, 629 (2001).
10. T. R. Vale, Ed., *Fire, Native Peoples, and the Natural Landscape* (Island Press, Washington, DC, 2002).
11. B. A. Black, C. M. Ruffner, M. D. Abrams, *Can. J. For. Res.* **36**, 1266 (2006).
12. M. B. Bush, M. R. Silman, *Front. Ecol. Environ* **5**, 457 (2007).
13. E. Jansen *et al.*, in *Climate Change 2007: The Physical Science Basis*, S. Solomon *et al.*, Eds. (Cambridge Univ. Press, Cambridge, 2007).
14. D. Foster *et al.*, *Bioscience* **53**, 77 (2003).
15. E. Dambrine *et al.*, *Ecology* **88**, 1430 (2007).
16. G. F. Peterken, *Glob. Ecol. Biogeogr.* **8**, 321 (1999).
17. Z. Naveh, *Restor. Ecol.* **13**, 228 (2005).
18. D. E. Schindler, R. A. Knapp, P. R. Leavitt, *Ecosystems* **4**, 308 (2001).
19. C. L. Schelske *et al.*, *Ambio* **34**, 192 (2005).
20. F. M. Chambers, D. Mauquoy, E. W. Cloutman, J. R. G. Daniell, P. S. Jones, *Biodivers. Conserv.* **16**, 2821 (2007).
21. National Oceanic and Atmospheric Administration, National Climatic Data Center, Paleoclimatology, www.ncdc.noaa.gov/paleo/paleo.html.
22. Neotoma Paleoecology Database, www.neotomadb.org.
23. J. W. Williams, B. Shuman, T. Webb III, P. J. Bartlein, P. L. Leduc, *Ecol. Monogr.* **74**, 309 (2004).
24. S. T. Jackson, *J. Veg. Sci.* **17**, 549 (2006).

25. J. W. Williams, S. T. Jackson, *Front. Ecol. Environ* **5**, 475 (2007).
26. S. T. Jackson, J. L. Betancourt, R. K. Booth, S. T. Gray, *Proc. Natl. Acad. Sci. U.S.A.* 10.1073/PNAS.0901644106 (2009).
27. B. Shuman, A. K. Henderson, C. Plank, I. Stefanova, S. S. Ziegler, *Ecology* **90**, 2792 (2009).
28. R. J. Hobbs *et al.*, *Glob. Ecol. Biogeogr.* **15**, 1 (2006).
29. T. R. Seastedt, R. J. Hobbs, K. N. Suding, *Front. Ecol. Environ* **6**, 547 (2008).
30. R. J. Hobbs, V. A. Cramer, *Annu. Rev. Environ. Resour.* **33**, 39 (2008).

31. R. H. W. Bradshaw, W. K. Lauenroth, J. A. Lockwood, J. McLachlan, J. T. Overpeck, W. A. Reiners, D. Sax, and J. W. Williams provided discussion and asked difficult questions.

10.1126/science.1172977

PERSPECTIVE

Species Invasions and the Limits to Restoration: Learning from the New Zealand Experience

David A. Norton

Species invasions impose key biotic thresholds limiting the success of ecological restoration projects. These thresholds may be difficult to reverse and will have long-term consequences for restoration because of invasion legacies such as extinctions; because most invasive species cannot be eliminated given current technology and resources; and because even when controlled to low levels, invasive species continue to exert substantial pressure on native biodiversity. Restoration outcomes in the face of biological invasions are likely to be novel and will require long-term resource commitment, as any letup in invasive species management will result in the loss of the conservation gains achieved.

Recent theoretical advances have emphasized thresholds and alternative stable states as key drivers influencing the outcomes of ecological restoration (*1*). One consequence of these emerging perspectives is the recognition that restoration must address not only the degrading factors but also the altered feedbacks that lead to self-perpetuating novel ecosystems—ecosystems that are different from those that would have existed before human impacts, especially as the impacts of climate change increasingly alter biotic interactions (*2*). The importance of addressing abiotic thresholds in restoration, such as those associated with changes in soil or water conditions, is widely recognized (*1*). Although some biotic thresholds can be easier to address than abiotic thresholds (*3*), biotic thresholds resulting from species invasions are likely to be difficult to reverse and have long-term consequences for restoration projects. Biological invasions can be both the cause of degradation (for example, through predation on native species) and the driver of ecosystem change during restoration (through altering the abundance of resident species or through the establishment of new species), and can result in irreversible changes in ecosystem composition and structure. As a result, the control of invasive species is a key focus of many ecological restoration projects (*4*).

Here I explore how species invasions can impose biotic thresholds limiting the success of ecological restoration projects. I use New Zealand as a case study because the impacts of biological invasions are particularly pronounced as a result of the archipelago's isolation, high endemism, and recent human settlement (within the past 700 to 800 years). New Zealand highlights the many challenges that biological invasions present both to other islands and increasingly to continental areas. At least 30 mammals, 34 birds, 2000 invertebrates, and 2200 plants are fully naturalized in New Zealand (*5*). Although control of these species is the major focus of ecological restoration, eradication is usually not possible except on some offshore islands or within fenced enclosures, and invasive species management therefore needs to be ongoing (*4*). Furthermore, control or eradication is usually able to target only a subset of invasive species (primarily mammalian predators and some plants), while others are left largely unmanaged (such as invasive birds or invertebrates).

A key consequence of biological invasions, especially on islands, has been the reduction in the abundance of, and in some cases the extinction of, resident biota (*6*). The long-term implications of this are poorly understood but are likely to be important for a range of ecological processes, including reproductive mutualisms (*7*). For example, large-fruited plants (>1 cm in diameter) in New Zealand, including some dominant forest canopy trees (Fig. 1), are now reliant on one avian disperser, the kereru (*Hemiphaga novaeseelandiae*). Other potential dispersers are either very rare or extinct [including the moa (Dinornithidae)] because of predation by invasive mammalian carnivores (*8*), and no invasive birds are capable of dispersing the fruit of these trees. Kereru themselves are far less abundant today than they were historically. Reduced dispersal is likely to result in long-term shifts in forest canopy composition. From a restoration perspective, it is clear that even with control of mammalian predators, the future composition of New Zealand forests will be different from that before invasion.

The need for intensive mammalian pest control in New Zealand is well supported by numerous examples contrasting the survival of indigenous biota in areas with and without such control (*5*). However, the impacts of animal pests may not be reversible, even when they are controlled to very low densities. For example, red deer (*Cervus elaphus scoticus*) are widely dispersed through native forests and have a strong negative influence on

Fig. 1. Forest canopy trees such as *Beilschmiedia tawa* are dependent on kereru (*H. novaeseelandiae*) for dispersal of their large (>1.4 cm in diameter) fruits, because other potential dispersers are extinct or very rare. [Photos: D. Norton and A. McIntosh]

Rural Ecology Research Group, School of Forestry, University of Canterbury, Private Bag 4800, Christchurch 8140, New Zealand. E-mail: david.norton@canterbury.ac.nz

populations of understory plants. Seedling growth is often very slow, and even at low densities, deer prevent regeneration because they consume almost all seedlings of preferred species that are present within the browse layer (*9*). As a result, reducing deer numbers, even to low levels, will not necessarily result in the restoration of pre-disturbance conditions. Changes in the abundance of seed dispersers will also limit restoration success in these forests, even if the elimination of deer were possible, because severely depleted plant species may not be able to reestablish themselves.

Invasive plants are very prevalent in New Zealand ecosystems. Although many naturalized plants appear to be having little obvious impact on native biodiversity, some present substantial challenges for restoration and limit the ability of restoration projects to achieve desired outcomes. Of particular concern are a suite of invasive grasses (such as *Dactylis glomerata*, *Bromus* spp., *Festuca rubra*, and *Holcus lanatus*) and forbs (such as *Echium vulgare*, *Hieracium* spp., and *Trifolium* spp.) that are now widespread through open communities (such as herbfield, grassland, and shrubland). An absence of natural enemies and adaptation to anthropogenic disturbances, including grazing, have favored these species. The long-term survival of native species such as the endangered limestone wheatgrass (*Australopyrum calcis*), which grows in naturally open sites associated with limestone outcrops, is seriously compromised by competition with these invasive plants (*10*). The restoration of open communities is very difficult without ongoing human intervention to control invasive plants and/or to establish seedlings of native plants. Even when native species have been established, further intervention will be required to ensure ongoing recruitment.

Fig. 2. Seedling of the native forest tree *Pittosporum eugenioides* regenerating under a canopy of the invasive woody weed gorse (*U. europaeus*) that has become established on abandoned farmland. As the gorse senesces, native forest species will replace it, although the subsequent forest composition may be different from that which develops through a succession dominated by native successional species. [Photo: D. Norton]

Some invasive species can play positive roles in restoration, although they may lead to unexpected outcomes. For example, the European legume gorse (*Ulex europaeus*) acts as a nurse plant for native forest regeneration in many areas of New Zealand, because it readily invades old fields once livestock grazing has been removed. Gorse shades out the invasive grass sward, creating suitable microsites for the regeneration of native woody species (Fig. 2). However, plant succession under gorse follows a different trajectory from that occurring under the native seral species kanuka (*Kunzea ericoides*), at least during the early stages of forest development, with a lower species richness of native forest species and an absence of some native species that are present in comparable kanuka successions (*11*). Furthermore, gorse-dominated successions are more invaded by bird-dispersed exotic woody plants than are kanuka-dominated successions.

Management responses to deal with the threats posed by invasive species present a number of challenges that need to be addressed if restoration is to be successful. Livestock exclusion is actively undertaken as part of restoration projects. However, livestock removal can have undesired outcomes; simply removing browsing animals may not solve the problem. For example, livestock exclusion was implemented to restore habitat for the threatened Whitaker's skink (*Cyclodina whitakeri*) at its last mainland site. However, monitoring over the following 22 years showed that this skink declined from 0.01 skinks per trap night (1984–1989) to 0.0005 skinks per trap night (2000–2006). Removing grazing animals did not restore skink abundance as intended; instead, reduced grazing allowed introduced pasture grasses to proliferate, resulting in periodic rodent irruptions supporting a guild of other introduced mammalian predators, which in turn depleted the Whitaker's skink population (*12*). The removal of livestock grazing can also have unintended consequences for native plants. For example, although restoration of the critically threatened shrub *Olearia adenocarpa* and its habitat requires the removal of grazing by domestic and invasive mammals to enable remaining mature plants to survive, the removal of grazing pressure also results in invasive grasses and herbs preventing the establishment of new plants (*13*).

Ecological restoration is a critical tool for mitigating native biodiversity loss in the face of anthropogenic impacts. Although it might be possible to reverse many abiotic thresholds (for example, through reinstating a disrupted disturbance or hydrological regime), reversing biotic thresholds that have been crossed as a result of the impacts of invasive species is very difficult. This occurs because of legacies resulting from invasions (such as species extinctions); because even when controlled to low levels, invasive species still exert substantial pressure on native biodiversity; and because most invasive species cannot be eliminated with current technology and resources. In these situations, the future ecosystem condition even with restorative management will be different from that which would have occurred at the site had biological invasions not occurred. The New Zealand examples highlight the magnitude of the challenges that face ecological restoration anywhere in the face of biological invasions, challenges that are likely to be even greater when biological invasions are coupled with other drivers of ecosystem change (*14*, *15*).

Three general predictions can be made about the outcomes of restoration in ecosystems that have undergone substantial biotic change as a result of species invasion.

1) Outcomes will be novel in that the ecosystems resulting from restoration will contain species assemblages and interactions that are new for the site and will include exotic species.

2) With multiple species invasions, control or eradication of one or some species will not necessarily result in desired outcomes because of changes in interactions among other species.

3) Where eradication is not possible, restoration will require ongoing management of invasive species if specific outcome conditions are desired.

To be successful with ecological restoration, we must recognize the severe limitations that species invasions impose on achieving traditional restoration outcomes. Ecological restoration in the face of biological invasion needs to be adaptable in the manner in which it sets outcome targets. These might range from establishing areas where restoration involves intensive and ongoing pest management, including the use of predator-proof fencing, to accepting the idea that native species can be sustained within novel ecosystems that include a range of exotic species. However, underscoring all restoration work involving invasive species is the need to ensure that resources are available to enable the ongoing sustainability of the project. Ecological restoration in systems with invasive species involves long-term resource commitment. Any letup in invasive species control, especially of mammalian predators, will result in the restored ecosystem quickly reverting to a highly degraded state as exotic species increase in abundance and/or reinvade, with the conservation gains achieved quickly lost.

References and Notes

1. K. N. Suding, R. J. Hobbs, *Trends Ecol. Evol.* **24**, 271 (2009).
2. T. R. Seastedt, R. J. Hobbs, K. N. Suding, *Front. Ecol. Environ* **6**, 547 (2008).
3. V. A. Cramer, R. J. Hobbs, R. J. Standish, *Trends Ecol. Evol.* **23**, 104 (2008).
4. A. Saunders, D. A. Norton, *Biol. Conserv.* **99**, 109 (2001).
5. R. B. Allen, W. G. Lee, Eds., *Biological Invasions in New Zealand* (Springer Verlag, Berlin, 2006).
6. D. F. Sax, S. D. Gaines, J. H. Brown, *Am. Nat.* **160**, 766 (2002).
7. A. Traveset, D. M. Richardson, *Trends Ecol. Evol.* **21**, 208 (2006).
8. M. N. Clout, J. R. Hay, *N. Z. J. Ecol.* **12** (suppl.), 27 (1989).
9. D. A. Coomes, R. B. Allen, D. M. Forsyth, W. G. Lee, *Conserv. Biol.* **17**, 450 (2003).

10. B. P. J. Molloy, *N.Z. J. Bot.* **32**, 37 (1994).
11. J. J. Sullivan, P. A. Williams, S. M. Timmins, *N.Z. J. Ecol.* **31**, 22 (2007).
12. J. M. Hoare, L. K. Adams, L. S. Bull, D. R. Towns, *J. Wildl. Manage.* **71**, 1576 (2007).
13. P. B. Heenan, B. P. J. Molloy, *N.Z. J. Bot.* **42**, 21 (2004).
14. R. K. Didham, R. M. Ewers, N. J. Gemmell, *Science* **307**, 1412a (2005).
15. J. J. Hellmann, J. E. Byers, B. G. Bierwagen, J. S. Dukes, *Conserv. Biol.* **22**, 534 (2008).

16. I thank R. Didham, R. Hobbs, E. Laliberté, and the members of my graduate restoration ecology class for helpful comments and discussion on this article.

10.1126/science.1172978

PERSPECTIVE

Pollination and Restoration

Kingsley W. Dixon

Pollination services underpin sustainability of restored ecosystems. Yet, outside of agri-environments, effective restoration of pollinator services in ecological restoration has received little attention. This deficiency in the knowledge needed to restore pollinator capability represents a major liability in restoration programs, particularly in regions where specialist invertebrate and vertebrate pollinators exist, such as global biodiversity hotspots. When compounded with the likely negative impacts of climate change on pollination services, the need to understand and manage pollinator services in restoration becomes paramount.

Robust pollination services underpin the plant reproductive continuity of a restored ecosystem and rely on an understanding of how to support pollination processes and vectors after restoration activities. In agriculture and horticulture, the economic value of pollination is well recognized, with 75% of crop species and 35% of crop value dependent on pollination by animals (*1*, *2*). The importance of pollinators in agricultural production has been highlighted by the emergence of colony collapse disorder and varroa mite infestation in honeybee hives (*3*). This has led to remediation measures that include importation of hives from countries free of these disorders to use of electric vibrators to replicate buzz pollination in tomato crops.

Conversely, reestablishment of pollination services in restored native ecosystems is not well understood, yet biotically driven pollination services, particularly animal-based pollination services, sustain reproductive potential and genetic resilience in many ecosystems. To date, little has been done in the restitution of pollinator services in ecological restoration projects (*4*, *5*). This is despite a plea 10 years ago for fauna-mediated pollination services to be "…[reintroduced] as part of critical habitat management and restoration plans" (*6*). For example, due to a lack of pollination knowledge, one of Australia's largest urban woodland restoration programs at Kings Park and Bold Park in Perth, involving $5 million and reestablishment of 1 million plants, could not consider pollinator enhancement as part of the programs.

Specialist pollinators are often the first casualties when ecosystems degrade. However, the most pervasive ecosystem impact will arise from the loss of generalist pollinators (*7*–*9*), as witnessed with colony collapse disorder and honeybees. Similar pollination consequences will occur in natural and restored natural ecosystems if generalist pollination services are disrupted.

For the global biodiversity hotspots that represent 44% of the world's vascular plant species and contain most of the specialized plant-pollinator mutualisms and interactions (*10*, *11*), restoring pollination services may be critical for ensuring restoration success. However, with 60% of global landscapes disturbed by humans and at least 70% of the land area in the 25 biodiversity hotspots cleared, future restoration capability will depend on the ability of pollinators to migrate and establish across often highly fragmented habitat matrices. In such fragmented landscapes, nonflying or restricted-range pollinators, such as terrestrial mammals, lizards, and many invertebrates, are doomed as pollinators particularly when the alienated matrix is ecologically hostile. In these cases, highly specific and obligate pollination interactions are most at risk and likely to pose the greatest challenge to conservation biologists and restoration ecologists.

Only a handful of research papers specifically investigate pollination networks and persistence in the face of climate change (*7*, *8*), yet climate change represents a major threat to pollination services. Climate-change trends predict alteration in timing of greening, flowering and senescence, and overall shortening of the growing season (*12*), factors with direct impact on pollination mutualisms. However, climate change will also lead to a decrease in precipitation and a shift in seasonality of rainfall, particularly in mediterranean regions, resulting in reduced plant vigor, delayed plant maturation, and a decline in nectar production capacity, with potentially devastating effects on nectar-dependent mutualists.

In addition, global warming may lead to partial or total asynchrony between pollinator life cycles and flowering phenologies. In the case of obligate pollination systems, this may lead to a breakdown of pollination mutualisms (*13*, *14*). Both have important implications for restoration, where species mixes may need to source nonlocal native plant species from a climate zone that matches the predicted new climate regime at the target restoration site. Such actions would necessitate the careful consideration of the invasive potential of introducing such plant species.

Ecosystems with high levels of specialized plant-pollinator interactions present substantial risks in achieving restoration success. These are heightened when the associations involve mutual dependencies between pollinator and plant leading to coextinction (*15*)—the "buy one, get one free" phenomenon. In turn, decay or shifts in pollinator assemblages servicing a plant species can lead to undesirable consequences such as lowered seed set or increased inbreeding, as seen in some plant species (*16*, *17*). In cases of one-on-one commensal relationships, as found in orchids, extinction risks for the plant partner can be substantial. This is exemplified in sexually deceptive orchid-wasp relationships in the southwest Australian biodiversity hotspot where the first recorded orchid extinction for the region may be a direct result of habitat loss, altered fire regimes (e.g., prescribed spring burning), and/or pollinator loss (*18*). Conservation and restoration of these highly specialized pollinator associations will require detailed knowledge of the ecological requirements for both plants and their pollinators.

Though many factors will influence the capacity of pollinator guilds to become established in restored landscapes, there are continental-scale trends that provide some guidance for restoration practitioners. For example, plants in biodiversity hotspots are more likely to exhibit higher levels of pollinator specialization due to increased competition for pollinator services in species-rich plant communities (*19*), resulting in ecological restoration that may involve specialized, obligate, and potentially unrecoverable pollinator associations. In the case of Southern Hemisphere continents, nonspecialist-to-specialist vertebrate pollination occurs along a continental gradient from east to west (*20*). Thus, in southwest Australia, which has the highest recorded incidence of bird pollination, 15% of plant species are pollinated by birds that exhibit generalist foraging strategies (*21*). In contrast, some tropical South American hummingbirds exhibit a high level of co-adapted dependency on particular plant species (*20*), placing these relationships at greater risk. Thus, undertaking restoration in a South American context is likely to involve more plant species where specialized vertebrate pollinator commensalisms and mutualisms need to be considered and factored in than for southern Australian ecosystem restoration.

A key component in facilitation of pollinator activity in restoration is proximity to natural landscapes that support pollinator communities (*22*).

School of Plant Biology, The University of Western Australia, Nedlands, 6009 Kings Park and Botanic Garden, West Perth 6005, Western Australia, Australia. E-mail: kingsley.dixon@bgpa.wa.gov.au

However, with habitat fragmentation rife in most of the world's ecosystems, ecological linkages may not adequately support pollinator migration to restored sites. Here, pollinator facilitation through intervention management may be required and involve establishment of corridors of pollinator-friendly plant species (*23*), including use of framework species (species that provide a major nectar or pollen source), bridging species (plants that provide resources over resource-limited times), and magnet species (*24*) (plants with attractive flowers associated with species with unattractive or small flowers). For example, in agri-environments, optimizing pollinator-friendly blends of plant species has provided improved forage opportunities for pollinators (*25*, (*26*), and similar "plant mixes" may enhance pollinator migration, colonization, and persistence in restoration programs. Alternatively, pollinator shifts have enabled replacement of extinct pollinators by extant species. In the case of *Freycinetia aborea* from Hawaii, the extinct bird pollinator was replaced by an introduced bird (*27*), suggesting that pollinator substitution may be an effective tool in restoration where native pollinators are absent. Such action needs to be considered with extreme caution, because introduced pollination surrogates such as honeybees have been implicated in the disruption of natural plant-pollinator mutualisms (*28*). In the event that pollinators fail to arrive in restored landscapes, unproven restoration technologies, such as captive breeding and reintroduction, are a last-resort and potentially costly solution for reinstating pollination capacity.

Ultimately, restoring pollination capability in restored landscapes will rely on research that addresses key information needs based on the following: (i) Understanding pollinator dispersability as a key predicator of natural migration of pollinators into restored landscapes (Fig. 1); (ii) restoring plant species that facilitate and assist pollinator migration across landscapes (identifying plants that operate as framework, bridging, and magnet species for pollinators); and (iii) ensuring that foraging patterns of pollinators optimize plant reproductive outputs (seed quality; heterozygosity).

Pollination research and restoration ecology need to find common ground if we are to avert a global meltdown in pollination capability in natural and restored ecosystems. By including pollination ecological considerations in ecological restoration planning, local abundance of pollinators can be increased and act as source populations to reinforce pollinators in nearby natural areas with potential pollination spin-offs for adjacent agri-environments (*2*).

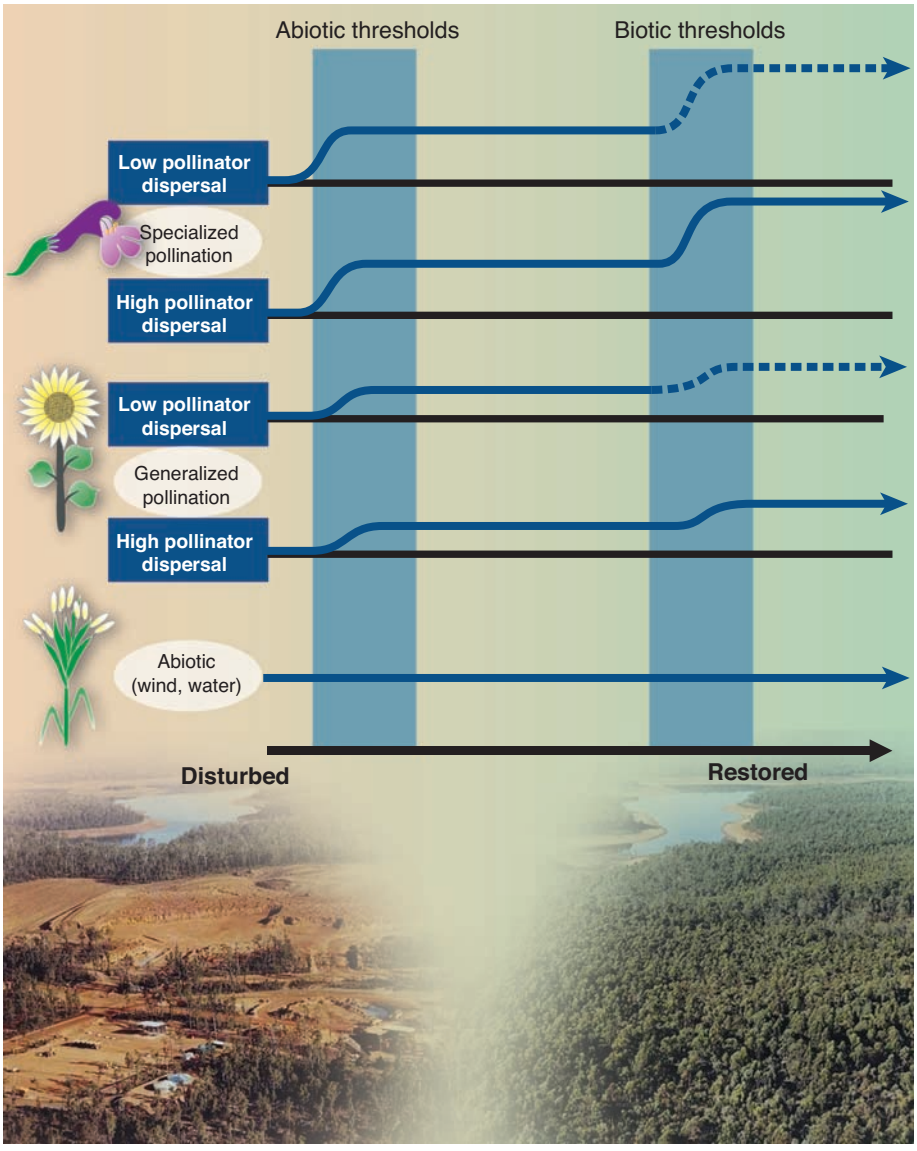

Fig. 1. Generalized models for restoration trajectories of pollination services where degree of pollinator specialization by plants when linked to natural dispersability of pollinators influences the capacity and complexity to achieve pollinator reinstatement. Achieving restoration outcomes will depend on establishing abiotic (soil, hydrology, topography) and biotic (living organisms necessary to maintain an ecosystem) thresholds, with level of technical difficulty represented by the relative height of each lift—the greater the lift, the greater the technical difficulty to achieve the outcome. Dashed lines indicate a very high degree of technological intervention or difficulty (captive breeding, translocation) to restore natural pollinators. (Photos) Postmining ecological restoration in the biodiversity hotspot of Western Australia, showing a bauxite extraction pit in jarrah forest (left) and restoration of the same area (right). [Photos: Alcoa World Alumina]

References

1. A. M. Klein *et al.*, *Proc. R. Soc. Lond. B. Biol. Sci.* **274**, 303 (2007).
2. C. Kremen, N. M. Williams, R. W. Thorp, *Proc. Natl. Acad. Sci. U.S.A.* **99**, 16812 (2002).
3. D. L. Cox-Foster *et al.*, *Science* **318**, 283 (2007).
4. M. L. Forup, K. S. E. Henson, P. G. Craze, J. Memmott, *J. Appl. Ecol.* **45**, 742 (2008).
5. M. L. Forup, J. Memmott, *Restor. Ecol.* **13**, 265 (2005).
6. G. Allen-Wardell *et al.*, *Conserv. Biol.* **12**, 8 (1998).
7. J. Memmott, P. G. Craze, N. M. Waser, M. V. Price, *Ecol. Lett.* **10**, 710 (2007).
8. J. Memmott, N. M. Waser, M. V. Price, *Proc. R. Soc. London Ser. B. Biol. Sci.* **271**, 2605 (2004).
9. C. Fontaine, I. Dajoz, J. Meriguet, M. Loreau, *PLoS Biol.* **4**, e1 (2006).
10. S. D. Johnson, K. E. Steiner, *Trends Ecol. Evol.* **15**, 140 (2000).
11. N. Myers, R. A. Mittermeier, C. G. Mittermeier, G. A. B. da Fonseca, J. Kent, *Nature* **403**, 853 (2000).
12. H. Steltzer, E. Post, *Science* **324**, 886 (2009).
13. S. J. Hegland, A. Nielsen, A. Lázaro, A.-L. Bjerknes, Ø. Totland, *Ecol. Lett.* **12**, 184 (2009).
14. Anonymous, "Status of Pollinators in North America" (National Academies Press, Washington, DC, 2007).
15. R. R. Dunn, N. C. Harris, R. K. Colwell, L. P. Koh, N. S. Sodhi, *Proc. R. Soc. London Ser. B* 10.1098/rspb.2009.0413 (2009).
16. B. B. Lamont, P. G. L. Klinkhamer, E. T. F. Witkowski, *Oecologia* **94**, 446 (1993).
17. C. Botes, S. D. Johnson, R. M. Cowling, *Int. J. Plant Sci.* **170**, 151 (2009).
18. A. D. Brown, P. Dundas, K. W. Dixon, S. D. Hopper, *An Illustrated Guide to the Orchids of Western Australia* (Univ. of Western Australia Press, Nedlands, Australia, 2008).

19. J. C. Vamosi *et al.*, *Proc. Natl. Acad. Sci. U.S.A.* **103**, 956 (2006).
20. T. H. Fleming, N. Muchhala, *J. Biogeogr.* **35**, 764 (2008).
21. E. M. Brown *et al.*, *Pollination in Western Australia: A Database of Animals Visiting Flowers* (Western Australia Naturalists' Club, Perth, Australia, 1997), Handbook No. 15.
22. C. Kremen, N. M. Williams, R. L. Bugg, J. P. Fay, R. W. Thorp, *Ecol. Lett.* **7**, 1109 (2004).
23. P. A. Townsend, D. J. Levey, *Ecology* **86**, 466 (2005).
24. M. A. Molina-Montenegro, E. I. Badano, L. A. Cavieres, *Oikos* **117**, 1833 (2008).
25. C. Carvell, W. R. Meek, R. F. Pywell, D. Goulson, M. Nowakowski, *J. Appl. Ecol.* **44**, 29 (2007).
26. C. Kremen *et al.*, *Ecol. Lett.* **10**, 299 (2007).
27. P. A. Cox, *Oikos* **41**, 195 (1983).
28. A. Traveset, D. M. Richardson, *Trends Ecol. Evol.* **21**, 208 (2006).

10.1126/science.1176295

PERSPECTIVE

Soil Microbial Communities and Restoration Ecology: Facilitators or Followers?

Jim Harris

Microorganisms have critical roles in the functioning of soil in nutrient cycling, structural formation, and plant interactions, both positive and negative. These roles are important in reestablishing function and biodiversity in ecosystem restoration. Measurement of the community indicates the status of the system in relation to restoration targets and the effectiveness of management interventions, and manipulation of the community shows promise in the enhancement of the rate of recovery of degraded systems.

Soil microbes ranging from free-living bacteria to single fungi covering several square kilometers are a vastly diverse group in terms of taxonomy, structure, and function. We know the biology of few species directly because most soil microbes are currently impossible to cultivate (less than 1% grow readily on agar plates), and we instead rely on indirect means of analyses, principally biochemical markers, and measurements of the whole, or selected parts, of the communities' metabolic activities. Does the soil microbial community merely reflect what is happening in the rest of the ecosystem, or could it be a key player in facilitating restoration objectives? We do know that microorganisms are essential to soil function, particularly in organic matter decomposition and nutrient cycling, and therefore in regulating plant productivity and community dynamics (*1*, *2*) and in soil structural generation (*3*). Hence, their study could be an essential part of any program aimed at the restoration of an ecosystem. However, soil microbes have only recently become a focus for restoration ecology, and research on the interactions between microorganisms and plants in both undisturbed and degraded ecosystems has begun to yield interesting results (*4*).

Department of Natural Resources, Cranfield University, Cranfield, Bedfordshire MK43 0AL, UK.

Recently, microbes have been investigated in two ways in relation to restoration: first to indicate the state of the ecosystem in reference to "target" sites or conditions, and second as a system component to be manipulated so as to enhance the speed with which the system can be moved along to the desired state by overcoming "biotic barriers," either the absence of desirable components (such as mutualists) or the presence of undesirables (such as invasive plants) (*5*). We can distinguish between studies carried out on restoration sites to elucidate mechanisms and those on "natural" sites, which have implications for restoration practice. Sometimes the division between the two is not clear cut; how might we classify an investigation in which the site of interest is field-abandoned for many years and now being "restored" to species-rich grassland? Restoration purists may regard this as reversing the wrong way down a successional gradient, away from a climax endpoint of mature forest in temperate ecosystems (of, for example, northern Europe), but the restoration of species-rich grassland is a common target for many conservation bodies.

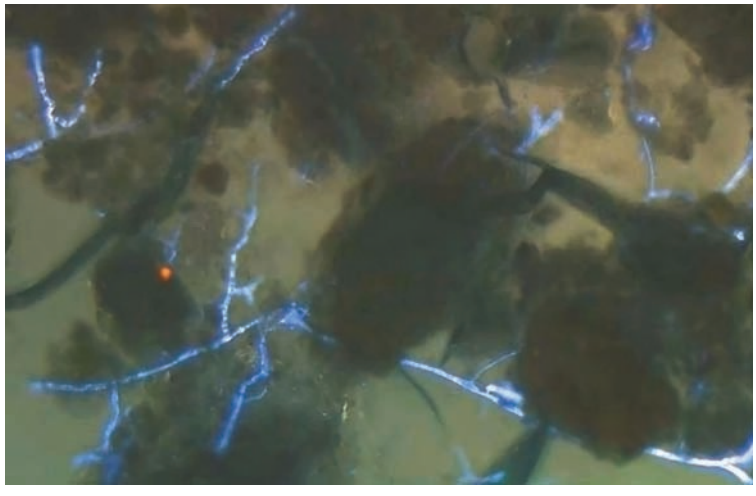

Fig. 1. Fungal hyphae ramify through soil, enmeshing and binding soil particles tighter so as to stabilize structure, accelerate decomposition, and affect plant diversity. [Image courtesy of K. Ritz, National Soil Resources Institute, Cranfield University]

There has been a long history of using analysis of the soil microbial community to indicate the condition of soil-based ecosystems. Work in this area provides clear evidence that as intensive use of sites is deliberately decreased in order to achieve a more natural state, there is an increase in the ratio of fungal to bacterial biomass (*6*) as more-complex organic material enters the soil matrix in these systems and physical perturbations decrease. The ratio increases further with scrub and forest development, which is consistent with the observation of a shift of resource and energy flows from root to fungal "energy channels" (*7*) as systems move from early to later successional stages. This work suggests that the microbial community "follows" and is dependent on what is going on in the above-ground community and can indicate the impact of restoration-management practices (*8*).

More difficult to assess is the role the microbial community plays in facilitating the establishment of plant communities at various successional stages and the possibilities for manipulation of the soil microbial community to "enhance" the rate at which a mature, stable ecosystem is established. In recent years, there has been an increasing focus on restoring ecosystem function, with associated flows of ecosystem goods and services, rather than "putting things back the way they were"—particularly in regard to shifting of species ranges caused by climate change and local extinction of key species. We are attempting to hit a moving target in this rapidly changing biophysical environment: Species assemblages that would have been found at a particular geographical location in the past may be impossible to reestablish under a changed climatic regime

and where key historical species components have become locally or totally extinct (*9*).

It has long been thought that one preeminent group of microorganisms, the mycorrhizae, could demonstrably improve the establishment, survival, and success of target plant species. In mycorrhizal relationships, which occur in most plant groups, fungal hyphae either penetrate or (in tree species) form sheaths around plant roots, then ramify out into the soil's mineral matrix. The fungi gain ready access to photosynthate; the plants gain access to mineral nutrients and protection from pathogens and drought; and thus both gain a competitive advantage. The links between mycorrhizae, plant diversity and productivity, and system heterogeneity are well established (*10*), and it follows that establishing a mycorrhizal community in an appropriate configuration is a prerequisite for establishing a target plant assemblage (*11*). In the restoration of extensively disturbed areas, such as large-scale mining, mycorrhizae offer a potentially low-cost means of establishing plant communities. The proximity of the restoration site to established mycorrhizal networks and propagule sources is an important factor in establishing new mycorrhizal relationships in restored systems (*12*). There are numerous cases in which the addition of mycorrhizae symbiont propagules has improved establishment, particularly in desert ecosystems (*13*). However, more recent work suggests that this effect may be more hit and miss than was previously thought (*14*) because of the complexity of plant-mycorrhizal symbioses, the multiplicity of plant-fungal specificity at different growth stages of the plant, and the prevailing soil/hydrological conditions (*15*). Although preinoculation of plants with mycobiont may help increase mycorrhizal diversity in soils with impoverished mycorrhizal communities, this approach appears to decrease mycorrhizal diversity when used in mature ecosystems (*16*). There is another dimension to these interactions, that of the role of bacteria that appear to help the formation of the mycorrhizal relationship (*17*), adding another layer of complexity to what we need to know before we can carry out manipulations with sufficient confidence that they will result in the desired ecosystem outcome. Fungi have a more general role to play in stabilizing soil structure by enmeshing and linking mineral particles in their hyphae; bacteria produce gums and mucilages that act as adhesives (Fig. 1).

Restoration sites using raw materials excavated by mining provide close if not precise analogies of those conditions occurring in systems that result from volcanic eruptions and the retreat of glaciers. Even here, past observations that autotrophs are the first to establish are being challenged; heterotrophic organisms arriving with organic matter may be a prerequisite for the establishment of later successional species (*18*). If this is the case, then accelerating succession by means of organic amendment may be an essential, not merely desirable, intervention on former mining sites. Such raw substrates offer a rich opportunity to explore the subtle interactions between above- and below-ground components in developing ecosystems without the constraints encountered in fragile or rare ecosystems. It is possible to manipulate carbon:nitrogen ratios so as to favor particular microbial groups capable of reducing the prevalence of invasive plants in abandoned fields; activated carbon added to soil has been shown to have the potential for reducing allelopathic compound concentrations produced by invasive plant species, reducing their competitiveness and thus lengthening the time available for the establishment of pathogens specific to invasive plants (*19*). The diversity of the bacterial community in general, and the nitrogen-fixing guild in particular, has been found to be positively correlated with the development of spatial heterogeneity and niche diversification in alpine grasslands (*20*).

Is it possible to shortcut succession in order to achieve desired ecosystem target states, or do ecosystems have to go through all successional stages (Fig. 2)? Accelerated succession may not always be possible, or at least easy to achieve. Kardol *et al.* (*21*) have observed that introducing soil or turves from target ecosystems with a high fungal content from a species-rich grassland site did not result in the establishment of the target-plant assemblages in the receptor site; it would appear that the mismatch in abiotic conditions between donor and receptor sites overwhelmed any biotic influence.

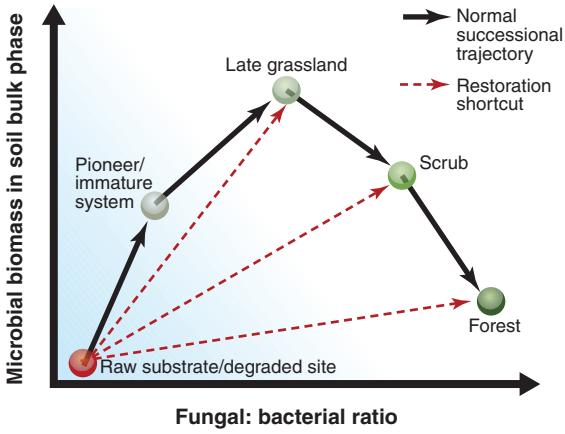

Fig. 2. As ecosystems mature, there is a switch in dominance from bacterial to fungal biomass; total microbial biomass in bulk (non-rhizosphere) soil peaks around midsuccession because this is the period in which root exudates in this phase peak. As fungal symbionts begin to dominate the rhizosphere, fewer plant exudates diffuse into the soil bulk phase. The aim of restoration to mature forest systems is to shortcut this trajectory by means of establishing fungal dominance at an early stage.

The investigation of soil microbial communities in systems undergoing restoration is providing fruitful insights into how "pristine" ecosystems work as well as the restored areas. Measurements of the size, composition, and activity of the soil microbial community accurately describe the status of restored systems in relation to target sites or systems, particularly when presented together in the form of two- or three-dimensional scatterplots (*8*), and work on this aspect of restoration ecology continues to be refined and extended. More work is needed to elucidate the role of microbes in generating soil structure in perturbed systems and their potential for enhancing the rate at which this proceeds. It is not yet clear that manipulation of microbial components of the soil subsystem can be guaranteed to effect enhanced ecosystem succession and function except in certain cases. There is a need for a more complete assessment of the role of all of the soil biological community and its interaction with the above-ground components and the mineral-organic matrix in the context of reversing ecosystem degradation, and there are clear signs that the research community is taking up this challenge.

References and Notes

1. D. A Wardle *et al*, *Science* **304**, 1629 (2004).
2. M. G. A. Van der Heijden, R. D. Bardgett, N. M. van Straalen, *Ecol. Lett.* **11**, 296 (2008).
3. D. S. Feeney *et al*., *Microb. Ecol.* **52**, 151 (2006).
4. L. Heneghan *et al*., *Restor. Ecol.* **16**, 608 (2008).
5. R. J. Hobbs, J. A. Harris, *Restor. Ecol.* **9**, 239 (2001).
6. A. Van der Wal *et al*., *Soil Biol. Biochem.* **40**, 2407 (2006).
7. R. Holtkamp *et al*., *Appl. Soil Ecol.* **39**, 23 (2008).
8. J. A. Harris, *Eur. J. Soil Sci.* **54**, 801 (2003).
9. J. A. Harris, R. J. Hobbs, J. Aronson, E. Higgs, *Restor. Ecol.* **14**, 170 (2006).
10. M. G. A. Van der Heijden *et al*., *Nature* **396**, 69 (1998).
11. B. S. Richter, J. C. Stutz, *Restor. Ecol.* **10**, 607 (2002).
12. F. P. Teste, S. W. Simard, *Oecologia* **158**, 193 (2008).
13. N. Requena, E. Perez-Solis, C. Azcon-Aguilar, P. Jeffries, J.-M. Barea, *Appl. Environ. Microbiol.* **67**, 495 (2001).
14. D. A. Jasper, *Restor. Ecol.* **15**, S74 (2007).
15. T. A. Ishida, K. Nara, T. Hogetsu, *New Phytol.* **174**, 430 (2007).
16. D. L. Mummey, P. M. Antunes, M. C. Rillig, *Soil Biol. Biochem.* **41**, 1173 (2009).
17. G. Bending, *New Phytol.* **174**, 707 (2007).
18. I. D. Hodkinson, N. R. Webb, S. J. Coulson, *J. Ecol.* **90**, 569 (2002).
19. A. Kulmatiski, K. H. Beard, *Restor. Ecol.* **14**, 251 (2006).
20. R. Gros, L. J. Monrozier, P. Faivre, *Environ. Microbiol.* **8**, 1889 (2006).
21. P. Kardol, T. M. Bezemer, W. Van Der Putten, *Restor. Ecol.* **17**, 258 (2009).
22. The author thanks K. Ritz, Cranfield University, for useful discussions and providing the photomicrograph shown as Fig. 1.

10.1126/science.1172975

PERSPECTIVE

Restoration of Ecosystem Services for Environmental Markets

Margaret A. Palmer[1,2]* and Solange Filoso[1]

Ecological restoration is an activity that ideally results in the return of an ecosystem to an undisturbed state. Ecosystem services are the benefits humans derive from ecosystems. The two have been joined to support growing environmental markets with the goal of creating restoration-based credits that can be bought and sold. However, the allure of these markets may be overshadowing shortcomings in the science and practice of ecological restoration. Before making risky investments, we must understand why and when restoration efforts fall short of recovering the full suite of ecosystem services, what can be done to improve restoration success, and why direct measurement of the biophysical processes that support ecosystem services is the only way to guarantee the future success of these markets. Without new science and an oversight framework to protect the ecosystem service assets on which people depend, markets could actually accelerate environmental degradation.

As early as the 1940s, Aldo Leopold (*1*) linked the concepts of human reliance on natural systems and restoration of those systems. Today, each of these two seemingly simple concepts is associated with scientific and management quandaries created by joining them as the restoration of ecosystem services. Ecological restoration is an activity or series of activities undertaken to return a degraded ecosystem to a healthy state. Ecosystem services are the benefits humans derive from ecosystems, which have been largely taken for granted, especially since the industrial revolution (*2*). However, as ecosystems become progressively more human-dominated, the services they provide are increasingly seen as something of economic value, which can be traded in ecosystem service markets (*3*). At present, the demand in these markets is driven by regulations that require those seeking permits to mitigate or provide offsets for their environmental impacts. Some hope that voluntary ecosystem service markets will expand outside of a regulatory context and result in a net gain of ecosystem services rather than just offsets for lost ones. The most prominent example of regulation-driven ecosystem service markets is for wetland mitigation, although stream mitigation banks are rapidly growing, and although not yet official, "early" trading involving carbon credits created through reforestation of land can be sold to offset CO_2 emissions (*4*, *5*).

We do not disagree about the potential for ecosystem service markets to help solve environmental problems, especially if markets can be created to provide incentives for conservation of natural resources rather than facilitating new environmental impacts because offsets are available. Our concern is that the flurry of interest in ecosystem markets supplied by restoration is out of step with the science and practice of ecological restoration, and so it is obscuring the fact that restoration projects, particularly those in aquatic ecosystems, are not providing all the services of healthy ecosystems (*6*, *7*). Stream and river restoration projects are often based on reshaping a channel and adding wood or rocks, yet there are few documented cases in which this has resulted in improved water quality or biodiversity comparable to those in undisturbed streams (*8*, *9*). In the case of wetlands, the success of restoration projects has been debated, largely because most are implemented for mitigation purposes, and although they may meet legal requirements, which are sometimes based on simple acre-for-acre compensations, they may not provide the full suite of ecological services (*10*, *11*).

The danger of marketing ecosystem services delivered through ecological restoration without properly understanding the potential shortfalls of restoration is that the level or quality of the ecosystem services provided as an offset may not correspond with the losses. If this happens, these markets may cause an increase rather than decrease in environmental degradation. Hence, before ecosystem service markets that rely on restoration expand further, we must understand why many restoration efforts are falling short and what should be done to improve restoration success.

The broadening definition of what counts as restoration and the limited scale of restoration both contribute to the inadequacy of restoration efforts. In its purest form, restoration refers to returning an ecosystem to an undisturbed or historic state, but today, diverse activities are routinely undertaken in the name of ecological restoration. For instance, "creation" of wetlands and streams where they did not previously exist is now considered a form of ecosystem restoration (*8*, *12*). Because the ecosystem services provided by wetlands and streams depend in critical ways on their context in natural landscapes, successful restoration of even a subset of the services is unlikely, unless there is very careful site selection and/or management actions at regional scales. Restoration efforts that target improvements on minimally degraded lands offer the most hope for recovering ecosystem services, whereas attempts to create ecosystems offer the least.

When restoration efforts target sites in watersheds with deforestation, mining, or development, it is unrealistic to assume that the full suite of ecosystem services can be restored, given the current state of the science. First, restoration actions that benefit one service may interfere with another (*13*). For example, wetland restoration undertaken to reduce nitrogen loads to adjacent coastal areas may also result in increasing the bioavailability of mercury to fish (*14*). Second, final ecosystem services are supported by a complex network of biophysical processes and ecosystem features (collectively referred to as ecosystem functions) (Fig. 1), many of which are not restored because restoration designs are typically not process-based. Instead, most designs are based on structural features of ecosystems or, at best, hydrological processes that may be necessary, but not sufficient, to recover desired ecosystem services (*15*). For example, river restorations are often based on recreating structural attributes like channel width, depth, and sinuosity, because of making the erroneous assumption that ecological functions will follow. Yet, how a stream looks is not the same as how it processes nutrients and supports life. Designs must focus on restoring processes that support ecosystem services of interest, and careful measurements of how targeted processes respond to restoration are critical to postproject monitoring for adaptive management (*16*).

It is important to emphasize that measuring ecological processes is not the same as measuring an ecosystem service. The former should be based on well-accepted scientific methods that provide information on how an ecosystem is performing, such as its rate of nutrient processing; the latter should be based on the delivery of a final service or good, like clean water to humans. The metrics of ecosystem service markets are the value or importance societies place on natural systems and associated products at specific locations (*2*, *3*). Without direct measurements of processes that lead to the production of ecosystem services, or surrogate measurements that have been shown to dependably represent the functions that support a service or suite of services (*16*, *17*), there is no way to know if restoration actions are actually leading to the delivery of services. The assumptions that simple proxies, like habitat descriptors, can be used to evaluate restoration success and that single ecological measures, like biodiversity, can be used to evaluate a full suite or "bundle" of ecosystem processes are not only naïve but have been demonstrated to be false for many ecosystems (*4*).

Despite progress in developing methods for the valuation of ecosystem services, we still lack a clear picture of what biophysical factors support services

[1]Chesapeake Biological Laboratory, University of Maryland Center for Environmental Science, Solomons, MD 20688, USA. [2]Department of Entomology, University of Maryland, College Park, MD 20742, USA.

*To whom correspondence should be addressed. E-mail: mpalmer@umd.edu

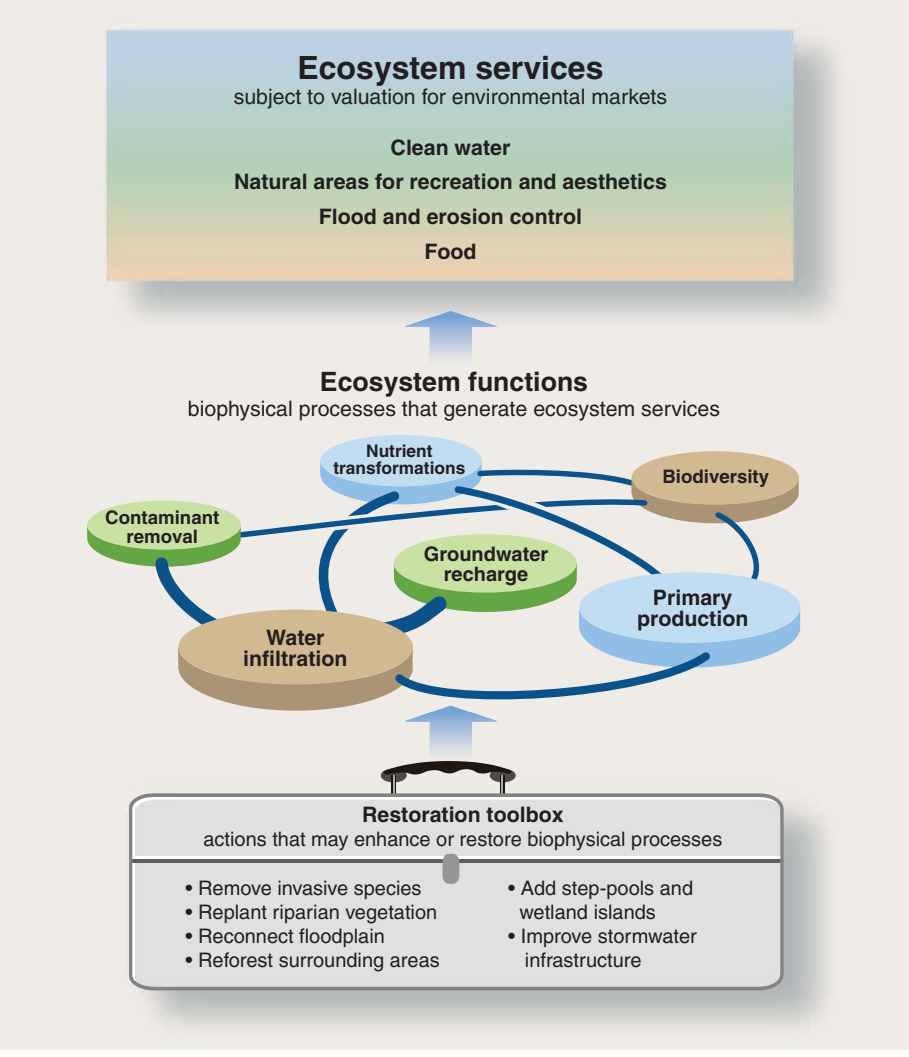

Fig. 1. Restoration of ecosystem services that can be bought, sold, or traded requires actions (use of "tools") that directly influence biophysical processes, such as microbial removal of excess dissolved nitrogen, the uptake of metals by plants, or the infiltration of rainwater into soils. These processes interact with ecosystem features (e.g., suites of species or surrounding land use) and are collectively called ecosystem functions or ecological processes. To ensure the value of an ecosystem service credit, direct measurements of the service (e.g., clean water without excessive nitrogen) or ecosystem functions that support the service (e.g., denitrification) must be made. For some services and landscape settings, researchers are only now identifying the most relevant ecological processes.

for different ecosystems and in what combinations. This kind of information is absolutely essential to create and/or support the restoration of a full suite of ecosystem services; for now, we can only apply a logical, data-driven approach to prioritize sites and particular services for restoration and to test the efficacy of various restoration tools in accelerating the recovery of biophysical processes critical to those services. As we start to build up a database on process-based responses to restoration treatments and relate these responses to data on a range of project characteristics, we can develop useful relations between local environmental conditions, restoration methods, and probabilities of outcomes.

Until this kind of information is available, the only way to ensure that credits generated by restoration of ecosystems can be associated with the delivery of ecosystem services is to have a third-party, unbiased entity verify, through direct measurements, that ecosystem functions were sufficiently restored. Independent and transparent evaluation approaches that do not rely on those who stand to profit or those tasked with regulation have been successfully employed for other environmental issues. For example, third-party, academic-based programs subject to routine peer review provide certification testing of ballast water treatment systems designed to prevent the introductions of non-native aquatic species by commercial ships in the United States (*18*). Even with such verification programs, the units of exchange in ecosystem service markets need to be fairly complex in order to account for uncertainties in success, as well as any environmental or social consequences of spatially redistributing ecosystem services (*19*). Furthermore, the rules of exchange need to contain clear liability guidelines to the buyer or the seller, and long-term monitoring of ecological processes must be required; otherwise, by default, the risks of environmental failure will fall on the general public (*20*).

Until there is a sound scientific basis for linking restoration actions to changes in biophysical processes and ecological features that result in the delivery of specific ecosystem services, restoration-based markets and trading schemes are a risky business. Devising methods to assign economic value or mitigation credits to an ecosystem service, like clean water, does not mean that the service will necessarily be restored.

References and Notes

1. A. Leopold, *A Sand County Almanac* (Ballantine Books, New York, 1949).
2. G. C. Daily, P. A. Matson, *Proc. Natl. Acad. Sci. U.S.A.* **105**, 9455 (2008).
3. L. A. Wainger, J. W. Boyd, in *Ecosystem-Based Management for the Oceans*, K. McLeod, H. Leslie, Eds. (Island Press, Washington, DC, 2009), chap. 6.
4. R. Lave, M. M. Robertson, M. W. Doyle, *Ecol. Restor.* **26**, 287 (2008).
5. C. Hepburn, *Annu. Rev. Environ. Resour.* **32**, 375 (2007).
6. S. Tischew, A. Baasch, M. K. Conrad, A. Kirmer, *Restor. Ecol.*, in press; published online 29 October 2008, 10.1111/j.1526-100X.2008.00462.x.
7. E. S. Bernhardt *et al.*, *Science* **308**, 636 (2005).
8. M. A. Palmer, *Estuaries Coasts* **32**, 1 (2009).
9. J. M. Rumps *et al.*, *Restor. Ecol.* **15**, 506 (2007).
10. J. A. Zinn, C. Copeland, *Wetlands: An Overview of Issues*, (publ. no. RL33483, Congressional Research Service, Washington, DC, 2008); www.nationalaglawcenter.org/assets/crs/RL33483.pdf.
11. R. F. Ambrose, J. C. Callaway, S. F. Lee, *An Evaluation of Compensatory Mitigation Projects Permitted by the California State Water Resources Control Board, 1991–2002* (California State Water Resources Control Board, Sacramento, CA, 2007).
12. Wetland creation has been an acceptable way to generate mitigation credits in the United States; stream creation was added by means of new regulatory guidelines in 2008 (*21*).
13. J. G. Ehrenfeld, *Restor. Ecol.* **8**, 2 (2000).
14. J. M. Helfield, M. L. Diamond, *Environ. Manage.* **21**, 329 (1997).
15. N. H. Euliss, L. M. Smith, D. A. Wilcox, B. A. Browne, *Wetlands* **28**, 553 (2008).
16. S. M. Hoeltje, C. A. Cole, *Environ. Manage.* **43**, 597 (2009).
17. Relations between ecosystem services and the biophysical processes and ecosystem features that produce services are called ecological production functions; production functions bridge the work of biophysical scientists studying ecosystems with social scientists engaged in developing valuation methods for ecosystem services (*22*).
18. The Maritime Environmental Resource Center in Maryland, U.S.A., for example (www.maritime-enviro.org/index.html).
19. T. BenDor, N. Brozović, V. G. Pallathucheril, *J. Am. Plann. Assoc.* **73**, 263 (2007).
20. D. M. King, *Environ. Law Report.* **32**, 11317 (2002).
21. U. S. Army Corps of Engineers and Environmental Protection Agency, *Fed. Regist.* **73**, 9594 (2008).
22. G. C. Daily *et al.*, *Front. Ecol. Environ.* **7**, 21 (2009).

23. Supported in part by DIVERSITAS and by a Collaborative Network for Sustainability grant from the Environmental Protection Agency, award 8832206. We thank M. Doyle, D. King, and L. Wainger for discussions on the topic and comments on the paper and F. Younger for the illustration.

10.1126/science.1172976

The Map of Altinum, Ancestor of Venice

Andrea Ninfo,* Alessandro Fontana, Paolo Mozzi, Francesco Ferrarese

The urban structure of Altinum [Fig. 1B and fig. S2 (*1*)], an important Roman harbor on the inner margin of the Lagoon of Venice [fig. S2 (*2*)], has until now been largely unknown. This city, Roman Municipium since the first century before the common era (B.C.E.), plays an important role in the early history of Venice because its inhabitants colonized the northern lagoon islands when fleeing from Barbarians [fifth to seventh century C.E. (*3*–*5*)]. We used visible and near-infrared (NIR) aerial photographs [Fig. 1A and fig. S1 (*1*)] and a digital elevation model (DEM) to reconstruct the urban topography and paleoenvironmental setting of Altinum.

The reuse of stones and bricks of the abandoned buildings for the construction of Venetian palaces and churches led to the dismantling of Altinum (*3*). The ruins of the city were partially drowned in the lagoon by relative sea-level rise (*5*). After 20th-century land reclamation, archaeological excavations were performed outside the city walls, centered on segments of the Roman roads (Via Annia and Augusta) and on the Roman and Iron Age necropolis and sanctuaries (*2*). With a size comparable to Pompeii, Altinum is the only large Roman city in Northern Italy and one of the few in Europe that has not been buried by medieval and modern cities. This setting allows spatial investigation through remote sensing.

Our images were taken at the end of July 2007, during severe drought, which caused water stress of the maize and soy crops in the area (fig. S3). The NIR radiation, which is highly sensitive to vegetation health, highlights the archaeological features. The lighter crop marks (Fig. 1A) show the subsurface presence of stones, bricks, or compacted soil; the dark ones correspond to depressed features like pits, spoliation hollows, canals, and paleo-channels filled with silty-clay sediments.

The images reveal ancient urban fabric and waterways (Fig. 1B), the city walls and gates, the street network, dwellings with their internal divisions, and monumental buildings (e.g., theater, odeon, amphitheater, forum with emporia, and basilica). The monumental buildings can be attributed to the period of maximum urban expansion [first century B.C.E. to first century C.E. (*2*)].

The city was surrounded by a complex network of rivers and canals (fig. S2); a large canal crossed the urban center, which connected it to the lagoon. The DEM shows that the city was on top of a 2- to 3-m-high rise. Considering the position of the coastline in Roman times (*6*, *7*), the lagoon probably extended to the foot of the mound. Altinum was partially surrounded by water as described by the geographer Strabo in the first century B.C.E.

Our results indicate the existence of a complex urban structure with varied and outstanding architecture that was adapted to the peculiarity of the lagoon environment. These data show that Romans successfully exploited the amphibious environment several centuries before the city of Venice started to emerge on the archipelago in the middle of the lagoon (*4*).

References and Notes

1. Materials and methods are available as supporting material on *Science* Online.
2. G. Cresci Marrone, M. Tirelli, Eds., *Vigilia di romanizzazione* (Quasar, Rome, 1999).
3. N. Christie, *From Constantine to Charlemagne: An Archaeology of Italy AD 300-800* (Aldershot, Ashgate, UK, 2006).
4. A. J. Ammerman, "Venice before the Grand Canal" (Memoirs of the American Academy in Rome, Rome, 2003), vol. 48, pp. 141–158.
5. R. Cessi, *Origo civitatum Italiae seu Venetiarum* (Chronicon Altinate, Rome, 1933).
6. F. Antonioli *et al.*, *Quat. Int.*, in press (10.1016/j.quaint.2008.11.008).
7. A. J. Ammerman *et al.*, *Antiquity* **73**, 303 (1999).

8. Research supported by ARCUS S.p.A., Veneto Region, and Municipality of Padua, within "Via Annia" project.

Supporting Online Material

www.sciencemag.org/cgi/content/full/325/5940/577/DC1
Materials and Methods
Figs. S1 to S3
References

30 March 2009; accepted 29 May 2009
10.1126/science.1174206

Department of Geography, Padua University, 35123 Padua, Italy.

*To whom correspondence should be addressed. E-mail: andrea.ninfo@unipd.it

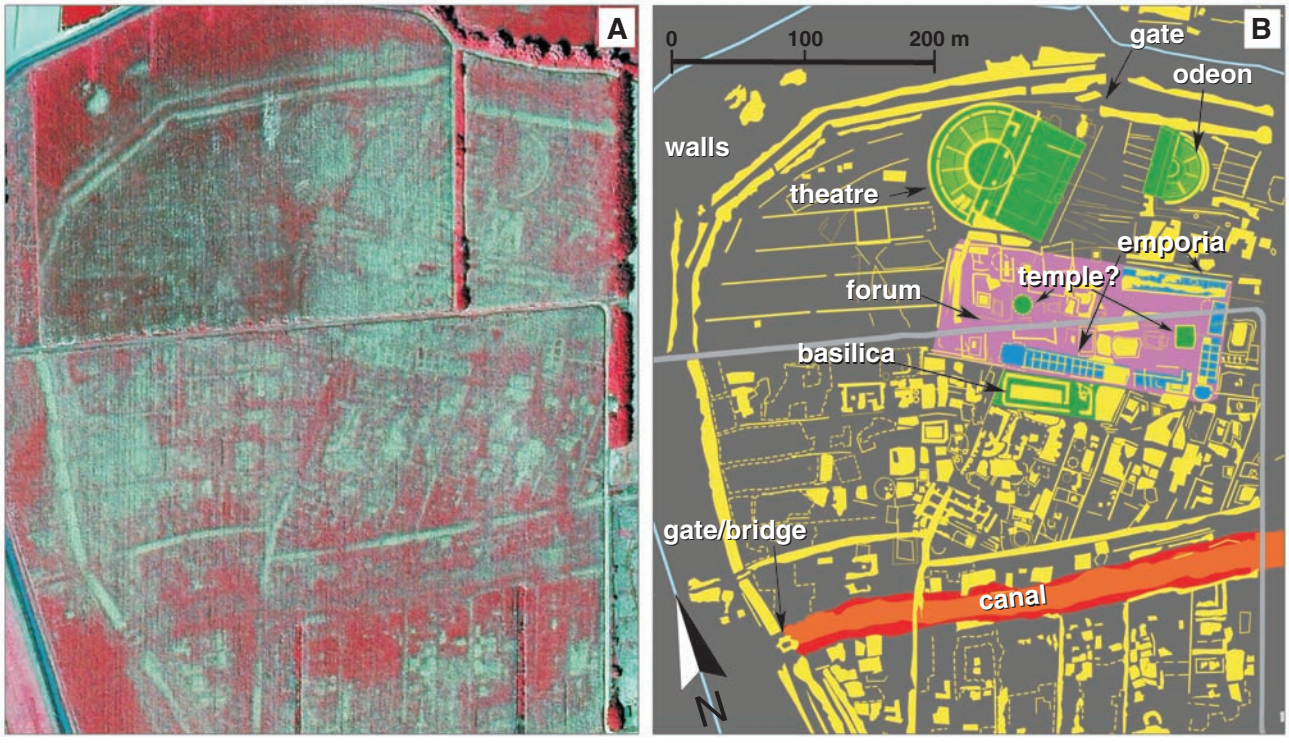

Fig. 1. (**A**) Digitally enhanced false-color composite image (NIR, red and green spectral bands) of the center of the Roman city (Realvista 2007, Telespazio S.p.A., Rome, Italy), with maize and soy crop marks. (**B**) Interpretation of (A).

Rebuilding Global Fisheries

Boris Worm,[1]* Ray Hilborn,[2]* Julia K. Baum,[3] Trevor A. Branch,[2] Jeremy S. Collie,[4] Christopher Costello,[5] Michael J. Fogarty,[6] Elizabeth A. Fulton,[7] Jeffrey A. Hutchings,[1] Simon Jennings,[8,9] Olaf P. Jensen,[2] Heike K. Lotze,[1] Pamela M. Mace,[10] Tim R. McClanahan,[11] Cóilín Minto,[1] Stephen R. Palumbi,[12] Ana M. Parma,[13] Daniel Ricard,[1] Andrew A. Rosenberg,[14] Reg Watson,[15] Dirk Zeller[15]

After a long history of overexploitation, increasing efforts to restore marine ecosystems and rebuild fisheries are under way. Here, we analyze current trends from a fisheries and conservation perspective. In 5 of 10 well-studied ecosystems, the average exploitation rate has recently declined and is now at or below the rate predicted to achieve maximum sustainable yield for seven systems. Yet 63% of assessed fish stocks worldwide still require rebuilding, and even lower exploitation rates are needed to reverse the collapse of vulnerable species. Combined fisheries and conservation objectives can be achieved by merging diverse management actions, including catch restrictions, gear modification, and closed areas, depending on local context. Impacts of international fleets and the lack of alternatives to fishing complicate prospects for rebuilding fisheries in many poorer regions, highlighting the need for a global perspective on rebuilding marine resources.

Overfishing has long been recognized as a leading environmental and socioeconomic problem in the marine realm and has reduced biodiversity and modified ecosystem functioning (*1*–*3*). Yet, current trends as well as future prospects for global fisheries remain controversial (*3*–*5*). Similarly, the solutions that hold promise for restoring marine fisheries and the ecosystems in which they are embedded are hotly debated (*4*–*6*). Such controversies date back more than a hundred years to the famous remarks of Thomas Huxley on the inexhaustible nature of sea fisheries (*7*) and various replies documenting their ongoing exhaustion. Although management authorities have since set goals for sustainable use, progress toward curbing overfishing has been hindered by an unwillingness or inability to bear the short-term social and economic costs of reducing fishing (*8*). However, recent commitments to adopting an ecosystem approach to fisheries may further influence progress because they have led to a reevaluation of management targets for fisheries and the role of managers in meeting broader conservation objectives for the marine environment (*9*).

In light of this debate, we strive here to join previously diverging perspectives and to provide an integrated assessment of the status, trends, and solutions in marine fisheries. We explore the prospects for rebuilding depleted marine fish populations (stocks) and for restoring the ecosystems of which they are part. In an attempt to unify our understanding of the global fisheries situation, we compiled and analyzed all available data types, namely global catch data (Fig. 1A), scientific stock assessments, and research trawl surveys (Fig. 1B), as well as data on small-scale fisheries (*10*). We further used published ecosystem models (Fig. 1B) to evaluate the effects of exploitation on marine communities. Available data sources are organized hierarchically like a Russian doll: Stock assessments provide the finest resolution but represent only a subset of species included in research surveys, which in turn represent only a small subset of species caught globally. These sources need to be interpreted further in light of historical fisheries before data collection and illegal or unreported fisheries operating today (*11*). We focus on two leading questions: (i) how do changes in exploitation rates impact fish populations, communities, and yields, and (ii) which solutions have proven successful in rebuilding exploited marine ecosystems?

Models. A range of models is available to analyze the effects of changes in exploitation rate on fish populations, communities, and ecosystems. Exploitation rate (u_t) is defined as the proportion of biomass that is removed per year, i.e., $u_t = C_t/B_t$ where C is the catch (or yield) and B is the available biomass in year t. Single-species models are often used to determine the exploitation rate u_{MSY} that provides the maximum sustainable yield (MSY) for a particular stock. Fishing for MSY results in a stock biomass, B_{MSY}, that is substantially (typically 50 to 75%) lower than the unfished biomass (B_0). It has been a traditional fisheries objective to achieve single-species MSY, and most management regimes have been built around this framework. Recently this focus has expanded toward assessing the effects of exploitation on communities and ecosystems (*9*).

Multispecies models can be used to predict the effects of exploitation on species composition, size structure, biomass, and other ecosystem properties. They range from simpler community models to more-complex ecosystem models (*12*). Figure 2 displays equilibrium solutions from a size-based community model, which assumes that fishing pressure is spread across species according to their size and that a subset of species remains unfished (*13*). Results of more-complex ecosystem models across 31 ecosystems and a range of different fishing scenarios were remarkably similar (fig. S1 and table S1). With increasing exploitation rate, total fish catch is predicted to increase toward the multispecies maximum sustainable yield (MMSY) and decrease thereafter. In this example, the corresponding exploitation rate that gives maximum yield u_{MMSY} is ~0.45, and total community biomass B_{MMSY} equilibrates at ~35% of unfished biomass (Fig. 2). Overfishing occurs when u exceeds u_{MMSY}, whereas rebuilding requires reducing exploitation below u_{MMSY}. An increasing exploitation rate causes a monotonic decline in total biomass and average body size, and an increasing proportion of species is predicted to collapse (Fig. 2). We used 10% of unfished biomass as a definition for collapse. At such low abundance, recruitment may be severely limited, and species may cease to play a substantial ecological role. This model suggests that a wide range of exploitation rates ($0.25 < u < 0.6$) yield ≥90% of maximum catch but with very different ecosystem consequences: whereas at $u = 0.6$ almost half of the species are predicted to collapse, reducing exploitation rates to $u = 0.25$ is predicted to rebuild total biomass, increase average body size, and strongly reduce species collapses with little loss in long-term yield (Fig. 2). In addition to reconciling fishery and conservation objectives, setting exploitation rate below u_{MMSY} reduces the cost of fishing and increases profit margins over the long term (*14*). This simple model does not incorporate fishing selectivity; however, in practice the proportion of collapsed species could be reduced further by increasing selectivity through improved gear technology (*15*), by closing areas frequented by vulnerable species, or through offering incentives to improve targeting practices (*16*). Such strategies allow for protection of vulnerable or collapsed species, while allowing for more intense exploitation of others.

[1]Biology Department, Dalhousie University, Halifax, NS B3H 4J1, Canada. [2]School of Aquatic and Fishery Sciences, University of Washington, Seattle, WA 98195–5020, USA. [3]Scripps Institution of Oceanography, University of California-San Diego, La Jolla, CA 92093–0202, USA. [4]Graduate School of Oceanography, University of Rhode Island, Narragansett, RI 02882, USA. [5]Donald Bren School of Environmental Science and Management, University of California, Santa Barbara, CA 93106–5131, USA. [6]National Marine Fisheries Service, National Oceanic and Atmospheric Administration, Woods Hole, MA 02543, USA. [7]Commonwealth Scientific and Industrial Research Organisation (CSIRO) Marine and Atmospheric Research, General Post Office Box 1538, Hobart, TAS 7001, Australia. [8]Centre for Environment, Fisheries and Aquaculture Science, Lowestoft NR33 0HT, UK. [9]School of Environmental Sciences, University of East Anglia, Norwich NR4 7TJ, UK. [10]Ministry of Fisheries, Post Office Box 1020, Wellington, New Zealand. [11]Wildlife Conservation Society Marine Programs, Post Office Box 99470, Mombasa, Kenya. [12]Hopkins Marine Station, Stanford University, Pacific Grove, CA 93950, USA. [13]Centro Nacional Patagónico, 9120 Puerto Madryn, Argentina. [14]Institute for the Study of Earth, Oceans, and Space, University of New Hampshire, Durham, NH 03824–3525, USA. [15]Fisheries Centre, University of British Columbia, Vancouver, BC V6T 1Z4, Canada.

*To whom correspondence should be addressed. E-mail: bworm@dal.ca (B.W.); rayh@u.washington.edu (R.H.)

These results suggest that there is a range of exploitation rates that achieve high yields and maintain most species. To test whether current fisheries fall within this range, we evaluated trends in 10 large marine ecosystems for which both ecosystem models and stock assessments were available (*10*). Figure 3A shows exploitation rate and biomass trajectories derived from 4 to 20 assessed fish or invertebrate stocks per ecosystem. These stocks typically represent most of the catch, and we assumed that trends in their exploitation rates represent the community as a whole. Ecosystem models were used to calculate u_{MMSY} (light blue bars) and the exploitation rate at which less than 10% of the fished species are predicted to be collapsed ($u_{conserve}$, dark blue bars). Across the 10 examined ecosystems, MMSY was predicted at multispecies exploitation rates of u_{MMSY} = 0.05 to 0.28 (mean of 0.16), whereas avoiding 10% collapse rates required much lower exploitation rates of $u_{conserve}$ = 0.02 to 0.05 (mean of 0.04).

Up to the 1990s, assessed species in 6 of the 10 ecosystems had exploitation rates substantially higher than those predicted to produce MMSY (Fig. 3A). Only the eastern Bering Sea has been consistently managed below that threshold. Since the 1990s, Iceland, Newfoundland-Labrador, the Northeast U.S. Shelf, the Southeast Australian Shelf, and California Current ecosystems have shown substantial declines in fishing pressure such that they are now at or below the modeled u_{MMSY}. However, only in the California Current and in New Zealand are current exploitation rates predicted to achieve a conservation target of less than 10% of stocks collapsed (Fig. 3A). Declining exploitation rates have contributed to the rebuilding of some depleted stocks, whereas others remain at low abundance. Averaged across all assessed species, biomass is still well below B_{MSY} in most regions. However, biomass has recently been increasing above the long-term average in Iceland, the Northeast U.S. Shelf, and the California Current, while remaining relatively stable or decreasing elsewhere (Fig. 3A).

Scientific stock assessments. Stock assessments quantify the population status (abundance, length, and age structure) of targeted fish or invertebrate stocks. We explored the status of 166 stocks worldwide for which we were able to obtain estimates of current biomass and exploitation rate (Fig. 3B). For about two-thirds of the examined stocks (63%), biomass (B) has dropped below the traditional single-species management target of MSY, that is, $B < B_{MSY}$. About half of those stocks (28% of total) have exploitation rates that would allow for rebuilding to B_{MSY}, that is, $u < u_{MSY}$, whereas overfishing continues in the remainder ($u > u_{MSY}$ in 35% of all stocks). Another 37% of assessed stocks have either not fallen below B_{MSY} or have recovered from previous depletion; most stocks in this category (77%) are in the Pacific. The weight of the evidence, as shown by the kernel density plot in Fig. 3B, indicates that most assessed stocks have

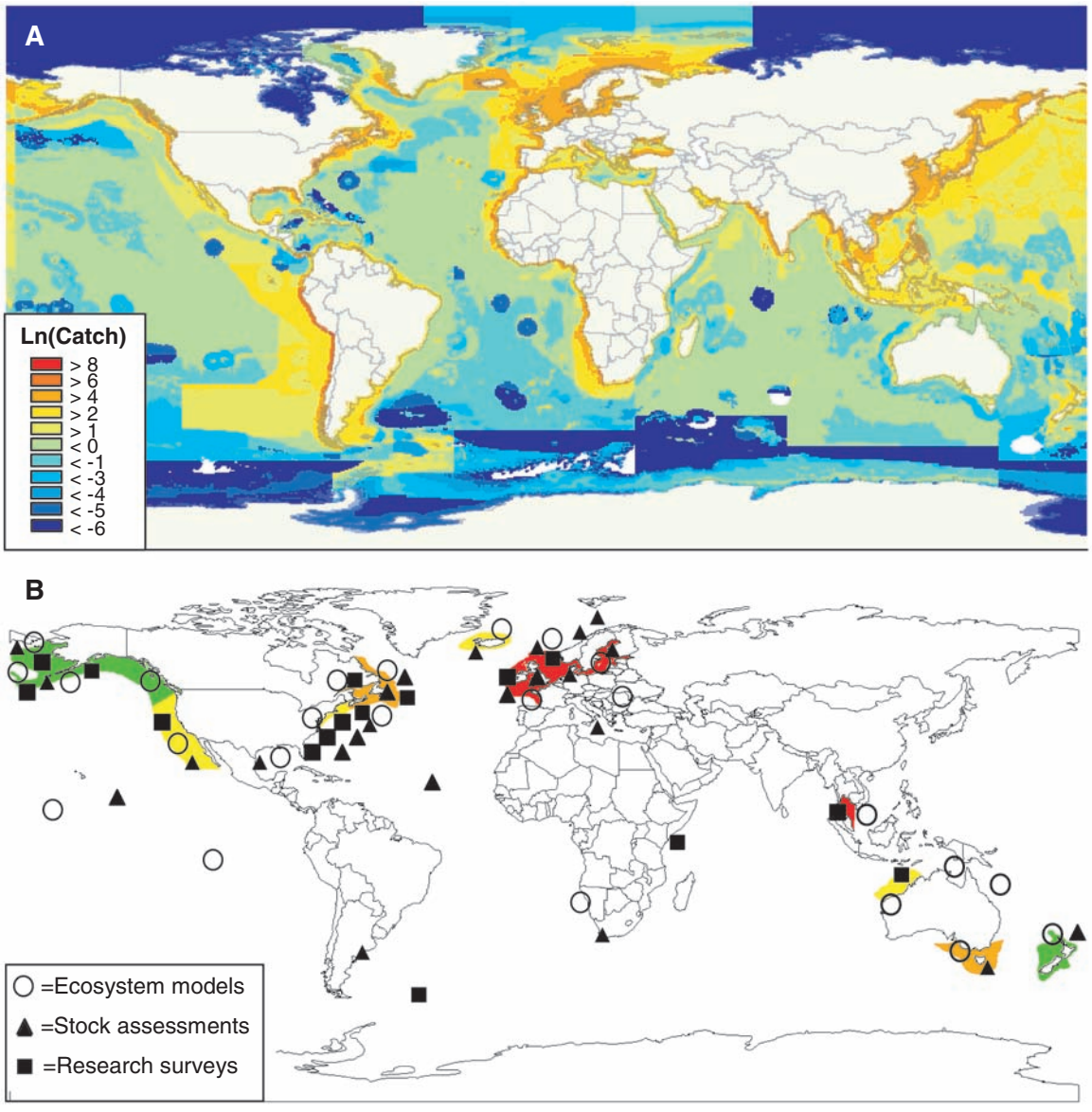

Fig. 1. Data sources used to evaluate global fisheries. (**A**) Global catch data; colors refer to the natural logarithm of the average reported catch (metric ton km^{-2} year^{-1}) from 1950 to 2004). (**B**) Other data: Stock assessments quantify the status of exploited populations; research trawl surveys are used to estimate fish community trends; ecosystem models are used to assess responses to fishing. Ecosystems that were analyzed in some detail are highlighted in green (not overfished), yellow (low exploitation rate, biomass rebuilding from overfishing), orange (low to moderate exploitation rate, not yet rebuilding), or red (high exploitation rate).

fallen below the biomass that supports maximum yield ($B < B_{MSY}$) but have the potential to recover, where low exploitation rates ($u < u_{MSY}$) are maintained. Note that most stock assessments come from intensely managed fisheries in developed countries, and therefore our results may not apply to stocks in many developing countries, which are often not assessed but fished at high exploitation rates and low biomass. Full results are provided in table S2.

When we combined the biomass estimates of stocks assessed since 1977 (n = 144, Fig. 4A), we observed an 11% decline in total biomass. This trend is mostly driven by declines in pelagic (mid-water) species, whereas large declines in demersal (bottom-associated) fish stocks in the North Atlantic were offset by an increase in demersal biomass in the North Pacific after 1977. This shows how a global average can mask considerable regional variation. Although some ecosystems showed relative stability (e.g., the eastern Bering Sea, Fig. 4B), some experienced a collapse of biomass (e.g., eastern Canada, Fig. 4C), whereas others indicated rebuilding of some dominant target species (e.g., Northeast U.S. Shelf, Fig. 4D). These regional examples illustrate different stages of exploitation and rebuilding.

Research trawl surveys. The best sources of information to assess the state of fished communities are repeated scientific surveys that include both target and nontarget species. We analyzed research trawl survey data from 19 ecosystems where such data were available (see Fig. 1B for locations and fig. S2 and table S3 for full data set). We found that community trends averaged across all surveys (Fig. 4E) were broadly similar to the combined biomass trends seen in the recent assessments (Fig. 4A), with similar signatures of stability (Fig. 4F), collapse (Fig. 4G), and recovery (Fig. 4H) in selected regional ecosystems. Few of these surveys, however, reached back to the beginning of large-scale industrial exploitation in the 1950s and early 1960s. Where they did, for example, in the Gulf of Thailand and in Newfoundland, they revealed a rapid decline in total biomass within the first 15 to 20 years of fishing (fig. S2) as predicted by ecosystem models (Fig. 2). These declines were typically most pronounced for large predators such as gadoids (codfishes) and elasmobranchs (sharks and rays). Subsequent to the initial decline, total biomass and community composition have often remained relatively stable (fig. S2), although there may be substantial species turnover and collapses of individual stocks (see below). Across all surveys combined (*10*), we documented a 32% decline in total biomass, a 56% decline in large demersal fish biomass (species ≥90 cm maximum length), 8% for medium-sized demersals (30 to 90 cm), and 1% for small demersals (≤30 cm), whereas invertebrates increased by 23% and pelagic species by 143% (Fig. 4E). Increases are likely due to prey release from demersal predators (*17*, *18*).

The trawl surveys also revealed changes in size structure that are consistent with model predictions: average maximum size (L_{max}) declined by 22% since 1959 when all communities were included (Fig. 4M). However, there were contrasting trends among our focal regions: L_{max} changed little in the eastern Bering Sea over the surveyed time period (Fig. 4N), dropped sharply in the southern Gulf of St. Lawrence, eastern Canada (Fig. 4O), as large demersal stocks collapsed, and increased because of rebuilding of large demersals (particularly haddock) on Georges Bank, Northeast U.S. Shelf (Fig. 4P). These trends included both target and nontarget species and show how changes in exploitation rates affect the broader community. Published analyses of the Gulf of St. Lawrence and adjacent areas in eastern Canada demonstrate that these community shifts involved large changes in predation regimes, leading to ecological surprises such as predator-prey reversals (*19*), trophic cascades (*17*), and the projected local extinction of formerly dominant species (*20*). Research on the Georges Bank closed area (*21*) and in marine protected areas worldwide (*22*) has shown how some of these changes may reverse when predatory fish are allowed to recover. This reveals top-down interactions cascading from fishers to predators and their multiple prey species as important structuring forces that affect community patterns of depletion and recovery (*18*).

Global fisheries catches. The benefits and costs involved in rebuilding depleted fisheries are demonstrated by an analysis of catch data. Global

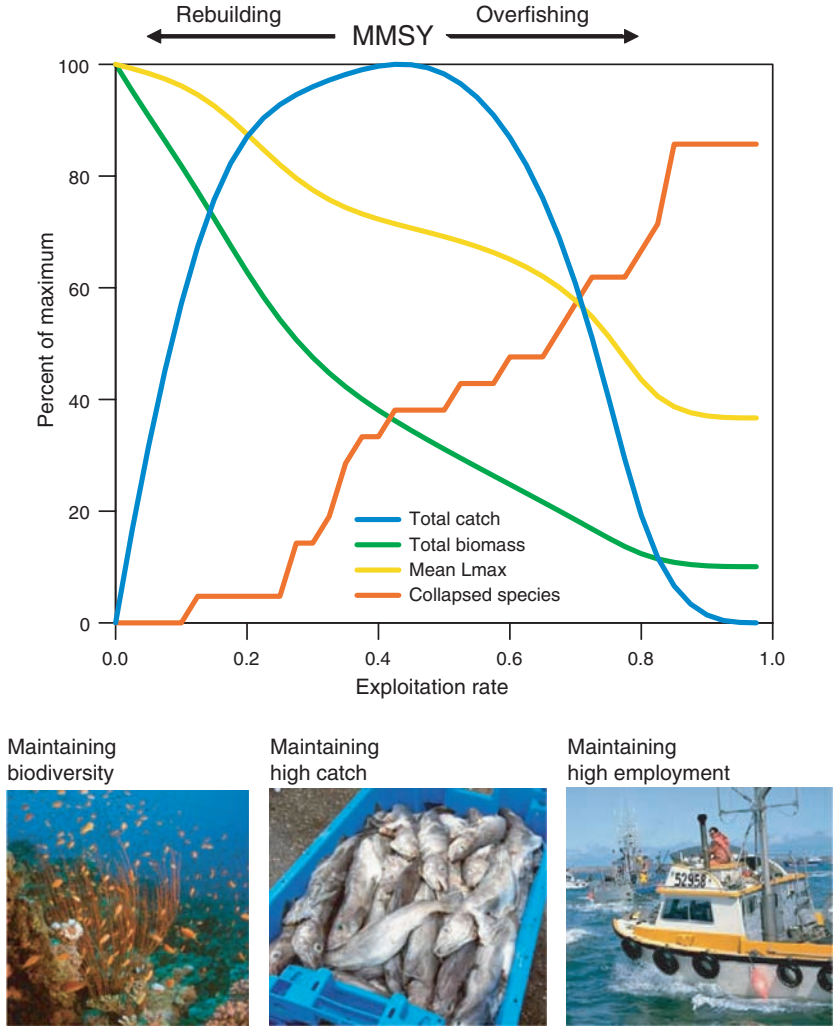

Fig. 2. Effects of increasing exploitation rate on a model fish community. Exploitation rate is the proportion of available fish biomass caught in each year. Mean L_{max} refers to the average maximum length that species in the community can attain. Collapsed species are those for which stock biomass has declined to less than 10% of their unfished biomass. This size-structured model was parameterized for 19 target and 2 nontarget species in the Georges Bank fish community (*13*). It includes size-dependent growth, maturation, predation, and fishing. Rebuilding can occur to the left, overfishing to the right, of the point of maximum catch. Three key objectives that inform current management are highlighted: biodiversity is maintained at low exploitation rate, maximum catch is maintained at intermediate exploitation rate, and high employment is often maintained at intermediate to high exploitation rate, because of the high fishing effort required.

catches have increased ~fivefold since 1950 as total biomass has been fished down (Fig. 4, A and E) then reached a plateau at ~80 million tons in the late 1980s (Fig. 4I). Catch composition with respect to the major species groups has remained relatively stable over time, with the exception of large demersal fishes, which have declined from 23 to 10% of total catch since 1950. Composition with respect to individual species, however, has fluctuated more widely owing to stock collapses (*3*) and expansion to new fisheries (*6*). Individual regions showed very different catch composition and trends, with large- and medium-sized demersal fish being historically dominant in the North Atlantic and North Pacific, small demersals being important in many tropical areas, and pelagic fish dominating the catch from oceanic and coastal upwelling systems (fig. S3). Among our focal regions, the eastern Bering Sea showed a high and stable proportion of large demersal fish (Fig. 4J), the Gulf of St. Lawrence displayed a collapse of the demersal catch and a replacement with small pelagic and invertebrate species (Fig. 4K), and Georges Bank (Fig. 4L) showed a large reduction in catch associated first with declining stocks and then with rebuilding efforts. These examples illustrate that the decline and rebuilding of fished stocks can incur significant costs because of lost catch, whereas sustained management for lower exploitation rates may promote greater stability with respect to both biomass and catches. Part of this stability may arise from the diversity of discrete populations and species that are more likely to persist in fisheries with low exploitation rates (*3*, *23*).

Trends in species collapses. Theory suggests that increases in fishing pressure, even at levels below MMSY, cause an increasing number of target and non-target species to collapse (Fig. 2). Reductions in fishing pressure are predicted to reverse this trajectory, at least partially. By using biomass data from stock assessments compared to estimates of unfished biomass (B_0) (*10*), we found an increasing trend of stock collapses over time, such that 14% of assessed stocks were collapsed in 2007, that is, $B/B_0 < 0.1$ (Fig. 4M). This estimate is in the same range as figures provided by the United Nations Food and Agriculture Organization (FAO), which estimated that 19% of stocks were overexploited and 9% depleted or recovering from depletion in 2007 (*24*). Collapse trends vary substantially by region: The eastern Bering Sea had few assessed fish stocks collapsed (Fig. 4N), whereas collapses strongly increased to more than 60% of assessed stocks in eastern Canada (Fig. 4O) and more than 25% on the Northeast U.S. Shelf (Fig. 4P).

It appears that recent rebuilding efforts, although successful in reducing exploitation rates in several ecosystems (Fig. 3A), have not yet reversed a general trend of increasing depletion of individual stocks (Fig. 4M). This matches the model-derived prediction that reduction of exploitation rate to the level that produces MMSY will still keep a number of vulnerable species collapsed (Fig. 2). Rebuilding these collapsed stocks may require trading off short-term yields for conservation benefits or, alternatively, more selective targeting of species that can sustain current levels of fishing pressure while protecting others from overexploitation.

Small-scale fisheries. Fish or invertebrate stocks that are scientifically assessed (n = 177 in our analysis) or appear in research trawl surveys (n = 1309 taxa-by-survey combinations in fig. S2) constitute only a fraction of fisheries worldwide, which is an important caveat to the above discussion. Moreover they represent a nonrandom sample dominated by valuable industrial fisheries with some form of management in developed countries. The information on other fisheries, particularly small-scale artisanal and recreational fisheries is scarcer, less accessible, and more difficult to interpret. This is because small-scale fisheries are harder to track, with 12 million fishers compared with 0.5 million in industrialized

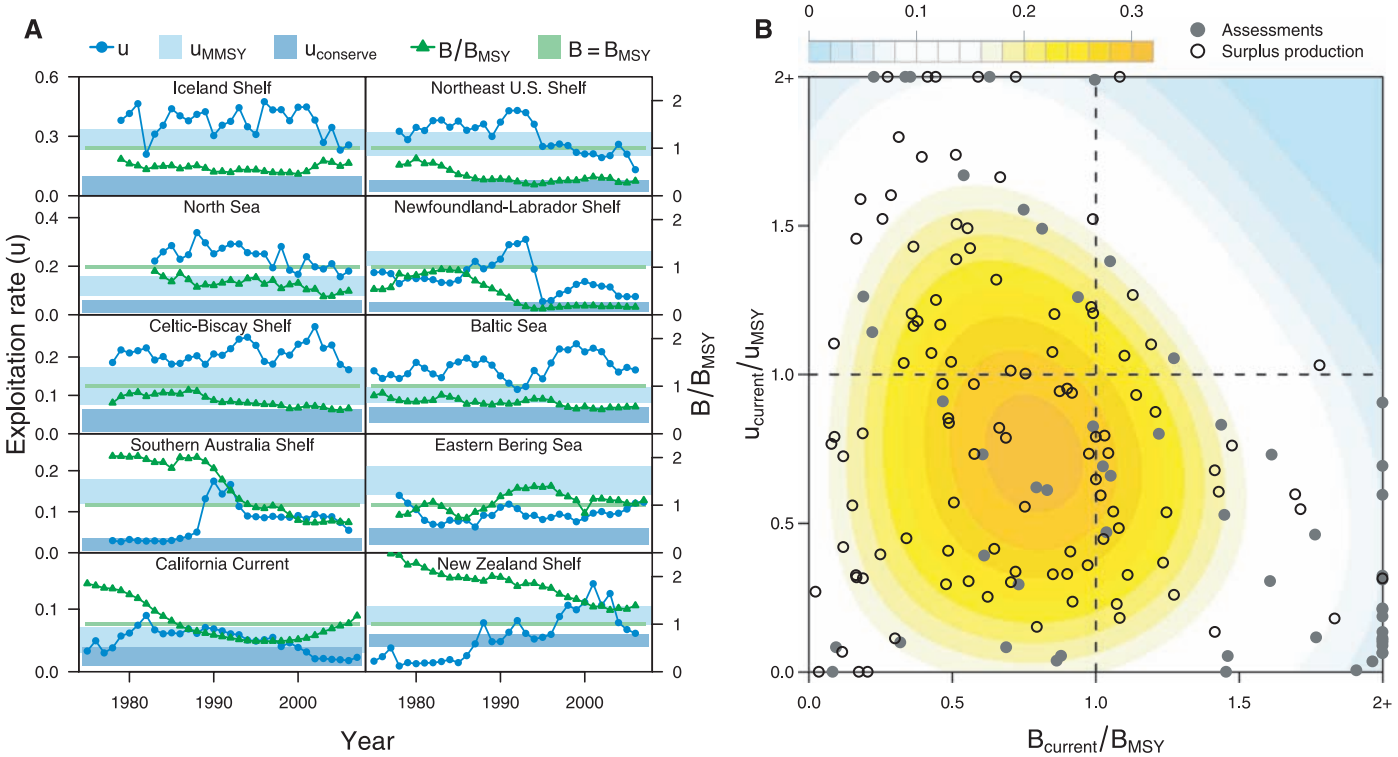

Fig. 3. Exploitation rate and biomass in large marine ecosystems and individual stocks. (**A**) Time trends of biomass (green triangles) are shown relative to the B_{MSY} (green band), exploitation rates (blue circles) relative to the u_{MMSY} (light blue band), and a hypothetical conservation objective at which less than 10% of species are collapsed ($u_{conserve}$, dark blue band). In each ecosystem, stock assessments were used to calculated average biomass relative to B_{MSY} and exploitation rate (total catch divided by total biomass) for assessed species. Reference points were calculated by using published ecosystem models; the width of the bands represents estimated uncertainty (*10*). (**B**) Current exploitation rate versus biomass for 166 individual stocks. Data are scaled relative to B_{MSY} and the exploitation rate (u_{MSY}) that allows for maximum sustainable yield. Colors indicate probability of occurrence as revealed by a kernel density smoothing function. Gray circles indicate that B_{MSY} and u_{MSY} estimates were obtained directly from assessments; open circles indicate that they were estimated from surplus production models (*10*).

fisheries (*25*), and assessments or survey data are often lacking. Small-scale fisheries catches are also poorly reported; the best global estimate is about 21 million tons in 2000 (*25*). Conventional management tools used for industrial fisheries are generally unenforceable in small-scale fisheries when implemented in a top-down manner. More successful forms of governance have involved local communities in a co-management arrangement with government or nongovernmental organizations (*26*). An example is the rebuilding of depleted fish stocks on Kenyan coral reefs (Fig. 5A). A network of closed areas and the exclusion of highly unselective beach seines were implemented in cooperation with local communities and led to a recovery of the biomass and size of available fish (*27*). This translated into steep increases in fishers' incomes, particularly in

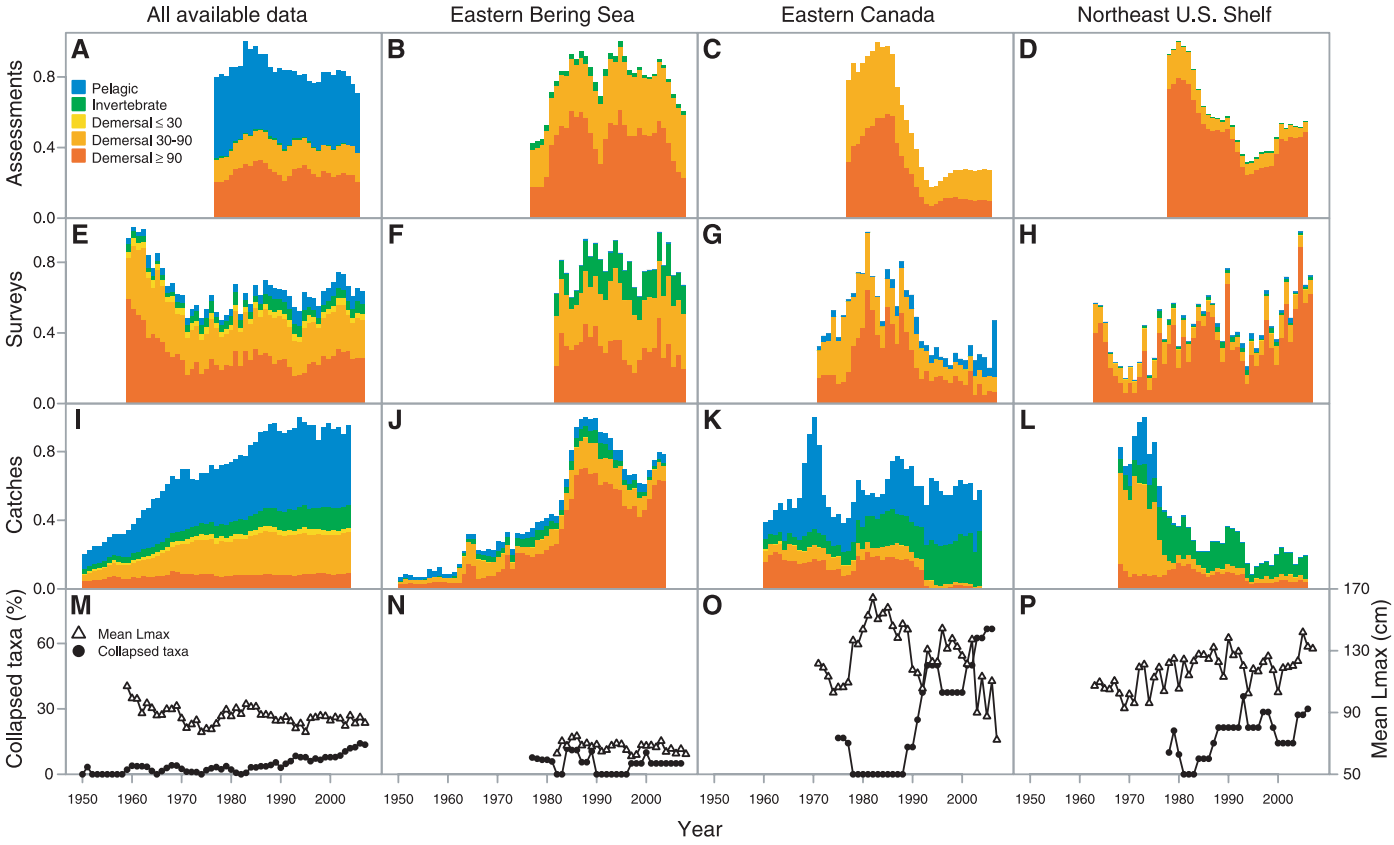

Fig. 4. Global and regional trends in fished ecosystems. Biomass trends computed from stock assessments (**A** to **D**), research surveys (**E** to **H**), as well as total catches (**I** to **L**) are depicted. Trends in the number of collapsed taxa (**M** to **P**, solid circles) were estimated from assessments, and changes in the average maximum size, L_{max} (M to P, open circles), were calculated from survey data (*10*). All data are scaled relative to the time series maximum. (G) and (K) represent the Southern Gulf of St. Lawrence (eastern Canada); (H) and (L), Georges Bank (Northeast U.S. Shelf) only. Collapsed taxa are defined as those where biomass declined to <10% of their unfished biomass. Colors refer to different species groups (demersal fish are split into small, medium, and large species based on the maximum length they can attain).

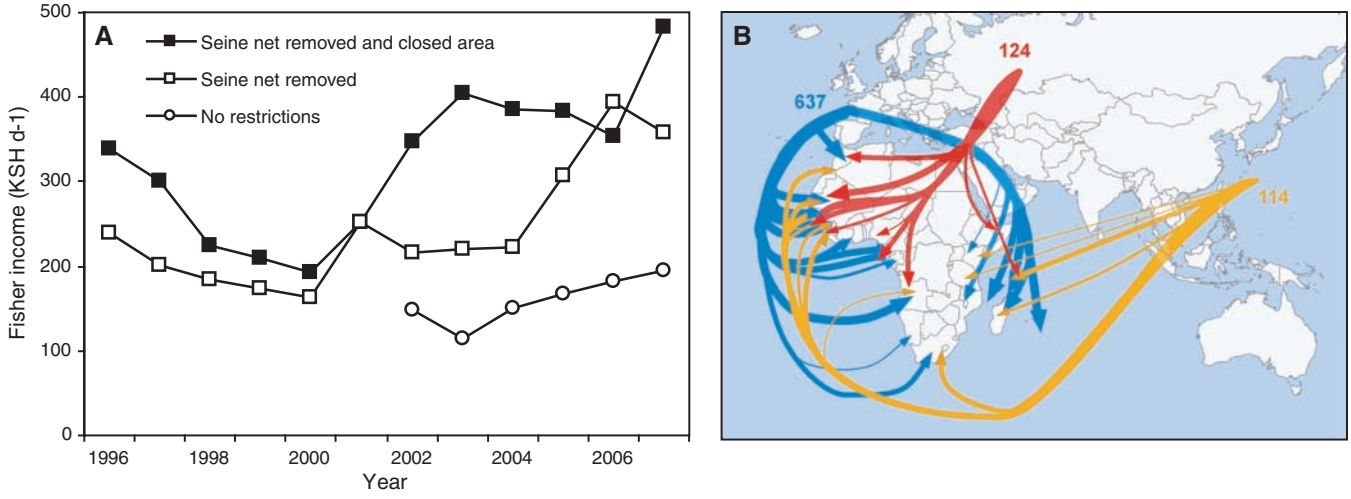

Fig. 5. Problems and solutions for small-scale fisheries. (**A**) Rebuilding of Kenyan small-scale fisheries through gear restrictions and closed area management. Updated, after (*27*). (**B**) Movement of fishing effort from developed nations to Africa in the 1990s. Data indicate total access years in distant-water fishing agreements. Updated, after (*39*).

Table 1. Management tools for rebuilding fisheries. Symbols indicate the contributions of a range of management tools to achieving reductions in exploitation rate: + tool contributed, ++ an important tool, or +++ an essential tool. Note that these examples are for industrialized fisheries, except Kenya, Chile, and Mexico. Ratings were supplied and checked by local experts.

Region	Gear restrictions	Capacity reduced	Total allowable catch reduced	Total fishing effort reduced	Closed areas	Catch shares	Fisheries certification	Community co-management
Bering Sea, Gulf of Alaska	+	++	+++		++	+++	+	+
California Current	+	++	+++		+++			
Northeast U.S. Shelf	+	++		+++	++			
North Sea, Celtic-Biscay	+	+	+++	++	+	+		+
Iceland	+	+	+++			+++		
Southeast Australian Shelf	+	+	+++		++	+++	+	
Northwest Australian Shelf	++				++			
New Zealand	+	+	+++			+++	+	
Kenya (Artisanal)	++				++			+++
Chile and Mexico (Artisanal)	+++				+			+++
Count	10	7	6	2	8	5	3	4
Total score	14	10	18	5	15	13	3	8

regions that had both closed areas and gear restrictions in place (Fig. 5A). Other examples of successful rebuilding come from Latin America, particularly Chile and Mexico, where open-access fisheries for valuable invertebrates were transformed by the establishment of spatial management units that had exclusive access by local fishing organizations (*26*). Despite these successes, rebuilding small-scale fisheries remains a significant challenge in developing countries where most fishers do not have access to alternative sources of food, income, and employment.

Tools for rebuilding. Management actions in a few ecosystems have prevented overfishing or, more commonly, reduced exploitation rates after a period of overfishing (Figs. 3 to 5). Diverse management tools have helped to achieve reductions in exploitation rates (Table 1). The most commonly used tools overall are gear restrictions, closed areas, and a reduction of fishing capacity, followed by reductions in total allowable catch and catch shares. Reductions in fishing capacity and allowable catch directly reduce the exploitation rate of target species by limiting catches. Gear modifications may be used to increase selectivity and reduce by-catch of nontarget species. Closed areas are either fully protected marine reserves (as in the Kenyan example discussed above) or are designed to exclude specific fisheries from certain areas. They can initiate recovery by providing refuge for overfished stocks (*21*, *28*), restoring community structure (*22*) and biodiversity (*3*), protecting important habitat features, and increasing ecosystem resilience (*29*). Assigning dedicated access privileges, such as catch shares or territorial fishing rights, to individual fishers or fishing communities has often provided economic incentives to reduce effort and exploitation rate (*30*) and may also improve compliance and participation in the management process (*31*). Likewise, the certification of sustainable fisheries is increasingly used as an incentive for improved management practices. Realigning economic incentives with resource conservation (rather than overexploitation) is increasingly recognized as a critical component of successful rebuilding efforts (*8*).

We emphasize that the feasibility and value of different management tools depends heavily on local characteristics of the fisheries, ecosystem, and governance system. For example, the most important element of small-scale fisheries success has been community-based management (Table 1), in which local communities develop context-dependent solutions for matching exploitation rates to the productivity of local resources (*26*). A combination of diverse tools, such as catch restrictions, gear modifications, and closed areas, is typically required to meet both fisheries and conservation objectives.

Here we have only identified the proximate tools, not the ultimate socioeconomic drivers that have enabled some regions to prevent or reduce overfishing while others remained overexploited. Yet it is generally evident that good local governance, enforcement, and compliance form the very basis for conservation and rebuilding efforts (*32*). Legislation that makes overexploitation illegal and specifies unambiguous control rules and rebuilding targets has also been critically important, for example, in the United States (*8*, *28*).

Most rebuilding efforts only begin after there is drastic and undeniable evidence of overexploitation. The inherent uncertainty in fisheries, however, requires that agencies act before it comes to that stage (*33*); this is especially true in light of accelerating global change (*34*). We found that only Alaska and New Zealand seemed to have acted with such foresight, whereas other regions experienced systemic overexploitation. The data that we have compiled cannot resolve why inherently complex fish-fisher-management systems (*35*) behaved differently in these cases; possible factors are a combination of abundant resources and low human population, slow development of domestic fisheries, and little interference from international fleets. It would be an important next step to dissect the underlying socioeconomic and ecological variables that enabled some regions to conserve, restore, and rebuild marine resources.

Problems for rebuilding. Despite local successes, it has also become evident that rebuilding efforts can encounter significant problems and

short-term costs. On a regional scale, the reduction of quotas, fishing effort, and overcapacity eliminates jobs, at least in the short term. Initial losses may create strong resistance from fisheries-dependent communities through the political process. For instance in the United States, where 67 overfished stocks have rebuilding plans, 45% of those were still being overfished in 2006, whereas only 3 stocks had been rebuilt at that time (*36*). This problem is exacerbated by the fact that the recovery of depleted stocks can take years or even decades (*28*, *37*), and during this time catches may be dramatically reduced (e.g., Fig. 4L). Furthermore, government subsidies often promote overfishing and overcapacity and need to be reduced against the interests of those who receive them (*38*). Lastly, there is the problem of unreported and illegal fishing, which can seriously undermine rebuilding efforts (*11*). Illegal and unreported catches vary between regions, ranging between an estimated 3% of total catch in the Northeast Pacific to 37% in the East Central Atlantic, with a global average of 18% in 2000–2003 (*11*).

On a global scale, a key problem for rebuilding is the movement of fishing effort from industrialized countries to the developing world (Fig. 5B). This north-south redistribution of fisheries has been accelerating since the 1960s (*39*) and could in part be a perverse side effect of efforts to restore depleted fisheries in the developed world, as some fishing effort is displaced to countries with weaker laws and enforcement capacity. The situation is particularly well documented for West Africa (*39*) and more recently East Africa, where local fisheries have seen increasing competition from foreign fleets operating under national access agreements (Fig. 5B) and where illegal and unreported catches are higher than anywhere else (*11*). Almost all of the fish caught by foreign fleets is consumed in industrialized countries and may threaten regional food security (*39*) and biodiversity (*40*) in the developing world. Clearly, more global oversight is needed to ensure that rebuilding efforts in some regions do not cause problems elsewhere. For example, fishing vessels removed in effort-reduction schemes would ideally be prohibited from migrating to other regions and exacerbating existing problems with overcapacity and overexploitation.

Open questions. Rebuilding efforts raise a number of scientific questions. Recovery of depleted stocks is still a poorly understood process, particularly for demersal species (*37*). It is potentially constrained by the magnitude of previous decline (*37*), the loss of biodiversity (*3*, *23*), species life histories (*37*), species interactions (*17*, *18*, *20*), and climate (*28*, *34*). Yet, many examples of recovery exist, both in protected areas (*3*, *21*, *22*) and in large-scale ecosystems where exploitation was substantially reduced (Fig. 3A). A better understanding of how to predict and better manage for recovery will require insight into the resilience and productivity of individual populations and their communities. This could be gained by more widespread spatial experimentation, involving proper controls, good monitoring, and adaptive management. Some of the most spectacular rebuilding efforts, such as those undertaken in California (*41*), the northeast United States (*21*), and northwest Australia (*42*), have involved bold experimentation with closed areas, gear and effort restrictions, and new approaches to catch allocation and enforcement. Science has a key role to play in guiding such policies, analyzing the effects of changes in management and advancing toward more general rules for rebuilding.

A second area of inquiry relates to the question of how to avoid contentious trade-offs between allowable catch and the conservation of vulnerable or collapsed species. Recovering these species while maintaining global catches may be possible through improved gear technology and a much more widespread use of ocean zoning into areas that are managed for fisheries benefits and others managed for species and habitat conservation. Designing appropriate incentives for fishers to avoid the catch of threatened species, for example, through tradable catch and by-catch quotas, has yielded good results in some regions (*16*). Temporary area closures can also be effective but require detailed mapping of the distribution of depleted populations and their habitats.

Conclusions. Marine ecosystems are currently subjected to a range of exploitation rates, resulting in a mosaic of stable, declining, collapsed, and rebuilding fish stocks and ecosystems. Management actions have achieved measurable reductions in exploitation rates in some regions, but a significant fraction of stocks will remain collapsed unless there are further reductions in exploitation rates. Unfortunately, effective controls on exploitation rates are still lacking in vast areas of the ocean, including those beyond national jurisdiction (*6*, *8*, *32*). Ecosystems examined in this paper account for less than a quarter of world fisheries area and catch, and lightly to moderately fished and rebuilding ecosystems (green and yellow areas in Fig. 1B) comprise less than half of those. They may best be interpreted as large-scale restoration experiments that demonstrate opportunities for successfully rebuilding marine resources elsewhere. Similar trajectories of recovery have been documented in protected areas around the world (*3*, *21*, *22*), which currently cover less than 1% of ocean area. Taken together, these examples provide hope that despite a long history of overexploitation (*1*, *2*) marine ecosystems can still recover if exploitation rates are reduced substantially. In fisheries science, there is a growing consensus that the exploitation rate that achieves maximum sustainable yield (u_{MSY}) should be reinterpreted as an upper limit rather than a management target. This requires overall reductions in exploitation rates, which can be achieved through a range of management tools. Finding the best management tools may depend on the local context. Most often, it appears that a combination of traditional approaches (catch quotas, community management) coupled with strategically placed fishing closures, more selective fishing gear, ocean zoning, and economic incentives holds much promise for restoring marine fisheries and ecosystems. Within science, a new cooperation of fisheries scientists and conservation biologists sharing the best available data, and bridging disciplinary divisions, will help to inform and improve ecosystem management. We envision a seascape where the rebuilding, conservation, and sustainable use of marine resources become unifying themes for science, management, and society. We caution that the road to recovery is not always simple and not without short-term costs. Yet, it remains our only option for insuring fisheries and marine ecosystems against further depletion and collapse.

References and Notes

1. J. B. C. Jackson *et al.*, *Science* **293**, 629 (2001).
2. H. K. Lotze *et al.*, *Science* **312**, 1806 (2006).
3. B. Worm *et al.*, *Science* **314**, 787 (2006).
4. R. Hilborn, *Ecosystems (N. Y., Print)* **10**, 1362 (2007).
5. S. Murawski *et al.*, *Science* **316**, 1281b (2007).
6. D. Pauly *et al.*, *Science* **302**, 1359 (2003).
7. T. H. Huxley, *Inaugural Meeting of the Fishery Congress: Address by Professor Huxley* (William Clowes and Sons, London, 1883).
8. J. R. Beddington, D. J. Agnew, C. W. Clark, *Science* **316**, 1713 (2007).
9. S. M. Garcia, A. Zerbi, C. Aliaume, T. Do Chi, G. Lasserre, "The ecosystem approach to fisheries" (FAO, Rome, 2003).
10. Details on methods and data sources are available as supporting online material on *Science* Online.
11. D. J. Agnew *et al.*, *PLoS One* **4**, e4570 (2009).
12. E. A. Fulton, A. D. M. Smith, C. R. Johnson, *Mar. Ecol. Prog. Ser.* **253**, 1 (2003).
13. S. J. Hall *et al.*, *Can. J. Fish. Aquat. Sci.* **63**, 1344 (2006).
14. R. Q. Grafton, T. Kompas, R. W. Hilborn, *Science* **318**, 1601 (2007).
15. S. Jennings, A. S. Revill, *ICES J. Mar. Sci.* **64**, 1525 (2007).
16. T. A. Branch, R. Hilborn, *Can. J. Fish. Aquat. Sci.* **65**, 1435 (2008).
17. K. T. Frank, B. Petrie, J. S. Choi, W. C. Leggett, *Science* **308**, 1621 (2005).
18. J. K. Baum, B. Worm, *J. Anim. Ecol.* **78**, 699 (2009).
19. D. P. Swain, A. F. Sinclair, *Can. J. Fish. Aquat. Sci.* **57**, 1321 (2000).
20. D. P. Swain, G. A. Chouinard, *Can. J. Fish. Aquat. Sci.* **65**, 2315 (2008).
21. S. A. Murawski, R. Brown, H.-L. Lai, P. J. Rago, L. Hendrickson, *Bull. Mar. Sci.* **66**, 775 (2000).
22. F. Micheli, B. S. Halpern, L. W. Botsford, R. R. Warner, *Ecol. Appl.* **14**, 1709 (2004).
23. R. Hilborn, T. P. Quinn, D. E. Schindler, D. E. Rogers, *Proc. Natl. Acad. Sci. U.S.A.* **100**, 6564 (2003).
24. FAO, *The State of World Fisheries and Aquaculture 2008* (FAO, Rome, 2009).
25. D. Pauly, *Marit. Stud.* **4**, 7 (2006).
26. O. Defeo, J. C. Castilla, *Rev. Fish Biol. Fish.* **15**, 265 (2005).
27. T. R. McClanahan, C. C. Hicks, E. S. Darling, *Ecol. Appl.* **18**, 1516 (2008).
28. J. F. Caddy, D. J. Agnew, *Rev. Fish Biol. Fish.* **14**, 43 (2004).
29. J. A. Ley, I. A. Halliday, A. J. Tobin, R. N. Garrett, N. A. Gribble, *Mar. Ecol. Prog. Ser.* **245**, 223 (2002).
30. C. Costello, S. D. Gaines, J. Lynham, *Science* **321**, 1678 (2008).
31. NRC, *Cooperative Research in the National Marine Fisheries Service* (National Research Council Press, Washington, DC, 2003).
32. C. Mora *et al.*, *PLoS Biol.* **7**, e1000131 (2009).

33. D. Ludwig, R. Hilborn, C. Walters, *Science* **260**, 17 (1993).
34. K. M. Brander, *Proc. Natl. Acad. Sci. U.S.A.* **104**, 19709 (2007).
35. P. A. Larkin, *Annu. Rev. Ecol. Syst.* **9**, 57 (1978).
36. A. A. Rosenberg, J. H. Swasey, M. Bowman, *Front. Ecol. Environ* **4**, 303 (2006).
37. J. A. Hutchings, J. D. Reynolds, *Bioscience* **54**, 297 (2004).
38. U. R. Sumaila *et al.*, *Fish. Res.* **88**, 1 (2007).
39. J. Alder, U. R. Sumaila, *J. Environ. Dev.* **13**, 156 (2004).
40. J. S. Brashares *et al.*, *Science* **306**, 1180 (2004).
41. M. Dalton, S. Ralston, *Mar. Resour. Econ.* **18**, 67 (2004).
42. K. J. Sainsbury, R. A. Campbell, R. Lindholm, A. W. Whitelaw, in *Fisheries Management: Global Trends*, E. K. Pikitch, D. D. Huppert, M. P. Sissenwine, Eds. (American Fisheries Society, Bethesda, MD, 1997), pp. 107–112.
43. This work was conducted as part of the "Finding common ground in marine conservation and management" Working Group supported by the National Center for Ecological Analysis and Synthesis funded by NSF, the University of California, and the Santa Barbara campus. The authors acknowledge the Natural Sciences and Engineering Research Council (NSERC) and the Canadian Foundation for Innovation for funding database development, the Sea Around Us Project funded by Pew Charitable Trusts for compiling global catch data, and numerous colleagues and institutions around the world for sharing fisheries assessment, catch, access, and survey data, and ecosystem models (see SOM for full acknowledgments).

Supporting Online Material
www.sciencemag.org/cgi/content/full/325/5940/578/DC1
Materials and Methods
Figs. S1 to S6
Tables S1 to S7
References and Notes

27 April 2009; accepted 22 June 2009
10.1126/science.1173146

Pre-Target Axon Sorting Establishes the Neural Map Topography

Takeshi Imai,[1]* Takahiro Yamazaki,[1]* Reiko Kobayakawa,[1] Ko Kobayakawa,[1] Takaya Abe,[2] Misao Suzuki,[3] Hitoshi Sakano[1]†

Sensory information detected by the peripheral nervous system is represented as a topographic map in the brain. It has long been thought that the topography of the map is determined by graded positional cues that are expressed by the target. Here, we analyzed the pre-target axon sorting for olfactory map formation in mice. In olfactory sensory neurons, an axon guidance receptor, Neuropilin-1, and its repulsive ligand, Semaphorin-3A, are expressed in a complementary manner. We found that expression levels of Neuropilin-1 determined both pre-target sorting and projection sites of axons. Olfactory sensory neuron–specific knockout of Semaphorin-3A perturbed axon sorting and altered the olfactory map topography. Thus, pre-target axon sorting plays an important role in establishing the topographic order based on the relative levels of guidance molecules expressed by axons.

In the vertebrate nervous system, sensory information is spatially encoded in the brain, forming topographic maps that are fundamental for cognition and higher-order processing of sensory information (*1*, *2*). Molecular mechanisms of topographic map formation have been extensively studied in the visual system. The visual image on the retina is roughly preserved in the tectum, which receives retinal ganglion cell axons. Nearly 50 years ago, Sperry proposed the "chemoaffinity hypothesis," in which target cells present chemical cues to guide axons to their destinations (*3*). Axonal projection of retinal ganglion cells is instructed by several pairs of axon guidance molecules that demonstrate graded expression in the retina and tectum (*1*, *2*).

Olfactory information is also encoded in a topographic map formed on the olfactory bulb (OB), a part of the forebrain. In rodents, odors are detected with ~1000 types of odorant receptors (ORs) expressed in olfactory sensory neurons (OSNs) in the olfactory epithelium (*4*). Each OSN expresses only one functional OR gene (*5*, *6*). Furthermore, OSNs expressing a given type of OR converge their axons to a specific glomerulus on each glomerular map in the OB (*7*–*9*). During olfactory development, OSN axons are guided to approximate locations in the OB by the combination of dorsal-ventral patterning, based on anatomical locations of OSNs in the olfactory epithelium (*10*), and anterior-posterior patterning, regulated by OR-derived cyclic adenosine monophosphate (cAMP) signals (*11*, *12*). The glomerular arrangement along the dorsal-ventral axis appears to be determined by axon guidance molecules expressed in a graded manner along the dorsomedial-ventrolateral axis in the olfactory epithelium, such as Robo-2 (*13*) and Neuropilin-2 (*14*). Unlike dorsal-ventral positioning, anterior-posterior positioning of glomeruli is independent of positional information in the olfactory epithelium. Instead, OR-specific cAMP signals determine the expression levels of Neuropilin-1 (Nrp1) in OSN axon termini, forming a gradient of Nrp1 (*11*). Thus, the olfactory system also uses gradients of axon guidance molecules to form the topographic map.

How then do guidance molecules regulate topographic map formation? Does map formation solely depend on axon-target interaction? Topographic order emerges in axon bundles, well before they reach the target (*15*, *16*). Here, we studied the pre-target sorting of OSN axons and its role in topographic map formation in the mouse olfactory system.

Nrp1 regulates axonal projection of OSNs along the anterior-posterior axis. OR-derived cAMP signals regulate the axonal projection of OSNs along the anterior-posterior axis in the OB; low cAMP leads to anterior positioning and high cAMP leads to posterior positioning (*11*). Furthermore, the levels of Nrp1 in OSN axon termini correlated with the level of cAMP signals (*11*).

We found that the Nrp1 levels determine the glomerular positioning along the anterior-posterior axis. When Nrp1 was overexpressed in OR-I7–expressing OSNs (fig. S1), projection sites shifted posteriorly relative to the control (Fig. 1A and fig. S2). In contrast, when Nrp1 was knocked out specifically in I7 OSNs, the projection sites shifted anteriorly relative to the control (Fig. 1A and fig. S2). In the pan-OSN Nrp1 knockout, however, projection sites for I7 often split into anterior and posterior areas (fig. S3). If absolute Nrp1 levels determine glomerular positioning, all glomeruli should form in the anterior OB in the pan-OSN knockout, and the results for I7 OSNs should be the same between the I7-specific knockout and pan-OSN knockout. These results indicate that the relative Nrp1 levels among axons determine the OSN projection sites.

Pre-target axon sorting in the bundle. How do the relative levels of Nrp1 determine the anterior-posterior positioning of glomeruli in the axonal projection of OSNs? To determine where the organization occurs for the olfactory map topography, we analyzed the axon bundles of dorsal-zone (D-zone) OSNs that project to the dorsal domain (D domain) of the OB. The D domain OB comprises two regions, DI and DII; DI is represented by class I ORs, and DII is represented by class II ORs. Class I and class II ORs are phylogenetically distinct and their glomeruli are segregated in the OB (*17*). We subdivided DII into two areas on the basis of Nrp1 expression level (*18*): DII-P is the posterior portion innervated by Nrp1-high axons, and DII-A is the anterior region innervated by Nrp1-low axons. Thus, the D domain can be divided into three areas: DI, DII-A, and DII-P (Fig. 1B).

Axon bundles that project to the D-domain OB were analyzed in neonatal mice by staining serial coronal sections from the anterior olfactory epithelium through the OB. Within the bundle,

[1]Department of Biophysics and Biochemistry, Graduate School of Science, University of Tokyo, Tokyo 113-0032, Japan. [2]Laboratory for Animal Resources and Genetic Engineering, Center for Developmental Biology, RIKEN, Kobe 650-0047, Japan. [3]Division of Transgenic Technology, Center for Animal Resources and Development, Kumamoto University, Kumamoto 860-0081, Japan.

*These authors contributed equally to this work.
†To whom correspondence should be addressed. E-mail: sakano@mail.ecc.u-tokyo.ac.jp

DI axons stained with DBA-lectin (fig. S4), DII-P axons stained with Nrp1 antibodies, and DII-A axons stained with neither. To visualize the Nrp1-low axon group (DII-A), we stained for yellow fluorescent protein (YFP)–positive OSNs that express the mutant OR gene *I7(RDY)-ires-gapYFP*; the I7(RDY) receptor is unable to activate downstream cAMP signals, thereby causing a lack of Nrp1 expression (*11*). Early in the trajectory of OSN projection, DI, DII-A, and DII-P axons were intermingled within the bundle. As the bundle progressed posteriorly, however, the axons segregated into a tripartite organization before they reached the target OB (Fig. 1B). Within the bundle, DI, DII-A, and DII-P axons were sorted to the medial, central, and lateral areas, respectively. Furthermore, there was a topographic order even within the DII-P axon group. Anterior-posterior positioning of glomeruli in the OB is well correlated with the central-lateral localization of axons in the bundle (fig. S5). Thus, the olfactory map topography emerges within the axon bundle prior to the axon-target interactions in the OB.

Heterotypic OSN axons segregate even without the OB (*19*, *20*). We analyzed the *Gli3* mutant mouse (*Pdn/Pdn*), where the OB is completely absent, and found that the pre-target axon sorting indeed occurred (Fig. 2A) (*21*). In the *Pdn/Pdn* mutant, OSN axons demonstrated a graded anterior-posterior topography among the olfactory fibers in the cranial cavity (Fig. 2B), which supports the notion that the anterior-posterior topography can be formed, at least partially, without axon-target interactions.

Nrp1 regulates pre-target axon sorting. Because Nrp1-high (DII-P) and Nrp1-low (DII-A) axons are segregated within the bundles, we investigated whether Nrp1 is involved in the pre-target axon sorting. Wild-type I7 axons were normally found among the Nrp1-positive DII-P axons in the lateral area in the bundle (Fig. 3A and fig. S6A). When Nrp1 was specifically knocked out in I7-expressing OSNs, these I7 axons moved to the central area (DII-A). In contrast to the wild-type I7, axons of the I7(RDY) mutant OSNs, which do not express Nrp1, were found in the central area (DII-A) of the bundle (Fig. 3B and fig. S6B). By simply expressing Nrp1 in these mutant OSNs with I7(RDY)-ires-Nrp1, axons moved to the lateral area (DII-P). Thus, Nrp1 indeed determines the sorting of DII-A (central) and DII-P (lateral) axons within the bundle.

Sema3A expressed by OSNs is required for axon sorting. Nrp1 is the receptor for the secreted repulsive ligand Semaphorin-3A (Sema3A) (*22*). Sema3A knockout disrupts proper targeting of OSNs (*23*, *24*). We studied the possible involvement of Sema3A in pre-target axon sorting. *Sema3A* is expressed not only in the target, but also in OSNs. Single-cell microarray analysis revealed that *Nrp1*

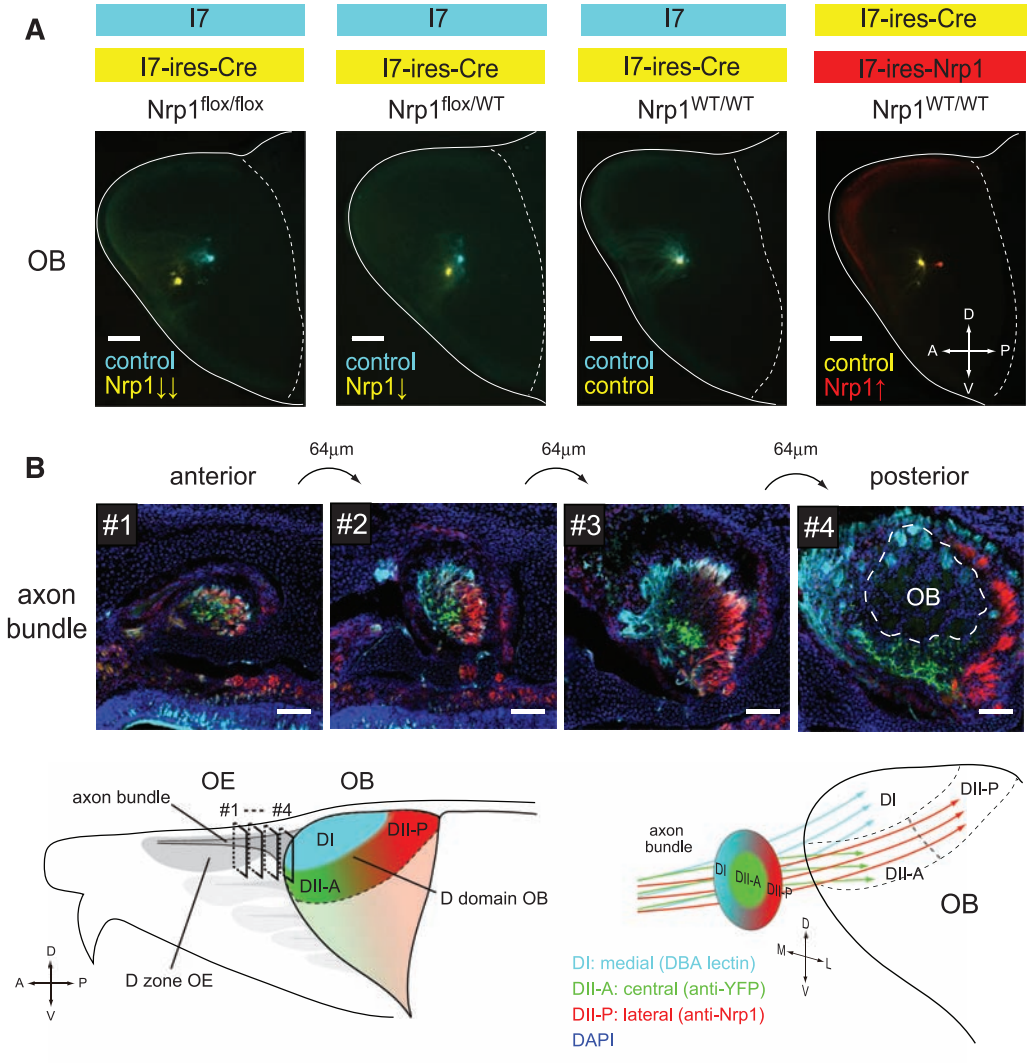

Fig. 1. Projection and axon sorting of OSNs. (**A**) Genetic manipulation of Nrp1 expression levels in OSNs. Whole-mount fluorescent views of OBs (medial surface) were analyzed [age, postnatal day 14 (P14)]. For the loss of function of Nrp1, an I7-ires-Cre mouse (labeled with gap-YFP; yellow) was crossed to the floxed Nrp1 line. The projection site for the I7 (labeled with gap-CFP; cyan) was analyzed as an internal control in the same animal. In the $Nrp1^{flox/flox}$ background, Nrp1 was specifically knocked out in OSNs expressing I7-ires-Cre. As a result, projection sites were shifted anteriorly in the OB. In the $Nrp1^{flox/WT}$ background, where the Nrp1 level was decreased by half, the anterior shifts were intermediate to those in the $Nrp1^{flox/flox}$ background. In the $Nrp1^{WT/WT}$ background, CFP- and YFP-labeled OSN axons coconverged. For the gain of function of Nrp1, we generated I7-ires-Nrp1 (labeled with gap-mCherry; red) and compared the projection site to that of the control construct, I7-ires-Cre. In the double transgenic mice, I7-ires-Nrp1 glomeruli were found posterior to the I7-ires-Cre glomeruli. Statistical data are in fig. S2. Scale bars, 500 μm. (**B**) Pre-target axon sorting of OSNs. The axons of dorsal-zone (D-zone) OSNs course through the bundle on the dorsal roof of the olfactory epithelium before projecting to the D domain of the OB. The D domain comprises DI and DII domains in the OB. The DI domain is located in the most dorsal part of the OB; the DII domain is just ventral to DI and is further divided into DII-P (Nrp1-high; posterior) and DII-A (Nrp1-low; anterior). DI axons were stained with DBA lectin (cyan). DII-P axons were immunostained with antibodies to Nrp1 (red). For labeling of DII-A axons, OSN axons expressing I7(RDY)-ires-gapYFP were immunostained with antibodies to YFP (green). Three types of axons projecting to the DI, DII, and DII-P regions in the OB are intermingled in the bundle near the olfactory epithelium but segregate to form a tripartite organization as they approach the OB. Coronal sections (#1 to #4, each separated by 64 μm) are shown. DI, DII-A, and DII-P axons are sorted to the medial, central, and lateral areas, respectively. Scale bars, 100 μm. OE, olfactory epithelium; A, anterior; P, posterior; D, dorsal; V, ventral; M, medial; L, lateral; ires, internal ribosome entry site.

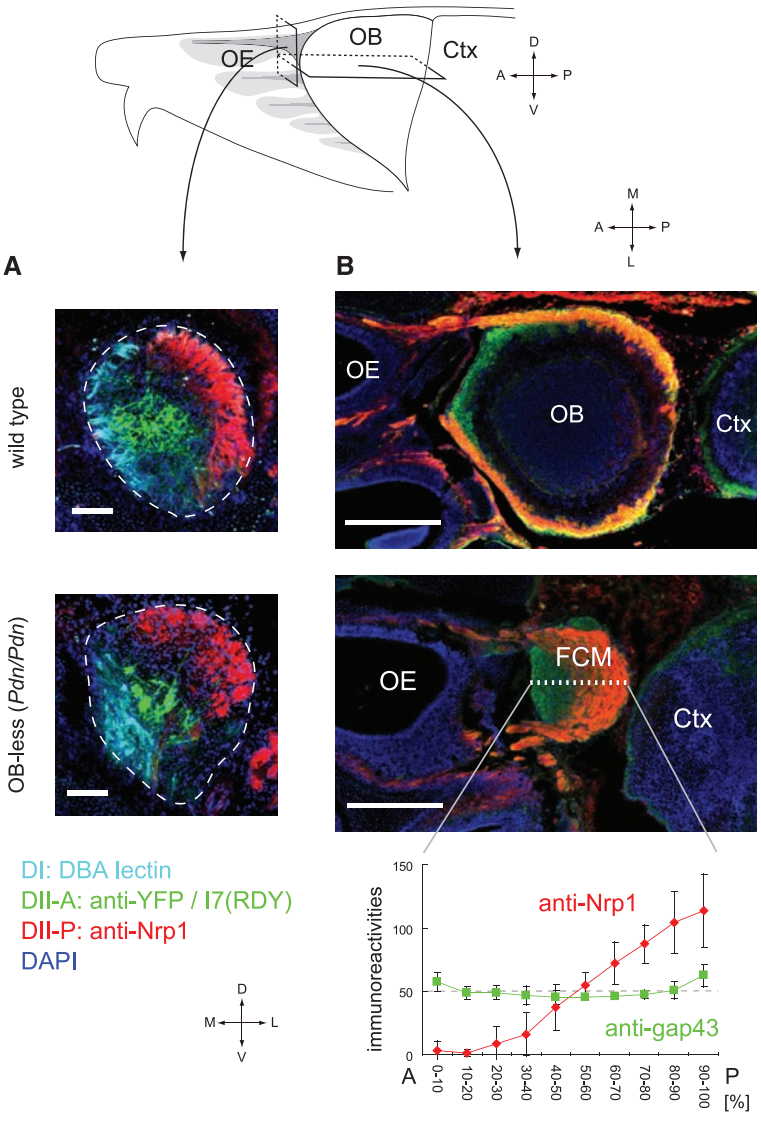

Fig. 2. Anterior-posterior topography is established without the OB. The OB-less mutant *Pdn/Pdn* was analyzed. The *Pdn/Pdn* mouse has an insertional mutation within the *Gli3* gene coding for a transcription factor (*21*), resulting in agenesis of the OB. In the cranial cavity of these mutant mice, OSN axons form a fibrocellular mass (FCM). (**A**) Coronal sections of axon bundles from the wild-type and *Pdn/Pdn* mutant mice were analyzed (age, P0). OSN axons expressing I7(RDY)-ires-gapYFP were immunostained with antibodies to YFP. Axonal segregation occurred without the OB in the *Pdn/Pdn* mutant (n = 6/6). Scale bars, 100 μm. (**B**) Horizontal OB sections of the wild-type and mutant mice (age, P0) were immunostained with antibodies to Nrp1 (red) and gap43 (green); gap43 is an axonal marker for OSNs. In the glomerular layer of the wild-type OB, Nrp1 shows an anterior-low–posterior-high gradient (*11*). Similarly, in the mutant mouse (*Pdn/Pdn*), Nrp1 demonstrates an anterior-low–posterior-high gradient within the FCM in the absence of the OB. Nrp1 and gap43 immunoreactivities were quantified along the anterior-posterior axis of the FCM (along the dotted line). Mean signal intensities are normalized to 50. Data are means ± SD (n = 8). OE, olfactory epithelium; Ctx, cerebral cortex. Scale bars, 500 μm.

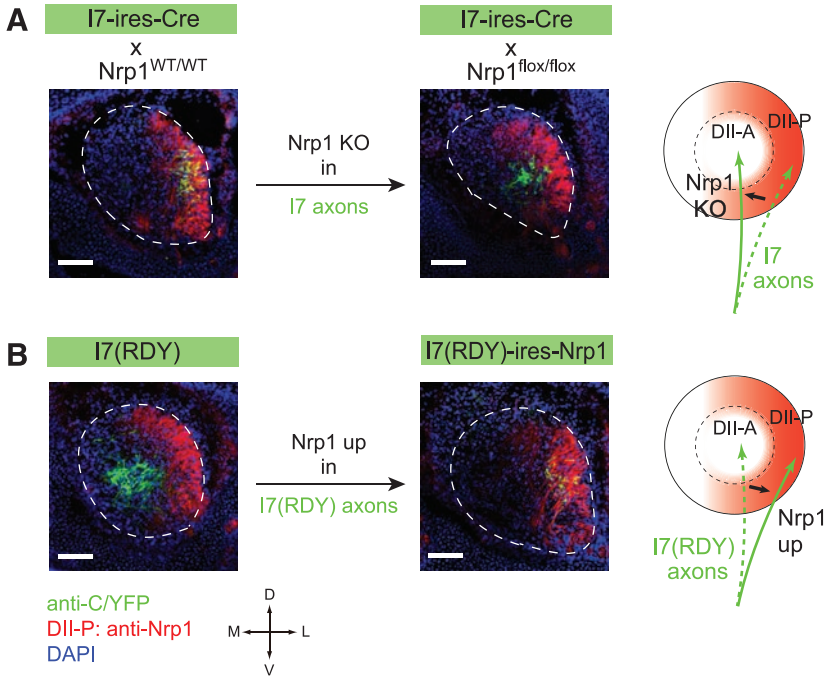

Fig. 3. Nrp1 regulates axon sorting in the bundle. (**A**) The loss-of-function experiment. Axons for I7-ires-Cre were sorted to the lateral peripheral area (DII-P). When Nrp1 was knocked out specifically in I7-ires-Cre OSNs, axons were sorted to the central region (DII-A). (**B**) The gain-of-function experiment. Axons for I7(RDY) that do not express Nrp1 were sorted to the central area of the bundle (DII-A). When Nrp1 was expressed specifically in I7(RDY) OSNs in the I7(RDY)-ires-Nrp1 mouse, axons were sorted to the lateral periphery (DII-P). Quantitative analyses are in fig. S6. Coronal sections of axon bundles (age, P0) were analyzed. Changes in axon sorting in the bundle are schematically shown at the right. Scale bars, 100 μm.

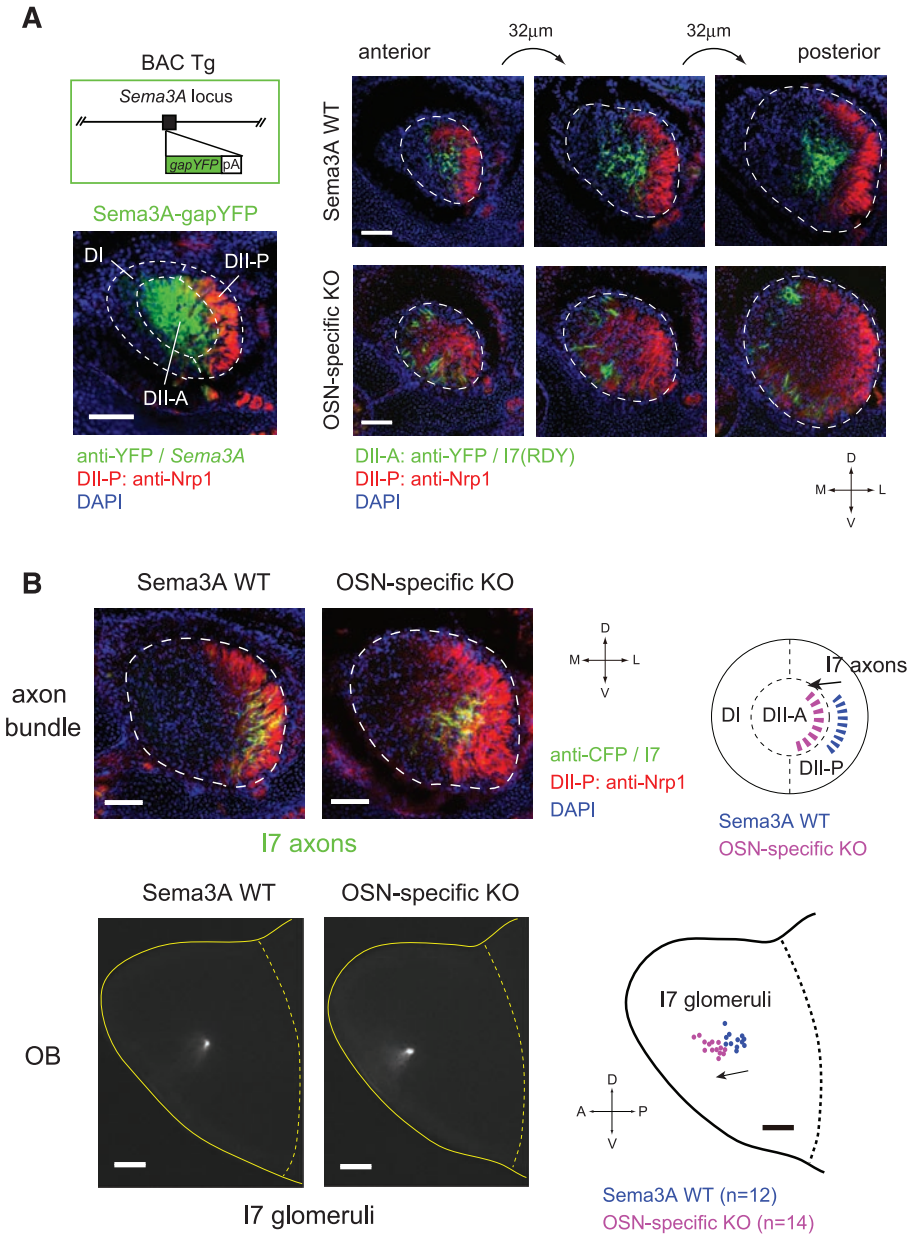

Fig. 4. OSN-derived Sema3A regulates not only pre-target axon sorting in the bundle, but also glomerular positioning in the OB. (**A**) Left panel: Segregation of Nrp1-expressing and Sema3A-expressing axons in the bundle (see also fig. S8B). The axonal marker protein gap-YFP was expressed under the *Sema3A* promoter in the BAC transgenic mice (age, P0). Nrp1-high DII-P axons were sorted to the lateral periphery (DII-P), whereas Sema3A-high axons were sorted to the central area (DII-A). Right panel: Axon sorting in the bundle in wild-type and OSN-specific Sema3A knockout mice. The conditional knockout mice were generated by crossing the OMACS-Cre line and the floxed Sema3A line (fig. S9). In the OSN-specific Sema3A knockout (age, P0), Nrp1-expressing axons (DII-P) spread out within the bundle, although they are still dense in the lateral region. I7(RDY) axons normally sorted to the central region (DII-A) are found in the medial region in the axon bundle. Scale bars, 100 μm. (**B**) Sorting and projection of I7-expressing OSN axons. In the wild-type mouse, I7 axons are sorted to the lateral periphery of the bundle. In contrast, in the OSN-specific Sema3A knockout, I7 axons are sorted to the central area, where DII-A axons are normally found (age, P0). Sorting patterns of I7 axons are schematically shown at the right (see also fig. S10B). Projection sites for I7 axons were analyzed in the OB (whole-mount medial views; age, P14). In the OSN-specific Sema3A knockout, I7 glomeruli were found anterior to the wild-type control. Results are summarized at the right; I7 glomeruli for the OSN-specific Sema3A knockout (14 bulbs, magenta) and wild-type littermates (12 bulbs, blue) are plotted on a schematic diagram of the medial OB (see also fig. S11A). Note that I7 OSN-specific Sema3A knockout did not affect the glomerular positioning (fig. S11B). Scale bars, 100 μm (axon bundles), 500 μm (OBs).

and *Sema3A* genes are regulated in a complementary manner by OR-derived cAMP signals (fig. S7) (*25*). In situ hybridization of embryonic olfactory epithelium demonstrated complementary expression of *Nrp1* and *Sema3A* (fig. S8A). To visualize the Sema3A-expressing OSN axons, we generated bacterial artificial chromosome (BAC) transgenic mice in which an axonal marker, *gap-YFP*, is expressed under the control of the *Sema3A* promoter (fig. S1). In the transgenic mouse, Sema3A-positive axons were found in the Nrp1-low area (DII-A) in the bundle (Fig. 4A and fig. S8B), which suggests that Nrp1-high axons (DII-P) are repelled by Sema3A-expressing axons (DII-A).

Because Sema3A is expressed in different cell types in olfactory tissues, we generated an OSN-specific knockout for Sema3A to investigate whether Sema3A in OSN axons is required for axon sorting within the bundle. We used the *OMACS* gene promoter, which is activated in the D-zone olfactory epithelium during early embryogenesis, to drive the expression of Cre recombinase (fig. S9) (*26*, *27*). The OMACS-Cre mouse was crossed to the floxed Sema3A mouse (*28*) to generate the OSN-specific conditional knockout. In wild-type mice, Nrp1-positive DII-P axons are sorted to the lateral periphery of the bundle. In the conditional Sema3A knockout, however, the DII-P axons were no longer confined to the lateral periphery (Fig. 4A). Concomitantly, DII-A axons spread to more medial areas in the bundle. Tripartite compartmentalization was not evident in the OSN-specific Sema3A knockout. Thus, Sema3A derived from OSN axons is required for pre-target axon sorting in the bundle.

Pre-target axon sorting affects the topographic map formation in the OB. We asked whether perturbation of axon sorting mediated by OSN-derived Sema3A affects glomerular map formation in the OB. In wild-type mice, I7 axons that coexpress gap-CFP (cyan fluorescent protein) were sorted to the lateral-peripheral compartment (DII-P) within the bundle. In the conditional Sema3A knockout, however, I7 axons were found in the central area where the DII-A axons are normally found (Fig. 4B and fig. S10B). When I7 glomeruli were analyzed in the OB, anterior shifts were observed in the conditional knockout (Fig. 4B and fig. S11A), consistent with the shift of I7 axons in the bundle. We also analyzed Nrp1-negative DII-A axons in the conditional knockout (fig. S12). These axons were confined to the central area in the wild-type bundle. However, they were scattered to both the central and medial areas in the conditional knockout. As a result, glomeruli were found not only in the anterior but also in the dorsal OB in the conditional knockout. Thus, positional changes within the axon bundle correlate well with positional changes of glomeruli in the OB.

Discussion. We found that pre-target axon sorting plays an important role in the organization of the topographic map. Nrp1 and its repulsive ligand Sema3A are both expressed in OSNs and are involved in axon sorting before targeting on the OB. Within the axon bundles

of D-zone OSNs, DII-A axons (Nrp1 low, Sema3A high) are sorted to the central compartment of the bundle, whereas DII-P axons (Nrp1 high, Sema3A low) are sorted to the lateral-peripheral compartment. This sorting appears to occur, at least in part, by the repulsive interaction between Sema3A and Nrp1. In addition to the repulsive interactions, Sema3A and Nrp1 signals may induce homophilic adhesion of axons with Nrp1 itself (*29*) or with other molecules such as L1 (*30*). Furthermore, additional guidance receptors such as Plexin-A1 (*16*) may be involved in the sorting of DII-A and DII-P axons (fig. S7). We assume that similar mechanisms are also at work in the sorting of DI and DII axons (Fig. 1B).

Once OSN axons are sorted in the bundle, they need to be oriented along the correct axis before projecting onto a topographic map on the OB. This probably requires positional cues that are derived from the target or that are found along the pathway between the olfactory epithelium and the OB. In the Sema3A total knockout, Nrp1-positive DII-P axons spread rather uniformly across diameter of the bundle (Fig. 5B) and consequently mistarget to the anterior region in the OB (*23*, *24*). The effect is different in the OSN-specific Sema3A knockout, where DII-P axons at least gravitate toward the lateral region in the bundle (Fig. 5B). Thus, Sema3A expressed by cells outside of the bundle likely functions as an additional guidance cue to orient the sorted axons along the correct axis for projection onto OB. In early embryos, but not in postnatal mice, *Sema3A* is expressed in the anterior OB (Fig. 5A). Furthermore, *Sema3A* is found in ensheathing glial cells along the medial side of the axon bundles (Fig. 5A) (*23*). Involvement of such intermediate cues has been reported for the thalamocortical projection (*31*, *32*).

In the *Drosophila* olfactory system, early-arriving OSN axons from the antenna repel late-arriving axons from the maxillary palp with Sema1a and Plexin-A, thereby segregating the two types of axons in the target (*33*). In the vertebrate retinotectal projection, target-derived guidance cues (e.g., ephrin-As) are thought to provide positional information. However, surgical and genetic studies indicated that projection sites for retinal ganglion cells are determined by relative, but not absolute, levels of guidance receptors, known as "axonal competition" (*34*, *35*). Furthermore, retinal axons are presorted before the target recognition (*15*). Although retinal ephrin-As are thought to antagonize Eph-A receptors in cis (*36*), they may also function in trans to segregate heterotypic axons (*37*–*39*). We propose that the axon-axon interaction is a general strategy to establish the topographic order based on the relative levels of guidance molecules expressed by axons (Fig. 5C).

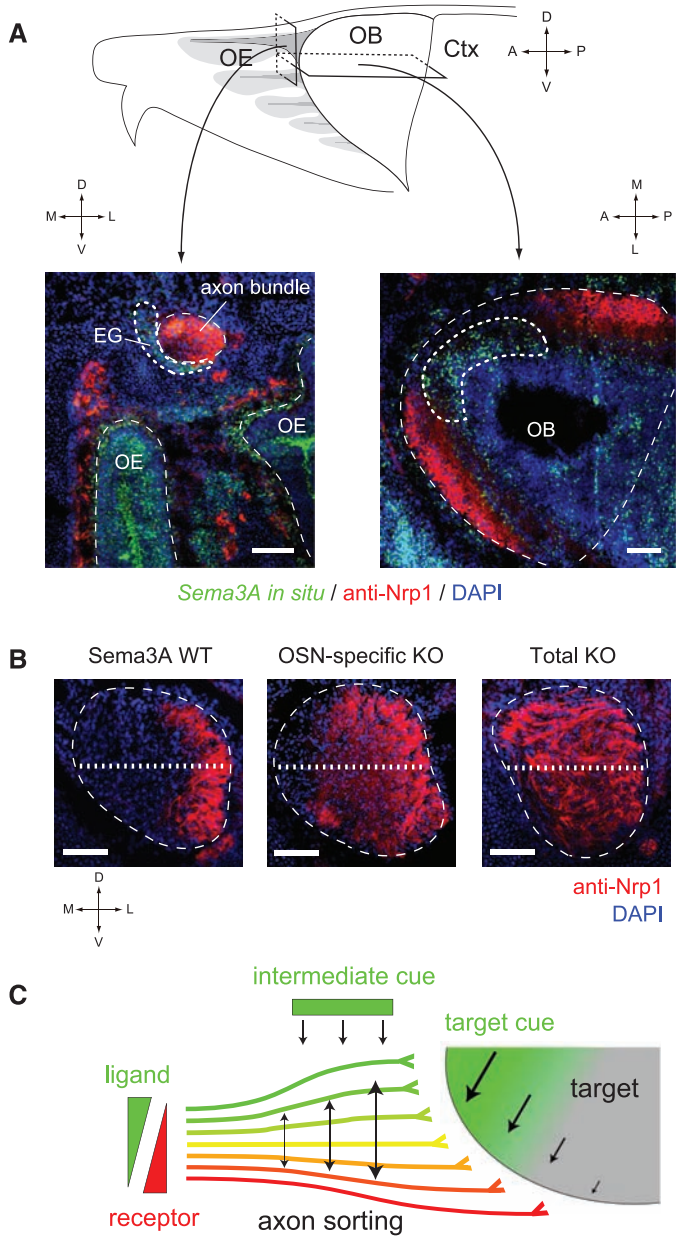

Fig. 5. Sema3A expressed by the non-OSN cells in the mouse olfactory system. (**A**) *Sema3A* mRNA is detected not only in OSNs, but also in the OB and ensheathing glia (EG) that surround axon bundles (age, E15). *Sema3A* expression is high on the medial side (Nrp1-low) of the axon bundle encircled by dotted line (left). In the OB, *Sema3A* is expressed in the anterior domain (encircled by dotted line) during early embryonic stages (right). Scale bars, 100 μm. The mouse olfactory system (lateral view) is schematically shown at the top. (**B**) Coronal sections of axon bundles stained with antibodies to Nrp1 (age, P0). In the total knockout of Sema3A, Nrp1-positive axons are spread uniformly within the bundle (right). However, in the OSN-specific Sema3A knockout, Nrp1-positive axons gravitate to the lateral side of the bundle (middle). Thus, non-OSN Sema3A may help to orient the axon bundle organization. Quantification of Nrp1 immunoreactivities (along the dotted lines) is shown in fig. S10A. Scale bars, 100 μm. (**C**) Possible mechanisms for topographic map formation in the brain. In the mouse olfactory system, a guidance receptor, Nrp1, and its repulsive ligand, Sema3A, are expressed in a complementary manner in OSNs. We propose that pre-target axon-axon interactions regulate the sorting of heterotypic axons. Target and intermediate cues may direct correct orientations of the map.

References and Notes

1. T. McLaughlin, D. D. O'Leary, *Annu. Rev. Neurosci.* **28**, 327 (2005).
2. L. Luo, J. G. Flanagan, *Neuron* **56**, 284 (2007).
3. R. W. Sperry, *Proc. Natl. Acad. Sci. U.S.A.* **50**, 703 (1963).
4. L. Buck, R. Axel, *Cell* **65**, 175 (1991).
5. B. Malnic, J. Hirono, T. Sato, L. B. Buck, *Cell* **96**, 713 (1999).
6. S. Serizawa *et al.*, *Science* **302**, 2088 (2003); published online 30 October 2003 (10.1126/science.1089122).
7. R. Vassar *et al.*, *Cell* **79**, 981 (1994).
8. K. J. Ressler, S. L. Sullivan, L. B. Buck, *Cell* **79**, 1245 (1994).
9. P. Mombaerts *et al.*, *Cell* **87**, 675 (1996).
10. K. Miyamichi, S. Serizawa, H. M. Kimura, H. Sakano, *J. Neurosci.* **25**, 3586 (2005).
11. T. Imai, M. Suzuki, H. Sakano, *Science* **314**, 657 (2006); published online 21 September 2006 (10.1126/science.1131794).
12. T. Imai, H. Sakano, *Curr. Opin. Neurobiol.* **17**, 507 (2007).
13. J. H. Cho, M. Lépine, W. Andrews, J. Parnavelas, J. F. Cloutier, *J. Neurosci.* **27**, 9094 (2007).
14. E. M. Norlin *et al.*, *Mol. Cell. Neurosci.* **18**, 283 (2001).
15. J. H. Scholes, *Nature* **278**, 620 (1979).
16. M. Satoda, S. Takagi, K. Ohta, T. Hirata, H. Fujisawa, *J. Neurosci.* **15**, 942 (1995).
17. A. Tsuboi, T. Miyazaki, T. Imai, H. Sakano, *Eur. J. Neurosci.* **23**, 1436 (2006).
18. H. Nagao, Y. Yoshihara, S. Mitsui, H. Fujisawa, K. Mori, *Neuroreport* **11**, 3023 (2000).
19. J. A. St John, H. J. Clarris, S. McKeown, S. Royal, B. Key, *J. Comp. Neurol.* **464**, 131 (2003).
20. S. Yoshihara, K. Omichi, M. Yanazawa, K. Kitamura, Y. Yoshihara, *Development* **132**, 751 (2005).
21. I. Naruse, K. Kato, T. Asano, F. Suzuki, Y. Kameyama, *Brain Res. Dev. Brain Res.* **51**, 253 (1990).
22. T. S. Tran, A. L. Kolodkin, R. Bharadwaj, *Annu. Rev. Cell Dev. Biol.* **23**, 263 (2007).
23. G. A. Schwarting *et al.*, *J. Neurosci.* **20**, 7691 (2000).
24. M. Taniguchi *et al.*, *J. Neurosci.* **23**, 1390 (2003).
25. See supporting material on *Science* Online.
26. Y. Oka *et al.*, *Eur. J. Biochem.* **270**, 1995 (2003).
27. K. Kobayakawa *et al.*, *Nature* **450**, 503 (2007).
28. M. Taniguchi *et al.*, *Neuron* **19**, 519 (1997).
29. S. Takagi *et al.*, *Dev. Biol.* **170**, 207 (1995).

30. V. Castellani, A. Chédotal, M. Schachner, C. Faivre-Sarrailh, G. Rougon, *Neuron* **27**, 237 (2000).
31. A. Dufour *et al.*, *Neuron* **39**, 453 (2003).
32. J. Seibt *et al.*, *Neuron* **39**, 439 (2003).
33. L. B. Sweeney *et al.*, *Neuron* **53**, 185 (2007).
34. M. G. Yoon, *J. Physiol.* **264**, 379 (1977).
35. A. Brown *et al.*, *Cell* **102**, 77 (2000).
36. M. R. Hornberger *et al.*, *Neuron* **22**, 731 (1999).
37. F. Bonhoeffer, J. Huf, *Nature* **315**, 409 (1985).
38. U. Drescher *et al.*, *Cell* **82**, 359 (1995).
39. B. W. Gallarda *et al.*, *Science* **320**, 233 (2008).
40. We thank D. D. Ginty and A. L. Kolodkin for Nrp1 mutant mice; M. Taniguchi and T. Yagi for Sema3A mutant mice; R. Y. Tsien for mCherry plasmid; and our laboratory members for valuable comments. Supported by the PREST program of the Japan Science and Technology Agency (R.K.), the Global COE program (K.K.), the Mitsubishi Foundation, and a Specially Promoted Research Grant from the Ministry of Education, Culture, Sports, Science and Technology of Japan.

Supporting Online Material
www.sciencemag.org/cgi/content/full/1173596/DC1
SOM Text
Figs. S1 to S12
References

16 March 2009; accepted 19 June 2009
Published online 9 July 2009;
10.1126/science.1173596
Include this information when citing this paper.

REPORTS

Grain Boundary Defect Elimination in a Zeolite Membrane by Rapid Thermal Processing

Jungkyu Choi,[1] Hae-Kwon Jeong,[2] Mark A. Snyder,[3] Jared A. Stoeger,[1] Richard I. Masel,[4] Michael Tsapatsis[1]*

Microporous molecular sieve catalysts and adsorbents discriminate molecules on the basis of size and shape. Interest in molecular sieve films stems from their potential for energy-efficient membrane separations. However, grain boundary defects, formed in response to stresses induced by heat treatment, compromise their selectivity by creating nonselective transport pathways for permeating molecules. We show that rapid thermal processing can improve the separation performance of thick columnar films of a certain zeolite (silicalite-1) by eliminating grain boundary defects, possibly by strengthening grain bonding at the grain boundaries. This methodology enables the preparation of silicalite-1 membranes with high separation performance for aromatic and linear versus branched hydrocarbon isomers and holds promise for realizing high-throughput and scalable production of these zeolite membranes with improved energy efficiency.

Polycrystalline zeolite films (*1*–*3*) are used as membranes for alcohol dehydration (*4*) and are considered among other emerging technologies for various other high-resolution molecular separations (*5*). They have also been implemented in membrane reactors (*6*, *7*) and used for a range of advanced applications (e.g., sensors, corrosion protection coatings, low-*k* dielectrics, and hosts for supramolecular organization of guest molecules) (*8*–*11*). A challenge stifling development and commercial realization of zeolite film technologies is the formation of cracks and/or grain boundary defects (*12*–*14*) during the thermal treatment required for removing structure-directing agents (SDAs) from zeolitic pores. Such defect structures are believed to degrade the separation performance of molecular sieve membranes by providing nonzeolitic and, often, nonselective transport pathways for permeating species. Successful approaches to minimizing the effects of grain boundaries and cracks on membrane performance rely on microstructural optimization during film growth, including control of grain orientation and the formation of nanocomposites with the zeolite crystals embedded in the support pores (*5*, *15*–*18*), as well as post-synthesis repair techniques (*14*, *19*, *20*). The complexity of these processes, however, hinders cost-effective and reliable scale-up of membrane production.

Heat treatment after hydrothermal film growth is a common technique for establishing accessible film microstructure. In this step, SDAs and/or other guest species occluded during crystal growth in the zeolite pores are removed. This calcination step is performed at very low heating rates in an attempt to minimize crack and other extra-zeolitic defect formation. Motivated by the persistence of defect structures despite such efforts to minimize their formation, we demonstrate the capabilities of rapid thermal processing (RTP) as a means for rapid microstructure development, substantial reduction of grain boundary defects, and marked improvements in membrane separation performance.

We demonstrate the influence of RTP on films of siliceous ZSM-5, also called silicalite-1. Silicalite-1 is an all-silica zeolite with the MFI framework topology [($Si_{96}O_{192}$)-MFI; for a description of MFI and other frameworks, see (*21*)]. MFI films are an excellent model system to investigate the effect of microstructure on film performance. Moreover, the ~6 Å pore opening of MFI enables separations of valuable components from commonly encountered chemical process streams like aromatic isomers and linear versus branched hydrocarbons. We focus on one class of siliceous MFI (hereafter referred to as MFI) films: *c*-out-of-plane–oriented films prepared by secondary growth of randomly oriented seeds (*14*, *22*). These films and the associated synthesis techniques were chosen as a test-bed for evaluating the RTP approach based on the extensive previous characterization of film-growth mechanisms and separation performance. In addition, the high degree of film reproducibility and the versatility in film formation on various substrates makes this approach more amenable to scale up than other methods for synthesizing zeolite membranes.

The presence of transverse grain boundary defects produced during conventional (slow rate) calcination for SDA removal is well documented and has been correlated with poor separation performance (*2*, *13*, *14*, *23*, *24*). These grain boundary defects are formed in response to tensile stresses caused mainly by the abrupt zeolite unit cell contraction upon SDA removal, as well as by the mismatch of thermal expansion coefficients between the substrate and the zeolite film (*13*, *25*). Depending on membrane operating conditions (temperature, pressure, mixture composition), the extrazeolitic pore openings at the grain boundaries may become substantially larger than the zeolite pores and, thus, compromise membrane performance (*14*). For example, the presence of grain boundary defects has been associated with the poor performance of *c*-oriented columnar membranes for xylene isomers (*p*- versus *o*-xylene) and the reduction of the mixture separation factor for butane isomers at elevated temperatures. For instance, despite the high single-component ideal selectivity (up to ~100) for xylene isomers, the separation factor for the corresponding binary mixture is less than 4 (*14*).

We explore the capabilities of RTP as the first heat treatment step after hydrothermal growth for reducing the formation of grain boundary

[1]Department of Chemical Engineering and Materials Science, University of Minnesota, 151 Amundson Hall, 421 Washington Avenue SE, Minneapolis, MN 55455, USA. [2]Artie McFerrin Department of Chemical Engineering, Texas A&M University, College Station, TX 77843–3122, USA. [3]Department of Chemical Engineering, Lehigh University, 111 Research Drive, Bethlehem, PA 18015, USA. [4]Department of Chemical and Biomolecular Engineering, University of Illinois at Urbana-Champaign, IL 61801, USA.

*To whom correspondence should be addressed. E-mail: tsapatsi@cems.umn.edu

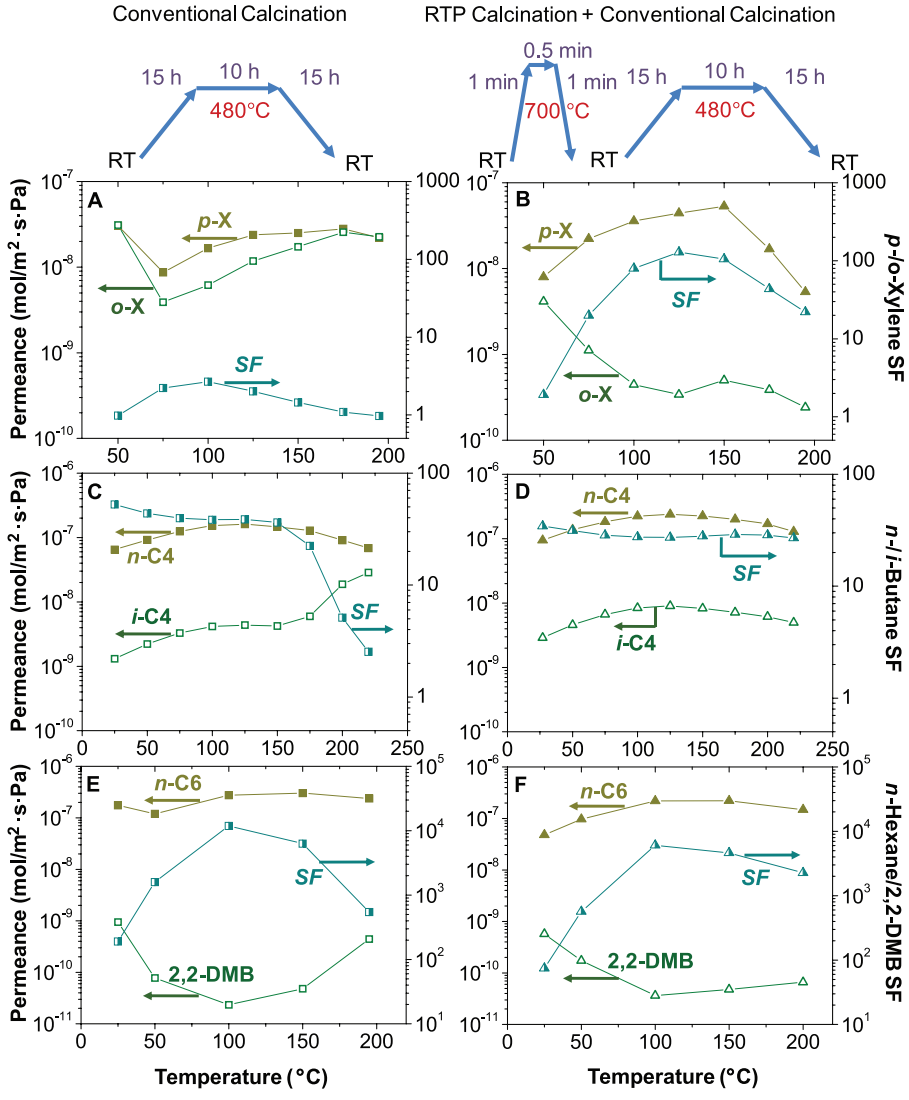

Fig. 1. Xylene (**A** and **B**), butane (**C** and **D**), and hexane (**E** and **F**) separation performance of conventionally calcined (0.5°C/min) (A, C, and E), and RTP-treated (700°C/min) and then conventionally calcined (0.5°C/min) (B, D, and F) *c*-oriented MFI membranes. The compositions of the feed mixtures were as follows: 0.50 kPa/0.50 kPa for *p*-xylene/*o*-xylene; 50 kPa/50 kPa for *n*-butane/*i*-butane; and 13 kPa/13 kPa for *n*-hexane/2,2-dimethylbutane (2,2-DMB). The permeation conditions, setup, and analysis procedure are described in (*30*) and references therein. All *c*-oriented membranes were made on homemade α-alumina disks (diameter: 22 mm; pore size: 150 to 200 nm; and membrane area: 3.8×10^{-4} m^2) by secondary growth as reported in (*30*). RTP was carried out with the use of an infrared chamber (E4-10 from Research Inc.) controlled by a Eurotherm temperature controller (Model 2404).

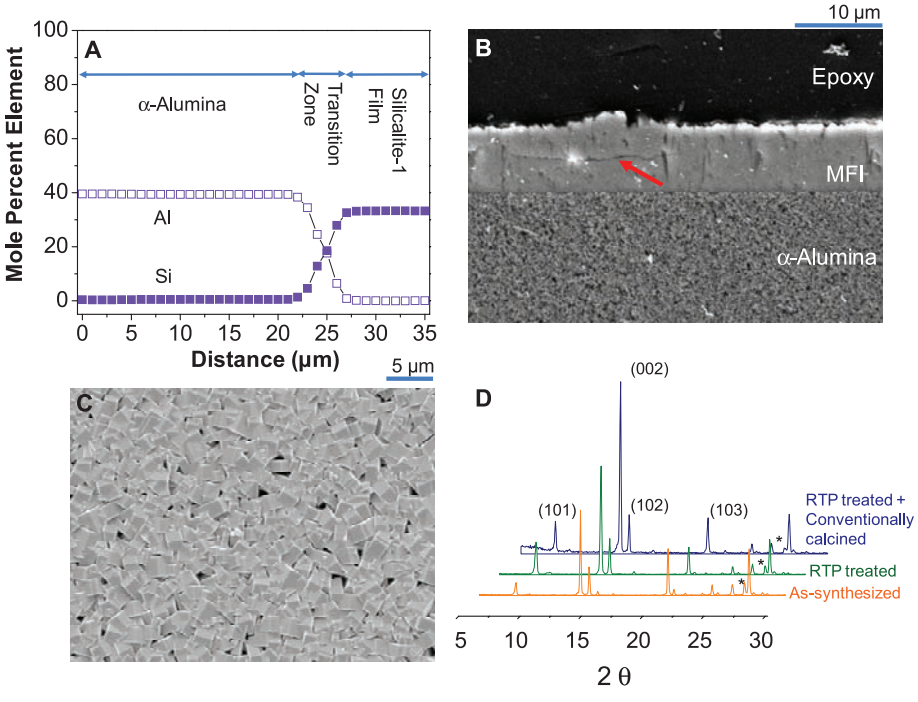

Fig. 2. (**A**) EPMA trace of composition across the membrane thickness and (**B**) SEM cross section of RTP-treated and then conventionally calcined membrane. A lateral delamination is marked by an arrow. The top view SEM is shown in (**C**), and the corresponding XRD traces are shown in (**D**). The XRD patterns in (D) were normalized by the porous α-alumina support peak designated by an asterisk (*) to discern the relative intensity differences at each stage: as-synthesized, RTP-treated, and RTP-treated with additional conventional calcination.

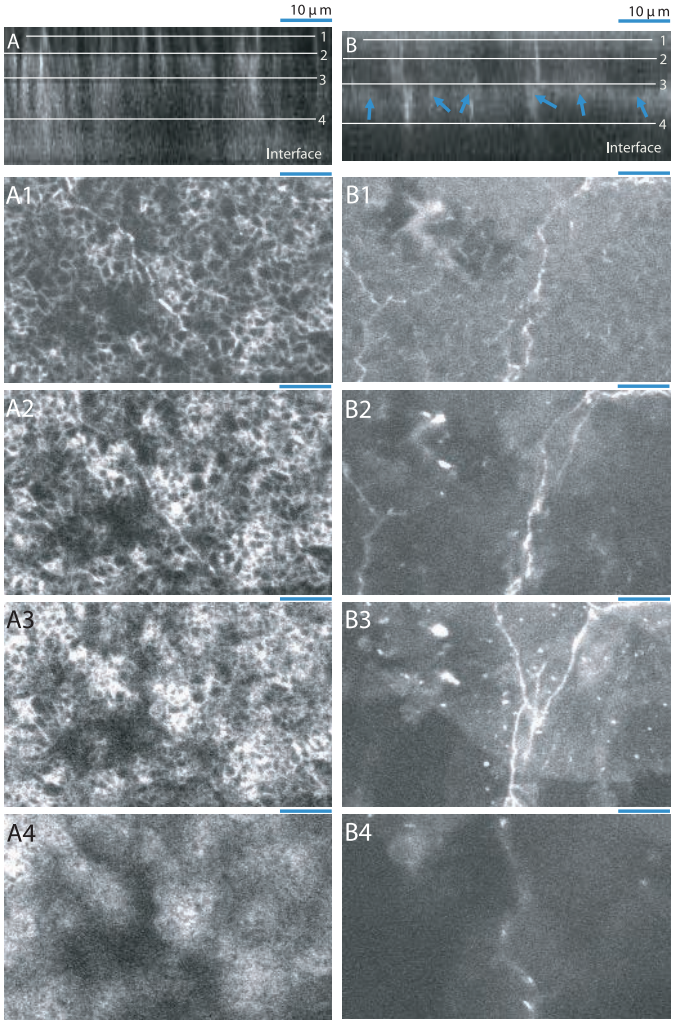

Fig. 3. FCOM cross sections of conventionally calcined (0.5°C/min) (**A**), and RTP-treated (700°C/min) and then conventionally calcined (0.5°C/min) (**B**), *c*-oriented MFI membranes along with the corresponding slices taken approximately at 2 μm (A-1, B-1), 6 μm (A-2, B-2), 10 μm (A-3, B-3), and 18 μm (A-4, B-4) from the surface as indicated by horizontal lines in (A) and (B), respectively. Lateral delaminations, observed approximately in the middle of the RTP-treated and then conventionally calcined *c*-oriented MFI film, are marked by blue arrows in (B). A discoid delamination is partially observed in (B-3) (see fig. S1 for the whole discoid delamination).

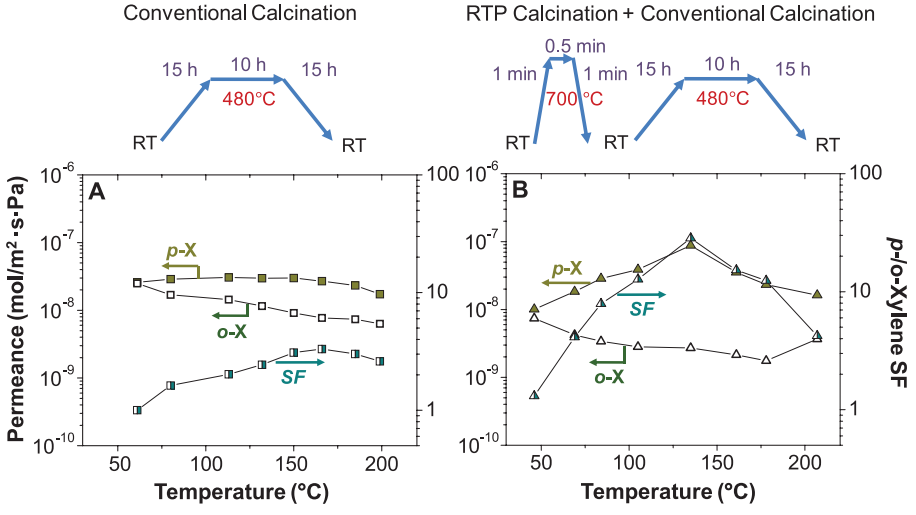

Fig. 4. Xylene separation performance of conventionally calcined (0.5°C/min) (**A**), and RTP-treated (700°C/min) and then conventionally calcined (0.5°C/min) (**B**), *c*-oriented MFI membranes on a tubular stainless-steel support. The composition of the feed mixtures was 0.50 kPa/0.50 kPa for *p*-xylene/*o*-xylene. The setup for permeation measurements was based on Wicke-Kallenbach mode with a homemade tubular quartz permeation cell. All *c*-oriented membranes were made on stainless-steel tubes (Pall Corp, ~1 μm pore size; 5-cm-long porous part with 1 cm outer diameter and two 2.5-cm-long nonporous parts at both ends) by secondary growth (*26*). The same RTP experimental setup given in Fig. 1 was used for *c*-oriented MFI membranes made on stainless-steel tubes.

defects. We hypothesized that the associated rapid temperature rise could result in condensation of Si-OH groups between adjacent crystal grains, thereby bolstering grain bonding before sufficient build-up of in-plane tensile stresses caused by the SDA removal. A possible and desirable outcome of such bond strengthening would be a reduced flexibility (i.e., reduced opening) of the grain boundaries during membrane operation for realizing high-selectivity separations.

Conventional calcination is typically performed at heating rates on the order of 1°C/min and by keeping the zeolite film isothermal at a temperature typically between 400° and 550°C for several hours. For the experiments reported here, the heating rate was 0.5°C/min, and the samples were kept isothermally at 480°C for 10 hours. For RTP treatment, an infrared lamp–based furnace was used to heat as-synthesized membranes up to 700°C within a minute, followed by soaking at that temperature for 30 s to 2 min, then cooling by water circulation (*26*).

Figure 1 illustrates the beneficial effect of the RTP step on membrane performance for otherwise similarly prepared *c*-oriented MFI membranes treated with conventional calcination. We observed an improvement in the separation of xylene isomers; separation factors for the *p*-/*o*-xylene mixture reached 128 in the case of RTP-treated membranes (Fig. 1B) compared with less than 4 for conventionally calcined membranes (Fig. 1A). A triplicate experiment (using three different membranes synthesized with the same procedure) gave highly reproducible separation performance within ~20% of the maximum separation factor presented in Fig. 1B. Moreover, the separation factors for butane and hexane isomer mixtures appear relatively insensitive to operating temperature in the case of RTP treatment, but displays a sharp decrease with increasing temperature in the case of conventional calcination. The combined selectivity for both xylenes (up to 128) and butanes (up to 34) cannot be achieved easily with a single membrane microstructure. For example, *b*-oriented MFI membranes that have a xylene separation factor up to 480 display a very small butane selectivity (up to 6) (*16*, *27*).

Electron probe microanalysis (EPMA), scanning electron microscopy (SEM), and x-ray diffraction (XRD) (Fig. 2) do not reveal any differences between the conventionally calcined and RTP-treated MFI membranes except for the presence of 10- to 100-μm lateral delaminations approximately in the middle of the RTP-treated membranes (Fig. 2B, arrow). Fluorescent confocal optical microscopy (FCOM) (Fig. 3 and fig. S1) confirms the presence, location, and lateral orientation (parallel to membrane/support interface) of these delaminations and reveals their disk shape. These defect structures may be due to local stress concentration developed during RTP treatment that results from disparate removal rates of SDA or its decomposition products from the membrane interior compared with

regions nearer the membrane surface. Concomitant mismatch in the extent of unit cell contraction between empty and SDA-filled regions could conceivably be relieved by film buckling and manifested as discoid delaminations.

Some SDA or SDA decomposition products remain in the RTP-treated films, and these are completely removed by subsequent conventional calcination, as shown by the relative intensity of the associated XRD peaks (Fig. 2D) as a function of calcination steps. For example, the intensity of the (002) reflection relative to the as-synthesized sample is observed to increase after RTP treatment and again after subsequent conventional calcination. Complete SDA removal can also be accomplished with a second RTP treatment instead of conventional calcination.

Figure 3 shows representative results from the examination of conventionally and RTP-treated membranes by FCOM. The images were taken after the membranes were brought into contact for 48 hours with a solution of a fluorescent dye (Fluorescein-Na salt), with an estimated kinetic diameter (~1 nm) nearly double the zeolitic pore size (~0.6 nm in size) (*12*). These probe molecules are, therefore, unable to enter the zeolite pores. In agreement with previous FCOM studies (*12*), the conventionally calcined membranes (Fig. 3A) prepared in this study display signature networks of grain boundaries propagating from the membrane surface to its support. Specifically, the fluorescent dye is readily detected, highlighting with bright fluorescence the grain boundaries extending across the transparent membrane thickness and indicating the presence of extrazeolitic transport pathways with pore openings that are or can become (upon dye adsorption) larger than the zeolite pores. By contrast, the RTP-treated (Fig. 3B), but otherwise similarly prepared films, show only sporadic penetration of the fluorescent dye through the membrane thickness, indicating less flexible and/or smaller grain boundary openings, a finding that correlates with the improved separation performance of the RTP-treated membranes. In addition, cracks in the RTP-treated membranes, highlighted by FCOM, are apparently only superficial; they fail to propagate completely through the thickness of the membrane, as reflected by their absence near the interface in Fig. 3B.

Although FCOM also reveals the presence of a large number of lateral discoidal delaminations described above and shown by SEM in Fig. 2B (and by FCOM in fig. S1), these are unlikely to compromise the separation performance because they do not span the transverse direction of the zeolite membrane. Although a cause-and-effect relation between the lateral discoid delaminations and the reduction of transverse grain boundary defects in RTP-treated membranes cannot be established, both are consistent with our initial hypothesis regarding strengthening of grain bonding at the grain boundaries before SDA removal.

We also explored whether performing calcination exclusively by RTP could replace the time-consuming and energy-intensive conventional calcination steps. After a single RTP step, however, the permeances of the faster-permeating species (e.g., *n*-butane) were measured to be an order of magnitude lower than those obtained after an additional calcination step, indicating that some SDA and/or SDA decomposition products remain in the zeolite pores after RTP treatment. This remnant SDA is most likely a result of mass-transport limitations on the rate of SDA release during the 1-min RTP treatment.

Although a calcination step after RTP seems to be necessary to completely open the micropores, preliminary results indicate that this second calcination can be performed by a second rapid treatment (fig. S2).

Examination of the RTP-treated membranes by FCOM before and after the conventional calcination step revealed no differences, suggesting that the lateral delaminations and the grain boundary cohesion characteristics develop only during the RTP step. Additional calcination is then only needed to remove the SDA remnants. The ramp rate of the first calcination step after hydrothermal growth appears to be the major factor affecting the formation of extrazeolitic porosity. This was confirmed by the consistent, albeit less pronounced, improvement of separation properties for membranes that were conventionally calcined at a ramp rate of 30°C/min versus 0.5°C/min (fig. S3).

It appears that the benefits of RTP calcination can be imparted to columnar membranes supported on tubular stainless-steel supports, which are of more practical interest. In preliminary experiments, porous stainless-steel tubes (without any coating to smoothen or otherwise modify their surfaces) were sonicated in a seed suspension before being subjected to hydrothermal growth. Owing to the roughness of the stainless-steel support, the sparse seed layer, and the use of only one secondary growth step, the separation factor of these membranes (Fig. 4) is lower than that of the membranes supported on the homemade flat α-alumina supports (Fig. 1B). Nevertheless, a considerable increase in *p*-xylene/*o*-xylene selectivity was observed for RTP-treated membranes, resulting in an attractive combination of *p*-xylene permeance (~8.7×10^{-8} mol·m^{-2}·s^{-1}·Pa^{-1}) and mixture separation factor (~28), whereas the mixture separation factor of the conventionally calcined membrane was about 3 (Fig. 4A). This performance of RTP-treated films is superior to that of conventionally calcined MFI films deposited on tubular stainless-steel supports through the use of more complicated seeding and multiple hydrothermal growths (separation factor of ~5) (*28*) and comparable to the best performance reported (separation factor of 27) (*29*) after further modification by ion exchange. The simplicity of the membrane preparation, robustness of the stainless-steel support, and good separation performance, therefore, make these membranes attractive for further development.

These findings suggest that the calcination ramp rate is an important means for controlling the grain boundary characteristics of zeolite films. The data demonstrate that RTP calcination can markedly improve the membrane-separation performance of columnar MFI films. If its beneficial effects on performance can be demonstrated for other zeolite types, compositions, and microstructures, RTP could contribute, in combination with fast one-step deposition methods, to the realization of large-scale production of zeolite membranes.

References and Notes

1. M. E. Davis, *Nature* **417**, 813 (2002).
2. J. Caro, M. Noack, *Microporous Mesoporous Mater.* **115**, 215 (2008).
3. M. A. Snyder, M. Tsapatsis, *Angew. Chem. Int. Ed.* **46**, 7560 (2007).
4. M. Kondo, M. Komori, H. Kita, K.-I. Okamoto, *J. Membr. Sci.* **133**, 133 (1997).
5. M. A. Carreon, S. Li, J. L. Falconer, R. D. Noble, *J. Am. Chem. Soc.* **130**, 5412 (2008).
6. J. Coronas, J. Santamaria, *Top. Catal.* **29**, 29 (2004).
7. J.-A. Dalmon *et al.*, *Appl. Catal. A* **325**, 198 (2007).
8. G. Calzaferri, H. Li, D. Bruhwiler, *Chem. Eur. J.* **14**, 7442 (2008).
9. J. S. Lee, H. Lim, K. Ha, H. Cheong, K. B. Yoon, *Angew. Chem. Int. Ed.* **45**, 5288 (2006).
10. Z. Li *et al.*, *Angew. Chem. Int. Ed.* **45**, 6329 (2006).
11. S. Mintova, T. Bein, *Microporous Mesoporous Mater.* **50**, 159 (2001).
12. G. Bonilla, M. Tsapatsis, D. G. Vlachos, G. Xomeritakis, *J. Membr. Sci.* **182**, 103 (2001).
13. J. Dong, Y. S. Lin, M. Z. C. Hu, R. A. Peascoe, E. A. Payzant, *Microporous Mesoporous Mater.* **34**, 241 (2000).
14. G. Xomeritakis, Z. Lai, M. Tsapatsis, *Ind. Eng. Chem. Res.* **40**, 544 (2001).
15. J. Hedlund *et al.*, *Microporous Mesoporous Mater.* **52**, 179 (2002).
16. Z. Lai *et al.*, *Science* **300**, 456 (2003).
17. S. Miachon *et al.*, *J. Membr. Sci.* **298**, 71 (2007).
18. N. Nishiyama, L. Gora, V. Teplyakov, F. Kapteijn, J. A. Moulijn, *Separ. Purif. Tech.* **22-23**, 295 (2001).
19. M. Nomura, T. Yamaguchi, S.-I. Nakao, *Ind. Eng. Chem. Res.* **36**, 4217 (1997).
20. Y. Yan, M. E. Davis, G. R. Gavalas, *J. Membr. Sci.* **123**, 95 (1997).
21. C. Baerlocher, L. B. McCusker, D. H. Olson, *Atlas of Zeolite Framework Types* (Elsevier, Amsterdam, ed. 6, 2007).
22. A. Gouzinis, M. Tsapatsis, *Chem. Mater.* **10**, 2497 (1998).
23. X. Gu, J. Dong, T. M. Nenoff, D. E. Ozokwelu, *J. Membr. Sci.* **280**, 624 (2006).
24. M. Lassinantti Gualtieri *et al.*, *J. Membr. Sci.* **290**, 95 (2007).
25. H.-K. Jeong, Z. Lai, M. Tsapatsis, J. C. Hanson, *Microporous Mesoporous Mater.* **84**, 332 (2005).
26. Materials and methods are available as supporting material on *Science* Online.
27. Z. Lai, M. Tsapatsis, *Ind. Eng. Chem. Res.* **43**, 3000 (2004).
28. A. M. Tarditi, E. A. Lombardo, *Separ. Purif. Tech.* **61**, 136 (2008).
29. A. M. Tarditi, G. I. Horowitz, E. A. Lombardo, *Catal. Lett.* **123**, 7 (2008).
30. J. Choi, S. Ghosh, L. King, M. Tsapatsis, *Adsorption* **12**, 339 (2006).

31. Funding for this work was provided by NSF (CBET-05 22518). All the characterizations were performed at the Minnesota Characterization Facility, which receives support from the NSF through the National Nanotechnology Infrastructure Network (NNIN).

Supporting Online Material

www.sciencemag.org/cgi/content/full/325/5940/590/DC1
Materials and Methods
Figs. S1 to S3
References

11 May 2009; accepted 18 June 2009
10.1126/science.1176095

Ultrasmooth Patterned Metals for Plasmonics and Metamaterials

Prashant Nagpal,[1] Nathan C. Lindquist,[2] Sang-Hyun Oh,[2] David J. Norris[1]*

Surface plasmons are electromagnetic waves that can exist at metal interfaces because of coupling between light and free electrons. Restricted to travel along the interface, these waves can be channeled, concentrated, or otherwise manipulated by surface patterning. However, because surface roughness and other inhomogeneities have so far limited surface-plasmon propagation in real plasmonic devices, simple high-throughput methods are needed to fabricate high-quality patterned metals. We combined template stripping with precisely patterned silicon substrates to obtain ultrasmooth pure metal films with grooves, bumps, pyramids, ridges, and holes. Measured surface-plasmon–propagation lengths on the resulting surfaces approach theoretical values for perfectly flat films. With the use of our method, we demonstrated structures that exhibit Raman scattering enhancements above 10^7 for sensing applications and multilayer films for optical metamaterials.

Plasmonic devices exploit electromagnetic waves known as surface plasmons that can propagate along a metal interface (*1*). Because these waves involve a mixture of both light and charge fluctuations on the metal surface, they have a unique hybrid character. Their photonic component allows them to interact with optical waves, whereas their electronic component allows these optical waves to be concentrated in volumes much smaller than the diffraction limit. This combination is useful for applications ranging from biosensing to solar cells (*2*–*6*). In a typical device, surface plasmons are created when a film of silver or gold is illuminated on its exposed surface. Although this excitation process is forbidden when the interface is perfectly flat, surface patterning on a suboptical length scale allows incident light to generate surface plasmons in the film (*1*). Patterning also provides a means to manipulate these plasmons, once they have been created. For example, surface structures can direct, channel, or focus the surface plasmons toward specific locations. However, because surface plasmons exist very close to the interface, they are extremely sensitive to surface inhomogeneities, which can cause absorption, scattering, and limited propagation. Consequently, fabrication of plasmonic devices requires metal films to be patterned while avoiding unwanted roughness and impurities that can seriously degrade their performance.

Unfortunately, metal films deposited by evaporation are inherently rough due to polycrystallinity. Moreover, when such films are patterned, for example by a focused ion beam (FIB), this roughness is increased as the grains are exposed. To avoid these problems, alternatives ranging from films with extremely small grains grown by fast sputtering (*7*) to large single crystals grown by the Czochralski process (*8*, *9*) have been explored. Although each of these alternatives can provide surfaces that are smoother than evaporated films, their devices still exhibit shorter-than-expected surface-plasmon propagation. In particular, ion impurities implanted in the metal during patterning introduce absorption. For sputtered films, plasmons can also scatter at the numerous grain boundaries. To increase the propagation, one solution is to use extremely thin metal films (~10 nm), in which long-range surface plasmons have been reported at infrared wavelengths (*10*). However, this occurs because most of the electromagnetic field from the surface plasmon is in the surrounding medium instead of the metal. For applications that exploit concentrated electromagnetic fields near a metal interface, thicker structures are required. All fabrication methods have also been limited to patterning one film at a time. This affects not only cost but also performance, because nanometer-scale differences between structures can influence the plasmons.

The emerging field of plasmonics needs simple, high-throughput, and reproducible approaches to obtain pure metallic films that are smooth yet patterned over large areas. Although techniques such as nanoimprinting and nanomolding can easily pattern metals on the proper length scales (*11*–*13*), none of these methods have been suitable. In most techniques, patterned polymeric molds are filled with metal to form a replica. This process introduces serious surface roughness because metals do not easily wet polymer interfaces. Even if this problem is avoided by substituting other mold materials, molds have to be etched away to release the metal structure. This reduces throughput and reproducibility because each mold generates only one device.

In contrast, a simple technique already exists to generate smooth unpatterned metallic films. Known as template stripping, this method makes use of the poor adhesion and good wettability of noble metals on solids such as mica, glass, and silicon (*14*). Typically, freshly cleaved mica is coated with a film of gold, and the exposed surface of gold is then attached to another substrate with an epoxy adhesive. When the mica and substrate are separated, the gold clings to the epoxy, and a metal interface that has formed on the mica is exposed. Because mica can be extremely smooth, ultraflat gold surfaces can be generated. These have been used widely in scanning probe experiments and studies of self-assembled monolayers.

However, it has not been realized that the same approach can produce smooth patterned metal films. Whereas template stripping was applied to form patterns on mica, complex multistep processes were employed (*15*–*17*). Instead of mica, we used inexpensive silicon wafers as the template to exploit the well-developed fabrication techniques for microelectronics. After the wafer is patterned (Fig. 1A), for example, with lithography or FIB, it is coated with a thin metal film and a layer of epoxy (*18*). The epoxy-metal bilayer can then be peeled off of the substrate to reveal a patterned structure with a surface roughness determined by the wafer template. Figure 1B shows a silicon substrate with circular concentric grooves defined by FIB. We thermally evaporated 275 nm of silver on this substrate, added epoxy, and peeled off the bilayer. Figure 1, C to E, indicates the quality of the silver "bull's eye" structure that results. Electron micrographs taken at glancing incidence (Fig. 1E) are extremely effective at exposing any surface roughness.

The evaporated silver film has a rough surface after deposition, but the device uses the opposite interface, which is smooth. If the film is thicker than ~100 nm, the rough side will not influence surface-plasmon propagation. Because the silicon wafer, and not the silver, is patterned by FIB or reactive ion etching (RIE), no ion impurities are implanted in the silver. We used x-ray photoelectron spectroscopy to analyze the surface composition of metal films patterned via RIE with SF_6 and found 49 atomic percent of fluoride ions within the top ~5 nm of the film, whereas template-stripped metals had no detectable surface impurities.

In addition to silver bull's eyes, we fabricated a variety of silver, copper, and gold plasmonic structures (Fig. 2). From the same patterned substrate, we have created more than 30 films without damage. If it was necessary to avoid epoxy, which remains attached to the metal and can be problematic for some applications, we used metal electrodeposition (*19*). For example, after a thin ~250-nm film of copper was evaporated onto a bull's eye template, we electrodeposited another ~1 mm of copper. The resulting patterned copper foil (Fig. 2A) could be peeled off directly, without the aid of epoxy. Similarly, a silver bump array (Fig. 2B) was produced on a free-standing ~100-μm-thick silver foil.

We also used simple chemical etching techniques to pattern the silicon substrate. When the surface of a [100]-oriented silicon wafer is exposed to a solution of KOH, anisotropic etching can lead to pyramidal divets or triangular grooves. We formed such patterns by coating a

[1]Department of Chemical Engineering and Materials Science, University of Minnesota, Minneapolis, MN 55455, USA. [2]Department of Electrical and Computer Engineering, University of Minnesota, Minneapolis, MN 55455, USA.

*To whom correspondence should be addressed. E-mail: dnorris@umn.edu

wafer with chromium and gold, selectively removing these layers with either FIB or photolithography, and immersing the substrate in KOH (*18*). Previously, pyramidal particles were created by depositing metals only at the bottom of such divets and then releasing the deposits to form a colloidal suspension (*20*, *21*). In our case, the divets were coated with ~250 nm of metal, which was removed with epoxy to produce silver (Fig. 2, C and D) or gold (Fig. 2E) pyramid arrays. (We also obtained similar structures with electrodeposition.) The pyramids were smooth, highly reproducible, and exhibited sharp tips with radii of curvature as small as 10 nm (Fig. 2D, inset).

The surfaces that are produced have a roughness that can approach that of the template, as confirmed by atomic force microscopy (AFM). For a silicon substrate with a root mean square (RMS) roughness of 0.19 nm, we measured 0.65 nm for the corresponding silver film. The largest contribution to this value was the grain boundaries in the polycrystalline silver. Within a single grain, the roughness was 0.26 nm, much closer to that of the silicon. These measurements were obtained for silver evaporated onto test-grade wafers at room temperature (*18*). Under slow-evaporation conditions with wafers heated to 75°C, the RMS roughness improved even further to 0.34 nm. Of course, the smoothness of the metal is affected by the method that we used to pattern the substrate. For example, the silicon bull's eye in Fig. 1B had an RMS roughness of 1.89 nm due to redeposition of material during patterning of the grooves with FIB. The corresponding silver film (Fig. 1C) had a roughness of 2.18 nm. Even in this case, the bull's eye, which is designed to have a sharp and directional absorption feature due to optical coupling to surface plasmons, exhibited a sharp absorption peak (fig. S1) that was not observed in the same structure made by standard methods (i.e., evaporated films patterned directly with FIB).

To quantify this further, we measured the propagation length of the surface plasmons. We prepared a 200-nm-thick ultrasmooth silver film on epoxy and then milled a series of identical slits through the metal with FIB. For each slit, we added a parallel groove in the film at a different fixed separation *d* (Fig. 3A). By illuminating the epoxy side of the bilayer with white light, surface plasmons could be launched on the film as light passed through the slits (*22*). When these propagating plasmons struck the grooves (Fig. 3A, inset), they scattered light that could be collected by a microscope. For each groove, we measured the spectrum of this light and, from an analysis of all such spectra, determined the scattered intensity as a function of *d*. Because this is directly related to the intensity of the surface plasmons at the

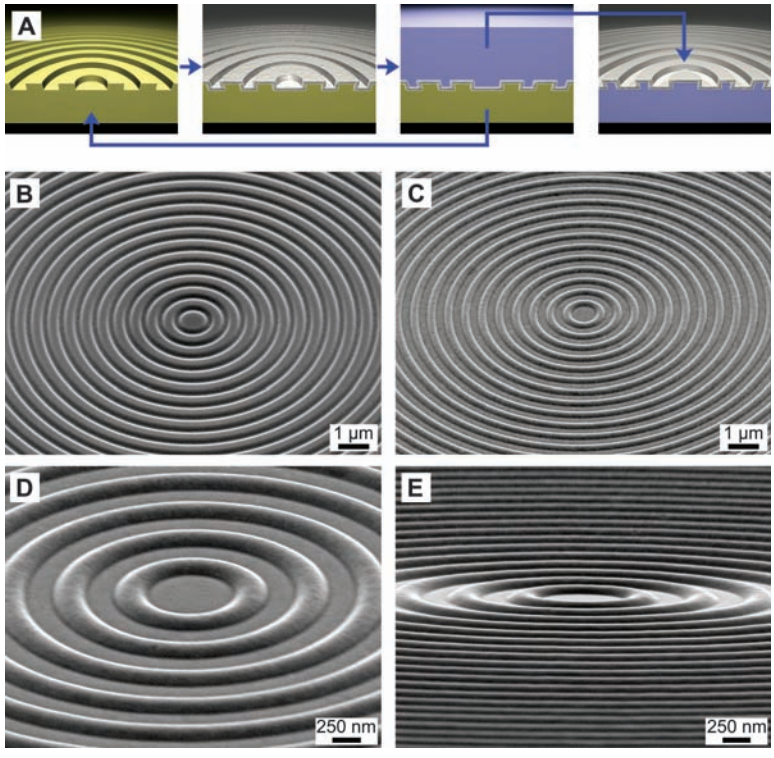

Fig. 1. (**A**) Schematic for fabricating ultrasmooth patterned plasmonic structures. After adding a desired pattern to a silicon wafer (green), a metal film is deposited and then coated with epoxy or additional metal (blue). The combined film can be peeled off of the substrate to reveal a smooth patterned surface. The substrate can be reused to form additional identical structures. (**B**) Electron micrograph of a silicon wafer patterned with circular grooves (bull's eye) by FIB. The grooves were 285 nm wide and spaced every 570 nm. (**C** to **E**) Electron micrographs of a silver bull's eye that was template stripped off of the silicon substrate in (B) using epoxy.

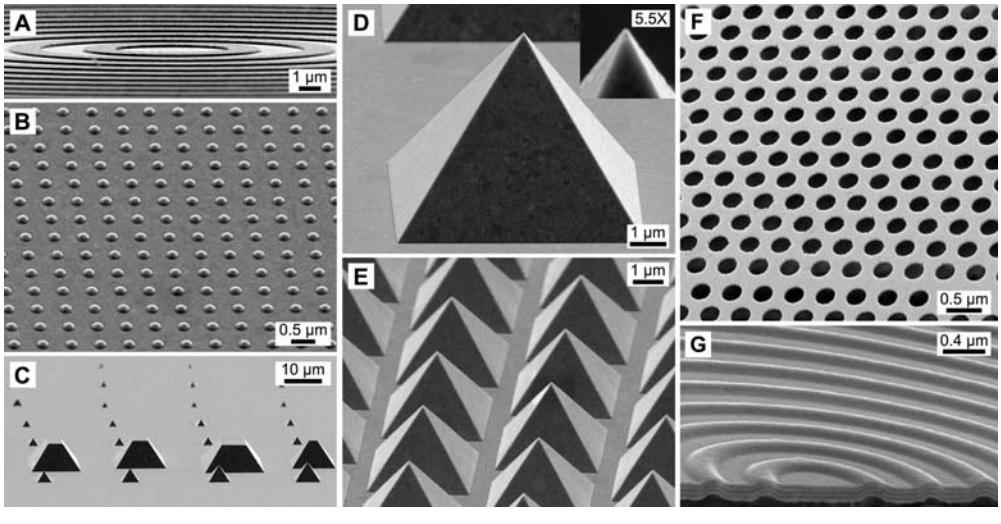

Fig. 2. Electron micrographs of various metal structures. (**A**) A copper bull's eye with 1.3-μm-wide circular grooves spaced every 3.5 μm; the template was patterned with photolithography and RIE. (**B**) A square silver array of 240-nm-diameter bumps spaced every 600 nm; the template was patterned with FIB. (**C** and **D**) A silver pyramid array made by anisotropic etching. A gold-on-chromium mask with square holes was formed with FIB on a silicon wafer and etched in KOH. The inset in (D) shows the tip of one of the pyramids. (**E**) A gold pyramid array made by anisotropic etching as in (C), except a chromium mask was patterned with a hexagonal array of 1-μm-diameter circles spaced by 2.25 μm using photolithography. (**F**) A thin silver nanohole array made with template stripping and nanosphere lithography. 265-nm-diameter holes spaced by 450 nm were formed in a 30-nm-thick silver film. (**G**) A multilayer bull's eye with alternating layers of silver (30 nm) and alumina (15 nm). A cross section etched by FIB shows seven layers.

grooves, the plasmon propagation length could be extracted for each wavelength. Figure 3B shows the measured propagation lengths for our template-stripped film. [Fringes appear in these data because of interference between surface plasmons propagating toward and away from the groove (*22*).] For comparison, we also plotted previously reported propagation lengths (*23*), as well as those that we obtained for a control film made by standard methods.

Due to roughness, propagating surface plasmons can be scattered in-plane (into other surface plasmons) or out-of-plane (into light). These losses can be quantified individually by propagation lengths L_{scat} and L_{rad}, respectively, that contribute to the overall propagation length L_{tot} (*1*, *24*). For a perfectly smooth single-crystalline film, L_{scat} and L_{rad} are infinite, and L_{tot} is limited by the ohmic losses (electron scattering) in the metal, described by L_{ohm}. If the dielectric properties of the film are known, L_{ohm} can be calculated directly (*18*). Using ellipsometry, we measured the dielectric function for our films and computed L_{ohm} (see figs. S2, S3, and S4). Figure 3B illustrates a comparison of our slit-groove data with L_{ohm} determined for a template-stripped film exposed to the same conditions. The measured values are close to L_{ohm}, especially at longer wavelengths.

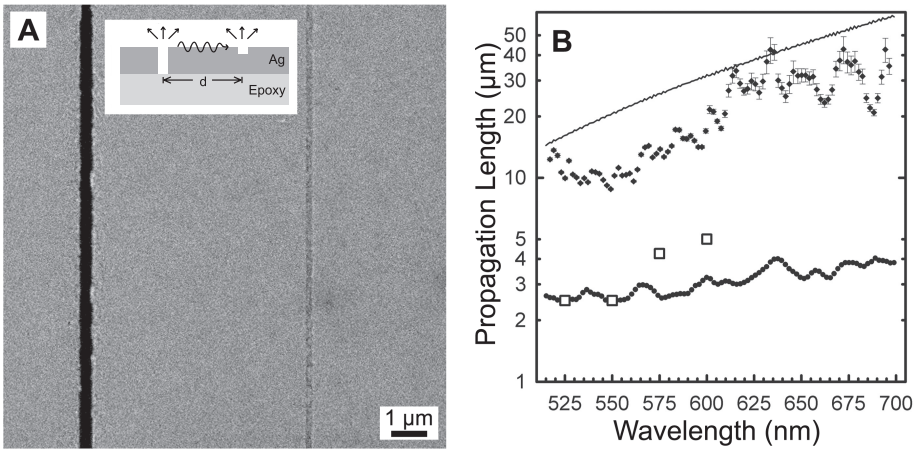

Fig. 3. (**A**) An electron micrograph of a slit-groove pair separated by 6 μm in a template-stripped 200-nm-thick silver (Ag) film. (**B**) Plot of propagation length versus wavelength extracted from a range of slit-groove separations, *d*. At every wavelength, we fit the decay of the scattered intensity with an exponential to extract the propagation length (diamonds). Error bars denote SE. Fringes appear in these data because of interference of surface plasmons propagating toward the groove and those reflected back, as confirmed by finite difference time-domain simulations. From the measured dielectric function of a template-stripped silver film treated to the same conditions, we determined the expected propagation length assuming only ohmic losses (solid curve) (*1*). Previously reported data (squares) (*23*) and values extracted from the rough side of a thermally evaporated control film (circles) are also shown. Error bars for the control data were smaller than the symbols in the plot and are not shown.

To confirm that the observed increase in propagation length is due to decreased roughness, we combined AFM and ellipsometry data to estimate the effect of different contributions to L_{tot} for template-stripped silver and gold samples, as well as standard films (*18*). From AFM scans (figs. S5 and S6), parameters describing the surface corrugation could be extracted (table S1) and used to estimate L_{scat} and L_{rad} within the single scattering approximation (*1*, *24*, *25*). L_{ohm} was determined separately from ellipsometry data. Table S2 shows that the reduction of surface roughness in template-stripped silver films should cause an increase in L_{tot} by a factor of 5 to 7, in agreement with Fig. 3B. For gold, which is inherently smoother than silver, the improvement is smaller. However, other benefits of template stripping may still be exploited. AFM scans (figs. S5 and S6) suggest a large increase in the grain size for template-stripped films. This occurred in silver during the mild heat treatment that we used to cure the epoxy (150°C). In gold, we intentionally annealed at 500°C. Unlike standard films, where thermal annealing under the same conditions increases roughness, template stripping allows grains to grow while constraining the surface. Because scattering of plasmons at grain boundaries can be an important loss mechanism on gold interfaces (*9*), grain growth can improve plasmon propagation. Assuming an increase in grain size from 80 to 1000 nm (fig. S6), L_{tot} should be improved by a factor of ~2 (table S3). The combined effect of larger grains, decreased roughness, and reduced impurities should also increase L_{ohm} due to reduced electron scattering. This increase and the preferred grain orientation (texturing) that we observe on template-stripped films offer additional advantages.

To demonstrate the utility of our approach, we fabricated large-area (square centimeters) substrates for surface-enhanced Raman scattering (SERS). In general, Raman scattering can identify molecules through their unique vibrational signatures. Because of the concentrated electric fields near patterned metal surfaces, gold and silver films have been studied for enhanced molecular and biological sensing (*26*). Signal enhancements above 10^8 for specific surface structures have been reported (*27*). However, more important for sensing applications is the ability to generate enhancements with films that are easily and reproducibly fabricated, and we illustrate this ability in Fig. 4. We first formed triangular grooves on a silicon wafer by combining photolithography and anisotropic etching (Fig. 4A). Figure 4B shows the smooth silver film with raised triangular ridges that was peeled off of this wafer. We then attached a self-assembled monolayer of benzenethiol to this surface and used scanning confocal Raman microscopy to collect the SERS signal as a function of position. The

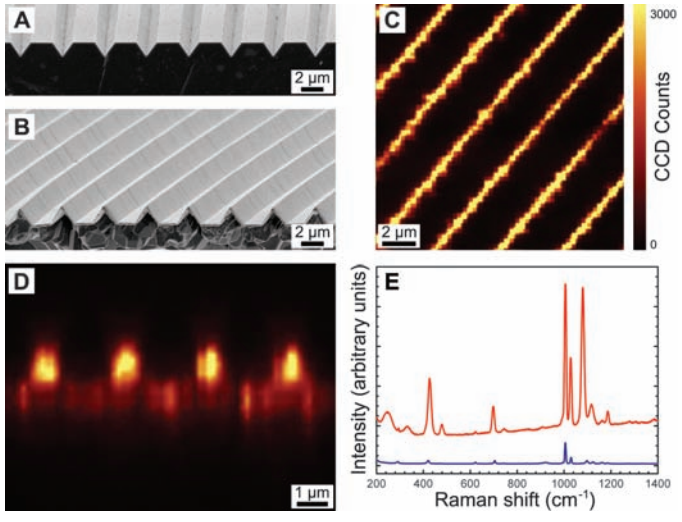

Fig. 4. (**A**) Electron micrograph of a silicon wafer patterned with a grating of triangular grooves by photolithography, lift-off, and anisotropic etching. The grooves cover 2 × 2 cm^2 on the wafer. (**B**) A silver film with triangular ridges formed from the wafer in (A). 280 nm of silver was evaporated, followed by 100 μm by electrodeposition. Due to slight misalignment of the grooves and the <110> direction of the wafer, step edges formed in the grooves during etching that are reproduced on the sides of the silver ridges. (**C** and **D**) Confocal Raman scattering microscopy scans of the film in (B) after incubation in 1 mM benzenethiol in ethanol for 16 hours. The excitation wavelength was 514 nm. The scan was in the plane of the ridge peaks in (C) and a cross section of the ridges in (D). CCD, charge-coupled device. (**E**) Raman scattering spectra for the same benzenethiol-coated silver film shown in (C) and (D) (red curve) and for neat benzenethiol (blue curve). The excitation wavelength was 532 nm.

resulting images for scans parallel to the ridge tops (Fig. 4C) reveal uniformly enhanced signals near the triangular peaks. More importantly, cross-sectional scans (Fig. 4D) show that the response is high at this peak while remaining low along the smooth sides of the ridges and the valleys in between. Using the protocol and apparatus in (*28*), we quantified the SERS enhancement by comparing the Raman signal from neat benzenethiol with that from our monolayer-coated substrate (Fig. 4E). After correcting for the number of molecules, we determined an enhancement factor of 1.4×10^7. Because this represents an average over the entire surface, the actual enhancement near the ridge peak should be much higher.

Whereas bumps, ridges, and grooves are clearly useful for these types of applications, different structural elements are necessary for others. For example, a nanoscale hole surrounded by surface structures can allow enhanced transmission of electromagnetic waves through a metal film (*3*). Figure 2F shows that we can also create such holes in thin smooth silver films. A hexagonal array of deep circular pits was formed on a silicon wafer with nanosphere lithography. By evaporating silver on top of such pits and adding epoxy, a thin silver film with a hole array was obtained. Although only one side of this film is ultrasmooth, which would affect its transmission properties, an additional absorbing layer such as Cr could be added to the rough side to minimize its effects. A second useful element is the multilayer structure. For example, thin patterned films with alternating layers of metal and insulator can exhibit a negative refractive index (*29*), which can lead to new optical phenomena (*30*). Our approach can also yield such structures, called metamaterials. After evaporating a thin film of silver on patterned silicon templates, we deposited alternating layers of alumina and silver. Because silver adheres to alumina better than silicon, the entire stack could be removed with epoxy. For example, a bull's eye (Fig. 2G) and a bump array (fig. S7) could be easily obtained, both of which have potential use as superlenses (*30*). As long as the adhesion requirement is satisfied, other materials besides alumina are also possible. The resulting films can lead to a variety of useful optoelectronic devices, especially considering that they are formed on flexible substrates with built-in metal contacts.

These results indicate that template stripping can be combined with silicon microfabrication methods to create ultrasmooth patterned metals for plasmonics and metamaterials. Although extremely simple, it provides a route to fabricate integrated metallic multilayer structures with designed grooves, bumps, tips, and holes with controlled spacings and orientations, while simultaneously avoiding previous problems because of roughness and impurities.

References and Notes

1. H. Raether, *Surface Plasmons* (Springer, Berlin, 1988).
2. H. A. Atwater, *Sci. Am.* **296**, 56 (2007).
3. C. Genet, T. W. Ebbesen, *Nature* **445**, 39 (2007).
4. E. Ozbay, *Science* **311**, 189 (2006).
5. N. Engheta, *Science* **317**, 1698 (2007).
6. A. Polman, *Science* **322**, 868 (2008).
7. L. Yin *et al.*, *Nano Lett.* **5**, 1399 (2005).
8. E. J. R. Vesseur *et al.*, *Appl. Phys. Lett.* **92**, 083110 (2008).
9. M. Kuttge *et al.*, *Appl. Phys. Lett.* **93**, 113110 (2008).
10. D. Sarid, *Phys. Rev. Lett.* **47**, 1927 (1981).
11. B. D. Gates *et al.*, *Chem. Rev.* **105**, 1171 (2005).
12. Y. L. Loo, R. L. Willett, K. W. Baldwin, J. A. Rogers, *J. Am. Chem. Soc.* **124**, 7654 (2002).
13. G. Kumar, H. X. Tang, J. Schroers, *Nature* **457**, 868 (2009).
14. M. Hegner, P. Wagner, G. Semenza, *Surf. Sci.* **291**, 39 (1993).
15. M. Graca, J. Turner, M. Marshall, S. Granick, *J. Appl. Phys.* **102**, 064909 (2007).
16. B. Jung, W. Frey, *Nanotechnology* **19**, 145303 (2008).
17. W. Frey, C. K. Woods, A. Chilkoti, *Adv. Mater.* **12**, 1515 (2000).
18. See supporting material on *Science* Online.
19. P. Samori, J. Diebel, H. Lowe, J. P. Rabe, *Langmuir* **15**, 2592 (1999).
20. Q. B. Xu, I. Tonks, M. J. Fuerstman, J. C. Love, G. M. Whitesides, *Nano Lett.* **4**, 2509 (2004).
21. J. Henzie, E. S. Kwak, T. W. Odom, *Nano Lett.* **5**, 1199 (2005).
22. V. V. Temnov, U. Woggon, J. Dintinger, E. Devaux, T. W. Ebbesen, *Opt. Lett.* **32**, 1235 (2007).
23. J. T. van Wijngaarden *et al.*, *Appl. Phys. Lett.* **88**, 221111 (2006).
24. D. L. Mills, *Phys. Rev. B* **12**, 4036 (1975).
25. H. Shiba, M. Haraguchi, M. Fukui, *J. Phys. Soc. Jpn.* **63**, 1400 (1994).
26. A. J. Haes *et al.*, *MRS Bull.* **30**, 368 (2005).
27. C. L. Haynes, R. P. Van Duyne, *J. Phys. Chem. B* **107**, 7426 (2003).
28. K. C. Bantz, C. L. Haynes, *Langmuir* **24**, 5862 (2008).
29. G. Dolling, M. Wegener, S. Linden, *Opt. Lett.* **32**, 551 (2007).
30. D. R. Smith, J. B. Pendry, M. C. K. Wiltshire, *Science* **305**, 788 (2004).

31. We thank K. Bantz and C. Haynes for help with SERS measurements and B. Carlson for help with x-ray photoelectron spectroscopy. This work was supported by the U.S. Department of Energy (grant DE-FG02-06ER46438) and used resources in the Institute of Technology at the University of Minnesota, including the Nanofabrication Center, which receives partial support from NSF through the National Nanotechnology Infrastructure Network program, and the Characterization Facility, which has received capital equipment funding from NSF through the Materials Research Science and Engineering Center, Major Research Instrumentation, and Engineering Research Center programs. S.-H.O. acknowledges support from a Minnesota Partnership for Biotechnology Award and a 3M Non-Tenured Faculty Award. P.N. and N.C.L. acknowledge support from a University of Minnesota doctoral dissertation fellowship and an NIH Biotechnology training grant, respectively. The authors have applied for a patent on the fabrication methods described.

Supporting Online Material

www.sciencemag.org/cgi/content/full/325/5940/594/DC1
Materials and Methods
Figs. S1 to S7
Tables S1 to S3
References

7 April 2009; accepted 16 June 2009
10.1126/science.1174655

Probing Spin-Charge Separation in a Tomonaga-Luttinger Liquid

Y. Jompol,[1]* C. J. B. Ford,[1] J. P. Griffiths,[1] I. Farrer,[1] G. A. C. Jones,[1] D. Anderson,[1] D. A. Ritchie,[1] T. W. Silk,[2] A. J. Schofield[2]

In a one-dimensional (1D) system of interacting electrons, excitations of spin and charge travel at different speeds, according to the theory of a Tomonaga-Luttinger liquid (TLL) at low energies. However, the clear observation of this spin-charge separation is an ongoing challenge experimentally. We have fabricated an electrostatically gated 1D system in which we observe spin-charge separation and also the predicted power-law suppression of tunneling into the 1D system. The spin-charge separation persists even beyond the low-energy regime where the TLL approximation should hold. TLL effects should therefore also be important in similar, but shorter, electrostatically gated wires, where interaction effects are being studied extensively worldwide.

The effects of interactions are almost impossible to calculate in a general many-particle system, although they cannot be ignored. However, for a one-dimensional (1D) system, Luttinger, building on an approximation scheme of Tomonaga, constructed a soluble 1D model with infinite linear dispersion and a restricted set of interactions. The solution has the remarkable property that the excitations of spin and charge behave independently and move with different speeds. It has been argued (*1*) that all 1D metals are adiabatically continuous with the Tomonaga-Luttinger model at low energies, and hence spin-charge separation should be observable in real systems. Determining the extent of its applicability would provide a major test of more general methods of modeling interaction effects, with relevance to quantum devices and the theory of high-temperature superconductivity. Recent work (*2*) presents a more general theory of 1D systems with a nonlinear dispersion, but the effects of spin are not yet included.

Some properties of the Tomonaga-Luttinger liquid (TLL), such as power-law behavior, have been observed and studied in a variety of systems,

[1]Cavendish Laboratory, University of Cambridge, J. J. Thomson Avenue, Cambridge CB3 0HE, UK. [2]School of Physics and Astronomy, University of Birmingham, Edgbaston, Birmingham B15 2TT, UK.

*To whom correspondence should be addressed. E-mail: yodchay.jompol@cantab.net

such as carbon nanotubes (*3*) and edge states in the fractional quantum Hall regime (*4*), but these experiments have not directly resolved the dispersion of the excitations in a TLL. Only a few experiments have attempted to detect the spin-charge separation directly, for example, by photoemission spectroscopy (*5*–*7*) and tunneling spectroscopy between a pair of closely spaced cleaved-edge-overgrown quantum wires (*8*–*10*). The latter 1D-1D tunneling results are striking and provide some evidence of dispersing spinons and holons—the excitations of a TLL. However, in these experiments TLLs act as both probe and subject, so an independent study—in a different geometry—of the excitation spectrum is vital to be sure of the interpretation.

We use a 2D electron gas (2DEG) as the (well-understood) probe layer. Use of an array of highly regular wires averages out impurity, length-resonance, and charging effects, and measurements of power-law behavior and spin-charge separation can be made with just the lowest 1D subband, without electrons becoming localized. Interpretation of TLL results is thus much easier, and results obtained in the nonlinear regime, where the theory is much less well developed, can be directly interpreted as a modification of the 1D elementary excitations. Our 1D wires are formed using split gates, where the confinement is much weaker than in the overgrown wires, making the results relevant to a broad range of other devices. The tunneling current I between the 1D wires and an adjacent low-disorder layer containing a 2DEG depends on the overlap between the spectral functions of the two systems. This overlap is varied by using an in-plane magnetic field B perpendicular to the wires to offset the two spectral functions in k space by $\Delta k = eBd/\hbar$ along the wires, where d is the center-to-center tunneling distance between the two systems (*11*). By applying a positive bias V_{dc} to the 2DEG relative to the wires, electrons tunnel into excited states of the 2DEG, from matching states below the Fermi energy in the 1D wires, allowing investigation of the energy dependence. Thus, the 2D system acts as a spectrometer, and the differential conductance G displays resonant-tunneling peaks corresponding to overlapping points in the offset dispersion relations, where energy and momentum are conserved.

Our devices contain an array of about 350 extremely regular quantum wires in the upper layer of a GaAs-AlGaAs double-quantum-well (DQW) structure (Fig. 1A). The two layers are separately contacted using a surface-gate depletion scheme (*12*–*14*). The wires, of length L = 17.5 μm and lithographic width 0.17 μm (device A) and 0.18 μm (device B), were squeezed by a negative gate voltage V_{wg}. There is an additional small ungated region p of width 0.9 μm, which provides a current path to the entrances to the 1D wires. The tunneling conductance $G = dI/dV_{dc}$ between the 1D wires and the 2D layer was measured as a function of source-drain bias V_{dc} in an in-plane magnetic field B perpendicular to the wires at lattice temperatures T down to ~40 mK.

First, the effect of the wire-gate voltage V_{wg} was characterized (Fig. 1). Initially, at small V_{wg}, the upper 2DEG screens the lower 2DEG. The first drop in G occurs at −0.40 V when the top well depopulates, leaving narrow 1D wires between the gates. Then, the bottom well is gradually depleted until it pinches off at −0.80 V. B was then swept at each V_{wg} (with V_{dc} = −0.3 mV, to avoid the zero-bias anomaly described later), revealing a series of peaks (Fig. 1B), one pair of peaks at $B_i^{\pm}$ for the ith 1D subband ($i \geq 1$). For this device (A, 0.17 μm wire width), six peaks are observed at V_{wg} = −0.49 V, corresponding to three occupied 1D subbands (*13*). With more negative V_{wg}, the 1D subband spacing increases and the 1D density decreases. Hence, the number of subbands can be reduced to just one. At $V_{wg} \sim -0.65$ V, the wires become insulating. The widths of the wire gates and of the long narrow 2D p region were chosen carefully such that even with just a single 1D subband in the top 2DEG there was minimal modulation of the lower 2DEG and current could still reach the wires. However, the p region inevitably contributes a 2D-2D parasitic tunneling current that appears in the measurements, but this is small and independent of the tunnel current from the wires, even after wire pinch-off, so it can be measured and allowed for.

We now choose V_{wg} = −0.62 V, well into the region where there is just one 1D subband. Figure 2, A and B, shows G as a function of the dc interlayer bias (V_{dc}) and B as color-scale plots, at high (1 K) and low (~40 mK) lattice temperatures, respectively. In the absence of interactions, there should be peaks in G that track the 1D and 2D parabolic dispersion relations; these are indicated with dashed and solid black curves, respectively. The parasitic 2D-2D tunneling in the ungated p region is also shown, as green dash-dotted lines labeled p. The crossing points along $V_{dc} = 0$ occur at $B^- = 1.08$ T and $B^+ = 3.62$ T (Fig. 2B). The 1D Fermi wave vector is $k_{F1D} = ed(B^+ - B^-)/2\hbar$, giving the approximate electron density in the wires $n_{1D} \cong 40\ \mu m^{-1}$ (from $k_{F1D} = \pi n_{1D}/2$). The up-turned (dashed) parabola maps the energy of the 1D wires as a function of wave vector k.

The curves drawn in Fig. 2 are those expected for single-particle tunneling. However, there is an additional region of high conductance to the right of B^+. It drops off along a straight line moving diagonally up and to the left from B^+ (indicated with an arrow). To show this more clearly, the data are differentiated with respect to B and plotted in Fig. 2C. We have taken detailed data in this region, sweeping B, in another device (B) in the same single-subband regime (Fig. 3B). We find a region of large negative dG/dB along a straight line to the right of the high-conductance region; this appears dark blue and is indicated by

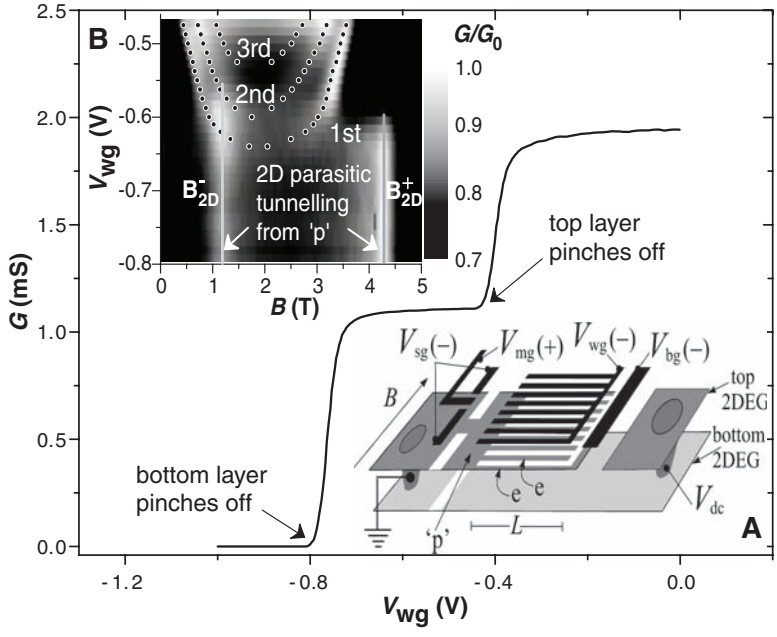

Fig. 1. The conductance, G, as a function of the wire-gate voltage V_{wg} (device A) with no other gates defined. It shows that the strip joining all the wire gates together (see inset A) is depleted at −0.4 V, blocking conduction along the top layer; electrons then have to tunnel to the bottom layer, which is only depleted at −0.8 V. (**Inset A**) Device layout showing gate positions in black; the signs beside the voltage symbols indicate the polarity of the various gate voltages. Current is injected into both layers at the left Ohmic contact, then three gates pinch off the lower layer so that electrons flow into the wires in the upper layer, tunnel to the lower 2DEG and then to the right contact. (**Inset B**) Gray-scale plot of the tunneling conductance showing resonant peaks (bright) as a function of transverse magnetic field measured at a lattice temperature of ~40 mK, with each trace normalized by the maximum height G_0. The dots indicate the features corresponding to the first, second, and third 1D subbands, as labeled, measured from the raw data. The 2D parasitic tunneling from region p does not change with V_{wg}. Its peaks stay at $B^-_{2D} = 1.27$ T and $B^+_{2D} = 4.31$ T, as indicated with vertical solid lines.

the red dashed line. We compare this with the theoretical prediction for noninteracting electrons, shown in Fig. 3A, where a similar dark blue feature also occurs. However, the latter tracks the 1D parabola along its length. In contrast, the feature in Fig. 3B disperses away from the 1D parabola. Because features in the conductance reflect singular features in the spectral function, we can conclude that the 1D parabola and the red dashed line track the dispersion of two independent excitations, which in the TLL framework correspond to the spinon and holon, for spin and charge excitations, respectively.

To confirm this interpretation, we have calculated the tunneling spectra for a TLL coupled to a 2D system of electrons. The framework for these calculations already exists in the literature (*15*, *16*), so we only describe the relevant details here. To compute the tunneling current, we require the spectral function of a TLL, which in general depends on four parameters: the spinon and holon velocities v_σ and v_ρ, respectively, plus two exponents γ_σ and

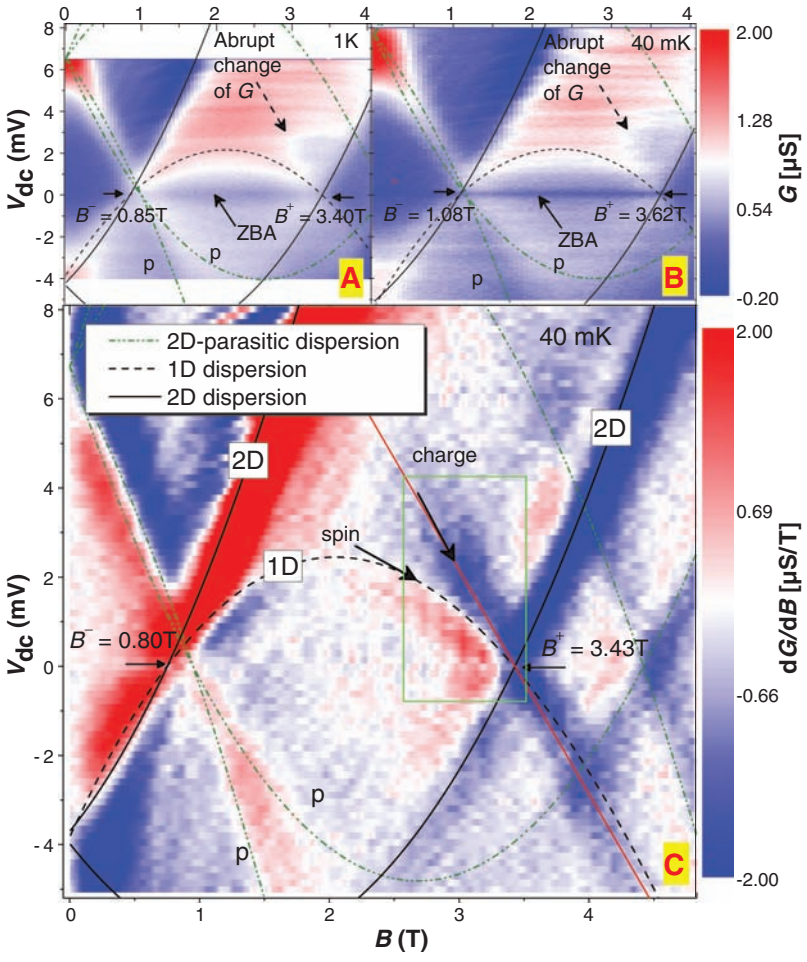

Fig. 2. (**A** and **B**) Color-scale plots of G versus V_{dc} and B at lattice temperatures of 1 K and 40 mK, respectively (device A, for V_{wg} = –0.62 V). Black lines (solid and dashed) indicate the locations of singularities predicted by the noninteracting model for tunneling between the wires and the 2DEG, whereas the green dash-dotted lines indicate the locations of the singularities associated with the parasitic 2D-2D tunneling. There is an additional abrupt decrease in G along the line indicated. In addition, G is suppressed at zero bias, labeled ZBA; this is another sign of interactions. (**C**) dG/dB (device A, for V_{wg} = –0.60 V). The noninteracting parabolae are shown as in (A) and labeled 1D or 2D to indicate which dispersion is being probed. The straight red line indicates the locus of the abrupt change in G indicated in (A) and (B) and is a factor of ~1.4 steeper than the 1D parabola at V_{dc} = 0. This feature clearly moves away from the 1D parabola. We identify it with the TLL charge excitation (holon), whereas the 1D parabola tracks the spin excitation (spinon).

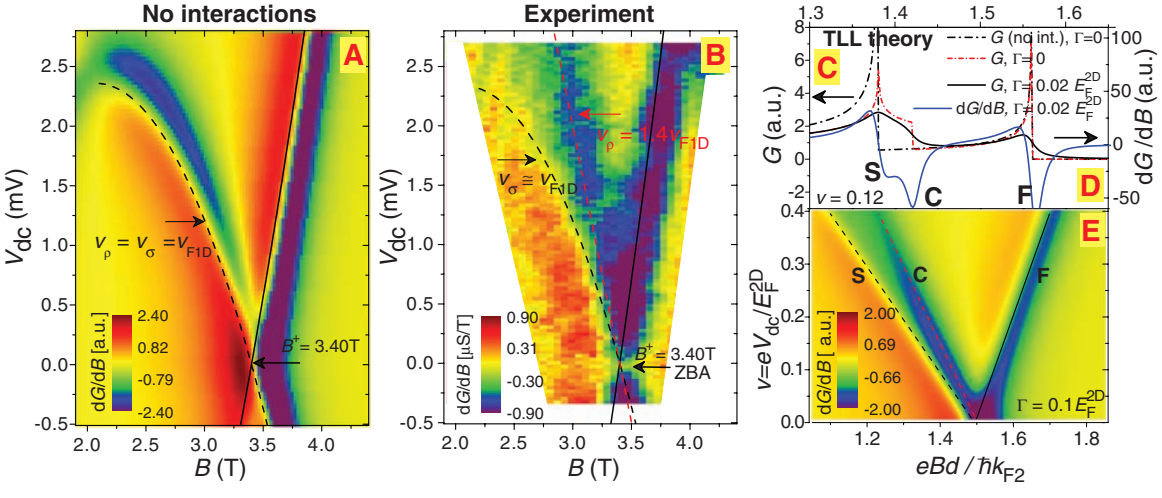

Fig. 3. Comparison of dG/dB for experiment and theory. (**A**) For noninteracting electrons, all features track the noninteracting parabolae (disorder broadening Γ = 0.6 meV). (**B**) dG/dB measured at high resolution while sweeping B, for device B. The red line marks a feature that does not track the noninteracting parabolae and is absent in (A). Calculation of G (**C**) and dG/dB (**D**) for noninteracting electrons and a TLL. The dimensionless bias $v = eV_{dc}/E_F^{2D} = 0.12$; Γ is indicated for each curve. For the TLL, the spinon velocity $v_\sigma = v_{F1D}$ and the chosen holon velocity $v_\rho = 1.4v_{F1D}$. Spin and charge excitations are labeled S and C, respectively. F labels the noninteracting 2D dispersion curve. (**E**) dG/dB as a function of B and v, showing the same charge feature (C) as in the experiment (B).

γ_ρ. We assume repulsive, spin-rotation-invariant interactions, which implies $\gamma_\sigma = 0$ and $v_\rho > v_\sigma$; in the absence of back-scattering, $v_\sigma \approx v_{F1D}$, the 1D Fermi velocity. For simplicity, we also neglect interbranch scattering processes, which sets $\gamma_\rho = 0$. The spectral function of the 2D system is taken to be a Lorentzian of width Γ, where Γ is the disorder-scattering rate in the 2D system (*17*).

This minimal model is convenient for analytical calculations and is expected to reproduce the main features of the tunneling spectra associated with spin-charge separation. It will not, however, capture the zero-bias anomaly, which is absent for $\gamma_\rho = 0$. Finite γ_ρ is also expected (*16*) to lead to a weakening of the singular features in the spectra, making our calculation the "optimum" case for observing spin-charge separation. Because the TLL model relies on the linearization of the spectrum at low energies, the model's results are only formally applicable in the low-bias part of the spectrum, where this linear approximation holds.

Figure 3C shows the calculated conductance in the vicinity of the B^+ point as a function of scaled magnetic field at fixed voltage for noninteracting electrons, a clean TLL, and a TLL with a little disorder broadening. The singular peak at high magnetic field is independent of the form of the excitations, and hence is common to both systems. The peak at lower magnetic field for the noninteracting system splits, in the TLL case, into a weakened singular peak (which for $v_\sigma = v_{F1D}$ occurs at the same magnetic field as the noninteracting peak), plus a finite discontinuity away from the peak. This sudden drop in the conductance away from the peak is precisely what is observed experimentally in Fig. 2, A and B. Figure 3D shows dG/dB with a little disorder. The spinon is identified as a maximum/minimum pair, which disperse together in the B-V_{dc} plane, as shown in Fig. 3E, for more realistic disorder broadening. The holon is identified as a single minimum, which disperses away from the spinon. We note that an extra feature is also predicted to occur at the B^- point. However, because all three features from this point remain in proximity to each other, it is difficult to resolve them individually.

The experimental results in Fig. 3B are consistent with the predictions in Fig. 3E, at least in the low-bias regime where the linear approximation is reasonable. We have observed this extra feature in the conductance in three devices, at temperatures between ~60 mK and 1.8 K, and on several thermal cycles. We thus conclude that we are observing spin-charge separation, the hallmark of a TLL.

An additional feature that cannot be explained in the noninteracting model is the zero-bias anomaly (ZBA), the strong suppression of conductance along $V_{dc} = 0$, visible as a dark-blue line in Fig. 2, A and B. This is likely to be related to the energy cost for an electron to tunnel into or out of a 1D wire, as it disturbs the line of electrons on either side of it. It has previously been observed in 1D-1D tunneling (*8*), and, for a TLL, G is expected to have identical power-law dependences on V_{dc} and temperature T.

Figure 4A shows the ZBA in the tunneling conductance G as a function of V_{dc} at various T, at a field midway between B^- and B^+. Figure 4, B and C, shows $G(V_{dc} = 0,T)$ and $G(|V_{dc}|, T < 70$ mK), respectively, on log-log plots. Both clearly vary as power laws, as labeled, over considerably more than one order of magnitude. The corresponding power-law exponents $\alpha_T \approx 0.45 \pm 0.04$ and $\alpha_V \approx 0.52 \pm 0.04$ are very similar, as expected. To illustrate that temperature and bias play a similar role in smearing the energy, $G(|V_{dc}|)$ is plotted in Fig. 4D as a function of $V'_{dc} = \sqrt{|V_{dc}|^2 + (3k_BT/e)^2 + V_{ac}^2}$, the simplest way of adding forms of energy smearing together as noise in quadrature. ($3k_BT$ is an estimate of the thermal energy spread, and the factor of 3 is chosen to match the offset between the curves in Fig. 4, B and C.)

The TLL is characterized by the "anomalous" exponent γ_ρ and the spinon and holon velocities. γ_ρ can be expressed in terms of an interaction parameter g [$\gamma_\rho = (g + 1/g - 2)/8$], which indicates the strength of the interactions ($g = 1$ for noninteracting particles). Accurate a priori calculation of g cannot be done in general. However, an estimate based on the 1D densities used suggests $g \sim 0.7$ (supporting online text). We now determine g from the various experimental results.

In TLL theory, the spin velocity v_σ is approximately equal to the Fermi velocity v_{F1D} for weak backscattering ($v_\sigma < v_{F1D}$ for stronger interactions) (*18*, *19*). Thus, the spin mode should follow the low-bias part of the noninteracting 1D parabola (or even lie below it). The charge mode should propagate faster than the spin mode for repulsive interactions. Thus, we label the curve that follows the 1D parabola "spin" and the extra line "charge." For device B, we deduce the velocities close to zero bias to be $v_\sigma \approx v_{F1D} = \hbar k_F/m_{1D} = 1.13 \times 10^5$ ms^{-1} and $v_\rho \approx 1.4\ v_{F1D}$, respectively. In a Galilean invariant system, $g = v_{F1D}/v_\rho$ (*19*), so this gives $g \approx 0.7$, which is consistent with the estimate given above. For device A, g is very similar to that of device B, as is the 1D electron density. Another device, with a thinner (7 nm) barrier, yields $g \approx 0.65$.

Within TLL theory, the power-law exponents extracted from the ZBA can also be directly related to g. The form of the exponent depends on whether the excitations are affected by the ends of the wire. This is determined by comparing the energy of the tunneling electron to $\Delta E = 2\hbar v_{F1D}/gL$, which is related to the inverse time scale for the holon to travel to the end of a

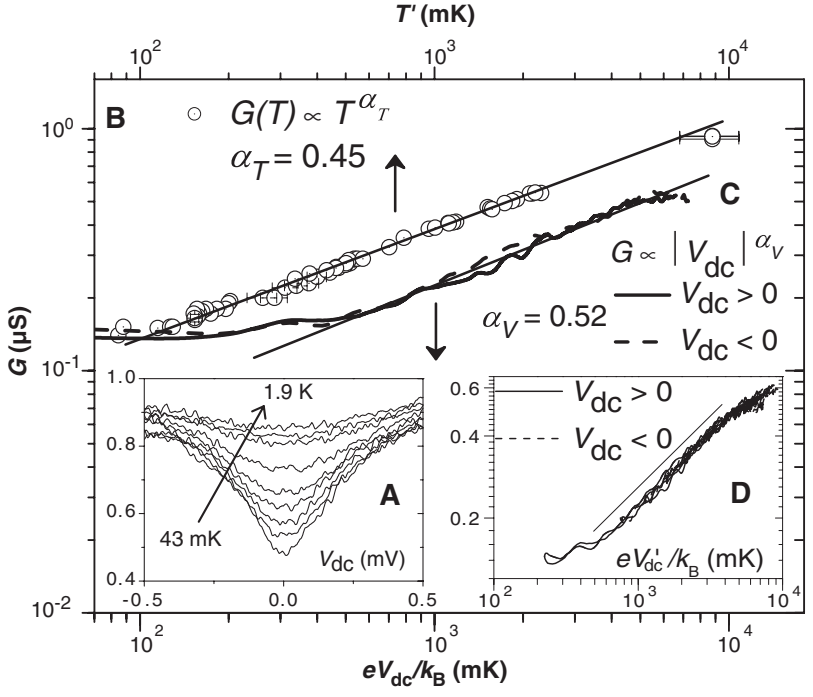

Fig. 4. The dependence of the conductance G on bias V_{dc} and temperature T (device B). (**A**) The ZBA at various T up to 1.9 K at $B = 2.33$ T. (**B**) Minima of the ZBA [$G(V_{dc} = 0)$] versus T. G varies as T^{α_T}, where $\alpha_T \approx 0.45$ over nearly two orders of magnitude. (**C**) $G(|V_{dc}|)$ on a log-log plot (with V_{dc} scaled to temperature using $eV_{dc} = k_BT$), on scales matching those in (B) for T, showing that it varies as $V_{dc}^{\alpha_V}$, where $\alpha_V \approx 0.52$ over more than one order of magnitude. (**D**) $G(|V_{dc}|)$ versus $V'_{dc} = \sqrt{|V_{dc}|^2 + (3k_BT/e)^2 + V_{ac}^2}$, the simplest way of adding the forms of energy smearing together as noise in quadrature. The value $3k_BT$ is chosen to superpose the lines in (B) and (C) and also all the curves in (D), where the lowest temperature has been adjusted from 43 mK to 70 mK to avoid saturation. Using the more complex scaling relation of equation 5 of (*3*) also gives a universal curve if $\alpha \approx 0.51$.

wire of length L (*8*, *20*). For k_BT, $eV_{dc} >> \Delta E$, the ends are unimportant and the process is called "bulk" tunneling, with an exponent $\alpha_{bulk} = (g + 1/g - 2)/4$. Taking $L = 17\mu m$ and $g = 0.7$ gives $\Delta E \approx 150$ mK for our device, and therefore almost all of our ZBA data shown in Fig. 4 are expected to be in the bulk-tunneling regime. The measured values of $\alpha_T = 0.45$ and $\alpha_V = 0.52$ (device B) give $g \approx 0.28$ and 0.26, respectively.

The values of g found from the ZBA exponents are much smaller than that extracted from the holon branch in Fig. 3. We briefly offer possible explanations for this [with more detail in (*14*)]. One possibility is that impurities and imperfections may make the effective length of each wire shorter than the lithographic length. It is well known that an impurity in a TLL will effectively cut it into two at low energies. Although at finite energies, electrons are able to tunnel through such constrictions, one might expect that the constrictions will modify the form of the ZBA exponent in a similar way to "ends." If we use the formula for ZBA exponent in the end-tunneling regime (*14*), the extracted values of g (0.53 from α_T and 0.49 from α_V) are more comparable to that extracted from the holon branch.

Alternatively, it may not be valid to extrapolate the higher-energy properties of the branches to low energies where the ZBA is measured. The interactions between the wires and/or between the wires and the 2DEG may become important, and may alter the form of the ZBA exponent (*21*). The effective dielectric constant of the material may also be energy dependent, changing the strength of the interactions at low energies.

TLL theory is based on the assumption of a linear dispersion relation about the Fermi energy. We go beyond that regime at high dc bias. There is very little work on interactions in 1D wires at high energy where the TLL approximation breaks down. Haldane (*1*) argued that all 1D metals are adiabatically continuous with the TLL, that is, perturbations such as the band curvature are only expected to lead to a renormalization of the TLL parameters, so spin-charge separation should persist; this is backed up by recent renormalization-group calculations (*22*). Recent theoretical work on spinless fermions for a curved band has shown an intriguing interplay of Fermi-liquid and TLL behavior (*2*, *23*). Numerical calculations have been performed in this regime (*24*) using quantum Monte Carlo methods, with results that resemble our experimental results—a parabolic spin branch and a fairly straight charge branch.

References and Notes

1. F. D. M. Haldane, *J. Phys. C Solid State Phys.* **14**, 2585 (1981).
2. A. Imambekov, L. I. Glazman, *Science* **323**, 228 (2009).
3. M. Bockrath *et al.*, *Nature* **397**, 598 (1999).
4. A. M. Chang, M. K. Wu, C. C. Chi, L. N. Pfeiffer, K. W. West, *Phys. Rev. Lett.* **86**, 143 (2001).
5. C. Kim *et al.*, *Phys. Rev. Lett.* **77**, 4054 (1996).
6. B. J. Kim *et al.*, *Nat. Phys.* **2**, 397 (2006).
7. P. Segovia, D. Purdie, M. Hengsberger, Y. Baer, *Nature* **402**, 504 (1999).
8. Y. Tserkovnyak, B. I. Halperin, O. M. Auslaender, A. Yacoby, *Phys. Rev. B* **68**, 125312 (2003).
9. O. M. Auslaender *et al.*, *Science* **295**, 825 (2002).
10. O. M. Auslaender *et al.*, *Science* **308**, 88 (2005).
11. B. Kardynal *et al.*, *Phys. Rev. Lett.* **76**, 3802 (1996).
12. S. A. Nield, J. T. Nicholls, W. R. Tribe, M. Y. Simmons, D. A. Ritchie, *J. Appl. Phys.* **87**, 4036 (2000).
13. Y. Jompol *et al.*, *Physica E* **40**, 1220 (2008).
14. Materials and methods are available as supporting material on *Science* Online.
15. A. Altland, C. H. W. Barnes, F. W. J. Hekking, A. J. Schofield, *Phys. Rev. Lett.* **83**, 1203 (1999).
16. S. A. Grigera, A. J. Schofield, S. Rabello, Q. Si, *Phys. Rev. B* **69**, 245109 (2004).
17. N. Turner *et al.*, *Phys. Rev. B* **54**, 10614 (1996).
18. J. Voit, *Phys. Rev. B* **47**, 6740 (1993).
19. C. E. Creffield, W. Häusler, A. H. MacDonald, *Europhys. Lett.* **53**, 221 (2001).
20. C. L. Kane, M. P. A. Fisher, *Phys. Rev. B* **46**, 15233 (1992).
21. D. Carpentier, C. Peça, L. Balents, *Phys. Rev. B* **66**, 153304 (2002).
22. H. Benthien, F. Gebhard, E. Jeckelmann, *Phys. Rev. Lett.* **92**, 256401 (2004).
23. M. Khodas, M. Pustilnik, A. Kamenev, L. I. Glazman, *Phys. Rev. B* **76**, 155402 (2007).
24. M. G. Zacher, E. Arrigoni, W. Hanke, J. R. Schrieffer, *Phys. Rev. B* **57**, 6370 (1998).

25. We acknowledge the UK Engineering and Physical Sciences Research Council for funding. Y.J. was supported by a scholarship from the Thai Ministry of Science. We thank F. Sfigakis for experimental assistance and B. E. Kardynal and C. H. W. Barnes for useful discussions.

Supporting Online Material

www.sciencemag.org/cgi/content/full/325/5940/597/DC1
Materials and Methods
SOM Text
References

3 February 2009; accepted 6 May 2009
10.1126/science.1171769

The Formation of Population III Binaries from Cosmological Initial Conditions

Matthew J. Turk,[1]* Tom Abel,[1] Brian O'Shea[2]

Previous high-resolution cosmological simulations predicted that the first stars to appear in the early universe were very massive and formed in isolation. Here, we discuss a cosmological simulation in which the central 50 $M_\odot$ (where $M_\odot$ is the mass of the Sun) clump breaks up into two cores having a mass ratio of two to one, with one fragment collapsing to densities of 10^{-8} grams per cubic centimeter. The second fragment, at a distance of ~800 astronomical units, is also optically thick to its own cooling radiation from molecular hydrogen lines but is still able to cool via collision-induced emission. The two dense peaks will continue to accrete from the surrounding cold gas reservoir over a period of ~10^5 years and will likely form a binary star system.

Hydrodynamical simulations that start from cosmological initial conditions have predicted that the first luminous objects in the universe were isolated stars with masses in the range of 30 to 300 $M_\odot$ (where $M_\odot$ is the mass of the Sun) on the basis of accretion rates calculated in the absence of accretion-inhibiting factors (*1*–*3*). Idealized protostellar evolution simulations suggest that accretion should end when the star reaches ~100 $M_\odot$ (*4*), but although most relevant feedback mechanisms of the protostars on their accretion flow are known (*5*), no fully self-consistent radiation hydrodynamical simulations reaching the main sequence have yet been possible, even in one dimension. The early stages of protostellar evolution, however, are understood in some detail from spherically symmetric calculations (*6*, *7*) as well as semi-analytic models (*8*).

The environment in which the first stars form is calculated by following early-universe evolution of the primordial gas and dark matter; by this means, the first stars are found to form in halos with a total mass of ~10^6 $M_\odot$, with collapse driven first by cooling via molecular hydrogen rovibrational lines and later by collision-induced emission (*6*, *9*, *10*). Although several tens of calculations (*1*, *11*, *12*) have followed the collapse of a primordial protostellar halo to relatively low densities (~10^{-12} g cm^{-3}), only two previous calculations have followed the collapse from cosmological initial conditions to protostellar densities (*2*, *13*). Both of these calculations used a chemical model that included the relevant medium- and high-density physics, such as heating from the formation of molecular hydrogen, collisionally induced emission, three-body molecular hydrogen formation, and gas opacity at high densities. Several simulations have followed the collapse of a single metal-free cloud starting from idealized initial conditions (*3*, *14*, *15*). Parameter studies of rotating cylinders have shown that metal-free gas can fragment (*16*) and have found fragmentation of spherical distributions of extremely low- and zero-metallicity gas (*17*), including in three-dimensional nested grid parameter studies (*18*). Additionally, studies of zero-metallicity gas collapsing in isolation have found fragmentation at low densities (~10^{-16} g cm^{-3}) (*19*). However, no previous simulation starting from cosmological

[1]Kavli Institute for Particle Astrophysics and Cosmology, Stanford University, 2575 Sand Hill Road, Menlo Park, CA 94025, USA. [2]Department of Physics and Astronomy, Michigan State University, East Lansing, MI 48824–2320, USA.

*To whom correspondence should be addressed. E-mail: mturk@slac.stanford.edu

initial conditions has shown fragmentation in a cosmological context.

We present simulations performed with the adaptive mesh refinement code Enzo (*20*). These simulations were initialized at a redshift of 99 in a box 300 kpc h^{-1} (comoving) on a side, where h is the Hubble constant unit (*21*). We stopped the simulation at a maximum (proper) baryon density of 1.61×10^{-8} g cm^{-3} at redshift $z = 19.08$ (189 million years after the Big Bang) and 1.72 $R_\odot$ (radius of the Sun proper) peak spatial resolution, where we resolved the first massive halo that forms in this simulation volume. The simulation presented here is explicitly a simulation of the first generation of Population III star formation. The second generation of Population III stars are still primordial in composition but are potentially affected by previous generation of stars, by effects such as kinetic energy injection, radiation backgrounds, or cosmic rays. We simulated five realizations of first-generation Population III stars that evolve to at least this density and found fragmentation in one. The dark matter halo merger history and the evolution of baryonic properties at redshifts above 20 are typical of previous simulations (*1*, *22*).

The collapsing halo fragmented at a density of $\simeq 2.0 \times 10^{-13}$ g cm^{-3} at $z = 19.08$, roughly. We conducted resolution studies, where we found fragmentation but a change in the separation of the identified cores (*21*). To study the fragmentation of the cloud, we identified gravitationally bound, topologically connected regions at or above a single density within the halo's virial radius. The density at which these regions diverged was $\sim 2.0 \times 10^{-13}$ g cm^{-3}; however, because the difference was only a thin strip of lower-density gas, we conducted all subsequent analysis on connected isodensity surfaces with minimum density of 3.0×10^{-13} g cm^{-3}. We selected material within two isodensity surfaces, hereafter referred to as core A and core B (Fig. 1). Core A is the more massive core, with a mass of 10.0 $M_\odot$, and core B has a mass of 6.3 $M_\odot$. Determining whether these two objects will ultimately merge is nontrivial, but estimates can be made on the basis of the current orbital mechanics as well as collapse conditions of each core in isolation. If these two objects form hydrostatically supported protostellar cores and most of the intervening gas is accreted onto them, they will remain separate and form a binary star system.

Both cores are oblate and are embedded in a crescent-shaped cloud. Although they cannot be reliably identified more than ~175 years before the end of the simulation, the beginning of fragmentation is already evident in both density and molecular hydrogen, where lower-density, mostly atomic regions are permeated by filaments of higher-molecular-fraction gas (Fig. 1, top row). Averaging over the time period during which the two cores are identifiable and distinct, core A experiences 0.061 $M_\odot$ year^{-1} mass flux across its density isosurface, whereas core B has mass flux of 0.049 $M_\odot$ year^{-1} (Fig. 2). The flow across both density isosurfaces is roughly linear. The peak densities in both cores evolve at close to free-fall trajectories, and core B collapses ~60 years after core A.

The separation of the centers of mass of the two cores is 800 astronomical units (AU). Within a minimally enclosing sphere of radius 780 AU located at the center of mass of the two cores, we find a total mass of 52 $M_\odot$; within a sphere of radius twice the separation of the cores, we find a mass of 99 $M_\odot$. By defining

$$\overline{R} = \left(\frac{3M_{\rm enc}}{4\pi\overline{\rho}}\right)^{1/3}$$

where $\overline{\rho}$ is the average mass density, we calculated the characteristic radius of each core. Core B, the lower-mass core, is at this time less dense then core A and has a smaller characteristic radius. Given its current angular momentum and assuming both angular momentum conservation and no material between the cores, its final Keplerian radius is given by

$$R_{\rm kep} = \frac{L_{\rm B}^2}{GM_{\rm A}}$$

where $L_{\rm B}$ is the specific angular momentum of core B in the rest frame of core A and $M_{\rm A}$ is the mass of core A. $R_{\rm kep}$ evaluates to 2400 AU, which is three times their current distance, indicating that the velocity of core B is super-Keplerian. The tangential velocity of core B with respect to core A is 5.9 km s^{-1}, and it has a radial velocity of -5.3 km s^{-1}. Given the current velocities, separation, and masses of the cores and the assumption that the two cores exist with their current trajectories in a vacuum, a simple orbit integration shows that their closest approach of 480 AU would

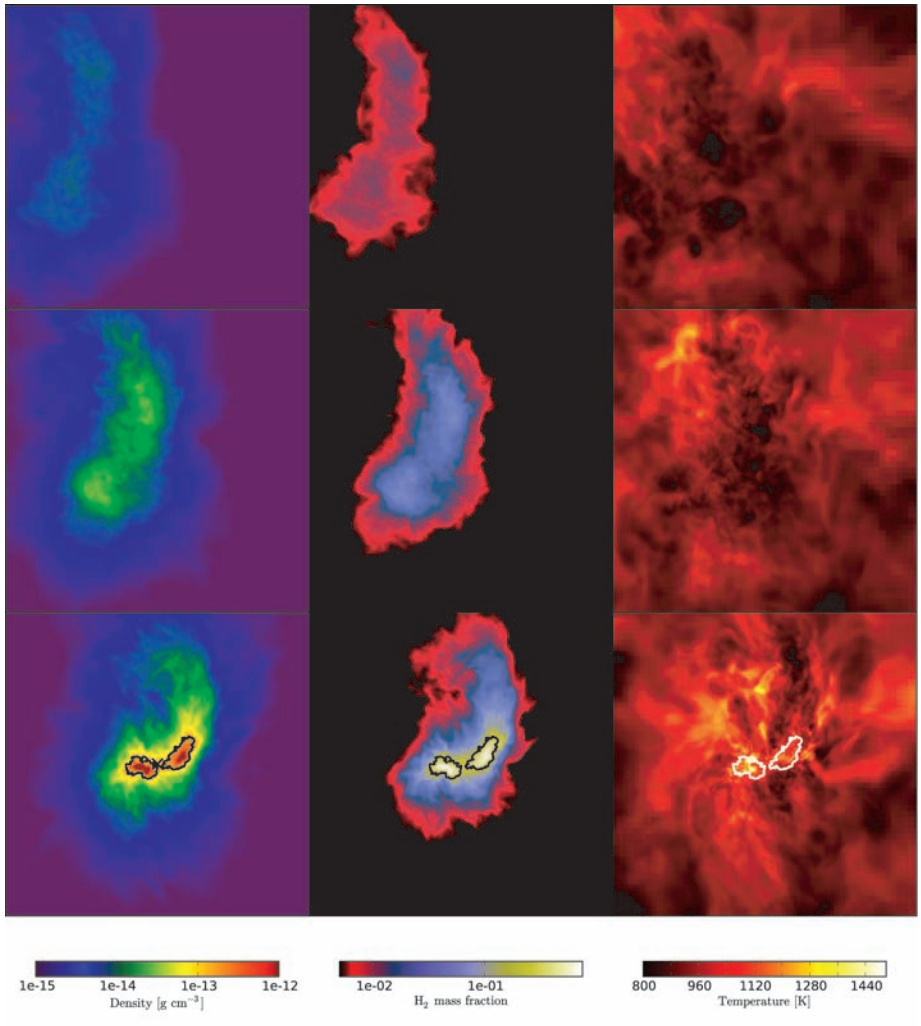

Fig. 1. Mass-weighted average density (left column), H_2 fraction (middle column), and temperature (right column) projected through a cube centered on the center of mass of the two-core system with a side length of 3500 AU. The bottom row is the final output of the simulation, the middle row is 555 years previous, and the top row is an additional 591 years before the middle row (1146 years before the end of the simulation). Gravitationally bound cores with a minimum density of 3.0×10^{-12} g cm^{-3} have been outlined with thick lines in the bottom row; core A is on the left, and core B is on the right. Field of view is 3500 AU.

occur after 360 years, more than 10 dynamical times of the lighter core. However, this vacuum assumption could be misleading. Another limit can be derived assuming the remaining 46-$M_\odot$ mass between cores A and B instantaneously was accreted onto only core A; then the orbit integrations show it would take over 400 years for B to come within 300 AU of A. Because the time scale of the formation of hydrostatically supported, protostellar cores in either core is close to the free-fall time, an accreting binary system will form. Following the formulation of the dynamical friction force on a massive perturber in a near-circular orbit (*23*), the loss of angular momentum through dynamical friction does not substantially increase the likelihood of a merger of the two cores; in fact, by providing an upper bound on the infall rate, we see that both cores will form protostars long before merging. We have calculated the average density of the background medium with use of spheres both two and five times the radius of the core separation and found that the two cores should not approach closer than 100 AU for at least 3600 years.

We plotted radially binned, mass-weighted average quantities at several epochs of the halo collapse (Fig. 3). The central bin was located at the most dense zone in the simulation at all times. After the cloud fragmented, this most-dense zone was always within core A. The location of core B is clearly visible as a spike in the density, temperature, and H_2 fraction and a slight enhancement in the enclosed mass at ~800 AU. The temperature plot shows a marked increase at high densities compared with those of both previous studies (*1*, *11*). This is likely a result not only of different molecular hydrogen formation and cooling rates but also the inclusion of the heating from the formation of molecular hydrogen and opacity to molecular hydrogen lines. These factors delay the conversion to a fully molecular state until the gas collapses to higher densities, reducing the efficiency of the rovibrational cooling and leading to higher temperatures. Furthermore, the average molecular hydrogen fraction of the cloud does not reach unity, as it has in previous calculations. At higher densities, the cooling from rovibrational lines is inefficient because of increased optical depth; this leads to an increase in the temperature and thus a drop in the molecular hydrogen fraction. There is no substantial dissociation at the final output of this simulation, but the inner region of the collapsing halo has a molecular hydrogen mass fraction of ~0.5. As the cloud collapses further, H_2 will dissociate at densities just slightly higher than those presented here. Following the prescription of (*9*), the peak density of the simulation provides an effective transmission coefficient of 2×10^{-3} for rovibrational cooling and a transmission coefficient of 0.94 for cooling from collision-induced emission.

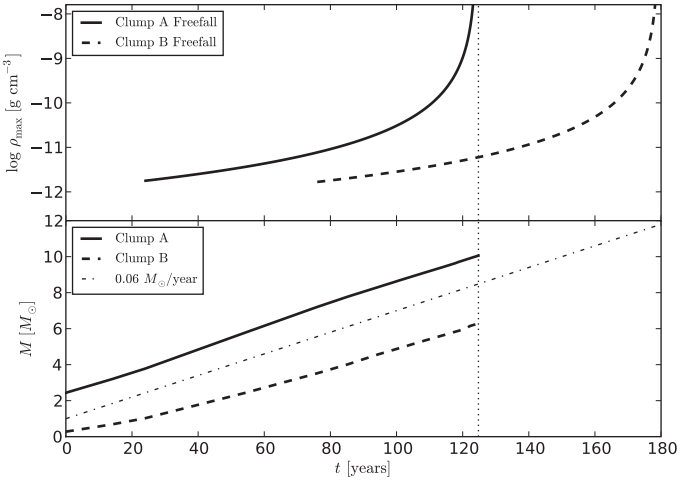

Fig. 2. (**Top**) Cores, identified by placing a minimum density cut at 3.0×10^{-13} g cm^{-3}, plotted over time. The *y* position denotes current maximum density; *x* position denotes time since the first core was identified. Overlaid is the predicted free-fall evolution of the peak density in each core starting from the first time when the maximum density is greater than 10^{-12} g cm^{-3}, governed by $\frac{d\rho}{dt} = \frac{\rho}{t_{ff}}$, where we use free-fall time $t_{ff} = \sqrt{\frac{3\pi}{32G\rho_{max}}}$. We have extended the free-fall trajectories past the end of the simulation, which is indicated by the vertical dotted line. (**Bottom**) Mass enclosed within identified cores as a function of time.

To estimate instabilities brought on by chemical and radiative mechanisms, we follow the methods of (*9*); when the characteristic time scales for the change in energy of the gas are less than the dynamical time, small perturbations can no longer be effectively suppressed and the gas is susceptible to fragmentation. The dynamical time is defined by

$$t_{dyn} \equiv \sqrt{\frac{3\pi}{16G\rho}}$$

where G is the gravitational constant. By defining E as the total thermal energy of the gas, $\dot{e}_{rad}$ as the radiative cooling from rovibrational lines and collision-induced emission, and $\dot{e}_{chem}$ as the heating or cooling due to chemical changes in the molecular hydrogen content of the gas (4.48 eV per molecule), we can write the molecular hydrogen time scale as

$$t_{H_2} = \frac{E}{\dot{e}_{rad} - \dot{e}_{chem}}$$

Comparing these two quantities (Fig. 4), we found that the ratio was around unity at most densities but that at the densities at which the gas fragmented this ratio changed sign abruptly. This is a steep transition, from being moderately prone to fragmentation to being dominated by the heating from the formation of H_2. However, as shown by (*24*), in isolation the thermal instability brought on by the onset of three-body heating and molecular line cooling would not be sufficient to cause the fragmentation of a collapsing gas cloud.

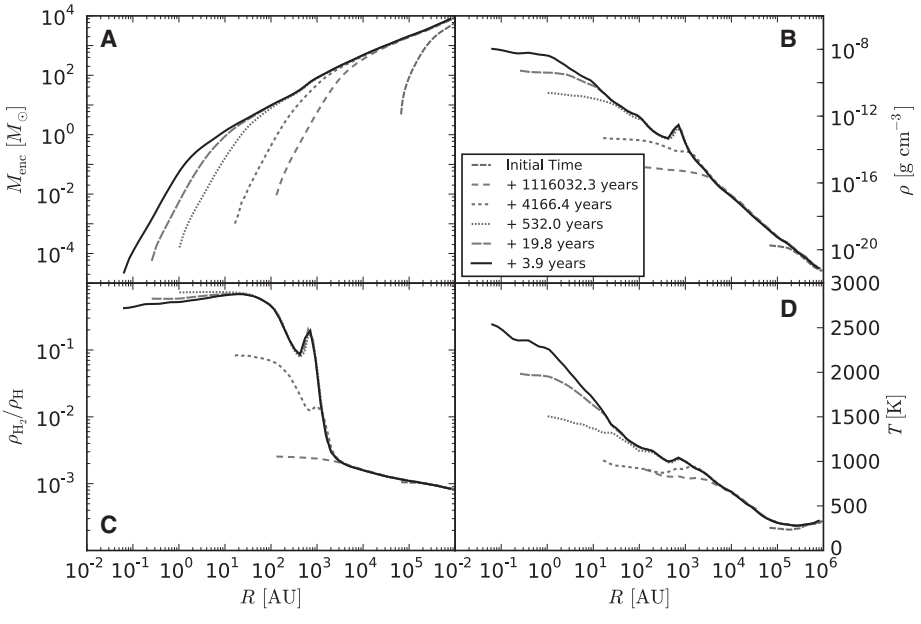

Fig. 3. Mass-weighted, spherically averaged quantities as a function of distance from the most dense point (which is located within core A after the cloud fragments) at different times in the simulation: mass-enclosed as a function of radius (**A**), density as a function of radius (**B**), molecular hydrogen mass fraction (**C**), and temperature (**D**).

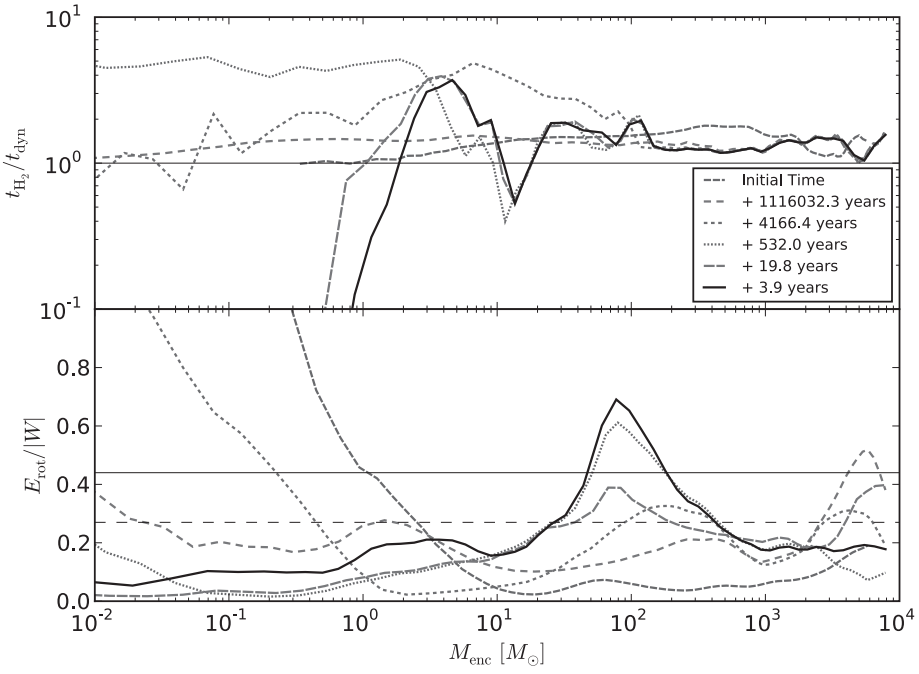

Fig. 4. Enclosed quantities as a function of mass enclosed, with respect to the most dense point (which is located within core A after the cloud fragments) and calculated in the rest frame of that point at different times in the simulation: the mass-weighted average ratio of the dynamical time of the gas divided by the cooling time of the molecular hydrogen, taking into account the heating from three-body formation processes (**top**) and rotational energy divided by gravitational binding energy (**bottom**). In the bottom graph, lines have been drawn to indicate ratios of 0.27 (thin dashed horizontal) and 0.44 (thin solid horizontal).

We define the rotational energy as

$$E_{\rm rot} \equiv \frac{1}{2}\omega \mathbf{I} \omega$$

where ω is the rotational velocity and **I** is the inertial tensor of the gas. For a sphere of radius r and mass M, the gravitational binding energy W is

$$W \equiv \frac{3}{5}\frac{GM^2}{r}$$

We compared these two quantities (Fig. 4, bottom) and indicated with thin lines the critical ratios of ~0.44 (*25*) and 0.27 (*26*) above which dynamical instabilities can become dominant in compressible toroids and compressible spheroids with a centrally concentrated mass. This ratio was at a maximum at an enclosed mass of about 100 $M_\odot$. The transition between instabilities identified above is within this radius. This halo fragments into multiple components because of the nesting of this marginal chemical instability within the radius of that of the rotational instability. However, more important is if an increase in this ratio is found exactly at the radii where the cloud has been identified as fragmenting. Although analytic estimates for the gravitational potential energy of a cloud vary by factors of order unity depending on the eccentricity and ellipticity of the cloud, the relative ratio traces the mass scales where fragmentation may occur.

The total number of first-generation Population III stars is likely to be substantially smaller than that of the second generation. Assuming no recombination, massive metal-free stars can ionize of order 10^7 $M_\odot$ of gas, which is between 100 to 1000 times the gas mass of a Population III star-forming halo (*27*), and thus will be outnumbered by a large factor by metal-free stars forming in preprocessed regions. Fragmentation in unprocessed, first-generation Population III stars thus indicates that fragmentation in preprocessed, second-generation Population III stars is also possible. This would ultimately be more important to structure formation and the star formation history of the universe and the chemical signature of metal-free stellar evolution in the fossil record of old stars in the Galaxy (*28*). By changing the size of the gas reservoirs from which the first-generation Population III protostars stars accrete, as well as the ultraviolet flux from the subsequent metal-free stars themselves, the long-term star formation environment for the next generation of Population III stars could be dramatically changed. A higher flux of ionizing photons could lead to more efficient cooling by molecular hydrogen in neighboring halos (*29*, *30*), but a lower metagalactic flux would likely lead to a higher global star formation rate and higher accretion rates (*31*).

We have shown that in a particular realization fragmentation occurs at relatively high densities. The separation and time scales are such that the two identified fragments are likely to form a binary stellar system. Improvements to chemical solvers at high densities and better laboratory values for the molecular hydrogen rate coefficients may change the details of the collapse, but these results demonstrate that fragmentation is possible in metal-free halos collapsing from realistic initial conditions. The frequency of such fragmentation, and thus that of metal-free binary systems, cannot be gauged by using the small number of simulations conducted thus far.

The problem of "finding" fragmentation in cosmological halos may be one of poor sampling; if fragmentation is rare, the small number of published calculations likely will not sample those halos in which it could occur. In particular, if fragmentation is more likely to occur in halos that undergo rapid merger history, the current means of ab initio simulation of Population III star formation may be ill equipped to study its likelihood and relevance. We have found fragmentation in one out of five realizations, suggesting that binaries are a formation channel that must be considered in population synthesis studies. From a set of only five realizations, an initial mass function cannot be estimated. However, we conclude by noting that the current means of conducting high-dynamic range simulations are biased against finding fragmentation in collapsing prestellar clouds. This simulation fragmented at a density of $\simeq 2.0 \times 10^{-13}$ g cm^{-3}, which corresponds to a dynamical time of 210 years; if the time delay between clump formation is greater than the approximate dynamical time, the current methods of simulating primordial star formation will not observe fragmentation. Consequently it is likely that a substantial fraction of Population III stars are forming binaries or event multiple systems.

References and Notes

1. T. Abel, G. L. Bryan, M. L. Norman, *Science* **295**, 93 (2002); published online 15 November 2001 (10.1126/science.1063991).
2. N. Yoshida, K. Omukai, L. Hernquist, *Science* **321**, 669 (2008).
3. V. Bromm, A. Loeb, *New Astron.* **9**, 353 (2004).
4. K. Omukai, F. Palla, *Astrophys. J.* **589**, 677 (2003).
5. C. F. McKee, J. C. Tan, *Astrophys. J.* **681**, 771 (2008).
6. K. Omukai, R. Nishi, *Astrophys. J.* **508**, 141 (1998).
7. E. Ripamonti, T. Abel, *Mon. Not. R. Astron. Soc.* **348**, 1019 (2004).
8. J. C. Tan, C. F. McKee, *Astrophys. J.* **603**, 383 (2004).
9. E. Ripamonti, T. Abel, *Mon. Not. R. Astron. Soc.* **348**, 1019 (2004).
10. S. Glover, in *First Stars III*, B. W. O'Shea, A. Heger, T. Abel, Eds. (American Institute of Physics Conference Series, American Institute of Physics, New York, 2008), vol. 990, pp. 25–29.
11. B. W. O'Shea, M. L. Norman, *Astrophys. J.* **654**, 66 (2007).
12. N. Yoshida, K. Omukai, L. Hernquist, T. Abel, *Astrophys. J.* **652**, 6 (2006).
13. M. J. Turk, T. Abel, B. W. O'Shea, in *First Stars III*, B. W. O'Shea, A. Heger, T. Abel, Eds. (American Institute of Physics Conference Series, American Institute of Physics, New York, 2008), vol. 990, pp. 16–20.
14. V. Bromm, P. S. Coppi, R. B. Larson, *Astrophys. J.* **564**, 23 (2002).
15. F. Nakamura, M. Umemura, *Astrophys. J.* **548**, 19 (2001).
16. K. Saigo, T. Matsumoto, M. Umemura, *Astrophys. J.* **615**, L65 (2004).

17. P. C. Clark, S. C. O. Glover, R. S. Klessen, *Astrophys. J.* **672**, 757 (2008).
18. M. N. Machida, K. Omukai, T. Matsumoto, S.-i. Inutsuka, *Astrophys. J.* **677**, 813 (2008).
19. V. Bromm, P. S. Coppi, R. B. Larson, *Astrophys. J.* **527**, L5 (1999).
20. B. W. O'Shea *et al*., in *Adaptive Mesh Refinement: Theory and Applications*, T. Plewa, T. Linde, G. Weirs, Eds. (Springer-Verlag, Berlin, 2004).
21. Detailed simulation parameters and methods are available as supporting material on *Science* Online.
22. N. Yoshida, T. Abel, L. Hernquist, N. Sugiyama, *Astrophys. J.* **592**, 645 (2003).
23. E. C. Ostriker, *Astrophys. J.* **513**, 252 (1999).
24. K. Omukai, Y. Yoshii, *Astrophys. J.* **599**, 746 (2003).
25. I. Hachisu, J. E. Tohline, Y. Eriguchi, *Astrophys. J. Suppl. Ser.* **66**, 315 (1988).
26. I. Hachisu, J. E. Tohline, Y. Eriguchi, *Astrophys. J.* **323**, 592 (1987).
27. T. Abel, J. H. Wise, G. L. Bryan, *Astrophys. J.* **659**, L87 (2007).
28. J. Tumlinson, *Astrophys. J.* **641**, 1 (2006).
29. B. W. O'Shea, T. Abel, D. Whalen, M. L. Norman, *Astrophys. J.* **628**, L5 (2005).
30. J. H. Wise, T. Abel, *Astrophys. J.* **685**, 40 (2008).
31. B. W. O'Shea, M. L. Norman, *Astrophys. J.* **673**, 14 (2008).
32. We thank V. Bromm, G. Bryan, A. Escala, S. Glover, C. McKee, J. Oishi, B. Smith, J. Tumlinson, and N. Yoshida for useful discussions. This work was partially supported by the U.S. Department of Energy (DOE) contract to Stanford Linear Accelerator Center no. DE-AC02-76SF00515, NASA Astrophysics Theory and Fundamental Physics grant NNX08AH26G, and NSF AST-0807312. B.W.O. and M.J.T. carried out this work in part under the auspices of the National Nuclear Security Administration of the DOE at Los Alamos National Laboratory (LANL) under contract no. DE-AC52-06NA25396. B.W.O. was partially supported by a LANL Director's Postdoctoral Fellowship (DOE LDRD grant 20051325PRD4).

Supporting Online Material
www.sciencemag.org/cgi/content/full/1173540/DC1
Materials and Methods
Table S1
References

13 March 2009; accepted 15 June 2009
Published online 9 July 2009;
10.1126/science.1173540
Include this information when citing this paper.

Water and the Oxidation State of Subduction Zone Magmas

Katherine A. Kelley[1]*† and Elizabeth Cottrell[2]*

Mantle oxygen fugacity exerts a primary control on mass exchange between Earth's surface and interior at subduction zones, but the major factors controlling mantle oxygen fugacity (such as volatiles and phase assemblages) and how tectonic cycles drive its secular evolution are still debated. We present integrated measurements of redox-sensitive ratios of oxidized iron to total iron ($Fe^{3+}/\Sigma Fe$), determined with Fe K-edge micro–x-ray absorption near-edge structure spectroscopy, and pre-eruptive magmatic H_2O contents of a global sampling of primitive undegassed basaltic glasses and melt inclusions covering a range of plate tectonic settings. Magmatic $Fe^{3+}/\Sigma Fe$ ratios increase toward subduction zones (at ridges, 0.13 to 0.17; at back arcs, 0.15 to 0.19; and at arcs, 0.18 to 0.32) and correlate linearly with H_2O content and element tracers of slab-derived fluids. These observations indicate a direct link between mass transfer from the subducted plate and oxidation of the mantle wedge.

Plate tectonics leads to a two-way geochemical exchange between Earth's interior and exterior. This process is driven by the formation of new oceanic crust by mantle melting at mid-ocean ridges, hydration and oxidative alteration of oceanic crust as it transits the seafloor, and the subsequent return of hydrated oxidized oceanic crust to the deep Earth at subduction zones (Fig. 1A) (*1*, *2*). How this exchange has affected the oxygen fugacity of the mantle spatially (*3*) and over time (*2*, *4*, *5*) remains unclear. Many lines of evidence point to oxidizing conditions in arc peridotites and magmas (*1*, *6*), but a quantitative link between oxidation state and the subduction process, although intuitive, has not been established. Here we provide coupled measurements of the redox-sensitive $Fe^{3+}/\Sigma Fe$ ratio and magmatic H_2O concentrations at the same spatial resolution in a global suite of undegassed basaltic glasses, in order to determine the current oxidation condition of the mantle as a function of tectonic regime.

The ratio of oxidized iron to total iron [$Fe^{3+}/\Sigma Fe = Fe^{3+}/(Fe^{3+} + Fe^{2+})$] in primary, mantle-derived basaltic melts reflects mantle oxygen fugacity, provided that magmas experience minimal modification as they ascend to the surface (*1*, *6*–*8*). Melts may, however, be oxidized by crustal assimilation, crystallization, or degassing during ascent (*3*, *8*, *9*). Interpretation of bulk measurements of $Fe^{3+}/\Sigma Fe$ ratios in lavas (for example, by wet chemistry or Mössbauer spectroscopy) can be complicated because many rock samples, even at small scales, are mixtures of crystals and glass that may not represent true magmatic liquids. Lavas erupted on land also extensively degas, which alters their primary $Fe^{3+}/\Sigma Fe$ ratios (*9*). Submarine pillow rim glasses and melt inclusions (Fig. 1), however, can preserve primitive, minimally degassed magmatic liquids (*10*, *11*).

We used synchrotron-based Fe K-edge micro–x-ray absorption near-edge structure (μ-XANES) spectroscopy to derive $Fe^{3+}/\Sigma Fe$ ratios from the valence-sensitive pre-edge feature corresponding to the $1s \rightarrow 3d$ electronic transition (*12*). The area-weighted average energy of the baseline-subtracted pre-edge feature (the centroid) shifts in energy as a function of Fe oxidation state in basaltic glass (*13*) (Fig. 2A). Natural basalt powders were equilibrated over 16 oxygen fugacities, between –3.5 and +4.5 log units relative to the quartz-fayalite-magnetite (QFM) buffer, to create a suite of calibration glasses of known $Fe^{3+}/\Sigma Fe$ ratios, independently determined by Mössbauer spectroscopy (*14*). Over this compositional range, neither H_2O content (*15*) nor basalt major or minor element concentrations (*14*) influence the relation between the energy of the area-weighted centroid and $Fe^{3+}/\Sigma Fe$. These reference glasses can be used to extract the $Fe^{3+}/\Sigma Fe$ ratio of basalts from multiple tectonic settings and with varying H_2O content, with a precision of ±0.0045, comparable to that determined by wet chemistry (*14*).

Our samples represent melts from a range of tectonic settings, including global submarine pillow-rim glasses from primitive [>6 weight percent (wt %) MgO] mid-ocean ridge basalts (MORBs) and Mariana Trough back-arc basin basalts (BABBs), as well as basaltic olivine-hosted melt inclusions from one MORB and a global suite of arc volcanoes (Fig. 1) (*12*). Based on μ-XANES spectral

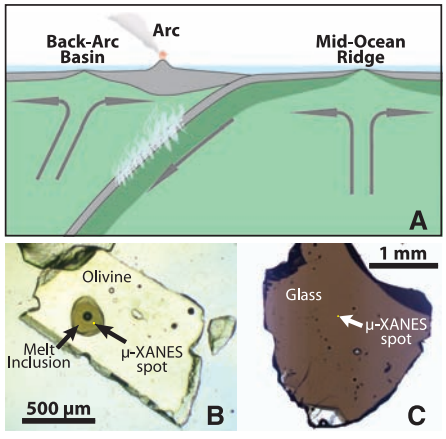

Fig. 1. (**A**) Cartoon showing plate tectonic settings of samples analyzed in this study. Mid-ocean ridges create oceanic crust through mantle upwelling. Hydrated and altered mid-ocean ridge crust is returned to the mantle by subduction, where H_2O released by metamorphic reactions enters the mantle sources of arc volcanoes and back-arc basins. (**B**) Photomicrograph of a double-polished, olivine-hosted arc melt inclusion (sample GUG-DB). The melt inclusion is originally glassy, free of daughter crystals, and contains a single vapor bubble caused by the contraction of the glass upon cooling. The size of the μ-XANES beam is shown for reference. (**C**) Photomicrograph of a wafered back-arc basin glass chip (sample ALV1839-21).

[1]Graduate School of Oceanography, University of Rhode Island, Narragansett, RI 02882, USA. [2]National Museum of Natural History, Smithsonian Institution, Washington, DC 20560, USA.

*These authors contributed equally to this work.
†To whom correspondence should be addressed. E-mail: kelley@gso.uri.edu

analysis, the $Fe^{3+}/\Sigma Fe$ ratio increases from the MORB (0.13 to 0.17) to BABB (0.15 to 0.19) to arc samples (0.18 to 0.32 (Fig. 2B and table S1), which is consistent with evidence that arc magmas are more oxidized than MORBs (*1*, *6*) and contrary to models based on V/Sc ratios (*3*).

Pre-eruptive magmatic concentrations of volatiles (such as H_2O) are also known to vary with tectonic setting, and specifically to increase at subduction zones (*10*, *11*). New measurements of the dissolved H_2O, CO_2, and S concentrations of basaltic glasses were also conducted, either by ion microprobe, following the methods of Hauri (*16*), or by Fourier transform infrared spectroscopy (FTIR) and electron microprobe, using the methods of Luhr (*10*), and were used in conjunction with previously published volatile data (*12*). These results show that magmatic H_2O content increases from MORBs (0.14 to 0.49 wt %) to BABBs (0.57 to 1.89 wt %) to arcs [2.23 to 5.39 wt %; except in one sample from an arc volcano that is known to be H_2O-poor (*17*)]. The oxidation state of Fe in the basaltic melts increases linearly with magmatic H_2O concentrations (Fig. 3). The high H_2O contents of subduction zone magmas have long been expected to relate to oxidized magmas and mantle sources (*1*, *6*, *18*), but these data provide a direct quantitative correlation between $Fe^{3+}/\Sigma Fe$ and water content in global basaltic melts. If the movement of volatiles from the subducted plate into the arc mantle can be linked to changes in Fe oxidation state, then the subduction process may play a central role in changing the mantle oxygen fugacity both across modern tectonic settings and throughout Earth history.

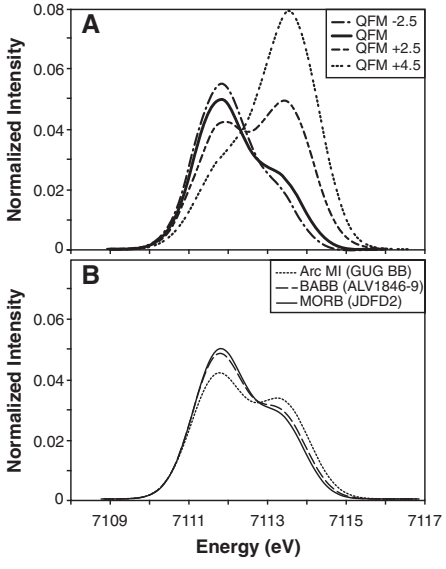

Fig. 2. Comparison of edge-step–normalized, baseline-subtracted, pre-edge μ-XANES spectra for basaltic glasses. The relative intensities of the two pre-edge peaks are diagnostic of the oxidation state of Fe in the glass. (**A**) Baseline-subtracted spectra for reference glasses of All-92-29-1 (*12*), equilibrated at QFM − 2.5 (dash-dot line), QFM (solid line), QFM + 2.5 (dash–double-dot line), and QFM + 4.5 (triple-dot line). (**B**) Baseline-subtracted spectra for natural samples, including a MORB glass (JDFD2, thin solid line), a BABB glass (ALV1846-9, thin dashed line), and an arc melt inclusion (GUG BB, thin dotted line).

Shallow magmatic processes could cause linear correlations between $Fe^{3+}/\Sigma Fe$ ratios and H_2O concentrations that are unrelated to the properties of the mantle source. Melt oxidation could occur through losses of some S species (such as H_2S) and H_2 driven by degassing or diffusion (*8*), but this would create an inverse relation between volatile content (such as H_2O) and $Fe^{3+}/\Sigma Fe$ ratio. We also excluded glasses showing evidence of H_2O degassing (low concentrations of earlier-degassing CO_2 or S). Small increases in $Fe^{3+}/\Sigma Fe$ ratios and H_2O contents are expected (and are observed within the MORB glasses) because Fe^{3+} and H_2O are incompatible in early-crystallizing olivine, whereas Fe^{2+} is compatible. The trajectories of both $Fe^{3+}/\Sigma Fe$ ratios and H_2O concentrations relative to MgO content, however, indicate that olivine fractional crystallization cannot explain the observed relation between Fe oxidation state and H_2O in BABBs and arc glasses. The melt inclusion samples could also have been modified by post-entrapment crystallization of olivine or diffusive loss of Fe^{2+}. Both of these processes can be detected, and the compositions can be corrected through analysis of melt compositions relative to their olivine hosts (*12*). In cases where Fe-Mg disequilibrium between a melt inclusion and its host olivine was evident, either equilibrium olivine or Fe^{2+} was added incrementally to each melt composition until equilibrium with the host olivine was achieved. On average, post-entrapment corrections resulted in <8% change in $Fe^{3+}/\Sigma Fe$ (table S2). Moreover, $Fe^{3+}/\Sigma Fe$ and H_2O measured on a MORB melt inclusion and the glass exterior to its olivine host directly overlap, suggesting that processes specific to melt inclusions are not the primary cause of the trend.

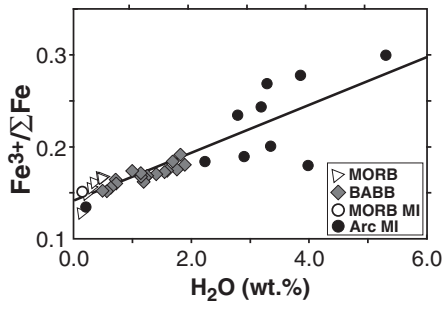

Fig. 3. Plot of measured H_2O concentrations versus $Fe^{3+}/\Sigma Fe$ determined by μ-XANES for MORB and BABB glasses, and olivine-hosted melt inclusions (MIs) from MORBs and global arc volcanoes. $Fe^{3+}/\Sigma Fe$ in MIs have been corrected for post-entrapment olivine crystallization or outward Fe^{2+} diffusion to place the melt compositions in equilibrium with the host olivine. Data for H_2O are published FTIR data from the literature or are FTIR or ion microprobe data from this study (*12*). Symbols exceed the size of the error bars in $Fe^{3+}/\Sigma Fe$ [±0.0045 (1σ)]. The solid line is a least-squares linear regression through all of the data, with equation $y = 0.026x + 0.14$ [correlation coefficient (r^2) = 0.72]. When only MORB and BABB data are used, linear regression gives $y = 0.018 + 0.14$ ($r^2 = 0.65$).

Rather than shallow or sample-specific processes, melt oxidation appears to be linked to the composition of the mantle source, an idea that is supported by trace element variations. For example, the ratio of Ba concentration (an element that is highly mobile in aqueous fluids) to La concentration (an element that is fluid-immobile) is a proxy for the influence of slab-derived fluid on the composition of the sub-arc mantle source. In the basalt samples from the Mariana arc and back-arc basin, Ba/La ratios of lavas (*12*) progressively increase with increasing $Fe^{3+}/\Sigma Fe$ ratios (Fig. 4 and table S3). Because the Ba/La ratio is minimally influenced by magmatic processes, it is considered a true reflection of the mantle source that gave rise to a given basalt. Covariation of the Ba/La ratio with $Fe^{3+}/\Sigma Fe$ thus suggests that oxidation is directly related to the addition of H_2O from the subducted slab.

The relation between H_2O, trace elements sensitive to slab additions, and Fe oxidation state requires that slab-derived fluids be directly linked to the oxidation process. The slope of the observed trend in $Fe^{3+}/\Sigma Fe$ ratio versus H_2O concentration indicates the magnitude of magmatic oxidation associated with the addition of fluids from the subducted plate. A simple linear regression of the global data yields a slope of 0.026 (that is, basalt $Fe^{3+}/\Sigma Fe$ increases on average by this amount with each weight % increase in magmatic H_2O). Arc melt inclusion data show more variation relative to the tightly correlated MORB and BABB glasses, which internally give a slope of 0.018. The scatter in the arc data probably reflects the geographical diversity of the arc samples, because each volcano samples a distinct combination of slab characteristics (such as plate age or sediment pile) and mantle inputs. Differing extents of fractional crystallization will also create small variations in both H_2O concentration and $Fe^{3+}/\Sigma Fe$ ratio, but we emphasize that such variability is minor relative to the observed trend.

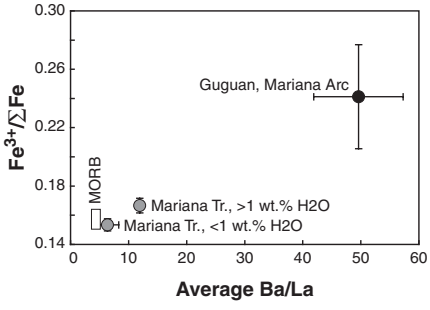

Fig. 4. Plot of average Ba/La ratio versus measured $Fe^{3+}/\Sigma Fe$ for MORBs, and subsets of BABB and arc basalts from the Mariana subduction zone. See supporting online material for sources of the Ba/La ranges for MORBs, the Guguan volcano, and the Mariana Trough. MORB and BABB glasses with 7.0 to 7.5 wt % MgO were used to average $Fe^{3+}/\Sigma Fe$.

Our data implicate the subduction process in the generation of magmas at higher oxygen fugacities than those of MORBs. If the mantle were equally reducing beneath ridges, back-arc basins, and arcs, then primitive undegassed basalts should have similar $Fe^{3+}/\Sigma Fe$ ratios in all three tectonic settings. At subduction zones, however, hydrated oxidized oceanic crust from Earth's surface is thrust into the mantle, where it contributes H_2O-rich fluids and/or melts, and its oxidized signature, to the mantle sources of arc volcanoes and back-arc spreading ridges (Fig. 1A). Indeed, undegassed BABBs and arc melts are systematically more oxidized than MORBs (Fig. 3). Differences between these tectonic regions may actually be underestimated, because H_2O acts to increase the extent of melting, leading to trace-element dilution at high melt fractions (*11*, *19*). If Fe^{3+} behaves strictly as an incompatible element, $Fe^{3+}/\Sigma Fe$ is expected to be higher in MORBs, where melt fractions are low, and to be lower in BABBs and arc basalts, where melt fractions are higher. On the other hand, H_2O may lower the activity coefficient of FeO during mantle melting, which could increase $Fe^{3+}/\Sigma Fe$ in hydrous mantle melts (*11*, *20*, *21*); however, experimental studies are not conclusive (*21*, *22*) and the effect of H_2O is likely to be minor relative to that of temperature (*21*).

Although H_2O concentrations and the oxidation state of Fe correlate linearly in these basalts, H_2O is not required to be the cause of oxidation. Water acts as an efficient oxidizing agent in many terrestrial environments, but not in Earth's upper mantle (*23*). For H_2O alone to play this role requires the efficient dissociation of H_2 from O^{2-}, followed by the efficient removal of H_2. Magmatic oxidation due to loss of H_2 may be responsible for oxidizing basalt pillow cores (*8*) at low pressure, but whether H_2O can dissociate to liberate H_2 in the mantle wedge remains controversial (*18*, *23*). The relation between Fe oxidation state and magmatic H_2O content at subduction zones may instead arise indirectly, as a consequence of the oxidized condition of the subducted oceanic lithosphere. Iron in marine sediments is highly oxidized [$Fe^{3+}/\Sigma Fe$ = ~82% (*2*)], and hydrothermal alteration of both basalt and peridotite results in a net oxidation of the oceanic lithosphere through the formation of Fe-oxyhydroxides and magnetite and the release of H_2 to the ocean (*2*, *24*). The subducting plate thus enters the mantle at intrinsically higher oxygen fugacity and clearly supplies the H_2O flux into the mantle wedge, but the associated transfer of the oxidized signature from the slab is poorly understood.

Dilute aqueous fluids are inefficient carriers of of Fe^{3+} (*25*), but as slab-derived components become more acidic, more saline, or more melt-like, Fe^{3+} may become highly mobile, as has been shown for other trivalent fluid-immobile elements (*26*, *27*). Transporting all of the Fe^{3+} that we observe in arc basalts in excess of MORBs directly from the slab into the mantle wedge would therefore require that slab-derived H_2O-rich components be hypersaline brines, supercritical fluids, or silicate melts of subducted sediments or the basaltic plate (*26*–*28*). Alternatively, fluid-mobile elements such as S could oxidize the mantle wedge of subduction zones without requiring direct transport of Fe^{3+}. If the intrinsic oxygen fugacity of fluids released from the descending slab is sufficiently high to carry S as sulfate (S^{6+}), then 1 mol of S has the potential to oxidize 8 mol of Fe^{2+} as sulfate in the fluid is reduced to form sulfide (S^{2-}) in the mantle. Sulfur reduction will take place provided that the oxygen fugacity of the mantle wedge remains below the sulfur-sulfur oxide buffer, or approximately QFM + 2 (*29*). From this perspective, if hydrous slab-derived components carry sufficient sulfate (*30*), direct addition of Fe^{3+} from the slab may not be required.

References and Notes

1. B. J. Wood, L. T. Bryndzia, K. E. Johnson, *Science* **248**, 337 (1990).
2. C. Lecuyer, Y. Ricard, *Earth Planet. Sci. Lett.* **165**, 197 (1999).
3. C.-T. A. Lee, W. P. Leeman, D. Canil, Z.-X. A. Li, *J. Petrol.* **46**, 2313 (2005).
4. D. Canil, *Earth Planet. Sci. Lett.* **195**, 75 (2002).
5. A. J. Berry, L. V. Danyushevsky, H. S. C. O'Neill, M. Newville, S. R. Sutton, *Nature* **455**, 960 (2008).
6. I. J. Parkinson, R. J. Arculus, *Chem. Geol.* **160**, 409 (1999).
7. V. C. Kress, I. S. E. Carmichael, *Contrib. Mineral. Petrol.* **108**, 82 (1991).
8. D. M. Christie, I. S. E. Carmichael, *Earth Planet. Sci. Lett.* **79**, 397 (1986).
9. M. Sato, T. L. Wright, *Science* **153**, 1103 (1966).
10. J. F. Luhr, *Contrib. Mineral. Petrol.* **142**, 261 (2001).
11. E. Stolper, S. Newman, *Earth Planet. Sci. Lett.* **121**, 293 (1994).
12. Materials and methods are available as supporting material on *Science* Online.
13. M. Wilke, G. M. Partzsch, R. Bernhardt, D. Lattard, *Chem. Geol.* **220**, 143 (2005).
14. E. Cottrell, K. A. Kelley, A. T. Lanzirotti, R. A. Fischer, *Chem. Geol.*, in press.
15. R. E. Botcharnikov, J. Koepke, F. Holtz, C. McCammon, M. Wilke, *Geochim. Cosmochim. Acta* **69**, 5071 (2005).
16. E. Hauri, *Chem. Geol.* **183**, 99 (2002).
17. T. W. Sisson, S. Bronto, *Nature* **391**, 883 (1998).
18. A. D. Brandon, D. S. Draper, *Geochim. Cosmochim. Acta* **62**, 333 (1998).
19. K. A. Kelley *et al.*, *J. Geophys. Res.* **111**, B09208 (2006).
20. I. Kushiro, *J. Petrol.* **13**, 311 (1972).
21. G. A. Gaetani, T. L. Grove, *Contrib. Mineral. Petrol.* **131**, 323 (1998).
22. K. Hirose, T. Kawamoto, *Earth Planet. Sci. Lett.* **133**, 463 (1995).
23. B. R. Frost, C. Ballhaus, *Geochim. Cosmochim. Acta* **62**, 329 (1998).
24. M. E. Berndt, D. E. Allen, W. E. Seyfried, *Geology* **24**, 351 (1996).
25. M. E. Schneider, D. H. Eggler, *Geochim. Cosmochim. Acta* **50**, 711 (1986).
26. M. C. Johnson, T. Plank, *Geochem. Geophys. Geosyst.* **1**, 10.1029/1999GC000014 (1999).
27. R. Kessel, M. W. Schmidt, P. Ulmer, T. Pettke, *Nature* **437**, 724 (2005).
28. C. E. Manning, *Earth Planet. Sci. Lett.* **223**, 1 (2004).
29. M. R. Carroll, M. J. Rutherford, *J. Petrol.* **28**, 781 (1987).
30. P. J. Wallace, *J. Volcanol. Geotherm. Res.* **140**, 217 (2005).

31. Thanks to R. Fischer and D. Kratzmann for beamline assistance and data processing; T. Gooding for sample preparation; A. Logan for electron microprobe assistance; D. Christie, T. Plank, L. Cooper, M. Zimmer, E. Hauri, M. Hirschmann, and C. Langmuir for samples, data, and discussion; and A. Lanzirotti for beamline method development. This work was supported by a Smithsonian Scholarly Studies Grant to E.C., a NSF ADVANCE fellowship to K.K., and NSF awards EAR-0841108 (K.K.) and EAR-0841006 (E.C.). NSF award OCE-0644625 provided curatorial support for marine geological samples at the University of Rhode Island. Beamline X26A is supported by the U.S. Department of Energy (DOE) Geosciences Division (grant DE-FG02-92ER14244 to the University of Chicago, Consortium for Advanced Radiation Sources). Use of the National Synchrotron Light Source was supported by DOE under contract no. DE-AC02-98CH10886.

Supporting Online Material

www.sciencemag.org/cgi/content/full/325/5940/605/DC1
Materials and Methods
Figs. S1 to S4
Tables S1 to S3
References

27 March 2009; accepted 10 June 2009
10.1126/science.1174156

The cAMP Sensor Epac2 Is a Direct Target of Antidiabetic Sulfonylurea Drugs

Chang-Liang Zhang,[1] Megumi Katoh,[1] Tadao Shibasaki,[1] Kohtaro Minami,[1] Yasuhiro Sunaga,[1]* Harumi Takahashi,[1] Norihide Yokoi,[1] Masahiro Iwasaki,[1] Takashi Miki,[1] Susumu Seino[1,2,3]†

Epac2, a guanine nucleotide exchange factor for the small guanosine triphosphatase Rap1, is activated by adenosine 3′,5′-monophosphate. Fluorescence resonance energy transfer and binding experiments revealed that sulfonylureas, widely used antidiabetic drugs, interact directly with Epac2. Sulfonylureas activated Rap1 specifically through Epac2. Sulfonylurea-stimulated insulin secretion was reduced both in vitro and in vivo in mice lacking Epac2, and the glucose-lowering effect of the sulfonylurea tolbutamide was decreased in these mice. Epac2 thus contributes to the effect of sulfonylureas to promote insulin secretion. Because Epac2 is also required for the action of incretins, gut hormones crucial for potentiating insulin secretion, it may be a promising target for antidiabetic drug development.

Epac is a guanine nucleotide exchange factor (GEF) for the Ras-like small guanosine triphosphatases Rap1 and Rap2 that is activated by the direct binding of adenosine 3′,5′-monophosphate (cAMP); two isoforms of Epac (also referred to as cAMP-GEF), Epac1 (cAMP-GEFI) and Epac2 (cAMP-GEFII), have been identified (*1*–*4*). Epac2 mediates the potentiation of

insulin secretion by cAMP in a protein kinase A (PKA)–independent pathway (*5*, *6*). Epac1 undergoes a conformational change upon cAMP binding, and partial and full-length Epac1 sandwiched between cyan fluorescent proteins (CFPs) and yellow fluorescent proteins (YFPs) act as fluorescence resonance energy transfer (FRET) sensors that monitor Epac1 activation in living cells (*7*–*9*). These sensors facilitate investigations of the mechanisms of cAMP signaling such as compartmentalization (*8*) and oscillation (*10*).

We generated a FRET sensor (termed C-Epac2-Y) using the full-length Epac2 (fig. S1A) (*11*, *12*). C-Epac2-Y was transiently expressed in simian kidney COS-1 cells, and we examined changes in FRET. Stimulation with 8-bromoadenosine 3′,5′-monophosphate (8-Br-cAMP), a cAMP analog, decreased FRET in C-Epac2-Y–expressing COS-1 cells (Fig. 1A and fig. S1B). In contrast, treatment of cells with 8-Br-cAMP did not alter FRET in COS-1 cells expressing mutant Epac2 (termed C-MtEpac2-Y), in which both cAMP-binding sites were disrupted (fig. S1, C and D) (*11*). These results show that cAMP induces a conformational change in Epac2, confirming that C-Epac2-Y functions as a sensor for monitoring Epac2 activation in living cells.

To search for agents that activate Epac2, we screened for effects of various insulin secretagogues on change in FRET in MIN6, mouse clonal pancreatic β cells, transfected with C-Epac2-Y. Tolbutamide (TLB) and glibenclamide (GLB), both of which are sulfonylureas used in treatment of diabetes, decreased FRET (Fig. 1B and fig. S1E). Because Epac2 was identified as a molecule interacting with the sulfonylurea receptor SUR1, a regulatory subunit of adenosine 5′-triphosphate (ATP)–sensitive K^+ (K_{ATP}) channels (*11*), we considered the possibility that TLB and GLB might have a secondary effect on FRET by affecting the interaction between exogenously introduced C-Epac2-Y and endogenously expressed SUR1 in the MIN6 cells. To clarify this, we examined the effect of these sulfonylureas on FRET in C-Epac2-Y–transfected COS-1 cells in which no endogenous SUR1 is expressed. Both TLB and GLB still decreased FRET (Fig. 1C), indicating that they might act directly on Epac2.

The possibility that sulfonylureas might decrease FRET by elevating intracellular cAMP levels was excluded (fig. S2). Other sulfonylureas, including acetohexamide, glipizide, and chlorpropamide, also decreased FRET to different degrees and with different kinetics (fig. S3A). However, neither nateglinide (NTG) nor repaglinide, glinide-derivatives lacking the sulfonylurea core structure that also stimulate insulin secretion by the closure of K_{ATP} channels through acting directly on SUR1 (*13*), affected FRET (fig. S3B). These results indicate that the core structure of sulfonylurea is required for binding to Epac2. The finding that gliclazide (GLC), a sulfonylurea that has a side chain on the urea group larger than that of other sulfonylureas (fig. S4), did not decrease FRET (Fig. 1C) suggests that the structure or size (or both) of the side chain on the urea group may determine capability of interaction between sulfonylureas and Epac2.

To test whether sulfonylureas bind to Epac2 directly, we performed binding experiments using radiolabeled GLB. GLB exhibited specific binding to the full-length Epac2 or SUR1 expressed in COS-1 cells (Fig. 2A). Binding of [^{3}H]glibenclamide

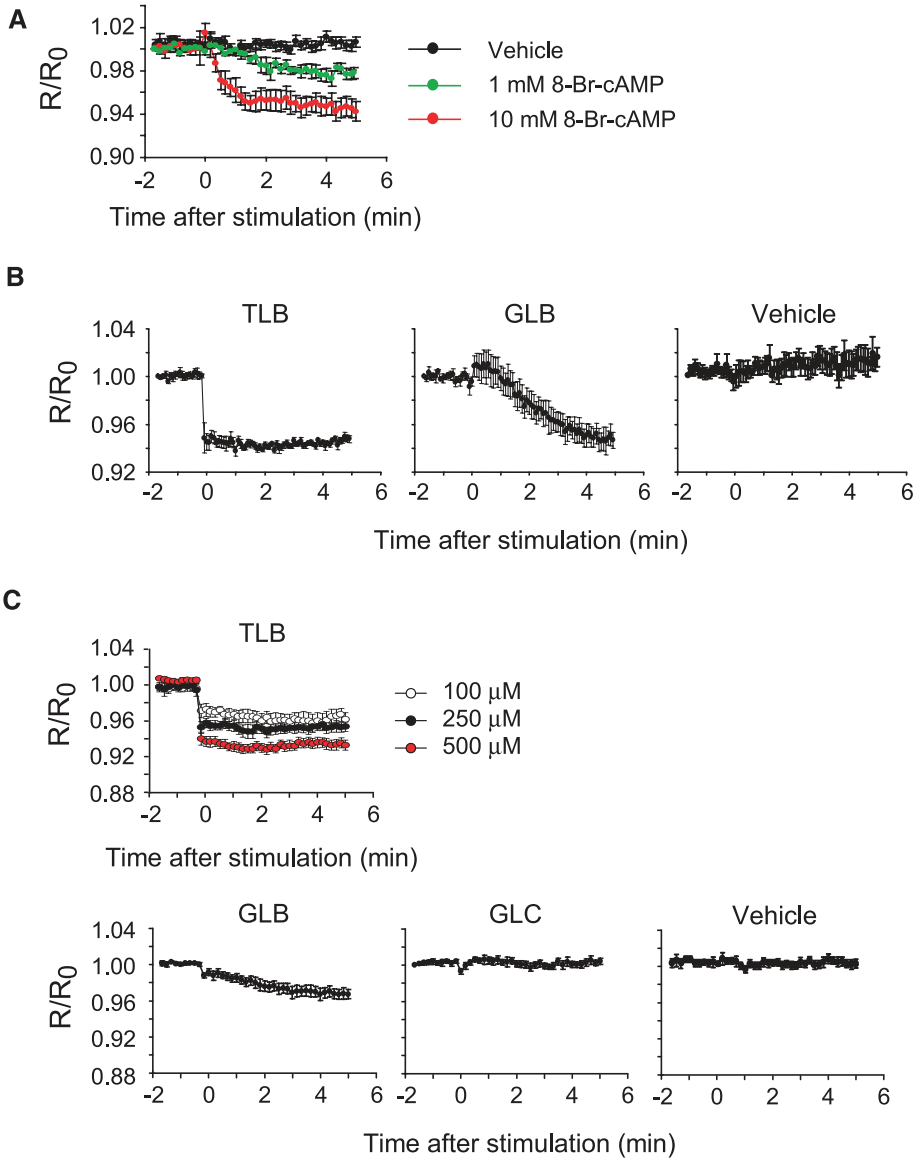

Fig. 1. Sulfonylureas induce changes in FRET in C-Epac2-Y. (**A**) Emission ratio time courses of C-Epac2-Y treated with 8-Br-cAMP or vehicle [dimethyl sulfoxide (DMSO)] in COS-1 cells. (**B**) Emission ratio time courses of C-Epac2-Y treated with 500 μM TLB, 100 nM GLB, or vehicle (DMSO) in MIN6 cells. (**C**) Emission ratio time courses of C-Epac2-Y treated with TLB (100 μM, 250 μM, or 500 μM), 100 nM GLB, 100 nM GLC, or vehicle (DMSO) in COS-1 cells. The YFP/CFP ratio (R) was normalized to R_0 to describe FRET efficiency changes (FRET change = R/R_0), where R_0 is the YFP/CFP ratio at time 0. FRET change was acquired every 5 s. Similar results were obtained in three independent experiments. Data are presented as mean ± SEM (n = 4 to 6 replications per experiment for each point).

[1]Division of Cellular and Molecular Medicine, Department of Physiology and Cell Biology, Kobe University Graduate School of Medicine, 7-5-1 Kusunoki-cho, Chuo-ku, Kobe 650-0017, Japan. [2]Division of Diabetes, Metabolism, and Endocrinology, Department of Internal Medicine, Kobe University Graduate School of Medicine, 7-5-1 Kusunoki-cho, Chuo-ku, Kobe 650-0017, Japan. [3]Core Research for Evolutional Science and Technology (CREST), Japan Science and Technology Agency, 4-1-8, Hon-cho, Kawaguchi, Saitama 332-0012, Japan.

*Present address: Cell Scale Team, Integrated Simulation of Living Matter Group, Computational Science Research Program, RIKEN, 2-1 Hirosawa, Wako-shi, Saitama 351-0198, Japan.

†To whom correspondence should be addressed. E-mail: seino@med.kobe-u.ac.jp

to Epac2 was inhibited by unlabeled TLB or unlabeled GLB in a concentration-dependent manner (Fig. 2B), indicating that TLB probably binds specifically to Epac2 at the same binding site as GLB. The median inhibitory concentration (IC_{50}) values of GLB and TLB for binding Epac2 were 25 nM and 240 μM, respectively, indicating lower affinities for binding Epac2 than for SUR1 (IC_{50} of GLB was 7.1 nM and of TLB was 140 μM) (*14*). Specific binding of GLB to Epac2 was not significantly inhibited in the presence of 8-Br-cAMP (Fig. 2B), suggesting that the sulfonylurea-binding site may be distinct from the cAMP-binding sites.

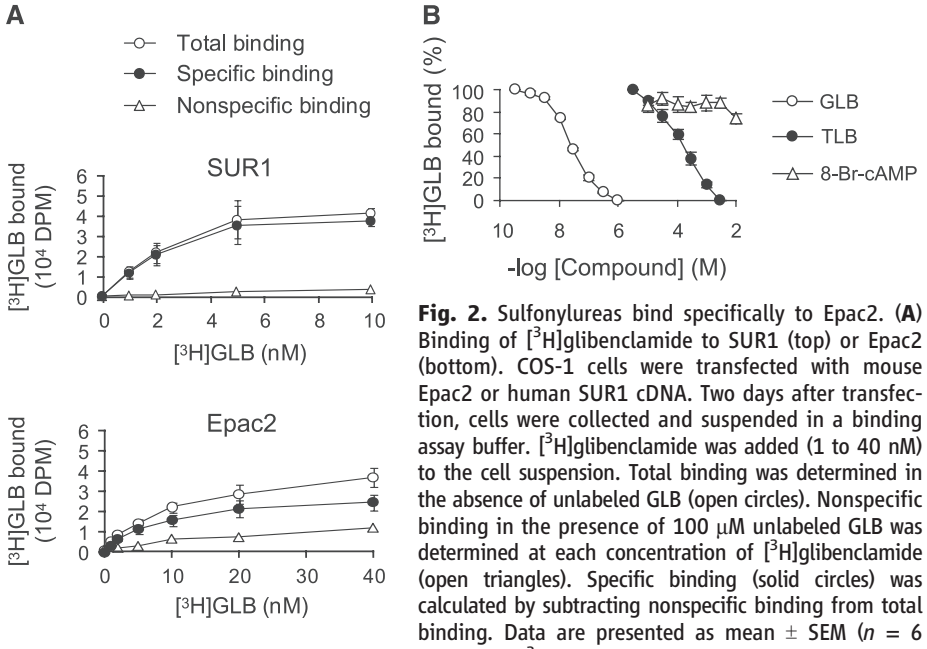

Fig. 2. Sulfonylureas bind specifically to Epac2. (**A**) Binding of [^{3}H]glibenclamide to SUR1 (top) or Epac2 (bottom). COS-1 cells were transfected with mouse Epac2 or human SUR1 cDNA. Two days after transfection, cells were collected and suspended in a binding assay buffer. [^{3}H]glibenclamide was added (1 to 40 nM) to the cell suspension. Total binding was determined in the absence of unlabeled GLB (open circles). Nonspecific binding in the presence of 100 μM unlabeled GLB was determined at each concentration of [^{3}H]glibenclamide (open triangles). Specific binding (solid circles) was calculated by subtracting nonspecific binding from total binding. Data are presented as mean ± SEM (n = 6 experiments for each point). (**B**) Displacement curves of [^{3}H]glibenclamide (10 nM) binding to Epac2 by unlabeled GLB, TLB, and 8-Br-cAMP. Data are presented as mean ± SEM (n = 3 experiments for each point).

Because Epac2 shows GEF activity toward Rap1 (*4*), we tested for possible sulfonylurea-induced activation of endogenous Rap1 in MIN6 cells. TLB activated Rap1 (Fig. 3A). The other sulfonylureas that decreased FRET all activated Rap1 significantly (fig. S5). GLB elicited activation at lower concentrations (10 to 100 nM) but not at higher concentrations (>200 nM). GLC, which did not decrease FRET, also had no effect on Rap1 activity. To determine whether activation of Rap1 by sulfonylureas is mediated through Epac2, we used *Epac2*-deficient, mouse clonal pancreatic β cells (*15*). No activation of Rap1 by either TLB or GLB was found in the *Epac2*-deficient cells, but activation of Rap1 by these sulfonylureas was detected after the adenoviral expression of wild-type (WT) Epac2 (Fig. 3B). Similar results were obtained with chlorpropamide, acetohexamide, and glipizide (fig. S6). NTG did not activate Rap1 even after the introduction of WT Epac2 into the *Epac2*-deficient cells (Fig. 3B). These results support the conclusion that sulfonylureas activate Rap1 at least in part through Epac2.

We investigated the role of Epac2 in stimulation of insulin secretion by sulfonylurea. Neither glucose- nor potassium-stimulated insulin secretion was different in pancreatic islets isolated from *Epac2*$^{-/-}$ mice and those from WT C57BL/6 mice (Fig. 4A). In contrast, both TLB-stimulated and GLB-stimulated insulin secretion from the pancreatic islets of *Epac2*$^{-/-}$ mice were significantly reduced as compared with those from the islets of control animals (Fig. 4, B and

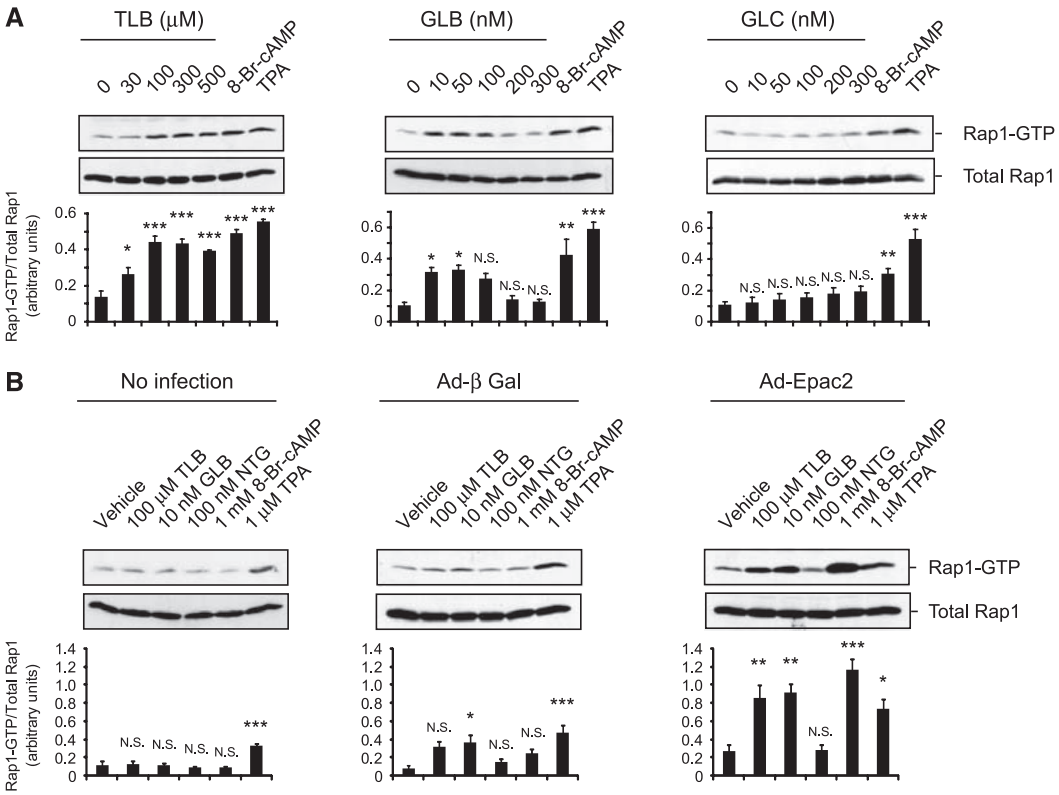

Fig. 3. Sulfonylureas activate Rap1 specifically through Epac2 in insulin-secreting cells. (**A**) Activation of Rap1 in MIN6 cells treated with TLB, GLB, or GLC. 8-Br-cAMP (1 mM) and 12-*O*-tetradecanoylphorbol-13-acetate (TPA) (1 μM) were used as positive controls. (**B**) Changes in activation of Rap1 by sulfonylureas through the introduction of Epac2 into *Epac2*-deficient mouse clonal β cells by means of adenovirus-based gene transfer. A representative blot for each experiment is shown. Similar results were obtained from three to seven independent experiments. Quantification of autoradiography is shown with corresponding bars positioned under the bands. The intensity of the Rap1-GTP signal was normalized by that of total Rap1. Data are presented as mean ± SEM (n = 3 to 7 experiments for each point). Dunnett's method was used for multiple comparisons with a control group (vehicle was DMSO). *P < 0.05; **P < 0.01; ***P < 0.001. N.S., not significant.

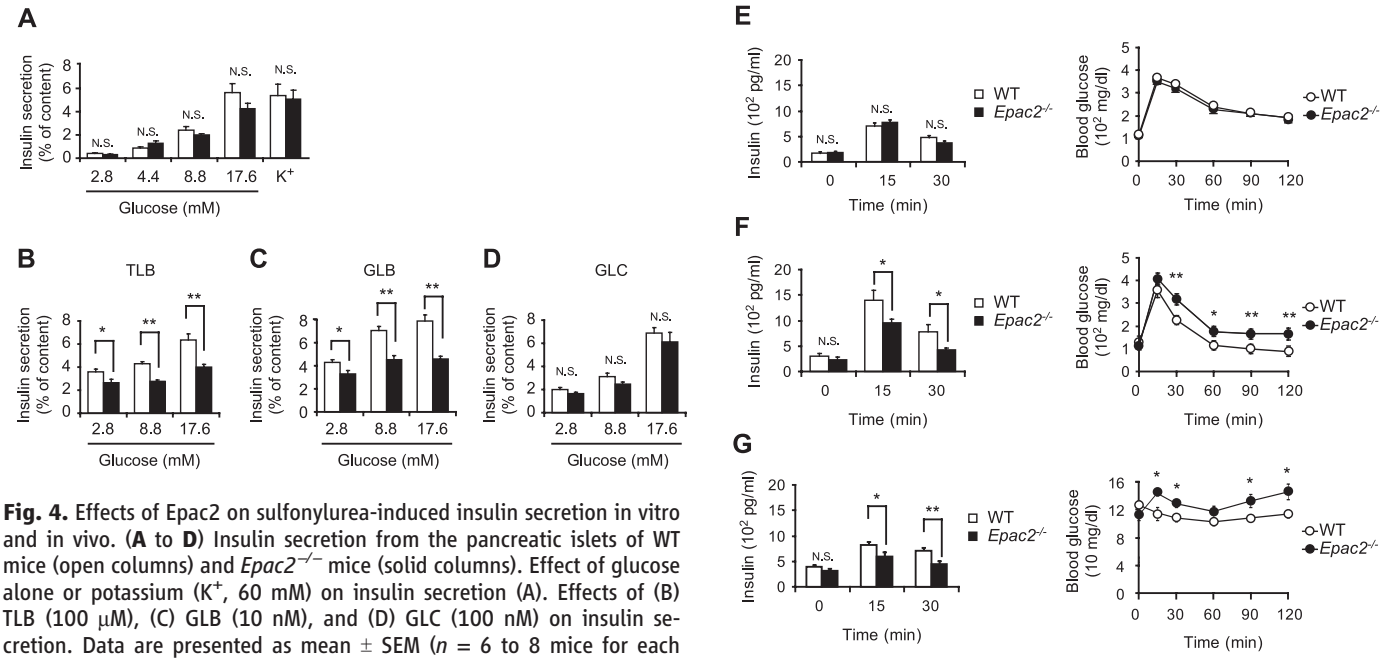

Fig. 4. Effects of Epac2 on sulfonylurea-induced insulin secretion in vitro and in vivo. (**A** to **D**) Insulin secretion from the pancreatic islets of WT mice (open columns) and *Epac2*$^{-/-}$ mice (solid columns). Effect of glucose alone or potassium (K^+, 60 mM) on insulin secretion (A). Effects of (B) TLB (100 μM), (C) GLB (10 nM), and (D) GLC (100 nM) on insulin secretion. Data are presented as mean ± SEM (n = 6 to 8 mice for each point). (**E** to **G**) Serum insulin and blood glucose responses to oral administration of glucose alone (E), concomitant administration of glucose and TLB (F), or TLB alone (G). Data are presented as mean ± SEM (n = 6 mice for each point). Unpaired student's t test was used for evaluation of statistical significance. *P < 0.05; **P < 0.01. Blood glucose level in WT mice decreased significantly 60 min after administration of TLB (0 versus 60 min, P = 0.019, paired t *test*), whereas that in *Epac2*$^{-/-}$ mice (G) did not (P = 0.36, paired t test).

C). Consistent with the findings of FRET response and Rap1 activity, there was no significant difference in insulin secretion in response to GLC (Fig. 4D). To clarify the role of Epac2 in modulating responses to sulfonylurea in vivo, we examined the effects of TLB on serum insulin and blood glucose in animals responding to oral intake of glucose. There were no significant differences in either serum insulin or blood glucose responses to the administration of glucose alone between *Epac2*$^{-/-}$ mice and WT mice (Fig. 4E). In contrast, the insulin response to concomitant administration of glucose and TLB in *Epac2*$^{-/-}$ mice was significantly reduced as compared with that in WT mice (Fig. 4F). In addition, the blood glucose levels after concomitant administration of glucose and TLB in *Epac2*$^{-/-}$ mice were significantly higher than those in WT mice (Fig. 4F). Furthermore, the glucose-lowering effect of TLB was not seen in *Epac2*$^{-/-}$ mice, and the insulin response to TLB was significantly reduced as compared with that in WT mice (Fig. 4G). These results show that the effects of Epac2 on responses to sulfonylurea operate in vivo.

Sulfonylureas stimulate insulin secretion by closing pancreatic β cell K_{ATP} channels through binding to SUR1 (*16*, *17*). Studies of mice lacking the inward rectifier K^+ channel member Kir6.2, the pore-forming subunit of K_{ATP} channels, and mice lacking SUR1 have shown that closure of the K_{ATP} channels is prerequisite for sulfonylureas to stimulate insulin secretion (*18*–*20*). Although sulfonylurea has also been suggested to act through an intracellular target (*21*–*26*), the target has not been identified. We identified Epac2 as a direct intracellular target of sulfonylureas. Considered together, in addition to closure of K_{ATP} channels, activation of Epac2 is required for sulfonylureas to exert their full effects on insulin secretion (fig. S7). Epac2 has also been implicated in the stimulation of insulin secretion through mechanisms not involving Rap1, such as the modulation of K_{ATP} channel activity (*27*). Because Epac2 also mediates the potentiation of insulin secretion by cAMP-increasing agents such as glucagon-like peptide 1 (*28*), analogs of which have been developed recently as new hypoglycemic agents (*29*), Epac2 may be a promising target for the development of drugs to treat diabetes.

References and Notes

1. J. de Rooij *et al.*, *Nature* **396**, 474 (1998).
2. H. Kawasaki *et al.*, *Science* **282**, 2275 (1998).
3. J. de Rooij *et al.*, *J. Biol. Chem.* **275**, 20829 (2000).
4. J. L. Bos, *Nat. Rev. Mol. Cell Biol.* **4**, 733 (2003).
5. E. Renstrom, L. Eliasson, P. Rorsman, *J. Physiol.* **502**, 105 (1997).
6. G. G. Holz, *Diabetes* **53**, 5 (2004).
7. V. O. Nikolaev, M. Bunemann, L. Hein, A. Hannawacker, M. J. Lohse, *J. Biol. Chem.* **279**, 37215 (2004).
8. L. M. DiPilato, X. Cheng, J. Zhang, *Proc. Natl. Acad. Sci. U.S.A.* **101**, 16513 (2004).
9. B. Ponsioen *et al.*, *EMBO Rep.* **5**, 1176 (2004).
10. L. R. Landa Jr. *et al.*, *J. Biol. Chem.* **280**, 31294 (2005).
11. N. Ozaki *et al.*, *Nat. Cell Biol.* **2**, 805 (2000).
12. Materials and methods are available as supporting material on *Science* Online.
13. P. Proks, F. Reimann, N. Green, F. Gribble, F. Ashcroft, *Diabetes* **51**, S368 (2002).
14. Y. Sunaga *et al.*, *Eur. J. Pharmacol.* **431**, 119 (2001).
15. T. Shibasaki *et al.*, *Proc. Natl. Acad. Sci. U.S.A.* **104**, 19333 (2007).
16. S. Seino, *Annu. Rev. Physiol.* **61**, 337 (1999).
17. J. C. Henquin, *Diabetes* **49**, 1751 (2000).
18. T. Miki *et al.*, *Proc. Natl. Acad. Sci. U.S.A.* **95**, 10402 (1998).
19. C. Shiota *et al.*, *J. Biol. Chem.* **277**, 37176 (2002).
20. V. Seghers, M. Nakazaki, F. DeMayo, L. Aguilar-Bryan, J. Bryan, *J. Biol. Chem.* **275**, 9270 (2000).
21. P. R. Flatt, O. Shibier, J. Szecowka, P. O. Berggren, *Diabete Metab.* **20**, 157 (1994).
22. S. E. Ozanne, P. C. Guest, J. C. Hutton, C. N. Hales, *Diabetologia* **38**, 277 (1995).
23. L. Eliasson *et al.*, *Science* **271**, 813 (1996).
24. X. Geng *et al.*, *Am. J. Physiol. Endocrinol. Metab.* **293**, E293 (2007).
25. L. Eliasson *et al.*, *J. Gen. Physiol.* **121**, 181 (2003).
26. X. Geng, L. Li, S. Watkins, P. D. Robbins, P. Drain, *Diabetes* **52**, 767 (2003).
27. G. Kang *et al.*, *J. Physiol.* **573**, 595 (2006).
28. Y. Kashima *et al.*, *J. Biol. Chem.* **276**, 46046 (2001).
29. D. J. Drucker, M. A. Nauck, *Lancet* **368**, 1696 (2006).

30. We thank L. H. Philipson for critical reading of the manuscript; T. Kataoka for RalGDS-RID cDNA; M. Matsuda, S. Nakajima, and H. Hiroaki for helpful advice; A. Tamamoto and Y. Takahashi for technical assistance; and G. K. Honkawa for assistance with the manuscript. This work was supported by a CREST grant from the Japan Science and Technology Agency and Grant-in-Aid for Scientific Research and by a grant for the Global Centers of Excellence Program "Global Center of Excellence for Education and Research on Signal Transduction Medicine in the Coming Generation" from the Ministry of Education, Culture, Sports, Science and Technology.

Supporting Online Material

www.sciencemag.org/cgi/content/full/325/5940/607/DC1
Materials and Methods
Figs. S1 to S7
References

13 February 2009; accepted 19 June 2009
10.1126/science.1172256

Flexible Learning of Multiple Speech Structures in Bilingual Infants

Ágnes Melinda Kovács* and Jacques Mehler

Children acquire their native language according to a well-defined time frame. Surprisingly, although children raised in bilingual environments have to learn roughly twice as much about language as their monolingual peers, the speed of acquisition is comparable in monolinguals and bilinguals. Here, we show that preverbal 12-month-old bilingual infants have become more flexible at learning speech structures than monolinguals. When given the opportunity to simultaneously learn two different regularities, bilingual infants learned both, whereas monolinguals learned only one of them. Hence, bilinguals may acquire two languages in the time in which monolinguals acquire one because they quickly become more flexible learners.

Although the remarkable performance of children acquiring one language is impressive, many children acquire more than one language simultaneously. As bilingual children presumably have to learn roughly twice as much as their monolingual peers (because they learn two languages instead of one), one would expect their language acquisition to be somewhat delayed. However, bilinguals pass the language development milestones at the same ages as their monolingual peers (*1*). For instance, infants produce their first words around 1 year of age and produce 50 words around 18 months, irrespective of whether they learn one language or two (*2*).

How do bilingual children succeed in acquiring two languages as fast as monolinguals learn one? An indication of how bilinguals may accomplish this feat comes from other cognitive domains, where increased experience in a domain leads to more efficient processing, such as chess masters who are better at memorizing chess configurations than novices.

Possibly, bilingual children efficiently acquire two languages because of their greater experience in learning from a mixed input. In fact, bilinguals have to learn a distinct set of properties for each of the languages from a multilanguage input, while avoiding interference between the two languages. Thus, they might recruit specific mechanisms that help them to simultaneously extract patterns from two languages even before they start speaking. If so, bilingual infants might show specific enhancements in dealing with multiple regularities in linguistic stimuli early on.

In an eye-tracking study, we explored whether 12-month-old bilingual infants are better at simultaneously learning multiple speech structures than monolinguals. In each trial, infants listened to a trisyllabic speech item while watching a central attention-getter stimulus. Following this, an attractive toy appeared on the left or the right side of the screen (Fig. 1A). The speech item's structure predicted the location of the toy. For example, if the speech item conformed to an ABA structure (where the first and the last syllables were identical), the toy appeared on the right side of the screen, whereas it appeared on the left side if the structure was AAB (experiment 1).

If infants have difficulties learning two structures simultaneously, they might still learn the structure they find easier to process [that is, AAB (*3*), although studies have suggested that infants can learn either structure when exposed to just one of them (*4*)]. Our crucial prediction, however, is that 12-month-old bilinguals are already flexible enough in dealing with multiple speech structures to learn two structures simultaneously.

Infants were first exposed to 36 AAB and ABA familiarization trials in pseudo-random order. Then, they were tested in eight trials with novel items. In these test trials, the toy did not appear after the speech item (*5*). To assess whether infants learned the structures, we measured where they looked after hearing a new item. During the test phase, infants can predict where the toy should appear only if they learn that the structures determine its location. Thus, for looking to the correct side, infants had to extract and generalize the two structures and to link each structure to one of the locations. Our principal measure to assess learning was infants' first look after hearing the new speech item. If they learned the structures, they should first search for the toy where it used to appear for that specific structure. Difference scores [(number of correct looks – number of incorrect looks)/

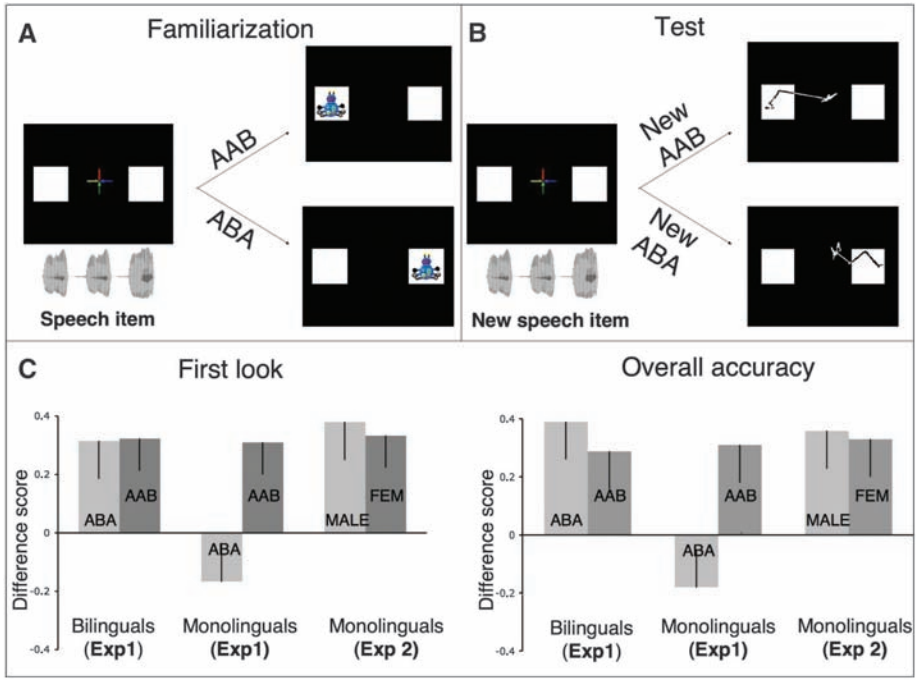

Fig. 1. (**A**) Familiarization phase of experiment 1. Infants listened to trisyllabic speech items where either the first two syllables were identical (i.e., an AAB structure, as in "lo-lo-vu") or the first and last syllables were identical (i.e., an ABA structure, as in "lo-vu-lo"). Speech items were followed by a toy appearing in one of two white squares that were displayed continuously on the screen. The location of the toy was predicted by the item's structure (e.g., left square for AAB, and right square for ABA). (**B**) Test phase of experiment 1. Infants were presented with new AAB and ABA items, but no toy followed the speech items. We used an eye-tracker to measure where the infants expected the toy to appear. On the right, two scan paths of an infant are depicted on two trials. (**C**) Measures of learning for the two structures or the two voice cues. Left: Difference scores for first looks [(number of correct looks – number of incorrect looks)/(number of correct looks + number of incorrect looks)] related to the chance level of 0 for ABA and AAB structures (experiment 1: bilinguals, $N = 22$; monolinguals, $N = 22$); and for male and female voices (experiment 2: monolinguals, $N = 20$). Right: Difference scores for overall accuracy for bilinguals and monolinguals in experiment 1 and for monolinguals in experiment 2. Error bars represent SE.

Scuola Internazionale Superiore di Studi Avanzati–SISSA, Via Beirut 4, 34014 Trieste, Italy.

*To whom correspondence should be addressed. E-mail: agneskovacs@mtapi.hu

(number of correct looks + number of incorrect looks)] were calculated for each structure and tested against a chance level of 0, as well as compared across groups and conditions. Second, we measured the infants' overall accuracy (*6*). That is, trials were scored as correct if the infant looked longer to the correct side within the 2 s after hearing a new item and before the start of the next trial. Difference scores were calculated for each structure as described above.

Bilinguals looked more often to the correct side for both structures during the test trials as shown by the first look analysis [AAB: $t(21) = 2.24$, $P = 0.03$; ABA: $t(21) = 3.76$, $P = 0.001$; Fig. 1C, left] and by the overall accuracy analysis [AAB: $t(21) = 2.14$, $P = 0.04$; ABA: $t(21) = 2.75$, $P = 0.01$; Fig. 1C, right]. Monolinguals, by contrast, looked more often to the correct side when the speech items had the structure AAB, but not when they had the structure ABA, as shown by the first look analysis [AAB: $t(21) = 2.37$, $P = 0.03$; ABA: $t(21) = -1.48$, $P = 0.15$] and by the overall accuracy analysis [AAB: $t(21) = 2.15$, $P = 0.04$; ABA: $t(21) = -1.43$, $P = 0.16$].

The overall analysis of variance with the factors Group (monolingual/bilingual) and Condition (AAB/ABA) on difference scores for first looks yielded a main effect of Group [$F(1,42) = 4.61$, $P = 0.03$] and, crucially, a Group × Condition interaction [$F(1,42) = 5.44$, $P = 0.02$]. Post hoc tests show that monolinguals' performance for the ABA structure was worse than for the AAB structure (Bonferroni $P = 0.03$) and worse than the bilinguals' performance for the ABA structure (Bonferroni $P = 0.02$).

To exclude the possibility that bilinguals' advantage reflects just a better learning of contingencies between sounds and locations, rather than their ability to learn multiple structural regularities, we ran an additional experiment involving only monolingual infants. In experiment 2, a new group of 12-month-old monolinguals heard speech items that differed not only in their structure but also in their pitch (e.g., female voice for ABA and male voice for AAB). Infants successfully learned to predict the toy locations based on the voices as shown by the first look analysis [female voice: $t(19) = 2.60$, $P = 0.01$; male voice: $t(19) = 2.94$, $P = 0.008$; Fig. 1C] and the overall accuracy analysis [female voice: $t(19) = 2.24$, $P = 0.03$; male voice: $t(19) = 2.59$, $P = 0.01$, Fig. 1C]. Together, the results of these experiments show that, in contrast to bilinguals, monolingual infants cannot learn two structures, although they can associate two speakers with different locations.

Twelve-month-old preverbal bilingual infants thus seem to be more flexible learners of multiple structural regularities than monolinguals. This flexibility might be related to different (mutually compatible) processes. Bilinguals might be better at learning two structures simultaneously. Alternatively, they might be better at avoiding interference between the two structures and quickly learn one of the structures and the corresponding toy location. This might even help them to learn the other structure and location. Although there is no evidence that such "reasoning by exclusion" is available to infants at this age, such ability might help infants to bootstrap new regularities from regularities they have already learned.

The advantage of bilinguals may be related to the precocious development of control and selection abilities, which has been documented in bilingual children (*7*) and infants (*8*). These abilities may allow bilinguals to take advantage of sources of information unavailable in monolingual settings and to become better at simultaneously monitoring different structural regularities. This in turn may help them to learn more efficiently each of their languages. Such powerful learning abilities allow bilinguals to pass the linguistic milestones at the same rate as monolinguals.

References and Notes

1. J. F. Werker, K. Byers-Heinlein, *Trends Cogn. Sci.* **12**, 144 (2008).
2. B. Z. Pearson, S. C. Fernandez, D. K. Oller, *Lang. Learn.* **43**, 93 (1993).
3. J. Gervain, F. Macagno, S. Cogoi, M. Peña, J. Mehler, *Proc. Natl. Acad. Sci. U.S.A.* **105**, 14222 (2008).
4. G. F. Marcus, S. Vijayan, S. Bandi Rao, P. M. Vishton, *Science* **283**, 77 (1999).
5. Materials and methods are available as supporting material on *Science* Online.
6. B. McMurray, R. N. Aslin, *Infancy* **6**, 203 (2004).
7. E. Bialystok, *Child Dev.* **70**, 636 (1999).
8. A. M. Kovács, J. Mehler, *Proc. Natl. Acad. Sci. U.S.A.* **106**, 6556 (2009).

9. We thank the parents and infants who participated in the study as well as A. D. Endress, G. Csibra, E. Téglás, and L. Bonatti for comments. We also thank the anonymous reviewers for helpful suggestions. This work was supported by the NEST PATHFINDER initiative "What it means to be human" (CALACEI), J. S. McDonnell Foundation, and Marie Curie 035975 DISCOS grants. Á.M.K. is currently at the Hungarian Academy of Sciences and at the Central European University, Budapest, Hungary.

Supporting Online Material
www.sciencemag.org/cgi/content/full/1173947/DC1
Materials and Methods

23 March 2009; accepted 19 June 2009
Published online 9 July 2009;
10.1126/science.1173947
Include this information when citing this paper.

Identification of Splenic Reservoir Monocytes and Their Deployment to Inflammatory Sites

Filip K. Swirski,[1]*† Matthias Nahrendorf,[1]* Martin Etzrodt,[1,2] Moritz Wildgruber,[1] Virna Cortez-Retamozo,[1] Peter Panizzi,[1] Jose-Luiz Figueiredo,[1] Rainer H. Kohler,[1] Aleksey Chudnovskiy,[1] Peter Waterman,[1] Elena Aikawa,[1] Thorsten R. Mempel,[1,3] Peter Libby,[4,5] Ralph Weissleder,[1,6]† Mikael J. Pittet[1]†

A current paradigm states that monocytes circulate freely and patrol blood vessels but differentiate irreversibly into dendritic cells (DCs) or macrophages upon tissue entry. Here we show that bona fide undifferentiated monocytes reside in the spleen and outnumber their equivalents in circulation. The reservoir monocytes assemble in clusters in the cords of the subcapsular red pulp and are distinct from macrophages and DCs. In response to ischemic myocardial injury, splenic monocytes increase their motility, exit the spleen en masse, accumulate in injured tissue, and participate in wound healing. These observations uncover a role for the spleen as a site for storage and rapid deployment of monocytes and identify splenic monocytes as a resource that the body exploits to regulate inflammation.

Protection of injured or infected tissue involves migratory leukocytes (*1*–*3*). Among them are blood monocytes, which consist of at least two functionally distinct subsets (*4*, *5*). Ly-6C^{high} (Gr-1^{+}) monocytes are inflammatory and migrate to injured (*6*, *7*) or infected (*8*–*10*) sites but also propagate chronic diseases (*11*–*13*). Ly-6C^{low} (Gr-1^{-}) monocytes patrol the resting vasculature (*14*), populate normal (*15*) or inflammatory sites (*14*), and participate in resolution of inflammation (*7*).

Tissue repair after myocardial infarction (MI) requires coordinated mobilization of both subsets: first, Ly-6C^{high} monocytes digest damaged tissue; second, Ly-6C^{low} monocytes promote wound healing (*7*). We observed that the ischemic myocardium accumulates Ly-6C^{high} monocytes in numbers that exceed their availability in circulation (Fig. 1A), which intrigued

[1]Center for Systems Biology, Massachusetts General Hospital and Harvard Medical School, Boston, MA 02114, USA. [2]Faculty of Biology and Medicine, University of Lausanne, CH-1015 Lausanne, Switzerland. [3]Center for Immunology and Inflammatory Diseases, Massachusetts General Hospital and Harvard Medical School, Charlestown, MA 02129, USA. [4]Cardiovascular Division, Department of Medicine, Brigham and Women's Hospital, Boston, MA 02115, USA. [5]Center for Excellence in Vascular Biology, Brigham and Women's Hospital, Boston, MA 02115, USA. [6]Department of Systems Biology, Harvard Medical School, Boston, MA 02115.

*These authors contributed equally to this work.
†To whom correspondence should be addressed. E-mail: fswirski@mgh.harvard.edu (F.K.S.); rweissleder@mgh.harvard.edu (R.W.); mpittet@mgh.harvard.edu (M.J.P.)

us. Although the bone marrow produces and contains numerous (pro)monocytes (*16*), we sought to identify compartmental reservoirs of extramedullary monocytes, as these could accommodate the demands of rapid-onset inflammation.

First, we screened candidate tissues for the presence of monocyte-like cells (*17*). Monocytes express CD11b and CD115 and are negative or

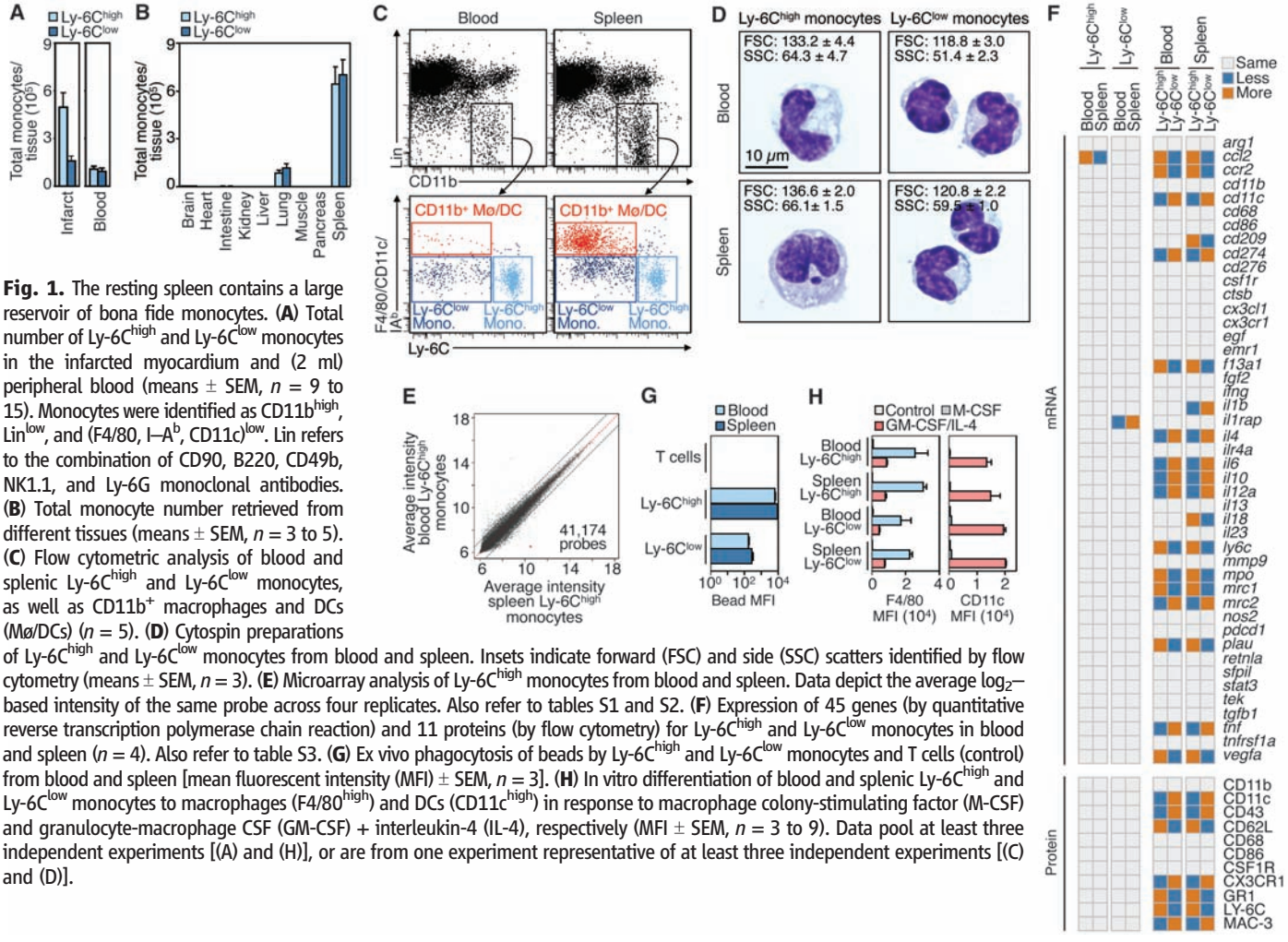

Fig. 1. The resting spleen contains a large reservoir of bona fide monocytes. (**A**) Total number of Ly-6C^{high} and Ly-6C^{low} monocytes in the infarcted myocardium and (2 ml) peripheral blood (means ± SEM, n = 9 to 15). Monocytes were identified as CD11b^{high}, Lin^{low}, and (F4/80, I–A^{b}, CD11c)^{low}. Lin refers to the combination of CD90, B220, CD49b, NK1.1, and Ly-6G monoclonal antibodies. (**B**) Total monocyte number retrieved from different tissues (means ± SEM, n = 3 to 5). (**C**) Flow cytometric analysis of blood and splenic Ly-6C^{high} and Ly-6C^{low} monocytes, as well as CD11b^{+} macrophages and DCs (Mø/DCs) (n = 5). (**D**) Cytospin preparations of Ly-6C^{high} and Ly-6C^{low} monocytes from blood and spleen. Insets indicate forward (FSC) and side (SSC) scatters identified by flow cytometry (means ± SEM, n = 3). (**E**) Microarray analysis of Ly-6C^{high} monocytes from blood and spleen. Data depict the average $\log_2$–based intensity of the same probe across four replicates. Also refer to tables S1 and S2. (**F**) Expression of 45 genes (by quantitative reverse transcription polymerase chain reaction) and 11 proteins (by flow cytometry) for Ly-6C^{high} and Ly-6C^{low} monocytes in blood and spleen (n = 4). Also refer to table S3. (**G**) Ex vivo phagocytosis of beads by Ly-6C^{high} and Ly-6C^{low} monocytes and T cells (control) from blood and spleen [mean fluorescent intensity (MFI) ± SEM, n = 3]. (**H**) In vitro differentiation of blood and splenic Ly-6C^{high} and Ly-6C^{low} monocytes to macrophages (F4/80^{high}) and DCs (CD11c^{high}) in response to macrophage colony-stimulating factor (M-CSF) and granulocyte-macrophage CSF (GM-CSF) + interleukin-4 (IL-4), respectively (MFI ± SEM, n = 3 to 9). Data pool at least three independent experiments [(A) and (H)], or are from one experiment representative of at least three independent experiments [(C) and (D)].

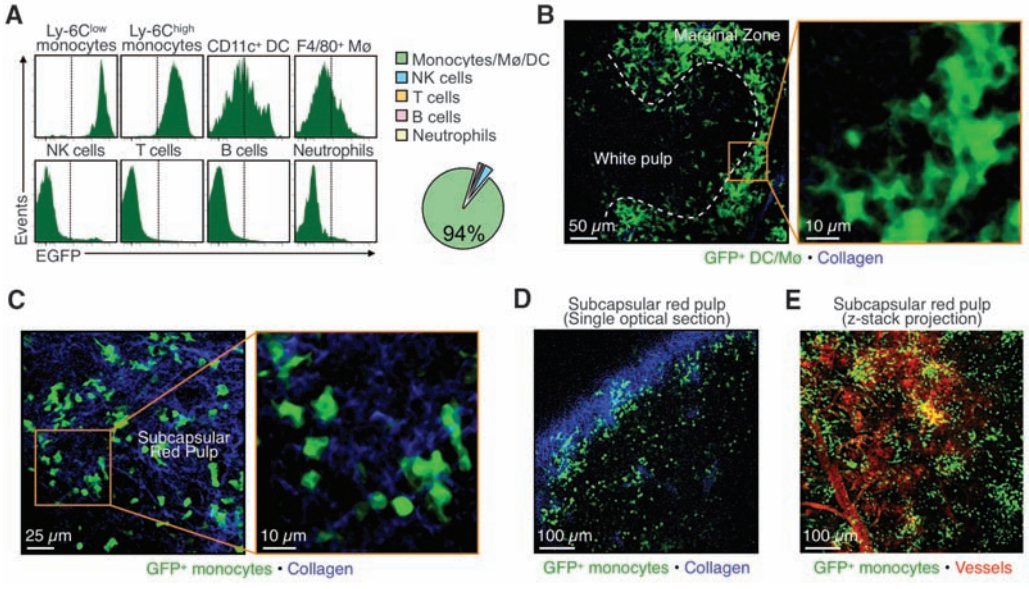

Fig. 2. Splenic monocytes cluster in the subcapsular red pulp. (**A**) Histograms depict flow cytometric analysis of GFP fluorescence of splenic leukocytes in *Cx$_3$cr1$^{gfp/+}$* mice (n = 3). The pie chart shows the relative proportions of various GFP^{+} populations. Also refer to figs. S2 and S3. (**B** and **C**) Multiphoton microscopy micrographs of *Cx$_3$cr1$^{gfp/+}$* mice show GFP^{+} Mø/DCs (green) in the marginal zones (B) and GFP^{+} monocytes (green) in the subcapsular red pulp (C). Collagen fibers appear in blue. (**D**) A single optical section shows GFP^{+} monocytes (green) in the subcapsular red pulp. The dense collagen network (blue) of the splenic capsule indicates the boundary of the organ. (**E**) An intravital micrograph of the spleen subcapsular red pulp shows GFP^{+} monocytes (green) organized in clusters and topographically distinct from blood vessels (red). All data are from one experiment representative of at least two independent experiments.

low for CD90, B220, CD49b, NK1.1, and Ly-6G surface proteins. They are distinct from macrophages and dendritic cells (DCs) on the basis of the F4/80 glycoprotein, CD11c, and major histocompatibility complex molecule I–A^b. Of all organs profiled, only the spleen contained cells that met these criteria and that were present in large quantities. The population included Ly-$6C^{high}$ and Ly-$6C^{low}$ subtypes in ratios similar to those in the blood (Fig. 1, B and C, and fig. S1).

The spleen's major known functions are removal of aging erythrocytes and recycling of iron, elicitation of immunity, and supply of erythrocytes after hemorrhagic shock (*18*). The presence of numerous monocytes in the spleen seems paradoxical, because monocytes are distinguished from lineage descendants on the basis of residency: Monocytes are considered circulating, whereas macrophages and DCs are tissue-resident and predominantly sessile (*5*, *14*, *19*). We therefore conducted additional experiments to characterize the monocyte-like cells in the spleen.

We found that splenic monocytes resembled their blood counterparts morphologically: Ly-$6C^{high}$ monocytes were larger than Ly-$6C^{low}$ monocytes, and both subsets had kidney- or horseshoe-shaped nuclei (Fig. 1D). Ly-$6C^{high}$ monocytes in blood and spleen had essentially indistinguishable transcriptomes (Fig. 1E and tables S1 and S2). Refined mRNA and protein analysis validated this similarity (Fig. 1F), although, as expected, Ly-$6C^{high}$ monocytes differed from their Ly-$6C^{low}$ counterparts (*5*) (Fig. 1F and table S3). Splenic Ly-$6C^{high}$ and Ly-$6C^{low}$ monocytes had phagocytic functions similar to those of their blood counterparts (Fig. 1G) and differentiated comparably into macrophages or DCs in vitro (Fig. 1H). We therefore concluded that the spleen contains a population of bona fide monocytes that coexists with, but is different from, macrophages and DCs and that outnumbers blood monocytes.

To determine where monocytes reside in the spleen, we used $Cx_3cr1^{gfp/+}$ mice in which nearly all fluorescent splenocytes are monocytes or their lineage descendents (Fig. 2A and figs. S2 and S3). We detected dense populations of green fluorescent protein–positive (GFP^+) cells in two regions, the marginal zone and the subcapsular red pulp. As expected, cells in the marginal zone were mostly macrophages and DCs (*18*): They were large and morphologically irregular; F4/80^{high} or CD11c^{high}, respectively; and localized around the white pulp (Fig. 2B, fig S3, and movie S1). The fluorescent cells in the subcapsular red pulp were mostly monocytes: They were devoid of dendrites; had kidney- or horseshoe-shaped nuclei; were $CD11b^+$ and F4/$80^{-/low}$ but $CD11c^-$; and were

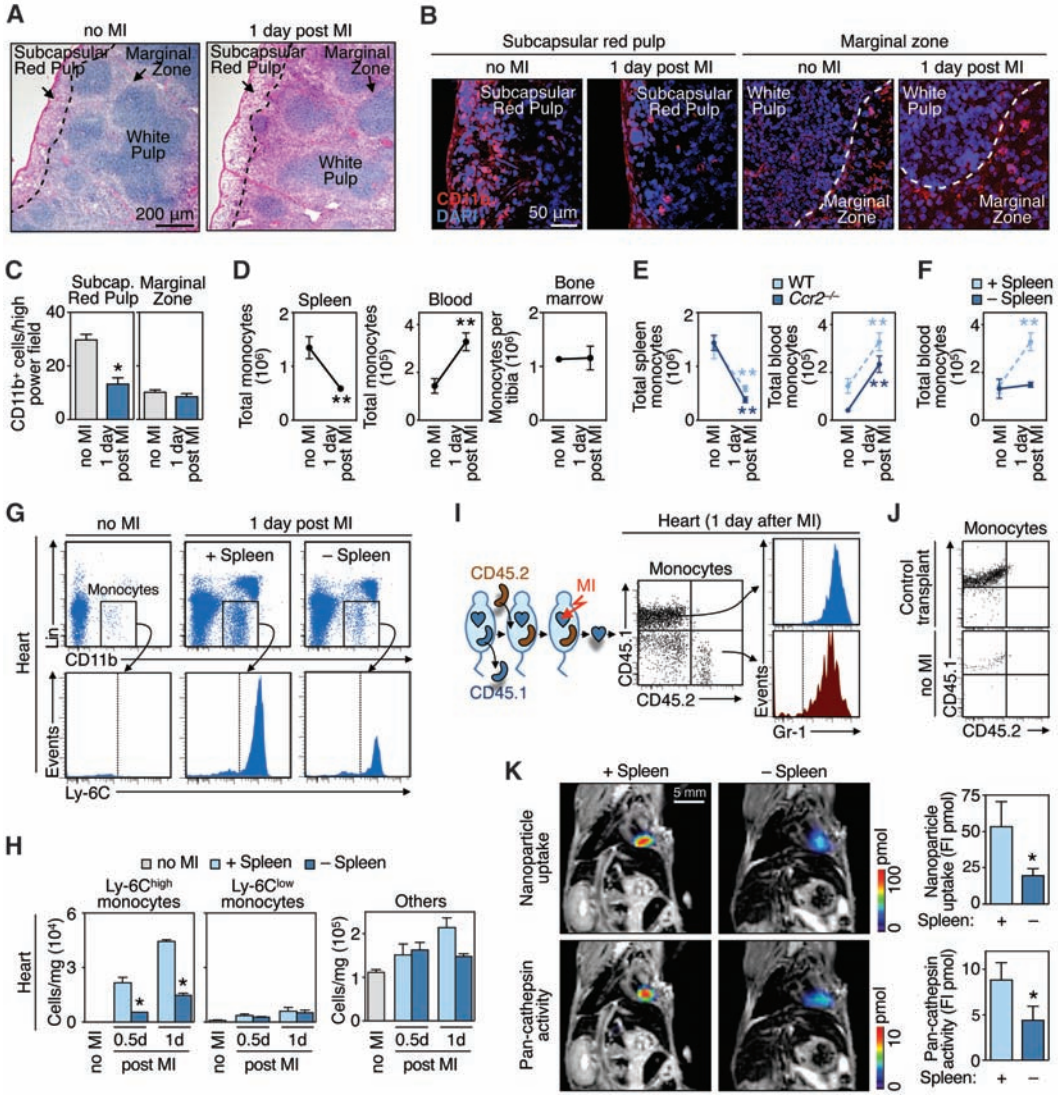

Fig. 3. Splenic reservoir monocytes emigrate from the subcapsular red pulp and populate inflammatory sites. (**A**) Splenic sections from mice without MI and 1 day after MI stained with hematoxylin and eosin. (**B**) Splenic sections stained with CD11b-specific antibodies (red) and 4′,6′-diamidino-2-phenylindole (DAPI) (blue) depict the subcapsular red pulp and the marginal zone from mice without MI and 1 day after MI. (**C**) Enumeration of $CD11b^+$ cells in the subcapsular red pulp and marginal zone (means ± SEM, n = 10 high-power fields). (**D**) Total number of monocytes in the spleen, blood, or bone marrow (tibia) in control mice (no MI) or 1 day after MI (means ± SEM, n = 6 to 15). (**E**) Total number of monocytes in the spleen or blood in wild-type (WT) and $Ccr2^{-/-}$ mice in response to MI (n = 3 to 6). (**F**) Total number of blood monocytes in splenectomized animals (–Spleen) and sham-operated controls (+Spleen) without MI or 1 day after MI (n = 3 to 6). (**G** and **H**) Accumulation of cells in heart in the same groups of mice as measured by flow cytometry [(G), n = 3] or by counts per mg tissue [(H), means ± SEM, n = 9]. (**I**) Accumulation of monocyte subsets originating exclusively from spleen as measured by flow cytometry. Dot plots (CD45.1 versus CD45.2) of gated monocytes and histograms (Gr-1) of each positive population. (**J**) CD45.1 versus CD45.2 profile of gated monocytes in a mouse receiving a control transplant (pancreas) and in a mouse not subjected to MI. Also refer to fig. S7. (**K**) FMT-MRI of in vivo phagocytic and proteolytic activities in infarcts. Fluorochrome concentration is shown in the infarcted area, on the basis of MRI-derived anatomy (n = 6). FI, fluorescence intensity. *P < 0.05; **P < 0.005. Data pool at least three independent experiments (D to F, and H), or are from one experiment representative of two [(I) and (J)] or at least three independent experiments [(A) to (C), and (G)].

arranged in clusters of ~20 to 50 cells along the perimeter of the organ (Fig. 2, C to E, fig. S3, and movies S2 and S3). They clustered mostly in the reticular fiber–rich pulp cords, just as iron-recycling CD163^{+} macrophages do (*20*) (fig. S3). Also, intravital microscopy and parabiosis experiments revealed that splenic monocytes resided in the spleen, rather than simply passed through the spleen within blood (fig. S4 and S5).

A hallmark of a reservoir population is its ability to deploy to distant sites. Thus, we tested whether splenic Ly-6C^{high} monocytes are mobilized in response to surgically induced ischemia of the myocardium. One day after coronary ligation, we observed reduced numbers of monocytes in the subcapsular red pulp of the spleen (Fig. 3, A to C) that could not be attributed to local cell differentiation or death (fig. S6) and, therefore, indicated exit. Entire organ enumeration after MI revealed monocyte loss in spleen, gain in blood, but no change in the bone marrow (Fig. 3D and fig. S6), which suggested mobilization of splenic, but not bone marrow, monocytes after tissue injury.

We next compared the relative contributions of the spleen and the bone marrow in response to MI by using mice in which only one of the two tissues can contribute monocytes. First, we evaluated *Ccr2*$^{-/-}$ mice, because the chemokine receptor mediates monocyte mobilization from the bone marrow (*9*, *21*), but not from the spleen (table S4). The number of blood monocytes comparably increased—and the number of splenic monocytes comparably decreased—after MI in both wild-type and *Ccr2*$^{-/-}$ mice (Fig. 3E). The released monocytes in *Ccr2*$^{-/-}$ mice did not accumulate in the ischemic myocardium, because infiltration depends on the chemokine CCR2 [table S4 and (*7*)]. Second, we evaluated animals splenectomized by a procedure that preserves the bone marrow and blood monocyte pools (fig. S7). After MI, blood monocyte numbers increased in control, but not splenectomized, animals (Fig. 3F). Analysis of the ischemic myocardium revealed a massive influx of Ly-6C^{high} monocytes in mice containing the spleen. However, this

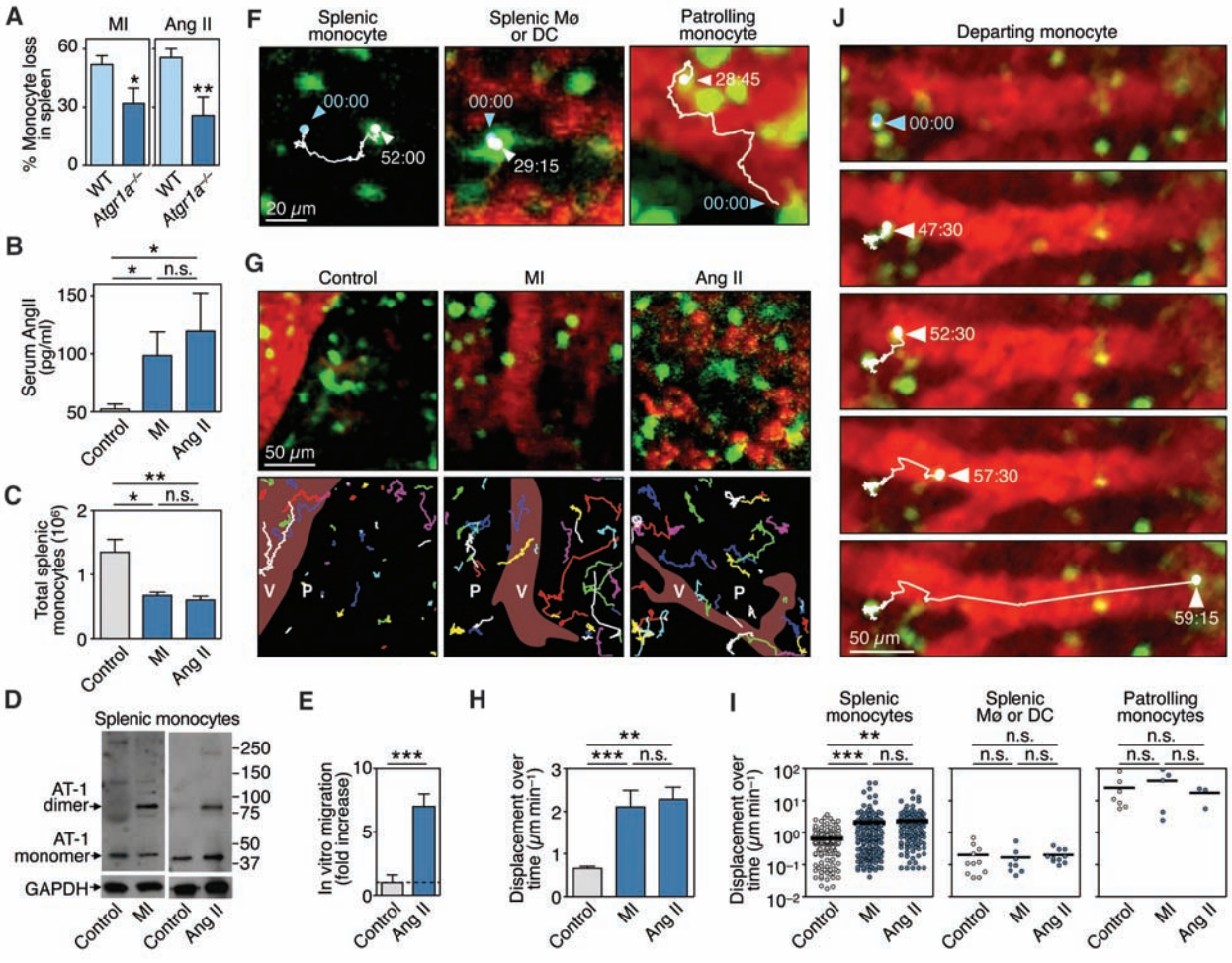

Fig. 4. Ang II–AT-1 receptor signaling promotes splenic monocyte motility and tissue emigration. (**A**) Percentage of monocytes lost from the spleen 1 day after MI or Ang II infusion in WT and *Atgr1a*$^{-/-}$ mice (means ± SEM, $n = 4$ to 9). (**B**) Serum Ang II concentrations in the steady-state (control), and 1 day after MI or infusion of Ang II ($n = 6$ to 9). (**C**) Total number of splenic monocytes (Ly-6C^{high} and Ly-6C^{low}) in the groups of mice mentioned above. (**D**) Western blot analysis of monomeric and dimeric forms of the AT-1 receptor on control splenic monocytes in the steady state (control), and 1 day after MI or infusion of Ang II, $n = 3$. (**E**) In vitro migration of splenic monocytes in response to Ang II (1 μM) (means ± SEM, $n = 6$). (**F**) Intravital microscopy of GFP^{+} cells (green) in the spleen subcapsular red pulp of an Ang II–treated *Cx$_3$cr1*$^{gfp/+}$ mouse. Images show a splenic monocyte, an Mø or DC, and a patrolling monocyte. Blood is shown in red. Tracks indicate the position of cell centroids at 15-s intervals (time in min:s). (**G**) (Top) Intravital micrographs of GFP^{+} cells in control mice and 1 day after MI or infusion of Ang II at the initial recording time point. (Bottom) Tracks for all GFP^{+} cells in the field of view and over 1 hour. Some cells entered or exited our imaging area during the recording and thus were followed for a shorter duration. V, vessel; P, parenchyma. (**H**) Average displacement over time of all GFP^{+} splenic monocytes [means ± SEM, $n = 143$ (control), 163 (MI), and 125 (Ang II) cells]. (**I**) Displacement over time of single splenic monocytes (left), splenic macrophages of DCs (middle), and patrolling monocytes (right). (**J**) Recording of a departing splenic monocyte. Tracks indicate the position of the cell centroid. *$P < 0.05$, **$P < 0.01$, ***$P < 0.001$. Data pool two [(A) to (C), and (E)] or at least three independent experiments [(H) and (I)], or are from one experiment representative of at least three independent experiments [(D), (F), and (G)].

number was decreased by 75% in splenectomized mice (Fig. 3, G and H). These findings indicate that the spleen mobilizes monocytes en masse after MI. Similar observations in rats argue for a generalizable existence of a splenic monocyte reservoir (fig. S8).

To track unambigously the fate of monocytes from the spleen to the heart, we studied CD45.1 mice that were splenectomized, given CD45.2 spleens by transplantation, and subjected to MI (fig. S9). We observed increased numbers of donor monocytes in the blood of animals after MI, which indicated that the injury triggered the release of splenic monocytes (fig. S10). The infarct accumulated donor (i.e., spleen-derived) and host monocytes, all of which were Gr-1^{+} (Ly-6C^{high}) (Fig. 3I). The transplantation procedure itself reduced the number of reservoir donor monocytes by a factor of 6.1, likely because of ischemia-related cell differentiation. Correcting for this, we calculated that the spleen contributed 41% of monocytes to the ischemic myocardium. Control experiments (transplanted pancreas or transplanted spleen but no MI) showed no accumulation of donor monocytes in the recipient heart (Fig. 3J). Noninvasive fluorescence molecular tomography–magnetic resonance imaging (FMT-MRI) three-dimensional fusion imaging (*22*) with phagocytosis and cathepsin-activatable sensors (*23*) revealed attenuated activities in infarcts of splenectomized mice (Fig. 3K), which indicates that splenic monocytes are biologically active when recruited to inflamed tissue. Thus, the spleen stores Ly-6C^{high} monocytes readily recruitable to augment inflammation at distant sites. The spleen does not likely produce monocytes, because donor spleens contained only host-derived cells as early as 3 weeks after transplantation (fig. S11).

The spleen did not contribute neutrophils significantly, which suggested selective mobilization of monocytes (fig. S12). Of these, both subsets (Ly-6C^{high} and Ly-6C^{low}) exited the spleen in response to MI, yet after 1 day, the ischemic myocardium recruited Ly-6C^{high} monocytes selectively (fig. S13). The excluded Ly-6C^{low} monocytes may have dispersed to other tissues, patrolled the vasculature, or accumulated in the infarct at a later time (*7*).

Monocytes express a wide variety of receptors (*24*), some of which may trigger splenic release. We focused on angiotensin II (Ang II), because (i) it induces cytoskeletal rearrangement and migration of monocytes in vitro (*25*), (ii) it augments monocyte-mediated inflammation (*26*), and (iii) its serum levels increase after MI (*27*). Ang II exerts its effects by binding to the angiotensin type 1 (AT-1) and AT-2 receptors.

Atgr1a$^{-/-}$ animals subjected to MI did not expel splenic monocytes efficiently (Fig. 4A) and accumulated only a few monocytes in the ischemic myocardium (fig. S14), which indicated that Ang II–AT-1 signaling contributes to expulsion in this model. Sustained exogenous administration of Ang II in wild-type mice reproduced monocyte egress; mice with Ang II concentrations comparable to those after MI (Fig. 4B) released splenic monocytes (Fig. 4C and fig. S15). Moreover, Ang II infusion or MI elicited AT-1 receptor dimerization in splenic monocytes in vivo (Fig. 4D), an event that stimulates a wide spectrum of intracellular responses (*26*). We also found that Ang II induced directional migration of splenic monocytes in vitro (Fig. 4E). These data support a direct link between Ang II, the AT-1 receptor, and splenic monocytes and prompted us to explore the effects of Ang II on cell behavior in vivo.

We developed a real-time intravital microscopy technique that allows observation of endogenous monocytes and vessels in the subcapsular red pulp of the spleen in live animals, at depths up to 100 μm below the fibrous capsule, while preserving organ temperature and blood flow. Spleens of *Cx$_3$cr1$^{gfp/+}$* mice contained three distinct GFP^{+} populations, based on their location and size (Fig. 4F, fig. S16, and movies S4 to 6). Real-time tracking of GFP^{+} cells in cluster-rich regions of the subcapsular red pulp revealed behavioral changes shortly after MI or after administration of Ang II (Fig. 4G). Splenic monocytes increased their displacement over time by more than threefold within 2 hours after either intervention (Fig. 4, G to I, movies S7 to 9 and fig. S17), which indicated that Ang II induced their migration in vivo. Conversely, splenic macrophages or DCs showed very low displacement that did not increase in response to intervention, whereas patrolling monocytes showed typically high displacement (Fig. 4I), as reported in dermal and mesenteric vessels (*14*). The motile splenic monocytes that responded to Ang II were more likely to encounter neighboring venous sinuses or collecting veins and to enter the blood stream to exit the spleen. Figure 4J and movie S10 show one example of a prototypical departing monocyte. The increased motility of splenic monocytes and subsequent egress led to a considerable loss of fluorescent cells in tissue (fig. S15).

Splenic contraction after hemorrhagic shock is associated with erythrocyte expulsion (*28*). Our intravital microscopy data show, however, that the subcapsular red pulp did not measurably contract when monocytes were already activated 1.5 hours after treatment with Ang II (fig. S18). A contraction-induced mechanism would also affect other leukocytes, but our neutrophil data indicate otherwise.

Our findings illuminate the body's ability to mobilize a reservoir of undifferentiated splenic monocytes in response to injury. Triggering of this reservoir likely provides a stochastic advantage for rapid monocyte accumulation, but such triggering is not necessarily desirable. Future studies should investigate the contribution of the splenic monocyte population in response to other inflammatory events and whether additional factors control monocyte migration, organization, and differentiation in the splenic environment. Understanding how an organism controls the quality and quantity of its immune players is essential to understanding homeostasis, and its perturbation and restoration following infection and tissue injury.

References and Notes

1. A. D. Luster, R. Alon, U. H. von Andrian, *Nat. Immunol.* **6**, 1182 (2005).
2. K. Ley, C. Laudanna, M. I. Cybulsky, S. Nourshargh, *Nat. Rev. Immunol.* **7**, 678 (2007).
3. A. J. Singer, R. A. Clark, *N. Engl. J. Med.* **341**, 738 (1999).
4. C. Auffray, M. H. Sieweke, F. Geissmann, *Annu. Rev. Immunol.* **27**, 669 (2009).
5. S. Gordon, P. R. Taylor, *Nat. Rev. Immunol.* **5**, 953 (2005).
6. L. Arnold *et al.*, *J. Exp. Med.* **204**, 1057 (2007).
7. M. Nahrendorf *et al.*, *J. Exp. Med.* **204**, 3037 (2007).
8. I. R. Dunay *et al.*, *Immunity* **29**, 306 (2008).
9. N. V. Serbina, E. G. Pamer, *Nat. Immunol.* **7**, 311 (2006).
10. C. Sunderkotter *et al.*, *J. Immunol.* **172**, 4410 (2004).
11. F. K. Swirski *et al.*, *J. Clin. Invest.* **117**, 195 (2007).
12. F. Tacke *et al.*, *J. Clin. Invest.* **117**, 185 (2007).
13. A. Mantovani, P. Allavena, A. Sica, F. Balkwill, *Nature* **454**, 436 (2008).
14. C. Auffray *et al.*, *Science* **317**, 666 (2007).
15. F. Geissmann, S. Jung, D. R. Littman, *Immunity* **19**, 71 (2003).
16. R. van Furth, Z. A. Cohn, *J. Exp. Med.* **128**, 415 (1968).
17. Materials and methods are available as supporting material on *Science* Online.
18. R. E. Mebius, G. Kraal, *Nat. Rev. Immunol.* **5**, 606 (2005).
19. D. M. Mosser, J. P. Edwards, *Nat. Rev. Immunol.* **8**, 958 (2008).
20. M. Kristiansen *et al.*, *Nature* **409**, 198 (2001).
21. C. L. Tsou *et al.*, *J. Clin. Invest.* **117**, 902 (2007).
22. R. Weissleder, M. J. Pittet, *Nature* **452**, 580 (2008).
23. M. Nahrendorf *et al.*, *Circ. Res.* **100**, 1218 (2007).
24. R. Medzhitov, *Nature* **454**, 428 (2008).
25. U. Kintscher *et al.*, *Hypertension* **37**, 587 (2001).
26. S. AbdAlla, H. Lother, A. Langer, Y. el Faramawy, U. Quitterer, *Cell* **119**, 343 (2004).
27. H. M. McAlpine, S. M. Cobbe, *Am. J. Med.* **84**, 61 (1988).
28. B. N. Davies, P. G. Withrington, *Pharmacol. Rev.* **25**, 373 (1973).

29. This work was supported in part by NIH grants U01 HL080731, P50 CA86355, R24 CA69246, U54 CA126515, and P01 A154904 (to R.W.), MGH-Center for Systems Biology (to M.J.P.), AHA SDG 0835623D (to M.N.), and NIH grant 1R01HL095612 (to F.K.S). The authors thank U. von Andrian for critical assessment of the manuscript; A. Luster for providing *Ccr2*$^{-/-}$ mice; D. Erle, A. Barcak, and C. Eisley for microarray hybridization and data analysis; M. Waring for sorting cells; A. Moseman for helpful discussion and feedback with parabiosis experiments; and A. Newton, C. Siegel, N. Sergeyev, and Y. Iwamoto for technical assistance. MIAME (minimum information about a microarray experiment)–compliant expression data have been deposited under accession no. GSE14850. This work is dedicated to the memory of Marc-Henri Pittet.

Supporting Online Material

www.sciencemag.org/cgi/content/full/325/5940/612/DC1
Materials and Methods
Figs. S1 to S18
Tables S1 to S4
References
Movies S1 to S10

20 April 2009; accepted 10 June 2009
10.1126/science.1175202

Innate and Adaptive Immunity Cooperate Flexibly to Maintain Host-Microbiota Mutualism

Emma Slack,[1,5]* Siegfried Hapfelmeier,[1,5] Bärbel Stecher,[2] Yuliya Velykoredko,[1] Maaike Stoel,[1] Melissa A. E. Lawson,[1] Markus B. Geuking,[1] Bruce Beutler,[3] Thomas F. Tedder,[4] Wolf-Dietrich Hardt,[2] Premysl Bercik,[1] Elena F. Verdu,[1] Kathy D. McCoy,[1] Andrew J. Macpherson[1,5]*

Commensal bacteria in the lower intestine of mammals are 10 times as numerous as the body's cells. We investigated the relative importance of different immune mechanisms in limiting the spread of the intestinal microbiota. Here, we reveal a flexible continuum between innate and adaptive immune function in containing commensal microbes. Mice deficient in critical innate immune functions such as Toll-like receptor signaling or oxidative burst production spontaneously produce high-titer serum antibodies against their commensal microbiota. These antibody responses are functionally essential to maintain host-commensal mutualism in vivo in the face of innate immune deficiency. Spontaneous hyper-activation of adaptive immunity against the intestinal microbiota, secondary to innate immune deficiency, may clarify the underlying mechanisms of inflammatory diseases where immune dysfunction is implicated.

Innate recognition of a few thousand bacteria in the blood and peripheral tissues results in an inflammatory response and, subsequently, induction of both cell-mediated and humoral adaptive immunity (*1*). Paradoxically, our trillions of intestinal bacteria do not normally induce spontaneous pathological inflammatory responses or high-titer serum antibody responses (*2*, *3*). Many layers of defense compartmentalize commensal bacteria within the gut lumen and mucosal immune compartment (Lamina propria, Peyer's patches, and mesenteric lymph nodes) (*3*). Thus, the paradigm emerged that minimizing microbial recognition within the specialized intestinal microenvironment is crucial to establishing mutualism (*4*), and consequently, it was no surprise that animals with deficient innate immunity successfully contain their microbiota. In contrast, we demonstrate that innate and adaptive immunity can function both sequentially (*5*), and in a compensatory manner, and the relative functionality of the two systems translates into a set point that permits mutualism.

To study how mammals can adapt to commensal intestinal bacteria in the absence of signaling through Toll-like receptors (TLRs), a major family of innate immune sensors, we maintained mice deficient in the TLR adaptor molecules MyD88 and Ticam1 (also known as TRIF) and control animals with different densities of intestinal commensal bacteria (*6*). We generated germ-free mice, who can be supposed to have never before encountered a live bacterium, "clean SPF" mice containing a very limited intestinal microbiota free of both *Enterococcus faecalis* and *Escherichia coli*, and "conventional SPF"

[1]Farncombe Family Digestive Health Research Institute, McMaster University, Hamilton, ON L8S 4L8, Canada. [2]Institute of Microbiology, ETH Zürich, 8032 Zürich, Switzerland. [3]Department of Genetics, The Scripps Research Institute, La Jolla, CA 92121, USA. [4]Department of Immunology, Duke University Medical Center, Durham, NC 27710, USA. [5]DKF (Department of Clinical Research), Maurice Müller Laboratories, Universitätsklinik für Viszerale Chirurgie und Medizin (UVCM), University of Bern, 3008 Bern, Switzerland.

*To whom correspondence should be addressed. E-mail: andrew.macpherson@insel.ch (A.J.M.); emma.slack@dkf.unibe.ch (E.S.)

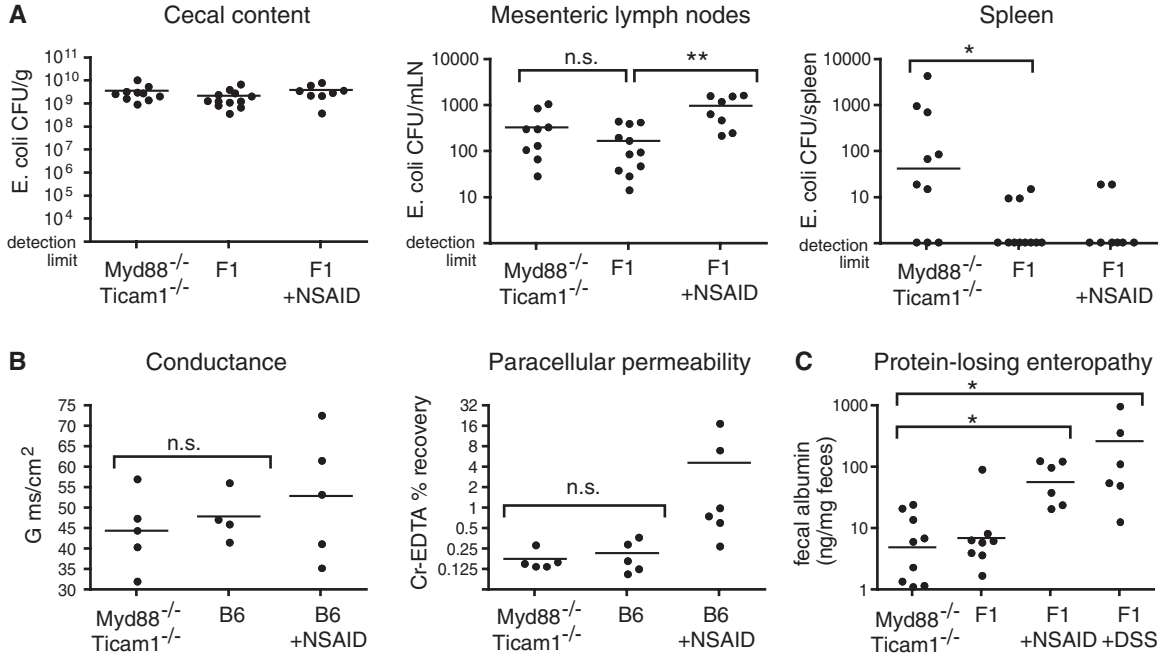

Fig. 1. Increased bacterial penetration in *Myd88*$^{-/-}$ *Ticam1*$^{-/-}$ mice is not dependent on increased intestinal permeability. (**A**) Clean SPF *Myd88*$^{-/-}$ *Ticam1*$^{-/-}$, F_1 control mice, and F_1 mice treated with 7.5 mg indomethacin per kg of body weight 24 hours earlier (F_1 + NSAID) were gavaged with 10^{10} ampicillin-resistant *E. coli* K-12. After 18 hours, the density of ampicillin-resistant *E. coli* in the cecal content, mesenteric lymph nodes, and spleen was determined by selective plating (*P < 0.027, **P < 0.002). Data are pooled from three independent experiments. CFU, colony-forming units; mLN, mesenteric lymph node; G, conductance. (**B**) Ussing chamber measurements of conductance and paracellular permeability, as assessed by serosal ^{51}Cr-EDTA recovery, of jejunum from *Myd88*$^{-/-}$ *Ticam1*$^{-/-}$ mice, cohoused C57BL/6 control mice (B6), and positive control (C57BL/6) mice treated with 7.5 mg/kg indomethacin (NSAID). Two or three matched mice were analyzed each day over 5 days. Each data point represents an individual mouse, and all collected data are shown. (**C**) Enzyme-linked immunosorbent assay (ELISA) for albumin presence in the feces of *Myd88*$^{-/-}$ *Ticam1*$^{-/-}$ mice, F_1 control mice, NSAID-treated control mice, or DSS-treated control mice. (*P < 0.05). Each data point represents an individual mouse, and all collected data pooled from three independent experiments are shown.

mice reared in standard clean animal house conditions and, thus, free of all monitored mouse pathogens.

To address whether mucosal containment of the microbiota was normal in TLR-deficient mice, we challenged clean SPF *Myd88*$^{-/-}$ *Ticam1*$^{-/-}$ mice intragastrically with high doses of a commensal bacterium to which they had never previously been exposed (*E. coli* K-12). In accordance with previous findings (*7*), both *Myd88*$^{-/-}$ *Ticam1*$^{-/-}$ and control mice had similar loads of culturable *E. coli* K-12 in the mesenteric lymph nodes 18 hours after challenge (Fig. 1A). In contrast, and in agreement with a recent publication from Vaishnava *et al*. (*8*), significantly more live bacteria were recovered from the spleens of *Myd88*$^{-/-}$ *Ticam1*$^{-/-}$ mice (Fig. 1A). Similar data were obtained when germ-free *Myd88*$^{-/-}$ *Ticam1*$^{-/-}$ mice were naturally colonized by cohousing with conventional SPF mice (fig. S1A), which ruled out any unphysiological complications due to gavage. These data demonstrate a dramatic failure to compartmentalize the intestinal microbiota within the mucosal immune compartment in *Myd88*$^{-/-}$ *Ticam1*$^{-/-}$ mice.

Alterations in epithelial proliferation and increased susceptibility to intestinal pathogens and

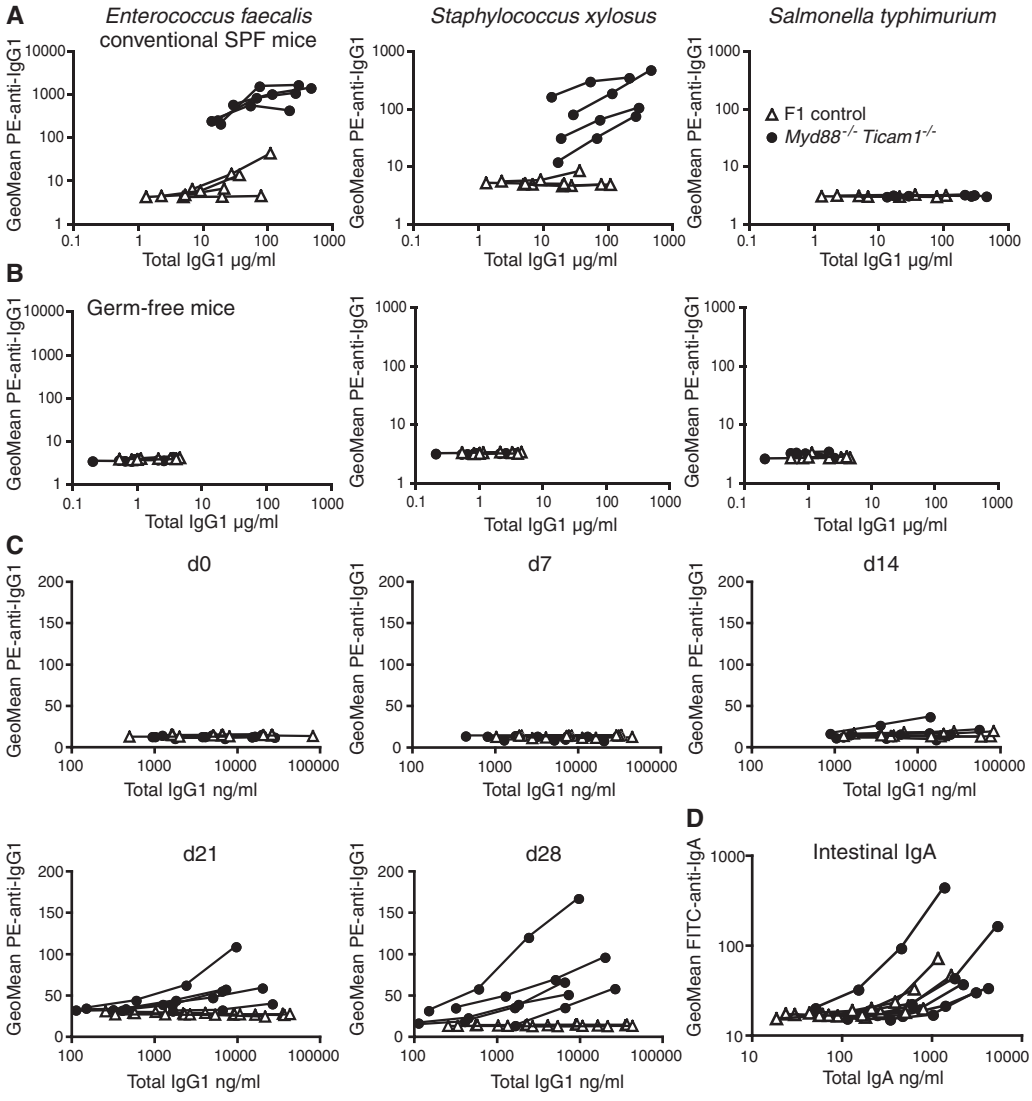

Fig. 2. *Myd88*$^{-/-}$ *Ticam1*$^{-/-}$ mice lose systemic ignorance to their commensal flora. (**A** and **B**). The commensal bacteria *E. faecalis* and *Staphylococcus xylosus* were stained with whole serum from *Myd88*$^{-/-}$ *Ticam1*$^{-/-}$ and control mice, followed by phycoerythrin (PE)–conjugated secondary antibody against a mouse IgG1 and analyzed by flow cytometry. Titrations *S. xylosus*, *E. faecalis*, and *Salmonella typhimurium* IgG1 reactivity from 24-week-old *Myd88*$^{-/-}$ *Ticam1*$^{-/-}$ or F_1 control mice housed in the indicated conditions. Each line represents an individual mouse. Data are representative of $n > 30$ mice. (**C**) Germ-free, 12-week-old *Myd88*$^{-/-}$ *Ticam1*$^{-/-}$ and *Myd88*$^{+/-}$ *Ticam1*$^{-/-}$ were monocolonized by cohousing with an *E. coli* K-12 monocolonized sentinel for the indicated amount of time (day 0, day 7, and so on). Serum was taken weekly to follow the development of *E. coli* K-12 IgG1 responses by bacterial flow cytometry and ELISA. Each line represents an individual mouse. Representative data of two independent experiments are shown. (**D**) *E. coli* K-12–specific IgA titers as determined by bacterial surface staining with cleared intestinal lavage from day 28 *E. coli*–monocolonized mice. Data shown are representative of two experiments.

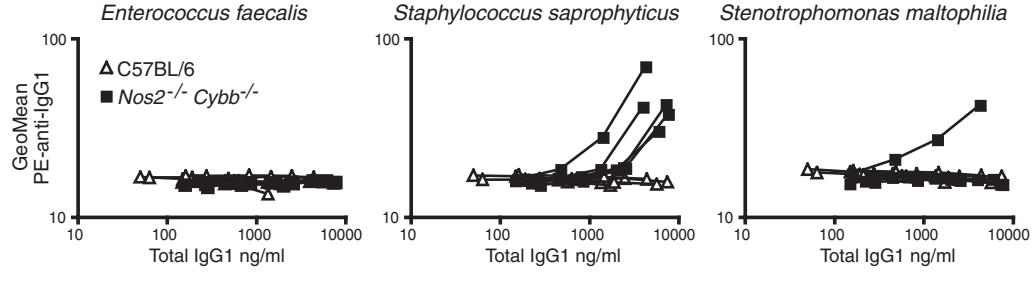

Fig. 3. *Nos2*$^{-/-}$ *Cybb*$^{-/-}$ mice exhibit serum antibodies directed against their commensal flora. Serum and feces were collected from 8-week-old *Nos2*$^{-/-}$ *Cybb*$^{-/-}$ mice and cohoused C57BL/6 controls. Isolates of *E. faecalis*, *Staphylococcus saprophyticus*, and *Stenotrophomonas maltophilia* were obtained by aerobic culture from feces, and pure cultures were stained with serum from *Nos2*$^{-/-}$ *Cybb*$^{-/-}$ and control C57BL/6 mice. Antibacterial IgG1 was quantified by flow cytometry. C57BL/6 controls ($n = 5$) and *NOS2Cybb* mice ($n = 5$). Representative data from two independent experiments are shown.

chemical damage have been reported in *Myd88*$^{-/-}$ mice (*9*, *10*). We therefore addressed whether altered intestinal barrier function was responsible for loss of mucosal compartmentalization in *Myd88*$^{-/-}$ *Ticam1*$^{-/-}$ mice. Treatment of clean SPF control mice with nonsteroidal anti-inflammatory drugs (NSAIDs) to increase small intestine permeability (*11*), before administering high numbers of *E. coli* K-12 intragastrically, resulted in increased recovery of live *E. coli* from mesenteric lymph nodes but not from the spleen (Fig. 1A). This suggested that a nonspecific increase in intestinal permeability was insufficient to cause high numbers of live intestinal bacteria to reach the spleen.

We carried out three additional independent measurements to assess intestinal permeability in *Myd88*$^{-/-}$ *Ticam1*$^{-/-}$ mice. We used Ussing chambers to measure permeability in vitro (Fig. 1B and fig. S1B), assessed permeability between the intestinal lumen and the vasculature ex vivo (fig. S1C), and directly measured serum protein loss into the intestinal lumen in vivo (Fig. 1C). In each case, the values were similar in *Myd88*$^{-/-}$ *Ticam1*$^{-/-}$ and C57BL/6 mice, but were elevated when permeability was increased by prior treatment of the animals with NSAIDs or dextran sodium sulfate (DSS). Histological examination of intestinal architecture and epithelial cell proliferation also revealed no differences between *Myd88*$^{-/-}$ *Ticam1*$^{-/-}$ mice and controls (fig. S1, D and E). Thus, although previous work demonstrated that MyD88 function is important in determining susceptibility to DSS-induced (*9*) and pathogen-induced (*10*) inflammation in the intestine, we found no evidence for altered intestinal barrier function in *Myd88*$^{-/-}$ *Ticam1*$^{-/-}$ mice with a limited defined intestinal flora. Therefore, our data suggest that loss of mucosal compartmentalization can occur in the presence of normal intestinal barrier function and in the absence of any measurable intestinal pathology.

Bacteria encountered in the blood and spleen induce strong adaptive immune responses (*1*). We therefore determined the serum titers of commensal bacteria–specific antibodies in conventional SPF *Myd88*$^{-/-}$ *Ticam1*$^{-/-}$ mice. To avoid detection of highly cross-reactive epitopes, we determined titers by surface staining of live bacteria and flow cytometric analysis (fig. S2). We found that as expected (*7*), conventional SPF F_1 control mice had no detectable serum antibodies to intestinal commensal bacterial species (Fig. 2A). In contrast, commensal-specific immunoglobulins G and M (IgGs and IgMs) were consistently present in conventional SPF unma-

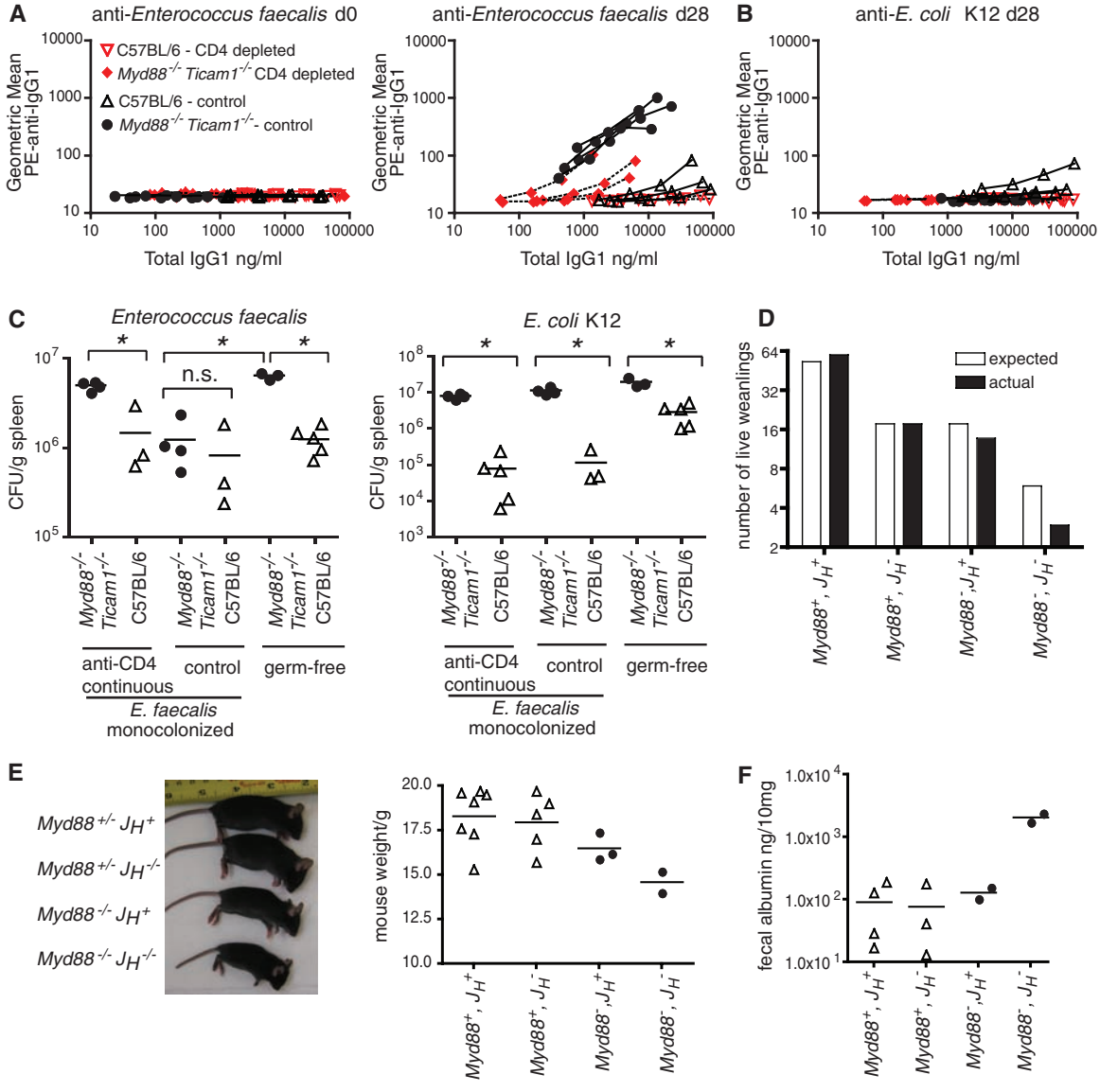

Fig. 4. Serum antibodies successfully protect *Myd88*$^{-/-}$ *Ticam1*$^{-/-}$ mice from bacteraemia. Germ-free, 12-week-old *Myd88*$^{-/-}$ *Ticam1*$^{-/-}$ and C57BL/6 mice were monocolonized with *E. faecalis* for 4 weeks by cohousing with monocolonized sentinel mice, with and without continuous CD4^{+} T cell depletion. (**A**) Serum antibodies against *E. faecalis* were quantified by bacterial flow cytometry at days 0 and 28 of colonization. (**B**) Serum antibodies against *E. coli* K-12 were quantified by bacterial flow cytometry at day 28 post colonization. (**C**) Germ-free mice that were monocolonized for 32 days and had been T cell–depleted, or mock-depleted, as indicated, were injected intravenously with a mixture of 10^7 CFU of nalidixic acid–resistant *E. faecalis* and 10^8 CFU of chloramphenicol-resistant *E. coli* K-12. Spleens were recovered 3 hours post injection and selectively plated (*$P < 0.01$). Data are representative of two independent experiments. (**D**) Total live mice of the indicated genotypes found at weaning (male and female mice). (**E**) Representative mice and weights of female mice at week 4 (7 days after weaning). (**F**) Protein-losing enteropathy quantified by measuring fecal albumin concentrations at 4 weeks of age. Total mice analyzed $N = 97$, including $n = 2$ MyD88$^{-/-}$]$_H^{-/-}$ mice.

nipulated *Myd88*$^{-/-}$ *Ticam1*$^{-/-}$ mice (Fig. 2A and S3A), at titers similar to those observed after intravenous vaccinations of control mice with bacteria (fig. S4). Furthermore, commensal-specific antibodies were also observed in clean SPF *Myd88*$^{-/-}$ *Ticam1*$^{-/-}$ mice and in an entirely independent colony of *Myd88*$^{-/-}$ mice (table S1). *MyD88* or *Ticam1* animals with a single gene deleted (single knockout) maintained under conventional SPF conditions also had spontaneous induction of commensal-specific antibodies, although at lower titers than *Myd88*$^{-/-}$ *Ticam1*$^{-/-}$ littermates (fig. S3B and C), which suggested an additive effect of the two genetic lesions.

Commensal bacteria–specific antibodies were shown to be a consequence of colonization with intestinal bacteria, because germ-free *Myd88*$^{-/-}$ *Ticam1*$^{-/-}$ mice had no detectable anti-commensal IgG (Fig. 2B). Furthermore, this phenomenon occurred independently of opportunistic pathogens in the microbiota, as we detected high titers of *E. coli* IgG in the serum of *Myd88*$^{-/-}$ *Ticam1*$^{-/-}$ mice monocolonized with the nonpathogen (*12*) *E. coli* K-12 (Fig. 2C). It was noteworthy that clean SPF *Myd88*$^{-/-}$ *Ticam1*$^{-/-}$ mice vaccinated intravenously with peracetic acid–killed bacteria required higher doses of killed bacteria to induce IgG1 antibody responses than control mice (fig. S4), which suggested that *Myd88*$^{-/-}$ *Ticam1*$^{-/-}$ mice must experience profoundly elevated systemic commensal bacterial–antigen loads. Intestinal and serum IgA was present at normal concentrations in clean SPF and monocolonized *MyD88*$^{-/-}$ *Ticam1*$^{-/-}$ mice (fig. S5) and with normal or elevated titers specific for colonizing organisms (Fig. 2D and fig. S5). This demonstrated that induction of commensal-specific antibodies is microbiota-dependent, but not due to microbial pathogenicity or IgA production defects. Furthermore, although TLR signaling increases the sensitivity of the host for induction of bacteria-specific antibodies (*5*, *13*–*16*), TLR-signaling is not essential for the induction of antibacterial IgG1 responses. This is presumably because of contributions of other innate immune detection pathways, such as the NOD-like receptors, which still operate in the absence of TLRs but with lower sensitivity.

Studies of bacterial infection in *MyD88*$^{-/-}$ mice imply that there is deficient bacterial clearance (*10*, *14*, *16*–*20*), which involves both hematopoietic and/or stromal cells. Indeed, intravenous injection of *E. coli* K-12 resulted in dramatically higher numbers of culturable bacteria in the spleens of clean SPF *MyD88*$^{-/-}$ *Ticam1*$^{-/-}$ mice than in spleens of clean SPF control mice (fig. S6). In addition, unmanipulated phagocyte oxidative burst–deficient mice (*21*) (*Nos2*$^{-/-}$ *Cybb*$^{-/-}$ mice) had serum antibodies specific for their commensal microbiota, whereas cohoused C57BL/6 controls did not (Fig. 3). This suggests that production of commensal-specific IgG in serum is a broad phenomenon associated with innate deficiency, causing impaired bacterial clearance.

To ask whether spontaneously induced anti-commensal immunity was functionally important, we determined whether commensal colonization of *Myd88*$^{-/-}$ *Ticam1*$^{-/-}$ mice could correct bacterial clearance defects. Germ-free *Myd88*$^{-/-}$ *Ticam1*$^{-/-}$ and C57BL/6 mice were depleted of CD4^{+} T cells or mock-depleted, and monocolonized with the typical commensal *Enterococcus faecalis* by cohousing. Four weeks after colonization, *Myd88*$^{-/-}$ *Ticam1*$^{-/-}$, but not C57BL/6 mice, had mounted a robust CD4^{+} T cell–dependent IgG response to *E. faecalis* (Fig. 4A and B). As expected, when infected intravenously with mixed *E. faecalis* and *E. coli* K-12, germ-free *Myd88*$^{-/-}$ *Ticam1*$^{-/-}$ mice had significantly higher splenic counts of both bacterial strains than C57BL/6 germ-free mice (Fig. 4C). In contrast, mock-depleted *E. faecalis* monocolonized *Myd88*$^{-/-}$ *Ticam1*$^{-/-}$ mice still did not clear *E. coli,* but could now clear *E. faecalis* from their spleens as efficiently as C57BL/6 mice (Fig. 4C). Monocolonized *Myd88*$^{-/-}$ *Ticam1*$^{-/-}$ mice that were depleted of CD4^{+} T cells (fig. S7A) and had not mounted strong IgG responses remained unprotected (Fig. 4C). Clearance did not require CD4^{+} T cells per se, as depletion just before challenge did not negatively influence protection (fig. S7, B to D). Further, coating of *E. faecalis* with serum from 28-day monocolonized *Myd88*$^{-/-}$ *Ticam1*$^{-/-}$ mice was sufficient to correct the bacterial clearance defect in *Myd88*$^{-/-}$ *Ticam1*$^{-/-}$ mice (fig. S7E). These data imply that adaptive immune responses, particularly high-titer T cell–dependent antibody responses, functionally compensate for the defect in bacterial clearance in *Myd88*$^{-/-}$ *Ticam1*$^{-/-}$ mice.

In order to confirm that this mechanism is functionally important in unmanipulated mice we bred the *Myd88*$^{-/-}$ $J_H^{-/-}$ double-deficient strain, which lacks antibody production beause of a deletion of the J segments of the immunoglobulin heavy-chain locus. Despite a clean SPF intestinal microbiota, *Myd88*$^{-/-}$$J_H^{-/-}$ offspring exhibited stunted growth, and only half the expected number survived to weaning (Fig. 4, D and E), whereas *Myd88*$^{-/-}$$J_H^{+/-}$ control littermates grew and survived normally. MyD88$^{-/-}$$J_H^{-/-}$ mice also displayed evidence of protein-losing enteropathy at weaning (Fig. 4F). These results suggest that antibody-mediated immunity is essential for TLR signaling–deficient mice to mutually coexist with their microbiota.

In this report, we have shown that adaptive immunity is critical for successful mutualism in TLR signaling–deficient mice. We conclude that TLR signaling is required for the normal elimination of low numbers of bacteria that are translocated from the intestinal lumen into the mucosa, but that commensal-specific serum IgG responses, induced in response to "escaped" intestinal bacteria, can restore effective bacterial clearance to wild-type levels. Thus, innate and adaptive immune mechanisms can complement each other to establish and maintain mutualism, as illustrated by the severe phenotype of the MyD88$^{-/-}$$J_H^{-/-}$ mouse. We suggest that there is a flexible set point between innate and adaptive immunity, determined by the functional performance of each system, that acts to protect the host. It is interesting to note that mutations in innate immunity genes are commonly associated with autoinflammatory diseases, the best characterized of which is the association of the non-TLR microbial recognition receptor NOD2 and Crohn's disease (*22*–*24*). Our work would clearly suggest that such patients would experience escape of a subset of the intestinal commensal flora, and the subsequent nature of immune responses induced may determine the presence or absence of disease.

References and Notes

1. R. Medzhitov, *Nature* **449**, 819 (2007).
2. W. B. Whitman, D. C. Coleman, W. J. Wiebe, *Proc. Natl. Acad. Sci. U.S.A.* **95**, 6578 (1998).
3. C. Mueller, A. J. Macpherson, *Gut* **55**, 276 (2006).
4. O. Shibolet, D. K. Podolsky, *Am. J. Physiol. Gastrointest. Liver Physiol.* **292**, G1469 (2007).
5. C. Pasare, R. Medzhitov, *Nature* **438**, 364 (2005).
6. Materials and methods are available as supporting material on *Science* Online.
7. A. J. Macpherson, T. Uhr, *Science* **303**, 1662 (2004).
8. S. Vaishnava, C. L. Behrendt, A. S. Ismail, L. Eckmann, L. V. Hooper, *Proc. Natl. Acad. Sci. U.S.A.* **105**, 20858 (2008).
9. S. Rakoff-Nahoum, J. Paglino, F. Eslami-Varzaneh, S. Edberg, R. Medzhitov, *Cell* **118**, 229 (2004).
10. D. L. Gibson *et al*., *Cell. Microbiol.* **10**, 618 (2008).
11. G. Sigthorsson *et al*., *Gastroenterology* **122**, 1913 (2002).
12. C. A. Fux, M. Shirtliff, P. Stoodley, J. W. Costerton, *Trends Microbiol.* **13**, 58 (2005).
13. A. L. Gavin *et al*., *Science* **314**, 1936 (2006).
14. S. L. Lebeis, B. Bommarius, C. A. Parkos, M. A. Sherman, D. Kalman, *J. Immunol.* **179**, 566 (2007).
15. A. Meyer-Bahlburg, S. Khim, D. J. Rawlings, *J. Exp. Med.* **204**, 3095 (2007).
16. H.-J. Ko *et al*., *J. Immunol.* **182**, 2305 (2009).
17. O. Takeuchi, K. Hoshino, S. Akira, *J. Immunol.* **165**, 5392 (2000).
18. K. Takeda, S. Akira, *Cell. Microbiol.* **5**, 143 (2003).
19. K. A. Archer, C. R. Roy, *Infect. Immun.* **74**, 3325 (2006).
20. H. von Bernuth *et al*., *Science* **321**, 691 (2008).
21. M. U. Shiloh *et al*., *Immunity* **10**, 29 (1999).
22. J. Hampe *et al*., *Lancet* **357**, 1925 (2001).
23. Y. Ogura *et al*., *Nature* **411**, 603 (2001).
24. J.-P. Hugot *et al*., *Nature* **411**, 599 (2001).

25. We thank J. Kirundi, J. Jury, and J. Lu for their technical support; A. G. Rolink and A. Strasser for providing reagents; and E. Denou, M. Heikenwälder, C. Reis e Sousa, D. Stetson, J. Danska, and C. Mueller for their helpful comments and editing of the manuscript. Grant support: Canadian Institutes of Health Research, Crohn's and Colitis Foundation of Canada, Genome Canada, Canada Research Chairs, Canadian Association of Gastroenterology, NIH grant numbers CA105001 and AI56363.

Supporting Online Material

www.sciencemag.org/cgi/content/full/325/5940/617/DC1
Materials and Methods
SOM Text
Figs. S1 to S7
Table S1
References

25 February 2009; accepted 15 June 2009
10.1126/science.1172747

Chronic Stress Causes Frontostriatal Reorganization and Affects Decision-Making

Eduardo Dias-Ferreira,[1,2,3] João C. Sousa,[1] Irene Melo,[1] Pedro Morgado,[1] Ana R. Mesquita,[1] João J. Cerqueira,[1] Rui M. Costa,[2,4]* Nuno Sousa[1]*

The ability to shift between different behavioral strategies is necessary for appropriate decision-making. Here, we show that chronic stress biases decision-making strategies, affecting the ability of stressed animals to perform actions on the basis of their consequences. Using two different operant tasks, we revealed that, in making choices, rats subjected to chronic stress became insensitive to changes in outcome value and resistant to changes in action-outcome contingency. Furthermore, chronic stress caused opposing structural changes in the associative and sensorimotor corticostriatal circuits underlying these different behavioral strategies, with atrophy of medial prefrontal cortex and the associative striatum and hypertrophy of the sensorimotor striatum. These data suggest that the relative advantage of circuits coursing through sensorimotor striatum observed after chronic stress leads to a bias in behavioral strategies toward habit.

In everyday life, we constantly have to select the appropriate actions to obtain specific outcomes. These actions can be selected on the basis of their consequences (*1*, *2*), e.g., when we press the elevator button to get to the particular floor of our new apartment. This goal-directed behavior is crucial to face the ever-changing environment, but demands an effortful control and monitoring of the response. One way to balance the need for flexibility and efficiency is through automatization of recurring decision processes as a rule or a habit (*3*). Habitual responses no longer need the evaluation of their consequences and can be elicited by particular situations or stimuli (*1*, *2*), e.g., after living for some time in that apartment, we automatically press the button of our home floor when we enter the elevator. The ability to shift between these two types of strategies is necessary for appropriate decision-making (*2*), and in some situations, it may be crucial to be able to inhibit a habit and use a goal-directed strategy, e.g., if we are visiting a new building, we should not press the button for our home floor.

Chronic stress, mainly through the release of corticosteroids, affects executive behavior through sequential structural modulation of brain networks (*4*, *5*). Stress-induced deficits in spatial reference and working memory (*6*) and behavioral flexibility (*7*) are associated with synaptic and/or dendritic reorganization in both the hippocampus (*8*) and the medial prefrontal cortex (mPFC) (*9*). However, the effects of chronic stress on action-selection strategies have not been investigated. Here, we examined whether previous exposure to chronic stress would affect the ability of animals to select the appropriate actions, based on the consequences of their choice. Because associative corticostriatal circuits involving the prelimbic (PL) cortex (*10*) and the dorsomedial striatum (DMS) (*11*) have been implicated in the acquisition and execution of goal-directed actions, whereas sensorimotor circuits, namely, the dorsolateral striatum (DLS) (*12*), are necessary for habit formation, we examined the effects of chronic stress on these brain areas.

In an attempt to mimic the variability of stressors encountered in daily life, adult rats assigned to the stress group were exposed to a well-established stress paradigm (*13*) that combines different stressors in an unpredictable manner to

[1]Life and Health Sciences Research Institute (ICVS), School of Health Sciences, University of Minho, 4710-057 Braga, Portugal. [2]Section on In Vivo Neural Function, Laboratory for Integrative Neuroscience, National Institute on Alcohol Abuse and Alcoholism, National Institutes of Health, Bethesda, MD 20852–9411, USA. [3]Ph.D. Programme in Experimental Biology and Biomedicine (PDBEB), Center for Neuroscience and Cell Biology, University of Coimbra, 3004-517 Coimbra, Portugal. [4]Champalimaud Neuroscience Programme at Instituto Gulbenkian de Ciência, Rua da Quinta Grande, 2780-901 Oeiras, Portugal.

*To whom correspondence should be addressed. E-mail: njcsousa@ecsaude.uminho.pt (N.S.) or costarui@mail.nih.gov (R.M.C.)

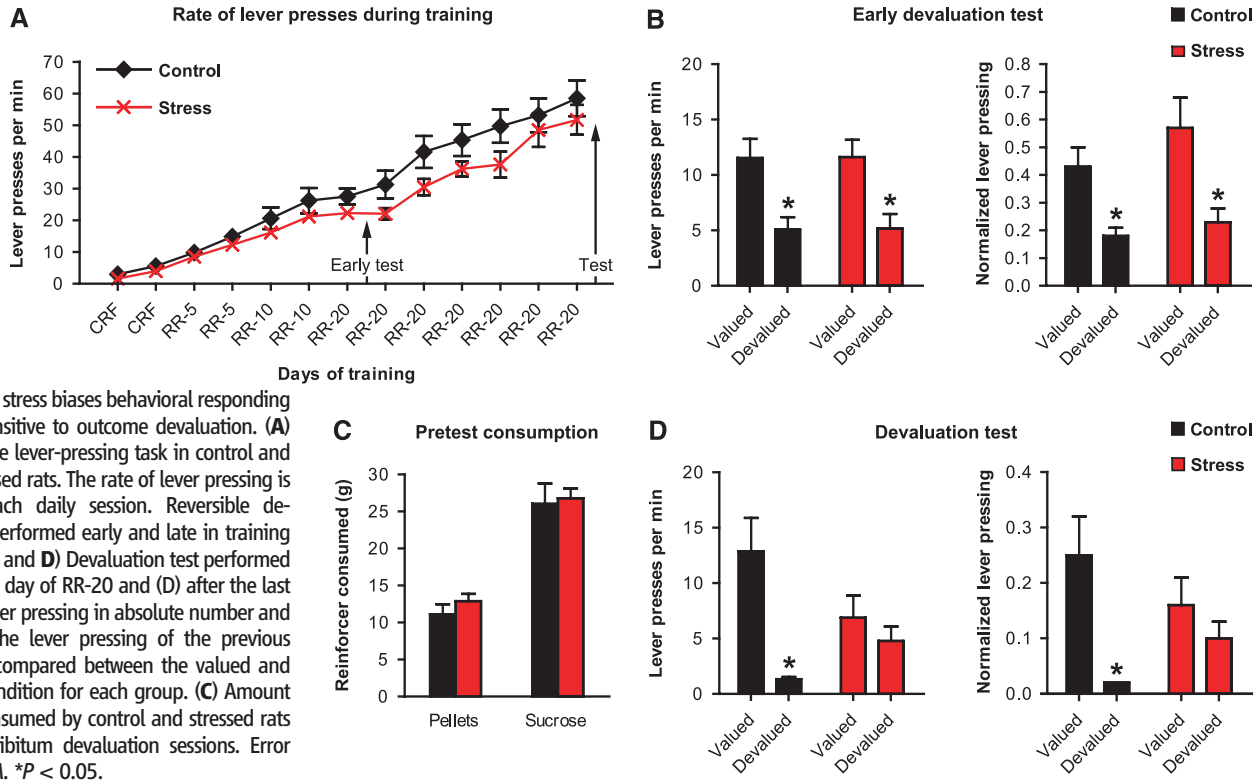

Fig. 1. Chronic stress biases behavioral responding to become insensitive to outcome devaluation. (**A**) Acquisition of the lever-pressing task in control and chronically stressed rats. The rate of lever pressing is depicted for each daily session. Reversible devaluation tests performed early and late in training are indicated. (**B** and **D**) Devaluation test performed (B) after the first day of RR-20 and (D) after the last training day. Lever pressing in absolute number and normalized to the lever pressing of the previous training day is compared between the valued and the devalued condition for each group. (**C**) Amount of reinforcer consumed by control and stressed rats during the ad libitum devaluation sessions. Error bars denote SEM. *$P < 0.05$.

avoid the resilient effect of behavioral control over stressors (*14*). Twenty-one days of stress exposure decreased body-weight gain (fig. S1A), reduced the thymus/body-weight ratio (fig. S1B), and resulted in persistently raised serum corticosterone levels (fig. S1C), when compared with attributes of handled controls. After stress exposure, we tested whether chronic stress affected the ability of animals to perform actions, based on the consequences of their behavior, using two different instrumental tasks.

We first examined whether previous exposure to chronic stress affected the ability of animals to perform actions based on the expected value of predicted outcomes (*1*, *15*). Rats ($n = 8$ per group) were trained to press a lever for a particular outcome (pellets or sucrose, counterbalanced) under a random ratio schedule that was previously shown to bias for goal-directed behavior (*3*, *15*, *16*). Training started with 2 days of continuous reinforcement (CRF) and progressed under increasing random ratio (RR) schedules of reinforcement to RR-20 (on average one reinforcer every 20 lever presses). Both groups increased lever pressing across training days ($F_{12,168} = 95.489$, $P < 0.001$), and there was no interaction with ($F_{12,3} = 1.089$, $P = 0.372$) or main effect of ($F_{1,14} = 3.094$, $P = 0.100$) stress treatment (Fig. 1A). To evaluate whether animals could learn to press for the specific outcome delivered contingent on lever pressing, we performed an early devaluation test after the first day of RR-20 (Fig. 1B). Both stressed animals and controls significantly reduced their responses after the outcome they pressed for during training was devalued by sensory-specific satiety (devalued condition), when compared with the situation when a different outcome was devalued (valued condition) (*13*) (lever presses per min: control, $t_7 = 3.197$, $P = 0.015$; stress, $t_7 = 2.931$, $P = 0.022$; normalized lever pressing: control, $t_7 = 3.106$, $P = 0.017$; stress, $t_7 = 2.694$, $P = 0.031$). With increased training and in accordance with previous studies (*3*, *15*, *16*), the actions of control animals became highly sensitive to sensory-specific satiety [(Fig. 1D) lever presses per min: $t_7 = 3.672$, $P = 0.008$; normalized lever pressing: $t_7 = 3.042$, $P = 0.019$]. In contrast, the actions of stressed animals became insensitive to the expected value of the outcome, as indicated by the lack of a devaluation effect [(Fig. 1D) lever presses per min: $t_7 = 0.984$, $P = 0.358$; normalized lever pressing: $t_7 = 1.095$, $P = 0.310$]. It is noteworthy that the early devaluation test demonstrates that this insensitivity did not arise from an inability of the stressed animals to learn the relation between the action and the outcome or from changes in motivation, food valuation, or hedonics (*17*), but rather because stressed animals rapidly shift to a habitual strategy as training progresses. The amount of reinforcer consumed during the ad libitum devaluation sessions was similar in stressed and control animals [(Fig. 1C) pellets: $t_{14} = -1.072$, $P = 0.302$; sucrose: $t_{14} = -0.252$, $P = 0.805$].

Although it seems unlikely that the results obtained in the test above were due to differences in hedonics or value processing, we used a different task to confirm whether animals previously exposed to chronic stress really had impairments performing actions on the basis of the consequences of their behavior. We therefore investigated whether the behavior of chronically stressed animals would depend on the contingency between getting the outcome and the previous execution of the action (*1*, *18*). We trained a separate group of rats ($n = 15$ per group) in a task in which one action (pressing the left lever) would lead to a particular outcome (i.e., pellets), and another action (pressing the right lever) would lead to a different outcome (i.e., sucrose). Every day animals had two training sessions, one for each action-outcome pair (counterbalanced). Both groups increased lever pressing as training progressed across days under increasing ratio schedules of reinforcement (pellets: $F_{11,308} = 138.213$, $P < 0.001$; sucrose: $F_{11,308} = 88.578$, $P < 0.001$), and there was no interaction with stress (pellets: $F_{11,18} = 0.419$, $P = 0.947$; sucrose: $F_{11,18} = 0.831$, $P = 0.609$), or main effect of stress (pellets: $F_{1,28} = 2.742$, $P = 0.109$; sucrose: $F_{1,28} = 0.781$, $P = 0.384$) on acquisition (Fig. 2A). Similar to the previous task, both controls and stressed animals were able to learn the action-outcome relation as shown by their clear preference toward the valued lever in an early devaluation test after the first day of RR-20 (lever presses per min: control valued, 15.73 ± 2.24; devalued, 4.88 ± 0.95; $t_{14} = 4.150$, $P = 0.001$; stress valued, 11.19 ± 1.40; devalued, 5.33 ± 0.77; $t_{14} = 4.262$, $P = 0.001$; normalized lever pressing: control valued, 0.41 ± 0.04; devalued, 0.14 ± 0.03; $t_{14} = 5.167$, $P < 0.001$; stress valued, 0.34 ± 0.04; devalued, 0.18 ± 0.03; $t_{14} = 4.133$, $P = 0.001$; results are means ± SEM). After the last day of acquisition, we tested whether stressed animals were performing actions because they were necessary to obtain the outcome or not. For each animal, we degraded the contingency between one of the actions and the respective outcome (degraded condition: to get this outcome, the animals no longer needed to press the lever), but not between the other action-outcome pair (non-degraded: to obtain this outcome, the animals needed to press the lever) (*13*). After 2 days of forced-choice degradation training in which

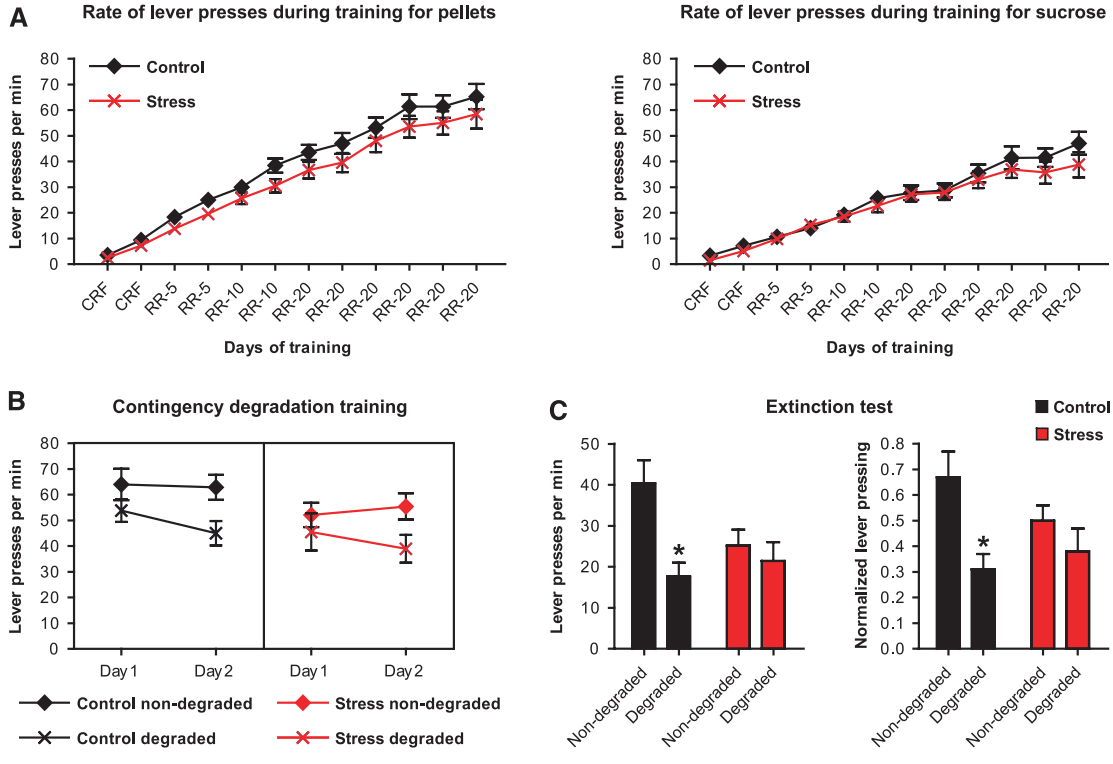

Fig. 2. Chronic stress predisposes choices to be insensitive to changes in action-outcome contingency. (**A**) Acquisition of the lever-pressing task in control and chronically stressed rats. The rate of lever pressing is depicted for each daily session for pellets and for sucrose. (**B**) Performance for each group during forced-choice sessions in which one instrumental outcome continued to be obtained in a RR-20 schedule (non-degraded) and the other outcome was delivered noncontiguously or freely (degraded). (**C**) Critical choice test between the lever for which the action-outcome contingency was preserved and the lever that had the contingency degraded. Lever pressing in absolute numbers and normalized to the lever pressing of the last acquisition training day is compared between levers for each group. Error bars denote SEM. *$P < 0.05$.

both groups changed their behavior [(Fig. 2B) degradation effect: control, $F_{1,28}$ = 4.342, P = 0.046; stress, $F_{1,28}$ = 2.189, P = 0.150; training × degradation interaction: control, $F_{1,28}$ = 2.396, P = 0.133; stress, $F_{1,28}$ = 5.580, P = 0.025], animals were given a free-choice test between the degraded and non-degraded lever, in extinction [to avoid the confounding effects of consumption and reinforcement (*11*)] (Fig. 2C). Control animals significantly reduced their responses on the degraded lever compared with the non-degraded (lever presses per min: t_{14} = 2.552, P = 0.023; normalized lever pressing: t_{14} = 2.645, P = 0.019). However, stressed animals pressed both levers similarly (lever presses per min: t_{14} = 0.808, P = 0.433; normalized lever pressing: t_{14} = 1.330, P = 0.205), which indicated that they failed to choose the action that was necessary to obtain the outcome and that their behavior was habitual.

These data indicate that previous exposure to chronic stress biases decision-making and pre-

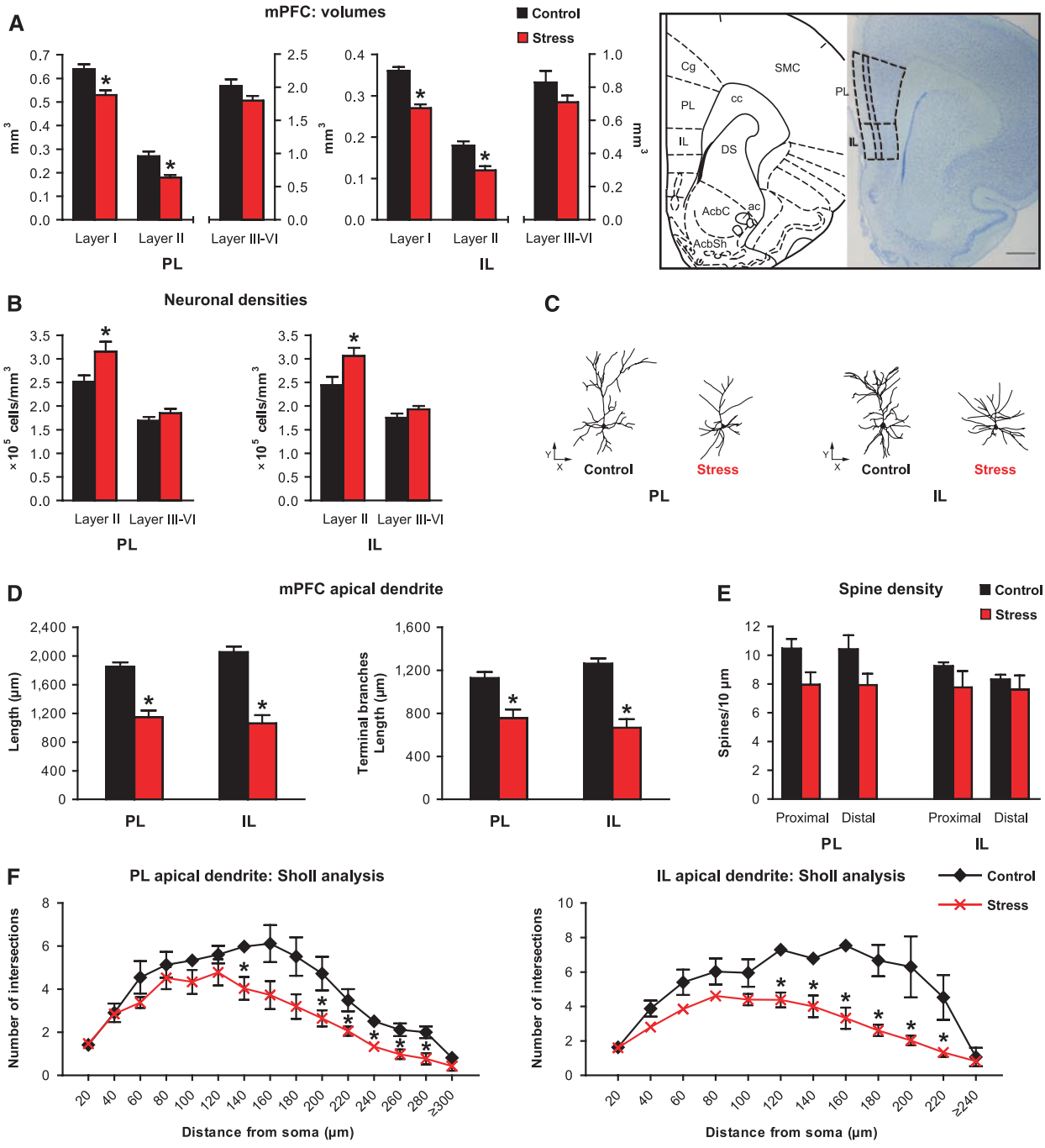

Fig. 3. Chronic stress results in selective atrophy within the external layers of both PL and IL mPFC subregions. Several structural measurements of control and chronically stressed rats are compared. (**A** and **B**) Stereological estimations of (A) volumes and (B) neuronal densities. (A, right) Outlining between regions and layers is represented; diagram was adapted from (*31*) and corresponding brain slice stained with Giemsa (2.20 mm from bregma). Cg, cingulate cortex; SMC, sensorimotor cortices; cc, corpus callosum; DS, dorsal striatum; AcbC, core, and AcbSh, shell, of nucleus accumbens; ac, anterior commissure. Scale bar, 800 µm. (**C** to **F**) Morphometric analysis in 3D of Golgi-stained pyramidal neurons of superficial layers (II/III). (C) Computer-assisted reconstructions of representative neurons depicted in the XY orthogonal plane. (D) Length, (E) spine density, and (F) differential rearrangement of apical dendrites. Error bars denote SEM. *P < 0.05.

disposes animals to more readily shift between goal-directed and habitual behavioral strategies as training progresses, similar to the effects observed after manipulations of the associative (*10*, *11*) or sensorimotor (*12*, *16*) corticostriatal circuits (*19*–*21*). Therefore, in a separate cohort of animals ($n = 5$ per group, submitted to chronic stress or handling but not submitted to instrumental training), we investigated the effects of chronic stress on the structure of cortical and striatal circuits known to be required for goal-directed actions and habits. Within the mPFC, the PL and infralimbic (IL) subregions have been implicated in instrumental behavior (*10*, *19*). Volumetric estimations showed a selective atrophy of external cortical layers in both mPFC subregions of stressed animals [(Fig. 3A) PL: layer I, $t_8 = 4.066$, $P = 0.004$; layer II, $t_8 = 3.697$, $P = 0.006$; layer III-VI, $t_8 = 1.725$, $P = 0.123$; IL: layer I, $t_8 = 6.225$, $P < 0.001$; layer II, $t_8 = 4.743$, $P = 0.001$; layer III-VI, $t_8 = 1.411$, $P = 0.196$]. Consistently, we observed an increase in neuronal density in these layers in the same animals [(Fig. 3B) PL: layer II, $t_8 = -2.602$, $P = 0.032$; layer III-VI, $t_8 = -1.383$, $P = 0.204$; IL: layer II, $t_8 = -2.488$, $P = 0.038$; layer III-VI, $t_8 = -1.688$, $P = 0.130$]. Three-dimensional (3D) morphometric analysis of dendritic arbors of layer II/III pyramidal cells in the mPFC indicated that these changes in volume and density could be ascribed to dendritic atrophy (PL: $t_8 = 6.457$, $P < 0.001$; IL: $t_8 = 7.021$, $P < 0.001$), particularly in terminal branches (PL: $t_8 = 3.851$, $P = 0.005$; IL: $t_8 = 6.389$, $P < 0.001$) of the apical tree (Fig. 3, C and D). These effects suggest a loss of neuronal connectivity that does not seem to result from spine loss [(Fig. 3E) PL: proximal, $t_8 = 2.290$, $P = 0.051$; distal, $t_8 = 1.960$, $P = 0.086$; IL: proximal, $t_8 = 1.270$, $P = 0.240$; distal, $t_8 = 0.669$, $P = 0.522$] or maturation (fig. S2A), but rather to an impoverished arborization confined to distal portions [(Fig. 3F) PL: stress effect, $F_{1,8} = 12.150$, $P = 0.008$; post hoc 140, 200 to 280 μm, $P < 0.05$; IL: stress effect, $F_{1,8} = 17.117$, $P = 0.003$; post hoc 120 to 220 μm, $P < 0.05$] of the apical tree. No consequences were observed in basal dendrites (fig. S3). Note that this atrophy was not generalized to all the regions of the frontal cortex. The orbitofrontal cortex (OFC), which is also a target of stress (*22*) and has been implicated in decision-making (*23*), showed a different pattern of change, with the most medial portions (medial orbital, MO) showing no alteration, whereas the most lateral regions (lateral orbital, LO) displayed a clear structural hypertrophy (fig. S4). In addition, no differences were found in the motor and somatosensory cortices (fig. S5).

We next examined the effects of chronic stress on the projection areas of these cortices into the dorsal striatum (DS), which has been previously implicated in controlling goal-directed and habitual strategies. We investigated more specifically the DMS, which receives input from the PL cortex (*24*) and has been implicated in goal-directed

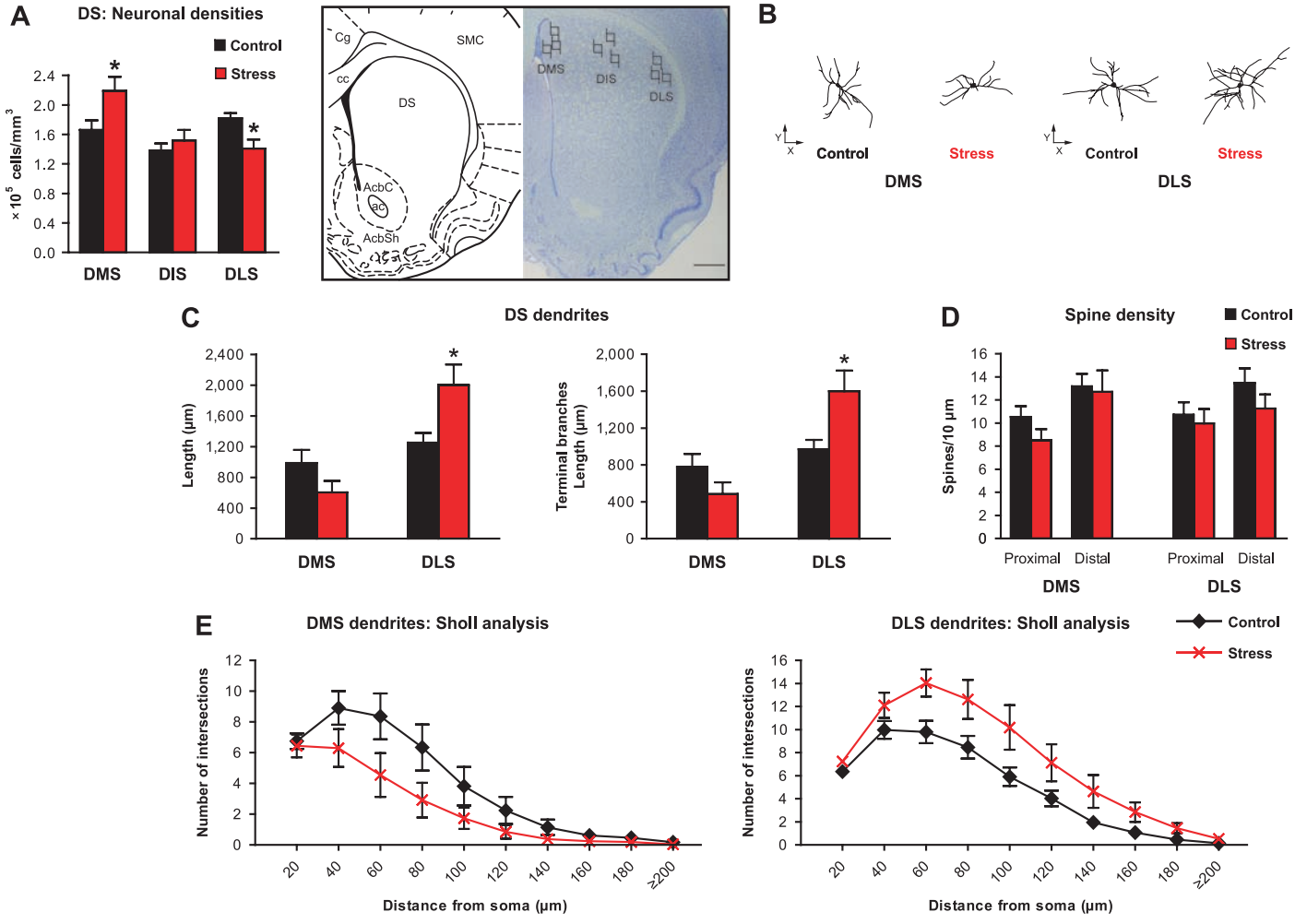

Fig. 4. Chronic stress induces opposing modulating effects in DMS and DLS networks. Several structural measurements of control and chronically stressed rats are compared. (**A**) (Left) Stereological estimation of neuronal densities. (Right) Sampling of the DMS, DIS, and DLS regions is illustrated; diagram was adapted from (*31*) and corresponding brain slice stained with Giemsa (1.00 mm from bregma). Abbreviations are as in Fig. 3. Scale bar, 800 μm. (**B** to **E**) Morphometric analysis in 3D of Golgi-stained MSNs [sampling following the same approach as for neuronal densities; for illustration, see (A)]. (B) Computer-assisted reconstructions of representative neurons depicted in the XY orthogonal plane. (C) Length, (D) spine density, and (E) differential rearrangement of dendrites. Error bars denote SEM. *$P < 0.05$.

actions (*11*), and the DLS or sensorimotor striatum, which is critical for habit formation (*12*) and receives input from the sensorimotor cortices (*24*) and, more laterally, from the LO cortex (*25*). Given the lack of precise anatomical landmarks delimiting these subregions in the DS, which could bias volumetric measures, we measured neuronal densities within the areas previously shown to be important for goal-directed and habitual behavior (Fig. 4A) (*11*–*13*) and found opposing effects of chronic stress in DMS and DLS. Neuronal density decreased in the DLS ($t_8 = 2.970$, $P = 0.018$) and increased in the DMS ($t_8 = -2.343$, $P = 0.047$) (Fig. 4A); these findings indicate atrophy of DMS and hypertrophy of DLS after stress exposure. These differences were not the result of generalized changes in the DS, because no differences in neuronal density were found in the intermediate area between medial and lateral regions (DIS: $t_8 = -0.802$, $P = 0.446$). To determine whether these changes in density were due to changes in dendritic arborization, we performed a 3D morphometric analysis of the medium spiny neurons (MSNs) within the same conservative limits for these DS subregions (Fig. 4, B, C, and E). We found a significant increase in dendritic arbors of DLS neurons [(Fig. 4C) length, $t_8 = -2.527$, $P = 0.035$; terminal branches length, $t_8 = -2.563$, $P = 0.033$; (Fig. 4E) $F_{1,8} = 5.016$, $P = 0.055$] and a nonsignificant trend toward a reduction in the dendrites in DMS neurons [(Fig. 4C) length, $t_8 = 1.682$, $P = 0.131$; terminal branches length, $t_8 = 1.550$, $P = 0.160$; (Fig. 4E) $F_{1,8} = 2.820$, $P = 0.132$] of stressed animals. No significant effects of stress were observed in spine density [(Fig. 4D) DMS: proximal, $t_8 = 1.504$, $P = 0.171$; distal, $t_8 = 0.221$, $P = 0.831$; DLS: proximal, $t_8 = 0.451$, $P = 0.664$; distal, $t_8 = 1.267$, $P = 0.241$] or morphology (fig. S2B). Taken together, the neuronal density and dendritic measures suggest a bidirectional modulation of neuronal connectivity in the DS expressed by a global hypertrophy of the DLS and shrinkage of the DMS.

The present results show a divergent structural reorganization of corticostriatal circuits after chronic stress, with atrophy of the associative corticostriatal circuits and hypertrophy of the circuits coursing through the sensorimotor striatum. This frontostriatal reorganization is accompanied by a shift toward habitual strategies, affecting the ability of stressed animals to perform actions based on their consequences. These data are consistent with previous studies showing that lesions of the PL cortex (*10*) and the DMS (*11*) can bias behavior to be more habitual, whereas inactivation of the DLS (*12*) can render the behavior of habitual animals goal-directed again, which suggest that competing corticostriatal circuits underlie the ability of animals to switch between these two modes of responding (*1*). Our results, using a natural model, indicate that the relative advantage of the sensorimotor network after chronic stress biases behavioral strategies toward habit and offer further insight into how chronic stress can lead to dysfunctional decision-making.

In addition to the role of the PL cortex (*10*), DMS (*11*), and DLS (*12*), the role of other brain regions affected by chronic stress in the behavioral bias herein described should be further investigated. For example, we did not observe changes in the sensorimotor cortices projecting to DLS but did find that the LO cortex, which also projects to the more lateral parts of the dorsal striatum (*25*), presents a clear hypertrophy. [The MO that projects to more medial striatal areas (*25*) does not.] Therefore, the role of the different subregions of the OFC in instrumental conditioning should be further explored, especially because although the atrophy of the PL cortex could contribute to the observed effects, the atrophy of IL cortex does not easily explain the bias toward habitual strategies, because lesions of this region have been shown to impair habit formation (*19*). Another possibility is that changes in the sensorimotor striatum relative to the associative striatum without parallel changes in the projecting cortices are sufficient to readily shift the behavioral strategies as training progresses. This is an interesting possibility given that more ventral striatal areas like the nucleus accumbens seem to have a more prominent role in appetitive Pavlovian responses than in control of instrumental behavior (*26*, *27*). Furthermore, a potential role of thalamic inputs to the sensorimotor striatum in mediating habitual strategies should not be discarded. Finally, the effects of chronic stress on the hippocampus (*8*) and amygdala (*28*) cannot easily explain the behavioral bias observed, because the early devaluation tests revealed that chronically stressed animals can learn action-outcome relations, and their behavior becomes biased as training progresses.

Optimization of decision-making processes confers an important advantage in response to a constantly changing environment. The ability to select the appropriate actions on the basis of their consequences and on our needs at the time of the decision allows us to respond in an efficient way to changing situations. However, the continuous control and attention that this process demands can result in an unnecessary expenditure of resources and can be inefficient in many situations. For instance, when behavior is repeated regularly for extensive periods without major changes in outcome value or contingency, or under uncertain situations where we cannot manipulate the probability of obtaining an outcome, general rules and habits can be advantageous (*3*). Thus, the more rapid shift to habits after chronic stress could be a coping mechanism to improve performance of well-trained behaviors, while increasing the bioavailability to acquire and process new information, which seems essential for adaptation to complex environments (*4*, *5*). However, when objectives need to be re-updated in order to make the most appropriate choice, the inability of stressed subjects to shift from habitual strategies to goal-directed behavior might be highly detrimental. Such impairment might be of relevance to understand the high comorbidity between stress-related disorders and addictive behavior or compulsivity (*29*, *30*), but certainly has a broader impact spanning activities from everyday life decisions to economics.

References and Notes

1. H. H. Yin, B. J. Knowlton, *Nat. Rev. Neurosci.* **7**, 464 (2006).
2. B. W. Balleine, M. R. Delgado, O. Hikosaka, *J. Neurosci.* **27**, 8161 (2007).
3. A. Dickinson, *Philos. Trans. R. Soc. London Ser. B Biol. Sci.* **308**, 67 (1985).
4. R. M. Sapolsky, *Why Zebras Don't Get Ulcers*. (Henry Holt, New York, ed. 3, 2004).
5. B. S. McEwen, *Physiol. Rev.* **87**, 873 (2007).
6. K. Mizoguchi *et al*., *J. Neurosci.* **20**, 1568 (2000).
7. J. J. Cerqueira, F. Mailliet, O. F. Almeida, T. M. Jay, N. Sousa, *J. Neurosci.* **27**, 2781 (2007).
8. N. Sousa, N. V. Lukoyanov, M. D. Madeira, O. F. Almeida, M. M. Paula-Barbosa, *Neuroscience* **97**, 253 (2000).
9. J. J. Radley *et al*., *Neuroscience* **125**, 1 (2004).
10. B. W. Balleine, A. Dickinson, *Neuropharmacology* **37**, 407 (1998).
11. H. H. Yin, S. B. Ostlund, B. J. Knowlton, B. W. Balleine, *Eur. J. Neurosci.* **22**, 513 (2005).
12. H. H. Yin, B. J. Knowlton, B. W. Balleine, *Behav. Brain Res.* **166**, 189 (2006).
13. Materials and methods are available as supporting material on *Science* Online.
14. J. Amat *et al*., *Nat. Neurosci.* **8**, 365 (2005).
15. C. D. Adams, A. Dickinson, *Q. J. Exp. Psychol.* **33**, 109 (1981).
16. M. R. Hilário, E. Clouse, H. H. Yin, R. M. Costa, *Front. Integr. Neurosci.* **1**, 6 (2007).
17. R. J. Katz, *Pharmacol. Biochem. Behav.* **16**, 965 (1982).
18. L. J. Hammond, *J. Exp. Anal. Behav.* **34**, 297 (1980).
19. S. Killcross, E. Coutureau, *Cereb. Cortex* **13**, 400 (2003).
20. A. Nelson, S. Killcross, *J. Neurosci.* **26**, 3805 (2006).
21. J. P. Jedynak, J. M. Uslaner, J. A. Esteban, T. E. Robinson, *Eur. J. Neurosci.* **25**, 847 (2007).
22. C. Liston *et al*., *J. Neurosci.* **26**, 7870 (2006).
23. A. Kepecs, N. Uchida, H. A. Zariwala, Z. F. Mainen, *Nature* **455**, 227 (2008).
24. P. Voorn, L. J. Vanderschuren, H. J. Groenewegen, T. W. Robbins, C. M. Pennartz, *Trends Neurosci.* **27**, 468 (2004).
25. E. A. Schilman, H. B. Uylings, Y. Galis-de Graaf, D. Joel, H. J. Groenewegen, *Neurosci. Lett.* **432**, 40 (2008).
26. L. H. Corbit, J. L. Muir, B. W. Balleine, *J. Neurosci.* **21**, 3251 (2001).
27. H. H. Yin, S. B. Ostlund, B. W. Balleine, *Eur. J. Neurosci.* **28**, 1437 (2008).
28. A. Vyas, R. Mitra, B. S. Shankaranarayana Rao, S. Chattarji, *J. Neurosci.* **22**, 6810 (2002).
29. J. N. Cleck, J. A. Blendy, *J. Clin. Invest.* **118**, 454 (2008).
30. G. F. Koob, *Neuron* **59**, 11 (2008).
31. G. Paxinos, C. Watson, *The Rat Brain in Stereotaxic Coordinates* (Academic Press, San Diego, ed. 4, 1998).

32. We thank M. Carlos, L. Martins, and L. G. Pinto for technical assistance and T. Gremel, X. Jin, and P. Fitzgerald for comments on the manuscript. E.D.-F., J.C.S., and A.R.M. received fellowships from the Portuguese Foundation for Science and Technology. This work was supported by the Bial Foundation (134/06), the ICVS, and the Division of Intramural Clinical and Basic Research, NIAAA, NIH. The authors declare that they have no conflicts of interest.

Supporting Online Material

www.sciencemag.org/cgi/content/full/325/5940/621/DC1
Materials and Methods
Figs. S1 to S5
References

21 January 2009; accepted 24 June 2009
10.1126/science.1171203

Nucleosomal Fluctuations Govern the Transcription Dynamics of RNA Polymerase II

Courtney Hodges,[1]* Lacramioara Bintu,[2]* Lucyna Lubkowska,[3] Mikhail Kashlev,[3] Carlos Bustamante[1,2,4]†

RNA polymerase II (Pol II) must overcome the barriers imposed by nucleosomes during transcription elongation. We have developed an optical tweezers assay to follow individual Pol II complexes as they transcribe nucleosomal DNA. Our results indicate that the nucleosome behaves as a fluctuating barrier that locally increases pause density, slows pause recovery, and reduces the apparent pause-free velocity of Pol II. The polymerase, rather than actively separating DNA from histones, functions instead as a ratchet that rectifies nucleosomal fluctuations. We also obtained direct evidence that transcription through a nucleosome involves transfer of the core histones behind the transcribing polymerase via a transient DNA loop. The interplay between polymerase dynamics and nucleosome fluctuations provides a physical basis for the regulation of eukaryotic transcription.

During transcription elongation in eukaryotes, RNA polymerase II (Pol II) must overcome the transcriptional barriers imposed by nucleosomes in chromatin. In vitro, a single nucleosome is sufficient to halt or greatly slow transcription by Pol II (*1*–*5*), and factors that restrict transcriptional backtracking relieve nucleosome-induced pauses and arrests, which suggests that the influence of the nucleosome is mediated through polymerase backtracking (*4*). Pol II also affects nucleosomal dynamics: Depletion and turnover of histones are seen in actively transcribed genes in vivo (*6*, *7*), and histones are often transferred behind transcribing polymerases in vitro (*2*). However, the mechanisms underlying the mutual influence between nucleosome and polymerase are not well understood.

Here, a dual-trap optical tweezers assay revealed real-time trajectories of individual Pol II complexes as they transcribed through single nucleosomes. A tether was created between two trapped beads—one attached to a stalled polymerase, the other to the upstream DNA (Fig. 1A) (*8*). Addition of ribonucleotide triphosphates induced the polymerase to move toward the nucleosomal positioning sequence (NPS), causing the force between the two beads to decrease. The position of the polymerase was calculated by fitting the measured force to the worm-like chain formula of DNA elasticity (*9*).

In the absence of a nucleosome, polymerases generally proceeded to the end of the DNA template, interrupted only by a few short pauses (Fig. 1B, black traces). When we preloaded a single core nucleosome onto the template, Pol II showed pronounced changes in its dynamics, ranging from one or two pauses to complete arrest at the nucleosome (Fig. 1B, colored traces). We observed a marked decrease in the frequency of nucleosomal arrest with increasing ionic strength (Fig. 1, C to E) (*2*, *5*). The influence of ionic strength on arrest parallels a decrease in the mechanical stability of the nucleosome with salt, but does not correlate with changes in the dynamics of transcription on bare DNA (*8*). Because a majority of polymerases were able to pass the nucleosome at 300 mM KCl, we conducted more detailed studies of nucleosomal transcription at this ionic strength.

To establish whether the nucleosome affected pause entry, we counted all pauses of at least 2 s and recorded their positions on the DNA template (Fig. 2A). The nucleosome locally increased the probability of Pol II to enter a paused state by a factor of ~3, from 0.0079 ± 0.002 bp^{-1} on bare DNA (bp, base pairs) to a peak of 0.022 ± 0.004 bp^{-1} at the nucleosome. The effect on pause density was strongest before the polymerase reached the dyad axis of the nucleosome (Fig. 2A) (*5*). Pause durations at the nucleosome were highly variable among trajectories and within a given trajectory. A comparison of the cumulative distributions of the pause durations shows that the nucleosome biases the polymerase toward longer pauses ($P < 0.001$, Fig. 2B), increasing the me-

[1]Jason L. Choy Laboratory of Single-Molecule Biophysics and Biophysics Graduate Group, University of California, Berkeley, CA 94720, USA. [2]Department of Physics, University of California, Berkeley, CA 94720, USA. [3]NCI Center for Cancer Research, National Cancer Institute–Frederick Cancer Research and Development Center, Frederick, MD 21702, USA. [4]Howard Hughes Medical Institute, Department of Chemistry and Molecular and Cell Biology, University of California, Berkeley, CA 94720, USA.

*These authors contributed equally to this work.
†To whom correspondence should be addressed. E-mail: carlos@alice.berkeley.edu

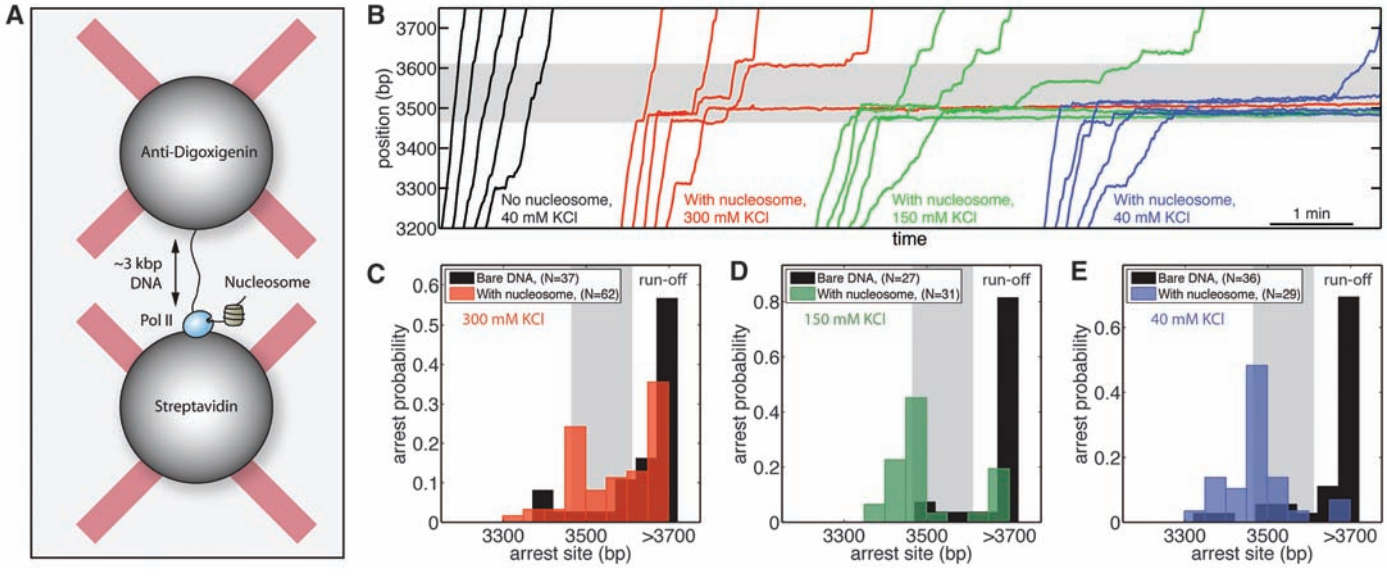

Fig. 1. Transcription through a nucleosome. (**A**) Geometry for the dual-trap optical tweezers experiments. (**B**) Representative trajectories of individual transcribing polymerases with or without the nucleosome at different ionic strengths. (**C** to **E**) Probability of arrest or termination as a function of polymerase position on the DNA template at 300, 150, and 40 mM KCl, respectively. Arrest is defined as a pause that lasts longer than 20 min or until the tether breaks. Data for transcription of bare DNA are in black; nucleosome data are in semitranslucent colors. The shaded region represents the NPS.

dian pause duration from 4.3 s on bare DNA to 8.1 s at the nucleosome. Thus, the nucleosome slows the underlying pause recovery mechanism of the polymerase. Finally, pause-free velocity at the NPS was reduced from 17.5 ± 2 bp s^{-1} on bare DNA to 10.5 ± 3 bp s^{-1} in the presence of a nucleosome (Fig. 2C) (*8*).

Many transcriptional pauses of Pol II on bare DNA are associated with backtracking of the enzyme along the DNA template (*10*–*12*). Pauses end when the polymerase diffusively realigns the dislocated 3′ end of the transcript with its active site and resumes elongation. The probability density of pause durations, $\psi(t)$, is equivalent to the distribution of first-passage times for return to the origin of a Poisson stepper that takes integral steps along a one-dimensional lattice (*13*, *14*), and is given by

$$\psi(t) = \sqrt{\frac{k_f}{k_b}}\,\frac{\exp[-(k_f + k_b)t]}{t}\,I_1\left(2t\sqrt{k_f k_b}\right) \quad (1)$$

where I_1 is the modified Bessel function of the first kind, and k_f and k_b are the forward and backward stepping rates, respectively, during a backtrack (Fig. 3). These rates depend on force according to

$$k_f = k_0 \exp\left(\frac{Fd}{k_B T}\right) \quad (2)$$

$$k_b = k_0 \exp\left(-\frac{Fd}{k_B T}\right) \quad (3)$$

where k_0 is the intrinsic zero-force stepping rate of Pol II diffusion along DNA during a backtrack, F is the force, and d is the distance to the transition state for a step (taken here to be 0.5 bp). For small forces, $\psi(t)$ reduces to the $t^{-3/2}$ power-law dependence previously reported (*10*). We maintained the applied force between 4 and 8 pN at the NPS and fit the cumulative distribution corresponding to $\psi(t)$ to the pause durations on bare DNA to determine $k_0 = 0.33 \pm 0.05$ s^{-1} (Fig. 2B); thus, our data confirm that pause recovery occurs through a diffusive mechanism that is slow relative to elongation.

A backtracked polymerase cannot actively separate downstream nucleosomal DNA from the surface of the histones because it possesses no energy source. Moreover, the DNA downstream of a backtracked polymerase can stochastically rewrap around the histones, restricting Pol II from diffusing back to the 3′ end of the nascent RNA to resume transcription, thereby increasing pause durations. Because local nucleosomal fluctuations are fast relative to the diffusive stepping rate k_0 (*15*), the nucleosome reaches fast local equilibrium between each backtracking step. Thus, we expect pause durations on nucleosomal DNA to be drawn from the same distribution as on bare DNA, but with a net forward stepping rate reduced by a factor corresponding to the fraction of time the local nucleosomal DNA is unwrapped, $\gamma_u = k_u/(k_u + k_w)$, where k_w and k_u are the rates of local wrapping and unwrapping of the DNA around the histones, respectively:

$$k_{f(nucl)} \rightarrow k_f \gamma_u \quad (4)$$

Using the value of k_0 determined above, the cumulative distribution of pause durations in the presence of a nucleosome at 300 mM KCl is correctly fit by the diffusive backtracking model when $\gamma_u = 0.48 \pm 0.05$, indicating that nucleosomal DNA is locally unwrapped half of the time immediately downstream of a polymerase.

During active transcription, forward elongation competes kinetically with pausing. Therefore, the increased pause density at a nucleosome can be used to infer changes in the net elongation rate, allowing us to discriminate between two possible scenarios: one in which Pol II can elongate only against a locally unwrapped nucleosome (Fig. 3), and another in which the polymerase can advance by actively unwrapping nucleosomal DNA (fig. S11). We first examine the predictions of the model where Pol II passively waits for unwrapping fluctuations of the nucleosome (Fig. 3). Here, pause density at the nucleosome has a similar form as on bare DNA, except with a dependence on γ_u (*8*):

$$P_{\text{bare DNA}} = \frac{k_b}{k_b + k_e} \quad (5)$$

$$P_{\text{nucleosome}} = \frac{k_b}{k_b + \gamma_u k_e} \quad (6)$$

We are able to verify the net irreversible elongation rate k_e by fitting the observed pause density on bare DNA to the above expression; we find $k_e = 16 \pm 5$ s^{-1}, in agreement with our measurements of pause-free velocity (Fig. 2C). Using this value of k_e, along with the values of k_b and γ_u obtained above, the model predicts a nucleosomal pause density of 0.017 ± 0.006 bp^{-1} for pauses longer than 2 s, a number that matches well our experimental measurements (Fig. 2A).

The alternative scenario, in which the polymerase can actively open a wrapped nucleosome and elongate through it with a rate $k_{e,w}$ (fig. S11), predicts a smaller pause density (*8*):

$$P_{\text{nucleosome, active unwrapping}} = \frac{k_b}{k_b + \gamma_u k_e + (1 - \gamma_u) k_{e,w}} \quad (7)$$

This prediction does not fit the observed peak value in pause density (above 0.02 bp^{-1}) unless $k_{e,w} = 0$ s^{-1}, which simplifies to the scheme shown in Fig. 3.

Local wrapping of the nucleosome prevents elongation, and because these nucleosomal fluctuations are very fast, the associated transcriptional delays are below the temporal resolution of our instrument. Instead, they have an impact on the apparent pause-free velocity of Pol II, reducing it to $k_e^{app} = \gamma_u k_e$ (*8*). Using our measurement of pause-free velocity on bare DNA (17.5 ± 2 bp s^{-1}), the model predicts an apparent pause-free velocity on nucleosomal DNA of 8.4 ± 1 bp s^{-1}, in close

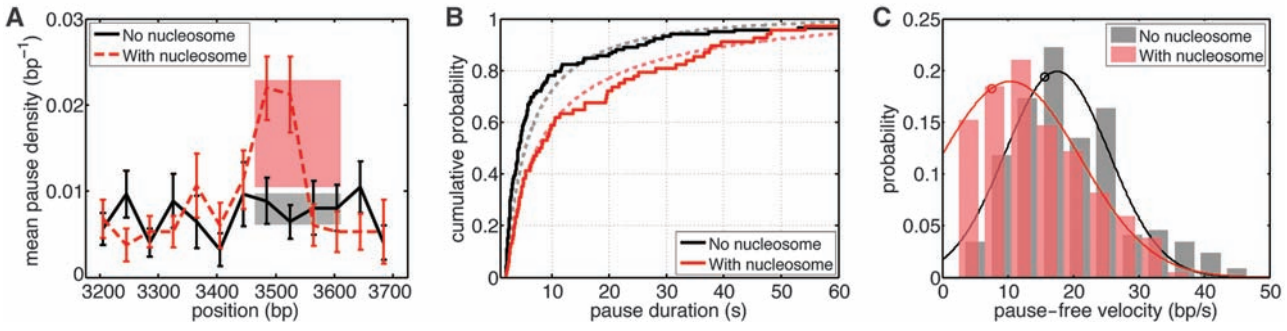

Fig. 2. Effect of the nucleosome on transcription dynamics. In each plot, only traces that passed the NPS are considered. (**A**) Pause density with a nucleosome (dashed red line) and on bare DNA (solid black line). The pink shaded area represents the pause density confidence interval at the nucleosome as predicted from the model presented in the text. The gray shaded region is the confidence interval for pause density on bare DNA used in the model. Error bars are SEM. (**B**) Cumulative distributions of pause durations with (solid red line) and without (solid black line) a nucleosome present. Theoretical cumulative distributions are shown for nucleosomal (pink dashed line) and non-nucleosomal (gray dashed line) pauses. (**C**) Pause-free velocities with (pink) and without (gray) a nucleosome with fits to normal distributions (solid lines). The predicted values based on the diffusive model with and without a nucleosome are shown as red and black circles, respectively.

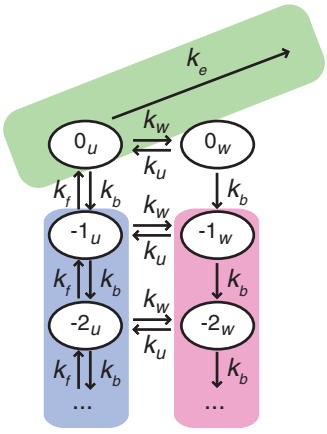

Fig. 3. Kinetic model of transcription through a nucleosome. The green area corresponds to on-pathway elongation (k_e). The pink and blue areas represent off-pathway paused states where Pol II is backtracked; negative numbers indicate how many bases Pol II has backtracked from the elongation competent state, denoted by 0. The subscript u refers to the nucleosome being locally unwrapped (blue area); w denotes the states where the nucleosome is wrapped in front of Pol II (pink area).

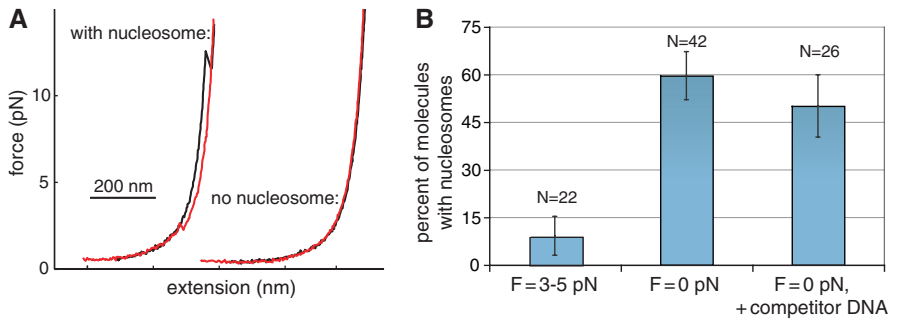

Fig. 4. Histone transfer during transcription. (**A**) Force-extension curves of transcribed DNA. Pulling curves are shown in black and relaxation curves in red. (**B**) Frequency of histone transfer as a function of applied force during transcription.

agreement with our experimental measurement of 10.5 ± 3 bp s^{-1} (Fig. 2C). Thus, during both backtracking and elongation, Pol II does not actively unwrap nucleosomal DNA, but instead waits for fluctuations that locally unwrap the nucleosome to advance, consistent with ratcheting mechanisms proposed for transcription elongation (*16*, *17*).

It has been proposed that a transient DNA loop (*18*, *19*) might allow the histones of a partially unwrapped nucleosome to contact DNA behind the polymerase and remain associated with the DNA after transcription (*2*, *4*, *5*, *18*). The probability of forming such a thermally induced DNA loop should be sensitive to forces as low as 0.2 pN (*20*). We designed a construct that stops the polymerase in a mechanically stable conformation after it has passed the nucleosome (*8*); this strategy allowed us to obtain force-extension curves of the transcribed DNA to determine the dependence of histone transfer on applied force.

We monitored transcription of the nucleosomal region at forces between 3 and 5 pN, then pulled on the transcribed DNA when Pol II reached the end of the template. Very few molecules displayed nucleosome unwrapping transitions (2 of 22) despite marked pausing at the NPS; instead, most showed monotonic force-extension curves, indicating that no nucleosome was present behind the polymerase (Fig. 4A). In contrast, when transcription proceeded in bulk before tether formation so that the DNA template was not under tension during transcription, a significant fraction of complexes showed nucleosomes upstream of the polymerase (25 of 42, $P < 0.0001$), indicating that histone transfer had occurred (Fig. 4B). Histone transfer was not significantly affected by an eightfold excess (50 ng/μl) of competitor DNA (13 of 26, $P < 0.0025$), a concentration sufficient to capture displaced histones (*18*). We conclude that histones are transferred in cis to DNA upstream of Pol II upon nucleosomal transcription, as the looping model proposes, and that tension inhibits formation of the looped intermediate necessary for transfer. This interpretation is consistent with the reduction in pause density as the polymerase advances through the NPS (Fig. 2A), because either the histones detach from the DNA, are transferred to DNA upstream of the enzyme, or are pushed to a lower-affinity (i.e., higher γ_u) downstream sequence.

Regulation of elongation and pausing is of great importance for cotranscriptional processes such as alternative splicing (*21*, *22*). Indeed, a large number of genes from different species are regulated during elongation by extended pausing, including many important developmental and heat shock–induced genes (*23*–*29*). Because nucleosomes are located at ubiquitous, well-defined positions in the genome and act as general repressors of transcription, they constitute a potential scaffold for the regulation of transcription elongation. Our study indicates that modulation of the wrapping/unwrapping equilibrium of DNA around the histone octamer constitutes the physical basis for regulation of transcription through nucleosomal DNA.

References and Notes

1. M. G. Izban, D. S. Luse, *Genes Dev.* **5**, 683 (1991).
2. M. L. Kireeva *et al.*, *Mol. Cell* **9**, 541 (2002).
3. W. Walter, M. L. Kireeva, V. M. Studitsky, M. Kashlev, *J. Biol. Chem.* **278**, 36148 (2003).
4. M. L. Kireeva *et al.*, *Mol. Cell* **18**, 97 (2005).
5. V. A. Bondarenko *et al.*, *Mol. Cell* **24**, 469 (2006).
6. R. M. Widmer *et al.*, *EMBO J.* **3**, 1635 (1984).
7. C. Thiriet, J. J. Hayes, *Genes Dev.* **19**, 677 (2005).
8. See supporting material on *Science* Online.
9. C. Bustamante, J. F. Marko, E. D. Siggia, S. Smith, *Science* **265**, 1599 (1994).
10. E. A. Galburt *et al.*, *Nature* **446**, 820 (2007).
11. N. Komissarova, M. Kashlev, *Proc. Natl. Acad. Sci. U.S.A.* **94**, 1755 (1997).
12. N. Komissarova, M. Kashlev, *J. Biol. Chem.* **272**, 15329 (1997).
13. W. Feller, *An Introduction to Probability Theory and Its Applications* (Wiley, New York, ed. 2, 1971), vol. 2, pp. 59–65.
14. M. Depken, E. A. Galburt, S. W. Grill, *Biophys. J.* **96**, 2189 (2009).
15. G. Li, M. Levitus, C. Bustamante, J. Widom, *Nat. Struct. Mol. Biol.* **12**, 46 (2004).
16. P. H. von Hippel, E. Delagoutte, *Cell* **104**, 177 (2001).
17. G. Bar-Nahum *et al.*, *Cell* **120**, 183 (2005).
18. V. M. Studitsky, D. J. Clark, G. Felsenfeld, *Cell* **76**, 371 (1994).
19. V. M. Studitsky, G. A. Kassavetis, E. P. Geiduschek, G. Felsenfeld, *Science* **278**, 1960 (1997).
20. J. Yan, R. Kawamura, J. F. Marko, *Phys. Rev. E* **71**, 061905 (2005).
21. G. Nogues, S. Kadener, P. Cramer, D. Bentley, A. R. Kornblihtt, *J. Biol. Chem.* **277**, 43110 (2002).
22. M. de la Mata *et al.*, *Mol. Cell* **12**, 525 (2003).
23. A. E. Rougvie, J. T. Lis, *Cell* **54**, 795 (1988).
24. A. Krumm, T. Meulia, M. Brunvand, M. Groudine, *Genes Dev.* **6**, 2201 (1992).
25. L. J. Strobl, D. Eick, *EMBO J.* **11**, 3307 (1992).
26. A. Plet, D. Eick, J. M. Blanchard, *Oncogene* **10**, 319 (1995).
27. D. L. Bentley, M. Groudine, *Nature* **321**, 702 (1986).
28. S. A. Brown, A. N. Imbalzano, R. E. Kingston, *Genes Dev.* **10**, 1479 (1996).
29. L. J. Core, J. T. Lis, *Science* **319**, 1791 (2008).

30. We thank E. Galburt, Y. Zhang, and M. Kireeva for helpful advice, as well as D. King, J. Choy, and S. Grill for technical assistance, and J. Wittmeyer for her gift of plasmids for histone proteins. Supported by NIH grant GM32543 (C.B.).

Supporting Online Material

www.sciencemag.org/cgi/content/full/325/5940/626/DC1
Materials and Methods
SOM Text
Figs. S1 to S13
References

2 March 2009; accepted 16 June 2009
10.1126/science.1172926

Confocal FRAP Imaging

The VT-HAWK combines high precision point-scanning fluorescence recovery after photobleaching (FRAP) with multibeam confocal imaging. The instrument's ability to switch between imaging and photo-bleach modes in seconds enables accurate quantitation of fluorescence intensity dynamics in precise, user-defined regions of the image. VT-HAWK supports FRAP, fluorescence loss in photobleaching, photo-activation, and photo-conversion techniques with selectable pinhole sizes for confocal imaging. The instrument's optics deliver optimal laser beam quality at the sample without compromising the performance of either mode. Options include a laser-merge module that houses up to six solid-state lasers.

VisiTech International
For information +44-(0)-191-5166255
www.visitech.co.uk

Interferon Kit

The VeriKine-HST Human Interferon-Beta Serum ELISA Kit is an enzyme-linked immunosorbent assay for measuring human interferon-beta in serum, plasma, and cell culture supernatant samples. It offers high sensitivity, detecting levels as low as 0.5 IU/ml, with an excellent coefficient of variation. It is not affected substantially by the presence of sample contaminants.

PBL InterferonSource
For information 877-725-8881
www.interferonsource.com

Electroelution of Nucleic Acids and Proteins

G-Capsule is a simple electroelution device that excises DNA or protein bands from agarose and polyacrylamide gels and elutes sample in a final volume of 30 µl. Gentle electroelution through G-Capsule eliminates the risks of damage to DNA or protein samples commonly encountered in the use of glass milk, spin columns, binding columns, and other popular techniques. The simple method eliminates washing, spinning, heating, and precipitation steps. The kit has two parts, G-Pick and G-Trap. The user picks up the protein or nucleic acid band with the G-Pick and assembles it with the G-Trap. The assembled G-Capsule is submerged in electrophoresis buffer on a horizontal electrophoresis system and the protein or nucleic acid is rapidly eluted into the G-Trap. The recovered DNA can be used in molecular manipulations such as ligation, restriction enzyme digestion, sequencing, amplification, random priming, and other enzymatic reactions.

G-Biosciences
For information 314-991-6034
www.GBiosciences.com

Magnetic Stirrers

A new line of magnetic stirrers comes in three sizes and four colors. They are available in sizes 120 mm, 170 mm, and 220 mm, with stirring capacities of 2 liters, 4 liters, and 5 liters, respectively. Stirring speed range is from 150 rpm to 2,500 rpm. The tops are made of polypropylene and come with two nonslip silicon covers (colored black and white) to prevent sliding of the sample vessel. A wide base and rubber feet make these quiet stirrers extremely stable.

Jeio Tech
For information 781-376-0700
www.jeiotech.com

High Throughput Electrophoresis

The CSL multiSUB4 is a compact electrophoresis gel system capable of running four gels in one tank for optimum throughput while saving time and space. The system can run up to 1,200 samples in four vertically stacked gel trays to provide high throughput electrophoresis with the space-saving advantage of a small unit. Each gel tray is ultraviolet-transparent to ensure easy visualization of samples directly on the transilluminator following electrophoresis. The inclusion of four double-sided, multichannel-pipette-compatible combs allows rapid sample loading from 96-well gel trays and thermal cycler blocks. The multiSUB system is available with two formats of double-sided combs, one with one marker and one sample lane for the large scale-up of nucleic acids that may be turned over for a 12-sample throughput, and another included with the unit that offers both eight-sample and 18-sample throughput.

Cleaver Scientific, Ltd.
For information +44-(0)-1788-565-300
www.cleaverscientific.com

Cell Culture Inserts

The Hanging Millicell Cell Culture Inserts are available preloaded into 24-well receiver trays to save time and labor in a range of experimental protocols. Millicell inserts are plastic cell culture wells with membrane bottoms designed to promote more natural cell behavior than plastic plates. The porous membrane allows cells to be fed from both the apical and basolateral sides. As a result, the cells form high-integrity membranes, and studies have shown that cell growth and function more closely resemble those of cells grown in vivo. The hanging, preloaded inserts are available with a polyethylene terephthalate (PET) membrane in two common pore sizes (0.4 and 8.0 micron). The insert's unique design allows easier basolateral access than other hanging inserts with less risk of contamination. The units are sterile and tissue-culture treated. The hanging inserts are recommended for coculture and permeability assays including angiogenesis, chemotaxis, invasion, feeder layers, immunohistochemistry, tumor cell metastasis, and invasion assays.

Millipore
For information 800-548-7853
www.millipore.com

Electronically submit your new product description or product literature information! Go to **www.sciencemag.org/products/newproducts.dtl** for more information.

Newly offered instrumentation, apparatus, and laboratory materials of interest to researchers in all disciplines in academic, industrial, and governmental organizations are featured in this space. Emphasis is given to purpose, chief characteristics, and availabilty of products and materials. Endorsement by *Science* or AAAS of any products or materials mentioned is not implied. Additional information may be obtained from the manufacturer or supplier.

POSITIONS OPEN

TEXAS A&M UNIVERSITY

PROFESSOR AND CHARLES R. PARENCIA CHAIR IN COTTON ENTOMOLOGY. The Department of Entomology at Texas A&M University seeks qualified applicants for this endowed chair position: 12-month, tenure-track, 75 percent research, 25 percent teaching. Applicants should possess a Ph.D. in entomology or closely related biological science from an accredited university, as well as professional expertise and recognition appropriate to a Professor and Chair at Texas A&M University. We seek applicants who can make significant and unique enhancements to the Department's existing scholarly activities in research, teaching and service. Upon hire the Chair holder is expected to conduct extramurally funded entomological research that will enhance cotton production and pest management programs. Classroom teaching responsibilities will be developed to match the professional background and expertise of the Chair with the academic needs of the Department; in addition the successful applicant will have responsibility for mentorship and leadership training of undergraduate and graduate students. As a result of these activities, the Chair is expected to provide state, national, and international leadership in cotton entomology. We seek applicants with demonstrated abilities to develop and work effectively with interdisciplinary teams; to operate easily across discovery, translational, and implementation research; and to communicate effectively among diverse audiences. Texas A&M University seeks individuals who will contribute to the diversity efforts of the University. See details at **website: http://insects.tamu.edu** for full description and instructions for submission of application materials. Applicant review will begin October 1, 2009.

FACULTY POSITION in Developmental Neurobiology. The George Washington University is accepting applications for a tenured or tenure-track faculty member at the rank of **PROFESSOR** with expertise in the field of developmental neurobiology. As part of a new initiative at GWU, the successful candidate will play a key role in organizing and expanding research relevant to autism and developmental brain disorders and will develop multi-investigator proposals for extramural funding. The candidate will also participate in medical and graduate student teaching and faculty mentorship. Basic qualifications for the position are a terminal degree (Ph.D. and/or M.D.) in an appropriate discipline and outstanding accomplishments in biomedical research as demonstrated by peer-reviewed publications as well as active and sustained competitive external funding. Preferred qualifications for the position include experience in an academic medical setting and participation and leadership in collaborative research activities such as NIH program project grants and centers. To be considered, send complete curriculum vitae, a statement of current and future research interests, and the names and addresses of three references electronically to **e-mail: phmvac@gwumc.edu** or by surface mail to: **Vincent A. Chiappinelli, Ph.D., Chair of Search Committee, Department of Pharmacology and Physiology, The George Washington University Medical Center, Suite 640, 2300 Eye Street, N.W., Washington, DC 20037.** Only complete applications will be considered. Review of applications will begin on August 31, 2009, and will continue until the position is filled. *The George Washington University is an Equal Opportunity/Affirmative Action Employer.*

Two **POSTDOCTORAL POSITIONS** are available in the laboratory of **Dr. Guoli Dai** in the Department of Biology and the Center for Regenerative Biology and Medicine at Indiana University–Purdue University Indianapolis (IUPUI). Research projects will focus on studying the molecular and cellular mechanisms responsible for liver injury and regeneration. Applicants must have a doctoral degree in life science with substantial research experience. Experience in liver biology and disease is desirable but not essential. Interested candidates should send their curriculum vitae and names of three references to **e-mail: gdai@iupui.edu.**

POSITIONS OPEN

Diabetes Center
University of California, San Francisco

ASSISTANT/ASSOCIATE PROFESSOR
Institute for Molecular Medicine

The Diabetes Center and Institute for Molecular Medicine at the University of California, San Francisco are recruiting an Assistant/Associate Professor with an M.D., Ph.D., or M.D.-Ph.D. degree whose research focuses on biomedical aspects of diabetes. The Center and Institute investigate both type 1 and type 2 diabetes, as well as the development, differentiation, and homeostasis of cell types and tissues manifesting these diseases. Research areas include immunology/inflammation, insulin resistance, obesity, and stem cell research relevant to diabetes. Successful candidates will commit to active participation in Diabetes Center and Department of Medicine affairs. The appointee will occupy space on the UCSF Parnassus Heights Campus and become a member of the Biomedical Sciences Graduate Program. Appointments at the Assistant and Associate Professor level will be considered.

Applications should include curriculum vitae, research accomplishments summary, future research plans, list of major publications, and three to five recommendation letters, submitted by October 1, 2009, to:

UCSF Diabetes Center
c/o Vivian Tucker - Reference M-3073
513 Parnassus Avenue, Room HSW 1117
San Francisco, CA 94143-0540

The University of California is an Equal Opportunity/Affirmative Action Employer. Women and underrepresented minorities are particularly encouraged to apply.

THE UNIVERSITY OF KANSAS
CANCER CENTER

The University of Kansas is seeking a **DEPUTY DIRECTOR** for its Cancer Center. The pursuit of NCI designation is the No. 1 priority of the University of Kansas and represents one of the fastest growing programs on the University of Kansas Medical Center campus.

The Deputy Director will be responsible for developing the vision for clinical research and care at KU and for insuring that the Cancer Center investigators have adequate infrastructure and facilities to achieve the goals and objectives of the Cancer Center. The division chiefs of medical oncology, surgical oncology, and radiation oncology will have reporting responsibilities to the Deputy Director, who is responsible for overall coordination of all clinical cancer care and clinical research activities.

Prior experience in an NCI-designated cancer center and administration of clinical cancer programs preferred. This is a tenure-track appointment at the **ASSOCIATE/FULL PROFESSOR** level. Minimum qualifications are M.D. or M.D.-Ph.D., participation in an NCI-designated cancer center, and a history of productive clinical cancer research. This is an endowed position with a nationally competitive salary and startup package.

To view the complete position description and apply online only, go to: **website: http://jobs.kumc.edu** and search for **position J0084078.** *An Equal Opportunity/Affirmative Action Employer.*

POSTDOCTORAL POSITION in cellular immunology to study the effector mechanisms involved in the induction and regulation of autoimmunity, including mechanisms of immunomodulation by antigens and natural plant extracts. Experience in tissue culture and handling of rodents desired. Recently graduated applicants preferred. Submit curriculum vitae and three letters of reference at **website: http://kmoud001@umaryland.edu. Kamal D. Moudgil, M.D., Ph.D., Associate Professor, Department of Microbiology and Immunology, University of Maryland School of Medicine, Baltimore, MD, U.S.A. Fax 410-706-2129.**

The European Commission is recruiting for

2 Senior Officials

in the Joint Research Centre (JRC)

1. Deputy Director General (AD15) from the EU Member States **– COM/2009/10204 – JO C 165 A of 17 July 2009 – deadline for submission 11 September 2009.**

The Joint Research Centre of the European Commission (JRC) provides scientific-technical advice and support to European policy makers. It comprises seven research institutes spread across 5 sites in Europe; the headquarters are in Brussels. It has a staff of 2,750 and an operating budget of €340M per annum. Based on solid in-house expertise, major research infrastructures and a network of collaborators in the EU and worldwide, the JRC works in a wide variety of areas, including energy, security, nuclear safety and security, reference materials and measurements, environment, health, food safety and consumer protection, competitiveness, and economic and policy analysis.

Candidates should have: proven experience in senior management, including direct responsibility for sizeable staff numbers and budgets, preferably in a scientific organisation or in a policy-making entity in a field relevant to the JRC; a demonstrated track record in a discipline of relevance to the JRC; high level scientific qualifications (PhD or equivalent experience) would be desirable; good knowledge of relevant European Union policies and Directorate Generals; excellent interpersonal, decision-making, communication and negotiating skills.

2. Director (AD14) of the Ispra Site Directorate (JRC.C) from the following Member States: Bulgaria, Czech Republic, Latvia, Lithuania, Malta, Poland, Romania and Slovak Republic **– COM/2009/10205 – JO C 170 A of 22 July 2009 – deadline for submission 15 September 2009.**

The JRC site in Ispra (near Milan, Italy) is the third largest site of the European Commission, hosting 1,800 Commission employees and 3 of the JRC's scientific institutes. The Ispra Site Directorate provides these institutes with a range of essential technical and support services and is responsible for the overall management and development of the Ispra campus. This includes the management of the site's nuclear decommissioning activities. Its mission is to make the Ispra site a safe, secure and attractive working environment by providing efficient customer-driven services to facilitate the current and future scientific activities of the Ispra Institutes. As part of an overall site development plan, the JRC has decided on important investments in the construction of new facilities and the refurbishment of old buildings.

Candidates should notably: be motivated to further develop the efficiency and quality of the site services and their customer orientation; have proven senior management experience, ideally in managing a facility; an engineering background would be an asset; have the necessary leadership to manage a sizeable number of staff and budget; have very good negotiation and communication skills; have a basic understanding of the specific needs of a research organisation; have a very good knowledge of English; a good knowledge of Italian would be an advantage.

A full job description, selection criteria and application details can be found in the Official Journal or on the EUROPA Website:
http://ec.europa.eu/dgs/personnel_administration/working_senior_mgt_en.htm

If you want to apply, you must register via the internet by going to the website:
https://ec.europa.eu/dgs/personnel_administration/seniormanagementvacancies/CV_Encadext/index.cfm

The closing date for applications is 11 September 2009 for COM/2009/10204 and 15 September 2009 for COM/2009/10205.

On-line application will not be possible after 12.00 noon Brussels time.

EUROPEAN COMMISSION

http://ec.europa.eu

Department of Health and Human Services
National Institutes of Health
Postdoctoral Fellow, National Cancer Institute

The National Institutes of Health (NIH) in Bethesda, Maryland, the world's largest medical research facility, seeks applications from exceptional candidates for the position of postdoctoral fellow in the Lewis laboratory of the Metabolism Branch, Center for Cancer Research, National Cancer Institute. The research interests of the lab revolve around the transcriptional regulation of eukaryotic genes by RNA polymerase II. The main focus is on understanding the transcriptional biochemistry of human promoters. This includes using crude and reconstituted in vitro transcription systems to study the factor requirements of promoter regulation (Lewis et al., Molecular Cell 18: 471, 2005; Lee et al., Mol. Cell Biol. 25: 9674, 2005; Pavri et al., Molecular Cell 18:83, 2005). Other complimentary techniques such as microarrays, siRNA knockdown, ChIP and ChIP/seq, FACS analysis of promoter regulation in vivo will be implemented to assess the in vivo and genome-wide regulation of various promoters. The lab will address both fundamental issues of transcriptional regulation and begin to address promoter regulation in tissue-specific contexts. The successful candidate will have a Ph.D. degree with a strong publication record in molecular biology and/or biochemistry and less than three years of postdoctoral experience. US citizenship is not required but proficiency in English is essential. Please submit curriculum vitae and three letters of reference to:

Brian A. Lewis, Ph.D.
Investigator and Head
Transcriptional Regulation and Biochemistry Unit
Metabolism Branch, CCR, NCI
9000 Rockville Pike
Bldg. 10, Rm. 6B05
Bethesda, MD 20892
lewisbri@mail.nih.gov

With nationwide responsibility for improving the health and well being of all Americans, the Department of Health and Human Services oversees the biomedical research programs of the National Institutes of Health.

Department of Health and Human Services
National Institutes of Health
National Cancer Institute
Staff Scientist Position

With nation-wide responsibility for improving the health and well being of all Americans, the Department of Health and Human Services oversees the biomedical research programs of the National Institute of Health and those of NIH's research Institutes.

The Surgery Branch in the Center for Cancer Research, National Cancer Institute of the National Institutes of Health is seeking a Staff Scientist to extend on going genomic (DNA and microRNA microarray) and functional genomic studies using human samples, cultured cells and in vitro and in vivo models of Endocrine Cancers. Experiments will focus on validation of genomic data, identification of novel candidate diagnostic markers and molecular targets using cultured cells as well as in specimens from patients. Candidate must be an experienced Molecular Biologist with experience in genomic and functional genomic approaches. Individuals must have a Ph.D. or M.D. with at least four years of experience. Salary is negotiable and commensurate with the candidate's level of experience. This position is subject to a background investigation.

Candidates should send a letter of interest, curriculum vitae, bibliography, two letters of reference, and copies of three published articles or book chapters. The completed application should be mailed to: **Electron Kebebew, M.D., Senior Investigator and Head, Endocrine Surgery Section, Surgery Branch, National Cancer Institute, Building 10, Room 2B-07, Bethesda, MD 20892-1502, Tel: 301-496-5049, Fax: 301-402-1788, E-mail: kebebewe@mail.nih.gov**.

Tenure-Track Principal Investigator Genetics Branch

The mission of the Genetics Branch (GB), Center for Cancer Research (CCR), National Cancer Institute (NCI) is to improve the understanding of cancer through basic and translational investigations spanning tumor genetics, molecular oncology, genome biology, and model organism genetics. The GB invites applications for a tenure track principal investigator position to conduct studies using genetic or genomic approaches to cancer research. Desirable areas of expertise and emphasis include genomics, chromatin/chromosome biology, genome instability, epigenetics, and functional genomics. To learn more about the Genetics Branch, please visit the CCR's website at: http://ccr.nci.nih.gov/, or the Genetics Branch's website at: http://ccr.cancer.gov/labs/lab.asp?labid=78.

About NCI's Center for Cancer Research

The NCI is part of the National Institutes of Health (NIH) in the Department of Health and Human Services (DHHS), a federal government agency. CCR is the largest component of the NCI intramural biomedical research effort at NIH and a major user of the NIH Clinical Research Center, a state-of-the-art research hospital on the campus of the NIH in Bethesda, MD. The CCR offers tremendous depth and breadth of intellectual and technological resources, as well as opportunities for collaboration with investigators both within and outside of the NIH.

Eligibility

Applicants must have an M.D. and/or Ph.D. in a relevant field with extensive post-doctoral experience, and a strong publication record demonstrating potential for creative independent research in the application of genetics or genomics to cancer research. The incumbent will direct an independent research program consisting of postdoctoral fellows and technicians funded by the NCI intramural research program. The incumbent will receive research support for developing a state-of-the-art laboratory that includes sufficient space, equipment, and supply budget in order to sustain a research program in Genetics. Salary is commensurate with research experience and accomplishments.

Application

Interested applicants should send a cover letter, curriculum vitae, a brief statement of research interests and future plans (1 to 2 pages), and request three letters of reference to be sent to Beverly Stalker electronically (preferred) or by mail to the address below. Position will remain open until filled. Review of applications is expected to begin **October 15, 2009**. **Dr. Snorri Thorgeirsson, Chair, Search Committee, Center for Cancer Research, NCI, Genetics Branch, c/o Beverly Stalker, stalkerb@mail.nih.gov. Executive Secretary, 37 Convent Dr., Bldg 37, Room 6138 MSC 4265, Bethesda, Maryland 20892-4265**.

DEPARTMENT OF HEALTH AND HUMAN SERVICES
NATIONAL INSTITUTES OF HEALTH (NIH)
National Center for Complementary and Alternative Medicine

The National Center for Complementary and Alternative Medicine (NCCAM), a component of the National Institutes of Health (NIH), Department of Health and Human Services, seeks an accomplished, innovative neuroscientist to serve as Scientific Director of its Intramural Research Program (IRP) and as senior investigator responsible for developing a new research program in mind-body medicine. This individual reports to the Director, NCCAM, and will serve as a member of the NCCAM leadership team.

As Scientific Director, you will articulate and implement a vision and oversee research infrastructure for highly unified and mutually supportive laboratory and clinical programs in the conduct of bench-to-bedside and bedside-to-bench research related to complementary and alternative medicine (CAM) therapies.

As Senior Investigator, you will have substantial committed resources to create a cutting-edge program of clinically oriented laboratory research and/or clinical studies that exploit the best current methods from the neuroscience disciplines to define the nature, mechanisms of action, safety, and efficacy of the CAM modalities that affect actions and interactions linking mind, body, and behavior.

This exceptional opportunity is available to an accomplished neuroscientist who has a demonstrated record of senior-level management of a large, nationally recognized research program, a commitment to both basic and clinical research, and leadership skills to forge team efforts with colleagues within intramural programs across the NIH.

The candidate will be given the necessary resources (space, budget, staff) to build the intramural research program anticipated to encompass three to five laboratory groups.

Applicants must possess an M.D., Ph.D., or equivalent degree in a biomedical field related to the mission of NCCAM and have professional experience reflecting a broad scientific background and experience in basic and/or clinical investigation. Applicants must be able to interact with full authority; have the demonstrated capability to plan and direct research programs of national and international importance; and have the ability to communicate with and obtain the cooperation of national and international organizations and individuals who represent wide-ranging views and competing priorities. Salary is commensurate with qualifications and experience. Full Federal benefits including leave, health and life insurance, long-term care insurance, retirement, and a savings plan (401k equivalent). Qualified individuals are encouraged to email their CV, bibliography, list of three references, and cover letter outlining their relevant experience and vision for leading the NCCAM IRP to: **nccamsrrecruits@mail.nih.gov, Subject Line: Scientific Director Search**. **Email receipt of applications and inquiries is preferred; however, candidates needing reasonable accommodation may fax application materials to 301-402-4741**.

Department of Health and Human Services
National Institutes of Health
National Institute of General Medical Sciences
Cell Biology and Biophysics Division
HEALTH SCIENTIST ADMINISTRATOR

The National Institute of General Medical Sciences (NIGMS), a major research component of the National Institutes of Health (NIH) and the Department of Health and Human Services (DHHS), is seeking applications from exceptional scientists to serve as **Chief of the Structural Genomics and Proteomics Technology Branch in the Division of Cell Biology and Biophysics Division**. This Branch supports research grant programs for the Protein Structure Initiative (PSI), a large, multi-component activity with the goal of making three-dimensional, atomic-level structures obtainable from knowledge of their corresponding DNA sequences. Information about the Protein Structure Initiative can be found at: http://www.nigms.nih.gov/Initiatives/PSI

The Institute is seeking an individual with scientific, administrative, and leadership credentials who can manage individual grant programs in structural biology, structural genomics, proteomics or bioinformatics as well as serve as Chief of the Structural Genomics and Proteomics Technology Branch and as Director of the PSI. Information about the Division of Cell Biology and Biophysics can be found at: http://www.nigms.nih.gov/About/Overview/CBB.htm.

Qualifications: The successful individual will possess a Ph.D., M.D. or equivalent degree in a field relevant to the position, have research experience in structural biology or related fields, a knowledge of biological processes, leadership and managerial skills, and strong oral and written communication skills. Applicants must be U.S. citizens.

Salary: The current salary range is $120,830 – $153,200, depending on experience and accomplishments; a full Civil Service package of benefits (including retirement, health, life and long term care insurance, Thrift Savings Plan participation, etc.) is available. Recruitment or relocation incentive may be awarded and moving expenses will be paid.

How to Apply: Position requirements and detailed application procedures are provided in vacancy announcement NIGMS-09-352072-DE-CR, which can be obtained by accessing the USAJOBS website at **http://www.usajobs.gov**. All applications and supplemental information must be received no later than **August 18, 2009**. For additional information, contact **Dawn White at 301-435-3415**.

Singapore Bioimaging Consortium

A*STAR

The Singapore Bioimaging Consortium (SBIC) is a member of the Agency for Science, Technology and Research (A*STAR). SBIC aims to harness existing imaging expertise and capabilities in Singapore and develop them into a focused national platform to support the growth of multi-disciplinary research activities and speed the development of biomedical research discoveries. The Consortium is under the chairmanship of Professor Sir George Radda, a noted expert on magnetic resonance in medicine who pioneered the use of the magnetic resonance spectroscopy technique to study the biochemistry of living tissues which led to the advances in treatment of a wide variety of diseases.

Due to formation of new research groups and expansion of research activities, we are looking for **Post Doctoral Research Fellows** in the following areas:

- **Magnetic Resonance Imaging Group (Headed by Dr Chuang Kai-Hsiang)**
  The research focuses on the development and application of MRI methods and imaging biomarkers for detection of neural plasticity, neurodegeneration and pharmaceutical effects in the brain using small animal disease models, as well as the translation between clinical investigations in Clinical Imaging Research Centre.
- **Translational Molecular Imaging Group (Headed by Dr Kishore Bhakoo)**
  The research focuses on the development of animal models and/or Stem cell biology for the study of Stem Cell applications in pre-clinical models of Neurodegenerative diseases, the translation of the technologies and findings to clinical investigations in Clinical Imaging Research.
- **PET and SPECT Imaging Group (Headed by Prof David Townsend)**
  The research focuses on the development of PET and SPECT imaging techniques with PET/CT and SPECT/CT pre-clinical instrumentation and their application to pre-clinical models of diseases that include diabetes, neurodegenerative and cancer.
- **Magnetic Resonance Spectroscopy and Metabolic Imaging Group (Headed by Dr Sendhil Velan)**
  The research focuses on the development of Magnetic Resonance Spectroscopy and advanced spectroscopic imaging approaches for the study of metabolic abnormalities in pre-clinical and/or clinical setting. Research will include models of diabetes, insulin resistance and neuronal insults, the translation of the technologies and findings to clinical investigations in Clinical Imaging Research Centre as well as to link up with the metabolic imaging in Singapore Institute for Clinical Sciences.
- **Laboratory of Metabolic Medicine (Headed by Dr Han Weiping)**
  The research focuses on the study of molecular regulation of hormone secretion and its role in the pathogenesis of diabetes and obesity using mouse genetic, biochemical, electrophysiological, optical imaging, molecular and cell biological approaches.
- **Laboratory of Bioimaging Probe Development (Headed by Dr Chang Young-Tae)**
  The research focuses on the development of novel bioimaging probes and discovery of new biomarkers for stem cells, diabetics, and various neuro dieseases.
- **Bio-optical Imaging Group (Headed by Prof Malini Olivo)**
  The research focuses on the development of Surface Enhanced Raman Spectroscopic (SERS) sensors for both small molecules and proteins involved in in vitro and in vivo models of diseases, and the study of the efficacy of a novel nanoparticle based biosensing using SERS of small molecules and proteins involved in metabolism.

Requirements:

- PhD in related discipline such as Physics, Chemistry, Neuroscience, Biophysics, Biomedical Engineering, Physiology, Biology, Cell biology, Biochemistry, Molecular genetics or Neurochemistry.
- Related field with emphasis in magnetic resonance, stem cells applications, PET/CT and SPECT/CT Imaging and Instrumentation, Bio-imaging, spectroscopic characterization or Bio-sensing.

For more details on job requirements and to apply, please visit the SBIC website at: **http://www.sbic.a-star.edu.sg/career.php**

UNIVERSITY OF OXFORD

www.ox.ac.uk/jobs

Mathematical, Physical and Life Sciences Division
Department of Physics in association with Keble College

University Lecturership In Experimental Quantum Physics

The Department of Physics proposes to appoint to a University Lecturership in Experimental Quantum Physics in the sub-department of Atomic and Laser Physics. The post will be held in conjunction with a (Tutorial) Fellowship at Keble College. The combined University and College salary will be on a scale up to £56,917 per annum, in addition to which the College pays a number of allowances as described in the Further Particulars. The successful applicant is expected to take up the appointment by 1 January 2010 or as soon as possible thereafter.

The advertised post is one of six Science and Innovation Lecturerships awarded to Oxford and Cambridge Universities and Imperial College, London under the theme of Quantum Coherence. The initiative provides an excellent opportunity to develop intra- and inter-institutional collaborative projects.

Preference will be given to experimentalists with recognized expertise in the study of quantum coherence, including ultracold matter and quantum optics, as well as applications in quantum technology, such as quantum simulations, metrology and information processing. He or she will be expected to lead an internationally excellent research effort, to be an effective teacher at both the undergraduate and postgraduate levels, and to participate fully in the life of the College. It is expected that the successful candidate will interact closely with existing experimental and theory programmes.

(See http://www.physics.ox.ac.uk/al/index.htm, for descriptions of current research in the department, and http://www.keble.ox.ac.uk/ for information about the College.)

Further particulars are available from http://www.physics.ox.ac.uk/al/vacs.htm. The application procedure is described therein. (Or they may be obtained from the Administrative Secretary, Atomic and Laser Physics, Clarendon Laboratory, Parks Road, Oxford, OX1 3PU, Tel: 01865 272254 Fax: 01865 272375, alp@physics.ox.ac.uk) Applications should be submitted by 30 September 2009. Please quote DU 09 010 on all correspondence.

The University of Oxford is an Equal Opportunity Employer.

MACQUARIE UNIVERSITY

FACULTY OF SCIENCE

Department of Physics & Engineering

Future Fellowship Candidate Search

Macquarie University in Sydney Australia, seeks applicants for Australian Research Council Future Fellowships in the areas of Astronomy & Astrophysics, Photonics and Quantum Science. Future Fellowships are prestigious four year awards aimed at mid-career researchers, particularly those with a demonstrated ability to build collaborations. Fellowships are awarded at the Senior Lecturer, Associate Professor and Full Professor levels and include $50,000/yr in research funding. We expect the University to offer continuing posts to Fellowship awardees.

The Physics Department (www.physics.mq.edu.au) includes twenty-six faculty and forty PhD students, with major strengths in photonics and laser physics; nanotech and biophotonics; astronomy, astrophysics & astrophotonics; and quantum science & quantum photonics.

Applicants will be assessed on their track record, collaborative history, research vision, and alignment with the Department's research strengths and goals.

Indicative Salary Packages
(including base salary, annual leave loading and 17% employer's superannuation)
Senior Lecturer: A$121,000 pa (base salary A$95,000 pa)
Associate Professor: A$147,000 pa (base salary A$115,000 pa)
Full Professor: A$172,000 pa (base salary $135,000 pa)

To apply: Interested candidates should email their CV with details of their short and long term research visions and collaboration record to research-phys@science.mq.edu.au by 9 Sept 2009.
Enquiries to the Research Coordinator: + 61 (2) 9850 8908 or **research-phys@science.mq.edu.au**

Candidates may care to read information and rules for last year's round at: **www.research.mq.edu.au/researchers/funding/arc_schemes/discovery_futures_fellowships** and **www.arc.gov.au/pdf/FT09_FundingRules.pdf.**

OAK RIDGE NATIONAL LABORATORY

Managed by UT-Battelle for the Department of Energy

Director BioEnergy Science Center

The Oak Ridge National Laboratory (ORNL) is seeking an outstanding research leader for the position of Director of the BioEnergy Science Center (BESC). BESC, which is aligned with ORNL's Biological and Environmental Sciences Directorate, is funded by the U.S. Department of Energy (DOE) Office of Science. BESC is a partnership for bioenergy solutions that's connecting the world's leading scientific minds and resources. Our mission is to revolutionize how bioenergy is processed within five years. To do that, we have assembled a world-class team of leading experts and facilities. This unique partnership and spirit of collaboration is backed by more than $80 million in investments from state and private-sector sources, all of which is going to develop alternative fuel solutions that create viable and affordable options to petroleum-based fuels. The BESC Director role provides a unique opportunity for a highly motivated research leader to shape the direction of an exceptional research program. Please visit www.bioenergycenter.org for more information on the center.

Director Biosciences Division

The Biosciences Division Director role provides a unique opportunity for a highly motivated research leader to shape the future of the division and lead a broad spectrum of current biological research programs including bioprocessing, bioinformation systems, computing and bioinformatics, enzyme improvement, gene expression, imaging and analytical technologies, microbial growth and strain development, nanoscale science, protein structure prediction, proteomics, and sensor development. Please visit http://www.ornl.gov/sci/besd/ for further details about our research programs.

BESC BioEnergy Science Center

For further consideration and full job descriptions, please visit **jobs.ornl.gov** , view open positions, and select position category Science- Biological and Environmental Sciences.

Oak Ridge National Laboratory is an Equal Opportunity Employer

Office of Science U.S. DEPARTMENT OF ENERGY

COLUMBIA UNIVERSITY
Tenure-Track Assistant/Associate Professor Faculty Position

The Institute for Cancer Genetics is inviting applications from outstanding scientists for a tenure-track assistant/associate-professor faculty position to direct a program in cancer research. The successful candidate will be offered a generous start-up package, laboratory space in the new Irving Cancer Research Center building, and will become a member of the Herbert Irving Comprehensive Cancer Center at Columbia University. Academic and/or joint appointment.

Please vist the following Web site to apply.
https://academicjobs.columbia.edu/applicants/Central?quickFind=51880

Columbia University is an affirmative action/equal opportunity employer.

The **Center for Ocean Solutions (COS)** and **Stanford University** seek applicants to be a collaborative leader and Science Director of the Center. The Science Director will be appointed to the faculty of a department at Stanford University and as a Senior Fellow in the Woods Institute for the Environment.

COS works to develop practical and sustainable solutions to the major environmental challenges facing the ocean through research, outreach, and education. A collaboration among Stanford University (including the Hopkins Marine Station and Woods Institute for the Environment), the Monterey Bay Aquarium, and the Monterey Bay Aquarium Research Institute (MBARI), COS combines Stanford's expertise in marine biology, oceanography, engineering, economics, law, and policy, with the Aquarium's success at public education and outreach, and MBARI's leadership in deep-sea technology, exploration, and monitoring. COS is headquartered in Monterey, California, near the Hopkins Marine Station, Aquarium, and MBARI. More information about COS is available at **www.centerforoceansolutions.org**.

We seek a motivated, broad-thinking scientist to establish a vigorous research program and provide scientific leadership for COS while complementing existing expertise at Stanford, the Aquarium, MBARI, and other nearby academic and research institutions. In addition to serving as Science Director, the successful candidate will teach classes at the graduate and undergraduate level and supervise research. We are particularly interested in candidates with a record of public engagement on scientific issues and a familiarity with the intersection of science and public policy.

Applicants in all areas of marine science and oceanography are welcome. The Science Director will collaborate with scientists and policy makers engaged in a broad range of activities, including observations, modeling, theory and laboratory experiments, technology development, and policy analysis and development. The Science Director will work closely with the Executive Director on the development, funding, and implementation of projects and initiatives undertaken by COS and in setting the science direction for COS. The Science Director will be based in Monterey, with research facilities at the Hopkins Marine Station, and will also be expected to maintain a presence on the main campus.

Applicants should have a doctoral degree and a publication record in the marine sciences or oceanography, a demonstrated track record of leadership, excellent communications and management skills, and experience in collaborative research and partnership building. The level and terms of appointment of a successful candidate will depend upon background and experience. Curriculum vitae should be sent by **August 15, 2009**, but applications will be considered until the position is filled. Interested candidates should submit materials to **Patti Hines** at **patti.hines@stanford.edu**.

Women and minority applicants are particularly encouraged to apply.

CARNEGIE INSTITUTION FOR SCIENCE | DEPARTMENT OF GLOBAL ECOLOGY

Faculty Position

We seek a scientist for a research-centered faculty position in global ecology. The search is open to scientists who work on a wide range of ecosystems using a wide range of approaches. The successful applicant will use some combination of experiments, observations, modeling, and synthesis to explore the interaction of ecological processes with other components of the Earth system. Areas of special interest include the world food system, coastal oceans, the large-scale distribution of ecosystems, and patterns of global biodiversity. The research tools can range from molecular biology techniques to satellite remote sensing but should include some combination of empirical and modeling approaches. The position is in a high-profile interdisciplinary department that includes expertise in ecology, biogeochemistry, climate, atmospheric sciences, and remote sensing. The search will focus on scientists early in their careers but with significant post-doctoral and/or faculty experience.

The Carnegie Institution for Science is a private, not-for-profit organization dedicated to basic research and "the application of knowledge to the improvement of mankind". Faculty positions at Carnegie are hard money and include support for research and associated staff. Located on the campus of Stanford University, the Department of Global Ecology (**http://www.dge.ciw.edu**) integrates its primary research mission with opportunities for graduate and undergraduate teaching at Stanford. We encourage collaboration both inside and outside the Institution.

Please submit applications or questions about the position by email to **Chris Field (cfield@ciw.edu), Director, Department of Global Ecology, 260 Panama Street, Stanford, CA 94305**. Applications should include a curriculum vitae, a statement outlining research interests, and the names and addresses of three or more references. The position will remain open until filled. To be assured full consideration, applications should be submitted by **October 1, 2009**.

The Carnegie Institution for Science has a strong institutional commitment to the principle of diversity. In that spirit, we particularly encourage applications from women, members of ethnic minorities, and individuals with disabilities.

UNITED NATIONS UNIVERSITY

International Recruitment

INTERNATIONAL INSTITUTE FOR SOFTWARE TECHNOLOGY (UNU-IIST)
(based in Macao, Special Administrative Region of China)

DIRECTOR (L-7)
(circa: US$ 131,245 to 152,671 p.a.)

UNU-IIST is searching for a new Director with a vision for building on the strengths of the Institute's existing research in ways that address key 21st century challenges of sustainable development in the application of and user engagement with computers and information technologies. More information about UNU-IIST can be found at its website: **http://www.iist.unu.edu**.

The Director of UNU-IIST is the chief academic and administrative officer and has overall responsibility for the direction, organisation, administration and programmes of UNU-IIST. The preferred candidate should have an established scientific profile in computer science and software engineering and allied fields, lending to UNU-IIST the necessary prestige in the international scholarly community; guaranteeing scientific excellence through internal quality control and providing leadership and guidance for the conduct of UNU-IIST.

Applicants should have a Ph.D. or equivalent in computer science or a related discipline with strong background or research and publications in areas related to UNU-IIST's interests with proven record of effective leadership and management experience at a senior level in academic or research institutions. Good communication skills, ability to work in multi-cultural environment and fluency in English are required. Knowledge of other United Nations official language is desirable.

Applications close on **15 September 2009**. Please refer to **http://unu.edu/employment/** for full details of the position and how to apply. All applications must be submitted with UN University P.11 form (available in our website) with a covering letter setting out how your qualifications and experience match the requirements. A brief vision for how UNU-IIST can best respond to 21st Century challenges should be included as part of the covering letter.

Washington University in St. Louis

Post-doctoral Fellowship Position

The Cardiac Bioelectricity and Arrhythmia Center (CBAC) of Washington University is an interdisciplinary center that conducts a cutting-edge research program with its focus on cardiac electrophysiology and arrhythmias (see **http://cbac.wustl.edu** and **http://rudylab.wustl.edu**). We currently have an opening for a post-doctoral fellow to work on projects involving mathematical modeling and computer simulations of cardiac electrophysiology, arrhythmia and calcium cycling. The research will be conducted in the laboratory of Dr Yoram Rudy (CBAC Director) located in the Department of Biomedical Engineering. A strong applicant will have research experience in computational biology, and strong background in mathematics, computing and physiology.

We are seeking PhD or DSc graduates with experience in the fields of biophysics and/or biomedical engineering. This position will be available starting September, 2009 for a period of 3 years.

Potential applicants should submit their CV with a cover letter with stated research interests, as well as three letters of recommendation to **Dr. Yoram Rudy** by email: **rudy@wustl.edu**.

Washington University is an EEO/AA Employer.

FACULTY POSITIONS IN THE DEPARTMENT OF MOLECULAR AND CELLULAR BIOLOGY UNIVERSITY OF ARIZONA

The Department of Molecular and Cellular Biology (**www.mcb.arizona.edu**) as part of a new initiative in Systems Biology is seeking to hire 2 tenure-track Assistant Professors with expertise in Bioinformatics or Systems Biology for appointment in 2010. Successful candidates can become members of the interdisciplinary Bio5 institute (**www.bio5.arizona.edu**) and/or the Arizona Cancer Center and may apply for a joint appointment in Mathematics, Computer Sciences, Electrical and Computer Engineering, Physics, or other relevant departments. The appointed individuals will be expected to establish independent and collaborative research programs and contribute to undergraduate, graduate and/or medical education. Opportunities for interaction and collaboration are particularly strong in the areas of functional genomics, genetics, DNA repair, and cancer research. To apply, submit an on-line faculty application for job number 43211 at **www.uacareertrack.com**. Applicants should be prepared to attach a curriculum vitae and a 1-2 page statement of research and teaching interests at the time of application. Separately, have at least three supporting letters sent via email to **dslay@email.arizona.edu**. To ensure consideration, complete applications should be received by **September 15, 2009**, although applications will be accepted until the positions are filled.

The University of Arizona is an EEO/AA Employer/M/W/D/V and is seeking individuals who are able to work with diverse students and colleagues and who have experience with a variety of teaching methods and curricular perspectives.



The Leopold Griffuel Award from the French Cancer Research Association (ARC)

The ARC –Leopold Griffuel Award is among the most respected science prizes in the world

The purpose of this award is the recognition of an investigator or a group whose work or contribution constitutes tangible achievement in the field of Cancer. Since 1970, the Griffuel Award has recognized the contributions of scientists and physicians who have made major advances in the understanding, diagnosis, treatment, cure and prevention of cancer disease. This award, like few others, presages future recognition by the Nobel committee.

Association pour la Recherche sur le Cancer

Deadline : Monday, September 28, 2009
ASSOCIATION POUR LA RECHERCHE SUR LE CANCER (Villejuif, France)
www.arc.asso.fr
E-mail: griffuel@arc.asso.fr

Information about the Prize:
http://www.arc.asso.fr/pages_chercheurs/griffuel_ang.htm

LAB STAFFING IN EUROPE:
Hiring and Retaining Top Academic Talent

Watch *Science* Careers' live webinar featuring a discussion among experts on staffing-related topics including strategies for productive interviews, motivating staff, mentoring, and conflict resolution.

26 August 2009 • 12 pm BST (GMT + 1)

Register for free—visit www.sciencecareers.org/webinar

Science Careers
From the journal *Science* AAAS

Produced by the *Science*/AAAS Business Office.

COURSE

OIST Winter Course "Evolution of Complex Systems"

Date: December 7 – 12, 2009
Location: OIST Seaside House, Onna, Okinawa, Japan
Sponsor: Okinawa Institute of Science and Technology (OIST)

The aim of the OIST Winter Course "Evolution of Complex Systems" (OWECS) is to provide opportunities for young researchers with biological backgrounds to learn the latest advances in the field of evolutionary developmental biology. The OWECS is a combination of lectures and workshops. We invite about 20 graduate students and postgraduate researchers. The sponsor will provide lodging and meals during the course and support travel for those without funding.

Confirmed lecturers: Nipam H. Patel, Robb Krumlauf, Shigeru Kuratani, Thomas C.G. Bosch, Mike Levine, Nori Satoh, Sydney Brenner

Apply to: http://www.irp.oist.jp/owecs/index.html
Deadline for application: September 20, 2009

More information can be obtained from **http://www.irp.oist.jp/owecs/index.html** or contact secretariat at **owecs2009@oist.jp**

POSITIONS OPEN

THE UNIVERSITY of TENNESSEE HEALTH SCIENCE CENTER

J. R. HYDE CHAIR OF EXCELLENCE
The University of Tennessee Health Science Center Department of Orthopaedic Surgery/Campbell Clinic

The University of Tennessee Health Science Center, Department of Orthopaedic Surgery seeks applications and/or nominations for the J. R. Hyde Chair of Excellence with an emphasis in research. UTHSC has established a Center of Excellence in Connective Tissue Diseases with the goal of developing one of the premier musculoskeletal research centers in the nation.

The successful candidate should hold the Ph.D., M.D., or M.D.-Ph.D. degree with a focus in orthopaedic research, a nationally and internationally recognized research program as evidenced by peer-reviewed publications, and a sustained history of external research funding. Applicants should have a demonstrated commitment to and knowledge of equal employment opportunity and affirmative action.

Interested candidates are encouraged to contact: **Steven J. Bares, Ph.D., telephone: 901-448-1799 or e-mail: sbares@utmem.edu.** Qualified applicants must submit a letter of interest accompanied by curriculum vitae and the names and addresses of at least three references to: **Polly A Hofmann, Ph.D., Associate Dean of Faculty Affairs College of Medicine, University of Tennessee Health Science Center, P.O. Box 63647, Memphis, TN 38163.** Review of applications will begin immediately and will continue until the position is filled.

The University of Tennessee is an Equal Employment Opportunity/Affirmative Action/Title VI/Title IX/Section 504 ADA/ADEA Institution in the provision of its education and employment programs and services.

USDA ARS Agricultural Research Service

The USDA, Agricultural Research Service, Plant Genetics Research Unit in St. Louis, Missouri, is seeking a **RESEARCH COMPUTATIONAL BIOLOGIST** at GS-12/13 (**Announcement Number ARS-X9W-0230**), salary range from $67,613.00 to $104,525.00, for placement in a group studying soybean seed development at the Donald Danforth Plant Science Center in St. Louis, Missouri. The research focus of the position is mathematical modeling and systems analyses of plant growth and development. Scientists with a strong quantitative biology, computer science, biostatistics, or bioinformatics background are additionally encouraged to apply. Applicants are expected to develop cutting-edge methods for integration of "omics" data, and ultimately predictive models that will be suitable for use in biotechnology or breeding-based programs to improve soybean yield or modify seed composition. The scientist is expected to establish collaborations with other ARS scientists, as well as with faculty members at the Danforth Center and the University of Missouri. Experience in the biological sciences is desirable but not necessary. *United States citizenship is required.* For information on the research program and/or position, contact **JoAnne Kniptash, telephone: 573-875-5293; e-mail: Joanne.Kniptash@ars.usda.gov.** Refer to **website: http://www.ars.usda.gov/Careers/Careers.htm** for further information and complete application instructions or call **telephone: 301-504-1583.** Send application materials to: **Latania Maise, USDA-ARS-HRD-WSB, 5601 Sunnyside Avenue, Stop #5106, Beltsville, MD 20705-5106** by August 26, 2009. *USDA/ARS is an Equal Opportunity Provider and Employer.*

POSITIONS OPEN

Cedars-Sinai Medical Center
Board of Governors' Gene Therapeutics Research Institute

Gene Therapeutics Research Institute, Cedars Sinai Medical Center; and Department of Molecular and Medical Pharmacology, School of Medicine, University of California at Los Angeles

POSTDOCTORAL POSITIONS are available in the Gene Therapeutics Research Institute and the Department of Molecular and Medical Pharmacology, University of California at Los Angeles to study the molecular and cellular mechanisms involved in brain tumor regression; the formation and function of specific immunological synapses in vivo; and the in vivo migration of immune cells into the tumor microenvironment. This project has a strong translational component to develop and implement novel immunotherapeutics in human clinical trials for brain cancer (*PLoS Medicine,* **6(1):**e10, 2009; *The Journal of Experimental Medicine,* **203:**2095–107, 2006; *Cancer Research,* **65:**7194–7204, 2005; *Nature Biotechnology,* **19:**582–585, 2001; *Proc. Natl. Acad. Sci. U.S.A.,* **97:**7482–7, 2000; *Nature Medicine,* **5:**1256–1263, 1999). A strong background in immunology, cancer biology, or imaging is preferred.

Our Institute is located at the Cedars Sinai Medical Center campus and offers state-of-the-art facilities in an exciting environment for postdoctoral research. Interested candidates should have a Ph.D and/or an M.D. and have under five years of experience. Salary is dependent on experience; range is from $38,000 to $48,000. Please submit a cover letter, full curriculum vitae, and contact information for three references to: **Pedro R. Lowenstein, M.D., Ph.D., or Maria G. Castro, Ph.D., Cedars Sinai Medical Center, 8700 Beverly Boulevard, Davis Building, Room 5090, Los Angeles, CA 90048. E-mail: lowensteinp@cshs.org or castromg@cshs.org.**

POSTDOCTORAL POSITION

An NIH-funded Postdoctoral position is available to study the role of transcription and signaling in the regulation of mammalian embryogenesis using molecular genetic approaches. Previous experience with the analysis of mouse development, molecular genetics, signal transduction, and/or transcription factors is required. The laboratory is located at the new Anschutz Medical Campus of the University of Colorado within sight of the Rocky Mountains (**website: http://www.uchsc.edu/cdb/People/Faculty/williams.html**). Applicants should submit curriculum vitae and the names and contact information for three references to **e-mail: trevor.williams@ucdenver.edu** or apply electronically at **website: http://www.jobsatcu.com;** refer to **job posting #807608.**

The University of Colorado is committed to diversity and equality in education and employment.

POSITIONS OPEN

POSTDOCTORAL POSITION, Cancer Research

The laboratory of **Gary Kruh** at University of Illinois at Chicago Cancer Center is seeking a highly motivated Postdoctoral Fellow with a Ph.D. and more than four years in biochemistry, molecular biology, or closely related biological sciences to conduct cancer research. Experience in molecular genetic techniques and cell culture systems are desirable. Send resume, cover letter with a statement of research interests, and names of three references by September 1, 2009, to: **Ms. Dorothy Sholeen-Modrzyk, UIC Cancer Center MC 700, 914 South Wood Street, Chicago, IL 60612. E-mail: cancer@uic.edu.** *UIC is an Affirmative Action/Equal Opportunity Employer.*

ANNOUNCEMENT

INDO-U.S. SCIENCE AND TECHNOLOGY FORUM
Fulbright House, 12 Hailey Road, New Delhi-110 001, India
Website: http://www.indousstf.org
THIRD CALL FOR PROPOSAL–2009

The Indo-U.S. Science and Technology Forum (IUSSTF), established under an agreement between the governments of India and the United States of America, is an autonomous grant-making organization that promotes and catalyzes the Indo-U.S. bilateral collaborations in science, technology, engineering, and biomedical research through substantive interaction among government, academia, and industry.

The IUSSTF seeks to support innovative programs aimed to stimulate interactions that have a strong potential for generating follow-on activities and building long-term Indo-U.S. S&T relationships.

The IUSSTF solicits proposals thrice a year (submission deadlines: 15 February, June, October) jointly submitted by U.S. and Indian principal investigators from academia, government funded institutions/laboratories, and private R&D entities for: (1) knowledge R&D networked and public-private networked Indo-U.S. centers; (2) Indo-U.S. workshop, conference, symposium; (3) training program/advanced schools; (4) travel grants (i) to avail already awarded fellowship and sabbatical positions in U.S./India; (ii) for selected U.S. participants to attend international conferences/events in India; (iii) for specific exploratory/planning visits aimed at large-scale collaborations.

Detailed format available at **website: http://www.indousstf.org.**

For further details and electronic submission: **Arabinda Mitra, e-mail: amitra@indousstf.org, and Michael Cheetham: e-mail: mcheetham@si.edu.**

Submission deadline, 15 October 2009, and award announcement, mid January 2010.

MARKETPLACE

Learn how current events are impacting your work.

***Science*Insider, the new policy blog from the journal *Science*,** is your source for breaking news and instant analysis from the nexus of politics and science.

Produced by an international team of science journalists, *Science*Insider offers hard-hitting coverage on a range of issues including climate change, bioterrorism, research funding, and more.

Before research happens at the bench, science policy is formulated in the halls of government. Make sure you understand how current events are impacting your work. Read *Science*Insider today.

www.ScienceInsider.org

*Science*Insider
Breaking news and analysis from the world of science policy

Science
AAAS

Epigenetics sample and assay technologies by QIAGEN

Trust in methylation analysis

Rely on QIAGEN epigenetics sample and assay technologies for:

- **DNA purification**
- **Bisulfite conversion**
- **Whole bisulfitome amplification**
- **Methylation-specific PCR**
- **Methylation detection and quantification with Pyrosequencing**

Making improvements in life possible — www.qiagen.com

QIAGEN®

Sample & Assay Technologies

ADNAEpigenetics0309S1WW